UNIVERSIDAD DE EXTREMADURA

Departamento de Ingeniería Química y Química Física

TESIS DOCTORAL

ELIMINACIÓN DE CONTAMINANTES EMERGENTES PRESENTES EN AGUAS POR MÉTODOS FÍSICOS Y QUÍMICOS

◈

REMOVAL OF EMERGING CONTAMINANTS IN WATERS BY MEANS OF PHYSICO-CHEMICAL PROCEDURES

ELENA RODRÍGUEZ PANIAGUA

Conformidad de los Directores

Fdo.: Juan Luis Acero Díaz   **Fdo.: F. Javier Benítez García**

Fdo.: Francisco J. Real Moñino

Badajoz, 2015

UNIVERSIDAD DE EXTREMADURA

UEX

Departamento de Ingeniería Química y Química Física

ELIMINACIÓN DE CONTAMINANTES EMERGENTES PRESENTES EN AGUAS POR MÉTODOS FÍSICOS Y QUÍMICOS

◈

REMOVAL OF EMERGING CONTAMINANTS IN WATERS BY MEANS OF PHYSICO-CHEMICAL PROCEDURES

MEMORIA PARA OPTAR AL GRADO DE
DOCTOR CON MENCIÓN INTERNACIONAL

ELENA RODRÍGUEZ PANIAGUA

Badajoz, 2015

A mis padres y a mis hermanas

A mis amigos Amaya, Joaquín, María y Víctor que siempre me han alentado a seguir. Gracias por las risas, las salidas, los consejos, los días de biblioteca, los desayunos, las cenas, los juegos y cada rato que hemos pasamos juntos. Sois los mejores amigos que se puede tener.

También quiero dar las gracias a Mely, Sandra, Yaiza, Javi, Isiki, Alex, Raúl y Carlos, con quienes he compartido tan buenos momentos y se han convertido en parte fundamental de mi vida. Que suerte he tenido de conoceros.

Muchísimas gracias a Juan Francisco, Antonio, Nati, Rafa, Jose, Patri y Miriam por acogerme con los brazos abiertos. Un ejemplo de unidad y trabajo. Con especial cariño a Jose y Miriam. Gracias Jose por tu alegría y por enseñarme tanto, y por mostrarme lo bonito que es Jaén. Gracias Miriam por cada momento, por cada risa, por contagiarme tu ilusión y tus ganas por el laboratorio, lo mejor de mi estancia en Jaén es tenerte como amiga.

Os meus agradecimentos não poderiam deixar de ser para todos aqueles que me acompanharam ao longo da minha passagem pelo LNEC. Muito obrigada a Maria João, Margarida, Elsa, Rui, Catarina, Victor, Laura, Ana e David. Obrigada por me fazerem sentir como uma mais a partir do primeiro dia, pela vossa atenção, ajuda e tempo. Maria João, muito obrigada pelo teu profissionalismo, tua disponibilidade, preocupação e simpatia. Obrigada Margarida por ser um exemplo de força e conhecimento, e obrigada Elsa por estar sempre disposta a ensinar-me. Tenho aprendido muito com cada um de vocês. Obrigada à Catarina por ser tão gentil e atenciosa, ao Rui pela sua disposição para responder a quaisquer perguntas e ao Victor por ser a alegria do laboratório. Com carinho especial para a Sara e para a Rita, que roubaram o meu coração, o melhor da minha estadia em Lisboa.

Gracias a Juana, Juanjo y Pepe por los buenos momentos que compartimos. Con muchísimo cariño a Cami, fuiste la alegría y la amiga que necesité en todo momento.

Para ti, Julio, no tengo palabras. Gracias por cada momento. Gracias por tu paciencia, tu cariño, por animarme y por creer en mí. A tu lado todo es más fácil. Gracias por hacerme feliz.

Por último, quiero dar las gracias a las personas más importantes en mi vida, a mis padres y a mis hermanas. A mis padres, Cándido y Ana, que son mi ejemplo de trabajo y esfuerzo, siempre animándonos a seguir y alcanzar nuestras metas; gracias por vuestras palabras y consejos, por quererme y por cuidarme. A mis hermanas, Ana y Rosa, que sois los centros de mi vida, muchísimas gracias por vuestro apoyo, por las alegrías y el cariño que me dais. Lo tengo todo, porque os tengo a vosotros.

INDICE

1. SUMMARY/RESUMEN

SUMMARY

This global report of Ph.D. Thesis work summarizes the objectives and the most representative results obtained in a research program, which basically consisted in a wide study about the removal of selected emerging contaminants in waters by means of physico-chemical methods. These organic compounds derived from domestic, commercial, and industrial uses are not commonly monitored in the environment, but have the potential to promote known or suspected adverse ecological and/or human health effects. The present work is part of a general research program, which has been developed by the Chemical Engineering Department of the University of Extremadura (Badajoz-Spain), consisting in the treatment of natural waters and wastewaters contaminated with different organic pollutants by using physical, chemical and biological technologies.

This research program has been financially supported by the project CTQ2010-14823, granted by the *Ministerio de Ciencia e Innovación* of Spain, as well as the projects RNM021 and GR10026 from *Gobierno de Extremadura*, Spain. Additionally, the author of this work, Chem. Engnr. Elena Rodríguez, is grateful to the *Gobierno de Extremadura* and *Fondo Social Europeo* for providing her with a FPI grant, and an additional grant within the project GR10026 for the necessary funds for a two-month stay in Jaén (Spain) and a four-month stay in Lisbon (Portugal). Thus, part of this research was conducted in the Department of Analytical Chemistry of University of Jaen (Jaen, Spain) and in the Unit of Quality and Water Treatment, of National Laboratory of Civil Engineering (LNEC, Lisbon, Portugal).

In this general context, the present work was focused on the removal of five emerging contaminants (ECs) from aquatic systems, which were selected as model pollutants that are present in natural water sources: 1-H-benzotriazole (BZ), nortriptyline hydrochloride (NH), N,N-diethyl-m-toluamide or DEET (DT), 3-methylindole (ML) and chlorophene (CP). These compounds were spiked to different types of waters and were

exposed, individually or together, to various chemical oxidation treatments and membrane technologies. The experimental processes carried out are summarized below.

In a first stage, the degradation of the target contaminants was carried out by using chemical oxidation processes, which are suitable for removing organic micropollutants from drinking waters and wastewaters. For this purpose, different oxidant reagents or combinations of oxidants were used, and chemical degradation experiments were designed for the removal of the target pollutants in ultra-pure water and real waters (reservoir water and two different secondary effluents from two WWTPs). Some operating variables were modified with the aim of establishing the optimal conditions for each chemical process; and basic kinetic parameters were determined, which are useful to design reactors and equipments for real water treatment plants.

First of all, the five selected emerging contaminants (benzotriazole, nortriptyline hydrochloride, DEET, methylindole and chlorophene) were photodegraded individually by UV irradiation in ultra-pure aqueous solutions, using a low pressure mercury vapor lamp. The application of the Line Source Spherical Emission Model allowed determining average values for quantum yields of each compound at 20 °C in the range pH 3-9 ($(53.8-9.4)\times10^{-3}$ mol E^{-1} for benzotriazole, $(525-469)\times10^{-3}$ mol E^{-1} for chlorophene, $(2.8-0.9)\times10^{-3}$ mol E^{-1} for DEET, $(108-165)\times10^{-3}$ mol E^{-1} for methylindole, and $(13.8-15.0)\times10^{-3}$ mol E^{-1} for nortriptyline). First-order rate constants of the photolysis reactions were calculated as well as degradation levels reached for the target compounds, which allowed the establishment of the influence of operating variables, such as pH, nature of the selected emerging contaminants and presence of different initial concentrations of H_2O_2. Moreover, the main by-products formed during the photodegradation process were identified for each compound and the evolution of the toxicity was studied. Photochemical experiments were also carried out in real waters in order to evaluate the effect of natural organic matter (NOM) on the degradation levels of the selected emerging compounds. Finally, a kinetic model was proposed for the prediction of the elimination of ECs in any type of water, which agreed satisfactory with the experimental results. In real water matrices, photodegradation turned out to be an effective process for the removal of nortriptyline, chlorophene, methylindole,

and to a certain extent, for benzotriazole. However, UV irradiation is not an effective option for DEET removal.

The second-order rate constants for the direct reactions between each selected EC and the hydroxyl radical (k_{OH-EC}) were later evaluated by competition kinetics. For that purpose, p-CBA was selected as a reference compound and OH radicals were produced by the Fenton's reaction. Thus, the following values were obtained: 8.24×10^9 M^{-1} s^{-1} for benzotriazole; 8.47×10^9 M^{-1} s^{-1} for chlorophene; 7.51×10^9 M^{-1} s^{-1} for DEET; 5.57×10^9 M^{-1} s^{-1} for methylindole, and 10.87×10^9 M^{-1} s^{-1} for nortriptyline.

As chlorination is a very common process for drinking water and wastewater disinfection, it was also investigated in the present work. In a first stage, the goal was to determine the apparent second-order rate constant for the reaction of each EC with chlorine in the pH range 3-11, and a strong pH dependence was found (values at pH 7-8 were $(13.6-4.4) \times 10^{-4}$, 0.15-0.12, 0.40-0.51, 38.8-59.0, $(5.75-3.21) \times 10^3$ M^{-1} s^{-1} for DEET, benzotriazole, nortriptyline, chlorophene and methylindole, respectively). Intrinsic rate constants for the reactions of HOCl with every specific compound species were also determined. In the next stage, apparent second-order rate constants for the reactions of each EC with HOBr were determined in the pH range 7-9 (values at pH 7-8 were 0.09-0.03, 7.4-8.3, 8.5-6.4, 193-445 and $(109-103) \times 10^6$ M^{-1} s^{-1} for DEET, benzotriazole, nortriptyline, chlorophene and methylindole, respectively). To complete this oxidation process, several experiments of chlorination of mixtures of ECs were conducted with the aim of establishing the influence of the type of water and determining the required initial chlorine dose, in order to avoid the dangerous formation of disinfection by-products (mainly trihalomethanes). Since low concentration of bromide in water systems enhances the chlorination process by formation of HOBr, chlorination of ECs in real waters was carried out with different initial concentration of bromide. Degradation of ECs increased in water matrices with low NOM content and with higher concentration of both, chlorine and bromide. It is finally concluded that chlorination is a good option for the removal of methylindole, and to a certain extent, for chlorophene and nortriptyline in real waters. However, chlorination is not an appropriate process for the degradation of benzotriazole and DEET.

The following oxidizing agent investigated was ozone. Two types of experiments were performed with different purposes. The first group of experiments consisted in the ozonation process of each EC dissolved in ultrapure water, at different pH, and in the presence of tert-butylalcohol, with the aim of determining second-order rate constants for the direct reactions between ozone and each compound. For those compounds exhibiting dissociation constants, the specific rate constants of the un-dissociated and dissociated species were also evaluated. Thus, in the case of benzotriazole (pK_a=8.2), rate constants varied from 20.1±0.4 $M^{-1} s^{-1}$ at pH=3 to 2143±23 $M^{-1} s^{-1}$ at pH=10, and specific rate constants of the un-dissociated and dissociated species were 20.1±2.0 and (2.0±0.3)x10^3 $M^{-1} s^{-1}$, respectively. For chlorophene (pK_a=9.8) rate constants values varied from 1.67x10^3 $M^{-1} s^{-1}$ at pH=3 to 1.82x10^5 $M^{-1} s^{-1}$ at pH=11, and the specific rate constants of the neutral and anionic species were 2.8x10^3 $M^{-1} s^{-1}$ and 2.5x10^5 $M^{-1} s^{-1}$. For nortriptyline (pK_a=10.2), values varying from 2.40x10^3 to 472x10^3 $M^{-1} s^{-1}$ in the pH range 2-11 were deduced, and the specific rate constants of the protonated and neutral species were 2.1x10^3 and 4.3x10^5 $M^{-1} s^{-1}$. Finally, for DEET and methylindole, which do not present acidic nature, rate constants remained almost unaffected with the pH. Thus, average values of 0.123±0.003 $M^{-1} s^{-1}$ and (4.90±0.7)x10^5 $M^{-1} s^{-1}$ were proposed for DEET and methylindole, respectively.

The second group of experiments consisted in the ozonation process of each EC dissolved in ultrapure water, and in absence of tert-butylalcohol, with the aim of evaluating the evolution of toxicity and identifying the by-products formed: thus, 6, 27, 14, 8 and 24 intermediates were identified by LC-TOF-MS for benzotriazole, nortriptyline, DEET, methylindole and chlorophene, respectively. Based on these identified by-products, tentative degradation pathways were proposed. It is concluded that ozonation was a suitable process for the removal of chlorophene, methylindole, nortriptyline; and to a certain extent, for benzotriazole. However, ozone is not an appropriate oxidant to eliminate DEET.

In order to complete chemical oxidation experiments, several oxidation systems (mainly AOPs) were applied to remove selected ECs from several water matrices. Specifically, the processes studied were UV radiation, Fenton's reagent, Fenton-like system, ozone and combinations such as O_3/H_2O_2, UV/H_2O_2, $O_3/UV/H_2O_2$, O_3/UV, UV/TiO_2, O_3/TiO_2,

UV/Fe^{2+}/H$_2$O$_2$, UV/Fe^{3+}/H$_2$O$_2$ and O$_3$/TiO$_2$/UV. A comparison of advanced oxidation processes based on first-order rate constants was accomplished, being the oxidation by means of individual oxidants agents less favourable than by the combinations of oxidants. In particular, UV/TiO$_2$, O$_3$/H$_2$O$_2$, and photo-Fenton systems provided higher removal rates of the selected compounds due to several individual reactions taking place: direct ozonation, direct photolysis and hydroxyl radical oxidation.

The second important stage of the present work was the removal of the five selected emerging contaminants in water systems by means of membrane technologies, specifically ultrafiltration (UF) and nanofiltration (NF) processes. UF and NF are adequate to retain organic molecules with different sizes, being able to split the feed stream into two different streams: the concentrate solution or retentate, and the filtered solution or permeate. Two experimental set ups were employed. On one hand, experiments carried out at the University of Extremadura (UEx, Badajoz, Spain) were conducted in a laboratory membrane device in cross-flow mode, with the permeate stream collected separately and the retentate stream recycled to the feed tank. On the other hand, experiments carried out at the National Laboratory for Civil Engineering (LNEC, Lisbon, Portugal) were conducted with a cellulose acetate hollow-fibre (inside-out configuration) UF membrane module.

The first part of this stage was carried out at UEx, employing different water matrices (surface water and two secondary effluents) and different membranes: three UF membranes (MWCOs of 20000, 5000 and 2000 Da) and three NF membranes (MWCOs in the range 150-300 Da). This stage was focused on the evaluation of the influence of some operating variables (nature and MWCO of the membranes, pH, presence of NOM) on the permeate flux and on the retention of the selected compounds. Slight different sequence of removals were determined for UF and NF processes, achieving retentions higher than 80% for chlorophene, methylindole and nortriptyline in both processes and for the three real water matrices used. Considering retention coefficients of both, ECs and DOC (dissolved organic carbon), the nanofiltration HL membrane was the most appropriate for the removal of the selected emerging contaminants from the waters tested, excepting benzotriazole (rejection around 20%).

The second part of this stage was carried out at LNEC, and the main goal was the evaluation of PAC/UF processes for removal of the five selected ECs in three different water matrices (secondary effluents of WWTP Beirolas (Lisbon)). Firstly, simultaneous removal of ECs in ultrapure water by different doses of two PACs was investigated, and the results were discussed. Once the most appropriate dose and PAC was established, PAC/UF experiments were carried out with the selected water matrices and the influence of NOM was investigated. In real waters, PAC/UF process resulted a plausible option for the removal of chlorophene, nortriptyline and methylindole (elimination above 95%); but not very effective for the removal benzotriazole and DEET (elimination around 60%).

The third and last stage of this Ph.D. Thesis work was the investigation of the performance of several sequential physico-chemical processes. These processes consisted in different sequences of individual treatments, in order to enhance the elimination of the target compounds in several water matrices and to obtain a final effluent useful for discharge or reuse. The main objective was to establish the influence of the previous stage on the subsequent step by considering the purification levels reached for the treated water in each individual step.

Firstly, a membrane filtration (UF or NF) pre-treatment was conducted, and both permeate and retentate were afterwards treated by chemical oxidation, using ozone or chlorine. The NF permeate treated with both ozone and chlorine showed completely removal of residual contaminants, excluding benzotriazole, whereas UF permeate chemically oxidized was free of nortriptyline, methylindole and chlorophene, but not of benzotriazole and DEET. Secondly, a chemical oxidation pre-treatment (by using ozone, chlorine, O_3/H_2O_2, UV irradiation or UV/H_2O_2) was applied followed by a nanofiltration process. In all cases, global removals higher than 97% were reached for DEET, chlorophene, methylindole and nortriptyline, although lower values were obtained for benzotriazole (29-95%). At the same time, an important reduction of NOM was also reached. Therefore, both sequential treatments are promising technologies to remove the selected micropollutants while reducing the chlorine doses needed to achieve final water disinfection.

RESUMEN

La presente Memoria de Tesis Doctoral expone y discute de forma detallada los resultados obtenidos en el trabajo de investigación realizado, el cual tiene como objetivo global el estudio de la eliminación de una selección de contaminantes emergentes presentes en diversas aguas mediante procesos físico-químicos. Estos compuestos orgánicos proceden del uso doméstico, comercial e industrial y habitualmente no son monitorizados en el medio ambiente, pero tienen un potencial, conocido o presumible, de causar efectos negativos tanto al medio ambiente como en la salud de los seres humanos. El presente estudio forma parte y se enmarca dentro de una línea de trabajo general más amplia que se viene desarrollando desde hace años en el Área de Ingeniería Química de la Universidad de Extremadura, y que consiste fundamentalmente en el tratamiento y eliminación de diferentes tipos de contaminantes que están presentes en aguas superficiales y residuales, empleando para ello métodos físicos, químicos y biológicos.

La presente investigación ha sido desarrollada a través del proyecto CTQ2010-14823, financiado por el *Ministerio de Ciencia e Innovación* de España, y también, mediante los proyectos RNM021 y GR10026 del Gobierno de Extremadura. Además, la autora de este trabajo, la Ingeniera Química Elena Rodríguez Paniagua, agradece al Gobierno de Extremadura y al Fondo Social Europeo la adjudicación de una beca FPI para el desarrollo de su Tesis doctoral, así como al proyecto GR10026 por los fondos necesarios para la realización de una estancia de dos meses en Jaén (España) y de cuatro meses en Lisboa (Portugal). De este modo, parte de esta investigación se llevó a cabo en el Departamento de Química Analítica de la Universidad de Jaén y en la Unidad de Calidad y Tratamiento de Aguas del Laboratorio Nacional de Ingeniería Civil (LNEC) de Lisboa.

En este contexto general, el presente trabajo se ha centrado en la eliminación de cinco contaminantes emergentes (ECs) en diferentes aguas, los cuales han sido seleccionados como contaminantes modelo al encontrarse presentes en diversas fuentes habituales de agua: 1-H-benzotriazol (BZ), nortriptilina clorhidrato (NH), N,N-dietil-m-

toluamida o DEET (DT), 3-metilindol (ML) y clorofeno (CP). Estos compuestos se disolvieron en diferentes tipos de aguas y fueron expuestos individualmente o de forma simultánea a diversos tratamientos de oxidación química y tecnologías de membrana. Los procesos experimentales llevados a cabo en este trabajo se resumen a continuación.

En una primera etapa se llevó a cabo la degradación de los contaminantes seleccionados mediante procesos de oxidación química, los cuales son muy adecuados para la eliminación en general de microcontaminantes orgánicos de las aguas potables y residuales. Para este propósito se utilizaron diferentes reactivos oxidantes y combinaciones de los mismos y se diseñaron experimentos de degradación química para la eliminación de los contaminantes en agua ultrapura y aguas reales (un agua superficial (pantano), y dos efluentes secundarios procedentes de dos EDAR). Algunas de las variables de operación fueron modificadas con el objetivo de establecer las condiciones óptimas para el proceso químico. Asimismo, se determinaron los parámetros cinéticos básicos, los cuales son útiles para el posterior diseño de reactores y equipos que están presentes en las estaciones de tratamiento de agua.

En primer lugar, los cinco contaminantes emergentes seleccionados (benzotriazol, nortriptilina, DEET, metilindol y clorofeno) fueron degradados individualmente mediante radiación UV en agua ultrapura, utilizando una lámpara de vapor de mercurio a baja presión. La aplicación del Modelo de Fuente Líneal de Emisión Esférica permitió la determinación de los valores medios para los rendimientos cuánticos de cada compuesto a 20 °C en el intervalo de pH 3-9, obteniéndose valores de $(53.8-9.4) \times 10^{-3}$ mol E^{-1} para benzotriazol, $(525-469) \times 10^{-3}$ mol E^{-1} para clorofeno, $(2.8-0.9) \times 10^{-3}$ mol E^{-1} para DEET, $(108-165) \times 10^{-3}$ mol E^{-1} para metilindol y $(13.8-15.0) \times 10^{-3}$ mol E^{-1} para nortriptilina. A su vez, las constantes de velocidad de primer orden de las reacciones fotoquímicas, así como los niveles de degradación alcanzados, se determinaron para cada uno de los ECs, estableciendo la influencia de variables de operación tales como el pH, la naturaleza de los contaminantes emergentes seleccionados y la presencia de diferentes concentraciones iniciales de H_2O_2. Además, para cada compuesto objeto de estudio se identificaron los intermedios de reacción formados durante el proceso de fotodegradación y se estudió la evolución de la toxicidad. Por último, se llevaron a cabo experimentos en aguas reales para

evaluar el efecto de la presencia de materia orgánica en los niveles de degradación obtenidos de los compuestos emergentes seleccionados. Finalmente, se propuso un modelo cinético para predecir la eliminación de los ECs en cualquier tipo de agua, el cual mostró resultados que coincidían satisfactoriamente con los valores experimentales. Por su parte, en aguas reales, la eficacia de la fotodegradación resultó ser elevada para la eliminación de los contaminantes nortriptilina, clorofeno y metilindol, moderada para benzotriazol y baja para DEET.

En una etapa posterior, la constante de velocidad de segundo orden para la reacción directa entre cada uno de los ECs seleccionados y los radicales hidroxilo (k_{OH-EC}) fue evaluada mediante un método competitivo, empleando p-CBA como compuesto de referencia. Siguiendo este procedimiento, se obtuvieron los siguientes valores: $8.24 \times 10^9\, M^{-1} s^{-1}$ para benzotriazol; $8.47 \times 10^9\, M^{-1}\, s^{-1}$ para clorofeno; $7.51 \times 10^9\, M^{-1} s^{-1}$ para DEET; $5.57 \times 10^9\, M^{-1} s^{-1}$ para metilindol, y $10.87 \times 10^9\, M^{-1} s^{-1}$ para nortriptilina.

Dado que el proceso de cloración es muy común en los tratamientos de desinfección de agua potable, también fue investigado en el presente trabajo. En la primera etapa, el objetivo fue determinar por un lado las constantes de velocidad de segundo orden aparente para la reacción de cada EC con el oxidante cloro en el intervalo de pH 3-11, encontrándose una fuerte dependencia del proceso con el cambio de pH, obteniéndose valores a pH 7-8 de $(13.6-4.4) \times 10^{-4}$, 0.15-0.12, 0.40-0.51, 38.8-59.0, $(5.75-3.21) \times 10^3\, M^{-1}\, s^{-1}$ para DT, BZ, NH, CP y ML, respectivamente. Asimismo, se determinaron las constantes de velocidad para las reacciones intrínsecas entre HOCl y las especies iónicas de cada EC, alcanzándose una buena concordancia entre los valores teóricos y experimentales. En la siguiente etapa se determinaron las constantes aparentes de velocidad de segundo orden para la reacción de cada EC con bromo en el intervalo de pH 7-9 (valores a pH 7-8 de 0.09-0.03, 7.4-8.3, 8.5-6.4, 193-445 y $(109-103) \times 10^6\, M^{-1}\, s^{-1}$ para DT, NH, BZ, CP y ML, respectivamente). Para completar este proceso de oxidación para la eliminación de los contaminantes seleccionados mediante cloro, se llevaron a cabo varios experimentos de cloración simultanea de los ECs en aguas reales con el objetivo de establecer la influencia del tipo de agua y las dosis iniciales de cloro adecuados con el fin de evitar la formación de productos de desinfección marcadamente peligrosos (principalmente trihalometanos).

Además, y dado que una baja concentración de bromuro en los sistemas de agua mejora el proceso de cloración, la cloración de los compuestos en aguas reales se llevó a cabo en presencia también de diferente concentración inicial de bromuro. Como cabría esperar, la degradación de los contaminantes emergentes fue mayor en aguas con bajo contenido en materia orgánica y tanto mayor al emplear mayor concentración de cloro y bromuro. En cualquiera de los casos estudiados, la concentración de trihalometanos no excedió el límite legal. En aguas reales, el proceso de cloración resultó ser una buena opción para la eliminación de metilindol, y en menor medida para clorofeno y nortriptilina, pero no es un proceso apropiado para la degradación de benzotriazol y DEET.

El siguiente oxidante empleado fue ozono. Dos tipos de experimentos se realizaron con diferentes propósitos. El primer grupo de experimentos consistió en el proceso de ozonización de cada EC disuelto en agua ultrapura, a diferentes pH, en presencia de terc-butanol, con el objetivo de determinar las constantes cinéticas para la reacción directa entre el ozono y cada compuesto. Para aquellos compuestos que muestran constante de disociación también se evaluaron las constantes de velocidad específicas de la especie disociada y no disociada. De este modo, en el caso de benzotriazol (pK_a=8.2), las constantes de velocidad variaron desde 20.1 ± 0.4 M^{-1} s^{-1} a pH=3 hasta 2143 ± 23 M^{-1} s^{-1} a pH=10; y las constantes de velocidad específicas de las especies disociada y no disociada fueron también evaluadas, siendo su valor 20.1 ± 2.0 y 2.0 ± 0.3 x 10^3 M^{-1} s^{-1}, respectivamente. Para clorofeno (pK_a=9.8), las constantes de velocidad variaron desde $1.67x10^3$ M^{-1} s^{-1} a pH=3 hasta $1.82x10^5$ M^{-1} s^{-1} a pH=11, y las constantes de velocidad específicas de la especie neutra e iónica fueron $2.8x10^3$ y $2.5x10^5$ M^{-1} s^{-1}, respectivamente. En el caso de nortriptilina (pK_a=10.2), los valores de la constante variaron desde $2.40x10^3$ a $472x10^3$ M^{-1} s^{-1} en el rango de pH 2-11 y las constantes de velocidad específicas de la especie protonada y neutra fueron $2.1x10^3$ y $4.3x10^5$ M^{-1} s^{-1}. Finalmente, para DEET y metilindol, los cuales no presentan naturaleza iónica, su eliminación mediante ozono no se vio afectada por el cambio de pH y por ello se propusieron valores medios para las constantes de velocidad, siendo dichos valores 0.123 ± 0.003 y $(4.90\pm0.7)x10^5$ M^{-1} s^{-1}, respectivamente.

El segundo grupo de experimentos consistió en la ozonación de cada EC disuelto en agua ultrapura y en ausencia de terc-butanol. Se estudió la evolución de la toxicidad y los

subproductos formados fueron identificados; en concreto, se identificaron 6, 27, 14, 8 y 24 intermedios mediante LC-TOFMS para benzotriazol, nortriptilina, DEET, metilindol y clorofeno, respectivamente. En base a los mismos, se propusieron los correspondientes mecanismos de reacción. En conjunto, la ozonación resultó ser un proceso adecuado para la eliminación de clorofeno, metilindol y nortriptilina, y en menor medida benzotriazol, pero no es adecuado para la eliminación DEET.

Con el fin de completar los experimentos de oxidación química, y de forma menos extensa pero con fines comparativos, se aplicaron varios sistemas de oxidación (principalmente POAs) para eliminar los ECs seleccionados en agua ultrapura y en aguas reales. En concreto, los procesos estudiados fueron la radiación UV, reactivo de Fenton, sistema Fenton-like, ozono y las combinaciones O_3/H_2O_2, UV/H_2O_2, $O_3/UV/H_2O_2$, O_3/UV, UV/TiO_2, O_3/TiO_2, $UV/Fe^{2+}/H_2O_2$, $UV/Fe^{3+}/H_2O_2$ y $O_3/TiO_2/UV$. Esta comparación de la eficacia de los tratamientos con POAs se llevó a cabo mediante la evaluación de las constantes aparentes de velocidad de primer orden, siendo la oxidación mediante agentes oxidantes individuales menos favorable que mediante las combinaciones de estos. En concreto, UV/TiO_2, O_3/H_2O_2 y el sistema foto-Fenton mostraron las tasas más altas de eliminación de los compuestos seleccionados debido a que varias reacciones tienen lugar de forma simultánea: ozonación directa, fotólisis directa y oxidación con radicales hidroxilo.

La segunda gran etapa de este trabajo fue la eliminación de los cinco contaminantes emergentes seleccionados mediante tecnologías de membrana, específicamente, ultrafiltración (UF) y nanofiltración (NF). Está ampliamente descrito que estos procesos de membrana son en general adecuados para retener moléculas orgánicas con diferente tamaño, siendo capaz de dividir la corriente de alimentación en dos corrientes diferentes: la solución concentrada o retenido y la solución filtrada o permeado. Se emplearon dos instalaciones experimentales: por un lado, los experimentos realizados en la Universidad de Extremadura (UEx) se llevaron a cabo en un equipo de membrana de laboratorio en modo concentración y flujo transversal; por otro lado, los experimentos realizados en el Laboratorio Nacional de Ingeniería Civil (LNEC, Lisboa, Portugal) se realizaron en un módulo de UF con una membrana de fibras huecas, configuración de "dentro a fuera".

La primera parte de esta etapa se llevó a cabo en la UEx, empleando diferentes matrices acuosas (un agua superficial y dos efluentes secundarios) y diferentes membranas: tres membranas de UF (MWCO de 20000, 5000 y 2000 Da) y tres membranas de NF (MWCO en el rango 150-300 Da). Esta etapa se centró en evaluar la influencia de algunas variables de operación (naturaleza y MWCO (tamaño de corte de peso molecular) de las membranas, pH, presencia de materia orgánica, etc.) sobre el flujo de permeado y la retención de los compuestos seleccionados. Se encontraron pequeñas diferencias en la secuencia de retención de los contaminantes para los procesos de UF y NF, lográndose eliminaciones superiores al 80% para clorofeno, metilindol y nortriptilina en ambos procesos y en las tres matrices acuosas empleadas. Bajo el punto de vista tanto de los coeficientes de retención como de eliminación de DOC, la membrana de nanofiltración HL resultó ser la más adecuada para la eliminación de estos contaminantes, a excepción de benzotriazol (eliminación en torno al 20%).

El segundo bloque experimental se llevó a cabo en el LNEC (Lisboa, Portugal) y se centró en evaluar los procesos PAC/UF para la eliminación de los cinco contaminantes emergentes seleccionados en tres matrices acuosas diferentes procedentes del efluente secundario de la EDAR Beirolas (Lisboa). En primer lugar, se estudió la eliminación simultánea de los ECs en agua ultrapura mediante dos carbones activos diferentes y con diferentes dosis. Una vez seleccionado el PAC y la dosis más apropiada se llevaron a cabo experimentos PAC/UF con las diferentes aguas de estudio y se evaluó la influencia de la materia orgánica natural presente. En aguas reales, el proceso PAC/UF resultó ser una gran opción para la eliminación de clorofeno, nortriptilina y metilindol (eliminación superior al 95%), pero no fue tan eficaz para la eliminación de benzotriazol y DEET (eliminación en torno al 60%).

En la tercera y última etapa de este Trabajo de Tesis Doctoral se llevó a cabo la investigación de varios procesos secuenciales físico-químicos. Estos procesos consistían en diferentes secuencias de tratamientos individuales, con el fin de mejorar la eliminación de los compuestos objeto de estudio en varias matrices acuosas (agua superficial y dos efluentes secundarios), y así obtener un efluente final útil para la descarga en efluentes públicos o para reutilización. El objetivo principal fue establecer la influencia de las etapas

previas sobre los procesos posteriores, teniendo en cuenta la eficiencia y los niveles de purificación alcanzados en el agua tratada.

En primer lugar, se realizó un pretratamiento de filtración mediante membranas de UF o NF, y tanto el permeado como el retenido fueron tratados posteriormente mediante oxidación química, empleando ozono o cloro. En los permeados obtenidos en la etapa de NF y tratados posteriormente con ozono y cloro se eliminaron por completo los contaminantes emergentes, excepto benzotriazol; mientras que en los permeados procedentes de UF y tratados mediante oxidación química se eliminaron completamente nortriptilina, metilindol y clorofeno, pero no benzotriazol y DEET. En segundo lugar, se aplicó un pretratamiento de oxidación química (mediante el uso de ozono, cloro, O_3/H_2O_2, radiación UV o UV/H_2O_2) seguido de un proceso de nanofiltración. Para todas las combinaciones químico-físicas, las eliminaciones globales fueron superiores al 97% para DEET, clorofeno, metilindol y nortriptilina, aunque se obtuvieron valores más bajos para benzotriazol (29-95%). Al mismo tiempo, se consiguió una reducción importante de la materia orgánica presente en el efluente final. Por lo tanto, puede concluirse que ambos procesos secuenciales resultaron ser tecnologías muy adecuadas para eliminar de forma eficaz los contaminantes emergentes seleccionados de diferentes matrices acuosas.

2. INTRODUCCIÓN

2.1. INTRODUCCIÓN.

El agua es esencial para la vida. Los ecosistemas, la sociedad y la economía necesitan del agua. Las fuentes de agua dulce son especialmente importantes, proporcionando una gama única y diversa de servicios de los que la sociedad humana depende (Vanneuville et al., 2012). Por ello, es necesario vigilar y cuidar la calidad de las aguas.

En Europa, el creciente desarrollo económico ha dado lugar a un aumento en la dependencia de los recursos hídricos y en determinadas zonas se ha puesto en peligro la calidad del agua. Dicha calidad del agua se ve comprometida debido a la contaminación procedente de diversas sustancias químicas tales como colorantes, disolventes, plaguicidas, fármacos, etc. como consecuencia del rápido incremento de la población, los avances tecnológicos, el inadecuado tratamiento de las aguas residuales, diferentes prácticas agrícolas, el uso inadecuado de fangos, etc. La mayor preocupación por la contaminación de las aguas es lógica si se tiene en cuenta que existen más de 30000 productos químicos producidos y comercializados en la Unión Europea; y es necesario identificar cuáles y en qué medida son dañinos para el medio ambiente y/o la salud humana.

La protección de los recursos hídricos y de su calidad ecológica en Europa requiere acciones a nivel de la UE. En el año 2000, en el marco de la política medioambiental europea, la WFD (Water Framework Directive, 2000/60/EC) fue la primera directiva en integrar la protección de ecosistemas acuáticos en términos de calidad de agua, cantidad de agua y su correspondiente papel para la población. En 2012, la Agencia Europea de Medioambiente (EEA, European Environment Agency) publicó "A Blueprint to Safeguard Europe's Water Resources" (COM(2012)673), que se centra en una política de acciones para la mejora de la implementación de la actual legislación del agua, y en la integración de los objetivos de la política del agua en otras políticas europeas. Todo ello enfocado hacia la gestión sostenible de los recursos hídricos en el marco temporal de la Estrategia UE 2020.

2.2. CONTAMINANTES EMERGENTES.

El crecimiento demográfico y el desarrollo industrial implican una cada vez mayor demanda de los recursos hídricos. Por ello es necesario investigar nuevos recursos a partir de aguas "deficientes" como los efluentes de aguas residuales, aguas salobres, etc. Si bien las investigaciones de calidad del agua se han centrado tradicionalmente en nutrientes, bacterias, metales pesados y contaminantes prioritarios (compuestos con efectos conocidos para la salud, tales como plaguicidas, productos químicos industriales, hidrocarburos derivados del petróleo), investigaciones más recientes han revelado la existencia de cientos de contaminantes orgánicos en aguas residuales y aguas superficiales.

Estos nuevos contaminantes pertenecen a diferentes clases de compuestos y se detectan normalmente a concentraciones en el rango de ng L^{-1} a µg L^{-1}, aunque las concentraciones alcanzan los 100 mg L^{-1} en algunos casos (Pal et al., 2014). Estos compuestos se conocen como contaminantes orgánicos emergentes (EOCs o ECs) e incluyen productos farmacéuticos y de cuidado personal (PPCPs), pesticidas, productos veterinarios, compuestos industriales, aditivos alimentarios, agentes tensioactivos y productos de desinfección entre otros (Lapworth et al., 2012), tal y como se muestra en la Tabla 1.

En general, no existe una regulación específica sobre su concentración permisible en aguas y se desconocen sus efectos sobre la salud humana y el medio ambiente, si bien se ha demostrado recientemente que tienen efectos ecotoxicológicos nocivos (Houtman, 2010). Además, estos compuestos pueden persistir o pseudo-persistir en las aguas porque su transformación/eliminación es compensada por su continua introducción en el medio (Stuart et al., 2012).

Por todo ello, es necesario monitorizar las diferentes aguas para evaluar la variedad y concentración de los diferentes contaminantes, así como investigar posibles tecnologías que permitan su eliminación o degradación en compuestos menos tóxicos o dañinos.

Tabla 1. Principales clases de contaminantes orgánicos emergentes.

Clase de compuesto	Ejemplos
Fármacos	Paracetamol, carbamazepina, diazepan, sulfametoxazol, amitriptilina clorhidrato.
Esteroides y hormonas	Estradiol, estrona, estriol, dietistilbestrol.
Drogas de abuso	Anfetamina, cocaína, tetrahidrocanabinol.
Fragancias	Almizcles policíclicos, macrocíclicos.
Filtros solares	3-Benzofenona, ácido octildimetil-p-aminobenzoico (ODPABA).
Antioxidantes y conservantes	Fenoles y parabenos.
Insecticidas y repelentes	Piretroides, N,N-dietil-m-toluamida (DEET).
Biocidas	Triclosán, clorofeno.
Detergentes, tensioactivos	Alquilfenoles y derivados.
Retardantes de llama	Éteres difenilo polibromados (PBDEs), ésteres organofosforados.
Plastificantes	Ftalatos, bisfenol A, ácido perfluorooctanoico (PFOA), perfluorooctanosulfonato (PFOS).
Aditivos y agentes industriales	Agentes quelantes, sulfonatos aromáticos, benzotriazoles, 1,4-dioxano.
Aditivos de la gasolina	Éteres de dialquilo, metil ter-butil éter (MTBE).
Subproductos de desinfección	Bromaldehídos, cianoformaldehído, bromoacetonitrílos bromoácidos.

2.2.1. Contaminantes emergentes seleccionados.

Recientes estudios han indicado que es necesario aplicar diferentes tratamientos (o una combinación de varios) para eliminar estos contaminantes, dependiendo de su naturaleza (Tijani et al., 2013). Para el estudio de eliminación de contaminantes emergentes en aguas se han seleccionado cinco contaminantes, cada uno de ellos perteneciente a una familia diferente y con diferentes propiedades físico-químicas. Cabe señalar que dos de ellos se encuentran entre los contaminantes más relevantes en términos de frecuencia de detección y concentración máxima en la UE, 1-H-Benzotriazol y DEET (Loos et al., 2010).

A continuación se describen la naturaleza química y algunas de las principales aplicaciones de los compuestos seleccionados.

1-H-Benzotriazol

Los benzotriazoles son derivados de un anillo de benceno en el que un par de átomos de carbono adyacentes se unen covalentemente a tres átomos de nitrógeno formando un anillo de cinco miembros (Figura 1). Se utilizan ampliamente como inhibidores de la corrosión, en fluidos para deshielo de aeronaves, anticongelantes de la automoción, sistemas de refrigeración industrial, agentes para lavavajillas domésticos (para la proteger la plata) (Matamoros et al., 2010) así como en revelado fotográfico, protectores solares, biocidas y como precursores de drogas (Asimakopoulos et al., 2013). Debido a su enorme volumen de producción son catalogados como HPV (High Production Volume) por la Agencia de Protección del Medioambiente de los EEUU.

El compuesto padre de esta familia es 1-H-Benzotriazol (BZ). Tanto él como sus derivados son considerados como potencialmente peligrosos para los organismos acuáticos, microorganismos y plantas; es cancerígeno y mutágeno en mamíferos, por lo que puede causar un considerable amenaza a la salud humana (Ding et al., 2010). En concentraciones de mg L^{-1} se ha demostrado que resulta tóxico para bacterias luminiscentes y organismos acuáticos, incluyendo plantas, peces y daphnia (Cancilla et al., 2003; Kadar et al., 2010; Seeland et al., 2012). Asimismo, Liang et al. (2014) han demostrado que actúa con disruptor endocrino en peces.

Debido a su carácter altamente polar, su solubilidad en agua, así como su estabilidad, BZ es uno de los benzotriazoles detectado con mayor frecuencia (Hart et al., 2004). A modo de ejemplo, se ha encontrado en aguas superficiales en concentraciones desde 24 a 304 ng L^{-1} en ríos alemanes (Wolschke et al., 2011) y de 17 a 44 µg L^{-1} en el pantano Wannsee, cercano a Berlín, (Reemtsma et al., 2010); en España se ha determinado en varios ríos alcanzando hasta 3.2 µg L^{-1} en el río Guadalquivir (Gorga et al., 2014). También se ha determinado a la entrada y salida de EDARs, por ejemplo en Beijing el influente y efluente presentaron concentraciones de 550-1380 ng L^{-1} y 226-520 ng L^{-1},

respectivamente (Qi et al., 2015); mientras que en Australia se ha determinado en concentraciones de 5706 ± 928 ng L^{-1} y 4164 ± 429 ng L^{-1} a la entrada y salida respectivamente (Liu et al., 2012) y de 4380 y 1514 ng L^{-1} a la entrada y salida de EDAR en Cataluña (Molins-Delgado et al., 2014).

Benzotriazol se caracteriza por una alta solubilidad en agua (28 g L^{-1}), baja presión de vapor, un coeficiente de partición octanol-agua bajo (log K_{ow}=1.23) y por ser un compuesto débilmente básico (pK_{a1}=0.4; pK_{a2}=8.2) (Weiss et al., 2006). Su peso molecular es de 119.12 g mol^{-1}.
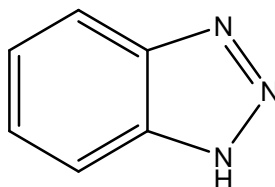
Figura 1. Estructura de 1-H-benzotriazol ($C_6H_5N_3$).

Nortriptilina Clorhidrato

Nortriptilina (NH) es un antidepresivo tricíclico (TCA) de segunda generación. Se comercializa como una sal de clorhidrato, como otros miembros de su familia. Los TCA se emplean desde el año 1950 para tratar la depresión, siendo el primer grupo de fármacos sintetizados con este fin específico. Su estructura básica se compone de un sistema lineal que consta de tres ciclos condensados, que se unen a una cadena con un nitrógeno terminal que contiene tres elementos (aminas terciarias) o dos elementos (aminas secundarias). Las aminas terciarias incluyen amitriptilina, imipramina, doxepina, trimipramina y clomipramina. Las aminas secundarias incluyen desipramina, protriptilina y nortriptilina.

Nortriptlina se utiliza en el tratamiento de la depresión severa y en niños que padecen enuresis nocturna; además se utiliza para enfermedades crónicas como fatiga, dolor crónico y migrañas. Actúa inhibiendo la recaptación de la norepinefrina (noradrenalina) y, en menor medida la serotonina. Nortriptilina se encuentra entre los 15

antidepresivos más vendidos en EEUU (SDI, Vector One: National, 2011) y además es el metabolito activo de amitriptilina (octavo antidepresivo más vendido en los Estados Unidos) formándose una vez que la amitriptilina se ha desmetilado en el hígado.

Este compuesto se ha hallado en el afluente de plantas de tratamiento de aguas en Canadá en concentraciones que alcanzan los 0.057 ng L^{-1} (Santos et al., 2010). También se ha encontrado en aguas superficiales del mismo país en concentraciones de 0.41 ng L^{-1} (Lajeunesse et al., 2008). En Europa se ha determinado en EDARs en Polonia en concentraciones de 0.25 a 0.97 ng L^{-1} (Giebułtowicz y Nałęcz-Jawecki, 2014) y en Reino Unido en concentraciones de hasta 185.8 ng L^{-1} (Baker y Kasprzyk-Hordern, 2013).

Nortriptilina (Figura 2) tiene una solubilidad en agua de 38.4 mg L^{-1}, un coeficiente de partición octanol-agua bajo (log K_{ow}=4.51) y tiene un valor de pK_a de 10.2. Su peso molecular es de 299.8 g mol^{-1}.
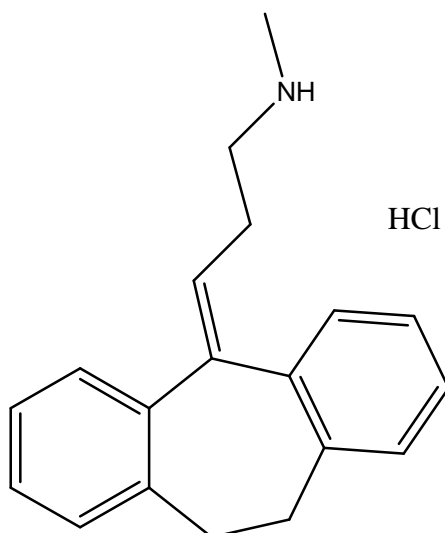
Figura 2. Estructura de Nortriptilina Clorhidrato ($C_{19}H_{21}N \cdot HCl$).

DEET

DEET (N,N-dietil-m-toluamida o DT) es el ingrediente activo en la mayoría de repelentes de insectos comerciales. Fue creado por el Departamento de Agricultura de los

EEUU en 1946 para el ejército estadounidense, para la protección contra las picaduras de insectos y la transmisión de enfermedades; en 1957 fue registrado para su uso por el público en general y para uso veterinario. En la actualidad, los productos que contienen DEET están a disposición en una gran variedad de formatos: líquidos, lociones, aerosoles, toallitas, aplicadores roll-on, etc. y las formulaciones registradas para la aplicación directa a la piel humana contienen del 4 al 100% de este ingrediente activo. Debido a su elevado consumo (solo en EEUU el uso de DEET se estima en 1.100 toneladas anuales) y a que solo el 20% de DEET es absorbido por la piel (Aronson et al., 2011), DEET es el contaminante emergente más frecuentemente detectado en los recursos hídricos en los Estados Unidos (Rivera-Cancelar et al., 2007).

El desarrollo y empleo de DEET ha salvado muchas vidas desde su introducción como repelente de insectos. Se han detectado algunos efectos secundarios cuando se utiliza en exceso, los cuales se atribuyen a interacciones antagonistas del DEET con la colinesterasa, una enzima necesaria para el funcionamiento apropiado del sistema nervioso en los seres humanos, otros vertebrados e insectos (Abou-Donia et al., 1996). Recientes estudios han demostrado que DEET puede potenciar la toxicidad de otras sustancias químicas y puede regular la absorción dérmica de fármacos y pesticidas (Baynes et al., 1997; Abou-Donia et al., 1996). Además, este contaminante presenta propiedades potencialmente cancerígenas en células de las mucosas nasales en humanos (Tisch et al., 2002).

Debido a su elevado consumo, este compuesto ha sido ampliamente determinado en estudios de monitorización de efluentes por todo el mundo. A modo de ejemplo cabe decir que en un río de Corea se ha detectado DEET con una concentración media de 56 ng L^{-1} (Yoon et al., 2010). Este contaminante se ha encontrado en España, en el río Guadalquivir, en concentraciones de hasta 5.7 ng L^{-1} (Robles-Molina et al., 2014). En concentraciones mucho mayores se ha detectado en China, alcanzando en agua superficial 255 ng L^{-1} (media de 122.4 ng L^{-1}) y en agua potable 24 ng L^{-1} (media de 0.5 ng L^{-1}) o en Arabia Saudí, encontrándose en concentraciones de hasta 415 ng L^{-1} en el efluente de una EDAR (Alidina et al., 2014).

DEET (Figura 3) presenta alta solubilidad en agua (912 mg L^{-1}), un coeficiente de partición octanol-agua medio (log K_{ow}=2.18), pK_a 0.6 y un peso molecular de 191.3 g mol^{-1} (Kim et al., 2009; Yoon et al., 2010).
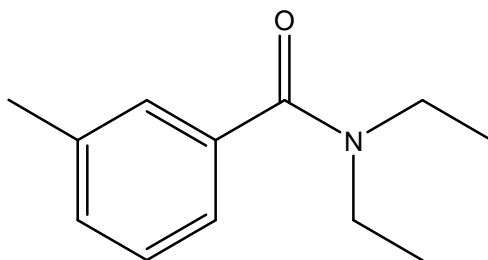
Figura 3. Estructura de DEET (C$_{12}$H$_{17}$NO).

3-Metilindol

Los indoles sustituidos se producen por la industria química para una variedad de aplicaciones, incluyendo productos farmacéuticos, cosméticos, fragancias, pesticidas, desinfectantes, productos agroquímicos, aditivos alimentarios y colorantes. 3-Metilindol o Skatole (ML) es un compuesto orgánico ligeramente tóxico que pertenece a la familia de los indoles. Se produce de forma natural en las heces de los mamíferos y tiene un olor fecal. Sin embargo, en bajas concentraciones posee un olor floral y se puede encontrar en varias flores (como el jazmín o la flor del naranjo) y en aceites esenciales. Principalmente se usa como componente en fragancias y para fijar el olor en los perfumes; otros usos de metilindol incluyen la fabricación de herbicidas, fungicidas, tintes, antidepresivos y fármacos anticancerígenos (Cui et al., 2013).

Se han encontrado efectos tóxicos de este compuesto en microorganismos y también se le considera agente implicado en ciertas afecciones de los rumiantes (vacas, cabras y ovejas) como por ejemplo, el edema pulmonar bovino y enfisema (ABPE) (Deslandes et al., 2001). En humanos, se ha determinado que las enzimas del citocromo P450 participan en la bioactivación de ML, formando intermedios que inician la apoptosis (muerte celular) en las células del pulmón humano (Nichols et al., 2003).

Este compuesto se ha hallado en concentraciones menores a 1 µg L^{-1} tanto en aguas residuales como en pozos de agua potable en Massachussets (Massachusetts Department of Environmental Protection, Bureau of Resource Protection and EPA Region I, 2010). En Croacia se han determinado concentraciones en la entrada y salida de una EDAR de 1 a 10 µg L^{-1} y de 0.1 a 1 µg L^{-1} respectivamente (Smital et al., 2011). En China se ha encontrado metilindol en efluentes secundarios de EDAR alcanzando concentraciones de hasta 370 ng L^{-1} (Yan et al., 2011).

Metilindol (Figura 4) presenta alta solubilidad en agua (498 mg L^{-1}), un valor del coeficiente de partición octanol-agua de 2.60 y un peso molecular de 131.1 g mol^{-1}.
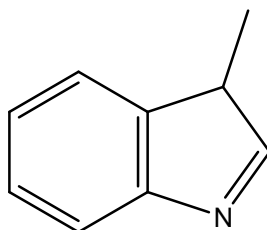
Figura 4. Estructura de 3-Metilindol (C$_9$H$_9$N).

Clorofeno

Los clorofenoles son sustancias orgánicas ampliamente utilizadas como desinfectantes o conservantes para la madera, pinturas, fibras vegetales y de cuero, como herbicidas, fungicidas e insecticidas, y como productos intermedios en la producción de productos farmacéuticos y colorantes. También son materias primas o productos intermedios de síntesis en muchos procesos industriales. Clorofeno, o o-benzil-p-clorofenol (CP), es un compuesto fenólico halogenado utilizado principalmente en productos para la limpieza y desinfección de hospitales y hogares, debido a su amplio espectro antimicrobiano, así como en la industria y la agricultura como agente activo en desinfectantes. Debido a su amplia aplicación en actividades diarias, clorofeno se descarga inevitablemente en el medio ambiente.

En referencia a los peligros que puede ocasionar CP como contaminante emergente, se ha determinado que posee potencial cancerígeno y actividad mutagénica en animales (Sires et al., 2007). En 2006, la EPA incluyó este pesticida en el grupo C: Posible carcinógeno humano (USEPA, 2006).

En España se ha encontrado en concentraciones superiores a 0.7 μg L^{-1} en influentes de EDAR (Martínez-Bueno et al., 2012). En la estación de tratamiento de aguas potables de Baltimore se han hallado concentraciones de 750 y 200 ng L^{-1} a la entrada y salida, respectivamente (Yu et al., 2006). En lo que respecta a aguas superficiales, se ha encontrado este compuesto en concentraciones cercanas a los 3 μg L^{-1} en los ríos Ely y Taff en Reino Unido (Kasprzyk-Hordern et al., 2009).

Clorofeno (Figura 5) presenta alta solubilidad en agua (149 mg L^{-1}), coeficiente de partición octanol-agua bastante alto (log K_{ow}=4.18), valor de pK_a de 9.8 y un peso molecular de 218.7 g mol^{-1}.
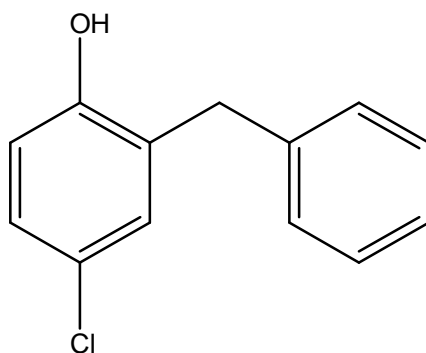
Figura 5. Estructura de clorofeno ($C_{13}H_{11}ClO$).

2.3. TRATAMIENTO DE AGUAS Y ELIMINACIÓN DE CONTAMINANTES EMERGENTES.

Las estaciones de depuración de aguas residuales y las estaciones de tratamiento de aguas potables han sido diseñadas para eliminar o reducir el nivel de contaminación de las aguas, de modo que pueda ser asimilado de forma natural por el cauce del río sobre el

que posteriormente será vertido o bien sean aptas para el consumo humano, cumpliendo los criterios que exige la legislación. Sin embargo, la aparición de nuevos microcontaminantes no regulados requiere un tratamiento más avanzado, empleando nuevas tecnologías. Además, hay que tener en cuenta que los contaminantes emergentes poseen una amplia gama de propiedades químicas y el éxito en la eliminación es muy variable en función de sus propiedades particulares y el grado de contaminación.

Los tratamientos primarios convencionales, que incluyen procesos como la coagulación-floculación, no son capaces de eliminar eficazmente los contaminantes emergentes. El principal mecanismo para la eliminación de microcontaminantes durante este proceso es su asociación o interacción con las superficies de las partículas en suspensión y los flóculos. En general, los compuestos que presentan alta hidrofobicidad (log K_{ow} > 6) y baja solubilidad en agua pueden ser eliminados en esta etapa (Snyder et al., 2007b). Por el contrario, la mayoría de pesticidas y productos farmacéuticos polares y semipolares permanecen en la fase acuosa (Stackelberg et al., 2007). Así, la eliminación de microcontaminantes durante los procesos de coagulación-floculación resulta inferior al 20% (Gasperi et al., 2010) y se producen lodos tóxicos, sin olvidar que los contaminantes se transforman de una fase a otra sin necesariamente ser descompuestos (Kasprzyk-Hordern et al., 2009; Maletz et al., 2013).

Los tratamientos biológicos son relativamente baratos y se emplean de forma frecuente en las plantas de tratamiento de aguas residuales para degradar compuestos orgánicos en general, tanto en medio aerobio como anaerobio. Por ejemplo, los lodos activados y filtros percoladores pueden convertir los contaminantes emergentes presentes en agua en biomasa, que es separada posteriormente (Helbling et al., 2010). Sin embargo, esta degradación microbiológica puede dar lugar a la formación de numerosos productos de degradación o de transformación (Bagnall et al., 2012) y aunque se adopte la mejor tecnología disponible, el tratamiento biológico elimina solo una parte de una amplia gama de contaminantes emergentes. En concreto los compuestos polares se descargan a través del efluente final (Petrovic et al., 2003). Por último, se generan lodos o fangos tóxicos que deben ser tratados.

Por otra parte, la oxidación química mediante tratamientos convencionales permite la descomposición de numerosos compuestos orgánicos y se lleva a cabo directamente sobre las aguas a tratar, empleando para ello ciertos agentes químicos que actúan como oxidantes o como catalizadores de la degradación, siendo el cloro el oxidante más común empleado en el tratamiento convencional del agua. La cloración permite eliminar más del 90% de los compuestos que presentan estructuras aromáticas con grupos hidróxido. Sin embargo su uso está limitado ya que se formar subproductos de reacción (cloroaminas, trihalometanos, etc.) que deben evitarse.

Los procesos de oxidación química para la eliminación de contaminantes emergentes presentan la ventaja de destruir el contaminante orgánico, frente a los procesos de separación física que transfieren el compuesto de una fase a otra y requieren de un posterior método de recuperación o destrucción del mismo. Además, los tratamientos de oxidación química son aptos para eliminar contaminantes tanto en la obtención de agua potable como en el tratamiento de efluentes industriales altamente contaminados. Sin embargo, las limitaciones más importantes son la cinética del proceso, que puede ser demasiado lenta en muchas ocasiones, y la formación de subproductos de reacción cuya toxicidad o efecto nocivo puede superar al contaminante de partida.

Actualmente, el desarrollo de las tecnologías de oxidación química para degradar contaminantes orgánicos emergentes en medio acuoso se basa en la introducción de uno o varios activadores de la reacción que actúan generando radicales intermedios muy reactivos, tales como los radicales hidroxilo, superóxido e hidroperóxido, los cuales son capaces de atacar con éxito a la mayor parte de las moléculas orgánicas, con constantes de velocidad de reacción muy elevadas que oscilan entre 10^6-10^9 M^{-1} s^{-1}. Estos tratamientos combinados constituyen los denominados Procesos de Oxidación Avanzada (POAs).

Hay que destacar que en ocasiones la mineralización total mediante oxidación química requiere una gran potencia y dosis de oxidante y, por lo tanto, elevado capital y costes de operación en comparación con otras tecnologías. Por ello es interesante evaluar la eficacia de otras tecnologías y la combinación de estas con los procesos de oxidación química.

De este modo, como alternativa a los procesos químicos, resulta interesante estudiar los tratamientos físicos para la purificación de aguas naturales y residuales, debido a que generalmente presentan un más bajo coste y conllevan poco impacto medioambiental. Estos procesos incluyen, por ejemplo, la adsorción mediante carbón activado o resinas y la tecnología de membranas.

Recientes estudios han demostrado que procesos de adsorción empleando carbón activado resultan efectivos para la eliminación de algunos contaminantes emergentes, pudiendo alcanzarse hasta el 90% de eliminación (Schafer et al., 2003). Sin embargo, la eficacia del carbón activado se puede ver reducida por la presencia de materia orgánica natural. La capacidad de eliminación de este proceso va a depender de la dosis de carbón activado, el tiempo de contacto, así como de la estructura molecular y comportamiento de los contaminantes (Snyder et al., 2007).

La aplicación de la tecnología de membranas para el tratamiento de aguas ha aumentado considerablemente en los últimos años. Una de las grandes ventajas que presentan los sistemas de filtración es que son capaces de retener un gran número de sustancias contaminantes en las aguas, entre ellas los contaminantes emergentes; sin embargo, no permiten la degradación de las mismas, por lo que dichos contaminantes se concentran en forma de residuos sólidos o líquido, requiriendo de un tratamiento adicional posterior (Homem y Santos, 2011). Especial interés suscitan los bioreactores de membrana (MBRs), al ser sistemas que combinan la filtración por membranas con la degradación biológica, usando fangos activos (Mutamim et al., 2012), y llevan a cabo tanto la retención física de los contaminantes como su biodegradación.

Tras esta panorámica general de los diversos tratamientos para la eliminación de microcontaminantes en aguas (naturales o residuales), se describen de forma más detallada los fundamentos y características de aquellos tratamientos de oxidación química y de filtración por membranas que han sido específicamente empleados en esta investigación para la eliminación de los contaminantes emergentes seleccionados.

2.4. TRATAMIENTOS DE OXIDACIÓN QUÍMICA DE AGUAS.

La elección del agente oxidante más adecuado depende de diversos factores, como la facilidad de aplicación técnica y económica o la posibilidad de actuar como desinfectante, pero especialmente de la naturaleza del agua a tratar y de los contaminantes presentes. Los agentes utilizados con más frecuencia son, entre otros: cloro, permanganato potásico, dióxido de cloro, ozono, radiación ultravioleta y peróxido de hidrógeno.

En este trabajo, se han empleado oxidantes individuales como cloro, ozono y radiación ultravioleta, así como las combinaciones de diversos agentes oxidantes que constituyen los denominados Procesos de Oxidación Avanzada (POA). Así, las combinaciones utilizadas han sido: O_3/H_2O_2, UV/H_2O_2, Fe^{2+}/H_2O_2, Fe^{3+}/H_2O_2, $UV/H_2O_2/Fe^{2+}$, $UV/H_2O_2/Fe^{3+}$, UV/TiO_2, O_3/TiO_2, UV/O_3 y $UV/H_2O_2/O_3$.

2.4.1. OZONO.

El ozono, forma alotrópica del oxígeno, es un oxidante muy enérgico. Es utilizado como tal en la desinfección del agua, dada su eficacia en oxidación de materias orgánicas e inorgánicas (entre éstas últimas destacan el hierro y manganeso). Su poder oxidante y desinfectante, mayor que el del cloro (potencial redox 2.07 V, mientras que el del cloro es 1.36 V), le hace más eficaz que éste en la eliminación del olor, sabor y color del agua, así como en la eliminación de bacterias, virus y otros microorganismos.

La vida media del ozono en el agua es muy variable, dependiendo de diversos factores (temperatura, pH, sustancias presentes en el agua, etc.). En condiciones estándar de temperatura y presión en agua destilada los valores la vida media de ozono varían entre 20 y 160 minutos, aumentando su inestabilidad en medio básico (Rodríguez, 2003). En la secuencia de tratamiento de aguas puede aplicarse como:

i. *Pre-tratamiento:* el objetivo en esta etapa es proporcionar una primera desinfección del agua, eliminar compuestos minerales, iones metálicos (Fe^{2+} y Mn^{2+}), color, turbidez, sólidos en suspensión, olores y sabores extraños, reducir la materia orgánica natural y mejorar los procesos de coagulación-floculación-decantación.

ii. *Oxidación intermedia*: se aplica antes de la etapa de filtración. Se utiliza principalmente para oxidar la materia orgánica (NOM), aumentando su biodegradabilidad y favoreciendo su eliminación biológica en los filtros. También se pretende degradar los microcontaminantes tóxicos que pudieran estar presentes y los precursores de trihalometanos.

iii. *Desinfección final:* para eliminar microorganismos patógenos y reducir los posibles subproductos de etapas anteriores.

En el proceso de ozonización hay que considerar dos posibles vías de acción oxidante: la directa debida a la reacción entre el ozono y los compuestos disueltos, donde se produce un ataque selectivo del ozono sobre moléculas orgánicas; y la vía radical derivada de las reacciones entre los radicales generados en la descomposición del ozono (radical hidroxilo, principalmente) y los propios compuestos disueltos. La combinación de ambas vías para la eliminación de compuestos dependerá de la naturaleza de los mismos, del pH del medio y de la dosis de ozono, principalmente.

Las reacciones por vía molecular son procesos más selectivos donde el ozono molecular puede actuar principalmente como dipolo (cicloadición sobre especies insaturadas) o como agente electrófilo (en sitios de alta densidad electrónica, sobre todo en anillos aromáticos activados). Presentan cinéticas de segundo orden y los principales sustratos que reaccionan con el ozono según esta vía son hidrocarburos insaturados e hidrocarburos aromáticos activados con grupos electrón-donadores (OH, NH_2).

La vía radicalaria son reacciones en las que las especies reaccionantes son radicales generados en la descomposición del ozono, principalmente el radical hidroxilo (E^o= +2.80 V). Estos radicales libres pueden reaccionar no selectivamente con los compuestos orgánicos (Andreozzi et al., 1999) y son reacciones muy rápidas, presentando cinéticas de segundo orden con valores de constantes $10^8 < k < 10^{10}$ M^{-1} s^{-1}. Algunos sustratos típicos que reaccionan con el ozono según esta vía son hidrocarburos saturados y derivados halogenados, ácidos alifáticos, aldehídos, cetonas, alcoholes, hidrocarburos aromáticos desactivados (con grupos electrón-atractores).

Varios factores favorecen que las reacciones vayan preferentemente por cada una de estas dos vías:

a) Factores que favorecen la vía molecular (inhiben la descomposición del ozono): medio ácido, secuestradores de radicales ("radical scavengers") como CO_3^{2-}, HCO_3^- (alcalinidad), t-BuOH, etc.

b) Factores que favorecen la vía radicalaria (promueven la descomposición del ozono): medio básico (OH^-), H_2O_2, radiación UV (253.7 nm), ácido fórmico, Fe^{2+}, etc. La descomposición del ozono puede asimismo ser adicionalmente acelerada por una reacción en cadena típicamente radicalaria en la cual los radicales libres producidos $^\bullet OH$ y $HO_2^\bullet$ son los que actúan como propagadores de la cadena. Las reacciones que intervienen en el mecanismo de la descomposición del ozono en radicales hidroxilo se muestran en la siguiente Tabla (Acero y von Gunten, 2000).

Tabla 2. Mecanismo de descomposición del ozono en radicales hidroxilo.

N°	Reacción			k; k_f, k_r, K_a
1	$O_3 + OH^-$	$\rightarrow$	$HO_2^- + O_2$	70 $M^{-1} s^{-1}$
2	$O_3 + HO_2^-$	$\rightarrow$	$O_3^{\bullet-} + HO_2^\bullet$	2.8 x10^6 $M^{-1} s^{-1}$
3	$O_3 + O_2^{\bullet-}$	$\rightarrow$	$O_3^{\bullet-} + O_2$	1.6 x10^9 $M^{-1} s^{-1}$
4	$O_3^{\bullet-} + H^+$	$\leftrightarrow$	$HO_3^\bullet$	5 x10^{10} $M^{-1} s^{-1}$; 3.3 x10^2 s^{-1}
5	$HO_3^\bullet$	$\rightarrow$	$^\bullet OH + O_2$	1.4 x10^5 s^{-1}
6	$O_3 + ^\bullet OH$	$\rightarrow$	$HO_2^\bullet + O_2$	2 x10^9 $M^{-1} s^{-1}$
7	$H_2O_2 + ^\bullet OH$	$\rightarrow$	$HO_2^\bullet + H_2O$	2.7 x10^7 $M^{-1} s^{-1}$
8	$HO_2^- + ^\bullet OH$	$\rightarrow$	$O_2^{\bullet-} + H_2O$	7.5 x10^9 $M^{-1} s^{-1}$
9	$HO_2^\bullet$	$\leftrightarrow$	$O_2^{\bullet-} + H^+$	1.6x10^{-5}
10	H_2O_2	$\leftrightarrow$	$O_2^- + H^+$	2.5 x10^{-12}

Con respecto a la ozonización de compuestos orgánicos en aguas naturales, parece más probable que el mecanismo radicalario juegue un papel dominante en las reacciones de ozonización; incluso en condiciones que favorecen la vía directa de actuación del ozono

se generan radicales (orgánicos e inorgánicos) que provocan la aparición de la vía indirecta de actuación del ozono (Rodríguez, 2003).

Las principales ventajas del empleo de ozono en el tratamiento de aguas incluyen:

- ✓ El proceso de ozonización utiliza un período corto de contacto (aproximadamente de 10 a 30 minutos).
- ✓ No necesita ser eliminado después del proceso de ozonización dado que el ozono se descompone rápidamente.
- ✓ El ozono es generado in situ, minimizando problemas de seguridad y costes asociados con el envío y el transporte.
- ✓ El proceso de ozonización eleva la concentración de oxígeno disuelto del efluente, pudiendo eliminar la necesidad de aireación.
- ✓ Es más eficaz que el cloro para la desinfección o destrucción de virus y bacterias: los microorganismos no crecen nuevamente, a excepción de aquellos que están protegidos por las partículas en la corriente de agua residual.
- ✓ No produce trihalometanos y además elimina sus precursores.
- ✓ No altera el pH del agua.
- ✓ Mejora la coagulación.
- ✓ Facilita la eliminación del hierro y manganeso y reduce en gran medida el olor, sabor y color del agua.

Como desventajas figuran:

- ▪ Su mayor coste, tanto en los equipos como en coste de operación (energía eléctrica).
- ▪ Puede formar otros subproductos tóxicos o nocivos, como el ion bromato.
- ▪ No mantiene una concentración residual persistente, lo que obliga a emplear cloro u otro desinfectante si se desea mantener un desinfectante residual.
- ▪ Puede formar óxido nítrico o ácido nítrico, que causan corrosión en los equipos.
- ▪ No resulta viable en aguas con altas concentraciones de sólidos en suspensión, demanda bioquímica de oxígeno, demanda química de oxígeno, o carbono orgánico total.
- ▪ Baja solubilidad en agua y relativamente inestable en disolución acuosa, motivo que obliga a generarle in situ.

2.4.2. RADIACION UV.

El proceso de degradación de contaminantes disueltos en agua mediante radiación UV se basa en proporcionar energía a los compuestos químicos en forma de radiación, que es absorbida por las distintas moléculas para alcanzar estados excitados el tiempo necesario para experimentar reacciones. La energía radiante es absorbida por las moléculas en forma de unidades cuantizadas denominadas fotones, los cuales contienen las cantidades de energía requeridas para excitar electrones específicos y formar radicales libres que experimentan una serie de reacciones en cadena para dar los productos de reacción. Estos radicales libres pueden generarse por homólisis de enlaces débiles, o bien por transferencia electrónica desde el estado excitado de la molécula orgánica hacia el oxígeno molecular, originándose el radical superóxido ($O_2^{\bullet -}$), o hacia otros reactivos químicos como el ozono o el peróxido de hidrógeno en cuyo caso se producen radicales hidroxilo ($^{\bullet}OH$).

El éxito de un método fotolítico radica en la capacidad de absorber radiación de la longitud de onda incidente por parte de los compuestos a degradar, en el rendimiento cuántico de los mismos y en la estabilidad y simplicidad de los productos de fotodegradación (Lemaire et al., 1982). De estos tres factores, el rendimiento cuántico (ϕ) es el factor más interesante a estudiar, el cual se define como la relación entre el número de moléculas que reaccionan y el número de fotones absorbidos. El rendimiento cuántico hace una función similar a la de la constante cinética en una reacción ordinaria, e incluso matemáticamente se puede relacionar con las distintas constantes de velocidad de las reacciones que intervienen en el mecanismo para explicar el proceso fotoquímico global. En bibliografía se han propuesto diferentes métodos de competición y métodos basados en diversos modelos de radiación para el cálculo de rendimientos cuánticos (Esplugas et al., 1983).

En sistemas fotoquímicos convencionales, el rendimiento cuántico es < 1 y suele ocurrir que solamente alrededor del 15% de la energía total de entrada se encuentra en la banda de absorción de la molécula. Por ello, para que un determinado proceso fotoquímico sea rentable, se requiere bien un alto precio del producto final, o bien un muy elevado rendimiento cuántico. La eficacia del proceso, por tanto, depende fundamentalmente de la

capacidad de absorción de radiación del sustrato y de la presencia de otros compuestos que absorben a la misma longitud de onda.

Las ventajas e inconvenientes del empleo de radiación UV en el tratamiento de aguas se muestran en la siguiente Tabla.

Tabla 3. Degradación mediante radiación UV. Ventajas e inconvenientes.

Ventajas
Al no introducirse reactivo ni materia extraña en la disolución, el carácter físico-químico no se ve modificado.
No se producen olores ni sabores desagradables.
No se generan lodos.
Metodología económica si se utiliza energía solar.
La sobredosificación no produce efectos perjudiciales

Inconvenientes
Baja eficiencia y procesos relativamente lentos.
La eficiencia de las lámparas disminuye con el tiempo por lo que es necesario un mantenimiento adecuado y continuo de las mismas.
Se precisa un preacondicionamiento del agua debido a que la radiación UV es absorbida por la materia orgánica y por las sustancias que originan turbidez.
Necesidad de capas finas de agua a tratar.
Aplicación limitada por factores climatológicos cuando utilizamos energía solar.

Puede concluirse, de forma general, que la radiación ultravioleta presenta baja eficacia en la degradación de compuestos orgánicos disueltos en agua en comparación con otros procesos que implican la generación de radicales hidroxilo, si bien la fotólisis puede resultar interesante en aquellos casos en que tanto el poder absorbente (coeficiente de extinción) como el rendimiento cuántico de los contaminantes tratados sea elevado. Además, resulta de gran interés la capacidad de desinfección de la radiación ultravioleta.

Para la generación de la radiación ultravioleta se dispone de lámparas de mercurio de baja y media presión o arcos de Xe/Hg, dependiendo de las longitudes de onda de la radiación deseada. La radiación de 254 nm es la más estudiada según refleja la bibliografía disponible. A continuación se describen las lámparas de mercurio, por ser la utilizada en el presente estudio.

Fuentes de radiación UV: lámparas de mercurio.

Una fuente de radiación, para su utilidad en reacciones fotoquímicas, debe tener las siguientes características: alta intensidad en la longitud de onda deseada, larga vida, dimensiones geométricas adecuadas para el proceso considerado, mínimo coste del equipo auxiliar necesario y facilidad de operación. Las fuentes actuales de radiación más importantes que cumplen tales condiciones, y por tanto las más utilizadas, son las lámparas de vapor de mercurio y la luz solar, especialmente las primeras.

De forma general, al hacer pasar una corriente eléctrica entre dos electrodos separados por un gas o vapor, se genera radiación ultravioleta. La intensidad y distribución de longitudes de onda de esta radiación dependerá de la naturaleza y presión del gas o vapor. Generalmente, ésta suele ser vapor de mercurio a diferentes presiones, ya que dicho vapor posee un espectro amplio en la zona ultravioleta y además no reacciona con los electrodos ni ataca al vidrio. A su vez, las lámparas de mercurio se subdividen en arcos de baja, media y alta presión.

Las lámparas de mercurio de baja presión operan a temperatura ambiente y a 0.001 atmósferas, emitiendo dos líneas principales de radiación a 253.6 y 184.9 nm, líneas que son interesantes para llevar a cabo reacciones fotosensibilizadas. Suelen refrigerarse por aire y su vida media es relativamente elevada, de 9500 a 12000 horas.

Por otra parte, las lámparas de mercurio de media presión operan a alrededor de 1 atmósfera. Tienen diversas líneas principales de radiación (253.7, 313, 365, 404.7, 435.8, 546.1 y 570.8 nm), y su vida media es de aproximadamente 1000 horas.

Finalmente, las lámparas de mercurio de alta presión son quizás las más importantes desde el punto de vista industrial, debido a su mayor potencia lumínica. Operan a presiones de entre 2 y 110 atmósferas, por lo que generalmente constan de un tubo de cuarzo de pequeño diámetro y pared gruesa que está rodeado de otro tubo de vidrio que hace las funciones de filtro de radiación, aislante de calor y protector en caso de rotura del tubo de cuarzo. Su espectro es más completo. Según sea la presión de la lámpara, la refrigeración será por aire o por agua, siendo su duración bastante más corta (de 100 a 200 horas).

Diseño de reactores fotoquímicos: modelos de radiación.

En el modelo matemático de un reactor convencional deben tenerse en cuenta los balances de materia y de energía y la ecuación cinética de la reacción o reacciones que tengan lugar. En el caso de un reactor fotoquímico hay que considerar además un balance de radiación, que depende del modelo que se proponga para describir la emisión y distribución de radiación en el reactor. En efecto, esta distribución de energía radiante en la masa de reacción no es uniforme debido a varias causas, como la atenuación debida a la absorción de luz por las especies del sistema, las propiedades físico-químicas del mismo sistema de reacción y las características geométricas del reactor y de la lámpara. En consecuencia, la energía radiante y por tanto la reacción de iniciación fotoquímica, no está distribuida homogéneamente en el reactor.

En la bibliografía se han propuesto una gran diversidad de modelos para describir la distribución de la energía radiante en el reactor. Éstos pueden clasificarse en dos grupos principales: a) modelos de incidencia, que suponen la existencia de una distribución de energía radiante dada en las proximidades del reactor; y b) modelos de emisión, que suponen una forma determinada de emisión de radiación por la lámpara, a partir de la cual se deduce la energía absorbida por la masa de reacción. De todos los modelos mencionados, los que reproducen con mayor precisión los resultados experimentales son los modelos de emisión (Spadoni et al., 1980); y de éstos, los que consideran una fuente de radiación con emisión esférica resultan ser los más apropiados para el diseño de reactores

fotoquímicos debido a su relativa simplicidad matemática. Entre ellos destaca el desarrollado por Jacob y Dranoff el cual ha sido empleado en el presente trabajo.

Modelo de Fuente Lineal de Emisión Esférica.

El modelo desarrollado por Jacob y Dranoff (1966, 1968, 1970) recibe el nombre de Modelo de Fuente Lineal de Emisión Esférica (LSSEM) y resulta ser el mejor que se adapta a las características geométricas del reactor y la lámpara usados en el presente trabajo. El mismo ha sido utilizado en diversos trabajos anteriores con resultados muy satisfactorios en la determinación de rendimientos cuánticos de reacciones individuales de degradación de compuestos orgánicos diversos mediante la acción oxidante de la radiación ultravioleta (Benítez et al., 2005; Real et al., 2010). Básicamente, supone una naturaleza tridimensional del proceso de emisión de energía, emitiendo la lámpara una radiación en todas las direcciones y de forma isotrópica. Dado que el reactor empleado en esta investigación es una columna de burbujeo que puede considerarse a todos los efectos como un reactor anular, el sistema de coordenadas más adecuado es el constituido por las coordenadas cilíndricas (Figura 6).

DIMENSIONES (cm)

R_1	1.85
R_0	3.50
L_0	7.60
L	4.00
H	11.60
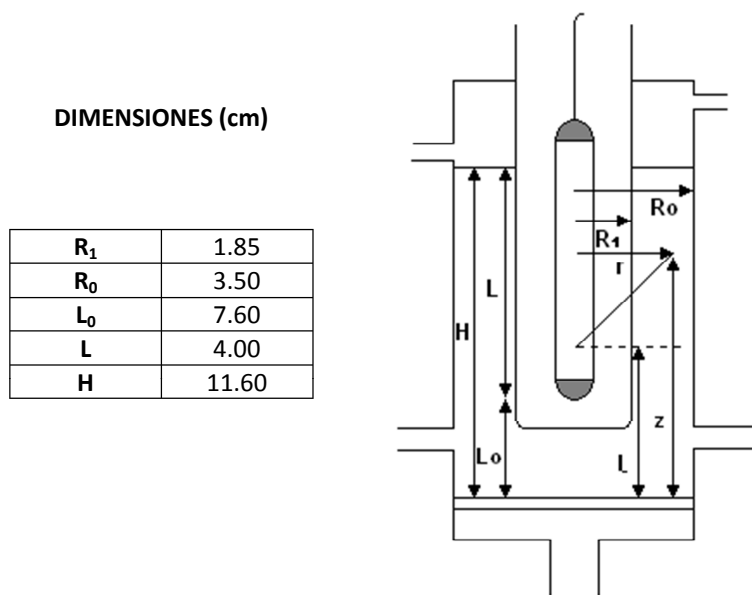
Figura 6. Coordenadas cilíndricas del reactor fotoquímico.

La aplicación del modelo de emisión esférica a un sistema de estas características geométricas permite deducir la expresión para el cálculo de la energía absorbida por la masa de reacción. De forma general, el caudal de energía radiante absorbida por un medio de reacción viene dado por la expresión:

$$W_{abs} = \Sigma\, W_{abs} = \Sigma \int_V \mu_i\, I_i\, dV \tag{1}$$

donde μ_i es la absorbancia del medio de reacción para cada longitud de onda de la radiación policromática, e I_i la intensidad de radiación para cada longitud de onda y en cada punto del reactor.

Teniendo en cuenta que la lámpara utilizada puede considerarse monocromática en la longitud de onda de 254 nm, la expresión (1) puede escribirse de la siguiente forma:

$$W_{abs} = \int_V \mu\, I\, dV \tag{2}$$

donde μ es la absorbancia del medio de reacción por unidad de longitud, e I la intensidad de radiación en cada punto del reactor.

Con objeto de evaluar W_{abs}, resulta necesario establecer y resolver el balance de radiación. De acuerdo con las características geométricas del reactor y con las hipótesis del modelo de emisión esférica (Jacob y Dranoff, 1968, 1970), y si μ es constante con la posición, resulta:

$$W_{abs} = 2\,\pi\,\mu \int_0^H \int_{R1}^{R0} I(r,\, z)\, r\, dr\, dz \tag{3}$$

donde $I(r,z)$ es la intensidad de radiación en cada punto del reactor e igual a:

$$I(r,\, z) = \frac{W_L}{4\,\pi\,L} \int_{L0}^{L0+L} \frac{\exp\left[-\mu\,(r - R_1)\cdot c\right]}{r^2 + (z - l)^2}\, dl \tag{4}$$

siendo el parámetro c igual a:

$$c = \frac{\left[r^2 + (z - l)^2\right]^{1/2}}{r} \tag{5}$$

En estas expresiones, r y z son las coordenadas radial y axial de un punto genérico considerado, y l la coordenada axial de la lámpara; L y L_0 son la longitud de la lámpara y la distancia de la base de la lámpara a la base del reactor; R_1 y R_0, los radios externo e interno del reactor fotoquímico, y H es la altura del reactor. Finalmente, W_L es el caudal total de radiación emitido por la lámpara.

Con objeto de simplificar, en lo sucesivo la integral triple que engloba a todos los términos geométricos se expresa mediante el parámetro N:

$$N = \int_0^H \int_{R1}^{R0} \int_{L0}^{L0+L} \frac{\exp[-\mu(r - R_1)\cdot c]}{r^2 + (z - l)^2}\ r\ dl\ dr\ dz \tag{6}$$

Por tanto, teniendo en cuenta las expresiones (3) a (6), el caudal de energía radiante absorbida puede evaluarse por la expresión reducida:

$$W_{abs} =\ W_L\ \frac{\mu\ N}{2\ L} \tag{7}$$

que permitirá determinar el caudal total de radiación absorbida, W_L, para cada tiempo de reacción fotoquímica en la longitud de onda a la que las disoluciones del compuesto orgánico estudiado absorben.

2.4.3. CLORO.

El cloro es el desinfectante más utilizado para el tratamiento del agua potable y su popularidad se debe al alto potencial de oxidación y a que provee el nivel necesario de concentración residual en el agua tratada, necesaria para evitar que se produzca una contaminación microbiológica dentro del sistema de distribución (Sadiq y Rodríguez, 2004). Además, se ha encontrado que el cloro también es útil para otros propósitos distintos al de la desinfección (USEPA, 1999), tales como:

- Control del olor y el sabor en el agua.
- Evita el crecimiento de algas manteniendo limpios los sistemas de tratamiento.
- Eliminación de hierro y manganeso por precipitación.
- Oxidación de sulfuro de hidrógeno.

- Mejora la eficiencia de la coagulación y la filtración.

El cloro adicionado al agua se transforma en varias formas diferentes a la especie elemental, como el ácido hipocloroso y el ión hipoclorito. En la actualidad su uso más frecuente es como gas, Cl_2 (g), generado por vaporización de cloro líquido almacenado bajo presión, y como sales, tanto hipoclorito de sodio, NaOCl, como hipoclorito de calcio, $Ca(OCl)_2$.

La forma en la que se adiciona el cloro al agua influye sobre ciertas propiedades químicas de ésta. La adición de cloro gaseoso a un agua disminuirá su alcalinidad:

$$Cl_{2(g)} + H_2O \leftrightarrow HOCl + H^+ + Cl^- \tag{8}$$
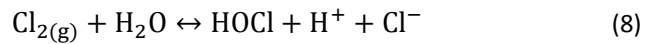
Sin embargo, si el cloro se dosifica como sal de ácido hipocloroso se tendrá:

$$NaOCl \leftrightarrow Na^+ + OCl^- \tag{9}$$

$$OCl^- + H_2O \leftrightarrow HOCl + OH^- \tag{10}$$
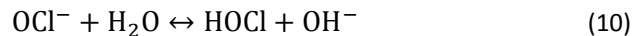
y habrá un aumento de la alcalinidad de acuerdo con el grado en el que el OCl^- reaccione con el H_2O.

Por otro lado, el valor de pK_a del equilibrio de disociación $HOCl/OCl^-$ (expresión 11) a 20 °C es 7.5. Por tanto, la cantidad relativa de las distintas especies cloradas oxidadas varía en función del pH del agua.

$$HOCl \leftrightarrow H^+ + OCl^- \tag{11}$$
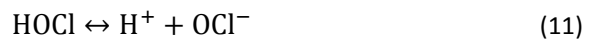
El ácido hipocloroso y el ión hipoclorito representan el "cloro libre residual" que es el desinfectante primario empleado. Así, se tiene que 3 < pH < 6 predomina el ácido hipocloroso y para pH > 9 predomina el ión hipoclorito. El ácido hipocloroso no disociado es alrededor de 80 a 100 veces más efectivo en la eliminación de bacterias indicadoras de contaminación fecal que el ión hipoclorito (Snoeyink y Jenkins, 2000), por ello, el intervalo óptimo de pH para la aplicación como desinfectante está en el rango de 6 a 8 tal y como se puede observar en la Figura 7.
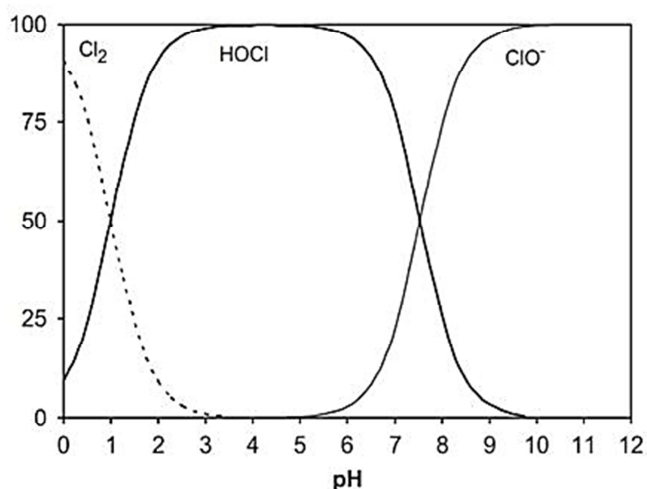
Figura 7. Porcentaje de especies de cloro presentes en el agua en función del pH.

El cloro participa en diferentes reacciones de oxidación-reducción con compuestos inorgánicos reducidos (Mn^{2+}, Fe^{2+}, S^{2-}, etc., en general se trata de reacciones muy rápidas) y con compuestos orgánicos (reacciona con el nitrógeno orgánico y con ciertas sustancias químicas perdiendo su poder oxidante para producir cloruro, ácido clorhídrico, óxidos de nitrógeno, cloro-orgánicos...). Pero sin duda las reacciones de oxidación-reducción con nitrógeno amoniacal son las más interesantes, al formarse una serie de compuestos denominados cloraminas, con cierto poder desinfectante.

Las cloraminas presentan un poder oxidante menor que el del ácido hipocloroso, pero son más estables en agua y por tanto tienen mayores tiempos de residencia. Presentan dos grandes inconvenientes: pueden dar lugar a olor y sabor en las aguas y son potencialmente toxicas. Las reacciones de formación de las cloraminas son:

Monocloramina
$$NH_3 + HOCl \leftrightarrow +ClNH_2 + H_2O \qquad (12)$$

Dicloramina
$$ClNH_2 + HOCl \leftrightarrow +Cl_2NH + H_2O \qquad (13)$$

Tricloramina
$$Cl_2NH + HOCl \leftrightarrow +Cl_3NH + H_2O \qquad (14)$$
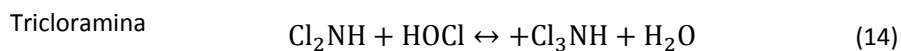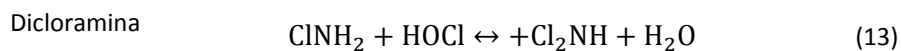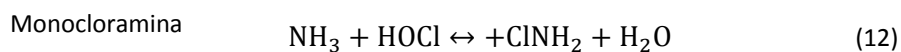
Su formación depende principalmente por la relación cloro/amoniaco presente en el agua, el pH y la temperatura. La monocloramina puede existir con relativa estabilidad combinada con cloro en soluciones neutrales o ligeramente alcalinas, y está generalmente presente como la especie química dominante en las operaciones de cloración. Cuando la concentración de cloro en el agua va aumentando se favorece la formación de dicloramina que es fácilmente oxidable a N_2 y NO_3^-.

El principal inconveniente del uso de cloro en el tratamiento de aguas recae en la formación de sustancias o subproductos de la desinfección que presentan posibles efectos genotóxicos para la salud de las personas. La naturaleza y la concentración de los compuestos formados son dependientes de variables fisicoquímicas de la materia orgánica, las cuales reaccionan originándose productos que son compuestos de diferente toxicidad, entre ellos mutagénicos y carcinogénicos; a todos en conjunto se les conoce como productos secundarios de cloración, que incluyen compuestos llamados trihalometanos (THM) y ácidos haloacéticos (HAA). Los THM originados durante este proceso de cloración incluyen cloroformo ($CHCl_3$), bromodiclorometano ($CHCl_2Br$), clorodibromometano ($CHClBr_2$) y bromoformo ($CHBr_3$), entre otros compuestos volátiles. Se ha descrito que el cloroformo en altas dosis es cancerígeno y que los otros THM son mutagénicos. Entre los HAAs el tricloroacético y dicloroacético son las especies encontradas en mayores concentraciones.

2.4.4. BROMO.

El bromo es un agente oxidante de eficacia similar al cloro. Cuando los iones bromuro se hallan en medio acuoso, el ácido hipobromoso (HOBr) se forma durante la cloración de agua (Heller-Grossman et al., 1993; von Gunten y Hoigné, 1996):

$$HOCl + Br^- \rightarrow HOBr + Cl^- \qquad (15)$$
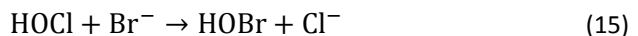
El poder de desinfección del ácido hipobromoso es muy alto, aunque ligeramente menor que el del hipocloroso. El HOBr no se usa extensamente como desinfectante y presenta un coste elevado. Al igual que el HOCl, conduce a la formación de productos de

desinfección bromados (Nawrocki y Bilozor, 1998) cuyos efectos para la salud humana no son todavía bien conocidos (Krasner et al., 1996). Los principales subproductos de desinfección que se forman en los procesos de bromación son bromoformo, diclorobromometano y dibromoclorometano; también reacciona con el amonio para formar bromoaminas, que son más desinfectantes que las cloraminas.

El equilibrio de disociación HOBr/OBr$^-$ posee un valor de pK$_a$=8.9 (Gallard et al., 2003), por lo que el HOBr es un ácido más débil que el HOCl (pK$_a$=7.5). Como ventajas destacan que es un biocida efectivo en un rango de pH más amplio que el ácido hipocloroso y que medioambientalmente es más aceptable que el cloro ya que se reduce la producción de halometano y las bromaminas que se pueden llegar a producir tienen un tiempo de vida media mucho más corto que las cloraminas.

Son particularmente peligrosos los bromatos, formados por oxidación de bromuro, ya que pueden causar afecciones carcinogenéticas. El agua no contiene bromato, pero puede formarse durante la ozonización si el agua contiene ión bromuro. En determinadas condiciones, también puede formarse bromato en las soluciones concentradas de hipoclorito que se utilizan para desinfectar el agua de consumo. Dada sus propiedades cancerígenas la WHO, UE y USEPA establecen su concentración máxima permisible en aguas de consumo en 10 µg L^{-1}.

2.4.5. PROCESOS DE OXIDACION AVANZADA (POAs).

Tal y como se ha señalado en el Apartado 2.3 los Procesos de Oxidación Avanzada (POAs) constituyen uno de los recursos tecnológicos más prometedores en el tratamiento de aguas contaminadas con productos orgánicos de vertidos industriales, urbanos o simplemente aguas superficiales o subterráneas contaminadas. Los POAs están especialmente indicados para tratar compuestos orgánicos que son especialmente resistentes y refractarios a la acción directa de los agentes oxidantes más frecuentes utilizados individualmente, siendo necesario el uso de otros oxidantes más fuertes, o bien la aplicación de nuevos procesos basados en combinaciones simultáneas de algunos de los oxidantes habituales.

Estas técnicas han demostrado ser muy efectividad en la destrucción de compuestos no biodegradables y refractarios (Glaze et al., 1982; Vallejo et al., 2015) y se caracterizan por generar principalmente radicales muy reactivos y oxidantes como son los radicales hidroxilo ($^\bullet OH$) que tras el flúor son los oxidantes más enérgicos. Existen diferentes alternativas para la formación de estos radicales, unas más eficaces que otras dependiendo del compuesto, como: UV/O_3, UV/H_2O_2, O_3/H_2O_2, Fe^{2+}/H_2O_2 (denominado reactivo de Fenton), UV/TiO_2, además de posibles combinaciones ternarias o cuaternarias de estos agentes.

Los POAs pueden clasificarse como fotoquímicos o no fotoquímicos dependiendo de si se irradia o no la muestra para la obtención del radical $^\bullet OH$ (ver Tabla 4). Los procesos fotoquímicos a su vez, pueden clasificarse en procesos fotocatalíticos o no fotocatalíticos, dependiendo de si utilizan o no un semiconductor o fotocatalizador para la absorción directa o indirecta de energía UV-Visible.

Tabla 4. Algunos de los POAs más conocidos.

Procesos fotoquímicos	Procesos no fotoquímicos
Fotólisis directa	Ozonización en medio alcalino (O_3/OH^-)
Fotólisis en el ultravioleta de vacío (UVV)	Ozonización con H_2O_2 (O_3/H_2O_2)
UV/H_2O_2	Reacción de Fenton ($Fe^{+2/+3}/H_2O_2$)
UV/O_3	Oxidación electroquímica
Foto-Fenton ($Fe^{+2/+3}/H_2O_2/UV$)	Radiolisis y tratamiento con haces de electrones
Fotocatálisis Heterogénea (TiO_2/UV)	Plasma no térmico
Oxidación en agua sub/ y supercrítica	Descarga electrohidráulica-ultrasonidos

En general, las ventajas que presentan los POAs incluyen:

- El contaminante se destruye, no se concentra ni cambia de medio.
- No generan lodos que a su vez requieren de un proceso de tratamiento posterior.
- Generalmente se puede conseguir la mineralización completa del contaminante orgánico, en especial de compuestos no biodegradables, y transformación de

compuestos inorgánicos hasta CO_2, H_2O e iones simples como cloruros, nitratos y otras sustancias más fácilmente tratables por otros métodos más económicos.

- Es una tecnología limpia y segura, y en algunos procesos como los fotocatalíticos, se puede emplear la radiación solar.

- Sirven para tratar contaminantes a muy bajas concentraciones.

- Eliminan los efectos perjudiciales sobre la salud, que presentan algunos desinfectantes y oxidantes residuales como el cloro.

El inconveniente principal de estos procesos es que los radicales $^{\bullet}OH$ son fácilmente atrapados por iones HCO_3^- y CO_3^{2-} abundantes en sistemas de tratamiento de aguas y/o residuos:

$$^{\bullet}OH + HCO_3^- \rightarrow H_2O + CO_3^{\bullet -} \tag{16}$$

$$^{\bullet}OH + CO_3^{2-} \rightarrow HO^- + CO_3^{\bullet -} \tag{17}$$
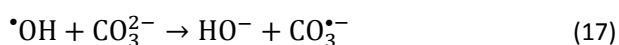
Se describen a continuación de forma más extensa los mecanismos de reacción y las etapas que tienen lugar en la oxidación general de compuestos orgánicos mediante los siguientes Procesos de Oxidación Avanzada: O_3/H_2O_2, UV/H_2O_2, Fe^{2+}/H_2O_2, Fe^{3+}/H_2O_2, $UV/H_2O_2/Fe^{2+}$, $UV/H_2O_2/Fe^{3+}$, UV/TiO_2, O_3/TiO_2, UV/O_3 y $UV/H_2O_2/O_3$, los cuales han sido empleados en el presente estudio.

2.4.5.1. Proceso de Oxidación Avanzada O_3/H_2O_2.

Es ampliamente conocido que la adición de H_2O_2 durante la ozonización de contaminantes incrementa considerablemente el rendimiento del proceso (Glaze et al., 1992). El H_2O_2 es un ácido débil ($pK_a=11.6$), un poderoso oxidante y un compuesto inestable, que dismuta con una velocidad máxima al pH correspondiente al valor de su pK_a:

$$H_2O + H_2O_2 \rightarrow HO_2^- + H_3O^+ \tag{18}$$

$$H_2O_2 + 2e^- + 2H^+ \rightarrow 2H_2O \tag{19}$$

$$H_2O_2 + HO_2^- \rightarrow H_2O + O_2 + HO^- \tag{20}$$
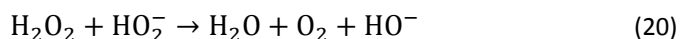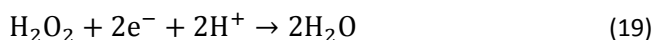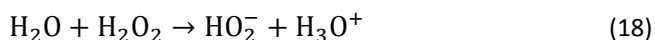
El uso de dos o más oxidantes combinados permite aprovechar los posibles efectos sinérgicos entre ellos, lo que produce una destrucción adicional de la carga orgánica del agua. Sin embargo, resulta difícil prever el rendimiento global del proceso, por ello, éste se debe determinar en ensayos de laboratorio.

El mecanismo de reacción del Proceso de Oxidación Avanzada constituido por la combinación de O_3/H_2O_2 es similar al descrito en el Apartado 3.1 para ozono individual. Existe una vía directa de ataque de ozono a la materia orgánica y una vía radicalaria mediante la cual el ozono se descompone formando radicales hidroxilos que actuarían como oxidantes secundarios (Tabla 2 y Figura 8). La vía radicalaria se encuentra favorecida en el presente sistema de oxidación respecto al proceso de ozonación simple por la presencia de peróxido de hidrógeno, el cual acelera la descomposición de ozono hacia la formación de radicales hidroxilo según se muestra en la Tabla 2 (reacción 2 y siguientes). Por tanto, la principal diferencia entre los procesos de ozonación simple y la combinación O_3/H_2O_2 es la reacción de iniciación de la descomposición de ozono; esto es, iones hidroxilo en ozonación simple y el anión peróxido en el proceso combinado (Staehelin y Hoigné, 1982).
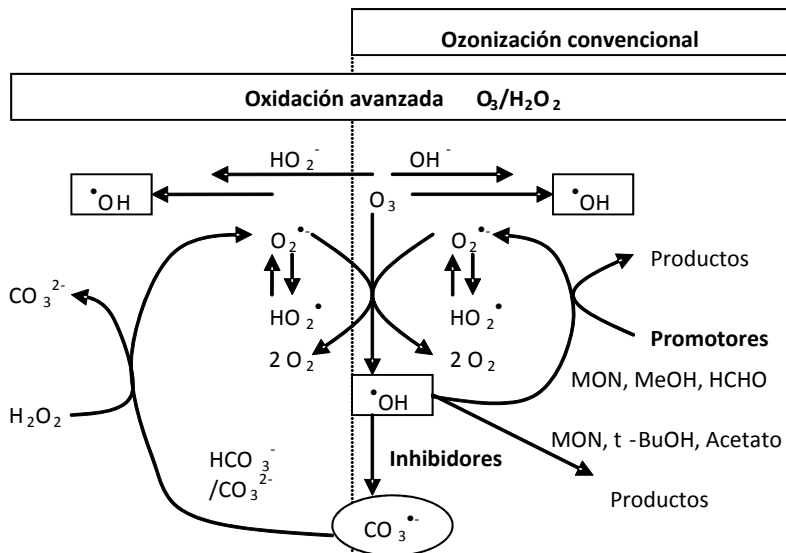
Figura 8. Esquema de las reacciones de descomposición de ozono en los sistemas de ozonación simple o del Proceso de Oxidación Avanzada O_3/H_2O_2.

Este POA conlleva un coste más elevado que la ozonización simple pero es más eficiente, pudiéndose tratar contaminantes orgánicos presentes en muy bajas concentraciones (ppb).

2.4.5.2. Proceso de Oxidación Avanzada UV/H$_2$O$_2$.

Entre los distintos procesos de aplicación para el tratamiento de aguas la combinación de la radiación ultravioleta y el peróxido de hidrógeno resulta ser muy interesante cuando se desea un agua con alto grado de pureza. Este POA implica la formación de radicales hidroxilo por fotólisis del peróxido de hidrógeno y consiguientes reacciones de propagación. El mecanismo más comúnmente aceptado para la fotólisis del peróxido de hidrógeno es la ruptura del enlace O-O por la acción de la radiación ultravioleta para formar dos radicales hidroxilo (presenta un rendimiento cuántico casi unitario ($\phi_{HO\bullet}$= 0.98 a 254 nm)):

$$H_2O_2 + h\upsilon \rightarrow 2 \ {}^\bullet OH \tag{19}$$

La fotolisis de un compuesto orgánico en disolución acuosa catalizada por la presencia de peróxido de hidrógeno es un proceso muy complejo que, de forma resumida, se esquematiza en la Figura 9, la cual muestra el mecanismo de reacciones más comúnmente aceptado para la misma (Legrini et al., 1993).
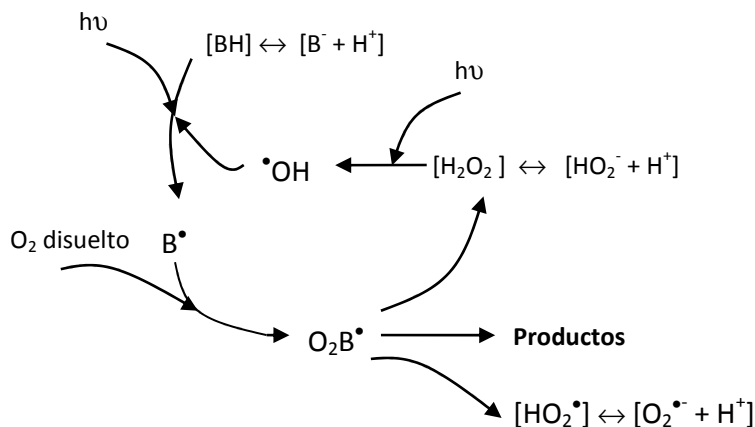
Figura 9. Mecanismo de reacción de la combinación UV/H$_2$O$_2$ sobre la materia orgánica.

Este mecanismo considera que en la primera etapa tiene lugar la degradación fotolítica de peróxido de hidrógeno que, mediante la escisión del mismo, produce dos radicales libres hidroxilo por cada molécula descompuesta (expresión 19).

Una vez formados estos radicales altamente reactivos, reaccionan a continuación con el compuesto orgánico mediante abstracción de un átomo de hidrógeno, adición a dobles enlaces C-C o transferencia de electrones, dependiendo de la naturaleza y grupos funcionales del compuesto orgánico. La vía de reacción más general es la abstracción de un átomo de hidrógeno y producción del consiguiente radical orgánico B$^{\bullet}$, que a su vez reacciona rápidamente con O_2 disuelto para formar el radical orgánico peróxido $O_2B^{\bullet}$ (Legrini et al., 1993). Estos radicales orgánicos descomponen mediante reacciones bimoleculares dando lugar a los diferentes productos de degradación del compuesto de partida junto con otros subproductos tales como peróxido de hidrógeno, radicales hidroperóxido, formaldehído, etc. (Von Sonntag y Schuchmann, 1997).

Los radicales $^{\bullet}OH$ generados, pueden actuar sobre el H_2O_2 remanente o adicionado a la solución, haciendo que se regenere y mantenga el ciclo de oxidación de los contaminantes orgánicos. En exceso de H_2O_2 y con elevadas concentraciones de radicales $^{\bullet}OH$, tienen lugar reacciones competitivas que producen un efecto inhibidor para la degradación de la materia orgánica (reacciones (20) a (23)) por lo que se debe determinar en cada caso la cantidad óptima de H_2O_2, para evitar un exceso que podría retardar la degradación (Baxendale et al., 1957). De la misma forma, se debe considerar el equilibrio ácido-base del peróxido de hidrógeno (ecuación 18), que está favorecido en medio básico, mientras que en medio ácido apenas tiene lugar. Por tanto, los $^{\bullet}OH$ son susceptibles de recombinarse o de reaccionar de acuerdo a las reacciones (19) a (23).

$$H_2O_2 + \ ^{\bullet}OH \rightarrow HO_2^{\bullet} + H_2O \qquad (20)$$

$$H_2O_2 + HO_2^{\bullet} \rightarrow \ ^{\bullet}OH + H_2O + O_2 \qquad (21)$$

$$2\ HO_2^{\bullet} \rightarrow H_2O_2 + O_2 \qquad (22)$$

$$HO_2^{\bullet} + \ ^{\bullet}OH \rightarrow H_2O + O_2 \qquad (23)$$
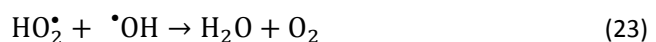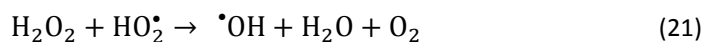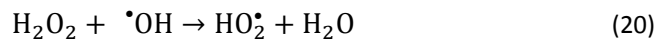
Debido al bajo coeficiente de absorción molar del H_2O_2 (ε=18.6 $M^{-1}cm^{-1}$ a 254 nm), es necesario establecer condiciones de flujo turbulento para evitar que zonas de la disolución queden sin tratar. Además, otras especies pueden absorber los fotones, siendo este proceso poco eficaz en aguas que presentan elevada absorbancia. El proceso fotoquímico es más eficiente en medio alcalino, ya que la base conjugada del peróxido de hidrógeno (HO_2^-) tiene una absortividad mayor (ε_{254}=240 $M^{-1}cm^{-1}$).

En resumen, existe un ciclo de descomposición y formación simultánea de peróxido de hidrógeno cuyo resultado global dependerá de diversas variables, como la intensidad de la radiación ultravioleta, la temperatura, el pH y la naturaleza de los compuestos orgánicos.

2.4.5.3. Proceso de Oxidación Avanzada H_2O_2/Fe^{2+} (reactivo de Fenton) y H_2O_2/Fe^{3+} (reactivo de Fenton-like).

El POA de catálisis homogénea Fenton (Fe(II)/H_2O_2) data de 1894, cuando Henry J. Fenton demostró que el peróxido de hidrógeno podía ser activado en presencia de sales de Fe(II) para oxidar ácido tartárico en rangos ácidos de pH (Fenton, 1894). En 1934 Haber y Weiss propusieron que el oxidante activo generado mediante la reacción de Fenton es el radical hidroxilo. Más tarde, Barb et al. (1949), revisaron el mecanismo original propuesto por Haber y Weiss para dar lugar a lo que actualmente se conoce como la reacción en cadena "clásica" o "vía radicales libres" de Fenton, en la que se considera como etapa clave del proceso la producción de radicales ($^{\bullet}$OH). La aplicación de la reacción de Fenton como proceso oxidante para la destrucción de sustancias orgánicas tóxicas comenzó a desarrollarse a mediados de los años 60 por Brown et al. (1964). Aunque el mecanismo exacto de la oxidación de un compuesto orgánico por dicho reactivo es complejo y no conocido de forma absoluta, diversos autores coinciden en las principales etapas del mismo:

$$H_2O_2 + Fe^{2+} \rightarrow {}^{\bullet}OH + OH^- + Fe^{3+} \tag{24}$$

Los radicales $^{\bullet}$OH así formados pueden reaccionar luego por dos vías: oxidando al Fe(II) (una reacción improductiva) y atacando a la materia orgánica:

$$^{\bullet}OH + Fe^{2+} \rightarrow OH^- + Fe^{3+} \tag{25}$$

$$RH + {}^{\bullet}OH + H_2O \rightarrow ROH + H_3O^+ \tag{26}$$
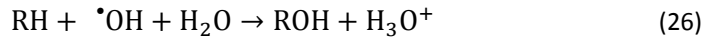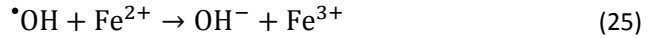
A pH < 3, la reacción es autocatalítica, ya que el Fe(III) descompone el H_2O_2 en O_2 y H_2O a través de un mecanismo en cadena:

$$H_2O_2 + Fe^{3+} \leftrightarrow FeOOH^{2+} + H^+ \tag{27}$$

$$FeOOH^{2+} \rightarrow HO_2^{\bullet} + Fe^{2+} \tag{28}$$

$$H_2O_2 + Fe^{2+} \rightarrow Fe^{3+} + HO^- + {}^{\bullet}OH \tag{29}$$

$$HO_2^{\bullet} + Fe^{3+} \rightarrow Fe^{2+} + H^+ + O_2 \tag{30}$$

$$^{\bullet}OH + H_2O_2 \rightarrow H_2O + HO_2^{\bullet} \tag{31}$$
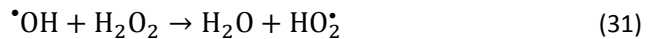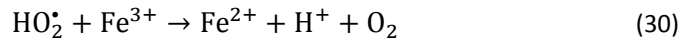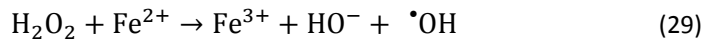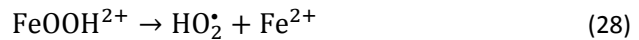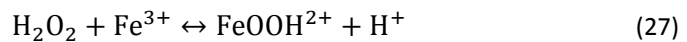
El ión hierro (III) puede reducirse por reacción con H_2O_2 y formar de nuevo ión hierro (II) y más radicales hidroxilo. Este segundo proceso se denomina Fenton-like. El proceso es potencialmente útil para destruir contaminantes, ya que es muy efectivo para la generación de $^{\bullet}$OH, pero un exceso de iones Fe^{2+}, H_2O_2, o halógenos si están presentes, pueden actuar como secuestradores de estos radicales (expresión 25).

En presencia de exceso de peróxido, la concentración de Fe^{2+} es pequeña en relación a la de Fe^{3+}, ya que la reacción (28) es más lenta que la (24). La constante de velocidad para la reacción de ión ferroso con H_2O_2 es alta, y el Fe(II) se oxida a Fe(III) en segundos o minutos en exceso de H_2O_2. Se cree por ello que la destrucción de contaminantes por reactivo de Fenton es simplemente un debido al ciclo catalítico de descomposición de H_2O_2, y que el reactivo de Fenton con exceso de H_2O_2, es esencialmente un proceso de Fe^{3+}/H_2O_2.

Como se ha señalado anteriormente, la actividad catalítica máxima del sistema Fe(II)/Fe(III)-H_2O_2 ocurre a pH 2.8-3.0. A pH > 5 se genera precipitado de Fe(III); si bien se

generan así barros que obligan a su posterior gestión, es frecuente alcalinizar las aguas al final del proceso con el agregado simultáneo de un floculante para eliminar el hierro remanente.

2.4.5.4. Proceso de Oxidación Avanzada UV/H_2O_2/Fe^{2+}: sistema foto-Fenton.

La velocidad de degradación de los contaminantes orgánicos se ve considerablemente aumentada cuando el reactivo Fenton se combina con la radiación UV visible debido a la regeneración continua del Fe^{2+}, como consecuencia del mecanismo de fotorreducción del Fe^{3+}, y la generación adicional de nuevos radicales hidroxilo ($^\bullet OH$) a partir de H_2O_2 (Pignatello, 1992). Este proceso se conoce como foto-Fenton, y en él los complejos de Fe^{3+} sufren una transferencia de carga ligando-metal, dando lugar a su disociación en Fe^{2+} y el ligando oxidado (Pignatello et al., 2006).

Los complejos de Fe^{3+} que se suelen formar en solución ácida son el $Fe(OH)^{2+}$ y $Fe_2(OH)_2^{4+}$, que absorben luz UV y visible, siendo la especie más importante el complejo $Fe(OH)^{2+}$ debido a la combinación entre su alto coeficiente de absorción y su alta concentración relativa con respecto a otras especies de Fe^{3+}:

$$Fe(OH)^{2+} + h\upsilon \rightarrow Fe^{2+} + \ ^\bullet OH \qquad (32)$$
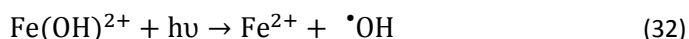
La oxidación de contaminantes orgánicos mediante Fenton o foto-Fenton, se inhibe por la presencia de iones inorgánicos tales como fosfato, sulfato, organosulfonato, fluoruro, bromuro y cloruro dependiendo de la concentración de los mismos. Estos aniones suelen encontrarse en las aguas residuales y también aparecen como productos de degradación durante la oxidación de las sustancias orgánicas. La inhibición que provocan estas especies suele deberse a la precipitación del hierro (por ejemplo, el Fe^{3+} forma complejos insolubles con el ión fosfato en medio ácido o neutro), o a la formación de complejos de coordinación con Fe^{3+} que son menos reactivos. En el caso del ión nitrato y perclorato, éstos no forman complejos con los iones Fe^{2+} y Fe^{3+}. La inhibición de las reacciones Fenton por la presencia de elevadas concentraciones de iones cloruro o bromuro, se debe a que estos iones reaccionan con los radicales $^\bullet OH$, ya que estas especies actúan como ligandos débiles para el Fe^{2+}.

Las principales ventajas que posee el presente sistema sobre el reactivo de Fenton son las siguientes:

- ✓ Fotólisis de peróxido de hidrógeno (si se usan radiaciones menores que 360 nm).
- ✓ Reducción de Fe^{3+} a Fe^{2+} mediante la radiación ultravioleta produciéndose radicales hidroxilo.
- ✓ Permite el uso de longitudes de onda desde 300 nm hasta el visible.
- ✓ Las concentraciones de Fe(II) a emplearse pueden ser órdenes de magnitud menores que en la reacción de Fenton convencional.

El sistema foto-Fenton tiene una gran aplicación futura en el tratamiento de depuración de aguas, al tratarse de un sistema donde los radicales hidroxilo se generan fácilmente y no se originan productos de oxidación secundarios clorados como en el caso de cloro o dióxido de cloro. En la actualidad se está comenzando a utilizar el sistema foto-Fenton con gran éxito en el tratamiento de aguas a escala planta piloto (Hernández-Rodríguez et al., 2014).

2.4.5.5. Proceso de Oxidación Avanzada $UV/H_2O_2/Fe^{3+}$: sistema foto Fenton-like.

La adición de luz al sistema Fenton-like, produce la regeneración de Fe (III) a través de un proceso fotorreductor (Amigó et al., 2008). Se trata de una reacción mucho más rápida que la de Fenton-like, y requiere la presencia de radiación de hasta 410 nm, por lo tanto se puede producir con la participación de la luz solar (Pignatello et al., 2006).

Paralelamente, la irradiación de hierro (III) con peróxido de hidrogeno da lugar a la formación de intermedios de hierro que poseen elevados estados de oxidación, los cuales son los responsables del ataque directo de la materia orgánica.

2.4.5.6. Proceso de Oxidación Avanzada UV/TiO_2.

El dióxido de titanio absorbe radiación en el ultravioleta cercano ($\lambda < 380$ nm) generando pares de electrón/hueco:

$$TiO_2 + h\upsilon \rightarrow TiO_2(e^- + h^+) \tag{33}$$
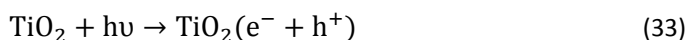
En presencia de especies redox adsorbidas en la partícula del semiconductor y bajo iluminación, se producen simultáneamente reacciones de oxidación y reducción en su superficie; los huecos fotogenerados dan lugar a reacciones de fotooxidación, mientras que los electrones de la banda de conducción dan lugar a las reacciones de fotorreducción, como se representa en la Figura 10.
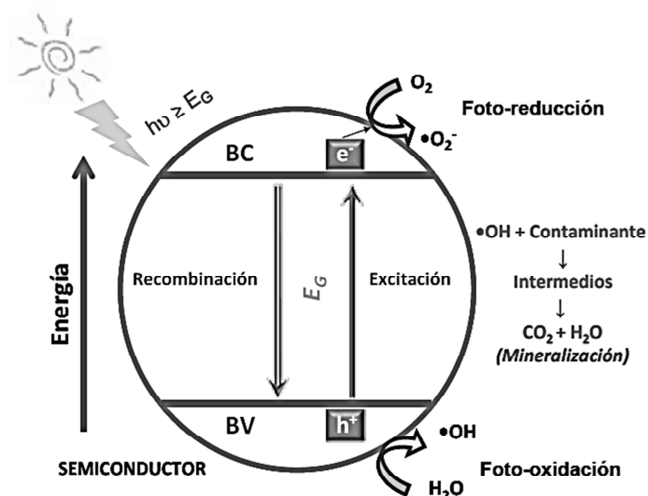
Figura 10. Esquema del proceso fotocatalítico sobre una partícula semiconductora de TiO$_2$.

Los huecos, después de migrar a la superficie, reaccionan con sustancias adsorbidas, en particular con el agua o con iones OH$^-$, generando radicales $^\bullet$OH:

$$TiO_2(h^+) + H_2O_{ad} \rightarrow TiO_2 + {}^\bullet OH_{ad} + H^+ \tag{34}$$

$$TiO_2(h^+) + OH^-_{ad} \rightarrow TiO_2 + {}^\bullet OH \tag{35}$$
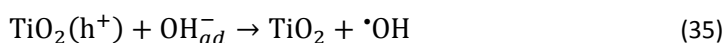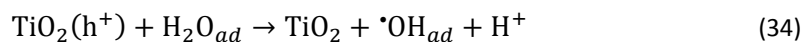
En aplicaciones ambientales, los procesos fotocatalíticos se llevan a cabo normalmente en ambientes aeróbicos, con lo cual el oxígeno adsorbido es la especie que actúa como receptora de electrones:

$$TiO_2(e^-) + O_2 \rightarrow TiO_2 + O_2^{\bullet -} \tag{36}$$
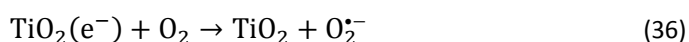
En resumen, la irradiación con un haz de luz de contenido energético apropiado sobre partículas semiconductoras es capaz de generar una serie de agentes oxidantes y reductores con suficiente vida media y reactividad para entrar en contacto con los contaminantes a través de la interfase sólido-fluido y proceder a su degradación. Además los huecos también pueden reaccionar directamente con las moléculas de contaminante adsorbidas en la superficie del catalizador. En el caso de contaminantes de naturaleza orgánica puede provocar, incluso, su mineralización total.

2.4.5.7. Proceso de Oxidación Avanzada O$_3$/TiO$_2$.

La combinación de ozono y dióxido de titanio no obedece a una simple reacción química o un proceso físico, pero es el resultado de una serie de diferentes reacciones. Primero, el ozono se adsorbe sobre la superficie del dióxido de titanio, esta adsorción superficial puede ser debida a:

- Adsorción física.
- Formación de enlaces de hidrógeno débiles con la superficie de los grupos hidroxilo.
- Adsorción disociativa en sitios ácidos de Lewis.

Cuando el ozono entra en contacto con la superficie del dióxido de titanio, un electrón de dicho compuesto genera el radical anión ozónido (expresión (37)), el cual genera en las siguientes etapas el radical hidroxilo (expresiones (38) y (39)):

$$\text{TiO}_2(\text{e}^-) + \text{O}_3 \rightarrow \text{TiO}_2 + \text{O}_3^{\bullet -} \qquad (37)$$

$$\text{O}_3^{\bullet -} + \text{H}^+ \rightarrow \text{HO}_3^{\bullet} \qquad (38)$$

$$\text{HO}_3^{\bullet} \rightarrow \text{O}_2 + {}^{\bullet}\text{OH} \qquad (39)$$
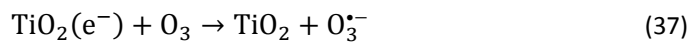
Además, si el oxígeno molecular acepta el electrón, se forma el anión superóxido (expresión (36)) que puede reaccionar con radicales de ozono para dar radicales hidroxilo en las etapas consecutivas:

$$\text{O}_2^{\bullet -} + \text{O}_3 \rightarrow \text{O}_3^{\bullet -} + \text{O}_2 \qquad (40)$$
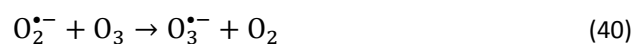
El ozono también puede reaccionar con el H_2O_2 (o con la base conjugada del H_2O_2) según la expresión (41), que se produce cuando el oxígeno molecular es reducido en la superficie del TiO_2, formando el radical anión ozónido que vuelve a generar radicales hidroxilo (Černigo et al., 2010):

$$O_3 + HO_2^- \rightarrow O_3^{\bullet -} + HO_2^{\bullet} \qquad (41)$$

2.4.5.8. Proceso de Oxidación Avanzada UV/O_3.

El proceso de oxidación en presencia de ozono y radiación ultravioleta se inicia a partir de la fotólisis de ozono. La irradiación de ozono en agua produce peróxido de hidrógeno en forma cuantitativa:

$$O_3 + h\upsilon + H_2O \rightarrow O_2 + H_2O_2 \qquad (42)$$
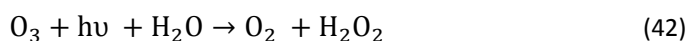
El H_2O_2 así generado se fotoliza a su vez generando radicales $^{\bullet}OH$, y reacciona con el exceso de ozono:

$$O_3 + H_2O_2 \rightarrow {}^{\bullet}OH + HO_2^{\bullet} + O_2 \qquad (43)$$
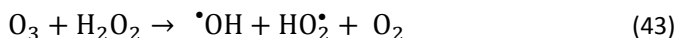
Este proceso podría considerarse en principio únicamente como un método de coste elevado para generar H_2O_2 y posteriormente $^{\bullet}OH$. En realidad, se trata de una combinación de los procesos UV/H_2O_2 y O_3/H_2O_2, con la ventaja de que el ozono posee un coeficiente de extinción molar de 3300 L mol^{-1} cm^{-1}, muy superior al del peróxido de hidrógeno (ε_{H2O2}=18.6 L mol^{-1} cm^{-1}) y puede ser empleado, por consiguiente, para tratar aguas que presentan alto valor de absorción de UV.

2.4.5.9. Proceso de Oxidación Avanzada UV/H_2O_2/O_3.

También puede utilizarse la combinación UV/H_2O_2/O_3, que acelera el proceso térmico: la adición de luz al proceso O_3/H_2O_2 produce un aumento en la velocidad de las reacciones, dado que son compuestos que absorben radiación ultravioleta y se descomponen originando radicales. Así, tanto la fotólisis del peróxido de hidrógeno como del ozono originan radicales hidroxilo (expresiones 19, 33 y 34).

La eficiencia del uso combinado de peróxido de hidrógeno y ozono con radiación ultravioleta, supone un incremento en la velocidad de degradación de ciertos compuestos orgánicos refractarios. Actualmente se están realizando estudios de aplicación a escala de planta piloto (Lucas et al., 2010).

2.4.6.   TECNOLOGIA DE MEMBRANAS.

Las primeras referencias existen sobre investigaciones relacionadas con el campo de las membranas datan de mediados del siglo XVIII, cuando Abbé Nolet, utilizó la palabra "ósmosis" para describir la permeación de agua a través de una membrana natural (Baker, 2004). A lo largo del siglo XIX, las membranas fueron utilizadas como herramientas de laboratorio para desarrollar teorías físico-químicas, pero no existían aplicaciones industriales ni comerciales.

El descubrimiento que permitió la transformación de una técnica de laboratorio en un proceso industrial se produjo en el comienzo de la década de 1960, con el desarrollo del proceso Loeb-Sourirajan para la fabricación de membranas de ósmosis inversa formadas por una capa selectiva ultrafina depositada sobre un soporte micro-poroso mucho más grueso pero a su vez mucho más permeable. El siguiente avance significativo se obtuvo en los métodos de empaquetado de las membranas (desarrollo de módulos de fibras huecas, enrollamientos en espiral o configuración de placas y marcos, entre otros) consiguiéndose en 1980 que la microfiltración (MF), la ultrafiltración (UF), la (osmosis inversa) OI y la electrodiálisis (ED) estuvieran establecidos como procesos a escala industrial (Urtiaga et al., 2010).

Actualmente, los avances basados en nuevos materiales y mejora de las técnicas de fabricación han generado un grado de durabilidad que hace que la tecnología de membrana se encuentran ampliamente extendidas en multitud de procesos de separación industriales. Son fundamentales para aplicaciones en la industria alimentaria, química, biotecnológica, farmacéutica, del automóvil, medicina y otras áreas en relación con energía y medio ambiente como células de combustibles y separación y purificación de gases. Con respecto al consumo de agua, las membranas semipermeables permiten hoy el suministro

de agua potable para millones de personas en el mundo gracias a la purificación y desalación. Los avances en este campo han sido posibles gracias al bajo coste (menos de 1$ m^{-3} de agua potable), bajo consumo energético y al alto rendimiento de esta tecnología.

Las operaciones de separación mediante membranas presentan una serie de ventajas que se enumeran a continuación:

- Bajo consumo de energía, puesto que la energía que hay que aportar habitualmente es la necesaria para conseguir el desplazamiento de las diferentes corrientes de fluido, ya que no suele ser necesario producir un cambio de estado de las fases implicadas.
- Condiciones de operación suaves, ya que con frecuencia la separación se lleva a cabo a temperatura ambiente.
- Posibilidad de obtener elevadas selectividades y eficacias en la separación mediante una correcta elección del tipo y características de la membrana a utilizar.
- Los equipos de membranas son compactos y modulares, por lo que ocupan poco espacio y se pueden acoplar fácilmente en instalaciones ya existentes. Asimismo, las inversiones de capital a realizar en la adquisición de estos equipos no son elevadas.
- Facilidad de montaje, desmontaje y operación.

La principal limitación de este tipo de separaciones reside en la sensibilidad de la membrana, ya que tiende a deteriorarse y/o ensuciarse con el paso del tiempo, siendo necesario reemplazarla con una cierta periodicidad. Además, estas membranas suelen presentar un coste elevado.

2.4.6.1. Definición de membrana.

Las membranas son barreras físicas semipermeables que separan dos fases, impidiendo su íntimo contacto y restringiendo el movimiento de las moléculas a través de ella de forma selectiva. Este hecho permite la separación de las sustancias contaminantes del agua, generando un efluente acuoso depurado.

El esquema básico de un proceso de separación con membranas se representa en la Figura 11: la membrana separa una corriente de alimentación en dos efluentes conocidos

como permeado y retenido. El permeado es el fluido que pasa a través de la membrana semipermeable, mientras que el retenido o rechazo contiene aquellos constituyentes rechazados. El transporte a través de la membrana se da mediante la acción de una fuerza impulsora, es decir, un gradiente de presión (ΔP), concentración (ΔC) o potencial eléctrico (ΔV).
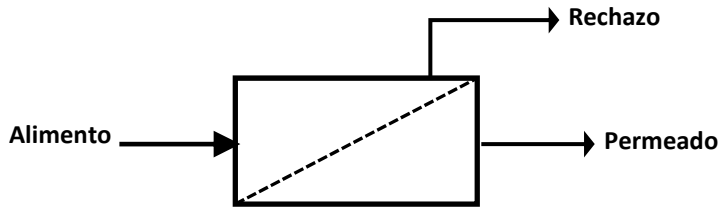
Figura 11. Principio de actuación de los procesos de membrana.

2.4.6.2. Operaciones de membrana.

Las operaciones de separación con membranas se pueden clasificar en tres grupos, dependiendo del objetivo perseguido en cada caso:

-*Operaciones de concentración de disoluciones:* se elimina parte del disolvente presente en la misma haciéndolo pasar a través de la membrana. El producto de interés en la separación es la disolución concentrada, que queda retenida por la membrana. A veces, se trata en realidad de una preconcentración, eliminándose el resto de disolvente mediante otra operación de separación posterior.

-*Operaciones de purificación o clarificación:* la separación tiene como objeto la eliminación de componentes no deseados, que habitualmente son rechazados y retenidos por la membrana, por lo que el producto con valor suele ser la fase que atraviesa la membrana. Este es el objetivo perseguido en el caso de sus aplicaciones para la purificación de aguas.

-*Operaciones de fraccionamiento:* en este caso se pretende conseguir la separación de determinados componentes presentes en el medio, resultando de interés tanto los retenidos por la membrana como los que pueden atravesarla.

Tal y como se ha señalado anteriormente, el desplazamiento a través de la membrana se da mediante la acción de una fuerza impulsora, la cual puede ser un gradiente de presión, concentración o potencial eléctrico. A diferencia de lo que sucede en las operaciones convencionales, en las separaciones mediante membranas no es necesario que las dos fases implicadas en el intercambio de materia sean inmiscibles entre sí, ya que no se encuentran en contacto directo, existiendo dos interfases: fase fluida 1/membrana (interfase 1) y membrana/fase fluida 2 (interfase 2).

Las diversas operaciones basadas en membranas se diferencian entre sí en el estado físico de las fases en contacto con la membrana, la fuerza impulsora del transporte de materia, el tipo de componentes que pueden atravesar la membrana y el tamaño de las especies que son rechazadas. En la siguiente Tabla se resumen las características más relevantes de los procesos de separación con membranas empleados en el tratamiento de agua.

Tabla 5. Características de las operaciones de separación con membranas.

Operación	Fuerza impulsora	Fases implicadas	Composición permeados	Estructura membrana
Diálisis	ΔC_i	L/M/L	Solutos	Porosa (0.1-10µm)
Electrodiálisis	ΔV	L/M/L	Iones	Intercambio iónico
Microfiltración	ΔP	L/M/L	Disolvente	Porosa (0.1-10µm)
Ultrafiltración	ΔP	L/M/L	Disolvente	Porosa (2-100µm)
Nanofiltración	ΔP	L/M/L	Disolvente	Porosa (<2nm)
Ósmosis inversa	ΔP	L/M/L	Disolvente	Densa (<1nm)

Además, mientras que las operaciones convencionales de separación suelen estar controladas por el equilibrio entre las fases, en las operaciones mediante membranas existe un control cinético, ya que la clave de la separación reside en las diferentes velocidades de transporte de los componentes a través de la membrana. La solubilidad es una variable de equilibrio que permite calcular la concentración de soluto en la interfase y depende de la afinidad química entre el soluto y la membrana. El equilibrio que se establece en la

interfase se suele describir por analogía con el equilibrio de otras operaciones: ley de Henry (destilación), isoterma de Langmuir (adsorción), etc. Por otro lado, la difusividad del soluto es un parámetro cinético relacionado con su movilidad en la membrana, por lo que depende de variables como el tamaño molecular y naturaleza del soluto, así como de la estructura de la membrana.

A continuación se explican brevemente las operaciones de membrana de más interés en el tratamiento de aguas, exponiéndose de forma más detallada los fundamentos de las dos operaciones empleadas en el presente trabajo: ultrafiltración y nanofiltración.

En microfiltración (MF) la fuerza impulsora es una diferencia de presiones hidrostáticas de hasta 2 bar, a través de membranas microporosas con tamaño de poro entre 0.1 μm y 10 μm, para la separación de coloides y partículas suspendidas. Se fabrican con materiales orgánicos (polímeros tales como el teflón, PTFE, fluoruro de polivinilideno, PVDF, polipropileno, PP, etc.) o inorgánicos (cerámicas, metales, vidrios, etc.). La microfiltración puede emplearse en cualquier escala (fermentaciones, clarificación y recuperación de biomasa, etc.). Se puede emplear para eliminar turbidez, bacterias y protozoos de aguas residuales, ya sea totalmente o de manera significativa.

En ultrafiltración (UF) la fuerza electromotriz es una diferencia de presiones hidrostáticas de 1 hasta 6 bar. El mecanismo de transporte es el mismo que el de MF, variando únicamente el tamaño de poro de las membranas que ahora se encuentra entre 2 nm y 0.1 μm. Se utilizan para eliminar partículas (clarificar) y desinfectar el agua. Estas membranas son porosas y eliminan bacterias, virus, sólidos en suspensión y partículas de hierro y manganeso, pero en general no son eficaces en la eliminación de compuestos orgánicos naturales o sintéticos. La UF es similar a la coagulación y la filtración de arena, en cuanto que se usa como pretratamiento para las aguas potables.

Las membranas más utilizadas en ultrafiltración son las anisótropas de tipo Loeb-Sourijan, donde una delgada capa de poros de pequeño diámetro se encuentra unida, sin discontinuidad, a otra capa más gruesa y microporosa. Los materiales habitualmente empleados en la fabricación de este tipo de membranas son: poliacrilonitrilo, polímeros de

polivinilclorudo/poliacrilonitrilo, polisulfonas, poliviniliden fluoruro, poliamidas aromáticas, acetato de celulosa y materiales cerámicos (óxidos de titanio, aluminio y silicio).

Según los objetivos que se pretendan, es importante el ahorro debido al tratamiento de las aguas residuales por UF (Laine et al., 2000):

- Reutilización de agua: reducción del coste del consumo de agua de la red municipal de abastecimiento.

- Tratamiento de agua caliente: en aguas de estas características, donde la temperatura puede ser de hasta 50 °C, es posible el tratamiento por UF sin tener que enfriarla previamente. Además del ahorro en energía, los menores problemas de ensuciamiento también reducirán los costes por reposición de membranas.

- Reducción de costes de tratamiento de efluentes industriales: la reutilización del agua evita, en gran parte, el vertido de efluentes a la red pública de saneamiento y, en la misma medida, los costes de tratamiento relativos al cumplimiento de la normativa sobre límites de vertido.

- Recuperación de productos: la UF permite la recuperación de productos valiosos que pueden reciclarse en el proceso de producción. La influencia de esta aplicación en la economía del proceso, dependerá del valor y cantidad del producto recuperado.

Los costes de capital y de operación en los tratamientos por UF son todavía demasiado altos para que pueda aplicarse como única tecnología de tratamiento de grandes caudales de agua residual, pero sí tiene ya un importante campo de aplicación, en combinación con otras tecnologías, como es el caso de los reactores biológicos de membrana o como pre-tratamiento en los procesos de OI. Como única tecnología se utiliza en el tratamiento de efluentes de aguas residuales de 2.5-25 m^3/día, sobre todo en aquellos casos como el tratamiento del agua caliente y recuperación de proteínas en la industria de la alimentación; recuperación de partículas de pintura del agua de los procesos de pintado de piezas industriales; recuperación de polímeros sintéticos en la industria textil; recuperación de aceites presentes en las aguas de proceso de la industria metalúrgica, etc.; donde se plantea el doble objetivo de recuperar un producto valioso y/o reutilizar el agua.

En nanofiltración (NF) se emplean membranas con un tamaño de poro inferior a 2 nm y las presiones que se les aplica se encuentran entre 5-25 bar. Resulta adecuada para eliminar dureza, metales pesados, materia orgánica natural, partículas y un gran número de compuestos orgánicos e inorgánicos. Presenta una elevada retención de iones divalentes y multivalentes, donde su retención es prácticamente total. Sin embargo, no es una tecnología adecuada para retener iones monovalentes, ofreciendo retenciones de NaCl moderadas o bajas, siendo mejores para este propósito las membranas de ósmosis inversa. De este modo, el proceso de nanofiltración es útil para el tratamiento de aguas subterráneas y superficiales con una elevada concentración de sólidos disueltos, pero con un bajo contenido en NaCl. Se utilizan membranas poliméricas con MWCO en el rango 150-1000 Da y coeficientes de retención de cloruro sódico de 0.2–0.8%.

En definitiva, la NF se utiliza principalmente en el tratamiento de aguas de consumo en pequeñas comunidades, en eliminación de la dureza del agua y como pre-tratamiento para la obtención de agua ultrapura. Recientes estudios han demostrado la viabilidad de empleo de este proceso; por ejemplo, García-Vaquero et al. (2014) estudiaron la eliminación de carbono orgánico disuelto (93%), iones (97%), metales (80-100%), color y turbidez (100%), THMs (53%) y microcontaminantes (15-100%) en una planta piloto de nanofiltración.

La ósmosis inversa (OI) es un proceso de filtración y difusión generalmente utilizado para aguas salobres y de mar. En este proceso la clave se encuentra en la gran diferencia de presiones que se utilizan con valores de hasta 80 bar, en el sentido contrario al que está actuando la presión osmótica. Las membranas de OI deben ser altamente selectivas, con gran afinidad y permeabilidad para el agua y gran tolerancia hacia los agentes oxidantes como el cloro, para permitir que las membranas puedan ser desinfectadas y limpiadas. La OI también se utiliza para purificar las aguas potables; en dicho caso se trabaja a baja presión (7 bar) y se consigue un 85-90% de rendimiento. Las unidades de OI eliminan contaminantes de hasta 0.0001 µm; esto incluye bacterias, virus y todos los compuestos orgánicos y de desinfección. Por lo anterior, la ósmosis inversa resulta también una técnica altamente eficaz para tratamientos de deshidratación,

concentración/separación de sustancias de bajo peso molecular en solución, o tratamiento de desechos.

A la vista de las principales aplicaciones de OI/NF, puede deducirse que las calidades del agua obtenida son suficientes para poder ser reutilizadas en las condiciones más exigentes. Además, el nivel de desarrollo alcanzado en los últimos años, como lo demuestra la aplicación de las membranas en nuevos procesos de separación (pervaporación, reactores de membranas, aplicaciones médicas, etc.), junto con la aparición de nuevos materiales que permitan, además de la depuración del agua, la recuperación de sustancias valiosas, hacen prever unas buenas perspectivas de futuro para estos procesos. Los aspectos más importantes a tener en cuenta para el diseño en plantas reales de NF son los caudales de agua potable requeridos y el nivel de retención de ciertos compuestos presentes en el agua bruta (van der Bruggen et al., 2001). La elección de la membrana más adecuada dependerá en gran medida de estas consideraciones, así como el cálculo de la superficie de la misma, que supone un coste importante.

En la siguiente Figura se muestra la relación existente entre las distintas impurezas que se puedan encontrar en las aguas a depurar y las operaciones de membranas más adecuadas que trabajan en el rango correspondiente, para el caso concreto de operaciones con membranas en las que la fuerza impulsora es una diferencia de presiones.
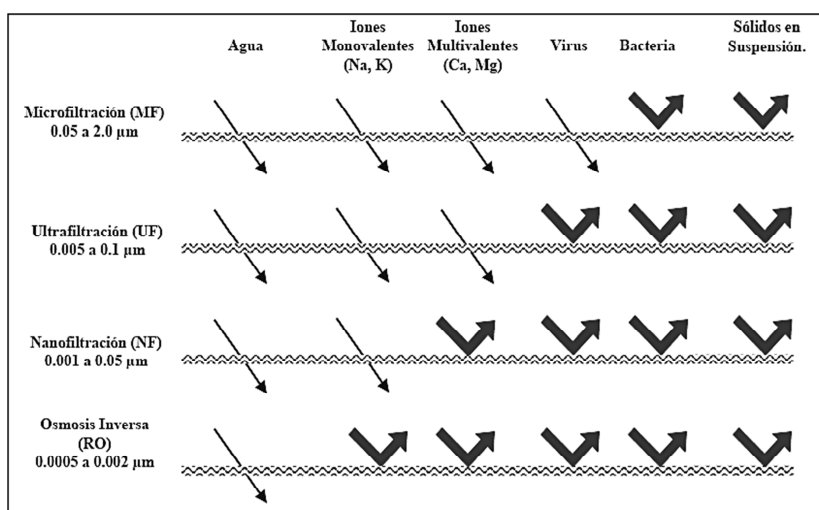
Figura 12. Relación entre tamaños de impurezas y membranas.

2.4.6.3. Clasificación de las membranas.

Las membranas pueden clasificarse de acuerdo a diferentes criterios tales como mecanismos de separación, tamaño de poro, morfología física y naturaleza química.

I. Según el mecanismo de separación

Hay tres mecanismos de separación que dependen de alguna propiedad específica de los componentes que serán eliminados o retenidos selectivamente por la membrana:

a) Separación fundamentada en grandes diferencias de tamaño, cuyas operaciones fundamentales son la microfiltración, ultrafiltración y nanofiltración.

b) Separación basada en las diferencias de solubilidad y difusividad de los materiales de la membrana (solución-difusión), caso típico de la ósmosis inversa.

c) Separación fundada en diferencias de cargas de las especies a separar (electrodiálisis).

La clasificación de las membranas basada en mecanismos de separación, se reduce a tres clases principales:

- *Membranas porosas*. Poseen poros finos de diferentes tamaños y realizan la filtración por medio del efecto criba: se distinguen macroporos, mayores de 50 nm (MF), mesoporos, en el rango de 2 a 50 nm (UF) y microporos, menores de 2 nm (NF).
- *Membranas no porosa*s. Estas membranas pueden considerarse como medios densos. La difusión de especies tiene lugar en el volumen libre que esté presente entre las cadenas macromoleculares del material de la membrana. La OI, entre otras, utilizan este tipo de membrana.
- *Membranas de intercambio iónico*. Son un tipo especial de membranas no porosas, de separación electroquímica, en la que los iones se transfieren a través de la membrana por medio de una tensión o corriente eléctrica continua.

II. Según el tamaño de poro

Las membranas pueden clasificarse por el tamaño de exclusión del soluto, que se denomina diámetro de poro. De forma habitual se indica el valor de corte de peso

molecular (MWCO), definido como el peso molecular de las proteínas, de tipo globular, que la membrana puede separar en un 90%.

III. Según su morfología

Debido a que la velocidad de paso de una sustancia a través de la membrana es inversamente proporcional a su espesor, las membranas deberán ser tan delgadas como sea posible. Mediante la fabricación de membranas anisotrópicas es posibles conseguir espesores de membranas inferiores a 20 mm, que son los espesores de las membranas convencionales (isotrópicas o simétricas: composición, estructura y demás propiedades son iguales en todos los puntos de la membrana). Debido a este tipo de membrana, se mejoraron los procesos de separación y se introdujeron a escala industrial.

Las membranas anisótropas son estructuras laminares o tubulares donde el tamaño de poro, la porosidad o la composición de la membrana cambia a lo largo de su espesor. Estas membranas constan de una capa muy fina, llamada película, soportada por otra capa subyacente más espesa y porosa. La capa pelicular es responsable de las funciones principales de la membrana, ya que el flujo y la selectividad sólo dependen de la estructura de esta capa. Su espesor está en el rango de 0.1 a 0.5 μm aproximadamente, lo cual corresponde al 1% del espesor de la capa porosa subyacente. La capa soportante presenta una resistencia despreciable a la transferencia de masa y está presente sólo como soporte mecánico. Se pueden distinguir dos tipos de membranas anisótropas:

- *Membranas asimétricas:* preparadas en base a un mismo material (membranas de Loeb-Sourirajan)
- *Membranas mixtas (composite):* en las cuales la capa superior y la subcapa son de material diferente. Cada capa puede ser optimizada independientemente y, generalmente, la capa porosa es una membrana asimétrica.

IV. Según su geometría

Un módulo de membrana es la unidad básica en un dispositivo de filtración. Los módulos contienen las membranas con sus soportes, así como las conducciones necesarias

para el flujo, y se sitúan en unos recipientes adecuados a las condiciones de operación. Deben ser lo más compacto posible (es decir, que incluya la mayor superficie de membrana por unidad de volumen de módulo), y también que su manipulación, en cuanto a sustitución y limpieza de membranas, sea sencilla, así como que tengan una buena compatibilidad química con los fluidos a tratar.

En principio los módulos se fabricaban con membranas planas, aunque las aplicaciones de éstos, debido a su escasa compacidad, se redujeron prácticamente a la escala de laboratorio. En la actualidad, los módulos que se comercializan son principalmente: módulo tubular, módulo con arrollamiento en espiral y módulo de fibra hueca.

- Planas: Es el tipo más sencillo. Se trata de membranas planas que se colocan dentro de un marco, circular o rectangular, que actúa como soporte de la membrana y le confiere rigidez y resistencia. Se colocan grupos de dos membranas de manera intercalada, con los lados del alimento encarados cada uno. En cada compartimento de alimento y permeado obtenido se coloca un espaciador. Su principal ventaja es que se obstruyen poco y además se limpian de forma relativamente fácil y eficaz en caso de ensuciamiento. El principal inconveniente es su baja capacidad productiva, debido a la baja área efectiva.
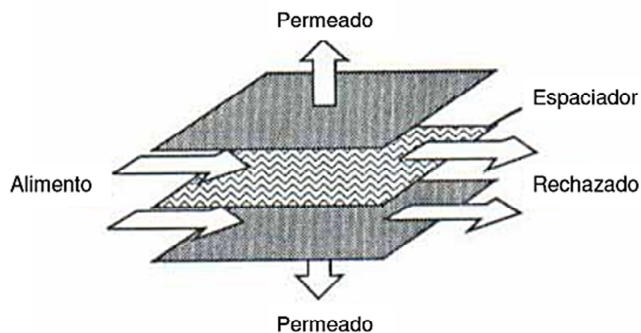
Figura 13. Esquema modulo con membranas planas.

- Tubulares. La membrana va alojada en el interior de un tubo de acero inoxidable o de PVC, que soporta la presión del proceso. El tubo va provisto de los orificios necesarios para la entrada y salida de los flujos de agua que intervienen en el proceso. El agua

fluye desde el interior de la configuración tubular hacia fuera. Su ventaja es que no se necesita una prefiltración fina de alimentación y son de fácil limpieza. Su desventaja es que tiene una baja densidad de compactado, por lo que incrementa el coste de inversión.
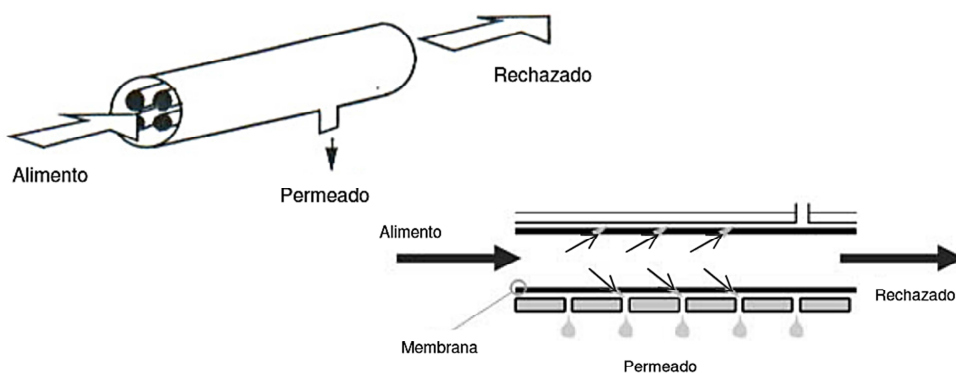
Figura 14. Esquema modulo y configuración tubular.

- Enrollamiento en espiral. Estos módulos se constituyen a partir de varias membranas planas rectangulares enrolladas alrededor de un eje cilíndrico provisto de perforaciones que permiten recoger el agua producto. Para el enrollamiento de las láminas de membrana se disponen éstas por parejas con sus capas activas hacia el exterior, alternadas con un separador impermeable y una malla. Esta malla plástica, de espesor entre 0.75 y 1.10 mm, constituye el canal por el que fluirá el conjunto alimentación-rechazo, y sirve además como elemento de ayuda en la formación de régimen de flujo turbulento de la alimentación, lo que reduce las posibilidades de obstrucción. El conjunto membranas, mallas y separadores se sella mediante un pegamento por tres de los lados, mientras que por el cuarto lado, que constituye la única salida posible para el agua que ha atravesado las membranas, se une al eje perforado que recoge y canaliza el permeado: el líquido de alimentación fluye longitudinalmente, en tanto que el permeado discurre entre las membranas hacia el tubo perforado.

Estos módulos pueden disponerse en serie, de manera que el líquido de alimentación puede pasar a través de un gran número de ellos. La longitud y el diámetro de esto módulos están limitados por la pérdida de carga que experimenta el líquido. El

arrollamiento permite introducir una gran superficie de membrana en un espacio reducido, resultado una compacidad elevada. El módulo arrollado en espiral es más sensible a la obstrucción que los sistemas planos, y no pueden utilizarse directamente con agua sin pretratamiento.
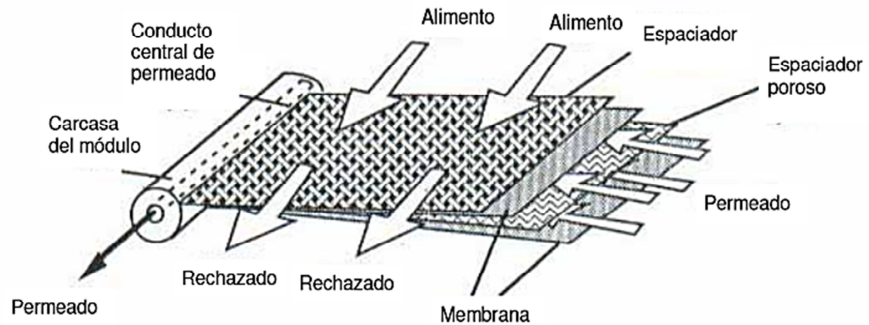
Figura 15. Esquema de un módulo en espiral.

- Fibras huecas. Estos módulos están constituidos por un haz de millones de tubos capilares, hueco interiormente. Las fibras huecas van empaquetadas en un tubo cilíndrico de un material plástico de alta resistencia como el poliéster reforzado con fibra de vidrio (PRFV), que constituye la carcasa protectora y permite la circulación de la disolución a tratar. El agua a presión se aplica a la membrana desde el exterior del capilar y la pared de la fibra actúa como membrana separadora reteniendo las sales mientras que por el interior circula el agua producto que ha atravesado la membrana. Estas unidades son muy compactas. Su caudal unitario es muy pequeño, pero debido al haz de fibras que constituyen la membrana, resulta un caudal total elevado. La desventaja es que tiene mayor tendencia al ensuciamiento.
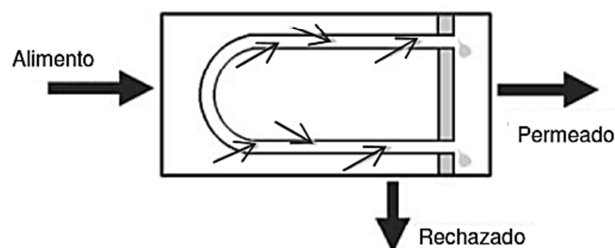
Figura 16. Configuración fibra hueca.

V. Según su naturaleza química

Las membranas sintéticas pueden construirse a partir de diferentes materiales orgánicos (polímeros) e inorgánicos (metales, cerámica, vidrio, etc.).

Membranas orgánicas: básicamente pueden ser utilizados todos los polímeros, pero en la práctica sólo se utiliza un número limitado de ellos. Los más usados son la celulosa y sus derivados. Estos polímeros hidrófilos presentan un bajo coste, poca tendencia a la adsorción y se utilizan no sólo en todos los procesos de presión, sino también en hemodiálisis y permeado gaseoso. En el tratamiento de aguas, las membranas de ésteres de la celulosa (principalmente di y triacetato) tienen la ventaja de ser relativamente resistentes al cloro y, a pesar de su sensibilidad a los ácidos, a la hidrólisis alcalina, a la temperatura y a la degradación biológica, se utilizan ampliamente para desalación, reducción de la dureza de las aguas, desinfección y clarificación.

Otra clase importante de membranas poliméricas son las realizadas con poliamidas. Son resistentes a la hidrólisis y al ataque de microorganismos, pueden tolerar condiciones alcalinas y temperaturas de hasta 50 °C. Sin embargo, son extremadamente sensibles a la presencia de cloruros, el grupo amida, la degradación oxidativa, y no toleran la exposición al cloro. Las poliamidas aromáticas se emplean fundamentalmente en separaciones de ósmosis inversa y las poliamidas alifáticas en microfiltración y ultrafiltración.

El poliacrilnitrilo (PAN) se utiliza también de forma común en las membranas de ultrafiltración y hemodiálisis. A pesar de la presencia del grupo nitrilo, fuertemente polar, este tipo de polímeros no es muy hidrofílico (menos que los dos polímeros anteriores). No tienen la propiedad de permeabilidad selectiva y no se usa en ósmosis inversa. Con frecuencia incorporan acetato de vinilo o metilmetacrilato como monómero para aumentar la flexibilidad de la cadena y el carácter hidrofílico.

Otros polímeros ampliamente utilizados son las polisulfonas (PSF) y las polietersulfonas (PES). Estos polímeros no son hidrofílicos y tienen una tendencia

relativamente alta a la adsorción, pero tienen muy buena estabilidad química, mecánica y térmica. Se usan normalmente como membranas de ultrafiltración, como soporte de membranas mixtas (composite) o como membranas de hemodiálisis.

Membranas inorgánicas: suelen poseer mayor estabilidad química, mecánica y térmica en comparación con los polímeros orgánicos. Sin embargo, tienen la desventaja de ser muy frágiles y más caras que las membranas orgánicas. Esto explica por qué su principal campo de aplicación está limitado a la industria química, para tratamiento de fluidos agresivos o de alta temperatura y a las industrias farmacéuticas y lácteas donde se precisa esterilización térmica. Las membranas cerámicas (óxidos, nitruros o carburos de metales, tales como aluminio, zirconio o titanio) son el tipo principal de membranas inorgánicas.

2.4.6.4. Modos de operación.

El principio de utilización del módulo de membranas es simple: una bomba asegura la presurización de la alimentación y circulación a lo largo de la membrana, colocándose una válvula sobre la línea de retenido (o concentrado) para mantener la presión dentro del módulo. El permeado sale a una presión generalmente cercana a la atmosférica (P_a). La elección de la bomba y la adaptación de la válvula permiten el ajuste independiente de la presión media a través de la membrana o presión trans-membrana (TMP). La presión trans-membrana se define como (Tasselli et al., 2007):

$$TMP = \frac{P_{entrada} + P_{salida}}{2} \tag{44}$$

donde $P_{entrada}$ es la presión a la entrada del módulo, y P_{salida} la presión a la salida.

En el tratamiento de aguas por operaciones de membrana se puede operar de dos formas (Figura 17):

- Filtración en línea o flujo final ciego. Las membranas se disponen en la línea de flujo del efluente que se desea tratar (alimentación), quedando las partículas contaminantes retenidas en el interior de las membranas y generándose una corriente

depurada o permeado. Las membranas utilizadas son de tipo filtro profundo, dispuestas en cartuchos.

- *Filtración tangencial*. El efluente que se desea tratar se hace circular tangencialmente a la membrana. Los contaminantes quedarán en la superficie de la membrana, siendo arrastrados por el flujo tangencial, evitándose en gran medida el ensuciamiento de la membrana. Esta forma de operar genera a partir de la alimentación dos corrientes o flujos: concentrado o rechazo, con una concentración de contaminantes mayor que en la alimentación, y permeado, con una baja concentración de contaminantes que hace posible su vertido o reutilización. Las membranas utilizadas son de tipo tamiz o densas.
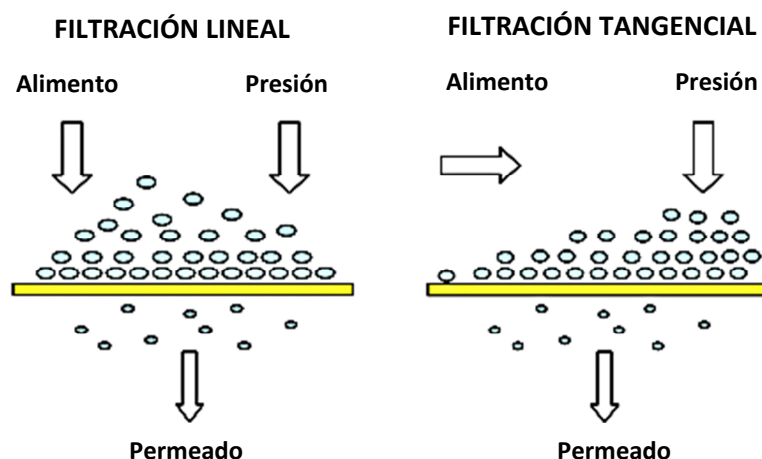
Figura 17. Esquema de filtración lineal y tangencial.

2.4.6.5. Factores que reducen las prestaciones de las membranas

El buen funcionamiento de una membrana se consigue cuando se mantiene el flujo de permeado y los factores de retención dentro de las condiciones de diseño de la operación, esto es, sin grandes modificaciones en la diferencia de propiedad (presión, potencial eléctrico) que genera el flujo de permeado (Rodríguez et al., 2006). El flujo de permeado (J_v) es el flujo de la solución que pasa la membrana, mientras que el coeficiente de retención (R) de un componente i que se desea excluir del permeado es una forma de

estimar el grado de separación conseguido por la membrana. A continuación se describe brevemente los dos principales factores que reducen las prestaciones de las membranas.

❖ Polarización de la concentración

Tiene lugar en aquellos procesos que operan en filtración tangencial. En las condiciones de trabajo de estos procesos es difícil evitar que los componentes de la alimentación que son rechazados por la membrana se acumulen en su superficie. El resultado es la creación de gradientes de concentración (polarización de la concentración) en el lado de la alimentación, que pueden disminuir la eficacia de separación de la membrana y el flujo de permeado (Thorsen, 2004). La Figura 18 representa la situación en la que un componente i de la alimentación, que es rechazado por la membrana, se acumula en su superficie, creándose un gradiente de concentración localizado en una película de espesor δ, próximo a la membrana.
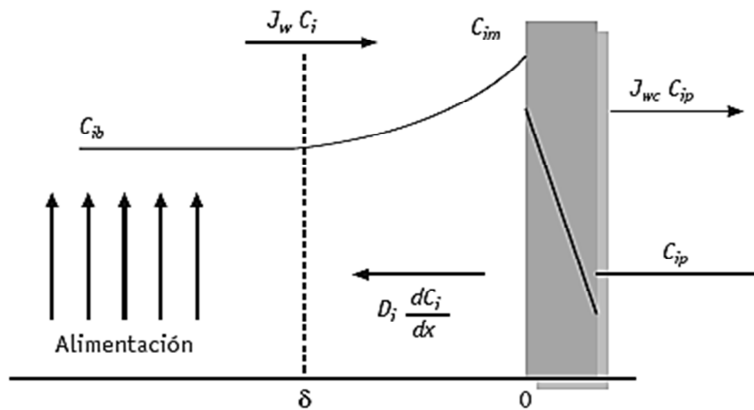
Figura 18. Creación de gradientes de concentración.

❖ Ensuciamiento de las membranas

El ensuciamiento de la membrana es debido a la presencia en la alimentación de sustancias que pueden interaccionar con ella, adsorbiéndose y/o precipitando en su superficie o penetrando en su interior. Los diferentes tipos de ensuciamiento se observan en la Figura 19.

- La formación de la capa de gel se produce cuando la concentración de ciertos componentes de naturaleza macromolecular se eleva demasiado, de manera que se alcanza su límite de solubilidad. Se forma así un depósito sobre la membrana que ejerce una resistencia hidráulica extra. Esto provoca una disminución del flujo de permeado. En principio, el ensuciamiento es reversible (limpieza con agua) pero puede ser irreversible si los componentes de la capa de gel reaccionan con otros formando una capa densa sobre la membrana que no es fácil de eliminar.

- Bloqueo de los poros, que generalmente es irreversible pero se puede llevar a cabo la inversión del sentido del flujo a través de la membrana, aunque no es aplicable a cualquier tipo de membranas. Además se debe considerar las incrustaciones inorgánicas debido a la precipitación de sales pocos solubles y metales, generalmente debidas a carbonato cálcico y sulfatos de bario, de calcio o de estroncio. Este tipo de ensuciamiento es especialmente importante en nanofiltracion y osmosis inversa.

- Adsorción de componentes, debido a lo cual se estrecha el radio del poro y se incrementa la resistencia hidráulica con la consecuente disminución del flujo. Se puede intentar la limpieza con productos específicos como sustancias fuertemente alcalinas o agentes ácidos a elevadas temperaturas.
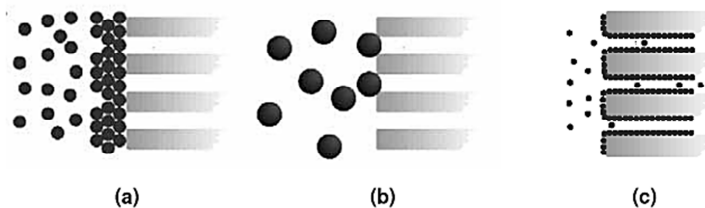
Figura 19. a) Formación de la capa de gel; b) Bloqueo de poros; c) Adsorción.

La consecuencia del ensuciamiento es una disminución del flujo de permeado, debido a una mayor resistencia de la membrana. Un aumento progresivo de la presión transmembrana, con el fin de mantener el flujo de permeado, acelerará el proceso de ensuciamiento, pudiéndose llegar a una situación irreversible de taponamiento de la membrana que haría necesaria su sustitución (Al-Amoudi y Lowitt, 2007).

2.4.7.   Carbón activo: PAC.

El carbón activo puede definirse como un material carbonoso poroso carbonizado, activado mediante la reacción con gases o por la adición de productos químicos, antes, durante o después del proceso de carbonización. Estos procesos confieren al material una elevada porosidad y extensa área superficial. El alcance de la activación condiciona la porosidad final del carbón, si bien, habitualmente presenta tres tipos de poros: microporo (diámetro <2nm), mesoporo (diámetro en el rango 2-50nm) y macroporo (diámetro >50nm). Aunque la mayor parte de la adsorción tiene lugar en los microporos, los mesoporos y macroporos juegan un papel crucial dado que sirven de camino del adsorbato hacia el interior de los microporos, los cuales apenas se encuentran en la superficie exterior del material.

La eficiencia de adsorción esta condiciona por diversos factores, tales como: superficie específica, tamaño y estructura de los poros, volumen del poro y reactividad de los diferentes componentes del material. Dentro de las características del adsorbato, que influyen en el proceso de adsorción, se incluyen: solubilidad, hidrofobicidad, estructura molecular, peso molecular, polaridad y grupos funcionales. Además de estos factores, las características del agua (conductividad, pH, temperatura, carbono orgánico disuelto, turbidez, metales disueltos etc.) también influyen en el proceso (Di Bernardo y Dantas, 2005).

Los adsorción con carbón activo es ampliamente empleada en el tratamiento de aguas, siendo su principal ventaja que no genera productos tóxicos y posee una elevada capacidad de adsorción (Estevinho et al., 2007). Por ello, numerosos estudios evalúan la adsorción de contaminantes emergentes (individuales o mezclas binarias) sobre carbones activados en agua ultrapura y en competencia con materia orgánica natural; sin embargo, se encuentran muy pocos estudios sobre la eliminación de mezclas de contaminantes (Rossner et al., 2009).

2.4.8. PAC/UF.

La combinación de ultrafiltración (UF) y carbón activo en polvo (PAC) ha ganado importancia en los últimos 15 años (Saravia et al., 2012). Los beneficios de la combinación PAC/UF se deben a la capacidad de adsorción de PAC y la capacidad de la membrana para retener compuestos de alto peso molecular y partículas (incluyendo el propio PAC). De este modo, la combinación PAC/UF permite la eliminación de compuestos de bajo peso molecular que no se pueden eliminar mediante ultrafiltración (Campinas y Rosa, 2010).

Los procesos híbridos PAC/UF mejoran el rendimiento de los procesos de membrana de ultrafiltración: mejora de la calidad de permeado (eliminación de contaminantes orgánicos) y la disminución del ensuciamiento de la membrana debido a la eliminación de sustancias que causan el ensuciamiento de la misma. Además, la dosis de PAC se puede ajustar a la calidad del agua a tratar en cada caso.

2.5. ESTUDIOS PREVIOS SOBRE ELIMINACIÓN DE CONTAMINANTES EMERGENTES MEDIANTE OXIDACIÓN QUÍMICA Y OPERACIONES DE MEMBRANA

En la bibliografía se encuentran diversos estudios sobre la creciente problemática de la contaminación de aguas mediante contaminantes emergentes, así como sobre su eliminación utilizando gran variedad de tratamientos, entre los cuales se encuentran la oxidación química y los procesos de membrana.

Con respecto a dicha problemática, en España se ha detectado una gran cantidad de contaminantes emergentes en aguas en los últimos años. Así, López-Roldán et al. (2010) detectaron 28 contaminantes en el río Llobregat determinando una concentración máxima de 8042 ng L^{-1} para el fármaco metoprolol; un año más tarde, en el mismo río los contaminantes emergentes detectados ascendieron a 47 (Calderón-Preciado et al., 2011). En el año 2012, un estudio de monitorización llevado a cabo en cinco efluentes de EDARs en España (en Almería, Cantabria, Barcelona y dos en Madrid) identificó la presencia de 100 contaminantes, entre los cuales se encontró amitriptilina clorhidrato en concentraciones en torno a 30 ng L^{-1} (Martínez-Bueno et al., 2012). López-Serna et al. (2013) encontraron 95

contaminantes cuando estudiaron tres aguas superficiales en el distrito de la ciudad de Barcelona. En 2014, numerosos estudios han sido publicados en relación a la presencia de contaminantes emergentes en agua; a modo de ejemplo, Köck-Schulmeyer et al. (2014) han identificado 22 pesticidas en aguas subterráneas de Cataluña; Robles-Molina et al. (2014) detectaron 53 contaminantes en agua de pantano (entre los cuales se encontraba DEET en concentraciones de hasta 43.5 ng L^{-1}), 26 contaminantes en humedales y 44 en el río Guadalquivir (entre ellos DEET, en concentraciones de hasta 5.7 ng L^{-1}) en la provincia de Jaén; Esteban et al. (2014) han encontrado 31 disruptores endocrinos al analizar aguas de los ríos Jarama y Manzanares (Madrid); y en Valencia, Carmona et al. (2014) han encontrado un total de 21 contaminantes al analizar muestras procedentes de agua potable, agua superficial y efluentes de estaciones depuradoras de aguas residuales.

En la bibliografía reciente se pueden encontrar algunos estudios para la eliminación de los contaminantes seleccionados, lo que indica el interés que suscitan, aunque en general los estudios son escasos y se centran en el grado de eliminación alcanzado.

1-H-Benzotriazol

En 1995 Naik y Moorthy, determinaron las constates de reacción de BZ con los radicales OH, aunque este primer estudio no estaba centrado en la eliminación del compuesto. Es a partir del año 2010 cuando aparecen los primeros estudios centrados en la eliminación del 1-H-Benzotriazol.

En lo que se refiere a estudios de oxidación química en agua ultrapura, Karpel Vel Leitner y Roshani (2010) estudiaron la ozonación de BZ determinando las constantes de reacción segundo orden a pH 2 y 5; Ding et al. (2010) estudiaron la degradación fotoelectrocatalítica de BZ con TiO_2 alcanzandose el 70% de eliminación en 180 min, y mayor eliminación de BZ (88%) consiguieron Xu et al. (2010) mediante adsorción en óxidos de metal Zn-Al-O.

La eliminación de BZ mediante aplicación de irradiación en presencia de $S_2O_8^{2-}$ fue estudiada por Roshani et al. (2011), alcanzandose una degradación en torno al 50%. Por su parte, Sichel et al. (2011) estudiaron la degradación alcanzada mediante UV/Cl_2 a pH 7 y Yang et al. (2011) evaluaron la oxidación de varios benzotriazoles con Fe (VI).

En 2012 Mawhinney et al. estudiaron la ozonación de BZ con distintas dosis de ozono e identificaron algunos intermedios de reacción. Al año siguiente, Xu et al. (2011) eliminaron el 90% de BZ mediante fotocatálisis con BiOBr y luz solar en 3 horas; idéntico tiempo y degradación consiguieron Wu et al. (2013) al aplicar un proceso Fenton-like catalizado con nanopartículas $ZnFe_2O_4$.

Mediante ozonación catalítica con Cu/Al_2O_3 Roshani et al. (2014) alcanzaron un 90% de degradación en 15 minutos. Al llevar a cabo la oxidación con permanganato catalizada por Ru-TiO_2, Zhang et al. (2014) alcanzaron un 60% de eliminación de BZ.

En cuanto a estudios de oxidación con aguas reales, De la Cruz et al. (2013) evaluaron la degradación mediante UV, UV/H_2O_2 y foto-Fenton en planta piloto. En 2014 Zúñiga-Benítez et al. aplicaron ultrasonidos a agua de río y consiguieron eliminar entre 40-90% de BZ en función del pH. En un efluente de EDAR, Altmann et al. (2014) determinaron que 40-50 mg L^{-1} de PAC son necesarios para eliminar el 90% de BZ; Ruhl et al. (2014) comprobaron la eliminación con 8 PAC diferentes encontrando eliminaciones entre 45-90% en efluente de EDAR.

En cuanto a procesos de membrana, Weiss y Reemtsma (2008) consiguieron degradar en torno a 60% mediante biorreactores de membrana en el efluente e influente procedente de una EDAR. Margot et al. (2013) y Löwenberg et al. (2014) consiguieron eliminaciones del 90% de BZ en el efluente de EDARs al aplicar procesos combinados PAC/UF.

Nortriptilina HCl

Dado que se trata de un antidepresivo de uso ampliamente extendido, existen numerosos estudios sobre su actividad y degradación metabólica y su presencia en diveros

tipos deagua (Linden et al., 2008; Lajeunesse et al., 2008; Santos et al., 2010; Baker y Kasprzyk-Hordern, 2013; Giebułtowicz y Nałęcz-Jawecki, 2014). Sin embargo, apenas existen estudios de tratamiento de aguas que aborden la eliminación de nortriptilina. En 2013 Lajeunesse et al. publicó un estudio sobre la oxidación de diferentes fármacos del efluente de una EDAR en el que se consiguió eliminar el 99% de NH con 5 mg L^{-1} de ozono.

DEET

Debido a su elevado consumo y a su frecuente aparición en aguas (Apartado 2.1), numerosos estudios se han llevado a cabo en los últimos años centrados principalmente en el grado de eliminación alcanzado.

Con respecto a la eliminación de DEET mediante oxidación química en agua ultrapura, Zhang y Lemley (2006) aplicaron un tratamiento anódico de Fenton (FAFT) consiguiendo eliminación completa en 20 minutos e identificando algunos intermedios de reacción mediante GC-MS. Kim et al. (2008) y Kim y Tanaka (2009) concluyeron que DEET es bastante resistente a la fotodegradación; Calza et al. (2014) identificaron algunos de los intermedios de reacción formados. Song et al. (2009) aplicaron radiación pulsada y radiación γ, determinando una constante de reacción con radicales OH de $4.6x10^{9}$ y $4.9x10^{9}$ $M^{-1}s^{-1}$, respectivamente. En ese mismo año, la ozonación (0.51-0.76 g h^{-1} de ozono) de DEET fue estudiada a cinco pH diferentes por Tay et al. (2009), quienes determinaron las constantes cinéticas de pseudo-primer orden e identificaron algunos subproductos de reacción mediante GC/MS. Yang et al. (2011b) indicaron que la adsorción con GAC no resulta un proceso viable para su eliminación. Su degradación fotocatalítica ha sido estudiada por Adams et al. (2009) empleando UV/Degussa P-25 TiO_2 y por Medana et al. (2010) y Antonopoulou et al. (2013) empleando UV/TiO_2, consiguiendo una degradación en torno al 80% tras 40 minutos de reacción. En 2014 Chen et al. obtuvieron eliminación total de DEET en una hora al aplicar determinadas condiciones de electrooxidación con electrodo de diamante dopado con boro.

La ozonación en agua de río fue estudiada por Snyder et al. (2006) alcanzando en torno al 80% de degradación. Kim y Tanaka (2010) alcanzaron el 46% de eliminación de

DEET de un efluente secundario al aplicar 6 mg L^{-1} de ozono. Wert et al. (2011) comprobaron que el proceso de coagulación en aguas residuales no mejoraba un posterior tratamiento de ozonación para la eliminación de DEET.

Ciertos procesos de membrana han sido asimismo estudiados. Yoon et al. (2006) estudiaron la eliminación de DEET en diferentes aguas reales mediante nanofiltración, alcanzando retenciones entre 20 y 80%, y mediante procesos de ultrafiltración, sin conseguir ninguna eliminación significativa. Por otro lado, Huang et al. (2011) alcanzaron retenciones del 83% tras aplicar cuatro etapas de OI.

3-Metilindol

Para metilindol se encuentran en bibliografía numerosos artículos sobre su actividad metabólica tanto en humanos como en animales (Lanza et al., 1999; Yan et al., 2007) y su degradación con microorganismos (Gu et al., 2002; Li et al., 2010). Sin embargo, los estudios sobre su eliminación mediante oxidación química son escasos y no existen estudios sobre su eliminación mediante procesos de membranas.

En 1997 Watkins et al. consiguieron la eliminación completa de ML mediante ozonación y Wu et al. (1999) lograron degradar el 50% de ML empleando oxígeno como agente oxidante.

Clorofeno

Para este compuesto se han encontrado algunos estudios previos sobre su oxidación química. Zhang y Huang (2003) determinaron el valor de la constante de primer orden de reacción de clorofeno con MnO_2 e identificaron algunos intermedios de reacción; en 2012 Taujale y Zhang emplearon otros óxidos de metales junto con el óxido de manganeso y estudiaron la degradación en el rango de pH 4-8. En 2007 Sires et al. evaluaron su eliminación a pH 3 mediante electro-Fenton con diferentes celdas electrolíticas. Su eliminación en biorreactores de membrana con óxidos de manganeso en efluentes de ETAP es superior al 75% (Forrez et al., 2011).

2.6. OBJETO Y ALCANCE DE LA PRESENTE INVESTIGACIÓN.

De acuerdo a todo lo anteriormente expuesto, existen escasos estudios de degradación los contaminantes emergentes seleccionados mediante los procesos de eliminación empleados en este estudio: radiación UV, ozonación, cloración, O_3/H_2O_2, UV/H_2O_2, nanofiltración, ultrafiltración y procesos combinados fisco-químicos/químico-físicos. Asimismo puede apreciarse que en su mayoría, estas investigaciones han centrado su interés en la determinación del grado de destrucción los contaminantes. Sin embargo los estudios cinéticos son escasos, y por lo tanto, pocos datos cinéticos están disponibles en la bibliografía para estos procesos, cuando precisamente esos parámetros son imprescindibles para el diseño de los equipos y dispositivos en los que llevar a cabo este tipo de operaciones. Al mismo tiempo, son escasos los estudios que investigan los productos intermedios de reacción y/o la evolución de la toxicidad.

Desde hace varios años, se viene desarrollando en el Área de Ingeniería Química de la UEx una amplia línea de investigación sobre la eliminación de contaminantes orgánicos en aguas naturales y residuales, mediante el empleo de tratamientos físicos, químicos y biológicos a escala laboratorio. Entre los múltiples contaminantes ensayados en estos trabajos pueden mencionarse: colorantes textiles, fenoles y polifenoles, ácidos, pesticidas, productos farmacéuticos, etc.

Los objetivos genéricos de todos estos estudios se centran fundamentalmente en medir los niveles de eliminación de los contaminantes estudiados que se alcanzan en los diversos tratamientos, así como la determinación de las condiciones operativas óptimas y la evaluación de una serie de parámetros cinéticos específicos. Como se ha comentado previamente, la importancia de estas determinaciones reside en que tales parámetros permiten llevar a cabo el diseño y la optimización de los dispositivos, equipos y reactores reales que se han de utilizar posteriormente en las plantas de tratamiento de aguas.

Dentro de este contexto general se enmarca la presente Tesis Doctoral, que se ha desarrollado a través del Proyecto CTQ2010-14823 financiado por el Ministerio de Ciencia e Innovación y titulado "Utilización de tecnologías avanzadas en aguas superficiales y tratadas

para la eliminación de contaminantes resistentes a métodos convencionales", y de los Proyectos RNM021 y GR10026 del Gobierno de Extremadura, Consejería de Empleo, Empresa e Innovación, cofinanciados por el Fondo Europeo de Desarrollo Regional "Apoyos a los Planes de Actuación de los Grupos Catalogados: Tecnología del medio ambiente e ingeniería química, GRUPO RNM021".

En esta Tesis se decidió investigar la eliminación de varios contaminantes emergentes pertenecientes a diferentes familias. Los tratamientos seleccionados para llevar a cabo su eliminación, tanto en agua ultrapura como en aguas reales, han sido los siguientes:

- Degradación de los contaminantes emergentes seleccionados mediante procesos de oxidación química, empleando los sistemas oxidantes: radiación ozono, radiación UV, O_3/H_2O_2, UV/H_2O_2, $O_3/UV/H_2O_2$, O_3/UV, UV/TiO_2, O_3/TiO_2, $O_3/UV/TiO_2$, $UV/S_2O_8^{2-}$ Fe^{2+}/H_2O_2, $UV/Fe^{2+}/H_2O_2$, Fe^{3+}/H_2O_2 y $UV/Fe^{3+}/H_2O_2$.

- Separación de los contaminantes emergentes seleccionados del medio acuoso mediante operaciones de filtración con membranas: ultrafiltración y nanofiltración.

- Eliminación de los contaminantes seleccionados mediante secuencias combinadas físico-químicas: pre-tratamiento químico (UV, O_3 O_3/H_2O_2, UV/H_2O_2 y cloro) seguido de nanofiltración por una parte; y por otra, ozonación o cloración de la corriente filtrada previamente en procesos de ultrafiltración y nanofiltración.

Los objetivos generales que se plantearon se pueden concretar en los siguientes objetivos específicos:

1) En la oxidación química individual de los productos farmacéuticos en agua ultra-pura:

    a) En el tratamiento con radiación UV, establecimiento de la influencia de las variables operativas sobre la degradación, obtención de las constantes de primer orden de reacción, así como los rendimientos cuánticos para la reacción individual de fotólisis de cada contaminante mediante la aplicación del modelo de Emisión Esférica. Determinación de subproductos de reacción.

    b) En los tratamientos de oxidación química con radicales hidroxilo generados mediante reactivo de Fenton y sistema foto-Fenton, evaluación de las

constantes de velocidad de la reacción radicalaria entre cada contaminante emergente y los radicales hidroxilos.

c) En el tratamiento con ozono, determinación de la constante aparente de velocidad de la reacción directa con este agente oxidante y las constantes específicas de reacción de las especies disociadas y neutras. Determinación de subproductos de reacción.

d) En los tratamientos de oxidación química con cloro, en ausencia y presencia de bromo, determinación de las constantes aparentes y las constantes de velocidad intrínseca para las reacciones elementales de las especies ionizadas y no ionizadas.

e) Comparación de la eficacia de sistemas oxidantes diversos: ozono, radiación UV, O_3/H_2O_2, UV/H_2O_2, $O_3/UV/H_2O_2$, O_3/UV, UV/TiO_2, O_3/TiO_2, $O_3/UV/TiO_2$, $UV/S_2O_8^{2-}Fe^{2+}/H_2O_2$, $UV/Fe^{2+}/H_2O_2$, Fe^{3+}/H_2O_2 y $UV/Fe^{3+}/H_2O_2$, en base a su contante de reacción.

2) En la oxidación química simultanea de los contaminantes emergentes en aguas reales (un agua superficial (pantano) y dos efluentes secundarios de EDARs):

a) Fotólisis simultánea de los ECs en las diferentes matrices acuosas, realización de un estudio cinético y desarrollo de un modelo para la predicción de la eliminación de los compuestos en sistemas reales mediante procesos de fotólisis.

b) Cloración simultánea de los ECs en las diferentes matrices acuosas y evaluación de la influencia de dicho proceso de oxidación en la formación de THM. Influencia de la presencia de bromuro en las aguas durante el proceso de cloración. Desarrollo de un modelo para la predicción de la eliminación de los contaminantes en sistemas reales.

c) Ozonación simultánea de los ECs en las diferentes matrices acuosas, realización de un estudio cinético y establecimiento de la contribución de los radicales hidroxilo a la reacción de oxidación global.

3) En la eliminación de contaminantes emergentes mediante procesos de membranas, tanto en agua UP como en aguas reales:

a) Aplicación de las técnicas de ultrafiltración y nanofiltración a los ECs disueltos en agua UP y en las diferentes matrices acuosas.

b) Determinación en todos los casos de los caudales y flujos de permeado obtenidos, así como establecimiento de la influencia del tamaño y de la naturaleza de las membranas utilizadas sobre los mencionados flujos de permeado y sobre los coeficientes de retención de los contaminantes emergentes seleccionados.

c) Análisis y evaluación de las distintas resistencias encontradas en ambos procesos de filtración.

d) Determinación de las masas adsorbidas en las membranas y discusión sobre los mecanismos de retención predominantes.

e) Aplicación de la técnica PAC/UF a los contaminantes emergentes disueltos en agua UP y en las diferentes matrices acuosas.

f) Determinación y análisis de la influencia de adición de carbón activado sobre el flujo de permeado y sobre los coeficientes de retención de los contaminantes emergentes seleccionados.

4) En los tratamientos combinados oxidación-filtración por membranas y filtración por membranas-oxidación química:

a) Determinación de los niveles globales de degradación, y de los valores adicionales obtenidos en tales tratamientos combinados con respecto a los que se obtuvieron en los procesos individuales.

b) Proposición de las secuencias más adecuadas de tratamientos que conduzca a los mejores resultados finales en las condiciones operativas más favorables.

REFERENCES

Abou-Donia, M.B.; Wilmarth, K.R.; Jensen, K.F.; Oehme, F.W.; Kurt, T.L. Neurotoxicity resulting from coexposure to pyridostigmine bromide, DEET, and permethrin: implications of Gulf War chemical exposures. J. Toxicol. Environ. Health **1996**, 48, 35-36.

Acero, J.L.; von Gunten, U. Influence of carbonate on the ozone/hydrogen peroxide based advanced oxidation process for drinking water treatment. Ozone Sci. Eng. **2000**, 22, 305-328.

Adams, W.A.; Impellitteri, C.A. The photocatalysis of N,N-diethyl-m-toluamide (DEET) using dispersions of Degussa P-25 TiO_2 particles. J. Photochem. Photobiol. A: Chem. **2009**, 202, 28-32.

Al-Amoudi, A.; Lowitt, R.W. Fouling strategies and the cleaning system of NF membranes factors affecting cleaning efficiency J. Membr. Sci. **2007**, 303, 4-28.

Alidina, M.; Hoppe-Jones, C.; Yoon, M.; Hamadeh A.F.; Li, D.; Drewes, J.E. The occurrence of emerging trace organic chemicals in wastewater effluents in Saudi Arabia. Sci. Total Environ. **2014**, 478, 152-162.

Altmann, J.; Ruhl, A.S.; Zietzschmann, F.; Jekel, M. Direct comparison of ozonation and adsorption onto powdered activated carbon for micropollutant removal in advanced wastewater treatment. Water Res. **2014**, 55, 185-19.

Amigó, J.; Buhigas, G.; Ortega, E. Tesis doctoral. Caracterización de la degradación de Sulfametazina mediante Foto-Fenton (POA's). Departamento de Ingeniería Química. Universidad Politécnica de Catalunya, (**2008**).

Andreozzi, R.; Caprio, V.; Insola, A.; Marotta, R. Advanced Oxidation Processes (AOP) for water purification and recovery. Catal. Today **1999**, 53, 51-59.

Antonopoulou, M.; Giannakas, A.; Deligiannakis, Y.; Konstantinou, I. Kinetic and mechanistic investigation of photocatalytic degradation of the N,N-diethyl-m-toluamide. Chem. Eng. J. **2013**, 231, 314-325.

Aronson, D.; Weeks, J.; Meylan, B.; Guiney, P.D.; Howard, P.H. Environmental release, environmental concentrations, and ecological risk of N,N-diethyl-m-toluamide (DEET). Integr. Environ. Assess. Manag. **2011**, 8, 135-166.

Asimakopoulos, A.G.; Ajibola, A.; Kannan, K.; Thomaidis, N. Occurrence and removal efficiencies of Benzotriazoles and Benzothiazoles in a wastewater treatment plant in Greece. Sci. Total Environ. **2013**, 452, 163-171.

Bagnall, J.P.; Evans, S.E.; Wort, M.T.; Lubben, A.T.; Kasprzyk-Hordern, B. Using chiral liquid chromatography quadrupole time-of-flight mass spectrometry for the analysis of pharmaceuticals and illicit drugs in surface and wastewater at the enantiomeric level. J. Chromatogr. A **2012**, 1249, 115-129.

Baker, D.R.; Kasprzyk-Hordern, B. Spatial and temporal occurrence of pharmaceuticals and illicit drugs in the aqueous environment and during wastewater treatment: New developments. Sci. Total Environ. **2013**, 454, 442-456.

Baker, R. Membrane technology and applications, 2nd edition. Ed. John Wiley &Sons. 2004.

Barb, W.G.; Baxendale, J.H.; George, P.; Hargrave, K.R. Reactions of ferrous and ferric ions with hydrogen peroxide. Nature **1949**, 163, 692-694.

Baxendale, J.H.; Wilson, J.A. Photolysis of hydrogen peroxide at high light intensities. Trans. Faraday. Soc. **1957**, 53, 344-356.

Baynes, R.E.; Halling, K.B.; Riviere, J.E. The influence of diethyl-*m*-toluamide (DEET) on the percutaneous absorption of permethrin and carbaryl. Toxicol. Appl. Pharmacol. **1997**, 144, 332-339.

Benitez, F.J.; Real, F.J.; Acero, J.L.; Leal, A.I.; Garcia, C. Gallic acid degradation in aqueous solutions by UV/H_2O_2 treatment, Fenton's reagent and the photo-Fenton system. J. Hazard. Mat. **2005**, 126, 31-39.

Bielski, B.H.J.; Cabello, D.E.; Arudi, R.L.; Ross, A.B. Pulse radiolysis study of the kinetics and mechanism of the reactions between manganese (II) complexes and perhydroxyl (HO_2)/hyperoxide (O_2^-) radicals. The phosphate complex and an overview. J. Phys. Chem. Ref. Data. **1985**, 14, 1041-1100.

Calderón-Preciado, D.; Matamoros, V.; Bayona, J.M. Occurrence and potential crop uptake of emerging contaminants and related compounds in an agricultural irrigation network. Sci. Total Environ. **2011**, 412, 14-19.

Calza, P.; Medana, C.; Sarro, M.; Baiocchi, C.; Minero, C. Photolytic degradation of N,N-diethyl-m-toluamide in ice and water: Implications in its environmental fate. J. Photochem. Photobiol. A: Chem. **2013**, 271, 99-104.

Campinas, M.; Rosa, M.J. Assessing PAC contribution to the NOM fouling control in PAC/UF systems, Water Res. **2010**, 44, 1636-1644.

Cancilla, D.A.; Baird, J.C.; Geis, S.W.; Corsi, S.R. Studies of the environmental fate and effect of aircraft deicing fluids: detection of 5-methyl-1H-benzotriazole in the fathead minnow (*Pimephales promelas*). Environ. Toxicol. Chem. **2003**, 22, 134-140.

Carmona, E.; Andreu, V.; Picó, Y. Occurrence of acidic pharmaceuticals and personal care products in Turia River Basin: From waste to drinking water. Sci. Total Environ. **2014**, 484, 53-63.

Černigoj, U., Štangar, U.L.; Jirkovský, J. Effect of dissolved ozone on ferric ions on photodegradation of thiacloprid in presence of different TiO_2 catalysts. J. Hazard. Mat. **2010,** 177, 399-406.

Chen, T.S.; Chen, P.H.; Huang, K. Electrochemical degradation of N,N-diethyl-m-toluamide on a boron-doped diamond electrode. J. Taiwan Inst. Chem. E. **2014**, 45, 2615-2621.

Christensen, H.S.; Sehested, H.; Corfitzan, H. Reactions of hydroxyl radicals with hydrogen peroxide at ambient and elevated temperatures. J. Phys. Chem. **1982**, 86, 15-88.

Cui, Y. X.; Li-Dong, S.; Qi, S.; Lei, S. Highly selective synthesis of 3-methylindole from glycerol and aniline over Cu/NaY modified by K_2O. Chin. Chem. Lett. **2013**, 24, 1127-1129.

De la Cruz, N; Esquius, L.; Grandjean, D.; Magnet, A.; Tungler, A.; de Alencastro, L.F.; Pulgarín, C. Degradation of emergent contaminants by UV, UV/H_2O_2 and neutral photo-Fenton at pilot scale in a domestic wastewater treatment plant. Water Res. **2013**, 47, 5836-5845.

Deslandes, B.; Gariépy, C.; Houde, A. Review of microbiological and biochemical effects of skatole on animal production. Livest. Prod. Sci. **2001**, 71, 193-200.

Di Bernardo, L.; Dantas, A.D.B. Métodos e técnicas de tratamento de água. Ed. São Carlos: Rima Editora. Vol. 2, **2005**.

Ding, Y.B.; Yang, C.Z.; Zhu, L.H.; Zhang, J.D. Photoelectrochemical activity of liquid phase deposited TiO_2 film for degradation of benzotriazole. J. Hazard. Mat. **2010**, 175, 96-103.

Esplugas, S.; Ibarz, A.; Vicente, M. Influence of lamp position on the performance of the annular photoreactor. Chem. Eng. J. **1983**, 27, 107-111.

Esteban, S.; Gorga, M.; Petrovic, M.; González-Alonso, S.; Barceló, D.; Valcárcel, Y. Analysis and occurrence of endocrine-disrupting compounds and estrogenic activity in the surface waters of Central Spain. Sci. Total Environ. **2014**, 466, 939-951.

Estevinho, B.N.; Martins, I.; Ratola, N.; Alves, A.; Santos, L. Removal of 2,4.dichlorophenol and pentachlorophenol from waters by sorption using coal fly ash froma Portuguese thermal power plant. J. Hazard. Mater. **2007**, 143, 533-540.

Farhataziz, T.; Ross, A.B. Selective specific rates of reactions of transients in water and aqueous solutions. III. Hydroxyl radical and perhydroxyl radical and their radicals ions. Natl. Stand. Ref. Data Ser. 59 (**1977**).

Fenton, H.J.H. Oxidation of tartaric acid in presence of iron. J. Chem. Soc. **1894**, 65, 899-910.

Forrez, I.; Carballa, M.; Fink, G.; Hennebel, T.; Vanhaecke, L.; Ternes, T.; Boon, N.; Verstraete, W. Biogenic metals for the oxidative and reductive removal of pharmaceuticals,

biocides and iodinated contrast media in a polishing membrane bioreactor. Water Res. **2011**, 45, 1763-1773.

Gallard, H.; Pellizzari, F.; Croué, J.P.; Legube, B. Rate constants of reactions of bromine with phenols in aqueous solution. Water Res. **2003**, 37, 2883-2892.

García-Vaquero, N.; Lee E., Jiménez Castañeda, R.; Cho J., López-Ramírez, J.A. Comparison of drinking water pollutant removal using a nanofiltration pilot plant powered by renewable energy and a conventional treatment facility. Desalination **2014**, 347, 94-10.

Gasperi, J.; Rocher, V.; Gilbert, S.; Azimi, S.; Chebbo, G. Occurrence and removal of priority pollutants by lamellar clarification and biofiltration. Water Res. **2010**, 44, 3065-3076.

Giebułtowicz, J; Nałęcz-Jawecki, G. Occurrence of antidepressant residues in the sewage-impacted Vistula and Utrata rivers and in tap water in Warsaw (Poland). Ecotox. Environ. Safe. **2014**, 104, 103-109.

Glaze, W.H.; Beltran, F.; Tuhkanen, T.; Kang, J. Chemical models of advanced oxidation processes. Water Pollut. Res. J. Canada **1992**, 27, 23-42.

Glaze, W.H.; Peyton, G.R.; Lin, S.; Huang, R.Y.; Burleson, K. Destruction of pollutants in water with ozone in combination with ultraviolet radiation. 2. Natural trihalomethane precursors. Environ. Sci. Technol. **1982**, 16, 454-458.

Gorga, M.; Insa, S.; Petrovic, M.; Barceló, D. Occurrence and spatial distribution of EDCs and related compounds in waters and sediments of Iberian rivers. Sci. Total Environ. **2015**, 503, 69-86.

Gu, J.D.; Fan, Y.; Shi, H. Relationship between structures of substituted indolic compounds and their degradation by marine anaerobic microorganisms. Mar. Pollut. Bull. **2002**, 45, 379-384.

Haber, F.; Weiss, J. The catalytic decomposition of hydrogen peroxide by iron salts. R. Soc. London Ser. **1934**, 147, 332-351.

Hart, D.S.; Davis, L.C.; Erickson, L.E.; Callender, T.M. Sorption and partitioning parameters of benzotriazole compounds. Microchem. J. **2004**, 77, 9-17.

Helbling, D.E.; Hollender, J.; Kohler, H.P.E.; Singer, H.; Fenner, K. High-throughput identification of microbial transformation products of organic micropollutants. Environ. Sci. Technol. **2010**, 44, 6621-6627.

Heller-Grossman, L.; Manka, J.; Limoni-Relis, B.; Rebhun, M. Formation and distribution of haloacetic acids, THM and tox in chlorination of bromide–rich lake water. Water Res. **1993**, 27, 1323-1331.

Hernández-Rodríguez, M.J.; Fernández-Rodríguez, C.; Doña-Rodríguez, J.M.; González-Díaz, O.M.; Zerbani, D.; Pérez Peña, J. Treatment of effluents from wool dyeing process by photo-Fenton at solar pilot plant. J. Environ. Chem. Eng. **2014**, 2, 163-171.

Homem, V.; Santos, L. Degradation and removal methods of antibiotics form aqueous matrices. A review. J. Environ. Manag. **2011**, 92, 2304-2347.

Houtman, C.J. Emerging contaminants in surface waters and their relevance for the production of drinking water in Europe. J. Integr. Environ. Sci. **2010**, 7, 271-95.

Huang, H.; Cho, H.; Schwaba, K.; Jacangelo, J.G. Effects of feedwater pretreatment on the removal of organic microconstituents by a low fouling reverse osmosis membrane. Desalination **2011**, 281, 446-454.

Jacob, S.M.; Dranoff, J.S. Design and analysis of perfectly mixed photochemical reactors. Chem. Eng. Prog. Sym. Ser. **1968**, 64, 54-63.

Jacob, S.M.; Dranoff, J.S. Light intensity profiles in a perfectly mixed photoreactor. AIChE J. **1970**, 16, 359-363.

Jacob, S.M.; Dranoff, J.S. Radial scale-up of perfectly mixed photochemical reactors. Chem. Eng. Prog. Symp. Ser. **1966**, 62, 47-55.

Kadar, E.; Dashfield, S.; Hutchinson, T. Developmental toxicity of benzotriazole in the protochordate *Ciona intestinalis* (Chordata, Ascidiae). Anal. Bioanal. Chem. **2010**, 396, 641-647.

Karpel Vel Leitner, N.; Roshani, B. Kinetic of benzotriazole oxidation by ozone and hydroxyl radical. Water Res. **2010**, 44, 2058-2066.

Kasprzyk-Hordern, B.; Dinsdale, R.M.; Guwy, A.J. The removal of pharmaceuticals, personal cares products, endocrine disruptors and illicit drugs during wastewater treatment and its impact on the quality of receiving waters. Water Res. **2009**, 43, 363-380.

Kim, I.; Tanaka, H. Document Photodegradation characteristics of PPCPs in water with UV treatment. Environ. Int. **2009**, 35, 793-802.

Kim, I.; Tanaka, H. Use of ozone-based processes for the removal of pharmaceuticals detected in a wastewater treatment plant. Water Environ. Res. **2010**, 82, 294-301.

Kim, I.H.; Tanaka, H.; Iwasaki, T.; Takubo, T.; Morioka, T.; Kato, Y. Classification of the degradability of 30 pharmaceuticals in water with ozone, UV and H_2O_2. Water Sci. Tech. **2008**, 57, 195-200.

Kim, S.D.; Cho, J.; Kim, I.S.; Vanderford B.J.; Snyder S.A. Occurrence and removal of pharmaceuticals and endocrine disruptors in South Korean surface, drinking, and waste waters. Water Res. **2007**, 41, 1013-1021.

Köck-Schulmeyer, M.; Ginebreda, A.; Postigo, C.; Garrido, T.; Fraile, J.; López de Alda, M.; Barceló, D. Four-year advanced monitoring program of polar pesticides in groundwater of Catalonia (NE-Spain). Sci. Total Environ. **2014**, 470, 1087-1098.

Krasner, S.W.; Owen, D.M.; Cromwell, J.E. Water disinfection and natural organic matter. Characterization and control. Ed. Roger A. Minear and Gary L. Amy. ACS Symposium Series, 649, 11–23. **1996.**

Laine, J.M.; Vial, D.; Moulart, P. Status after 10 years of operation–overview of UF technology today. Desalinaton **2000**, 131, 17-25.

Lajeunesse, A.; Blais, M.; Barbeau, B.; Sauvé, S.; Gagnon, C. Ozone oxidation of antidepressants in wastewater-treatment evaluation and characterization of new by-products by LC-QToFMS. Chem. Cent. J. **2013**, 7:15, 1-11.

Lajeunesse, A.; Gagnon, C.; Sauve, S. Determination of basic antidepressants and their *N*-desmethyl metabolites in raw sewage and wastewater using solid-phase extraction and liquid chromatography-tandem mass spectrometry. Anal. Chem. **2008**, 80, 5325-5333.

Lanza, D.L.; Code, E.; Crespi, C.L.; Gonzalez, F.J.; Yost, G.S. Specific dehydrogenation of 3-methylindole and epoxidation of naphthalene by recombinant human CYP2F1 expressed in lymphoblastoid cells. Drug Metab. Dispos. **1999**, 27, 798-803.

Lapworth, D.J.; Baran, N.; Stuart, M.E.; Ward, R.S. Emerging organic contaminants in groundwater: A review of sources, fate and occurrence. Environ. Pollut. **2012**, 163, 287-303.

Legrini, O.; Oliveros, E.; Braun, A.M. Photochemical processes for water treatment. Chem. Rev. **1993**, 93, 671-698.

Lemaire, J.; Campbell, I.; Hulpke, H.; Guth, J.A.; Merz, W.; Philip, J.; Von Waldow, C. An assessment of test methods for photodegradation of chemicals in the environment. Chemosphere **1982**, 11, 119-164.

Li, P.; Tong, L.; Liu, K.; Wang, Y. Biodegradation of 3-methylindole by Pseudomonas putida LPC24 under oxygen limited conditions. Fresen. Environ. Bull. **2010**, 19, 238-242.

Liang, X.; Wang, M.; Chen, X.; Zha, J.; Chen, H.; Zhu, L.; Wang, Z. Endocrine disrupting effects of benzotriazole in rare minnow (Gobiocypris rarus) in a sex-dependent manner. Chemosphere **2014**, 112, 154-162.

Linden, R.; Antunes, M.V.; Ziulkoski, A.L.; Wingert, M.; Tonello, P.; Tzvetkov, M.; Souto, A. A. Determination of amitriptyline and its main metabolites in human plasma samples using HPLC-DAD: application to the determination of metabolic ratios after single oral dose of amitriptyline. J. Braz. Chem. Soc. **2008**, 19, 35-41.

Liu, Y.S.; Ying, G.G.; Shareef, A.; Kookana, R.S. Occurrence and removal of benzotriazoles and ultraviolet filters in a municipal wastewater treatment plant. Environ. Pollut. **2012**, 165, 225-232.

Loos, R.; Locoro, G.; Comero, S.; Contini, S.; Schwesig, D.; Werres, F.; Balsaa, P.; Gans, O.; Weiss, S.; Blaha, L.; Bolchi, M.; Gawlik, B.M. Pan-European survey on the occurrence of selected polar organic persistent pollutants in ground water. Water Res. **2010**, 44, 4115-4126.

López-Roldán, R.; López de Alda, M.; Gros, M.; Petrovic, M.; Martín-Alonso, J.; Barceló, D. Advanced monitoring of pharmaceuticals and estrogens in the Llobregat River basin (Spain) by liquid chromatography–triple quadrupole-tandem mass spectrometry in combination with ultra-performance liquid chromatography-time of flight-mass spectrometry. Chemosphere **2010**, 80, 1337-1344.

López-Serna, R.; Jurado, A.; Vázquez-Suñé, E.; Carrera, J.; Petrović, M.; Barceló, D. Occurrence of 95 pharmaceuticals and transformation products in urban groundwaters underlying the metropolis of Barcelona. Environ. Pollut. **2013**, 174, 305-315.

Löwenberg, J.; Zenker, A., Baggenstos, M.; Koch, G.; Kazner, C.; Wintgens, T. Comparison of two PAC/UF processes for the removal of micropollutants from wastewater treatment plant effluent: Process performance and removal efficiency. Water Res. **2014**, 56, 26-36.

Löwenberg, J.; Zenker, A.; Baggenstos, M.; Koch, G.; Kazner, C.; Wintgens, T. Comparison of two PAC/UF processes for the removal of micropollutants from wastewater treatment plant effluent: Process performance and removal efficiency. Water Res. **2014**, 56, 26-36.

Lucas, M.S.; Peres, J.A.; Li Puma, G. Treatment of winery wastewater by ozone-based advanced oxidation processes (O_3, O_3/UV and O_3/UV/H_2O_2) in a pilot-scale bubble column reactor and process economics. Sep. Purif. Technol. **2010**, 72, 235-241.

Maletz, S.; Floehr, T.; Beier, S.; Klumper, C.; Brouwer, A.; Behnisch, P.; Higley, E.; Giesy, J.P.; Hecker, M.; Gebhardt, L.V.; Pinnekamp, J.; Hollert, H. In vitro characterization of the effectiveness of enhanced sewage treatment processes to eliminate endocrine activity of hospital effluents. Water Res. **2013**, 47, 1545-1557.

Margot, J.; Kienle, C.; Magnet, A.; Weil, M.; Rossi, L.; Alencastro, L.F.; Abegglen, C.; Thonney, D.; Chèvre, N.; Schärer, M.; Barrya, D.A. Treatment of micropollutants in municipal wastewater: Ozone or powdered activated carbon?. Sci. Total Environ. **2013**, 461, 480-498.

Martínez Bueno, M.J.; Gomez, M.J.; Herrera, S.; Hernando, M.D.; Agüera, A.; Fernández-Alba, A.R. Occurrence and persistence of organic emerging contaminants and priority pollutants in five sewage treatment plants of Spain: Two years pilot survey monitoring. Environ. Pollut. **2012**, 164, 267-273.

Matamoros, V.; Jover, E.; Bayona, J.M. Occurrence and fate of benzothiazoles and benzotriazoles in constructed wetlands. Water Sci. Technol. **2010**, 61, 191-198.

Mawhinney, D.B.; Vanderford, B.J.; Snyder, S.A. Transformation of 1H-benzotriazole by ozone in aqueous solution. Environ. Sci. Tech. **2012**, 46, 7102-7111.

Medana, C.; Calza, P.; Dal Bello, F.; Raso, E.; Minero, C.; Baiocchi, C. Multiple unknown degradants generated from the insect repellent DEET by photoinduced processes on TiO_2. J. Mass Spectrom. **2011**, 46, 24-40.

Molins-Delgado, D.; Díaz-Cruz, M.S.; Barceló, D. Removal of polar UV stabilizers in biological wastewater treatments and ecotoxicological implications. Chemosphere 2015, 119, S51-S57.

Mutamim, N.S.A.; Noor, Z.Z.; Hassan, M.A.A.; Olsson G. Application of membrane bioreactor technology in treating high strength industrial wastewater: a performance review. Desalination **2012**. 305, 1-11.

Naik, D.B.; Moorthy, P.N. Studies on the transient species formed in the pulse radiolysis of benzotriazole. Radiat. Phys. Chem. **1995**, 46, 353-357.

Nawrocki, J.; Bilozor, S. Brominated oxidation by-products in drinking water treatment. Aqua **1998**, 47, 304-323.

Neyens, E.; Baeyens, J.A review of classic Fenton's peroxidation as an advanced oxidation technique. J. Hazard. Mat. **2003**, 98, 33-50.

Nichols, W.K.; Mehta. R.; Skordos, K.; Macé, K.; Pfeifer, A.M.; Carr, B.A.; Minko, T.; Burchiel, S.W.; Yost, G.S. 3-methylindole-induced toxicity to human bronchial epithelial cell lines. Toxicol. Sci. **2003**, 71, 229-36.

Pal, A.; He, Y.; Jekel, M.; Reinhard, M.; Yew-Hoong Gin, K. Emerging contaminants of public health significance as water quality indicator compounds in the urban water cycle. Environ. Int. **2014**, 71, 46-62.

Petrovic, M.; Gonzales, S.; Barcelo, D. Analysis and removal of emerging contaminants in wastewater and drinking water. Trends Anal. Chem. **2003**, 22, 685-696.

Pignatello, J.J. Dark and photoassisted Fe^{3+}-catalyzed degradation of chlorophenoxy herbicides by hydrogen peroxide. Environ. Sci. Technol. **1992**, 26, 944-951.

Pignatello, J.J.; Oliveros, E.; Mackay, A. Advanced Oxidation Processes for organic contaminant destruction based on the Fenton reaction and related chemistry. Environ. Sci. Techol. **2006,** 35, 1-84**.**

Qi, W.; Singer, H.; Berg, M.; Müller, B.; Pernet-Coudrier, B.; Liu, H.; Qu, J. Elimination of polar micropollutants and anthropogenic markers by wastewater treatment in Beijing, China. Chemosphere **2015**, 119, 1054-1061.

Real, F.J.; Acero, J.L.; Benitez, F.J.; Roldán, G.; Fernández, L.C. Oxidation of hydrochlorothiazide by UV radiation, hydroxyl radicals and ozone: Kinetics and elimination from water systems. Chem. Eng. J. **2010**, 160, 1, 72-78.

Reemtsma, T.; Miehe, U.; Duennbier, U.; Jekel M. Polar pollutants in municipal wastewater and the water cycle: occurrence and removal of benzotriazoles. Water Res. **2010**, 44, 596-604.

Rivera-Cancel, G.; Bocioaga, A.G. Bacterial degradation of N,N-diethyl-m-toluamide (DEET): cloning and heterologous expression of DEET hydrolase. Appl. Environ. Microbiol. **2007**, 73, 3105-3108.

Robles-Molina, J.; Gilbert-López, B.; García-Reyes, J.F.; Molina-Díaz, A. Monitoring of selected priority and emerging contaminants in the Guadalquivir River and other related surface waters in the province of Jaén, South East Spain. Sci. Total Environ. **2014**, 479, 247-257.

Rodríguez, A.; Letón, P.; Rosal, R.; Dorado, M.; Villar, S.; Sanz, J.M. Tratamientos avanzados de aguas residuales industriales. Informe de Vigilancia Ambiental. Universidad de Alcalá del Círculo de Innovación en Tecnologías Medioambientales y Energía (CITME): 1-136. **2006**.

Rodríguez, F.J. Potabilización del agua e influencia del tratamiento de ozonación. Ed. Díaz de Santos, S.A. **2003**.

Roshani, B.; Karpel Vel Leitner, N. Effect of persulfate on the oxidation of benzotriazole and humic acid by e-beam irradiation. J. Hazard. Mat. **2011**, 190, 403-408.

Roshani, B.; McMaster, I.; Rezaei, E.; Soltan, J. Catalytic ozonation of benzotriazole over alumina supported transition metal oxide catalysts in water. Sep. Purif. Techol. **2014**, 135, 158-164.

Rossner, A.; Snyder, S.; Knappe, D. Removal of emerging contaminants of concern by alternative adsorbents. Water Research. **2009**, 43, 3787-3796.

Ruhl, A.S.; Zietzschmann, F.; Hilbrandt, I.; Meinel, F.; Altmann, J.; Sperlich, A.; Jekel, M. Targeted testing of activated carbons for advanced wastewater treatment. Chem. Eng. J. **2014**, 257, 184-190.

Sadiq, R.; Rodriguez, M.J. Disinfection by-products (DBPs) in drinking water and predictive models for their occurrence: A review. Sci. Total Environ. **2004**, 321, 21-46.

Santos, L.; Araújo, A.N.; Fachini, A.; Pena, A.; Delerue-Matos, C. Ecotoxicological aspects related to the presence of pharmaceuticals in the aquatic environment. J. Hazard. Mat. **2010**, 175, 45-95.

Saravia, F.; Zwiener, C.; Frimmel, F.H. Influence of PAC properties on membrane performance in a PAC/UF hybrid system. Water Sci. Technol. **2012**, 12, 496-503.

Schäfer, A.I.; Nghiem, L.D.; Waite, T.D. Removal of the natural hormone estrone from aqueous solutions using nanofiltration and reverse osmosis. Environ. Sci. Technol. **2003**, 37, 182-188.

SDI, Vector One®: National. Top 200 branded drugs by total prescriptions. Drug topics. 2011.

Seeland, A.; Oetken, M.; Kiss, A.; Fries, E.; Oehlmann, J. Acute and chronic toxicity of benzotriazoles to aquatic organisms. Environ. Sci. Pollut. Res. **2012**, 19, 1781-1790.

Sichel, C.; Garcia, C.; Andre, K. Feasibility studies: UV/chlorine advanced oxidation treatment for the removal of emerging contaminants. Water Res. **2011**, 45, 6371-6380.

Sirés, I.; Garrido, J.A.; Rodríguez, R.M.; Brillas, E.; Oturan, N.; Oturan, M.A. Catalytic behavior of the Fe^{3+}/Fe^{2+} system in the electro-Fenton degradation of the antimicrobial chlorophene. Appl. Catal. B: Environ. **2007**, 72, 382-394.

Smital, T.; Terzic S.; Zaja, R.; Senta, I.; Pivcevic, B.; Popovic, M.; Mikac, I.; Tollefsen, K.E.; Thomas, K.V.; Ahel M. Assessment of toxicological profiles of the municipal wastewater effluents using chemical analyses and bioassays. Ecotoxicol. Environ. Saf. **2011**, 74, 844-851.

Snoeyink, V.L.; Jenkins, D. Química del agua. Mexico, Ed. LIMUSA. **2000**.

Snyder, S.A.; Adham, S.; Redding, A.M.; Cannon, F.S.; De Carolis, J.; Oppenheimer, J.; Wert, E.C.; Yoon, Y. Role of membranes and activated carbon in the removal of endocrine disruptors and pharmaceuticals. Desalination **2007**, 202, 8156-181.

Snyder, S.A.; Wert, E.C.; Lei, H.; Westerhoff, P.; Yoon, Y. Removal of EDCs and pharmaceuticals in drinking and reuse treatment processes. Foundation, W.R, Denver, CO. **2007b.**

Snyder, S.A.; Wert, E.C.; Rexing, D.J.; Zegers, R.E.; Drury, D.D. Ozone oxidation of endocrine disruptors and pharmaceuticals in surface water and wastewater. Ozone Sci. Eng. **2006**, 28, 445-460.

Song, W.; Cooper, W.J.; Peake, B. M.; Mezyk, S.P.; Nickelsen, M.G.; O'Shea, K.E. Free-radical-induced oxidative and reductive degradation of N,N'-diethyl-m-toluamide (DEET): Kinetic studies and degradation pathway. Water Res. **2009**, 43, 635-642.

Spadoni, G.; Stramigioli, C.; Santarelli, F. Rigorous and simplified approach to the modelling of continuous photoreactors. Chem. Eng. Sci. **1980**, 35, 925-931.

Stackelberg, P.E.; Gibs, J.; Furlong, E.T.; Meyer, M.T.; Zaugg, S.D.; Lippincot, R.L. Efficiency of conventional drinking-water-treatment processes in removal of pharmaceuticals and other organic compounds. Sci. Total Environ. **2007**, 377, 255-272.

Staehelin, J.; Hoigné, J. Decomposition of ozone in water: rate of initiation by hydroxide ions and hydrogen peroxide. Environ. Sci. Technol. **1982**, 16, 676-681.

Stuart, M.; Lapworth, D.; Crane, E.; Hart, A. Review of risk from potential emerging contaminants in UK groundwater. Sci. Total Environ. **2012**, 416, 1-21.

Tasselli, F.; Cassano, A.; Drioli, E. Ultrafiltration of kiwifruit juice using modified poly(ether ether ketone) hollow fibre membranes. Sep. Purif. Technol. **2007**, 57, 94-102.

Taujale, S.; Zhang, H. Impact of interactions between metal oxides to oxidative reactivity of manganese dioxide. Environ. Sci. Tech. **2012**, 46, 2764-2771.

Thorsen, T. Concentration polarisation by natural organic matter (NOM) in NF and UF. J. Membr. Sci. **2004**, 233, 79-91.

Tijani J.O.; Fatoba O.O.; Petrik, L.F. A Review of pharmaceuticals and endocrine-disrupting compounds: sources, effects, removal, and detections. Water Air Soil Pollut. **2013**, 224, 1770, 1-29.

Tisch M.; Schmezer P.; Faulde M.; Groh A.; Maier H. Genotoxicity studies on permehtrin, DEET and diazinon in primary human nasal mucosal cells. Eur. Arch. Oto-rhino-l. **2002**, 259, 150-153.

Urtiaga; Ibáñez, R.; Ortiz, I.; Acero, J.L.; Teva, F.; Benítez, F.J. Tecnología de membranas: ultrafiltración, nanofiltración, ósmosis inversa. Tecnologías de tratamiento de agua para su reutilización. Programa Consolider Tragua. Cap. 7. **2010**.

USEPA Office of Pesticide Programs, Health Effects Division, Science Information Management Branch: Chemicals Evaluated for Carcinogenic Potential. **2006**.

USEPA., Office of Water, Guidance Manual. Alternative Disinfectantes and Oxidants 815-R-99-014. Cap. 8, 1-25. **1999**.

Vallejo, M.; Fresnedo San Román, M.; Ortiz, I.; Irabien, A. Overview of the PCDD/Fs degradation potential and formation risk in the application of advanced oxidation processes (AOPs) to wastewater treatment. Chemosphere **2015**, 118, 44-56.

van der Bruggen, B.; Everaert, K.; Wilms, D.; Vandecasteele, C. Application of nanofiltration for removal of pesticides, nitrate and hardness from ground water: rejection properties and economic evaluation. J. Membr. Sci. **2001**, 193, 239-248.

Vanneuville W.; Werner B.; Uhel R. Water resources in Europe in the context of vulnerability. EEA Report 11/**2012**.

von Gunten, U.; Hoigné, J. Ozonation of bromide-containing waters: bromate formation through ozone and hydroxyl radicals. In Roger A. Minear and Gary L. Disinfection by-products in water treatment. The chemistry of their formation and control. Ed. Lewis Publishers. **1996**.

von Sonntag, C.; Schuchmann, H.P. The Chemistry of free radicals: Peroxyl radicals in aqueous solutions. Ed. Z.B. Alfassi. **1997**.

Watkins, B.D.; Hengemuehle, S.M.; Person, H.L.; Yokoyama, M.T.; Masten, S.J. Ozonation of swine manure wastes to control odors and reduce the concentrations of pathogens and toxic fermentation metabolites. Ozone Sci. Eng. **1997**, 19, 425-437.

Weiss, S.; Jakobs, J.; Reemtsma, T. Discharge of three benzotriazole corrosion inhibitors with municipal wastewater and improvements by membrane bioreactor treatment and ozonation. Environ. Sci. Technol. **2006**, 40, 7193-7199.

Weiss, S.; Reemtsma, T. Membrane bioreactors for municipal wastewater treatment – A viable option to reduce the amount of polar pollutants discharged into surface waters? Water Res. **2008**, 42, 3837-3847.

Wert, E.C.; Gonzales, S.; Dong, M.M.; Rosario-Ortiz, F.L. Evaluation of enhanced coagulation pretreatment to improve ozone oxidation efficiency in wastewater. Water Res. **2011**, 45, 5191-519.

Wolschke, H.; Xie, Z.; Möller, A.; Sturm, R.; Ebinghaus, R. Occurrence, distribution and fluxes of benzotriazoles along the German large river basins into the North Sea. Water Res. **2011**, 45, 6259-6266.

Wu, J.; Pu, W.; Yang, C.; Zhang, M.; Zhang, J. Removal of benzotriazole by heterogeneous photoelectro-Fenton like process using $ZnFe_2O_4$ nanoparticles as catalyst. J. Environ. Sci. **2013**, 25, 801-807.

Wu, J.J.; Park, S.; Hengemuehle, S.M.; Yokoyama, M.T.; Person, H.L.; Gerrish, J.B.; Masten, S.J. The use of ozone to reduce the concentration of malodorous metabolites in swine manure slurry. J. Agric. Eng. Res. **1999**, 72,317-327.

Xu, B.; Wu, F.; Zhao, X.; Liao, H. Benzotriazole removal from water by Zn–Al–O binary metal oxide adsorbent: Behavior, kinetics and mechanism. J. Hazard. Mat. **2010**, 184, 147-155.

Xu, J.; Li, L.; Guo, C.; Zhang, Y.; Wang, S. Removal of benzotriazole from solution by BiOBr photocatalysis under simulated solar irradiation. Chem. Eng. J. **2013**, 221, 230-237.

Yan, Z.; Easterwood, L.M.; Maher, N., Torres, R.; Huebert, N.; Yost, G.S. Metabolism and bioactivation of 3-methylindole by human liver microsomes. Chem. Res. Tox. **2007**, 20, 140-148.

Yan, Z.; Yu Z.; Yu, J.; Yuan, H.; Yang, M. Identification of odorous compounds in reclaimed water using FPA combined with sensory GC-MS. J. Environ. Sci. **2011**, 23, 1600-1604.

Yang, B.; Ying, G.G.; Zhang, L.J.; Zhou, L.J.; Liu, S.; Fang, Y.X. Kinetics modeling and reaction mechanism of ferrate(VI) oxidation of benzotriazoles. Water Res. 45, **2011**, 2261-2269.

Yang, X.; Flowers, R.C.; Weinberg, H.S.; Singer, P.C. Occurrence and removal of pharmaceuticals and personal care products (PPCPs) in an advanced wastewater reclamation plant. Water Res. **2011**, 4, 5218-5228.

Yoon, Y.; Ryu, J.; Oh, J.; Choi, B-G.; Snyder, S.A. Occurrence of endocrine disrupting compounds, pharmaceuticals, and personal care products in the Han River (Seoul, South Korea). Sci. Total Environ. **2010**, 408, 636-643.

Yoon, Y.; Westerhoff, P.; Snyder, S.A.; Wert, E.C. Nanofiltration and ultrafiltration of endocrine disrupting compounds, pharmaceuticals and personal care products. J. Membr. Sci. **2006**, 270, 88-100.

Yu, J.T.; Bouwer, E.J.; Coelhan, M. Occurrence and biodegradability studies of selected pharmaceuticals and personal care products in sewage effluent. Agr. Water Manage. **2006**, 86, 16, 72-80.

Zhang, H.; Huang, C.H. Oxidative transformation of triclosan and chlorophene by manganese oxides. Environ. Sci. Tech. **2003**, 37, 2421-2430.

Zhang, H.; Lemley, A.T. Reaction mechanism and kinetic modeling of DEET degradation by flow-through anodic Fenton treatment (FAFT). Environ. Sci. Technol. **2006**, 40, 4488-4494.

Zhang, J.; Sun, B.; Xiong, X.; Gao, N.; Song, W.; Du, E.; Guan, X.; Zhou, G. Removal of emerging pollutants by Ru/TiO$_2$-catalyzed permanganate oxidation. Water Res. **2014**, 63, 262-270.

Zúñiga-Benítez, H.; Soltan, J.; Peñuela, G. Ultrasonic degradation of 1-H-benzotriazole in water. Water Sci. Techol. **2014**, 70, 152-159.

3. RESULTADOS Y DISCUSIÓN

3.1. Resumen.

Este Capítulo recoge los principales resultados obtenidos en el trabajo de investigación de esta Tesis Doctoral, el cual tiene como objetivo global el estudio de la eliminación de una selección de cinco contaminantes emergentes (benzotriazol, nortriptilina clorhidrato, N,N-dietil-m-toluamida (DEET), metilindol y clorofeno) presentes en diversas aguas, mediante procesos químicos y físicos típicamente empleados en el tratamiento de aguas, tanto residuales como superficiales. Entre los procesos químicos cabe destacar el empleo de diversos oxidantes químicos utilizados de forma individual, así como diversas combinaciones de los mismos en lo que constituyen los Procesos de Oxidación Avanzada (POAs). Por su parte, entre los procedimientos físicos se encuentra la adsorción sobre carbón activo en polvo (PAC) y la filtración mediante membranas. Finalmente se han aplicado diversas secuencias de tratamientos físicos y químicos con el objeto de alcanzar una elevada eliminación de los contaminantes. A continuación se describen brevemente los diversos procesos de tratamiento aplicados y los resultados obtenidos, los cuales han dado lugar a las publicaciones científicas que se muestran en los siguientes Capítulos de la Tesis Doctoral.

El primer agente empleado fue la radiación UVC, el cual resulta ser un proceso eficaz en la eliminación de contaminantes y además presenta un efecto germicida de interés en el tratamiento de aguas, por lo que en la actualidad está muy extendido su uso como desinfectante. Este estudio ha cristalizado en las dos publicaciones que se muestran en los Apartados 3.2 y 3.3 de la presente Memoria. En concreto, los cinco contaminantes emergentes seleccionados fueron degradados individualmente mediante radiación UVC (254 nm) en agua ultrapura a diferentes pH (3, 5, 7 y 9), utilizando una lámpara de vapor de mercurio a baja presión, en ausencia y presencia de terc-butanol. La aplicación del Modelo de Fuente Lineal de Emisión Esférica en los ensayos realizados en presencia de terc-butanol (que garantiza que la única vía de degradación significativa es la fotólisis directa) permitió la determinación de los valores de los rendimientos cuánticos para cada compuesto a 20 °C en el intervalo de pH 3-9, resultando ser: $(53.8-9.4)x10^{-3}$ mol E^{-1} para benzotriazol, $(525-469)x10^{-3}$ mol E^{-1} para clorofeno, $(2.8-0.9)x10^{-3}$ mol E^{-1} para DEET, $(108-165)x10^{-3}$ mol E^{-1} para metilindol y $(13.8-15.0)x10^{-3}$ mol E^{-1} para nortriptilina. De forma específica, los valores

obtenidos a pH 7 se muestran en la Tabla 1. Estos valores de rendimientos cuánticos permiten deducir el siguiente orden de reactividad: clorofeno > metilindol > benzotriazol > nortriptilina > DEET.

Además de los mencionados rendimientos cuánticos, en los experimentos de fotólisis se determinaron también las constantes de velocidad de primer orden, así como los niveles de degradación alcanzados para cada uno de los contaminantes emergentes en presencia y ausencia de terc-butanol a diferentes pH (3, 5, 7 y 9). Así, en presencia de este secuestrador de radicales, el orden de reactividad de los contaminantes coincide con el orden de los rendimientos cuánticos; sin embargo, cuando tiene lugar también la degradación por vía radicalaria, la secuencia de degradación cambia ligeramente (clorofeno > metilindol > nortriptilina > benzotriazol > DEET). La variación de pH no influyó significativamente en el valor de las constantes y la adición de diferentes concentraciones iniciales de H_2O_2, como cabría esperar, ejerció una influencia positiva en la eliminación de todos los contaminantes al favorecer la degradación por vía radicalaria, debido a la presencia de radicales hidroxilo procedentes de la fotólisis del H_2O_2.

Para finalizar el estudio de la aplicación de UVC en los contaminantes disueltos en agua ultrapura, se identificaron los intermedios de reacción formados en la fotólisis de cada compuesto a pH 7 mediante LC-QTOF-MS. Tal y como se detalla en el Apartado 3.2, se consiguieron identificar 2, 2, 4, 7 y 2 intermedios formados en la fotodegradación de benzotriazol, nortriptilina, DEET, metilindol y clorofeno, respectivamente. También se evaluó la evolución de la toxicidad mediante inhibición de la bacteria *Vibrio fischeri*, encontrándose un aumento inicial de la toxicidad para luego disminuir, a excepción del caso de nortriptilina clorhidrato, cuya fotodegradación aumentó la toxicidad de forma continua a lo largo del proceso.

Por otro lado, se llevaron a cabo experimentos con reactivo de Fenton con el objeto de determinar la constante de velocidad de segundo orden para la reacción directa entre cada uno de los ECs seleccionados y los radicales hidroxilo (k_{OH}). Para ello se utilizó un método competitivo, empleando p-CBA como compuesto de referencia, a pH 3 y con dos concentraciones iniciales de H_2O_2 diferentes. Los resultados detallados de este este estudio

se encuentran en la publicación mostrada en el Apartado 3.3, y los valores obtenidos para la constante de reacción de los ECs con los radicales OH aparecen también recogidos en la Tabla 1.

Tabla 1. Rendimientos cuánticos y constantes de reacción con radicales hidroxilo, cloro, bromo y ozono de los contaminantes emergentes seleccionados (T=20 °C y pH=7).

EC	$\phi \cdot 10^3$ (mol E^{-1})	$k_{OH} \times 10^{-9}$ (M^{-1}s^{-1})	$k_{app\ Cl}$ (M^{-1}s^{-1})	$k_{app\ Br}$ (M^{-1}s^{-1})	$k_{app\ O3}$ (M^{-1}s^{-1})
BZ	29.4	8.24 ± 0.04	0.15 ± 0.01	8.50 ± 0.33	79.6
CP	429	8.47 ± 0.19	38.8 ± 1.0	193 ± 16	3.12×10^3
DT	1.2	7.51 ± 0.07	$(13.6 \pm 1.7) \times 10^{-4}$	0.09 ± 0.02	0.126
ML	105	5.57 ± 0.53	$(5.75 \pm 0.52) \times 10^3$	$(109 \pm 11) \times 10^6$	5.34×10^5
NH	13.6	10.87 ± 0.08	0.40 ± 0.06	7.42 ± 0.25	2.73×10^3

En la siguiente etapa se llevaron a cabo experimentos con los compuestos modelo presentes en tres aguas reales diferentes (un agua superficial de pantano y dos efluentes secundarios procedentes de las EDAR de La Albuera y de Badajoz) para evaluar el efecto de la presencia en mayor o menor medida de materia orgánica sobre los niveles de degradación. Los resultados obtenidos están detallados en el Apartado 3.3. En concordancia con el contenido en materia orgánica, se alcanzó una eliminación similar en las dos primeras matrices acuosas (agua de pantano y efluente de La Albuera) y se consiguió una menor degradación al emplear el efluente secundario de la EDAR de Badajoz. La propuesta de un modelo cinético para predecir la eliminación de los contaminantes emergentes en cualquiera de las matrices acuosas proporcionó resultados que coincidían satisfactoriamente con los valores experimentales obtenidos. Estos resultados permiten deducir que en aguas reales el proceso de fotodegradación alcanza una eficacia elevada para la eliminación de los contaminantes nortriptilina, clorofeno y metilindol, moderada para benzotriazol y baja para DEET. Al mismo tiempo, la aplicación de radiación UVC no permite conseguir un alto grado de mineralización de la materia orgánica presente en las aguas, por lo que se decidió investigar la eficacia de otros agentes oxidantes.

El siguiente proceso desarrollado fue la cloración, tratamiento ampliamente aplicado en la desinfección de agua potable y de efluentes secundarios procedentes de EDAR. Los resultados obtenidos se encuentran ampliamente explicados en el Apartado 3.4. En primer lugar, se llevaron a cabo ensayos de reacción entre cloro y cada contaminante emergente en el intervalo de pH 3-11 en agua ultrapura. Se determinaron las constantes aparentes de velocidad de segundo orden, encontrándose una fuerte dependencia del proceso con el cambio de pH. Los valores obtenidos de las constantes aparentes a pH 7 se muestran igualmente en la Tabla 1, cumpliéndose la secuencia de reactividad DEET < benzotriazol < nortriptilina < clorofeno < metilindol. Además de estas constantes aparentes, se evaluaron las constantes específicas de velocidad para las reacciones intrínsecas entre HOCl y las especies iónicas de cada contaminante emergente. Para ello se propuso un modelo cinético que tenía en cuenta tanto las constantes aparentes como los equilibrios de disociación de cada contaminante y del cloro. La bondad del modelo quedó corroborada al encontrarse una satisfactoria concordancia entre los valores experimentales de dichas constantes aparentes y los valores teóricos calculados a partir de las propias constantes específicas.

Dado que una baja concentración de bromuro presente en el agua puede mejorar el rendimiento del proceso de cloración debido a la formación de bromo, y este oxidante ha resultado efectivo en la eliminación de ECs, igualmente se evaluaron las constantes aparentes de velocidad de segundo orden para la reacción de cada contaminante emergente con bromo en el rango de pH 7-9. Si bien los valores resultantes para las constantes aparentes de bromación se encuentran detallados en el Apartado 3.4, a modo de resumen los resultados obtenidos para las mismas a pH 7 se muestran asimismo en la Tabla 1. La secuencia de reactividad coincide con la del proceso de cloración, aunque las constantes presentan valores más elevados, lo cual pone de manifiesto el mayor poder oxidante del bromo.

Para completar el estudio de este proceso de oxidación, se llevaron a cabo varios experimentos de cloración simultánea de los contaminantes emergentes en aguas reales. Como cabría esperar, una mayor dosis inicial de cloro da lugar a una mayor eliminación de contaminantes y, al mismo tiempo, mayor formación de trihalometanos, cuya

concentración en ningún caso excedió el límite legal de la UE (100 µg L^{-1}). La formación de cloraminas fue consonante al contenido de amonio de las diferentes matrices acuosas empleadas, siendo significativa en el efluente procedente de la EDAR de Badajoz. La secuencia de reactividad coincidió con la establecida previamente en agua ultrapura. En cuanto a la influencia de la matriz acuosa empleada, se consiguió mayor eliminación en el efluente secundario de la EDAR de La Albuera, menor cuando se empleó agua de pantano y aún menor al emplear el efluente de la EDAR de Badajoz, lo cual está en concordancia con el contenido en materia orgánica presente en cada una de estas aguas. La elevada eliminación alcanzada en el efluente de la EDAR de La Albuera se atribuye en parte a la presencia natural de una baja concentración de bromuro, lo cual favorece la degradación de los contaminantes.

Para corroborar la influencia de la presencia del ión bromuro, se realizaron experimentos de cloración de los contaminantes en las aguas reales mencionadas y en presencia de diferentes dosis de bromuro (0-3.75 µM). La degradación alcanzada fue mayor al aumentar la dosis de bromuro, lo cual pone de manifiesto la formación de bromo que reacciona con los contaminantes con mayor velocidad que el cloro. Finalmente, a partir de las constantes de cloración aparentes determinadas se propuso un modelo cinético que permitió simular la degradación de los contaminantes estudiados en las diferentes matrices acuosas empleadas, obteniéndose una gran concordancia entre los perfiles teóricos y experimentales de la evolución de concentración de contaminantes. Este hecho confirma que las constantes cinéticas aparentes determinadas en agua ultrapura pueden ser empleadas para predecir la eliminación de los contaminantes durante la cloración de aguas reales. Finalmente, se concluye a partir de los resultados obtenidos que el proceso de cloración es una buena opción para la eliminación de metilindol y en menor medida para clorofeno y nortriptilina, pero no es un proceso adecuado para la degradación de benzotriazol y DEET.

El ozono es un agente oxidante altamente eficaz para la eliminación de numerosos microcontaminantes, motivo por el cual también fue seleccionado en este trabajo de Tesis Doctoral. Se llevó a cabo un amplio estudio de ozonación de los contaminantes seleccionados que dio lugar a las publicaciones que se muestran en los Apartados 3.5

(clorofeno), 3.6 (DEET y nortriptilina) y 3.7 (benzotriazol y metilindol). En primer lugar se llevó a cabo la ozonación individual de cada contaminante en agua ultrapura y en presencia de terc-butanol en condiciones homogéneas, con el objetivo de determinar las constantes cinéticas aparentes de reacción directa entre el ozono y cada compuesto para cada pH, así como las constantes de velocidad específicas de la especie disociada y no disociada de aquellos compuestos que presentan constante de disociación en el rango de pH estudiado (benzotriazol, nortriptilina y clorofeno). Los resultados obtenidos para estas constantes de reacción a pH 7 y 20°C se muestran de igual forma en la Tabla 1. De la observación de estos valores se deduce que la ozonación es un proceso adecuado para la eliminación de metilindol, clorofeno y nortriptilina, y en menor medida benzotriazol, no siendo adecuado para la eliminación de DEET.

Un segundo grupo de experimentos consistió en la ozonación individual de cada contaminante emergente disuelto en agua ultrapura, y en ausencia de terc-butanol, empleando altas concentraciones tanto del contaminante como de ozono en régimen heterogéneo, con el objeto de determinar la toxicidad y de identificar los intermedios de reacción. En cuanto a la evolución de la toxicidad, se encontraron diferentes comportamientos según el compuesto estudiado: en el caso de nortriptilina y clorofeno la toxicidad disminuyó un 75% y 50%, respectivamente; para metilindol y benzotriazol no se apreció variación significativa de la toxicidad con el transcurso de la ozonación; y en el caso de DEET la toxicidad aumentó con el tiempo de reacción.

Los intermedios de reacción fueron analizados mediante LC-TOF-MS. La identificación se realizó limitando el tipo de átomos presentes a los del compuesto de partida, el agente oxidante empleado y el medio de reacción. Además, se estudió la presencia de patrones isotópicos característicos y se tuvo en cuenta el parámetro DBE (dobles enlaces equivalentes) y la presencia de iones fragmento e iones diagnóstico para la propuesta de estructuras moleculares. Siguiendo este procedimiento, para benzotriazol se identificaron 6 intermedios de reacción, todos ellos de abundancia relativa mucho menor que el compuesto de partida, siendo el más abundante el correspondiente a benzotriazol trihidroxilado. Para nortriptilina clorhidrato y DEET, 27 y 14 subproductos fueron identificados respectivamente, siendo el intermedio más relevante en términos de

abundancia relativa en ambos casos la especie monohidroxilada. En el caso de metilindol y clorofeno, 8 y 24 subproductos fueron identificados, siendo C_8H_9NO (m/z 136.0757) y $C_{12}H_7ClO_{10}$ (m/z 344.9639), respectivamente, los subproductos más importantes en términos de abundancia relativa. En base a los intermedios identificados para cada compuesto, se propusieron los correspondientes mecanismos de reacción que se detallan en los mencionados Apartados 3.5, 3.6 Y 3.7.

Finalmente, de forma menos exhaustiva y con fines comparativos en términos de eficacia de degradación, se aplicaron varios sistemas de oxidación (principalmente Procesos de Oxidación Avanzada) para eliminar los contaminantes emergentes seleccionados en agua ultrapura y en aguas reales (pantano y dos efluentes secundarios de la EDAR Badajoz y La Albuera). Este estudio comparativo generó la publicación que se muestra en el Apartado 3.8, en la cual se comentan de forma detallada los resultados obtenidos. En concreto, los procesos estudiados fueron la radiación UV, reactivo de Fenton, sistema Fenton-like, ozono, así como diversas combinaciones de los agentes anteriores tales como O_3/H_2O_2, UV/H_2O_2, $O_3/UV/H_2O_2$, O_3/UV, UV/TiO_2, O_3/TiO_2, $UV/S_2O_8^{2-}$, $UV/Fe^{2+}/H_2O_2$, $UV/Fe^{3+}/H_2O_2$ y $O_3/TiO_2/UV$. Para cada sistema de oxidación se determinaron las constantes de reacción de primer orden y el tiempo de vida medio, tanto en agua ultrapura como en las matrices reales empleadas. En general, los resultados más favorables se obtuvieron al aplicar POAs, lográndose mayores niveles de degradación que con los oxidantes individuales, como cabría esperar. En concreto, en las condiciones experimentales empleadas (pH 3 y 20°C) los procesos de oxidación avanzada UV/TiO_2, $UV/S_2O_8^{2-}$, $O_3/UV/H_2O_2$ y el sistema foto-Fenton mostraron las tasas más altas de eliminación de los compuestos seleccionados y las mayores velocidades de degradación, debido a la contribución de diversas reacciones directas y radicalarias que incluso presentan un efecto sinérgico.

De forma general, y a partir de los valores de constantes cinéticas expuestos en la Tabla 1, puede establecerse que el radical hidroxilo no reacciona selectivamente con los compuestos orgánicos, pues todos los valores oscilan en el rango $(5-10)x10^9$ M^{-1} s^{-1}. Sin embargo, ozono, cloro y bromo sí son agentes oxidantes selectivos, y sus valores de contantes cinéticas con diferentes grupos orgánicos oscilan en varios órdenes de magnitud. Estos oxidantes con carácter electrofílico, que reaccionan preferentemente con

compuestos insaturados, compuestos aromáticos activados y con aminas orgánicas, presentan el siguiente orden de poder oxidante con los contaminantes emergentes seleccionados: ozono > bromo > cloro.

Una vez estudiados diversos procesos de oxidación química para la eliminación de los compuestos seleccionados, se inició un estudio basado en la aplicación de tecnologías de membrana, específicamente ultrafiltración (UF) y nanofiltración (NF). Los principales objetivos planteados fueron la evaluación tanto del flujo de permeado y ensuciamiento de las membranas como la determinación de los coeficientes de retención de los contaminantes. Con esta información obtenida se propusieron a continuación los mecanismos de ensuciamiento de la membrana y de la propia retención de los contaminantes.

En primer lugar se empleó un equipo de filtración mediante membrana de laboratorio que operaba en modo concentración y flujo transversal, y se realizó un estudio centrado en la evaluación de la influencia de algunas variables de operación (naturaleza y MWCO (tamaño de corte de peso molecular) de las membranas, pH, presencia de materia orgánica y Ca^{2+}) sobre el flujo de permeado y la retención de los compuestos seleccionados. Para ello, se emplearon diferentes matrices acuosas (agua ultrapura, agua sintética, agua superficial y dos efluentes secundarios procedentes de la EDAR Badajoz y La Albuera) y diferentes membranas: tres membranas de ultrafiltración (PW, PT y GK, con un MWCO de 20000, 5000 y 2000 Da, respectivamente); y tres membranas de nanofiltración (DK, CK y HL, con un MWCO en el rango 150-300 Da). Los resultados obtenidos en este estudio se recogen y discuten de forma detallada en la publicación que se muestra en el Apartado 3.9.

Aunque las membranas de UF presentaban un MWCO muy superior al tamaño de los contaminantes estudiados, todos ellos fueron retenidos en mayor o menor medida, alcanzando retenciones superiores al 70% en el caso de clorofeno y metilindol. Este hecho sugiere que el principal mecanismo de retención en estas membranas de UF es la adsorción, siendo la secuencia de retención: clorofeno > metilindol > nortriptilina > DEET > benzotriazol. Entre las membranas de ultrafiltración empleadas, la más eficaz fue la membrana PT (5 kDa). Por su parte, en el proceso de NF imperan como mecanismos de

retención la exclusión por tamaño y la repulsión electrostática de especies negativas a elevados valores de pH, siendo la secuencia de retención similar a la obtenida en UF: clorofeno > nortriptilina > metilindol > DEET > benzotriazol. Entre las membranas de NF empleadas, la más eficaz fue la membrana HL, pues dio como resultado los valores más elevados tanto de retención de contaminantes como de flujo de permeado. En cuanto al mecanismo de ensuciamiento de las membranas, se propuso que el bloqueo de poros y la formación de una capa de torta sobre la superficie de la membrana eran responsables del rápido ensuciamiento al inicio de los experimentos, y que únicamente la formación continuada de torta era la causante del ensuciamiento posterior.

Por otra parte, la presencia de materia orgánica natural incrementó la retención de los compuestos, probablemente debido a la interacción de estos con los ácidos húmicos. Sin embargo, la presencia adicional de iones de calcio disminuyó la retención de contaminantes, lo cual puede deberse a la interacción de estos iones con los ácidos húmicos, que a su vez dificulta la interacción entre ácidos húmicos y contaminantes. Además, la presencia conjunta de NOM y de iones calcio aumentó considerablemente el ensuciamiento de las membranas debido a la formación de la capa de torta, pues el ensuciamiento era principalmente de carácter externo y reversible. Con respecto a la eliminación de contaminantes en aguas reales, las membranas seleccionadas PT y HL, para ultrafiltración y nanofiltración respectivamente, lograron eliminaciones superiores al 80% para clorofeno, metilindol y nortriptilina en ambos procesos y en las tres matrices acuosas empleadas. Bajo el punto de vista tanto de los coeficientes de retención como de eliminación de NOM, la membrana de nanofiltración HL resultó ser la más eficiente entre las empleadas, siendo capaz de retener los tres compuestos anteriores con rendimientos superiores al 85%; y de DEET alrededor del 80%, si bien para benzotriazol se obtuvo un bajo coeficiente de retención (eliminación en torno al 25%). Asimismo, la membrana HL dio como resultado reducciones de materia orgánica elevadas, pues se consiguió eliminar DQO y TOC en un 80%, y absorbancia a 254nm en un 90%, por lo que es una membrana muy adecuada en la depuración de efluentes secundarios para su reutilización, así como en el tratamiento de aguas superficiales para su potabilización.

En segundo lugar, se empleó un módulo de ultrafiltración con una membrana de fibra hueca para llevar a cabo el estudio de la aplicación del proceso híbrido adsorción mediante carbón activado/ultrafiltración (PAC/UF) con el objeto de eliminar la NOM y los cinco contaminantes emergentes seleccionados en diferentes matrices acuosas procedentes del efluente secundario de la EDAR de Beirolas (Lisboa). Estos experimentos fueron realizados en el UQTA (Unidad de Calidad y Tratamiento de Aguas) del Laboratorio Nacional de Ingeniería Civil (LNEC, Lisboa, Portugal), y se incluyen en la publicación en preparación que se muestra en el Apartado 3.10. Se estudió la eliminación simultánea de los contaminantes emergentes en tres matrices acuosas mediante dos carbones activos en polvo (PAC) diferentes (SA Super y SAE Super) y con distintas dosis (3, 5, 7, 10 y 15 ppm). Ambos PAC, con volumen de mesoporos similar, apenas mostraron diferencia en cuanto a la cinética de adsorción de contaminantes, aunque sí mostraron diferencias en la adsorción de NOM hidrófoba. La secuencia de adsorción de los contaminantes emergentes obtenida con ambos PAC fue: benzotriazol < DEET < metilindol < nortriptilina < clorofeno, que se corresponde con el carácter hidrofóbico y aromaticidad de las sustancias estudiadas.

Una vez seleccionado el PAC más eficaz (SA Super) y la dosis más apropiada (10 ppm), se llevaron a cabo experimentos PAC/UF con las diferentes aguas de estudio en ausencia y presencia de contaminantes emergentes. Se comprobó que la adición de PAC no afectaba significativamente al flujo de permeado en las tres matrices acuosas empleadas, a pesar de las características diferentes de la materia orgánica presente (tamaño, hidrofobicidad). En general, el proceso híbrido PAC/UF resultó ser una gran opción para la eliminación de clorofeno, nortriptilina y metilindol (eliminación superior al 95%), pero no fue tan eficaz para la eliminación de benzotriazol y DEET (eliminación en torno al 60%).

Con el fin de mejorar la eliminación de los contaminantes, la última parte de este trabajo de Tesis Doctoral se centró en la investigación de varios procesos secuenciales físico-químicos, cuyo objetivo principal fue establecer la influencia de las etapas previas sobre los procesos posteriores, teniendo en cuenta la eficiencia de cada etapa y los niveles de purificación alcanzados en el efluente final. Estos ensayos se realizaron en diferentes matrices acuosas (agua superficial y dos efluentes secundarios). Los resultados obtenidos

en este estudio han dado lugar a la publicación que se muestra en el Apartado 3.11, en la que se detallan y discuten todos los resultados obtenidos.

En primer lugar, se llevó a cabo un pretratamiento mediante membranas de ultrafiltración (PT) y nanofiltración (HL), y tanto el permeado como el retenido resultantes fueron sometidos posteriormente a un tratamiento de oxidación química con ozono o cloro. Cuando se emplearon membranas de NF, el permeado, tras ser sometido a oxidación química, proporcionó un efluente exento de contaminantes emergentes, excepto en el caso de benzotriazol, para el cual se alcanzó una eliminación entre 30-68% dependiendo de la matriz acuosa empleada. Por su parte, en el proceso secuencial constituido por una etapa de UF seguida de oxidación química del permeado se logró la eliminación total de nortriptilina, metilindol y clorofeno, pero no de benzotriazol y DEET (eliminaciones en el rango 35-63%). La reducción de TOC en estos procesos secuenciales fue superior al 50% en el caso de pretratamiento mediante UF y superior al 70% en el caso de pretratamiento con NF. Como se ha comentado, los retenidos obtenidos en las etapas previas de UF y NF fueron sometidos asimismo a una etapa de oxidación química. En este caso, y debido a su elevada carga contaminante, se aplicó una dosis de oxidante mayor que en el tratamiento de los permeados, y se obtuvo como resultado la eliminación total de metilindol y clorofeno (salvo en la cloración del retenido procedente de la NF del efluente de EDAR Badajoz); y retenciones entre el 2-85%, 10-100% y 1-56% para benzotriazol, nortriptilina y DEET, respectivamente, dependiendo de las variables operativas utilizadas. Por lo tanto, una etapa de oxidación química, especialmente mediante ozono, puede conducir a una eliminación importante de los contaminantes emergentes presentes en el retenido procedente de la filtración mediante membranas. Como consecuencia, la aplicación de esta etapa de ozonación final del retenido soluciona satisfactoriamente el problema que origina su evacuación. En el caso particular de la aplicación del proceso secuencial filtración/oxidación en la depuración de efluentes secundarios, la ozonación del retenido conduciría a un efluente prácticamente exento de contaminantes emergentes que se podría recircular a la etapa de tratamiento secundario, evitándose así su descarga a cauces públicos.

En segundo lugar se investigó la secuencia inversa, aplicando un pretratamiento de oxidación química mediante el uso de ozono, cloro, O_3/H_2O_2, radiación UV o UV/H_2O_2 seguido de una etapa de nanofiltración con la membrana HL. En estos tratamientos secuenciales, la eliminación global de contaminantes emergentes fue superior al 97% para DEET, clorofeno, metilindol y nortriptilina, mientras que se obtuvieron valores inferiores para benzotriazol (en el rango 29-95%), especialmente en aquellas matrices acuosas con mayor contenido en materia orgánica. También se obtuvo una reducción importante de la materia orgánica presente en el permeado final, superior al 70% expresada como TOC, lo cual permite su reutilización. Al mismo tiempo, el retenido final presenta mejor calidad y mayor biodegradabilidad que el retenido obtenido en la filtración simple, por lo que requiere un tratamiento final más suave antes de proceder a su vertido.

En conclusión, ambas secuencias de procesos físico-químicos resultaron ser tecnologías adecuadas para eliminar los contaminantes emergentes presentes en diferentes matrices acuosas, y generar efluentes finales que pueden ser reutilizados en diferentes usos. Bien es cierto que, ante un problema real y concreto de tratamiento de agua, habría que elucidar cuál sería la secuencia más adecuada para resolverlo, teniendo en cuenta no solamente factores tecnológicos como los desarrollados en este trabajo, sino también factores económicos.

A la vista de todas las reactividades comentadas que presentan los contaminantes emergentes seleccionados con los diversos agentes oxidantes empleados, y de su retención con las diferentes membranas utilizadas, así como los carbones activados ensayados, se puede concluir de forma muy general que metilindol, clorofeno y nortriptilina se pueden eliminar de diferentes matrices acuosas mediante procesos químicos o físicos individuales. Sin embargo, para una eliminación eficaz de benzotriazol y DEET resultaría necesaria la aplicación de los procesos secuenciales aplicados en la última fase del presente trabajo.

3.2. Photolysis of model emerging contaminants in ultra-pure water: kinetics, by-products formation and degradation pathways.

3.2. PHOTOLYSIS OF MODEL EMERGING CONTAMINANTS IN ULTRA-PURE WATER: KINETICS, BY-PRODUCTS FORMATION AND DEGRADATION PATHWAYS

F. Javier Benítez, Juan L. Acero, Francisco J. Real, Gloria Roldan, Elena Rodríguez.

Departamento de Ingeniería Química, Universidad de Extremadura, Badajoz.

The photolysis of five frequent emerging contaminants (benzotriazole, chlorophene, N,N-diethyl-m-toluamide or DEET, methylindole, and nortriptyline hidrochloride) was investigated in ultrapure water under monochromatic ultraviolet radiation at 254 nm and by a combination of UV and hydrogen peroxide. The results revealed that the photolysis rates followed first-order kinetics, with rate constant values depending on the nature of the specific compound, the pH, and the presence or absence of the scavenger tert-butanol. Quantum yields were also determined and values in the range of 53.8×10^{-3} - 9.4×10^{-3} mol E^{-1} for benzotriazole, 525×10^{-3} - 469×10^{-3} mol E^{-1} for chlorophene, 2.8×10^{-3} - 0.9×10^{-3} mol E^{-1} for DEET, 108×10^{-3} - 165×10^{-3} mol E^{-1} for methylindole, and 13.8×10^{-3} - 15.0×10^{-3} mol E^{-1} for nortriptyline were obtained. The study also found that the UV/H_2O_2 process enhanced the oxidation rate in comparison to direct photolysis. High-performance liquid chromatography coupled to electrospray ionization quadrupole time-of-flight mass spectrometry (HPLC-ESI-QTOF-MS) technique was applied to the concentrations evaluation and further identification of the parent compounds and their by-products, which allowed the proposal of the degradation pathways for each compound. Finally, in order to assess the aquatic toxicity in the photodegradation of these compounds, the *V. fischeri* acute toxicity test was used, and the results indicated an initial increase of this parameter in all cases, followed by a decrease in the specific case of benzotriazole, DEET, methylindole, and chlorophene.

1. INTRODUCTION.

The so-called emerging contaminants (ECs) is a wide group of numerous chemical substances, that includes prescription and therapeutic drugs (pharmaceuticals), veterinary drugs, dietary supplements, consumer products such as fragrances, topical agents such as cosmetics and sunscreens (personal care products), laundry and cleaning products, flame retardants, corrosion inhibitors, etc. Once they are consumed by humans for personal health or cosmetic reasons, and also, by agribusiness to enhance growth or health of livestock, they are incorporated into the water environment in a variety of ways. Their presence in water effluents is mainly attributed to their incomplete removal through conventional methods in wastewater treatment plants (Suarez et al., 2008), and consequently, these compounds are increasingly found in water systems (Nakada et al., 2007), affecting the quality of drinking water supplies (Heberer, 2002). Therefore, a public health concern has recently increased in relation to this problem, since little is known about potential effects of these substances in humans and animals; their elimination from waters, together with other priority pollutants, is an emerging issue in environmental technology.

This elimination can be achieved by appropriate physical or chemical methods. One of the chemical techniques is the photodegradation process, based on UV radiation, which is very effective in advanced water treatment technologies for groundwater and drinking water remediation (Legrini et al., 1993). Mercury vapor lamps emitting at 254 nm are the most common sources used for photolysis processes, alone or combined with hydrogen peroxide. This UV/H_2O_2 combination is characterized by the generation of hydroxyl radicals which can oxidize organic compounds more effectively.

The present work was designed to study the photodegradation by UV radiation alone and UV radiation combined with H_2O_2 of five model ECs, selected because of their frequent presence in water systems. They were: benzotriazole (BZ), a corrosion inhibitor for copper or silver material, widely used in cooling and hydraulic fluids, antifreezing products and anti-icer fluid, and as dishwasher detergent, with large amounts detected in municipal WWTPs via household wastewater or indirect discharge from industry (Loos et al., 2009). N,N-diethyl-m-toluamide or DEET (DT), that constitutes an active compound in insect

repellents, and is used for protection against insect bites, the presence of which has been reported in various aquatic environments (Costanzo et al., 2007). Chlorophene (CF), a widespread broad-spectrum antimicrobial pharmaceutical, commonly used in hospitals and households for general cleaning and disinfecting, as well as in industrial and farming environments as an active agent in disinfectant formulations (Boehmer et al., 2004). Methylindole (ML), with potential application as perfume and for the synthesis of anti-inflammatory drug, antibiotic, dye, plant growth hormone, herbicide, antidiuretic, stimulant antihypertensive, muscular relaxant, respiratory inhibitor and heart stimulant medicaments (Wenhui et al., 2009). And finally, nortriptyline (NH), a tricyclic antidepressant still used in treatments against depression, that has been detected at high concentrations in WWTP effluents (Langford and Thomas, 2009).

The main objectives pursued in this research were to conduct a broad kinetic study of the photodegradation of these substances in ultra-pure water, by UV radiation alone and combined with H_2O_2, with the aim of determining the rate constants and quantum yields; to identify some of the by-products formed for each compound during the photolytic process, and to propose the degradation pathways in accordance to these by-products. Toxicity measurements are also included, which allowed the assessment of the evolution of the toxicity of the reaction mixtures through the photodegradation process for the five selected ECs.

2. MATERIALS AND METHODS.

2.1. Chemicals and reagents.

The selected ECs of the highest purity available (99%) were purchased from Sigma-Aldrich (Germany). The chemicals used for the solutions (hydrogen peroxide, eluents and buffers) were of reagent grade, also from Sigma-Aldrich. For toxicity measurements, freeze-dried bacteria, reconstitution solutions, diluents (2% NaCl) and osmotic adjusting solution (22% sodium chloride) were obtained from Strategic Diagnostics Inc (USA). Ultra pure water for preparing the EC working solutions was obtained from a Milli-Q System (Waters, Millipore) with a specific resistance of 18 MΩ·cm. Organic solvents and other chemicals

used in the analysis, either HPLC or analytical grade, were supplied from Merck (Germany), selected ECs of the highest purity available (99%) were purchased from Sigma-Aldrich, and all of the other chemicals used for the solutions (hydrogen peroxide, p-chlorobenzoic acid, ferrous salts, eluents, buffers, etc.) were of reagent grade.

2.2. Photolysis experiments.

The irradiation experiments of the selected ECs were carried out in a 500 cm^3 cylindrical glass reactor. The radiation source, placed axially within the reactor and covered by a quartz sleeve, was a low pressure mercury vapor lamp (Hanau TNN 15/32) with an electrical power of 15 W. This lamp emitted a monochromatic radiation at 254 nm. Previous chemical actinometry experiments, using hydrogen peroxide as actinometer (Nicole et al., 1990), were conducted to determine the radiation intensity I_0 emitted by the lamp into the reactor, and the value obtained was 1.73×10^{-6} E s^{-1}. The reactor was filled with 350 cm^3 of an aqueous solution of each one of the selected compounds (1×10^{-6} M) and thermostated at the desired temperature of 20 °C. In order to attain the required pH (in the range 3-9), the solutions were previously buffered with a phosphoric acid/phosphate buffer (10 mM). The radical scavenger effect of this low buffer concentration is not appreciable.

The experiments started when the lamp was connected, and during each experiment, samples were withdrawn at regular times for assay. In some experiments, tert-butanol (t-BuOH, 0.01 M) was added as radical scavenger. Similar UV photolysis experiments were performed at pH 7 for toxicity analysis. In the combined UV/H_2O_2 system, the amounts of H_2O_2 required to reach the desired initial concentrations (1×10^{-5} and 5×10^{-5} M) were initially added to the EC solutions. At regular times, 2 mL samples were withdrawn and rapidly transferred to HPLC vials containing 10 μL of sodium thiosulfate (0.1 M) to stop the reaction. Finally, in the single UV photolysis experiments with the purpose of indentifying the degradation by-products ([EC]$_0$=1×10^{-5} M, without buffering), samples were taken at regular times from the batch reactor, and were analyzed by HPLC-QTOF-MS.

2.3. Analytical Methods.

Analysis of ECs

In the photolysis experiments conducted for the kinetic study, the concentration of ECs in each sample was determined by HPLC, using a Waters Chromatograph equipped with a 996 Photodiode Array Detector and a Phenomenex Gemini C18 Column (5μm, 150mm×3mm). The analysis was performed in gradient mode with acetonitrile as mobile-phase A and 25 mM formic acid as mobile-phase B, at a flow rate of 0.2 mL min^{-1} and at a column temperature of 20 °C. Each run started with an initial mobile-phase composition of 10% A, which was linearly increased to 30% A in 3 min, followed by another linear gradient to 40% A in 5 min, to 70% A in 4 min and 90% A in 5 min. Finally, the mobile-phase composition was maintained at 90% A for 5min. A 5 min post-run time back to the initial mobile-phase composition was used after each analysis. The volume of injection was 100 μL in all cases. Detection was made at 250 nm for BZ, NH, and DT; and at 280 nm for ML and CF.

Photolysis products identification

A liquid chromatography - electrospray ionization – quadrupole - time of flight mass spectrometer (HPLC-ESI-QTOF-MS) was used in the photodegradation experiments conducted for the identification of the target compounds and the by-products formed. Ion Max Electrospray Ionization (ESI) was applied in the negative ionization mode to the acidic compound CF; on the contrary, positive ionization mode was used for the four remaining basic compounds. The separation of the analytes was performed by using a HPLC system (Agilent Technologies 1200 Series) in gradient mode, also with acetonitrile as mobile-phase A and 25 mM formic acid as mobile-phase B at a flow rate of 0.2 mL min^{-1}. The column used to separate the analytes was the same described in the HPLC analysis. For the analysis in positive mode, the optimized chromatographic method was exactly the same as described in previous Section (Analysis of ECs). Slight differences were introduced in negative mode LC gradient, which remained with 30% A for 5 min, was increased to 90% in 4 min, and finally, was maintained for 2 min. The volume of injection was again 100 μL.

This HPLC system was connected to a quadrupole-time-of-flight mass spectrometer (Agilent Technologies 6520, Accurate-Mass Q-TOF LC/MS) equipped with a dual ESI electrospray interface with the following conditions: capillary 3500 V; nebulizer, 30 psi; gas flow, 5 L min^{-1}; gas temperature 300 ^{o}C; skimmer voltage, 65 V; octapole rf, 750 V; fragmentor, 100 V. The mass axis was calibrated by using the mixture provided by the manufacturer, over the *m/z* 50-3200 range. A second orthogonal sprayer with a reference solution was used as a continuous calibration in positive ion mode, by using the following reference masses: 121.0509 and 922.0098 *m/z*. With the electrospray source in negative ion mode, reference masses were 119.036 320 and 966.000 725 *m/z,* as proposed by Martinez Bueno et al. (2007). The full-scan accurate mass spectra were processed by using the Agilent Mass Hunter Qualitative Analysis B.04.00 software. After following this protocol, possible degradation by-products were recognized by full scan chromatograms; and for the postulation of these by-products several tools were taken into account: some specific known reactions of UV radiation with the selected ECs described in literature, other general oxidation reactions of organic compounds*,* exact masses, abundances and retention times.

Toxicity tests

Toxicity of unirradiated ECs solutions, as well as of several samples collected after different irradiation times (at 15, 30 and 90 min) were assayed by Microtox Model 500 Toxicity Analyzer, which measures the ability of solutions to inhibit the bioluminescence of the bacterium *V. fischeri*. These assays are based on the decay of the light emitted by the bacterium when exposed to toxic chemical compounds. The luminescence was recorded after 30 min of incubation at room temperature (20 °C) and the percentage of inhibition was calculated by following the established protocol by the equipment manufacturer (Microtox, 1992).

3. RESULTS AND DISCUSSION.

3.1. Photodegradation of individual ECs in ultra-pure water by UV radiation and UV/H₂O₂

Single UV radiation treatment.

The selected ECs were subjected to individual photolysis in ultra-pure water at 20 °C by varying the pH and with the absence and presence of 0.01 M t-BuOH. Table 1 compiles the experiments performed with the specification of the pH used. In a first step, the role of t-BuOH is discussed. As is well known, this substance is a scavenger of hydroxyl radicals (Staehelin and Hoigne, 1985), and direct photolysis is expected to be the only significant pathway for the photodegradation process when t-BuOH is present in the reaction. Figure 1 presents the decay curves against reaction time for BZ (taken as example) in these single photolysis experiments, with similar plots for the remaining substances. It can be observed that for a specific pH, the degradation curves in the experiments with t-BuOH (solid lines) present lower degradation rate than those without this radical scavenger (dashed lines), specially at pH 3, and 5.
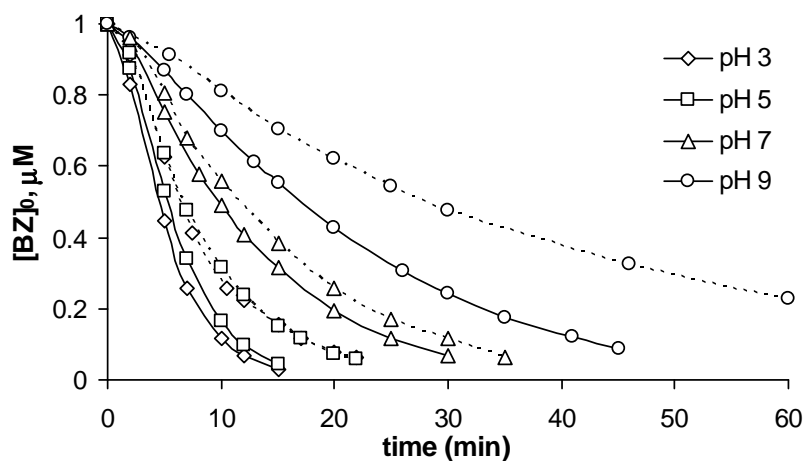
Figure 1. Influence of the presence of t-BuOH in the single photolysis of BZ at different pHs in ultra-pure water.

Table 1. Photolysis of ECs by single UV radiation, with and without t-BuOH. $[EC]_0=1\mu M$, T=20 °C.

Compound	pH	Without t-BuOH		With t-BuOH		
		Exp.	k_{UV} (min^{-1})	Exp.	k_{UV} (min^{-1})	$\phi \cdot 10^3$ (mol E^{-1})
BZ	3	BZ-1	0.264	BZt-1	0.135	53.8
BZ	5	BZ-2	0.231	BZt-2	0.141	53.5
BZ	7	BZ-3	0.094	BZt-3	0.080	29.4
BZ	9	BZ-4	0.056	BZt-4	0.027	9.4
CF	3	CF-1	0.414	CFt-1	0.381	525
CF	5	CF-2	0.389	CFt-2	0.346	494
CF	7	CF-3	0.397	CFt-3	0.334	429
CF	9	CF-4	0.392	CFt-4	0.327	469
DT	3	DT-1	0.116	DTt-1	0.0022	2.8
DT	5	DT-2	0.085	DTt-2	0.0011	1.3
DT	7	DT-3	0.063	DTt-3	0.0008	1.2
DT	9	DT-4	0.054	DTt-4	0.0007	0.9
ML	3	ML-1	0.226	MLt-1	0.166	108
ML	5	ML-2	0.132	MLt-2	0.109	73.7
ML	7	ML-3	0.197	MLt-3	0.153	105
ML	9	ML-4	0.271	MLt-4	0.251	165
NH	3	NH-1	0.125	NHt-1	0.046	13.8
NH	5	NH-2	0.133	NHt-2	0.039	11.3
NH	7	NH-3	0.153	NHt-3	0.046	13.6
NH	9	NH-4	0.166	NHt-4	0.056	15.0

This trend is also confirmed by a kinetic study. In a first approach, it is assumed that the photochemical reaction of organic compounds follows first-order kinetics. According to this model, a plot of ln $[P]_o/[P]$ *vs* reaction time should result in a straight line, whose slope provides the first-order rate constant k_{UV}. Following this kinetics, and after regression analysis ($r^2>0.99$ in all cases), the rate constants k_{UV} were deduced and

summarized in Table 1 for both types of experiments, with and without t-BuOH. These values clearly confirm the trend previously commented, with lower reaction rate constants for the experiments performed in the presence of t-BuOH. Then, it can be assumed that there is a significant contribution of the radical pathway to the overall reaction rate in the photodegradation process, which varies depending on the specific compound considered: it is low for CF, intermediate for ML and BZ, and more significant for DT and NH. These results can be explained by the fact that some amount of hydroxyl radicals are produced in the photodegradation of these pollutants, even in the case of UV radiation alone. Similarly, singlet oxygen, and superoxide radical are all generated in UV photolysis. Therefore, both pathways (direct photochemical and radical pathway) contribute to their degradation. Radical pathway plays a more significant contribution in those compounds that present very low reactivity towards UV radiation (DT and NH). Nevertheless, the reaction between ECs triplet state and an alcohol could also inhibit the direct photolysis of the substrate in case that it proceeds through the triplet state, and regenerates the substrate (Vione et al, 2010).

The rate constant values summarized in Table 1 also show the influence of pH on the photodegradation process. This effect is quite different depending on the nature of the selected ECs. Thus, it is seen in Figure 1 for BZ taken as example (and also from values in Table 1) that pH promoted a negative effect on the photodegradation, with increasing rates when the pH decreased. Similarly, slight decreases in the degradation rates were also obtained for DT with increasing pH. However, less clear effects were observed for CF, NH and ML, with similar reaction rates obtained at different pH values. It must be taken into account that BZ has two dissociation constants with $pK_{a1}=0.4$ and $pK_{a2}=8.20$. However, NH, CF and DT present one dissociation constant ($pK_a=10.21$ for NH; $pK_a=9.81$ for CF and $pK_a=0.67$ for DT), and ML does not present any pK_a value. No direct relationship could be found between rate constants and pK_a values, probably due to the different contribution of the reaction pathways discussed above. On the other hand, the resulting k_{UV} values reveal the following global sequence of reactivity for ECs photolysis: CF > ML > BZ > NH > DT.

In a next step, a more rigorous kinetic study was conducted with the objective of evaluating the quantum yields (ϕ) of the ECs photodegradation. This kinetic parameter represents the ratio between the total number of compound molecules degraded to the

total number of photons absorbed by the compounds present in the solution. As it only takes into account the direct photolysis, without contribution of the radical pathway, this analysis must be carried out with the experiments performed in the presence of t-BuOH. For the evaluation of ϕ the reaction model described in detail elsewhere was used (Benitez et al., 2006), which proposes the following general equation for the disappearance rate of any compound P as a function of the absorbed radiation flux W_{abs}:

$$[P] = [P]_0 - \frac{\Phi}{V} \int W_{abs} dt \tag{1}$$

A radiation source model, which describes the distribution of radiant energy within the reactor, was used for the determination of W_{abs}, which depends on [P] (Benitez et al., 2006). Once the values of W_{abs} were determined, the integral term $\int W_{abs} \cdot dt$ was calculated numerically. Finally, a plot of the ECs concentration [P] *vs* the corresponding integral $\int W_{abs} \cdot dt$ led to a straight line, whose slope provided the quantum yield ϕ for each compound. Following this procedure, and after regression analysis with correlation coefficients $r^2 > 0.99$ for all the experiments, the quantum yields ϕ were evaluated, and their values are also summarized in Table 1. It can be seen that the sequence of reactivity observed for the rate constants k_{UV} is again reproduced for these quantum yields; *i.e.*, CF > ML > BZ > NH>DT.

Combined UV/H$_2$O$_2$ treatment

Another group of individual ECs photodegradation experiments was performed at T=20 ^{o}C and pH=7, without t-BuOH, using the same UV radiation source, with the additional presence of hydrogen peroxide (initial concentrations of 1 x 10^{-5} and 5x10^{-5} mol L^{-1}). These experiments are summarized in Table 2. The molar extinction coefficients of the selected ECs at 254 nm were found to be very similar at different pH. The average values were 5083, 1350, 1641, 2725, and 7058 M^{-1}cm^{-1} for BZ, CF, DT, ML, and NH respectively. The molar extinction coefficient of H$_2$O$_2$ at 254nm is 19.6 M^{-1} cm^{-1}, which is very low, compared to the molar extinction coefficients of the selected ECs. Therefore, the UV light absorbed by the

selected ECs was higher than that absorbed by H_2O_2, even when the highest concentration of H_2O_2 was used.

Table 2. Photodegradation of ECs by the combination UV/H_2O_2. [ECs]$_0$=1 µM, T=20 °C, pH=7, without t-BuOH.

Compound	Exp.	Oxidation system	k_{UV} (min^{-1})	k_T (min^{-1})	k'_{OH} (min^{-1})
BZ	BZt-3	UV	0.080	-	-
BZ	BZH-1	UV+H_2O_2 (10 µM)	-	0.263	0.183
BZ	BZH-2	UV+H_2O_2 (50 µM)	-	0.522	0.442
CF	CFt-3	UV	0.334	-	-
CF	CFH-1	UV+H_2O_2 (10 µM)	-	0.468	0.134
CF	CFH-2	UV+H_2O_2 (50 µM)	-	0.562	0.228
DT	DTt-3	UV	0.0008	-	-
DT	DTH-1	UV+H_2O_2 (10 µM)	-	0.1869	0.1861
DT	DTH-2	UV+H_2O_2 (50 µM)	-	0.4877	0.4869
ML	MLt-3	UV	0.153	-	-
ML	MLH-1	UV+H_2O_2 (10 µM)	-	0.276	0.123
ML	MLH-2	UV+H_2O_2 (50 µM)	-	0.735	0.582
NH	NHt-3	UV	0.046	-	-
NH	NHH-1	UV+H_2O_2 (10 µM)	-	0.271	0.225
NH	NHH-2	UV+H_2O_2 (50 µM)	-	0.727	0.681

Following the same first-order kinetic model, the rate constants (k_T) were determined after regression analysis of the experimental results. These rate constant values k_T are also compiled in Table 2, as well as the k_{UV} values obtained in the same experiments with UV radiation alone (at pH=7) and with t-BuOH (experiments BZt-3, CFt-3, DTt-3, MLt-3 and NHt-3, respectively), in order to compare the degradation rate obtained by the single photolysis and by the global photodegradation process (direct photolysis plus radical pathway) for each compound. The rate constants contained in Table 2 show the positive influence of the combination UV/H_2O_2 on the photodegradation process: in fact, the k_T

values are higher in all cases than k_{UV} of direct photolysis. The difference is even higher in the experiments with the higher H_2O_2 concentration used (5×10^{-5} M). It demonstrates that the ECs photodegradation is greatly enhanced by the hydroxyl radicals generated by the AOP constituted by the combination of UV radiation plus hydrogen peroxide.

Under a kinetic point of view, this enhancement of oxidation provided by the presence of H_2O_2 can be determined from the rate constants values. For this purpose, a simple oxidation mechanism previously proposed and used by several authors (Rosenfeld and Linden, 2007; Chelme-Ayala et al., 2010), was applied. It considers that the oxidation rate is the result of the contribution of both reaction pathways: direct photolysis (r_{UV}) and hydroxyl radical attack (r_R). Thus, the overall oxidation rate of a compound P in any AOP can be represented by the expression:

$$-\frac{d[P]}{dt} = -\left(r_{UV} + r_R\right) = k_{UV}[P] + k_{OH}[^\bullet OH][P] = k_{UV}[P] + k'_{OH}[P] \qquad (2)$$

where k_{OH} is the second-order rate constant for the reaction between hydroxyl radicals and the substance P to be oxidized. Due to the fact that the OH radical concentration is assumed to be constant during the reaction, the term $k_{OH}[\cdot OH]$ can be transformed into a pseudo-first-order rate constant k'_{OH}. With this approach, the integration of Equation (2) leads to the following expression for the photochemical degradation of the compound P:

$$\ln \frac{[P]_0}{[P]} = k_{UV} t + k'_{OH} t = (k_{UV} + k'_{OH}) t = k_T t \qquad (3)$$

According to Equation (3), the rate constant for the radical reaction k'_{OH} can be easily deduced by subtracting the previously known value of k_{UV} (experiments performed with t-BuOH) from the overall rate constant k_T, which values are shown in Table 2. After following this procedure, Table 2 also shows the resulting k'_{OH} values. The observation of these rate constants also reveals the increase in the reaction rate when H_2O_2 concentration is increased. In fact, for BZ taken as an example, the contribution to the overall reaction rate of the direct photolysis was 30% compared to the 70% of the radical pathway in Expt. BZH-1. However, in Expt. BZH-2 with more H_2O_2, it was 15% while the radical pathway contributed the remaining 85%. Similar considerations can be made for the remaining
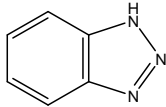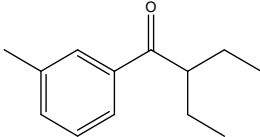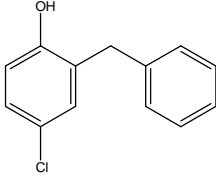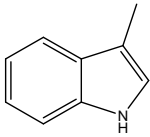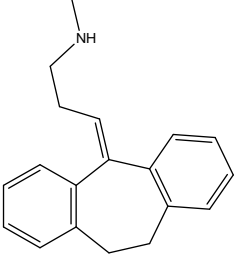
compounds, and it is a consequence of the OH generation caused by the photolysis of hydrogen peroxide, which is higher with the presence of a greater amount of H_2O_2.

3.2. By-products identification and degradation pathways of single UV photolysis.

Several studies previously reported were focused on the identification of various emerging compounds and their oxidation by-products (Pérez-Estrada et al., 2008; Yuan et al., 2009). However, only a few references have been found about the photodegradation of the selected ECs of the present study and their by-products. In order to accomplish this objective, the reaction samples from single UV experiments were analyzed by HPLC-QTOF-MS as described in the Experimental Section, due to the capacity of this technique to identify of unknown compounds. Table 3 compiles the retention times of the selected ECs, as well as the accuracies obtained in the mass measurements of their ionized molecules. These accurate mass measurements were carried out by following the procedure described previously (Ferrer et al., 2005), and the errors obtained were less than 3 ppm in all cases. As the widely accepted accuracy threshold for confirmation of elemental composition has been established at 5 ppm, it is concluded that the mass measurement accuracy, along with the characteristic retention time, provide useful tools for the elemental composition assignments of the selected ECs and their by-products. TOC analysis was also performed in most of the samples generated in the present work. However, TOC variation in each experiment was rather low (below 10%), indicating a low mineralization level.

The results of the analysis applied to the samples obtained in each individual photodegradation process of the five ECs showed the formation of a very complex reaction mixture, as a consequence of the strong photolytic reactivity of these compounds. Figures 2A-6A show the evolution of the chromatographic areas (normalized results to the highest value observed, mean of two replicates) with photodegradation time for the parent compounds and their most significant degradation by-products. Meanwhile, Figures 2B-6B show the degradation pathways tentatively proposed for each selected compound. Due to the large number of these degradation by-products detected in each case, it is not possible to describe all of them, and this study is only focused in the by-products which structure could be identified.

Table 3. LC/TOF-MS accurate mass measurements for the compounds studied.

Compound (acronym)	Ion	Chemical Structure	Retention time, min	m/z theoretical experimental	Error, ppm
Benzotriazole (BZ)	[M+H]$^+$		12.3	120.0556 120.0555	-0.8
DEET (DT)	[M+H]$^+$		20.3	192.1383 192.1380	-1.6
Chlorophene (CF)	[M-H]$^-$		23.9	217.0426 217.0430	1.8
Methylindole (ML)	[M+H]$^+$		21.9	132.0808 132.0805	-2.3
Nortriptyline HCl (NH)	[M+H]$^+$	HCl	13.6	264.1747 264.1744	-1.1

Firstly, Figure 2 shows the results concerning DT. As observed in the degradation curves shown in Figure 2A, the parent compound DT (MW=191) decreased slowly with reaction time, which is in agreement with its slow photodegradation rate, already discussed in the previous evaluation of the first-order rate constants k_{UV} and quantum yields (ϕ). In fact, DT had the lowest degradation rate among the five selected ECs. At the same time, it is

observed a continuous formation of a by-product with MW=207 during the whole reaction process (around 2 h); and a rapid formation of three by-products (MW= 135, 163 and 177) which reached a maximum after 30 min of reaction, followed by a slow decrease in their concentrations. These several intense peaks detected could explain the routes of oxidation that are shown in Figure 2B. On the one hand, it could be proposed that the product with MW=207 is the result of the OH radical attack to the aromatic ring, as proposed by Zhang and Lemley (2006). Alternatively, hydroxyderivatives could also arise upon reaction between DT triplet state and water (Bedini et al., 2012). On the other hand, the compound with MW=163 was attributed to the side chain oxidation and further hydrolysis causing removal of the ethyl group from the nitrogen (Song et al., 2009). Within the next steps, two new routes are suggested: a ring methyl oxidation through the formation of the proposed intermediate with MW=179 (not detected), which finally resulted in the identified product with MW=177 (Agency for Toxic Substances and Disease Registry, 2004); and a new N-dealkylation route, which is produced throughout the process resulting in the identified product with MW=135.

Figure 2. UV photolysis of DT: A) Products time profiles: chromatographic areas normalized to the highest value observed
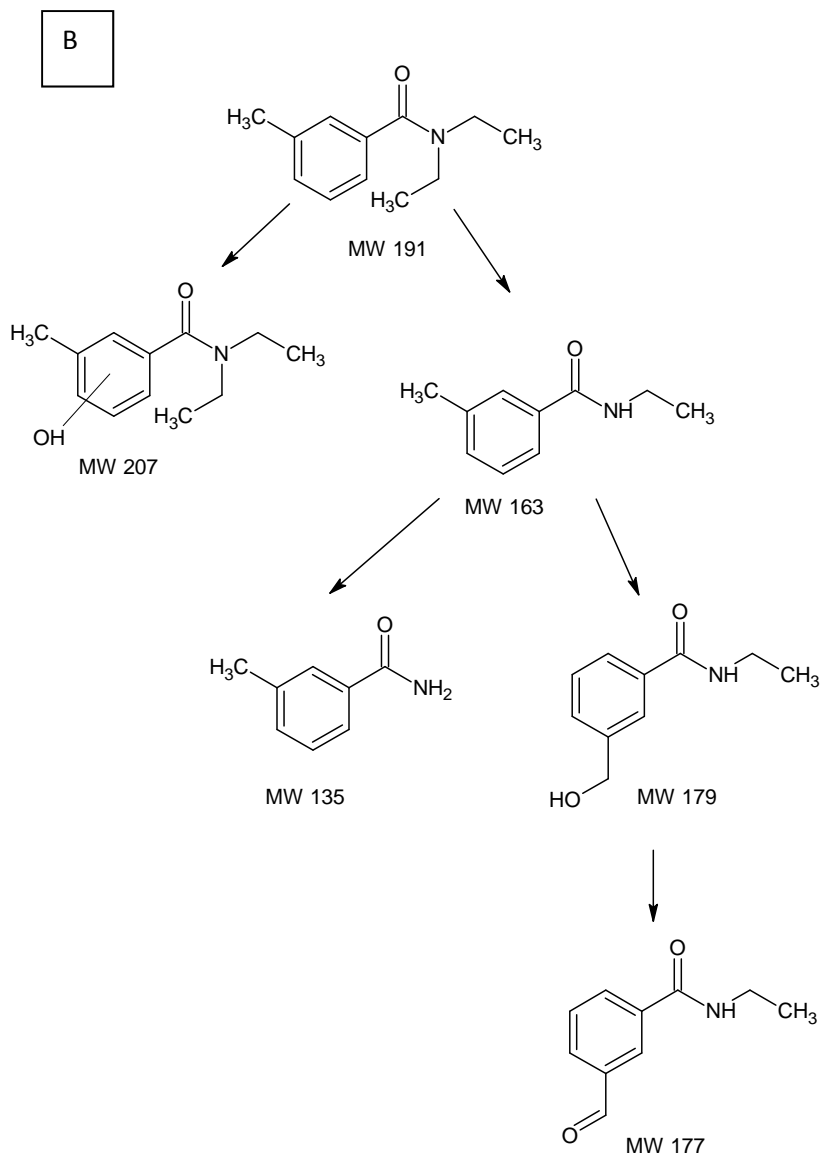
Figure 2. UV photolysis of DT: B) Degradation pathway proposed.

The evolution followed by ML and its degradation by-products is shown in Figure 3A: it is observed a rapid decrease of the parent compound ML (MW=131), which is almost totally consumed after 30 min of reaction. This corresponds to its high degradation rate, determined previously by the quantum yield. Several by-products were identified (MW=135, 147, 137, 179 and 119, and two different intermediates with MW=163). An increase in their concentrations was observed in this time interval, reaching maximum values between 30 and 60 min; it is followed by the decrease in the concentration at later times. According to these identified by-products, two degradation pathways can be proposed for ML (Figure 3B). Firstly, as Nemoto et al. (1991) had previously proposed, the oxidation of ML produces 2-formylaminoacetophenone (MW 163), which later leads to 2-aminoacetophenone (MW 135); and following this route, 2-aminobenzoic acid (MW=137) could be formed, which subsequently loses a water molecule yielding the product with MW=119. At the same time, a radical route based on a successive hydroxylation of the aromatic ring takes place, resulting successively in the by-products with MW=147, 163 and 179. An alternative for this hydroxylation pathway could be the reaction of ML triplet state and water.
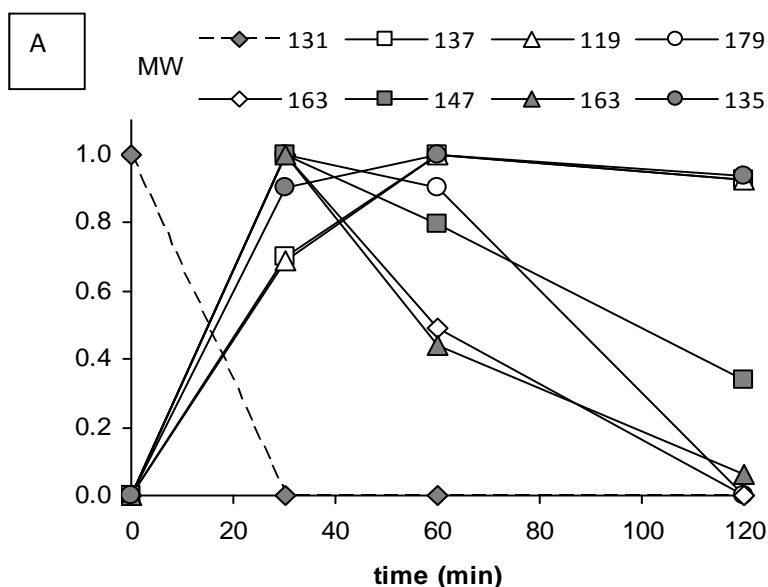
Figure 3. UV photolysis of ML: A) Products time profiles: chromatographic areas normalized to the highest value observed
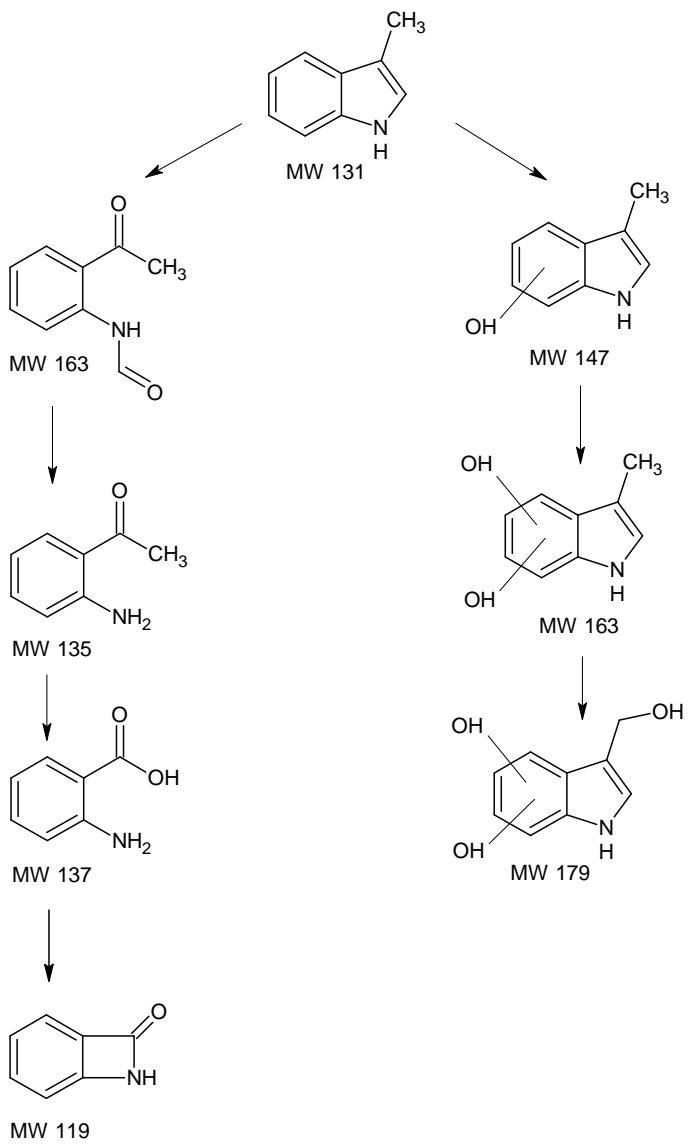
Figure 3. UV photolysis of ML: B) Degradation pathway proposed.

On the other hand, Figure 4A shows the degradation evolution of BZ, where a decrease in its concentration is observed (MW=119) in the first 30 min. Simultaneously, two identified by-products with MW=109 and 180 are formed, and later degraded. As shown in the reaction pathway proposed in Figure 4B, the prolonged irradiation of this parent compound could lead to two different routes of degradation: nitrogen elimination followed by hydroxylation, leading to a product with MW=109; and a dimerization process that leads to the formation of the product with MW=180. According to Wang et al., 2000, it must be noted that the loss of the nitrogen molecule from BZ at 254 nm does not take place directly, but it occurs through the intermediate with MW=93 (not detected) as shown in Figure 4B.
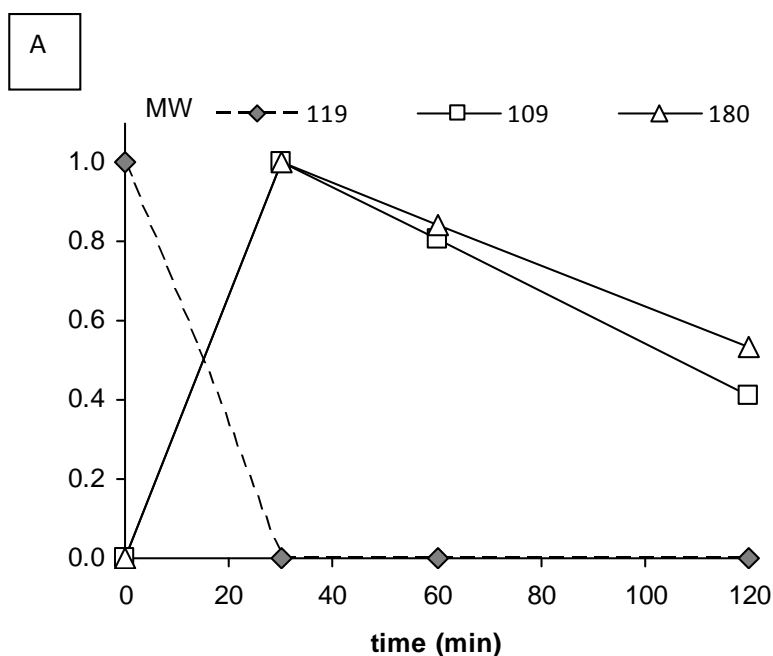
Figure 4. UV photolysis of BZ: A) Products time profiles: chromatographic areas normalized to the highest value observed.
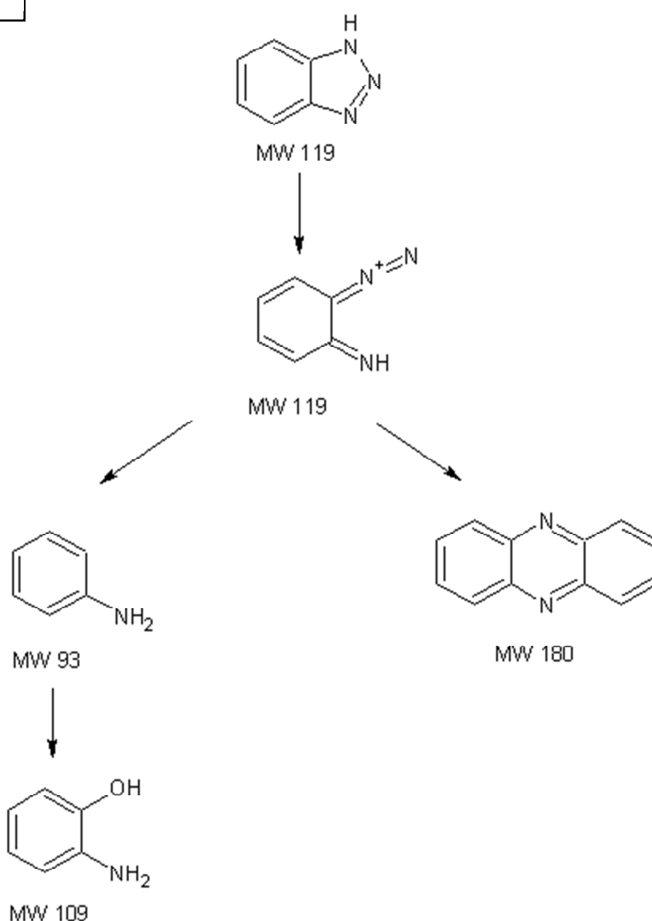
Figure 4. UV photolysis of BZ: B) Degradation pathway proposed.

In the case of NT, the degradation curves (Figure 5A) reveal a moderate degradation rate of the parent compound (MW=263) and the formation of two identified by-products during the first 30 min, which later were eliminated (MW=232 and 281). It can be proposed that the compound with MW=232 is the result of the loss of a fragment of the chain linked to the cycloheptane ring, while the substance with MW=281 might be generated from hydroxylation of this cycloheptane ring (see Figure 5B).
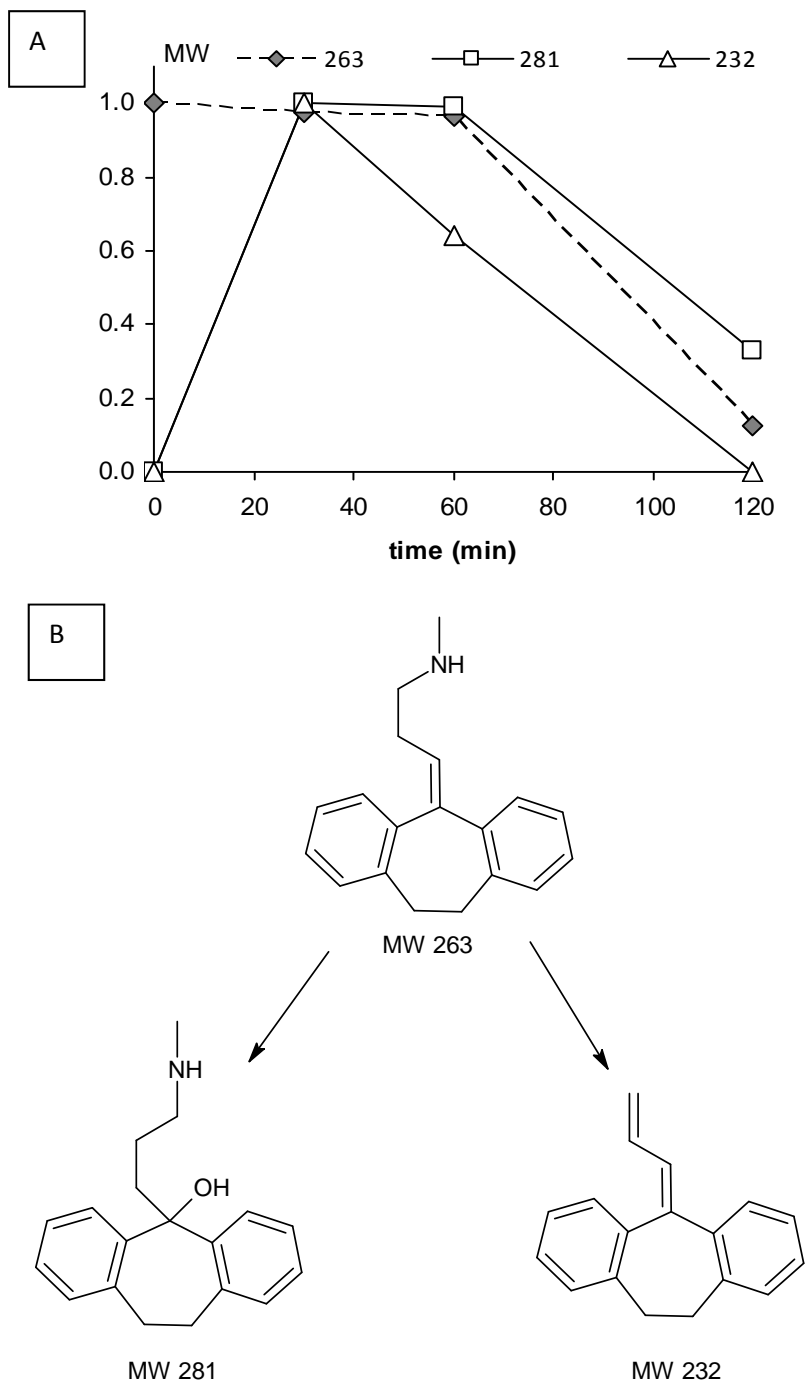
Figure 5. UV photolysis of NH: A) Products time profiles: chromatographic areas normalized to the highest value observed. B) Degradation pathway proposed.

Finally, the degradation curves of CF and their by-products (Figure 6A) show a rapid elimination of the parent compound (MW=218), in complete agreement with its highest degradation rate among the five selected ECs; and the appearance of two identified by-products (MW=234 and 216) during the first 30 min of reaction, which later were continuously degraded. A plausible reaction sequence for this photodegradation process (see Figure 6B) is that CF can undergo a parallel attack of OH radical on its meta and/or orto positions of the aromatic ring, resulting in two products with the same MW=234. These products could also be originated from the reaction of CF triplet state and water. The subsequent hydroxylation step with dechlorination of these products could lead to the same compound with MW=216. This reaction sequence is very similar to that reported in the oxidation of clofibric acid (Sirés et al., 2006), a substance with a similar chemical structure than CF.
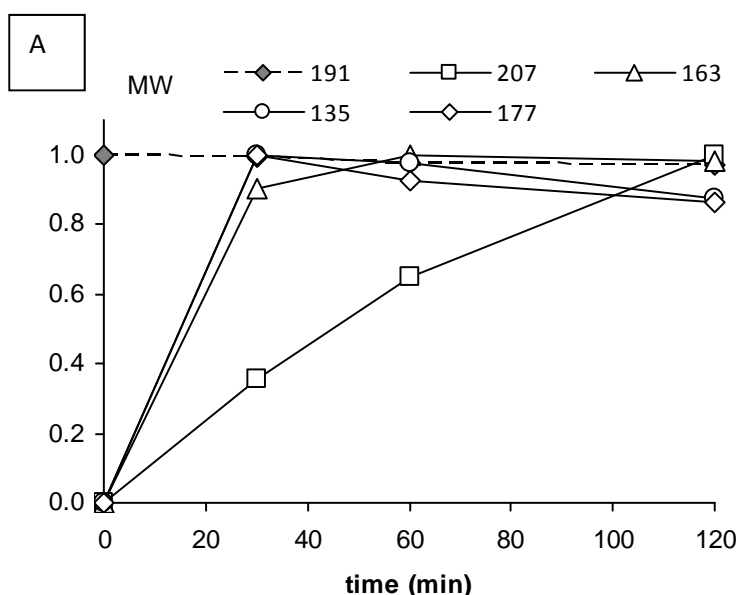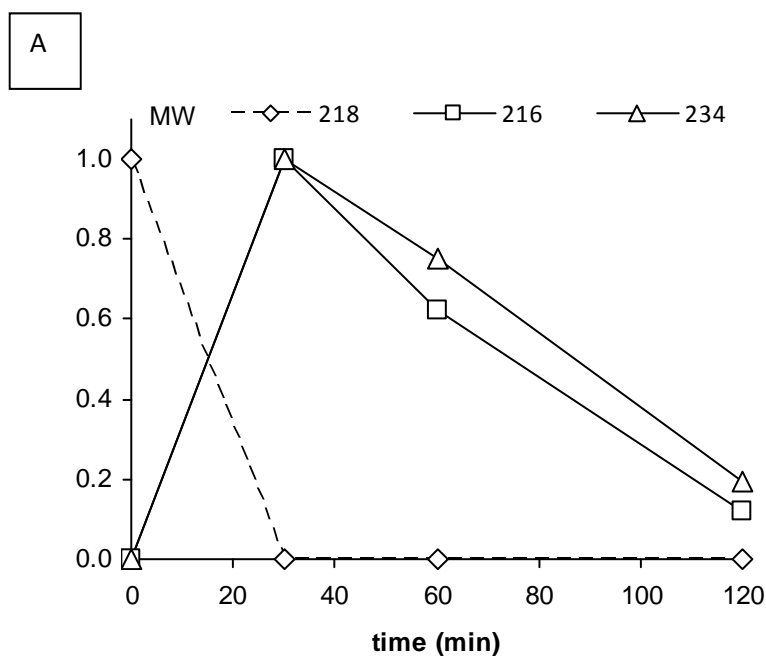

Figure 6. UV photolysis of CF: A) Products time profiles: chromatographic areas normalized to the highest value observed.
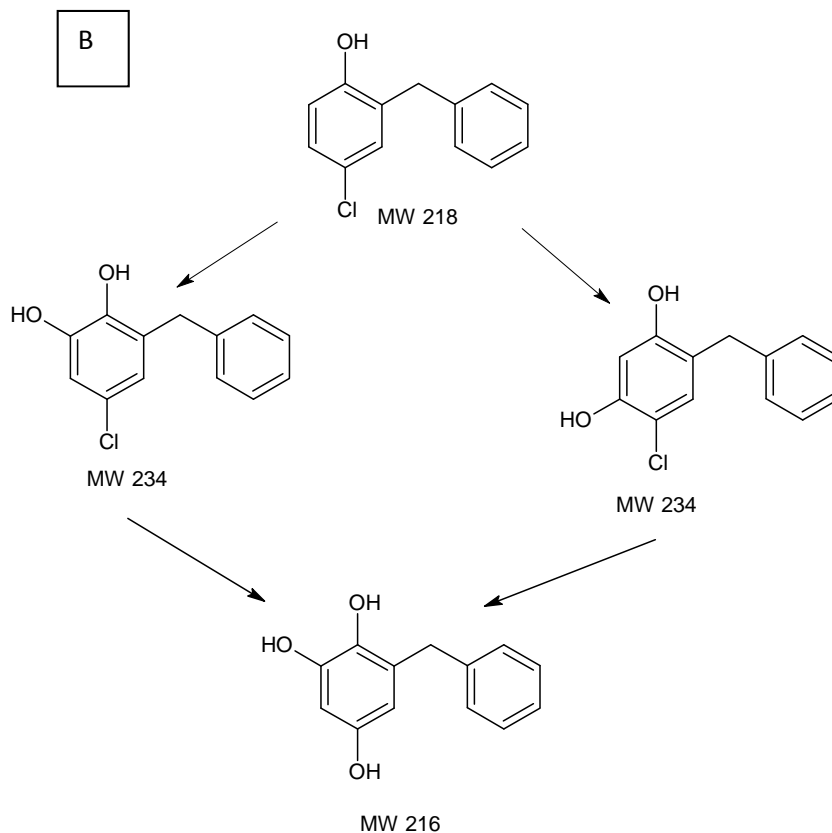
Figure 6. UV photolysis of CF: B) Degradation pathway proposed.

3.3. Toxicity evaluation.

The evolution of the toxicity in the individual photodegradation of the ECs by single UV radiation was studied in a group of experiments performed at pH=7. This toxicity was evaluated by measuring changes in the natural emission of the luminescent bacteria *V. fischeri* in samples collected at different irradiation times (0, 15, 30 and 90 min). Table 4 shows the percentages of inhibition of the natural emission in these samples for the five selected compounds, together with the percentage of ECs removal. As it is observed, the initial inhibition percentages were low for DT, CF and MT (values lower than 30%), or moderate for NH and BZ (32 and 34%, respectively). These percentages were increased in all cases during the initial period (0-15 min), when most of ECs were considerably degraded, which indicates that the first-generation by-products formed were more toxic than the

parent compounds. At more advanced reaction times, two different evolutions can be observed: on one hand, in the case of BZ, DT, CF and ML, and after reaching a maximum for this inhibition percentage value, the toxicity decreased at higher reaction times, suggesting that the intermediates were degraded to less toxic products. On the contrary, the toxicity values increased continuously for NH, which is an indication of continuous formation of intermediates more toxic than the initial parent compound. Further systematic study on the degradation intermediates should be performed in order to clarify in a major extent the evolution of toxicity in these photolysis processes.

Table 4. Toxicity evolution during the photolysis of ECs: light inhibition of the bacterium *Vibrio fischeri*. % represents the inhibition percentage and the number in parenthesis corresponds to the percentage of EC removal (single UV photolysis, pH=7, $[ECs]_0=1$ μM).

BZ		CF		DT		ML		NH	
t, min	%	t, min	%	t, min	%	t, min	%	t, min	%
0	34 (0)	0	25 (0)	0	22 (0)	0	26 (0)	0	32 (0)
15	36 (95)	15	70 (100)	15	36 (47)	15	50 (91)	15	41 (77)
30	40 (100)	30	54 (100)	30	32 (77)	30	40 (100)	30	51 (100)
90	31 (100)	90	39 (100)	90	35 (100)	90	30 (100)	90	54 (100)

4. CONCLUSIONS.

The results of the photodegradation processes, by UV radiation alone and the combined UV/H_2O_2 system, of the five emerging contaminants selected (benzotriazole, DEET, chlorophene, methylindole, and nortriptyline HCl) in ultra-pure water allowed the following conclusions to be drawn:

i. The single photolysis process of the ECs in ultra-pure water at different pH values by a monochromatic UV radiation at 254 nm revealed the following sequence of degradation: CF > ML > BZ > NH > DT.

ii. The presence of t-BuOH in the solutions decreased the degradation rates. As this substance is a scavenger of hydroxyl radicals, it might indicate that there is a

significant contribution of the radical pathway to the overall reaction rate. Further oxidant species, such as singlet oxygen and superoxide radical are all generated in UV photolysis. In addition, reaction between ECs triplet state and water has to be considered.

iii. The photodegradation process can be represented by first-order kinetics, with rate constants values and quantum yields that varied depending on the pH of the solution and the nature of each specific compound.

iv. The combined UV/H_2O_2 process provided a significant increase in the reaction rates, as a consequence of the hydroxyl radicals generated by this AOP.

v. Analysis by HPLC-QTOF-MS technique of the reaction samples allowed the determination and identification of the main intermediates generated. From the by-products identified, the degradation pathways are proposed for each specific case.

vi. The V. fischeri screening test was conducted to assess the toxicity of the untreated and treated samples. The results show an initial increase of this parameter in all cases, followed by a decrease in the toxicity of the samples for most of the compounds with the exception of NH.

REFERENCES

Agency for Toxic Substances and Disease Registry. DEET (N,N-Diethyl-meta-toluamide): Chemical Technical Summary for Public Health and Public Safety Professionals. Atlanta, Georgia. **2004.**

Bedini, A.; De Laurentiis, E.; Sur, B.; Maurino, C.; Brigante, M.; Mailhot, G.; Vione, D. Phototransformation of anthraquinone-2-sulphonate in aqueous solution. Photochem. Photobiol. Sci. **2012**, 11, 1445-1453.

Benítez, F.J.; Real, F.J.; Acero, J.L.; García, C. Photochemical oxidation processes for the elimination of phenyl-urea herbicides in waters. J. Hazard. Mater. **2006**, 138, 278-87.

Boehmer, W.; Ruedel, H.; Wenzel, A.; Schröeter-Kermani, C. Retrospective Monitoring of Triclosan and Methyl-triclosan in Fish: Results from the German Environmental Specimen Bank. Organohalogen. Comp. **2004**, 66, 1489-1494.

Chelme-Ayala, P.; El-Din, M.G.; Smith, D.W. Degradation of bromoxynil and trifluralin in natural water by direct photolysis and UV plus H_2O_2 advanced oxidation process. Water Res. **2010**, 44, 2221-2228.

Costanzo, S.D.; Watkinson, A.J.; Murby, E.J.; Kolpin, D.W.; Sandstrom, M.W. Is there a risk associated with the insect repellent DEET (N,N-diethyl-m-toluamide) commonly found in aquatic environments?. Sci. Total Environ. **2007**, 384, 214-220.

Ferrer, I.: García-Reyes, J.F.; Mezcua, M.; Thurman, E.M.; Fernández-Alba, A.R. Multi-residue pesticide analysis in fruits and vegetables by liquid chromatography time-of-flight mass spectrometry. J. Chromatography A **2005**, 1082, 81-90.

Heberer, T. Occurrence, fate, and removal of pharmaceutical residues in the aquatic environment: a review of recent research data. Toxicol. Lett. **2002**, 131, 5-17.

Langford, K.H.; Thomas, K.V. Determination of pharmaceutical compounds in hospital effluents and their contribution to wastewater treatment works. Environ. Int. **2009**, 35, 766-770.

Legrini, O.; Oliveros, E.; Braun, A.M. Photochemical processes for water treatment. Chem. Rev. **1993**, 93, 671-698.

Loos, R.; Gawlik, B.M.; Locoro, G.; Rimaviciute, E.; Contini, S.; Bidoglio, G. EU wide survey of polar organic persistent pollutants in European river waters. Environ. Pollut. **2009**, 157, 561-568.

Martínez Bueno, M.J.; Agüera, A.; Gómez, M.J.; Hernando, M.D.; García-Reyes, J.F.; Fernández-Alba, A.R. Application of liquid chromatography/quadrupole-linear ion trap mass spectrometry and time-of-flight mass spectrometry to the determination of

pharmaceuticals and related contaminants in wastewater. Anal. Chem. **2007**, 79, 9372-9384.

Microtox [TM] Manual: A toxicity Testing Handbook. 1992. Details Protocols, Vol. I-IV Microbics. Corp. Carlsbad CA, USA.

Nakada, N.; Komori, K.; Suzuki, Y.; Konishi, C.; Houwa, I.; Tanaka, H. Occurrence of 70 pharmaceutical and personal care products in Tone River basin in Japan. Water Sci. Technol. **2007**, 56, 133-40.

Nemoto, N.; Asakura, T.; Tobita, K.; Ueno, Y.; Ikeda, K.; Takamiya, N.; Ohkatsu, Y. Oxygenation of 3-methylindole catalyzed by cobalt(II) phthalocyanine attached to polyorganosiloxane Part 2. Mechanism for addition of oxygen to 3-methylindole. J. Molec. Catalysis **1991**, 70, 151-158.

Nicole, I.; De Laat, J.; Dore, M.; Duguet, J.P.; Bonnel, C. Use of UV radiation in water treatment: measurement of photonic flux by hydrogen peroxide actinometry. Water Res. **1990**, 24, 157-168.

Pérez-Estrada, L.A.; Agüera, A.; Hernando, M.D.; Malato, S.; Fernández-Alba, A.R. Photodegradation of malachite green under natural sunlight irradiation: Kinetic and toxicity of the transformation products. Chemosphere **2008**, 70, 2068-2075.

Rosenfeld, E.J.; Linden, K.G. The $R_{OH,UV}$ concept to characterize and the model UV/H_2O_2 process in natural waters. Environ. Sci. Technol. **2007**, 41, 2548-53.

Sirés, I.; Cabot, P.L.; Centellas, F.; Garrido, J.A.; Rodríguez, R.M.; Arias, C.; Brillas, E. Electrochemical degradation of clofibric acid in water by anodic oxidation: Comparative study with platinum and boron-doped diamond electrodes. Electrochim. Acta **2006**, 52, 75-85.

Song, W.; Cooper, W.J.; Peake, B.M.; Mezyk, S.P.; Nickelsen, M.G.; O'Shea, K.E. Free-radical-induced oxidative and reductive degradation of N,N-diethyl-m-toluamide (DEET): Kinetic studies and degradation pathway. Water Res. **2009**, 43, 635-642.

Staehelin, J.; Hoigne, J. Decomposition of ozone in water in the presence of organic solutes acting as promoters and inhibitors of radical chain reactions. Environ. Sci. Technol. **1985**, 19, 1206-1213.

Suárez, S.; Carballa, M.; Omil, F.; Lema, J.M. How are pharmaceutical and personal care products (PPCPs) removed from urban wastewaters? Environ. Sci. Biotechnol. **2008**, 7, 125-138.

Vione, D.; Khanra, S.; Das, R.; Minero, C.; Maurino, V.; Brigante, M.; Mailhot, G. Effect of dissolved organic compounds on the photodegradation of the herbicide MCPA in aqueous solution. Water Res. **2010**, 44, 6053-6062.

Wang, H.; Burda, C.; Persy, G.; Wirz, J. Photochemistry of 1H-Benzotriazole in aqueous solution: A Photolatent Base. J. Am. Chem. Society **2000**, 122, 5849-5855.

Yuan, F.; Hu, C.; Hu, X.; Qu, J.; Yang, M. Degradation of selected pharmaceuticals in aqueous solution with UV and UV/H_2O_2. Water Res. **2009**, 43, 1766-1774.

Zhang, H.; Lemley, A.T. Reaction mechanism and kinetic modeling of DEET degradation by flow-through anodic fenton treatment (FAFT). Environ. Sci. Technol. **2006**, 40, 4488-4494.

3.3. Modeling the photodegradation of emerging contaminants in waters by UV radiation and UV/H$_2$O$_2$ system.

3.3. MODELING THE PHOTODEGRADATION OF EMERGING CONTAMINANTS IN WATERS BY UV RADIATION AND UV/H₂O₂ SYSTEM

F. Javier Benítez, Juan L. Acero, Francisco J. Real, Gloria Roldan, Elena Rodríguez.

Departamento de Ingeniería Química, Universidad de Extremadura, Badajoz.

Five emerging contaminants (1-H-benzotriazole, N,N-diethyl-m-toluamide or DEET, chlorophene, 3-methylindole, and nortriptyline HCl), frequently found in surface waters and wastewaters, were selected to be photooxidized in several water matrices. Previous degradation experiments of these compounds individually dissolved in ultra pure water were performed by using UV radiation at 254 nm and the Fenton´s reagent. These oxidation systems allowed the determination of the quantum yields and the rate constants for the radical reaction between each compound and hydroxyl radicals. Later, the simultaneous photodegradation of mixtures of the selected ECs in several types of water (ultrapure water, reservoir water, and two effluents from WWTPs) was carried out and a kinetic study was conducted. A model is proposed for the ECs elimination, and the theoretically calculated concentrations with this model agreed well with the experimental results obtained, which confirmed that it constitutes an excellent tool to predict the elimination of these compounds in waters.

1. INTRODUCTION.

Emerging contaminants (ECs) constitute a diverse group of numerous chemical substances that include nanomaterials, pesticides, pharmaceuticals and personal care products, industrial compounds, fragrances water treatment by-products, flame retardants and surfactants, etc. (Stuart et al., 2012). These products have been labelled as emerging

contaminants, which means that they are still unregulated or in the process of being regulated. They are frequently found in treated wastewater, surface and ground waters, and even in drinking water (Fatta-Kassinos et al., 2011; Barceló, 2003), although their main source is through municipal sewage, because it is recognized that wastewater treatment plant technologies are very often unable to entirely degrade such persistent substances. Consequently, they accumulate in the aquatic environment where they may cause ecological risk (Hansen et al., 2007), such as interferences with endocrine system of higher organisms, micro-biological resistance and accumulation in soil, plants and animals (Camacho-Munoz et al., 2010).

An increasing public health concern has grown in relation to these compounds, since little is known about their potential effects in humans and animals; and their elimination from waters, together with other priority pollutants, is an emerging issue in environmental technology. Consequently, alternative advanced technologies for tertiary treatment of WWTP effluents are necessary. In this way, single oxidation treatments and advanced oxidation processes (AOPs) have been proposed as valuable methods for the elimination of persistent organic compounds, because unselective hydroxyl radicals are able to promote organic matter oxidation at high reaction rates.

Among the chemical procedures tested, UV radiation is very effective and widely applied to induce photoreactions of organic pollutants in advanced water treatment technologies for groundwater and drinking water remediation (Legrini et al., 1993). For this purpose, mercury lamps emitting at 254 nm are the UV sources most commonly used. Additionally, the use of UV radiation in combination with hydrogen peroxide is also a very promising technique for the oxidative degradation of organic compounds. In that case, the UV radiation dissociates H_2O_2 and generates hydroxyl radicals which can oxidize organic compounds more effectively (Rosenfeldt et al., 2006).

Although some information on the removal of ECs using UV radiation is reported in the literature (Kim et al., 2009; Yuan et al., 2009), this information is not abundant, even nonexistent for some specific substances. With these considerations in mind, the present study was designed with the main objective to investigate the degradation, during single UV

and combined UV/H$_2$O$_2$ treatments, of five selected ECs commonly found in water environments. These ECs, whose chemical structures are shown in Table 1, were selected as model pollutants of this group because of their common usages and frequent presences in waters.

Table 1. Chemical structures of the selected ECs.

Compound	Formula	Chemical structure
1-H-benzotriazole	C$_6$H$_5$N$_3$	
Chlorophene	C$_{13}$H$_{11}$ClO	
DEET	C$_{12}$H$_{17}$NO	
3-methylindole	C$_9$H$_9$N	
Nortriptyline·HCl	C$_{19}$H$_{21}$N·HCl	

Thus specifically, 1-H-benzotriazole (BZ) is an EC, well known as corrosion inhibitor for copper or silver material, and has been widely used in cooling and hydraulic fluids, antifreezing products, aircraft deicer and anti-icer fluid, as well as dishwasher detergent. It is also applied as antifogging agent and as intermediate for the synthesis of various chemicals. Some carcinogenic and mutagenic effects in mammals have been reported (Sills et al., 1999), and therefore, may cause a considerable threat to human health (Davis et al., 1997). Large amount of BZ has also been detected in municipal WWTPs via household wastewater, indirect discharge from industry, or surface runoff collected in combined sewer systems; and also, in surface waters due to incomplete removal during the wastewater treatment operations (Loos et al., 2009). Consequently, BZ has recently been listed as an emerging contaminant (Voutsa et al., 2066), which needs to develop appropriate effective treatment techniques.

On the other hand, N,N-diethyl-m-toluamide or DEET (DT) is an active compound in insect repellents, and has been used for more than 50 years for protection against insect bites. It has been reported to have potential carcinogenic properties in human nasal mucosal cells (Tisch et al., 2002). Contaminations of DT have been studied and reported in various aquatic environments, such as groundwater (Constanzo et al., 2007), streams (Kolpin et al., 2004), seawater, and even drinking water treated by conventional water treatment systems (Stackelberg et al., 2004). Thus, greater attention should be paid to removing this chemical, especially in the production of drinking water.

Additionally, chlorophene (CF) was chosen since it is a widespread broad-spectrum antimicrobial pharmaceutical, commonly used in hospitals and households for general cleaning and disinfecting, as well as in industrial and farming environments as an active agent in disinfectant formulations (Boehmer et al., 2004). Although CF is expected to present a low toxicity for humans, evidence of its carcinogenic and mutagenic activity in animals is documented (Yamarik et al., 2004). To avoid its dangerous accumulation in the aquatic environment, this compound and its by-products need to be removed from wastewaters by potent and viable oxidation methods.

Also, 3-methylindole (ML) is a malodorous chemical and degradation product of tryptophan formed in the rumen of cattle and goats, and is well-known as a highly selective pulmonary toxicant for ruminants (Carlson et al., 1972). It has received considerable attention owing to its potential application as perfume and synthesizing anti-inflammatory drugs, antibiotics, dyes, plant growth hormones, herbicides, antidiuretic, stimulant antihypertensive, muscular relaxant, respiratory inhibitor and heart stimulant medicaments, etc. (Wenhui et al., 2009).

And finally, the pharmaceutical nortriptyline HCl (NH) belongs to the group of tricyclic antidepressants (TCAs), which are still used as effective treatments against depression since their introduction 50 years ago (Jornil et al., 2011). It was detected at higher concentrations in WWTP effluents than were measured in the influent samples (Langford et al., 2009), and therefore, must be eliminated through later treatments.

2. MATERIALS AND METHODS.

2.1. ECs and water systems.

The selected ECs of the highest purity available (99%) were purchased from Sigma-Aldrich, and all of the other chemicals used for the solutions (hydrogen peroxide, p-chlorobenzoic acid, ferrous salts, eluents, buffers, etc.) were of reagent grade.

The water matrices used were: ultrapure water (UP), a natural water (PA) collected from the public reservoir lake "Peña del Aguila", located in the Extremadura Community, SW Spain; and two secondary effluents (BA and LA) collected from two WWTPs, located in Badajoz and La Albuera, both also in the Extremadura Community. These water matrices were shipped in 20 L bottles, previously filtered through a 0.45 μm cellulose nitrate filter within 24 h after sampling and stored in a refrigerator at 4 °C until the experiments were performed. Their main quality parameters are compiled in Table 2. Chemical oxygen demand (COD), total organic carbon (TOC) and absorbance at 254 nm (A254) constitute a significant indication of the total dissolved organic matter (DOM) present in these waters.

The measured values for these parameters revealed that the sequence of the dissolved organic matter content was: BA > PA > LA > UP.

Table 2. Characterization of the water matrices used.

	PA	LA	BA
pH	7.4	7.9	8.3
Conductivity (μS cm^{-1})	80.2	570	550
A$_{254\ nm}$ (cm^{-1})	0.187	0.041	0.245
COD (mg O$_2$ L^{-1})	18	7	56
Alkalinity (mg CaCO$_3$ L^{-1})	30	335	325
TOC (mg L^{-1})	5.2	2.8	11.1
Total nitrogen (mg L^{-1})	1.51	21.3	35.5
Phosphorus (mg L^{-1})	0.041	0.156	1.76

2.2. Experimental procedures.

As will be described later in the development of the kinetic model for predicting the elimination of the ECs, it is necessary to know in advance some specific parameters: the UV energy absorption for each compound, which is expressed as molar extinction coefficients (ε), the quantum yields (ϕ), and the second order rate constants between each one of these compounds and the hydroxyl radicals.

For the determination of the molar extinction coefficients, absorbances of known concentration of ECs solutions were spectrophotometrically measured. Then, and according to the Lambert-Beer law, the slopes of the linear regressions of these absorbances against the concentrations provided the desired molar extinction coefficients. The average values obtained by using this procedure were: 5083, 1642, 1350, 2725, and 7058 M^{-1} cm^{-1} for BZ, DT, CF, ML and NH, respectively. These values were almost constants at all pH values as no significant differences in the absorbance were found for each compound in the UV spectrum at the pH values tested.

The evaluation of the quantum yields (ϕ) was obtained by conducting photodegradation experiments of each one of the EC individually dissolved in UP water (Milli-Q water system, Millipore) and in the presence of tert-butanol. The radiation source used was a low pressure mercury vapor lamp (Hanau TNN 15/32) with an electrical power of 15 W. This lamp emitted a monochromatic radiation at 254 nm. As described in a previous work (Benitez et al., 2006), chemical actinometry experiments by using hydrogen peroxide as actinometer were conducted to determine the radiation intensity I_0 emitted by the lamp into the reactor, and the value obtained was 2.03×10^{-6} Einstein s^{-1}. In these experiments, the reactor was thermostatted at the desired temperature of 20 °C and at constant pH of 7 with a phosphoric acid/phosphate buffer (0.05 M) buffer. During each experiment, samples were withdrawn from the reactor at regular times for assay.

For the determination of the OH radical rate constants, oxidation experiments of each individual ECs dissolved together in UP water with p-chlorobenzoic acid (p-ClBz) (used as reference compound) were conducted by using the standard Fenton´s system. They were carried out in 250 mL Erlenmeyer flasks, at a constant temperature of 20 °C. Each flask was filled with an aqueous solution of ECs and p-ClBz at the desired initial concentrations, and adjusted to the pH=3 by adding perchloric acid/perchlorate (0.05 M). The required amounts of ferrous ion and hydrogen peroxide were also added to the reactor, and the reaction mixtures were homogenized using a magnetic stirrer. At regular times, samples were removed from the flasks for analysis. The reaction was stopped by adding sodium sulfite, which reacts quickly with the remaining hydrogen peroxide. The evaluation of these rate constants was carried out by using the competition kinetics method already reported elsewhere (Benitez et al., 2007), that will be described later in Results and Discussion Section.

The simultaneous photodegradation experiments of mixtures the ECs (1 µM of each compound) dissolved in the water matrices already described at the natural pH of each water (see Table 2), were carried out at a constant temperature of 20 °C, and by using UV radiation alone and combined with H₂O₂, with two different initial concentrations of hydrogen peroxide (1×10^{-5} and 5×10^{-5} M). Regularly, samples were retired from the reactor in order to analyze the concentrations of the different substances.

2.3. Analytical Methods.

The concentration of ECs in each sample, as well as p-ClBz (when used as a probe compound in the Fenton system), were determined by HPLC, using a Waters Chromatograph equipped with a 996 Photodiode Array Detector and a Phenomenex Gemini C18 Column (5μm, 150mm×3mm). The analysis was performed in gradient mode with acetonitrile as mobile-phase A and 25 mM acid formic as mobile-phase B, at a flow rate of 0.2 mL min^{-1} and at a column temperature of 20 °C. Each run started with an initial mobile-phase composition of 10% A, and linearly was increased to 30% A in 3 min, followed by another linear gradient to 40% A in 5 min, to 70% A in 4 min and 90% A in 5 min. Finally, the mobile-phase composition was maintained at 90% A for 5min. The volume of injection was of 100 μL in all cases. Detection was made at 250 nm for BZ, NH, and DT; and 280 nm for ML and CF. Similarly, the concentration of p-ClBz in the samples was also assayed by HPLC, with the detection carried out at 238 nm.

3. RESULTS AND DISCUSSION.

3.1. Degradation of individual ECs in ultra-pure water by UV radiation and Fenton's reagent.

As was already stated, previous objectives pursued in the present work were the evaluation of the quantum yield and the second-order rate constant for the direct reaction between each one of the selected ECs and the hydroxyl radicals (k_{OH-P}).

The evaluation of the quantum yields was performed in experiments where the selected ECs were subjected to individual photolysis in UP water at 20 °C and pH=7, as described in the Experimental Procedures Section. The quantum yield represents the ratio between the total numbers of molecules of the compound degraded to the total numbers of photons absorbed by the solution due to the compound's presence. As it only takes into account the direct photolysis, without any contribution of radical pathways, these experiments were carried out with the presence of a scavenger, being tert-butanol selected in this work (Staehelin and Hoigne, 1985). The evaluation of ϕ was made by following the

procedure described in detail elsewhere (Benitez et al., 2006), and the values obtained were: 429×10^{-3}, 105×10^{-3}, 29×10^{-3}, 14×10^{-3}, and 1.2×10^{-3} mol Einstein^{-1} for CF, ML, BZ, NH and DT respectively.

On the other hand, the Fenton´s reagent and the competition kinetics method widely described in the literature (Benitez et al., 2007) was used for the determination of the rate constant between each EC and the hydroxyl radicals. Basically, this oxidation system uses ferrous ion to react with hydrogen peroxide for the generation of OH radicals (Walling, 1975):

$$H_2O_2 + Fe^{2+} \rightarrow OH^- + \cdot OH + Fe^{3+} \tag{1}$$
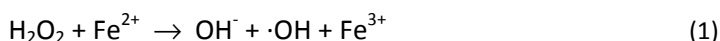
Reaction (1) is a very simplified scheme of this process, whose mechanism is described in detail elsewhere (Benitez et al., 2007), where reactions and rate constants values reported by previous works in the field were compiled. These radicals generated through reaction (1) oxidize most organic compounds:

$$P + \cdot OH \xrightarrow{\quad k_{OH} \quad} P_{oxid} \tag{2}$$
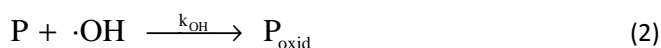
On the other hand, the mentioned competition kinetics method is based on the simultaneous oxidation of a target compound (P) with an unknown rate constant (each ECs in the present study), and a reference compound (R) which radical rate constant is perfectly known. The reference compound selected was p-ClBz, with a value of 5×10^9 L mol^{-1} s^{-1} for its rate constant for the reaction with hydroxyl radicals (Buxton et al., 1988).

The application of this competition kinetics method leads to the following relationship:

$$\ln \frac{[P]_0}{[P]_t} = \frac{k_{OH-P}}{k_{OH-R}} = \ln \frac{[R]_0}{[R]_t} \tag{3}$$

where the symbols P and R refer to the target (EC) and reference (p-ClBz) compounds; and 0 and t indicate concentrations at the initial and at any reaction time.

In order to determine these k_{OH-P} rate constans, two experiments at 20 °C and pH=3 were carried out for the simultaneous oxidation of each one of the selected ECs and p-ClBz by the mentioned Fenton´s reagent. Table 3 summarizes these experiments with the initial hydrogen peroxide concentration used. After regularly measuring the concentrations of P and R through every experiment, and according to Equation (3), values of ln $([P]_0/[P]_t)$ vs ln $([R]_0/[R]_t)$ were plotted. After linear regression analysis, the slopes k_{OH-P}/k_{OH-R} were deduced, and by using the known value of 5×10^9 L mol^{-1} s^{-1} for k_{OH-R}, the corresponding values of k_{OH-P} were determined and are also shown in Table 3. From both values for each compound, the final average rate constants k_{OH-P} are proposed.

Table 3. Second-order rate constants for the reaction between hydroxyl radicals and each EC. $[P]_0=[p-ClBz\ acid]_0=1\ \mu M$, $[Fe^{2+}]_0=50\ \mu M$, T=20 °C, pH=3.

ECs	Exp.	$[H_2O_2]_0$ (μM)	k_{OH-P}/k_{OH-R}	$k_{OH-P} \times 10^{-9}$ (L mol^{-1} s^{-1})	$k_{OH-P} \times 10^{-9}$ (L mol^{-1} s^{-1})
1-H-benzotriazole	FBZ-1	10	1.64	8.21	8.24 ± 0.04
	FBZ-2	50	1.65	8.27	
Chlorophene	FCF-1	10	1.72	8.61	8.47 ± 0.19
	FCF-2	50	1.67	8.34	
DEET	FDT-1	10	1.49	7.46	7.51 ± 0.07
	FDT-2	50	1.51	7.56	
3-methylindole	FML-1	10	1.04	5.20	5.57 ± 0.53
	FML-2	50	1.19	5.95	
Nortriptyline·HCl	FNH-1	10	2.16	10.82	10.87 ± 0.08
	FNH-2	50	2.19	10.93	

3.2. Photochemical oxidation of ECs mixtures in different water matrices.

Influence of independent variables

The photolysis of mixtures of the selected pollutants (initial concentrations of 1µM for each compound) dissolved in different types of waters was carried out at T=20 °C and the natural pH of each water (see Table 2). As was noted in Materials and Methods Section, these water matrices were: ultra-pure water (UP), reservoir water (PA), and two secondary effluents from municipal WWTPs (BA and LA). The photodegradation process was conducted by using UV radiation alone, and UV radiation combined with two different concentrations of H_2O_2 (1×10^{-5} and 5×10^{-5} M) in order to generate hydroxyl radicals.

Figure 1 shows the decrease of BZ and ML concentrations with reaction time in experiments carried out with UV radiation alone and in combination with hydrogen peroxide in PA water, with similar results for the rest of compounds and waters. It is clearly observed the expected positive effect of the combined UV/H_2O_2 system in comparison to the photodegradation by UV radiation alone. Moreover, the greater initial concentration of H_2O_2 when using the combined UV/H_2O_2 process provided a higher disappearance rate.
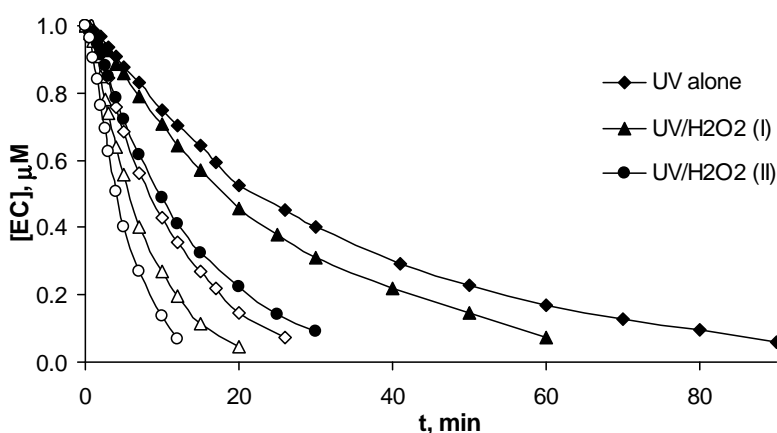
Figure 1. Evolution of concentrations in the photodegradation of BZ (black symbol) and ML (white symbols) in PA water by UV and UV/H_2O_2 systems. Influence of the type of degradation process. (I):$[H_2O_2]_0 = 1 \times 10^{-5}$ M. (II):$[H_2O_2]_0 = 5 \times 10^{-5}$ M.

Similarly, it is interesting to establish the influence of the nature of the ECs on the photodegradation rate. Thus, Figure 2 shows the degradation curves for the five compounds in the photodegradation by the UV/H_2O_2 combination (with the initial hydrogen peroxide concentration of 5×10^{-5} M) in BA water, taken as example. As it is seen, DT presented the lowest elimination rate, while CF reached the highest elimination rate, with similar results in the remaining water systems tested. In general terms, this disappearance rate sequence obtained completely agrees with the sequence of quantum yields for CF, ML and DT during the individual photodegradation of these ECs in UP water. However, there is an exception for NH and BZ: in effect, NH presented a slightly higher disappearance rate than BZ, while the quantum yields presented the inverse order: 29×10^{-3} mol Einstein^{-1} for BZ and 14×10^{-3} mol Einstein^{-1} for NH. This result can be explained by taking into account that the elimination rate in the UV/H_2O_2 combined process is the result of two contributions: direct photolysis and radical pathway. In the specific case of NH, its quantum yield (direct photolysis) is lower than that of BZ as mentioned before; however, its radical rate constant (radical pathway) is higher than that of BZ (10.87×10^9 L mol^{-1} s^{-1} *vs.* 8.24×10^9 L mol^{-1} s^{-1}, see Table 3). Therefore, it can be assumed that there is a more significant contribution of the radical pathway in the global elimination rate of NH than in the case of BZ.
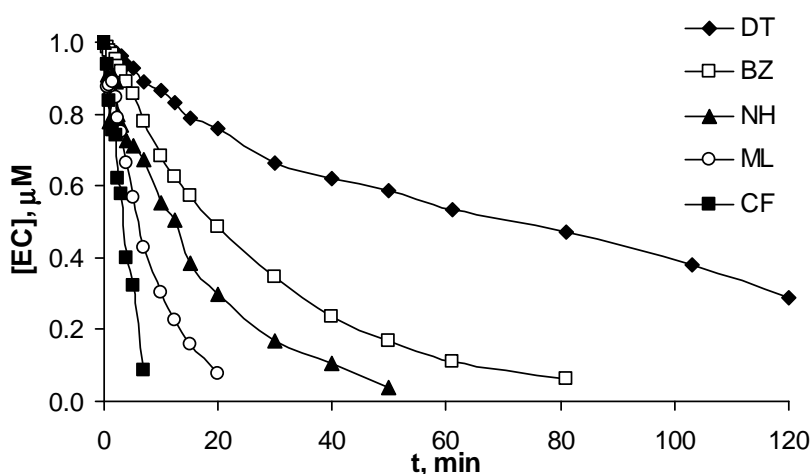
Figure 2. Evolution of concentrations in the photodegradation of ECs in BA water by UV/H_2O_2 system ([H_2O_2]$_0$=5×10^{-5}M). Influence of the nature of the selected compounds.

Finally, the effect of the water matrix nature on the ECs decomposition is shown in Figure 3, where the elimination curves of BZ, taken as example, are plotted *vs.* reaction time in experiments performed with the UV/H₂O₂ system ($[H_2O_2]_0=1 \times 10^{-5}$ M). It can be observed the fastest degradation in UP water, followed by PA and LA waters with similar rates, and the slowest elimination in BA water. Similar results were obtained for the remaining ECs with both, UV radiation alone and combined with H_2O_2, with the two initial concentrations.

As expected, the highest rates of ECs removal were obtained in UP water, which is due to the almost total absence of organic and inorganic matters that could consume radiation and hydroxyl radicals. On the contrary, in the lake water and wastewaters, with some organic compounds and bicarbonate ion content, the OH radical concentration available to react with the pollutants is smaller, and therefore, a lower degradation rate was obtained. Consequently, higher doses of oxidants are required for the removal of pollutant substances in natural water matrices. These results are confirmed by the measured absorbances at 254 nm of these waters, which were: 0.0, 0.041, 0.187 and 0.245 for UP, LA, PA, and BA respectively. It indicates that ECs and hydrogen peroxide are competing with the organic matter present for the absorption of UV. Particularly, more UV radiation is available for the oxidation of ECs and hydrogen peroxide in UP water, with the lowest absorbance value.
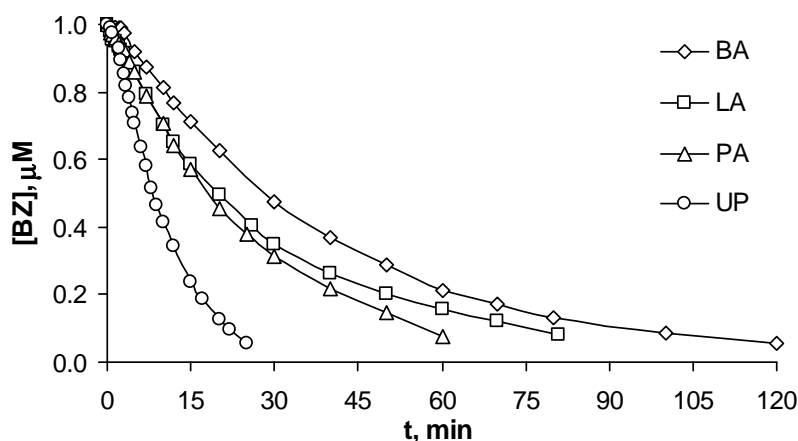
Figure 3. Evolution of concentrations in the photodegradation of BZ in different water matrices by the combination UV/H₂O₂ ($[H_2O_2]_0=1 \times 10^{-5}$ M). Influence of the water matrix.

Modeling and prediction of the ECs mixtures elimination

The following kinetic study was performed with the main goal of determining several rate constants for one specific substance (taken as reference compound); and later, to predict and model the photodegradation rate of some pollutants (specifically, the selected ECs) in a mixture of organic contaminants that could be present in any kind of water. These pollutant substances may be simultaneously photodegraded in a general purification process by each one of the oxidant systems used in the present work (UV radiation alone or combined with H_2O_2). The final objective of this study will be the theoretical evaluation of the concentration profile for each compound at any reaction time.

The kinetic model for the photodegradation process to be used has been proposed and described elsewhere (Staehelin and Hoigne, 1985) and is based on two initial conditions. Firstly, the overall degradation of each substance in a mixture by any combination of oxidants is the result of the contribution of two individual reaction pathways: direct photochemical reaction and radical reaction, the latest being the result of the reaction between the selected substance and hydroxyl radicals generated in the UV/H_2O_2 system. And secondly, in the oxidation of these mixtures, one of the substances is considered as a reference compound R, with known degradation rate constants; and the remaining substances are considered as target compounds P, with unknown rate constants. This procedure is reliable when measuring the rates of fast reactions in aqueous solutions, with overall second-order kinetics, and first-order with respect to both reactants (Staehelin and Hoigne, 1985; Peijnemburg et al., 1992).

With these conditions, the following rate Equation for the elimination of the reference compound is established by the referred kinetic model:

$$\ln \frac{[R]_o}{[R]} = k'_R\, t = \ln \frac{[R]_0}{[R]}\bigg|_d + \ln \frac{[R]_0}{[R]}\bigg|_r = (k'_{\phi-R} + k'_{OH-R})\, t \qquad (4)$$

where k'_R, $k'_{\phi-R}$ and k'_{OH-R} are the apparent first-order rate constants for the overall photodecomposition, the direct photochemical decomposition (subscript d) and the radical decomposition (subscript r) reactions, respectively. These rate constants are unknown and

must be evaluated for the selected reference compound. Similarly, the decomposition rate for any target compound can be expressed in the form reactants (Staehelin and Hoigne, 1985):

$$\ln \frac{[P]_o}{[P]} = k'_P \, t = \frac{\Phi_P \, \varepsilon_P}{\Phi_R \, \varepsilon_R} k'_{\Phi\text{-}R} \, t + \frac{k_{OH\text{-}P}}{k_{OH\text{-}R}} k'_{OH\text{-}R} \, t \qquad (5)$$

where k′$_P$ is the first-order rate constant for the overall decomposition reaction, which can be evaluated as a function of ϕ_P and ε_P, and ϕ_R and ε_R (quantum yields and molar extinction coefficients for the target and reference compounds, respectively); k$_{OH\text{-}P}$ and k$_{OH\text{-}R}$ are the true second-order rate constants for the radical reaction between OH radicals and the target and the reference compounds, respectively; and k′$_{\phi\text{-}R}$ and k′$_{OH\text{-}R}$ are the already mentioned apparent rate constants for the reference compound.

Once the kinetic rate constants (k′$_{\phi\text{-}R}$ and k′$_{OH\text{-}R}$) that characterize the photodegradation of a reference compound in a specific water are known, the overall rate constant k′$_P$ for any target compound in that water matrix can be evaluated if the quantum yields ϕ_R and ϕ_P, molar extinction coefficients ε_R and ε_P, and rate constants with OH radicals k$_{OH\text{-}R}$ and k$_{OH\text{-}P}$ are previously known for both, the reference and the target compounds. And with the value of k′$_P$, the concentration of P at any reaction time can also be theoretically predicted by using that Equation (5).

The described model is used in the present study, being NH selected as the reference compound R because of its intermediate oxidation rate. Then, and according to Equation (4), plots of ln ([R]$_o$/[R]) *vs* reaction time for NH photolysis experiments gave straight lines, and after regression analysis, the rate constants k′$_R$ were deduced, and their values are compiled in Table 4.

On one hand, the contribution of the radical pathway to the overall reaction can be neglected in the photodegradation experiments by UV radiation alone, and consequently, in these single photolysis experiments, it is deduced from Equation (4) that k′$_{OH\text{-}R}$=0, and k′$_R$=k′$_{\phi\text{-}R}$. Later, the radical pathway rate constant k′$_{OH\text{-}R}$ in experiments performed with both UV/H$_2$O$_2$ with different initial concentrations of H$_2$O$_2$ can be

determined by subtracting the rate constant $k'_{\phi-R}$ from the overall rate constants k'_R, values which are also summarized in Table 4 for NH. As it is expected, the experiments with higher initial hydrogen peroxide concentration provided higher values for k'_{OH-R}, as a consequence of a greater generation of hydroxyl radicals.

Table 4. First-order rate constants obtained for the reference compound (NH) in the selected water matrices. $[NH]_0=1\mu M$, T=20 °C.

Water matrix	$k'_R x10^{3\ (1)}$ min^{-1}	$k'_R x10^{3\ (2)}$ min^{-1}	$k'_{OH-R} x10^{3\ (2)}$ min^{-1}	$k'_R x10^{3\ (3)}$ min^{-1}	$k'_{OH-R} x10^{3\ (3)}$ min^{-1}
UP	86.5	100.4	13.9	255.2	168.7
PA	48.6	62.0	13.4	96.4	47.8
LA	52.8	57.1	4.3	68.4	15.6
BA	46.7	49.3	2.6	60.5	13.8

(1) Experiments with UV radiation alone, and therefore, $k'_R x10^3 = k'_{\phi-R} x10^3$.
(2) Experiments with UV/H_2O_2 system: $[H_2O_2]_0 = 10\ \mu M$.
(3) Experiments with UV/H_2O_2 system: $[H_2O_2]_0 = 50\ \mu M$.

Later, the elimination of the remaining ECs in the mixtures can be theoretically predicted by using Equation (5), on the basis that several parameters contained in that Equation (5) are perfectly known in advance. In effect, ε_R and ε_P were determined and are provided in Experimental and methods Section, while the quantum yields ϕ_R and ϕ_P were evaluated for each compound and are already reported: $\phi_R = 14x10^{-3}$ mol Einstein^{-1} for NH; and $\phi_P = 429x10^{-3}$, $105x10^{-3}$, $29x10^{-3}$, and $1.2x10^{-3}$ mol Einstein^{-1} for CF, ML, BZ, and DT respectively. Finally, the second-order rate constants for the reaction between each compound and OH radicals (*i.e.*, k_{OH-R} for NH, and k_{OH-P} for the rest of the substances) were also previously evaluated and compiled in Table 3. With all these parameters previously known, the application of Equation (5) to the four remaining target compounds provided the k'_P rate constants, which are summarized in Table 5. Once again, higher oxidation rates were obtained with the UV/H_2O_2 system with $[H_2O_2]_0 = 5x10^{-5}$M, as a consequence of an increasing generation of hydroxyl radicals with a greater contribution of the radical reaction pathway.

Table 5. Calculated values obtained for the first order rate constants for benzotriazole, chlorophene, DEET and methylindole. $[P]_0=1\mu M$, T=20 °C.

Compounds	Water matrix	k'_P x 10^3 [1], min^{-1}	k'_P x 10^3 [2], min^{-1}	k'_P x 10^3 [3], min^{-1}
1-H-benzotriazole	UP	45.1	55.6	172.6
	PA	25.3	35.5	61.4
	LA	27.5	30.8	39.3
	BA	24.3	26.3	34.8
Chlorophene	UP	514.2	525.0	645.3
	PA	288.9	299.4	326.1
	LA	313.8	317.1	325.9
	BA	277.6	279.6	288.3
DEET	UP	1.8	11.4	118.1
	PA	1.0	10.2	33.9
	LA	1.1	4.1	11.9
	BA	1.0	2.8	10.5
3-methylindole	UP	258.5	265.6	344.7
	PA	145.3	152.1	169.7
	LA	157.8	159.9	165.7
	BA	139.6	140.9	146.6

(1) Experiments with UV radiation alone, and therefore, $k'_R x10^3 = k'_{\phi-R} x10^3$.

(2) Experiments with UV/H₂O₂ system: $[H_2O_2]_0=10$ μM.

(3) Experiments with UV/H₂O₂ system: $[H_2O_2]_0=50$ μM

In order to check the utility of Equations (4) and (5), and the proposed model, Figure 4 shows, as examples, the concentration decay curves of BZ, DT, ML and CF predicted theoretically (lines) and the experimental values (symbols) obtained during the treatment of the PA water by UV radiation combined with H_2O_2 (1×10⁻⁵ M) (Figure 4a), and the same curves corresponding to the ECs concentration in the BA water when treated with the combination UV/H₂O₂ (5×10⁻⁵ M) (Figure 4b). Similar plots were obtained for the other waters and oxidation systems.
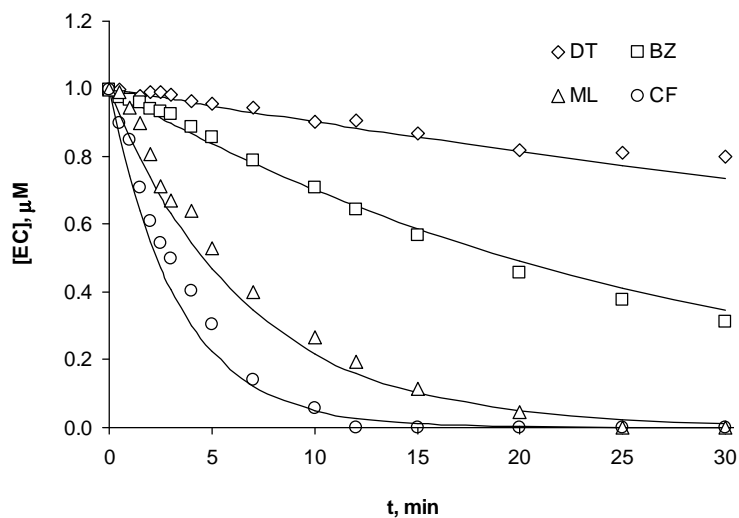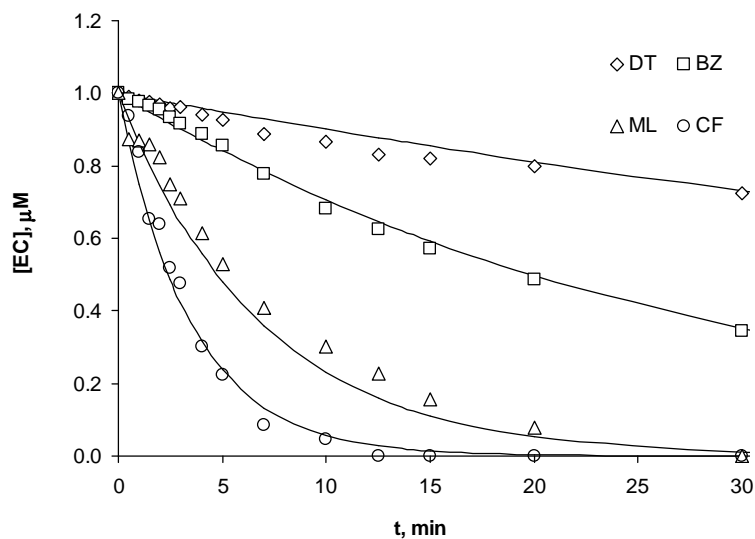
Figure 4. Comparison of the predicted (lines) and experimental (symbols) concentrations of the target compounds. 4a) Reservoir water (PA), UV/H$_2$O$_2$ system ([H$_2$O$_2$]$_0$=1x10^{-5} M). 4b) Effluent from WWTP (BA), UV/H$_2$O$_2$ system ([H$_2$O$_2$]$_0$=5x10^{-5} M).

A very satisfactory agreement between the predicted and experimental values can be appreciated, with deviations lower than 5% in all cases, confirming the goodness of the proposed model. Then, it can be concluded that the proposed kinetic approach permits the

prediction of the elimination rate for micropollutants (ECs compounds in the present study) in any kind of water during photochemical treatments, by conducting a reduced set of experiments with the selected water matrix in the presence of a reference compound, and by the application of UV radiation alone and the combination UV/H₂O₂.

4. CONCLUSIONS.

The results of the photodegradation processes, by UV radiation alone and the combined UV/H₂O₂ system, of the five emerging contaminants selected (1-H-benzotriazole, N-diethyl-m-toluamide or DEET, chlorophene, 3-methylindole, and nortriptyline HCl) allowed the following conclusions to be drawn:

i. The single photolysis process of the ECs in UP water, evaluated by the quantum yields, revealed the following sequence of degradation: CF > ML > BZ > NH > DT.

ii. The use of Fenton´s reagent applied to the oxidation of these ECs, and a competition kinetics method, allowed the determination of the rate constants for the radical reaction between each compound and the hydroxyl radicals, the values obtained being: $8.24 \times 10^{9}\,mol^{-1}\,L\,s^{-1}$ for BZ; $8.47 \times 10^{9}\,mol^{-1}\,L\,s^{-1}$ for CF; $7.51 \times 10^{9}\,mol^{-1}\,L\,s^{-1}$ for DT; $5.57 \times 10^{9}\,mol^{-1}\,L\,s^{-1}$ for ML, and $10.87 \times 10^{9}\,mol^{-1}\,L\,s^{-1}$ for NH.

iii. In the simultaneous photodegradation of mixtures of these ECs in different water matrices (UP water, reservoir water, and two effluents from WWTPs), a positive effect of the combined UV/H₂O₂ system in comparison to the photodegradation by UV radiation alone is deduced. Additionally, the higher initial concentration of H₂O₂ in the combined UV/H₂O₂ process yielded a greater disappearance rate.

iv. In these systems, a higher oxidation rate was found in the UP water, followed by PA and LA waters with similar rates, and the slowest elimination in the BA water, this sequence being consistent with their relative organic matter contents.

v. A kinetic model is proposed for the prediction of the elimination of ECs in any type of water, using some of the basic parameters determined previously (radical rate constants and quantum yields). The concentrations predicted with this model agreed well with the experimental results, indicating that the model could be useful for the prediction of ECs removal in water purification plants.

REFERENCES

Barcelo, D. Emerging pollutants in water analysis. Trends Anal. Chem. **2003**, 22, 14-16.

Boehmer, W.; Ruedel, H.; Wenzel, A.; Schröeter-Kermani, C. Retrospective Monitoring of Triclosan and Methyl-triclosan in Fish: Results from the German Environmental Specimen Bank. Organohalogen Comp. **2004**, 66, 1489-1494.

Camacho-Munoz, M.D.; Santos, J.L.; Aparicio, I.; Alonso, E. Presence of pharmaceutically active compounds in Donana Park (Spain) main watersheds. J. Hazard. Mater. **2010**, 177, 1159-2116.

Carlson, J.R.; Yokoyama, M.T.; Dickinson, E.O. Induction of pulmonary edema and emphysema in cattle and goats with 3-methylindole. Science **1972**, 176, 298-299.

Costanzo, S.D.; Watkinson, A.J.; Murby, E.J.; Kolpin, D.W.; Sandstrom, M.W. Is there a risk associated with the insect repellent DEET (N,N-diethyl-mtoluamide) commonly found in aquatic environments? Sci. Total Environ. **2007**, 384, 214-220.

Davis, L.N.; Santodonato, J.; Howard, P.H.; Saxena, J. Investigations of selected potential environmental contaminants: benzotriazoles. Office of Toxic Substances, USEPA, EPA Document 560, **1997**/277001.

Fatta-Kassinos, D.; Meric, S.; Nikolaou, A. Pharmaceutical residues in environmental waters and wastewater: current state of knowledge and future research. Anal. Bioanal. Chem. **2011**, 399, 251-275.

Hansen, P.D. Risk assessment of emerging contaminants in aquatic systems. Trends Anal. Chem. **2007**, 26, 1095-1099.

Jornil, J.; Jensen, K.G.; Larsen, F.; Linnet, K. Risk assessment of accidental nortriptyline poisoning: The importance of cytochrome P450 for nortriptyline elimination investigated using a population-based pharmacokinetic simulator. Eur. J. Pharm. Sci. **2011**, 44, 265-272.

Kim, I.; Yamashita, N.; Tanaka, H. Photodegradation of pharmaceuticals and personal care products during UV and UV/H$_2$O$_2$ treatments. Chemosphere **2009**, 77, 518-525.

Kolpin, D.W.; Skopec, M.; Meyer, M.T.; Furlong, E.T.; Zaugg, S.D. Urban contribution of pharmaceuticals and other organic wastewater contaminants to streams during differing flow conditions. Sci. Total Environ. **2004**, 328, 119-130.

Langford, K.H.; Thomas, K.V. Determination of pharmaceutical compounds in hospital effluents and their contribution to wastewater treatment works. Environ. Int. **2009**, 35, 766-770.

Legrini, O.; Oliveros, E.; Braun, A.M. Photochemical processes for water treatment. Chem. Rev. **1993**, 93, 671-698.

Loos, R.; Gawlik, B.M.; Locoro, G.; Rimaviciute, E.; Contini, S.; Bidoglio, G. EU wide survey of polar organic persistent pollutants in European river waters. Environ. Pollut. **2009**, 157, 561-568.

Rosenfeldt, E.J.; Linden, K.G.; Canonica, S.; von Gunten, U. Comparison of the efficiency of ·OH radical formation during ozonation and the advanced oxidation processes O$_3$/H$_2$O$_2$ and UV/H$_2$O$_2$. Water Res. **2006**, 40, 3695-3704.

Sills, R.C.; Hailey, J.R.; Neal, J.; Boorman, G.A.; Haseman, J.K.; Melnick, R.L. Examination of low incidence brain tumor responses in F344 rats following chemical exposures in national toxicology program carcinogenicity studies. Toxicol. Pathol. **1999**, 27, 589-599.

Stackelberg, P.E.; Furlong, E.T.; Meyer, M.T.; Zaugg, S.D.; Henderson, A.K.; Reissman, D.B. Persistence of pharmaceutical compounds and other organic wastewater contaminants in a conventional drinking-water-treatment plant. Sci. Total Environ. **2004**, 329, 99-113.

Stuart, M.; Lapworth, D.; Crane, E.; Hart, A. Review of risk from potential emerging contaminants in UK groundwater. Sci. Total Environ. **2012**, 416, 1-21.

Tisch, M.; Schmezer, P.; Faulde, M.; Groh, A.; Maier, H. Genotoxicity studies on permehtrin, DEET and diazinon in primary human nasal mucosal cells. Eur. Arch. Oto-rhino-l. **2002**, 259, 150-153.

Voutsa, D.; Hartmann, P.; Schaffner, C.; Giger, W. Benzotriazoles, alkylphenols and bisphenol A in municipal wastewaters and in the River Glatt Switzerland. Environ. Sci. Pollut. Res. **2006**, 13, 333-341.

Wenhui, L.; Xinghai, L.; Dongyan, L.; Lei, S.; Qi, S. Vapor-Phase Synthesis of 3-Methylindole over Fe-, Co-, or Ni-Promoted Ag/SiO$_2$. Chin. J. Catal. **2009**, 30, 1287-1290.

Yamarik, T.A. Safety assessment of dichlorophene and chlorophene. Int. J. Toxicol. **2004**, 23, 1-27.

Yuan, F.; Hu, C.; Hu, X.; Qu, J.; Yang, M. Degradation of selected pharmaceuticals in aqueous solution with UV and UV/H$_2$O$_2$. Water Res. **2009**, 43, 1766-1774.

3.4. Chlorination and bromination kinetics of emerging contaminants in aqueous systems.

3.4. CHLORINATION AND BROMINATION KINETICS OF EMERGING CONTAMINANTS IN AQUEOUS SYSTEMS

Juan L. Acero, F. Javier Benítez, Francisco J. Real, Gloria Roldan, Elena Rodríguez.

Departamento de Ingeniería Química, Universidad de Extremadura, Badajoz.

Second-order rate reaction constants of micropollutants with chlorine are essential for evaluating their removal efficiencies from water during chlorine disinfection. In this study, the reactions of five selected emerging contaminants with unavailable kinetic data (benzotriazole, N, N-diethyl-m-toluamide or DEET, chlorophene, 3-methylindole, and nortriptyline HCl) with chlorine and bromine have been investigated, and their apparent second-order rate constants have been determined as a function of the pH. For the chlorination process, the intrinsic rate constants for the elementary reactions of the ionized and neutral species were also evaluated. The sequence of reaction rates was methylindole > chlorophene > nortriptyline HCl > benzotriazole > DEET. The bromination of the selected emerging contaminants in ultrapure water provided exactly the same sequence of reaction rates as in the chlorination process, although higher values of rate constants. The efficiency of the chlorination process for the degradation of these ECs when present in several aqueous systems (surface water from a public reservoir, and two effluents from municipal wastewater treatment plants) was investigated. During wastewater or drinking water treatment, chlorine is a good option for the degradation of methylindole, and in a lower extent for chlorophene and nortriptyline. However, it is not a suitable oxidant for the abatement of benzotriazole and DEET. Finally, chlorination in the presence of bromide revealed that low bromide concentrations enhanced slightly the degradation of the selected compounds during chlorine oxidation.

1. INTRODUCTION.

Chemical oxidants are commonly used in water treatments because of their potential for destruction of micropollutants. Some of the oxidation systems include UV radiation, ozonation, and advanced oxidation processes (AOPs), such as O_3/H_2O_2, UV/H_2O_2 or Fenton's reagent. Most of these AOPs have demonstrated high effectiveness in the degradation of organic compounds present in water systems which are oxidized to readily biodegradable and less toxic compounds (Wols et al., 2012)]. Although less reactive than ozone, chlorine (Cl_2) as gaseous chlorine or hypochlorite has also been frequently used in water treatments (Sharma, 2008; Deborde and von Gunten, 2008). Chlorine hydrolyzes in water and forms hypochlorous acid:
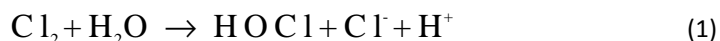
$$Cl_2 + H_2O \rightarrow HOCl + Cl^- + H^+ \qquad (1)$$

Moreover, hypochlorous acid is a weak acid that dissociates in aqueous solutions:

$$HOCl \Leftrightarrow ClO^- + H^+ \qquad (2)$$

This equilibrium presents a dissociation constant $K_{HOCl}=2.9x10^{-8}$ (pK_a=7.54 at 25 °C). In the pH range 6-9 (typical of water treatment conditions), hypochlorous acid and hypochlorite are the main chlorine species present (Deborde and von Gunten, 2008). Besides its low cost, the great advantage of chlorine is the reaction with numerous inorganic and organic micropollutants present in waters. However, its main disadvantage is the formation of possible harmful disinfection by-products (DBPs), such as halogenated organic compounds, some of which exhibit a potentially carcinogenic activity (trihalomethanes (THMs) and haloacetic acids (HAAs)) (Bougeard et al., 2010).

Although in a minor extent than chlorination, the involvement of bromination reactions in the oxidation of water pollutants has also deserved an increasing interest, especially in waters with a high bromide (Br^-) content (Lee and von Gunten, 2009). In general, the oxidation of bromide with chlorine leads to the formation of aqueous bromine (HOBr + OBr$^-$) (Deborde and von Gunten, 2008):

$$HOCl + Br^- \rightarrow HOBr + Cl^- \qquad k=1.55x10^3 \, M^{-1} \, s^{-1} \qquad (3)$$
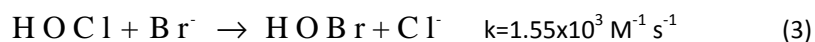
At the same time, the dissociation equilibrium HOBr/OBr⁻ presents a pK_a value of 8.9, which indicates that HOBr is a weaker acid than HOCl.

Recently, an increasing attention has been paid to a wide group of numerous chemical substances, including prescription and therapeutic drugs, veterinary drugs, dietary supplements, consumer products such as fragrances, topical agents such as cosmetics and sunscreens, laundry and cleaning products, etc. (Bolong et al., 2009). All of them constitute the so-called group of the emerging contaminants (ECs), since they are still unregulated or in the process of being regulated. ECs are not entirely metabolized, and consequently, they are excreted to water effluents and later have to be treated into municipal wastewater treatment plants. However, several studies have revealed that they are not removed quantitatively in conventional water treatment processes (Bolong et al., 2009; Ikehata et al., 2008). Consequently, they can be found in secondary effluents and in surface waters (Nakada et al., 2007; Yang et al., 2011). As these aquatic streams could be latter used as drinking water source, ECs constitute a potential risk for human health, since they can cause unexpected physiological consequences.

According to the increasing interest in the chlorination and bromination of pollutants in waters, the degradation of five frequently found ECs in water systems by means of chlorine and bromine has been investigated. The ECs selected (structures shown in Figure 1) were: benzotriazole (BZ), a well known corrosion inhibitor for copper or silver material, widely used in cooling and hydraulic fluids, anti-freezing products, aircraft deicer and anti-ice fluid, and dishwasher detergents (Loos et al., 2009); N,N-diethyl-m-toluamide or DEET (DT), an active compound in insect repellents, and largely used for more than 50 years for protection against insect bites (Constanzo et al., 2007); chlorophene (CF), a widespread broad-spectrum antimicrobial pharmaceutical, used in hospitals and households for general cleaning and as active agent in disinfectant formulations (Boehmer et al., 2004); 3-methylindole (ML), used as perfume and synthesizing anti-inflammatory drug, antibiotic, dye, plant growth hormone, herbicide, muscular relaxant, respiratory inhibitor and heart stimulant medicaments (Wenhui et al., 2009); and the pharmaceutical nortriptyline HCl (NH), which belongs to the group of tricyclic antidepressants (TCAs), and used in treatments against depression since its introduction around 50 years ago (Langford

et al., 2009). To the best of our knowledge, the kinetics of chlorination and bromination of these compounds has not been investigated.

Therefore, the reactions in ultra-pure (UP) water of these compounds with aqueous chlorine and bromine were investigated with the objective of determining the unknown apparent rate constants as a function of the pH. In the case of chlorine, the influence of pH on the calculated rate constants was established, and the intrinsic rate constants for the elementary reactions were evaluated. The following objective was to establish the efficiency of the chlorination process for the degradation of these ECs when present in several aqueous systems (a reservoir water, and two secondary effluents from two municipal wastewater treatment plants (WWTP)) and to assess the formation of THM as the main disinfection by-products. In addition, a reaction model that predicts the degradation of these ECs with the use of the previously determined rate constants has been proposed and validated. Finally, chlorination experiments were performed in the presence of low bromide concentrations to study the effect of bromide on the fate of ECs during water chlorination.

2. MATERIALS AND METHODS.

2.1. ECs and water matrices.

The selected ECs and the reference compounds were purchased of the highest purity available (Sigma-Aldrich, Germany). The chemicals used for the solutions (eluents and buffers) were of reagent grade, and also from Sigma-Aldrich. In contrast, the water matrices used were a natural water (PA) collected from the public reservoir lake "Peña del Aguila", located in the Extremadura Community, SW Spain; and two secondary effluents (BA and LA) from WWTPs corresponding to the cities of Badajoz and La Albuera, in the same Extremadura Community. These waters were analyzed for a variety of general water quality parameters, such as pH, total organic carbon (TOC), absorbance at 254 nm ($UV_{254 \, nm}$), chemical oxygen demand (COD), alkalinity, conductivity, ammonia, total nitrogen, total phosphorus and bromide (Clesceri et al., 1989). After replicated analysis, the average values

depicted in Table 1 were measured. This data revealed that the sequence of the dissolved organic matter (DOM) content was: BA > PA > LA.

Table 1. Characterization of the selected water matrices.

	PA	LA	BA
pH	7.4	7.9	8.3
TOC (mg L^{-1})	5.17	2.86	11.09
UV$_{254\ nm}$ absorbance	0.187	0.041	0.245
COD (mg L^{-1})	18	7	56
Alkalinity (mg CaCO$_3$ L^{-1})	30	335	325
Conductivity (μS)	80.2	570	550
NH$_4^+$-N (mg L^{-1})	0.08	0.16	5.79
Total nitrogen (mg L^{-1})	1.51	21.3	35.5
Phosphorus (mg L^{-1})	0.041	0.156	1.76
Bromide (μg L^{-1})	n.d.	330	n.d.

n.d.: not determined

2.2. Experimental procedures.

In a first stage, experiments were carried out to determine the individual chlorination rate constants of each selected EC in UP water. For this purpose, chlorine stock solutions (0.01 M) were prepared by diluting a commercial solution of sodium hypochlorite (Panreac, nominally 10% w/w chlorine). At the same time, stock solutions of each compound (1x10^{-4} M) were also prepared by dissolving them in UP water, which was produced from a Milli-Q (Millipore) water purification system. As the reactivity towards chlorine of the five selected ECs was quite different, two types of experiments were conducted according to the specific reaction rate of these substances: a first group of experiments called "slow reactions", which corresponded to CF, NH, BZ and DT, as a consequence of their lower reaction rates with chlorine; and a second group of experiments called "fast reactions", which corresponded to ML because of its higher reaction rate towards chlorine.

The "slow reactions" experiments were carried out under first-order conditions, with chlorine added in excess (at least twenty-fold) with respect to the EC. A certain volume of the chlorine stock solution was added to a 250 mL flask reactor containing 200 mL of the EC solution (1 µM) at the desired temperature and pH (adjusted by using a phosphoric acid/phosphate buffer 10 mM). At regular reaction times, 2 mL samples were taken from the reactor and rapidly transferred into HPLC vials containing 10 µL of sodium thiosulfate (0.1 M) to stop the reaction. The residual EC concentration was analyzed directly by HPLC. In the specific case of CF and NH, experiments were performed varying temperature and modifying the initial concentration of chlorine. However, BZ and DT experiments were performed at 20 °C with a constant chlorine concentration.

In the "fast reactions" experiments with ML, the rate constants were determined by applying a competition kinetics method. In the present work, naproxen and orcinol (depending on the pH of the experiment) were selected as references compounds. In these cases, the reference compound was simultaneously dissolved with ML (both 1 µM) in UP water. The experiments were performed in 20 mL flask reactors at a constant temperature of 20 °C. The desired pH was adjusted by means of phosphoric acid/phosphate buffer. Each reaction started by injecting a variable volume of the chlorine stock solution. After complete chlorine consumption, residual concentrations of ML and reference compound were analyzed.

A similar experimental procedure was followed to determine bromination rate constants: the experiments were carried out under first-order conditions for CF, NH, BZ and DT, in which the total bromine concentration was in excess with respect to the EC concentration. However, since the bromination reaction of ML was faster, the experiments were conducted with the additional presence of the reference compound amoxicillin. Previously, a stock solution of bromine was prepared by addition of a 0.8 mM ozone solution to a 0.7 mM solution of potassium bromide at pH=4, according to the procedure described by Pinkernell et al. 2000. This concentrated ozone stock solutions was prepared in advance by bubbling a gas mixture of oxygen-ozone through UP water in a flask placed in an ice bath.

The second stage of this work was focused in the simultaneous degradation of the five selected ECs (1 µM) by chlorine in the water matrices previously described. Two types of experiments were also performed in this stage. In the "static dose", the ECs were dissolved into the waters and the volume of the chlorine stock solution required to achieve the desired initial chlorine concentration (0-5 mg L^{-1}, as typically applied in real water treatment) was injected into the reactor. After sufficient time for complete chlorine consumption (24 h), the residual concentration of ECs and THMs (chloroform, bromodichloromethane, chlorodibromomethane, and bromoform) was analyzed. In the "time dependant" experiments, chlorine (5 mg L^{-1}) was injected in the reaction flask containing the ECs dissolved in the selected water. Samples were regularly taken from the reactor, and the concentration of remaining ECs, total chlorine, free chlorine and chloramines was analyzed.

Finally, chlorination experiments with the three water matrices varying bromide concentration were performed. The experimental conditions were pH=7, 20 °C, initial chlorine dose of 70 µM (5 mg L^{-1}), and a bromide dose in the range 0–3.75 µM (0–300 µg L^{-1}), values typically found in real waters. Residual concentration of ECs was determined in these samples after total chlorine consumption (24 h).

2.3. Analytical Methods.

The concentration of ECs in each sample was determined by HPLC, using a Waters Chromatograph equipped with a 996 Photodiode Array Detector and a Phenomenex Gemini C18 Column (5µm, 150mm×3mm). The mobile phase was a mixture of water/acetonitrile with formic acid (2.5x10^{-2} M) in gradient mode at a flow rate of 0.2 cm^3 min^{-1}. Detection was performed at 250 nm for BZ, NH, and DT; and 280 nm for ML and CF. Similarly, the concentration of the reference compounds was also evaluated by HPLC, being the detection performed at 250 nm for naproxen and amoxicillin, and 280 nm for orcinol. THMs were measured by gas chromatography (GC System Agilent 6890 Series), using head space injection and electron capture detection (Golfinopoulos et al., 2001). And chlorine and chloramines concentration in real waters was determined spectrophotometrically according

to the ABTS [2,2-azino-bis(3-ethylbenzothiazoline)-6-sulfonic acid diammonium salt] method (Pinkernell et al., 2000).

Bromine stock solution was standardized by direct photometric determination of the hypobromite at 329 nm, and chlorine stock solution was analyzed spectrophotometrically in presence of excess of iodide to form triiodine (ε at 351 nm = 25700 M^{-1} cm^{-1}) according to the procedure described by Bichsel and von Gunten (Bichsel and von Gunten, 1999).

3. RESULTS AND DISCUSSION.

3.1. Kinetics of the reaction between emerging contaminants and chlorine.

The reaction between chlorine and most of inorganic and organic compounds generally follows second-order kinetics, and first-order with respect to both reactants (Deborde and von Gunten, 2008; Lee and von Gunten, 2009; Acero et al., 2010). Therefore, the chlorination rate of the selected ECs can be written in the form:

$$-\frac{d[P]}{dt} = k_{app}[P]_t[Cl_2]_t = k_{obs}[P]_t \tag{4}$$

where $[Cl_2]_t$ is the total concentration of chlorine species (HOCl + ClO$^-$), $[P]_t$ the total concentration of the target EC, by considering the different species present in the solution, and k_{app} is the apparent second-order rate constant. If $[Cl_2]_t$ is in excess with respect to $[P]_t$, the total concentration of chlorine remains almost constant during the reaction and pseudo-first-order kinetics takes place, being k_{obs} the corresponding pseudo first-order rate constant.

As mentioned previously, the first goal of this study was the determination of k_{app} for the chlorination of the selected ECs in UP water at different pH values. Thus, the so-called "slow reactions" experiments for CF, NH, BZ and DT (see Section 2.2) were performed under first-order conditions (i.e. $[Cl_2]_t \gg [P]_t$). In these experiments, and after integration of Equation (4), a plot of $\ln([P]_0/[P])$ vs. reaction time led to a straight line for each experiment ($R^2 > 0.99$), and after linear regression analysis, the values of k_{obs} were deduced. As the $[Cl_2]_t$

remained almost constant during the reaction time, k_{app} was directly determined by dividing the value of k_{obs} by the total initial chlorine concentration. In those cases in which the initial concentration of chlorine was modified, a linear regression analysis of k_{obs} values vs. $[Cl_2]_t$ provided the apparent second-order rate constants.

The values of k_{app} obtained are compiled in the Supporting Information (SI), Table SI1. As observed, CF presented the highest rate constants values at neutral pH, followed by NH, BZ and DT. The highest reactivity of CF was observed at pH around 8, typical of phenolic compounds (Deborde and von Gunten, 2008). Moreover, the chlorination rate constants were evaluated at different temperatures for NH and CF at pH=7, and the values obtained were adjusted to an Arrhenius expression. After regression analysis, the activation energies were calculated to be 23.2 kJ mol^{-1} for NH and 31.9 kJ mol^{-1} for CF. Similar values of activation energy were found in a previous study carried out with different pharmaceutical compounds (Acero et al., 2010).

The so-called "fast reactions" experiments for ML were conducted by following competition kinetics for the determination of k_{app}. The model, described in detail elsewhere (Acero et al., 2010; Dodd et al., 2005), leads to the final expression:

$$\ln \frac{[P]_0}{[P]} = \frac{k_{app}}{k_{app-R}} \ln \frac{[R]_0}{[R]} \tag{5}$$

In this Equation (5), k_{app} and k_{app-R} represents the apparent chlorination rate constants for the target and reference compounds, respectively. As the reactivity with chlorine of the reference compound must be in the same order of magnitude with that of the target compound, naproxen and orcinol were selected as reference compounds, depending on the pH of work. Specifically, the rate constants for these reference compounds were determined and reported by Acero et al. 2010 for naproxen, and Rebenne et al. 1996 for orcinol, and are summarized in Table SI2 for each pH. According to Eq. (5), plots of $\ln([P]_0/[P])$ vs. $\ln([R]_0/[R])$ were conducted, and after regression analysis, the values of k_{app} for ML included in Table 3 were determined. ML presented higher reaction rates than the remaining ECs compiled in Table SI1.

From the results in Tables SI1 and SI2, a strong dependence of k_{app} on the pH for each selected compound is observed. This dependence is represented in Figure 1 where curves with different shape, as a consequence of the different nature of each EC, can be observed. In effect, each substance can dissociate depending on the pH of work, and their several ionized and un-ionized forms present different reactivity towards chlorine.
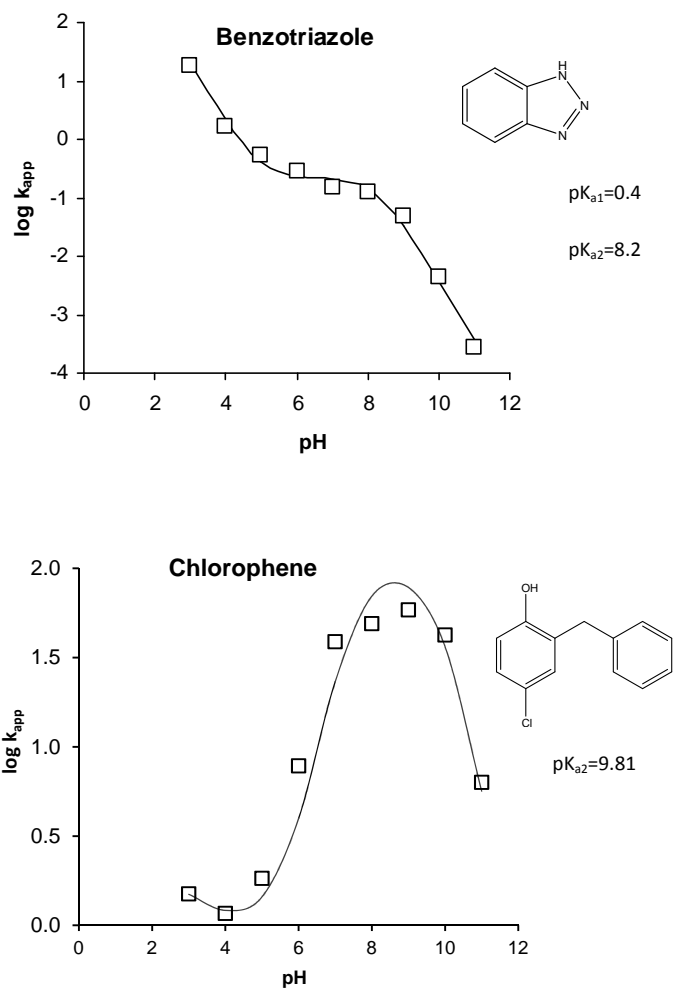
Figure 1. pH dependence of the apparent rate constants for the reactions of chlorine with the selected emerging compounds.
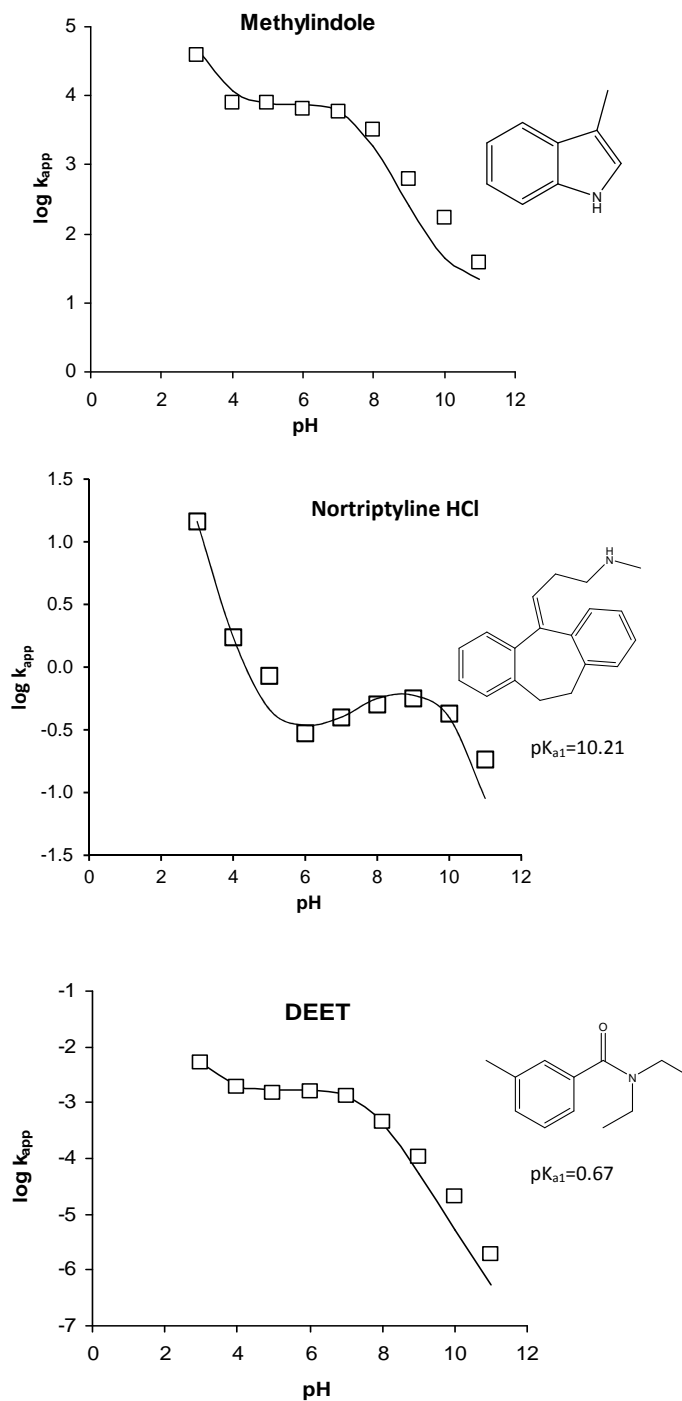
Figure 1 (cont.). pH dependence of the apparent rate constants for the reactions of chlorine with the selected emerging compounds.

Therefore, the next goal was the evaluation of the intrinsic rate constants for the different species present. For this purpose, a global reaction mechanism must be proposed, starting with the different dissociation equilibrium reactions. At this point, it must be taken into account that BZ has two dissociation constants with $pK_{a1}=0.4$ and $pK_{a2}=8.20$:

$$PH_2^+ \xleftrightarrow{ka1} PH + H^+ \tag{6}$$

$$PH \xleftrightarrow{ka2} P^- + H^+ \tag{7}$$

According to Equations (6)-(7), three possible species can be present in solution depending on the pH: PH_2^+, PH, and P^-. On the other hand, NH, CF and DT present one dissociation constant ($pK_{a1}=10.21$ for NH; $pK_{a2}=9.81$ for CF and $pK_{a1}=0.67$ for DT). Consequently, only Equation (6) takes place for NH and DT, and two species are present for each substance: PH_2^+ and PH; and Eq (7) takes place for CF, with PH and P^- species. Finally, ML does not present any pK_a value, and PH is the only specie present in solution.

In addition, the dissociation of hypochlorous acid (reaction 2) must be also taken into account, whose $pK_a=7.54$. Due to the low reactivity of OCl^- compared to HOCl, the reactions with OCl^- were assumed to be negligible (Deborde and von Gunten, 2008), and therefore, only the reactions with HOCl have been considered. These reactions for the species of BZ are:

$$PH_2^+ + HOCl \xrightarrow{k_1} Products \tag{8}$$

$$PH + HOCl \xrightarrow{k_2} Products \tag{9}$$

$$P^- + HOCl \xrightarrow{k_3} Products \tag{10}$$
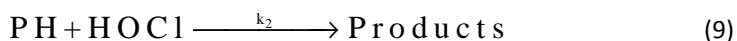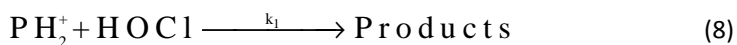
On the contrary, for NH and DT, reaction (10) does not exist, and only reactions (8) and (9) must be taken into account. Similarly, reactions (9) and (10) are applied for CF. In the case of ML only reaction (9) must be considered.

Finally, the whole reaction mechanism must be completed with the acid-catalyzed reaction of HOCl with each emerging contaminant in its protonated form, which is also present in some extent:

$$PH_2^+ + HOCl + H^+ \xrightarrow{\quad k_c \quad} Products \qquad (11)$$
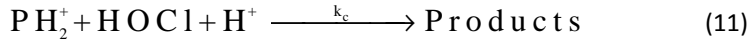
From this reaction mechanism, Equations (6)-(11), the degradation of any compound can be represented by the general equation:

$$\frac{d[P]}{dt} = k_1[PH_2^+][HOCl] + k_2[PH][HOCl] + k_3[P^-][HOCl] +$$
$$+ k_c[PH_2^+]\,[HOCl][H^+] \qquad (12)$$

By equaling Equations (4) and (12), and introducing the equilibrium constants of reactions (2) and (6)-(7), a general equation for k_{app} can be deduced. This equation for the specific case of BZ is:

$$k_{app} = \frac{\left\{k_1[H^+]^2 + k_2K_{a1}[H^+] + k_3K_{a1}K_{a2} + k_c[H^+]^3\right\}\left\{\dfrac{[H^+]}{[H^+] + K_{HOCl}}\right\}}{[H^+]^2 + K_{a1}[H^+] + K_{a1}K_{a2}} \qquad (13)$$

Similarly, the expression for NH and DT is:

$$k_{app} = \frac{\left\{k_1[H^+] + k_2K_{a1} + k_c[H^+]^2\right\}\left\{\dfrac{[H^+]}{[H^+] + K_{HOCl}}\right\}}{[H^+] + K_{a1}} \qquad (14)$$

A similar expression is deduced for CF. Finally for ML, as reactions (6) and (7) do not occur, and only reactions (2), (9) and (11) are applied, the expression for k_{app} is reduced to:

$$k_{app} = \left\{ k_2 + k_c [H^+] \right\} \left\{ \frac{[H^+]}{[H^+] + K_{HOCl}} \right\} \qquad (15)$$

The application of this model allowed the determination of the intrinsic rate constants k_c and k_i (being i=1, 2 and 3). For this purpose, the values of k_{app}, K_{a1}, and K_{a2} were introduced in the proposed equations for each specific substance, as well as $[H^+]$ for each pH. After non-linear least squares regression analysis, the values of the intrinsic rate constants were deduced and are summarized in Table 2. In order to check the results obtained, these intrinsic rate constants were introduced in Equations (13), (14) or (15) (depending on each selected EC), and the k_{app} values were determined. Figure 2 also shows these k_{app} values theoretically evaluated (lines) vs. pH. As observed, there is a quite good agreement between calculations and experimental results, which confirms the goodness of the proposed reaction mechanism.

Table 2. Intrinsic rate constant for the reactions of HOCl with EC species (reactions (8)-(11)), and calculated k_{app} at pH 7.

ECs	k_1, $M^{-1} s^{-1}$	k_2, $M^{-1} s^{-1}$	k_3, $M^{-1} s^{-1}$	k_c, $M^{-2} s^{-1}$	k_{app}, $M^{-1} s^{-1}$
BZ	8000 ± 2000	0.22 ± 0.03	1.20 ± 0.20	< 2 x10^5	0.20
CF		1.15 ± 0.10	19000 ± 3500	340 ± 80	28.4
DT	0.71 ± 0.25	0.0016 ± 0.0003		< 200	1.30x10^{-3}
ML		7500 ± 2000		(4 ± 1)x10^7	5.75x10^3
NH	0.32 ± 0.03	330 ± 30		147000 ± 2000	0.40

a)

b)

c)
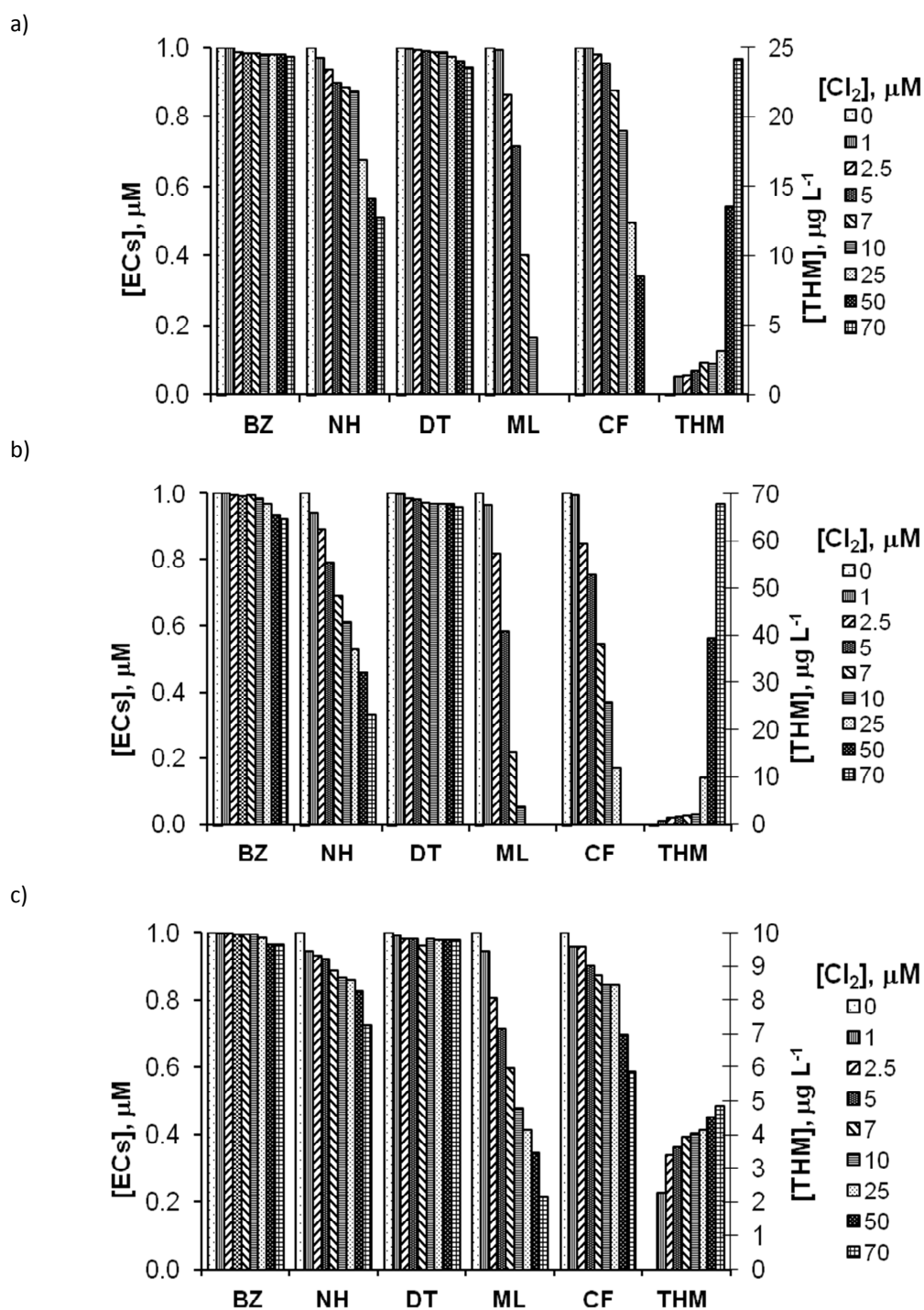
Figure 2. Influence of initial chlorine dose on the ECs oxidation and THMs formation in experiments performed with PA water (a) and the secondary effluents LA (b) and BA (c).

3.2. Kinetics of the reaction between emerging contaminants and bromine.

In a similar way as in the chlorination process, the kinetics of the reaction between the selected ECs and bromine was also investigated in UP water at pH 7, 8 and 9, which is the usual pH range of real water systems. As it has been reported previously, bromination of organic compounds also follows second-order kinetics (Gallard et al., 2003; Acero et al., 2007). Then, and similarly to Equation (4) for the chlorination system, the reaction rate can be written in the form:

$$-\frac{d[P]}{dt}=k_{app}[P]_t[Br_2]_t=k_{obs}[P]_t \tag{16}$$

where $[P]_t$ and $[Br_2]_t$ represent the total concentration of the target compound (ECs) and bromine, respectively; and k_{app} is again the apparent second-order rate constant of the reaction.

In order to determine k_{app} for CF, NH, BZ and DT, experiments were carried out under first-order conditions (initial $[Br_2]_t \gg [P]_t$). Following a similar procedure as with chlorine, the values of k_{app} obtained for the four mentioned compounds are summarized in Table 3. It is interesting to note that these rate constants follow a quite similar trend with the sequence observed in the chlorination reaction: in effect, CF presented the highest values, followed by NH and BZ, whose rate constants were in the same range; and finally, DT presented the lowest rate constants.

Competition kinetics was applied for ML, as a consequence of its higher reaction rate. For this purpose, amoxicillin was selected as reference compound, since its rate constants with bromine are known (Benitez et al., 2011), and are similar to those of ML. This competition kinetics model was described above for the chlorination reaction and leads to the same final Equation (5). Following this procedure, the values of k_{app} obtained for ML are also compiled in Table 3. The results confirm that the reaction rates for ML, with apparent rate constants in the range 10^6-10^8 M^{-1} s^{-1}, were much greater than those of the four remaining ECs.

Table 3. Apparent second-order rate constants (k_{app}) for the reactions of selected ECs with aqueous bromine.

k_{app}, $M^{-1}s^{-1}$				
pH	Nortriptyline HCl	Chlorophene	Benzotriazole	DEET
7	7.42± 0.25	193± 16	8.50± 0.33	0.09± 0.02
8	8.33± 0.36	445± 25	6.42± 0.29	0.03± 0.01
9	11.7± 0.55	790± 46	5.08± 0.24	0.01± 0.01
pH	Reference comp.	$k_{app\text{-}R}x10^{-6}$ (a), $M^{-1}s^{-1}$	Target comp.	$k_{app}x10^{-6}$, $M^{-1}s^{-1}$
7	Amoxicillin	6.71	Methylindole	109± 11
8		58.1		103± 10
9		276		62.2± 5.7

(a) Benitez et al. 2011.

3.3. Chlorination of emerging contaminants in water matrices.

The chlorination of the selected ECs was later studied in the water matrices described in the Experimental Section (i.e. a surface water from a public reservoir PA, and two effluents from municipal wastewater treatment plants, BA and LA). The goal was to investigate the efficiency of chlorination during wastewater and drinking water treatment not only in terms of ECs degradation, but also in terms of disinfection by-products formation, mainly THMs. For this purpose, chlorination experiments were conducted at T=20 °C and natural pH of the waters (in the range pH 7.4-8.3).

Figure 2 shows the results obtained for the three water matrices in experiments carried out in "static dose". Several trends can be clearly observed: firstly, the increase in the initial chlorine dose provided an increase in the degradation of the five ECs, as could be expected. Secondly, the degradation level of each substance in the three water matrices tested was in accordance with the rate constants of the chlorination reaction that were deduced in the preceding Section 3.1 at pH=8 (see Tables S1 and S2): thus, the highest

degradation with the higher chlorine dose (70 μM) was obtained for ML, with a chlorination rate constant at pH=8 of 3210 L mol^{-1} s^{-1}. Intermediate degradation levels were obtained for CF and NH, with chlorination rate constants of 49.0 and 0.50 L mol^{-1} s^{-1}, respectively. Finally, very low degradations, even with the highest chlorine dose, were reached for BZ and DT, consistent with their lower chlorination rates: 0.12 and 3.4x10^{-4} L mol^{-1} s^{-1}, respectively. In relation to the water matrix nature, it is also interesting to remark that the decay in the ECs concentration was higher in LA water, intermediate in PA water, and low in BA water. This trend is in agreement with the organic content of the water matrices measured by the COD and TOC parameters (see values in Table 1). In effect, the higher organic matter content in BA water leads to a lower oxidant exposure for the degradation of the ECs, and subsequently, to a lower decay in the concentration of these substances. On the contrary, the lowest content in organic matter of LA water provides more chlorine available for the oxidation of the ECs. The presence of bromide in LA water could also enhance the degradation of ECs as will be discussed later.

Figure 2 also shows the total concentration of THMs formed in the chlorination process in the three water matrices. The total THMs concentration increased continuously with the increase in the chlorine dose. In addition, it was obtained that the highest chlorine dose of 70 μM provided final THMs concentrations of 68, 24 and 4.8 μg L^{-1} for LA, PA and BA waters respectively. Therefore, for a certain chlorine dose, the formation of THMs was more important in the water with lower DOC. It must be noted that the total THMs concentration was below 100 μg L^{-1} (the maximum value permitted by EU regulations in drinking water). In conclusion, THMs formation is below the minimum EU limit for all the chlorine doses used in this study (0-5 mg·L^{-1} as typically applied in water treatment). It must be noticed that chloroform was the main specie formed in PA and BA waters, followed by bromodichloromethane, while the formation of chlorodibromomethane and bromoform was not significant. On the contrary, the main species generated in the LA water were bromodichloromethane and chlorodibromomethane, as a consequence of the bromide content in this effluent (see Table 1). Therefore, higher bromide levels lead to higher concentrations of brominated DBPs as found previously in the literature (Bougeard et al., 2010).

Another group of chlorination experiments of the selected ECs in the three water systems was carried out by using a constant initial chlorine dose of 5 mg L^{-1} ("time dependant" experiments), in order to establish the changes of the chlorine decay and the formation of chloramines during the chlorination process. The results are compiled in Figure 3 which shows, on one hand, the normalized concentration of free chlorine (free chlorine concentration divided by total initial chlorine dose, being the free chlorine measured as the difference between the concentrations of total chlorine and chloramines formed) vs. reaction time; and on the other hand, the normalized concentration of chloramine (chloramine concentration divided by total initial chlorine dose) vs. reaction time. Regarding to the chlorine concentration changes, a continuous decay in LA and PA waters can be observed, with lower consumption in LA water, as a consequence of its lower organic matter content. In the case of BA, an instantaneous decay was observed, due to its higher organic and inorganic content, and the fast reactions among chlorine and the pollutant matter present in this water (instantaneous chlorine demand).
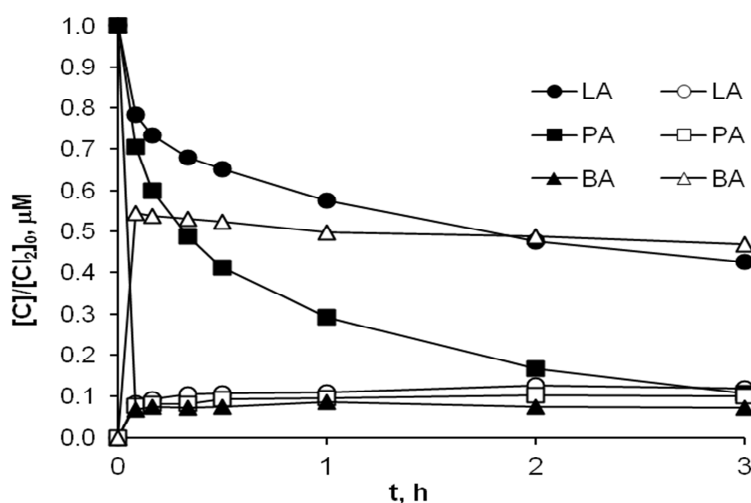
Figure 3. Changes of chloramines (open symbols) and free chlorine (solid symbols) in the "time dependant" experiments. Influence of the quality of the selected waters. Concentrations normalized by the initial chlorine dose (5 mg L^{-1}). The term [C] stands for either chlorine or chloramine.

For chloramines, a higher formation in the case of BA water and low formation for LA and PA waters is observed, as could be expected by taking into account the ammonia content in these waters (see Table 1). In effect, BA water presented the highest level of ammonia which led to a higher formation of chloramines. On the contrary, low levels of ammonia in the LA and PA waters provided almost negligible amounts of chloramines.

In order to predict the degradation of the selected ECs in these water matrices, a kinetic model is proposed which takes into account the chlorine concentration decay during an experiment and the previously evaluated rate constants k_{app}. This chlorine concentration allows to determine the chlorine exposure (CT parameter) which is defined as the integral of chlorine concentration over the reaction time (CT=∫[Cl$_2$]·dt). With CT evaluated and the known values of k_{app} (values theoretically calculated by using Equations (13)-(15) for each specific compound and the intrinsic rate constants reported in Table 2), the concentration profile of a specific compound can be theoretically determined by the equation:

$$[P] = [P]_0 \exp(-k_{app} \, CT) = [P]_0 \exp\left(-k_{app} \int_0^t [Cl_2] dt\right) \qquad (17)$$

Following this procedure in the three water systems, the changes of the concentration of each substance were evaluated. Figure 4 shows the results for PA water taken as example (symbols represent experimental data; lines represent theoretical predictions), with similar plots for BA and LA waters. As observed, there is a good agreement between experimental and theoretical values which confirms that the rate constants determined in pure water can be used to predict the degradation of the selected ECs during chlorination of real waters.
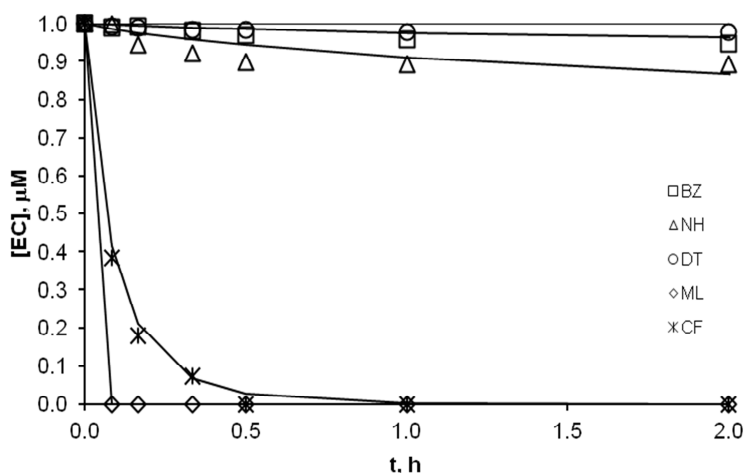
**Figure 4. Changes of ECs concentration in the chlorination of PA water. T=20 °C;
$[EC]_0=1\mu M$; $[Cl_2]_0=5$ mg L^{-1}. Symbols represent experimental data; lines represent
theoretical predictions.**

3.4. Chlorination in presence of bromide.

Finally, a new group of oxidation experiments was conducted in the three water systems by using chlorine (70 µM or 5 mg L^{-1}) in the presence of bromide (0 to 3.75 µM or 0-300 µg L^{-1}). The goal of these experiments was to evaluate the influence of the presence of bromide on the chlorination of contaminants in real waters, since chlorine reacts with bromide yielding bromine according to Equation (3).

Figure 5 shows the residual concentrations of the selected ECs in the three water systems after total chlorine consumption. The presence of bromine enhanced the oxidation of the ECs in relation to the single presence of chlorine as oxidant agent, with a more pronounced effect for increasing bromide concentrations. This positive effect of bromine is due to the higher values of bromination rate constants compared to chlorination. Once again, a total degradation of ML was obtained, as well as significant degradations of CF and NH, moderate degradation of BZ, and low degradation of DT. This trend for the degradation of ECs is in accordance with their sequences of reactivity, for both, chlorination and bromination processes (see rate constants with chlorine and bromine, Tables SI1, SI2 and 3).
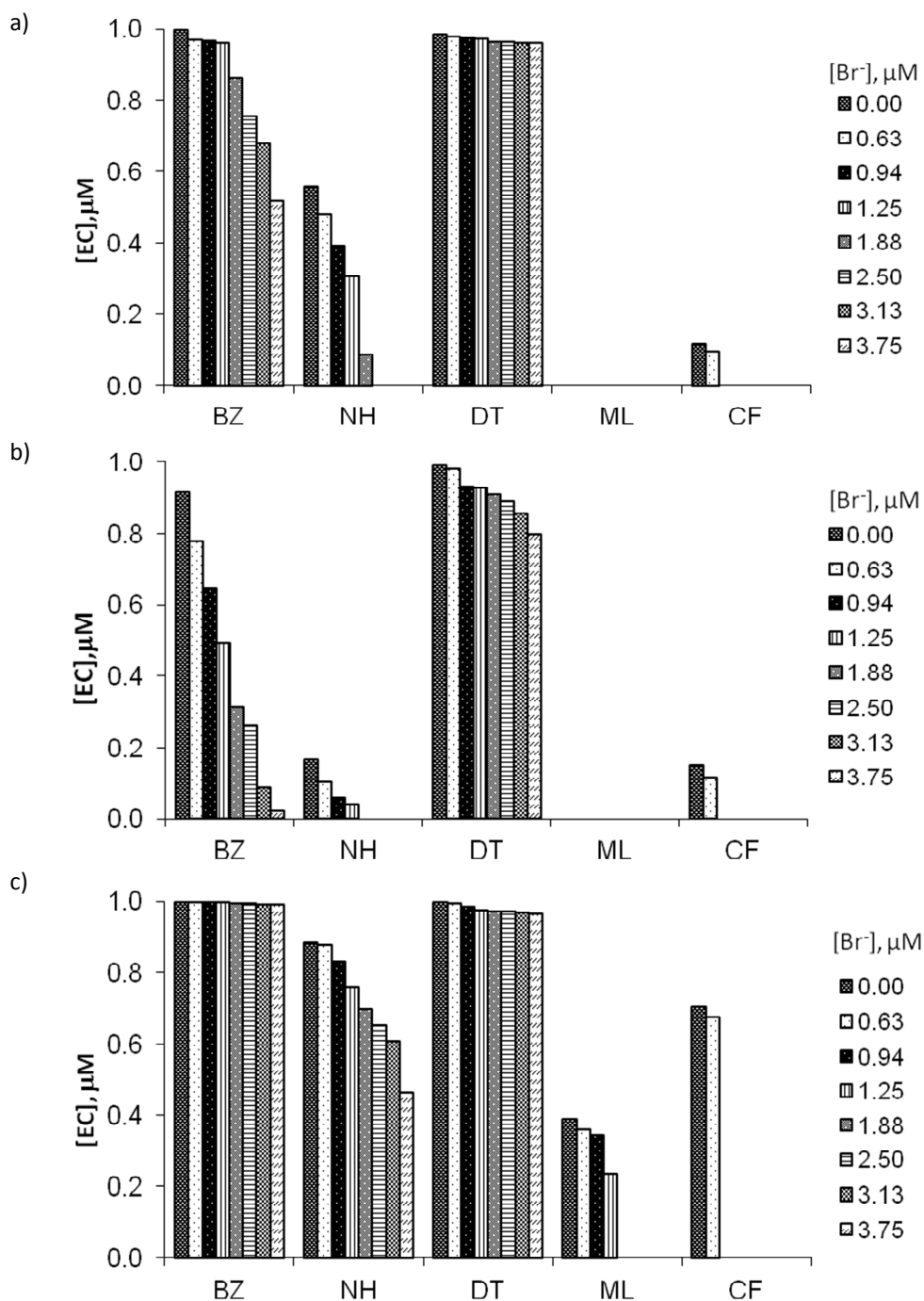
Figure 5. Influence of bromide concentration (0 to 3.75 µM or 0-300 µg L^{-1}) on the residual concentration of the selected ECs during chlorination of reservoir water PA (a) and secondary effluents, LA (b) and BA (c).

The positive effect of the increasing bromide concentration in the total degradation of the ECs was more pronounced in LA water, intermediate in PA water, and lower in BA water, in perfect agreement with their organic matter and ammonia contents. Therefore, the positive effect on the degradation of ECs due to the presence of bromide leading to bromine oxidation is partially hindered by the more rapid reactions of bromine than chlorine with reactive moieties of the NOM such as amine or phenolic moieties. As a consequence, competitive reactions of bromine with NOM and ammonia lead to lower degradation of micropollutants.

In general, any compound that reacts with chlorine or bromine (NOM, ammonia) decreases the oxidant exposure, and therefore, higher oxidant dose must be added to the water to reach the required ECs degradation. In presence of ammonia, chloramines are formed, which act as a chlorine sink and are not effective in ECs degradation. It is necessary to calibrate each water with respect to the rate of chlorine depletion in order to determine the initial dose that leads to the required oxidant exposure. In any case, chlorine is a plausible option for the degradation of ML, and in a lower extent for CF and NH. However, it is not a suitable oxidant for the abatement of BZ and DT.

4. CONCLUSIONS.

The results obtained in this study lead to the following main conclusions:

i. The chlorination of the selected ECs in UP water provided a wide range of apparent second-order rate constants depending on the pH and the nature of each compound. The sequence of reaction rates was 3-methylindole > chlorophene > nortriptyline HCl > benzotriazole >> DEET. Hypochlorous acid was the reactive aqueous chlorine species.

ii. The bromination of the selected ECs in UP water provided exactly the same sequence of reaction rates as in the chlorination process, although higher values of rate constants (one order of magnitude higher for NH, CF, BZ and DT and three for ML).

iii. In the chlorination of the selected contaminants simultaneously present in three water systems, the contaminants degradation decreased according to the sequence LA > PA > BA, which agreed with the sequence of increasing DOC present.

iv. According to the results of ECs degradation in real waters, chlorine is a good option for the oxidation of ML, and in a lower extent for CF and NH. However, it is not a suitable oxidant for the abatement of BZ and DT.

v. THMs concentrations increased continuously when chlorine doses were increased, being in all cases below 100 μg L^{-1}.

vi. The presence of low concentration of bromide in aqueous systems accelerated slightly the abatement of the selected contaminants during chlorine disinfection, specially in those waters with low NOM and ammonia content.

vii. It is necessary to calibrate each wastewater or drinking water with respect to the rate of chlorine depletion in order to determine the initial dose that leads to the required micropollutant degradation.

REFERENCES

Acero, J.L.; Benitez, F.J.; Real. F.J.; Roldan, G. Kinetics of aqueous chlorination of some pharmaceuticals and their elimination from water matrices. Water Res. **2010**, 44, 4158-4170.

Acero, J.L.; Real, F.J.; Benitez. F.J.; Gonzalez, M. Kinetics of the reaction between chlorine or bromine and the herbicides diuron and isoproturon. J. Chem. Technol. Biotechnol. **2007**, 82, 214-222.

Benitez, F.J.; Acero, J.L.; Real. F.J.; Roldan, G.; Casas, F. Bromination of selected pharmaceuticals in water matrices. Chemosphere **2011**, 85, 1430-1437.

Bichsel, Y.; von Gunten, U. Determination of iodine and iodate by ion chromatography with postcolumn reaction and UV/visible detection. Anal. Chem. **1999**, 71, 34-38.

Boehmer, W.; Ruedel, H.; Wenzel, A.; Schröeter-Kermani, C. Retrospective Monitoring of Triclosan and Methyl-triclosan in Fish: Results from the German Environmental Specimen Bank. Organohalogen. Comp. **2004**, 66, 1489-1494.

Bolong, N.; Ismail, A.F.; Salim, M.R.; Matsuura, T. A review of the effects of emerging contaminants in wastewater and options for their removal. Desalination **2009**, 239, 229-246.

Bougeard, C.M.M.; Goslan, E.H.; Jefferson, B.; Parsons S.A. Comparison of the disinfection by-product formation potential of treated waters exposed to chlorine and monochloramine. Water Res. **2010**, 44, 729-740.

Clesceri, L.S.; Greenberg, A.E.; Trussell, R.R. Standard Methods for the Examination of Water and Wastewater, 17th ed., APHA, AWWA, WPCF, Washington DC, **1989**.

Costanzo, S.D.; Watkinson, A.J.; Murby, E.J.; Kolpin, D.W.; Sandstrom, M.W. Is there a risk associated with the insect repellent DEET (N,N-diethyl-m-toluamide) commonly found in aquatic environments?. Sci. Total Environ. **2007**, 384, 214-220.

Deborde, M.; von Gunten, U. Reactions of chlorine with inorganic and organic compounds during water treatment-Kinetics and mechanism: A critical review. Water Res. **2008**, 42, 13-51.

Dodd, M.C.; Shah, A.D.; von Gunten, U., Huang, C-H. Interactions of fluoroquinolone antibacterial agents with aqueous chlorine: reaction kinetics, mechanisms, and transformation pathways, Environ. Sci. Technol. **2005**, 39, 7065-7076.

Gallard, H.; Pellizzari, F.; Croue, J.P.; Legube, B. Rate constants of reaction of bromine with phenols in aqueous solutions. Water Res. **2003**, 37, 2883-2892.

Golfinopoulos, S.K.; Lekkas, T.D.; Nikolaou, A.D. Comparison of methods for determination of volatile organic compounds in drinking water. Chemosphere **2001**, 45, 275-284.

Ikehata, K.; Gamal El-Din, M.; Snyder, S.A. Ozonation and advanced oxidation treatment of emerging organic pollutants in water and wastewater. Ozone Sci. Eng. **2008**, 30, 21-26.

Langford, K.H.; Thomas, K.V. Determination of pharmaceutical compounds in hospital effluents and their contribution to wastewater treatment works. Environ. Int. **2009**, 35, 766-770.

Lee, Y.; von Gunten, U. Transformation of 17α-Ethinylestradiol during water chlorination: effects of bromide on kinetics, products, and transformation pathways. Environ. Sci. Technol. **2009**, 43, 480-487.

Loos, R.; Gawlik, B.M.; Locoro, G.; Rimaviciute, E.; Contini, S.; Bidoglio, G. EU wide survey of polar organic persistent pollutants in European river waters. Environ. Pollut. **2009**, 157, 561-568.

Nakada, N.; Komori, K.; Suzuki, Y.; Konishi, C.; Houwa, I.; Tanaka H. Occurrence of 70 pharmaceutical and personal care products in Tone River basin in Japan. Water Sci. Technol. **2007**, 56, 133-40.

Pinkernell, U.; Nowack, B.; Gallard, H.; von Gunten, U. Methods for the photometric determination of reactive bromine and chlorine species with ABTS. Water Res. **2000**, 34, 4343-4350.

Rebenne, L.M.; Gonzalez, A.; Olson T.M. Aqueous chlorination kinetics and mechanism of substituted dihydrobenzenes. Environ. Sci. Technol. **1996**, 30, 2236-2242.

Sharma, V.K. Oxidative transformation of environmental pharmaceuticals by Cl_2, ClO_2, O_3, and Fe (VI): Kinetics assessment. Chemosphere **2008**, 73, 1379-1386.

Wenhui, L.; Xinghai, L.; Dongyan, L.; Lei, S.; Qi, S. Vapor-Phase Synthesis of 3-Methylindole over Fe-, Co-, or Ni-Promoted Ag/SiO$_2$. Chin. J. Catal. **2009**, 30, 1287-1290.

Wols, B.A.; Hofman-Caris, C.H.M. Review of photochemical reaction constants of organic micropollutants required for UV advanced oxidation processes in water. Water Res. **2012**, 46, 2815-2827.

Yang, X.; Flowers, R.C.; Weinberg, H.S.; Singer, P.C. Occurrence and removal of pharmaceuticals and personal care products (PPCPs) in an advanced wastewater reclamation plant. Water Res. **2011**, 45, 5218-5228.

SUPPLEMENTARY INFORMATION

Table S1. Apparent second-order rate constants (k_{app}) for the reactions of nortriptyline, chlorophene, benzotriazole and DEET with chlorine. $[Cl_2]_0=10^{-4}$ M for NH, CF and BZ and $[Cl_2]_0=10^{-3}$ M for DT.

pH	T, °C	Nortriptyline HCl k_{app}, $M^{-1}s^{-1}$	Chlorophene k_{app}, $M^{-1}s^{-1}$
3	20	14.5 ± 0.4	1.50 ± 0.20
4	20	1.72 ± 0.07	1.17 ± 0.18
5	20	0.65 ± 0.06	1.83 ± 0.10
6	20	0.29 ± 0.02	7.03 ± 0.60
7	20	0.40 ± 0.06	38.8 ± 1.0
8	20	0.51 ± 0.04	59.0 ± 0.7
9	20	0.56 ± 0.07	68.5 ± 1.2
10	20	0.43 ± 0.03	42.3 ± 1.8
11	20	0.18 ± 0.02	6.30 ± 0.15
7	10	0.33 ± 0.02	19.8 ± 1.0
7	30	0.65 ± 0.07	62.3 ± 3.0
7	40	0.84 ± 0.06	72.2 ± 3.7

pH	T, °C	Benzotriazole k_{app}, $M^{-1}s^{-1}$	DEET k_{app} x 10^4, $M^{-1}s^{-1}$
3	20	18.5 ± 2.8	51.5 ± 3.3
4	20	1.67 ± 0.28	19.0 ± 2.3
5	20	0.55 ± 0.09	14.6 ± 2.4
6	20	0.28 ± 0.07	14.9 ± 1.1
7	20	0.15 ± 0.01	13.6 ± 1.7
8	20	0.12 ± 0.03	4.41 ± 0.3
9	20	$(4.8 ± 0.4) \times 10^{-2}$	1.05 ± 0.15
10	20	$(4.4 ± 0.4) \times 10^{-3}$	0.26 ± 0.03
11	20	$(2.7 ± 0.2) \times 10^{-3}$	0.02 ± 0.003

Table S2. Apparent second-order rate constants (k_{app}) for the reactions of methylindole with chlorine, determined by competition kinetics.

pH	Reference comp.	$k_{app-R} \times 10^{-3}$ (a), $M^{-1}s^{-1}$	Target comp.	$k_{app} \times 10^{-3}$, $M^{-1}s^{-1}$
3	Naproxen	1.56	Methylindole	39.3 ± 2.3
4		0.18		8.01 ± 0.82
5		0.08		7.95 ± 0.99
pH	**Reference comp.**	$k_{app-R} \times 10^{-4}$ (b), $M^{-1}s^{-1}$	**Target comp.**	$k_{app} \times 10^{-3}$, $M^{-1}s^{-1}$
6	Orcinol	0.35	Methylindole	6.30 ± 0.58
7		1.85		5.75 ± 0.52
8		5.49		3.21 ± 0.43
9		6.16		0.62 ± 0.06
10		4.64		0.17 ± 0.01
11		3.26		0.04 ± 0.004

(a) Acero et al., 2010.
(b) Rebenne et al., 1996.

3.5. Oxidation of chlorophene by ozonation: kinetics, identification of by-products and reaction pathways.

3.5. OXIDATION OF CHLOROPHENE BY OZONATION: KINETICS, IDENTIFICATION OF BY-PRODUCTS AND REACTION PATHWAYS

F. Javier Benítez, Juan L. Acero, J. Francisco García†, Francisco J. Real, Gloria Roldan, Elena Rodríguez, Antonio Molina-Díaz†.

Departamento de Ingeniería Química, Universidad de Extremadura, Badajoz.

†Grupo de Investigación de Química Analítica, Universidad de Jaén, Jaén.

The ozonation of chlorophene, an emerging contaminant frequently present in aquatic systems because of its numerous uses nowadays, is studied. The kinetic experiments allowed the determination of the apparent rate constants for its reaction with ozone in the pH range 3-11. The rate constants values obtained varied from 1.67×10^3 L mol^{-1} s^{-1} at pH=3 to 1.82×10^5 L mol^{-1} s^{-1} at pH=11. As a consequence of its acidic nature (pK$_a$=9.81), the degree of dissociation of this pollutant was determined at every pH of work, and the specific rate constants of the neutral and anionic species were evaluated, being these rate constants $k_1=2.8 \times 10^3$ L mol^{-1} s^{-1} and $k_2=2.5 \times 10^5$ L mol^{-1} s^{-1}. Up to 24 by-products formed in the ozonation reaction were identified by liquid chromatography/mass spectrometry using a high-resolution time of flight analyzer (LC-TOFMS). From these intermediates identified, the degradation pathways are proposed and discussed. Toxicity measurements of the ozonated chlorophene solutions revealed that these by-products are less toxic than the parent compound.

1. INTRODUCTION.

Emerging contaminants (ECs) is a wide group of chemical substances, that includes prescription and therapeutic drugs (pharmaceuticals), veterinary drugs, dietary

supplements, consumer products, cosmetics and sunscreens (personal care products), laundry and cleaning products, and corrosion inhibitors. One of these ECs is chlorophene, a halogenated phenolic compound that presents multiple applications: in personal care, in household products for general cleaning and disinfecting, as antimicrobial substance, and as an active agent in disinfectant formulations in industrial and farming environments (Boehmer et al., 2004; Zhang and Huang, 2003; Amold et al., 2003). Due to these numerous usages, it is inevitably discharged into aquatic systems in the environment, Similarly to the rest of chlorophenols, it is toxic and poorly biodegradable, and therefore, remains for long periods in the environment, in both, soils and waters (He et al., 2011). Chlorophene concentrations of 50 mg L^{-1} have been found in activated sludge sewage systems, as well as 10 μg L^{-1} in sewage treatment plant effluent and rivers (Sirés et al., 2007).

In order to avoid the accumulation in the environment of ECs in general, and chlorophene in particular, there is an increasing interest in developing new technologies for their removal. Specifically for the elimination of chlorophene from waters, several studies can be found in the literature, which are focused in the degradation of this compound by a variety of chemical procedures, such as oxidation by manganese oxides (Zhang and Huang, 2003), oxidation by the combined system Fe^{3+}/Fe^{2+} (Sirés et al., 2007) or photochemical degradation (He et al., 2011). More recently, two studies focused on the chemical degradation of five model ECs, including chlorophene, by UV radiation by itself or combined with H_2O_2 (Benítez et al., 2013), and by chlorine (Acero et al., 2013), have been reported.

Inside this general field of work, focused on the application of chemical oxidation processes, other different oxidation technologies are recommended to be tested for the elimination of this substance, such as ozonation and Advanced Oxidation Processes (AOPs) (Glaze et al., 1987). In effect, ozone is an efficient oxidant for the purification of surface and drinking waters (von Gunten, 2003) because, in addition to the direct reaction with the organic pollutants, its decomposition is initially fast and produces another strong oxidant, the OH radical. Thus, ozonation processes include both, ozone and OH radical pathways; and consequently, they have demonstrated a high effectiveness in the degradation of different groups of organic contaminants (Ikehata et al., 2006; Esplugas et al., 2007).

In view of these considerations, chlorophene was chosen in the present work as a model EC with the aim of evaluating the efficiency of the ozonation process for its effective oxidation, with the following objectives: (i) to determine the rate constants for the reaction of chlorophene and ozone in ultra-pure water as a function of the pH of work, (ii) to identify the main by-products generated in the ozonation process, (iii) to propose the reaction mechanism for the degradation with ozone in accordance to the by-products identified, and (iv) to assess the toxicity of degradation products.

2. MATERIALS AND METHODS.

2.1. Chemicals and reagents.

Chlorophene of the highest purity available (99%) was purchased from Sigma-Aldrich (Germany). The chemicals used for the solutions (buffers) were of reagent grade, also from Sigma-Aldrich. Ultra-pure (UP) water for preparing chlorophene solutions was obtained from a Milli-Q System (Millipore) with a specific resistance of 18 MΩ·cm. Organic solvents and other chemicals used in the analysis, either HPLC or analytical grade, were supplied from Merck (Germany).

2.2. Experimental procedures.

Two different groups of ozonation experiments of chlorophene were carried out. In the first group, focused in the kinetic study for the determination of the rate constant for the direct reaction between ozone and this substance, the experiments were conducted in homogeneous conditions. A competition kinetics model was applied, which needed the presence of a reference compound whose rate constant with ozone was previously known. In the present work, this reference compound was metoprolol, being its rate constant for the ozonation reaction previously reported by Benitez et al. (2009).

Mixtures of chlorophene and metoprolol (1×10^{-5} M) were previously dissolved in UP water in 25 mL flasks. The initial concentration used for both substances was 10 µM. Tert-butyl-alcohol (0.1 M) was also added to the solution as OH radical scavenger (Staehelin and Hoigne, 1985). At the same time, ozone stock solutions were generated by dissolving

an ozone gas stream in ice-cooled UP water until the saturation was reached. The experiments were conducted at 20 °C and different pH values in the range 3-11. For this purpose, the solutions were buffered with a phosphoric acid/phosphate buffer (0.05 M) at the desired pH. Each run was initiated by injecting a variable volume of the ozone stock solution, necessary to achieve the desired initial O_3 dose into the flask (0-2x10^{-4} M or 0-10 mg L^{-1}). After complete ozone consumption, the residual concentrations of chlorophene and metoprolol were analyzed.

The second group of experiments was focused in the identification of by-products generated during the ozonation of chlorophene. These experiments were performed in heterogeneous conditions at 20 °C and without buffering. Thus, chlorophene (10 mg L^{-1}) was dissolved in UP water, and ozone, produced from an air stream in an ozone generator (Sander, mod. 300.5), was continuously bubbled into the solutions through a gas-dispersion plate located at the bottom of the reactor. The mass flow rate applied in all cases was 0.7 g m^{-3}, which is equivalent to a volume flow rate of 1.8 L h^{-1} of ozone. At regular reaction times, samples were withdrawn from the reactor to be analysed.

2.3. Analytical methods.

Kinetic experiments

In the ozonation experiments conducted for the kinetic study, the chlorophene and metoprolol concentrations were determined by HPLC with a Waters Chromatograph equipped with a 996 Photodiode Array Detector and a Phenomenex Gemini C18 Column (5μm, 150mm x 3mm). The injection volume was 100 μL and the detection was made at 280 nm. A gradient mode was applied and the mobile-phase consisted of acetonitrile (A) and water containing 25 mM formic acid (B). The global flow rate was 0.2 mL min^{-1} and the column temperature 20 °C. Each run started with an initial mobile-phase composition of 70% A, which was held for 3 min and then linearly increased up to 90% A in 3 min and held for 4 min. Then back to initial conditions for 2 min and finally, it was held at 70% A for equilibration (4 min).

Identification of by-products using liquid chromatography time-of-flight mass spectrometry

In the ozonation experiments carried out for the by-products identification, relative abundances of chlorophene and its intermediates generated during the ozonation process were analyzed by a HPLC system (Agilent 1290 Infinity) equipped with a XDB-C$_{18}$ analytical column (1.8 μm, 50 mm x 4.6 mm). Mobile-phases A and B were respectively, water with 0.1% formic acid and acetonitrile, at a flow rate of 0.5 mL min^{-1}. The chromatographic method started with an initial mobile-phase composition of 10% B for 3 min, followed by a linear gradient to 100% B up to 25 min and then held for 3 min. A post-run time of 10 min at initial mobile phase composition was included after each run. The HPLC system was connected to a time of-flight mass spectrometer (Agilent 6220 accurate mass TOF) equipped with an electrospray interface operating in either, positive and negative ionization modes. The following operation parameters were used: capillary voltage, 4000 V(+)/3000 V(-); nebulizer pressure, 40 psig; drying gas flow rate, 9.0 L min^{-1}; gas temperature, 325 °C; skimmer voltage, 65 V; octapole 1 rf, 250 V; fragmentor voltages: 160, 200 and 240 V. LC–MS accurate mass spectra were recorded across the m/z range of 50–1000 in positive ion mode and 50–1100 in negative ion mode. The instrument performed the internal mass calibration automatically, by using a dual-nebulizer electrospray source with an automated calibrate delivery system. The calibrating solution contained the internal reference masses TFANH$_4$ (ammonium trifluoroacetate, C$_2$O$_2$F$_3$NH$_4$, at m/z 112.985587 in negative ion mode), purine (C$_5$H$_4$N$_4$, at m/z 121.050873, in positive ion mode) and HP-0921 (Hexakis- (1H,1H,3H-tetrafluoropropoxy) phosphazine, C$_{18}$H$_{18}$O$_6$N$_3$P$_3$F$_{24}$, at m/z 922.009798 in positive ion mode and 1033.988109 in negative mode). The full scan data were recorded with Agilent Mass Hunter Data Acquisition software (version B.04.00) and processed with Agilent Mass Hunter Qualitative Analysis software (version B.04.00). Samples were directly analyzed without previous treatment.

Measurements of toxicity

With the aim of evaluating the toxicity of the solutions after ozonation of chlorophene, some experiments were carried out with different O$_3$/TOC ratios (mg O$_3$/mg TOC corresponding to the initial chlorophene solution), from 0 to 0.6. In these experiments

the initial concentration of chlorophene was maintained constant at 10 mg L^{-1}, and the pH value was 7.

After the total consumption of ozone, the removal of the initial chlorophene was measured by HPLC, and the toxicity was evaluated by a Microtox Model 500 Toxicity Analyzer, which measures the ability of solutions to inhibit the bioluminescence of the marine bacterium *Vibrio fischeri*. The procedure is based on the decay of the light emitted by the bacterium when exposed to toxic chemical compounds. The luminescence was recorded after 15 min of incubation at room temperature (20 °C), and the percentage of inhibition was determined.

3. RESULTS AND DISCUSSION.

3.1. Reaction kinetics between chlorophene and ozone.

Competition kinetics was applied to the evaluation of the rate constants for the direct reaction between chlorophene and ozone at different pH values. This procedure was initially proposed by Gurol and Nekouinaini (1984), and later widely used in other studies (De Laat et al., 1996; Karpel and Roshani, 2010). It is based on the simultaneous oxidation of a reference compound, whose rate constant with the oxidant is previously known, and a target compound (chlorophene in the present study). The model is previously described in detail elsewhere (Benitez et al., 2003), and leads to the final expression:

$$\ln \frac{[CP]_0}{[CP]} = \frac{k_{CP}}{k_R} \ln \frac{[R]_0}{[R]} \qquad (1)$$

In this Equation (1), [CP] and [R] represent the concentrations of chlorophene and the reference compound; and k_{CP} and k_R represent the oxidation rate constants for chlorophene and the reference compound, respectively. Then, and according to Equation (1), a plot of ln ([CP]$_0$/[CP]) against ln ([R]$_0$/[R]) must lead to a straight line whose slope provides the rate constant ratio k_{CP}/k_R; and later, if the value of k_R is previously known, the rate constant k_{CP} can be easily evaluated. In this method, an important condition to be fullfilled is that both substances, the target and reference compounds, must present

reactivities towards ozone in the same order of magnitude. Due to this fact, metoprolol was used as reference compound in the present work, whose rate constants for its reaction with ozone k_R at different pH and 20 °C were previously determined (Benítez et al., 2009), and are depicted in Table 1.

Table 1. Apparent second-order rate constants k_{cp} for the reaction between chlorophene and ozone at different pH values.

pH	k_Rx10^{-2}, L mol^{-1} s^{-1}	k_{CP}/k_R	k_{CP}x10^{-3}, L mol^{-1} s^{-1}
3	2.55	6.52	1.67
4	2.56	11.54	2.95
5	2.59	12.29	3.18
6	2.81	11.21	3.15
7	5.07	6.15	3.12
8	27.3	4.49	9.39
9	213	1.21	25.8
10	844	1.89	160
11	1200	1.27	182

The application of competition kinetics to the ozonation experiments of chlorophene at different pH values provided the slopes k_{CP}/k_R which are reported in Table 1, along with the deduced k_{CP} values. The rate constants revealed that the reactivity between chlorophene and ozone clearly increases with increasing pH values of the solution, which is a consequence of the acidic nature of the selected EC, which presents one dissociation constant (pK_a=9.81). Then, it is interesting to evaluate the specific rate constants for the elementary reactions between ozone and the neutral and anionic species of this substance.

For this purpose, the model initially proposed by Hoigne and Bader (1983) and later successfully applied by other authors (Benner et al., 2008) can be used. This model establishes that:

$$k_{CP} = \alpha_1 \, k_1 + \alpha_2 \, k_2 \tag{2}$$

where k_{CP} is the previously obtained apparent rate constant for the reaction between chlorophene and ozone; k_1 is the specific rate constant for the neutral form, and k_2 is the rate constant for the anionic form; and α_1 and α_2 are the respective fractions of chlorophene species at the specific pH of each experiment. The values of α_1 and α_2 can be obtained by using the concentration of H^+ and the dissociation constant K_a. A non-linear least squares regression analysis of Equation (2) was applied by using the deduced rate constants k_{CP} and the corresponding values of α_1 and α_2 for each pH. Following this procedure the specific rate constants for the two species of chlorophene were determined, and the values obtained were $k_1 = 2.8 \times 10^3$ L mol^{-1} s^{-1} and $k_2 = 2.5 \times 10^5$ L mol^{-1} s^{-1}.

In order to check the results obtained, Figure 1 shows the plot of the rate constants k_{CP} for each pH of work, in the range 3-11: symbols represent the experimentally deduced values shown in Table 1, while the continuous lines represent the theoretical values obtained after applying Equation (2) with the specific rate constants k_1 and k_2 previously determined. It can be observed an excellent agreement between both, the experimental and theoretical values, which confirms the goodness of the evaluated specific rate constants.
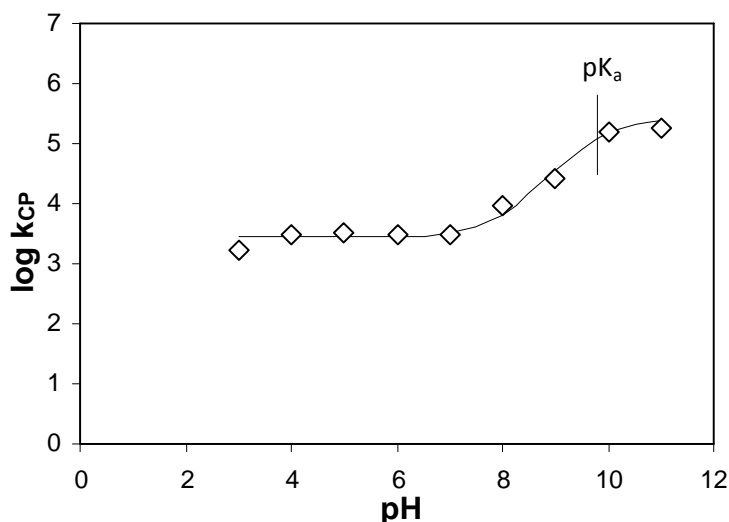
Figure 1. Rate constants for the ozonation reaction of chlorophene with the variation of the pH: a comparison among theoretical and experimental values.

3.2. Ozonation by-products.

The following step of this study was focused on the identification of the intermediate by-products generated during the ozonation of chlorophene. In order to accomplish this objective, reaction samples were collected at regular reaction times and analyzed by HPLC with a high-resolution time of flight analyzer (LC-TOFMS), as described in the Experimental Section, which permitted accurate mass measurements of the intermediates formed and the subsequent elemental compositions. In order to reduce the number of possible molecular formulas for each m/z value, the structure of the parent compound and the specific characteristics of the oxidation process were taken into account. Moreover, two additional tools were also used in order to identify these intermediates, and to assign the specific structures: (i) the DBE value (Double Bond Equivalent parameter), which provides information about the double bonds and rings that are present in the molecule; and (ii) in-source CID fragmentation experiments (pseudo MS/MS experiments) which provides additional fragmentation information for structure elucidation purposes (Abranko et al., 2011). Three voltages were applied: 160, 200, and 240 V. The evaluation of the LC-MS chromatograms obtained at different reaction times in both, positive and negative ionization modes, combined with the use of the above mentioned tools, allowed the identification of the numerous intermediates, which are summarized in Table 2, including elemental compositions and tentative structures proposed. It must be noted that all these compounds were identified in negative ionization mode.

Additionally, Figures 2A-2B show the evolution of the time profiles for these chlorophene by-products, expressed as relative abundance of chromatographic areas (mean of two replicates) with reaction time. Note that an exact quantitation of each individual intermediate cannot be accomplished due to the lack of standards, so relative abundance from mass spectra is used assuming that the detector response of the different intermediates is not significantly different. Due to the large number of these substances detected, Figure 2A compiles the compounds that were found in a larger amount, while Figure 2B shows the less abundant by-products. As observed in the time profile curves shown in Figue 2A, the parent compound CP decreased continuously with reaction time as could be expected; and the C9 intermediate was the by-product generated in a greater

extent, with an initial increase in its concentration, followed by a continuous decrease after around 30 min of reaction.

Table 2. Degradation by-products identified during chlorophene ozonation.

	R_t (min)	Molecular Formula [M]	m/z theoretical experimental	Error (ppm)	DBE	Tentative structure [M]
CF	17.2	$C_{13}H_{11}ClO$	217.0426 217.0428	-0.92	8	
C1	11.66	$C_7H_5ClO_3$	170.9854 170.9857	-1.75	5	
C2	9.55	C_6H_5ClO	142.9905 142.9908	-0.08	4	
C3 **C4** **C5** **C6**	13.82 14.06 15.02 15.74	$C_{13}H_{11}ClO_2$	233.0375 233.0384	-3.86	8	
C7 **C8**	12.08 13.18	$C_{13}H_{10}O_4$	229.0506 229.0515	-3.64	9	
C9	9.94	$C_{12}H_7ClO_{10}$	344.9655 344.9639	4.82	9	

Table 2 (cont). Degradation by-products identified during chlorophene ozonation.

	R_t (min)	Molecular Formula [M]	m/z theoretical experimental	Error (ppm)	DBE	Tentative structure [M]
C10 **C11** **C12**	9.77 10.2 11.4	$C_{12}H_{12}O_3$	203.0714 203.0720	-3.01	7	
C13	8.74	$C_{11}H_{10}O_4$	205.0506 205.0514	-2.90	7	
C14 **C15** **C16**	9.88 11.18 11.35	$C_{12}H_8O_{10}$	311.0045 311.0023	-4.41	9	
C17 **C18**	7.49 7.75	$C_{12}H_{12}O_5$	235.0612 235.0620	-3.71	7	
C19 **C20** **C21** **C22** **C23**	5.04 6.03 6.59 7.47 8.43	$C_{11}H_{10}O_5$	221.0455 221.0461	-2.71	7	
C24	10.05	$C_9H_{12}O_{10}$	279.0358 279.0351	2.43	4	
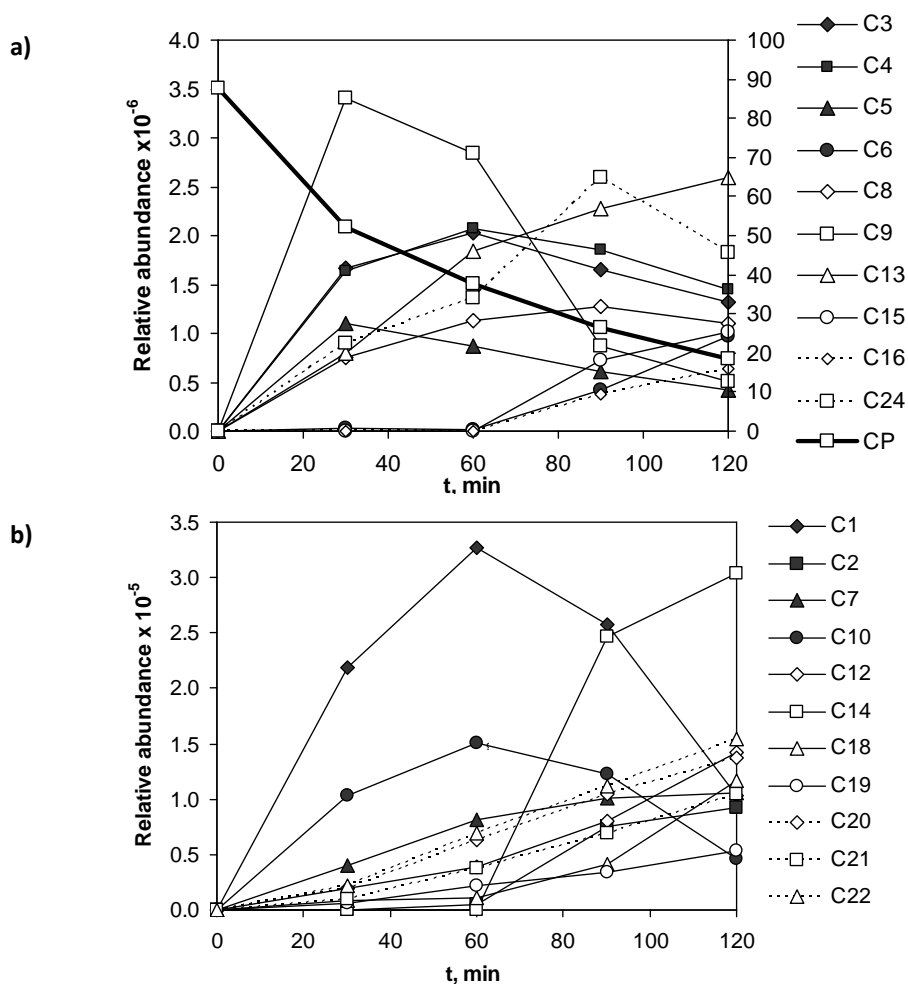
Figure 2. Quantitative analysis of derivatives detected during the ozonation process: time profiles for chlorophene by-products: major(a) and minor (b) intermediates formed.

Other relevant by-products generated and later consumed were: C24, which was also initially formed, followed by a decrease after around 90 min of reaction; C3 and C4 isomers, and C8, which also reached important amounts during the first hour of reaction, followed by a decrease in their concentrations, these aspects being later explained in the reaction mechanism proposed. On the contrary, the C13 compound showed a continuous increase in its concentration since the initial reaction time. Less significant amounts were detected for the remaining by-products shown in this Figure 2A: C5, C6, C15 and C16. On the other hand, Figure 2B shows great amounts generated for C1 and C14 compounds:

however, it must be remarked that the values of the relative abundance in this Figure 2B are ten times lower than those in Figure 2A. Therefore, the concentrations determined for the rest of identified by-products that are shown in this Figure 2B are less significant.

3.3. Ozonation pathways.

On the basis of the above mentioned by-products identified, Figure 3 shows the proposed mechanism for the ozonation of chlorophene. Among the primary oxidation products, it can be expected that hydroxyl-chlorophene is formed, as reported by Zhang et al. (2003). Hydroxyl-chlorophene has been found in this study, being four isomers identified (C3 to C6 in Table 2, with molecular formula $C_{13}H_{11}ClO_2$ and m/z 233.0375). This oxidation product, together with p-quinone and p-hydroquinone of chlorophene (S1 and S2 by-products shown in Figure 3, but not identified in this study) are analogous to those formed in the oxidation of 4-chlorophenol, as reported by Satuf et al. (2008). As observed in Figure 2A, C4 was obtained in a slightly higher concentration than C3 isomer, and much in greater extent than C5 and C6 isomers. In a first approach, this major isomer corresponds to the molecular structure proposed in the tentatively reaction pathway shown in Figure 3. In effect, as Catrinescu et al. (2011) pointed out, it can be supposed that the hydroxyl radical attack is directed by the position of the hydroxyl group, which is a stronger ortho-para director than chlorine. Several oxidation steps of isomers C3 to C6 and the subsequent loss of a carbon atom could lead to the formation of C9 product, with molecular formula of $C_{12}H_7ClO_{10}$ and m/z 344.9639, which is the major intermediate found as was previously mentioned. A latter loss of the chlorine atom by a hydroxyl radical resulted in the isomers C14 to C16 with molecular formula $C_{12}H_8O_{10,}$ m/z=311.0023 and a value of DBE=9.

Although in a minor extent, other identified by-products with chlorine atoms in their molecules were C1 ($C_7H_5ClO_3$, m/z 170.9857) and C2 (C_6H_5ClO, m/z 142.9908). It could be expected that these intermediates were formed either, from the parent compound chlorophene or from the isomers C3-C6 with m/z 233.0384, in both cases after oxidation and subsequent cleavage of the molecules involved. The presence of Cl atom in these degradation products (C1 to C6, and C9) is confirmed by their mass spectra, which show the characteristic isotopic patterns of chlorine.
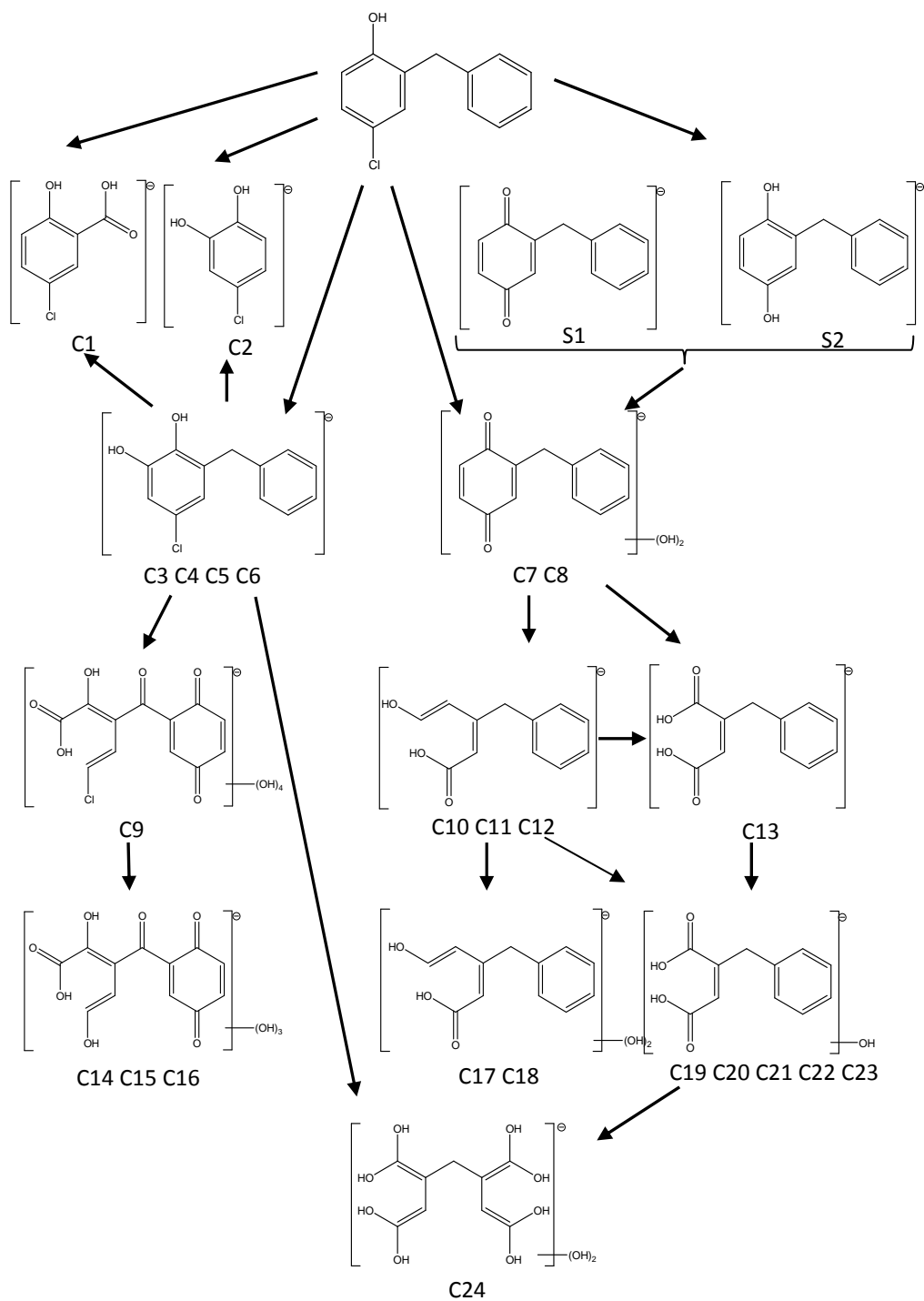
Figure 3. Degradation pathways proposed for the ozonation of chlorophene.

As an example, Figure 4 shows the chromatogram of the isomers C3 to C6, as well as the mass spectrum for the specific degradation product C5, whose retention time was 15.03 min. As can be seen in this Figure 4, the accurate mass of isomer C5 was 233.0365, together with a ^{37}Cl isotope signal of 235.0341, the last one presenting relative intensity of about one-third of the main peak. Moreover, the difference between both mass signals is 1.9976, close to the exact mass difference between ^{35}Cl (34.9689) and ^{37}Cl (36.9659) which is 1.9970.
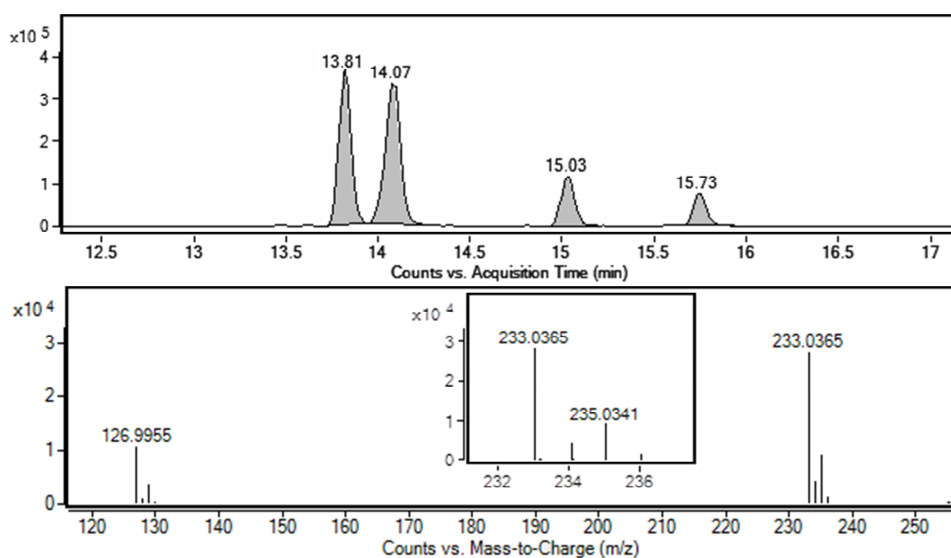
Figure 4. Extracted ion chromatogram for m/z 233.0365 and mass spectrum of degradation product C5.

This evidence confirmed that the C5 compound unequivocally contains chlorine atom. The same procedure was followed for the remaining compounds containing Cl atoms (C1 to C6, and C9) and the same confirmation about the presence of this chlorine was deduced (see supplementary information, Figure S1). In addition, as can be seen in Figure 4 a fragment with m/z 126.9955 was found for C5 isomer (which also appeared in the mass spectrum of C6 isomer, shown in Figure S1). This fragment also presented the characteristic isotopic patterns of chlorine, and its exact mass corresponded to chlorophenol C_6H_5ClO. This fact supports that the hydroxylation did not occur in the aromatic ring containing the chlorine atom in these C5 and C6 isomers.

As confirmed by their mass spectra, the remaining degradation products identified have lost the chlorine atom. Thus, the formation of isomers C7 and C8 ($C_{13}H_{10}O_4$, with m/z 229.0506 and DBE of 9) can be justified as the result of several hydroxylation steps of the previously mentioned oxidation products S1 and S2 (not identified in this work), as well as directly from chlorophene, by replacement of the chlorine atom and two hydroxylations. Later, the ring cleavage of the S1 and S2 intermediates (or their hydroxylation transformation products C7 and C8) may lead to the degradation product C13 (molecular formula $C_{11}H_{10}O_4$, m/z 205.0512), whose mass spectrum is shown in Figure 5. This intermediate has two carboxyl groups, as can be deduced from the two fragments found (see Figure 5, m/z 161.0610 and 117.0711), which resulted from the loss of two carboxyl groups (m/z 43.9904) in C13. Later, a hydroxylation of C13 resulted in isomers C19 to C23 ($C_{11}H_{10}O_5$, m/z 221.0455). Once again, their mass spectra confirmed the presence of two carboxyl groups (spectra shown in Figure S1). A final step in the degradation process led to the opening of the aromatic ring with the loss of two terminal carbons, resulting in C24 ($C_9H_{12}O_{10}$, m/z 279.0351). Moreover, this intermediate can also be generated from isomers C3 to C6 by hydroxylation and aromatic ring fission plus loss of carbon.
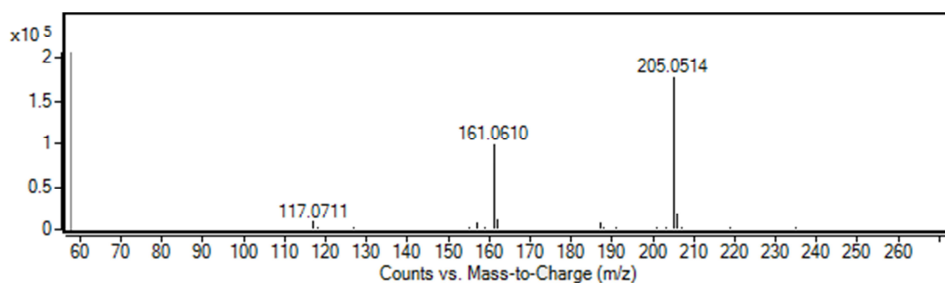
Figure 5. Mass spectrum of degradation product C13 with m/z 205.0514.

At the same time, the identified degradation products C10 to C12 ($C_{12}H_{12}O_3$, m/z 203.0714) may correspond to the loss of chlorine and one carbon, and to the increase in two oxygen atoms from C7 and C8 intermediates. Once again, the fragments found in their mass spectra evidenced the presence of a carboxyl group (spectra shown in Figure S1). Finally, the hydroxylation of these transformation products C10-C12 resulted in the isomers C17 and C18 ($C_{12}H_{12}O_5$, m/z 235.0612, with the same DBE=7); or even, the loss of a carbonyl

group followed by oxidation of terminal carbon and hydroxylation could result in the formation of isomers C19 to C23 ($C_{11}H_{10}O_5$, m/z 221.0455) which were also generated through another pathway, as previously discussed.

3.4. Toxicity measurements.

Finally, the evolution of the toxicity during the ozonation of chlorophene was also followed, by conducting specific experiments for this purpose, as was explained in the Experimental Section. In these experiments, the initial ozone doses were varied according to the ratio O_3/TOC which ranged between 0 and 0.6. The initial TOC due exclusively to the presence of chlorophene was around 6 mg L^{-1}. After total ozone consumption (more than ten hours of reactions), the resulting reacting solution was inoculated with the bacteria *Vibrio fischeri*, and the luminescence inhibition was evaluated after 15 min. At the same, the removal percentage of chlorophene was also determined. The results obtained are shown in Figure 6, and several conclusions can be obtained. Analysis of TOC were also performed for the reaction samples, and the value kept fairly constant (data not shown).
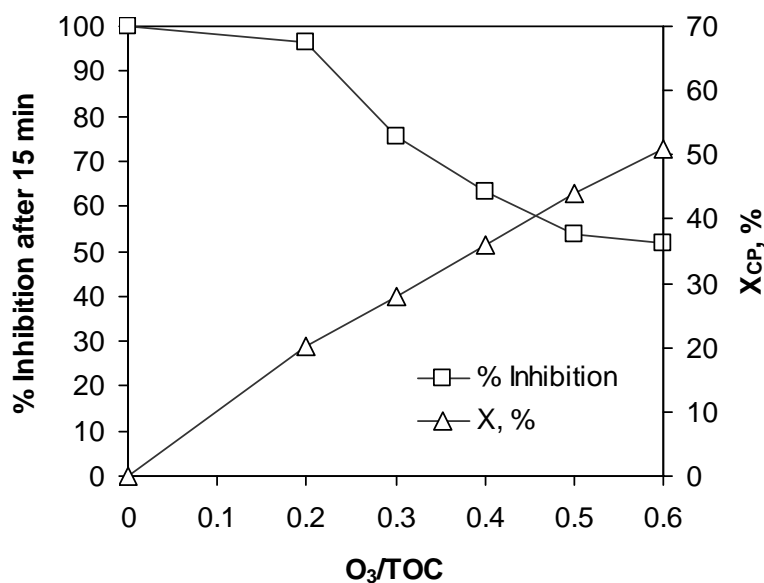
Figure 6. Toxicity evolution during ozonation of chlorophene for different ozone/Total Organic Carbon ratio. (pH=7, [CP]$_0$=10 mg L^{-1}).

As can be observed in Figure 6, the removal of chlorophene increased continuously with the increase in the ozone dose, as could be expected, reaching 51% for the ratio O_3/TOC=0.6. At the same time, the inhibition percentage decreased with the increase in the mentioned ozone dose. Chlorophene is a toxic compound, and the initial bioluminescence inhibition, without the presence of ozone, was around 100%. However, after reaction with ozone the toxicity decreased to 51.8% inhibition of *V. fisheri* bioluminescence with a ratio O_3/TOC of 0.6. It does mean that a higher amount of ozone promotes a higher chlorophene removal and the subsequent formation of by-products which are less toxic than the parent compound. It can also be appreciated in Figure 6 a very small decrease of toxicity with the lowest ozone dose, which implies that the first-generation by-products present a toxicity similar to chlorophene. Only when the ozone dose is higher and the ozonation process advances further, the bioluminecence inhibition decreases faster, which means that the second-generation by-products are considerably less toxic than chlorophene.

From the results obtained, it is deduced that ozone is a plausible option for the degradation of chlorophene due the high values of rate constants and the decrease of the toxicity of the degradation products. Similar results (high reactivity and toxicity decrease) are also expected during drinking water or wastewater contaminated with chlorophene. In general, any compound that reacts with ozone (NOM) decreases the oxidant exposure, and therefore, higher oxidant dose must be added to the water to reach the required contaminant degradation. It is necessary to calibrate each water with respect to the rate of ozone depletion in order to determine the initial dose that leads to the required oxidant exposure.

4. CONCLUSIONS.

Ozonation can be successfully used to oxidize the emerging contaminant chlorophene in ultra-pure water, being able to obtain an important level of degradation of this substance in short or moderate reaction times, depending on the pH of work. The apparent rate constants for this reaction between ozone and this contaminant in the pH range 3-11 varied from 1.67×10^3 L·mol^{-1} s^{-1} at pH=3 to 1.82×10^5 L mol^{-1} s^{-1} at pH=11. Due to its acidic nature, with a pK_a=9.81, the degree of dissociation can be determined at every pH

of work, and the specific rate constants of the neutral and anionic species of chlorophene have been determined, being their values $k_1=2.8\times10^3$ L mol^{-1} s^{-1} and $k_2=2.5\times10^5$ L mol^{-1} s^{-1}. Analysis by HPLC-QTOF-MS technique of the reaction samples allowed the determination and identification of 24 intermediate by-products. Taking into account the molecular formulas and chemical structures of these intermediates, the degradation pathway and general reaction mechanism of this ozonation process can be proposed. Toxicity measurements reveal that the ozonation process generates intermediate products less toxic than the parent compound. This work reveals the plausible successful application of ozone for the abatement of chlorophene in drinking water and wastewater treatment due the high values of rate constants and the decrease of the toxicity of the degradation products.

REFERENCES

Abranko, L.; García-Reyes, J.F.; Molina-Díaz, A. In-source fragmentation and accurate mass analysis of multiclass flavonoid conjugates by electrospray ionization time-of-flight mass spectrometry. J. Mass Spectrom. **2011**, 46, 478-488.

Acero, J.L.; Benítez, F.J.; Real, F.J.; Acero, J.L.; Roldán, G.; Rodríguez, E. Chlorination and bromination kinetics of emerging contaminants in aqueous systems. Chem. Eng. J. **2013**, 219, 43-50.

Arnold, W.A.; McNeil, K.; Packer, J.L.; Latch, D.E.; Boreen, A.L. Report of the USGS-WRRI 104G, National Grants Competition, 18, **2003**.

Benítez, F.J.; Acero, J.L.; Real, F.J.; Garcia, J. Kinetics of photodegradation and ozonation of pentachlorophenol. Chemosphere **2003**, 51, 651-662.

Benítez, F.J.; Acero, J.L.; Real, F.J.; Roldán, G. Ozonation of pharmaceutical compounds: Rate constants and elimination in various water matrices. Chemosphere **2009**, 77, 53-59.

Benítez, F.J.; Acero, J.L.; Real, F.J.; Roldán, G.; Rodríguez, E. Photolysis of model emerging contaminants in ultra-pure water: Kinetics, by-products formation and degradation pathways. Water Res. **2013**, 47, 870-880.

Benner, J.; Salhi, E.; Ternes, T.; von Gunten, U. Ozonation of reverse osmosis concentrate: kinetics and efficiency of beta blocker oxidation. Water Res. **2008**, 42, 3003-3012.

Boehmer, W.; Ruedel, H.; Wenzel, A.; Schröeter-Kermani, C. Retrospective Monitoring of Triclosan and Methyl-triclosan in Fish: Results from the German Environmental Specimen Bank. Organohalogen Comp. **2004**, 66, 1489-1494.

Catrinescu, C.; Arsene, D.; Teodosiu, C. Catalytic wet hydrogen peroxide oxidation of para-chlorophenol over Al/Fe pillared clays prepared from different host clays. Appl. Catal. B: Environ. **2011**, 101, 451-460.

De Laat, J.; Maouala-Makata, P.; Dore, M. Rate constants for reactions of ozone and hydroxyl radicals with several phenyl-ureas and acetamides. Environ. Technol. **1996**, 17, 707-716.

Esplugas, S.; Bila, D.M.; Krause, L.G.T.; Dezotti, M. Ozonation and advanced oxidation technologies to remove endocrine disrupting chemicals (EDCs) and pharmaceuticals and personal care products (PPCPs) in water effluents. J. Hazard. Mater. **2007**, 149, 631-642.

Glaze, W.H.; Kang, J-W.; Chapin, D.H. Chemistry of water treatment processes involving ozone, hydrogen peroxide and ultraviolet radiation, Ozone Sci. Engin. **1987**, 9, 335-352.

Gurol, M.; Nekouinaini, S. Kinetic behavior of ozone in aqueous solutions of substituted phenols. Ind. Eng. Chem. Fund. **1984**, 23, 54-60.

He, Z.; Zhang, A.; Li, Y.; Song, S.; Liu, Z.; Chen, J.; Xu, X. Chlorophene degradation by combined ultraviolet irradiation and ozonation, J. Environ. Sci. Health A: Tox. Hazard. Subst. Environ. Eng. **2011**, 46, 1-8.

Hoigné, J.; Bader, H. Rate constants of reactions of ozone with organic and inorganic compounds in water - II. Dissociating organic compounds. Water Res. **1983**, 17, 185-194.

Ikehata, K.; Nagashkar, N.J.; Gamal El-Din, M. Degradation of aqueous pharmaceuticals by ozonation and advanced oxidation processes: a review. Ozone Sci. Eng. **2006**, 28, 353-414.

Karpel Vel Leitner, N.; Roshani, B. Kinetic of benzotriazole oxidation by ozone and hydroxyl radical, Water Res. **2010**, 44, 2058-2066.

Satuf, M.L.; Brandi, R.J.; Cassano, A.E.; Alfano, O.M. Photocatalytic degradation of 4-chlorophenol: A kinect study. Appl. Catal. B: Environ. **2008**, 82, 37-49.

Sirés, I. ; Garrido, J.A.; Rodríguez, R.M.; Brillas, E.; Oturan, N.; Oturan, M. Catalytic behavior of the Fe^{3+}/Fe^{2+} system in the electro-Fenton degradation of the antimicrobial chlorophene, Appl. Catal. B: Environ. **2007**, 72, 382-394.

Staehelin, J.; Hoige, J. Decomposition of ozone in water in the presence of organic solutes acting as promoters and inhibitors of radical chain reactions. Environ. Sci. Technol. **1985**, 19, 1206-1213.

von Gunten, U. Ozonation of drinking water. Part I. Oxidation kinetics and product formation. Water Res. **2003**, 37, 1443-1467.

Zhang, H.; Huang, C.H. Oxidative transformation of triclosan and chlorophene by manganese oxides. Environ. Sci. Technol. **2003**, 37, 2421-2430.

SUPPLEMENTARY INFORMATION

Chlorophene:
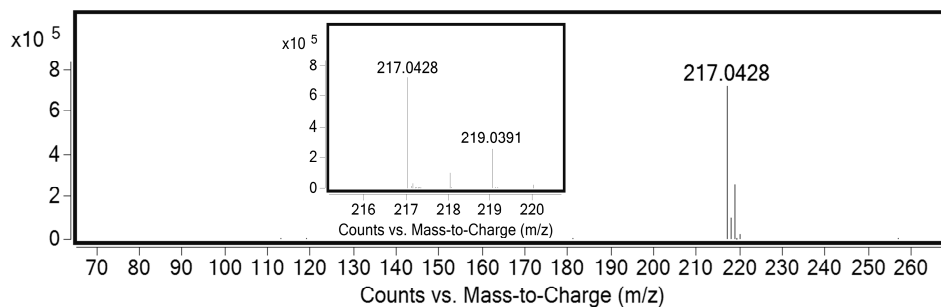
C1:
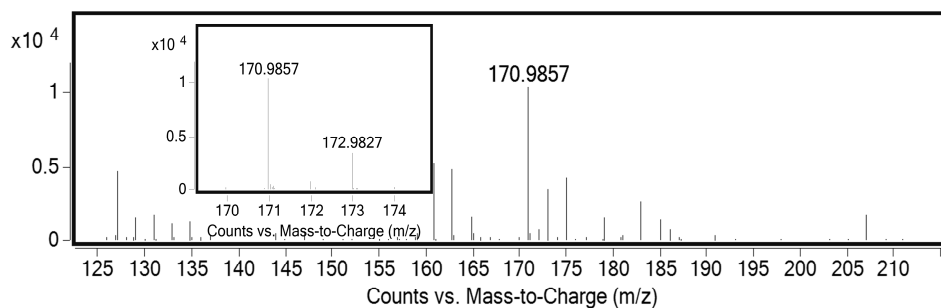
C2:
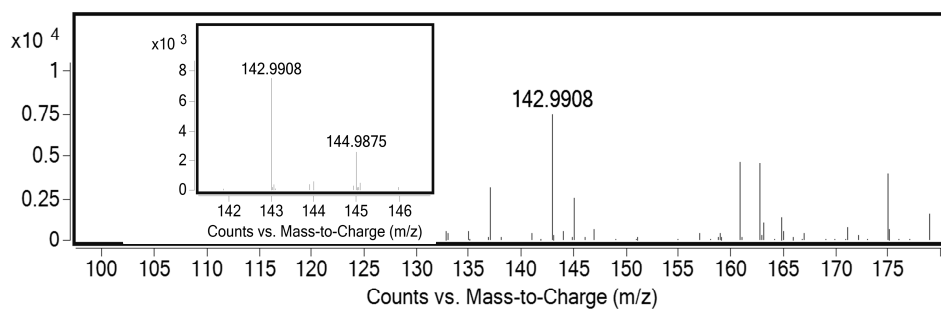
C3:
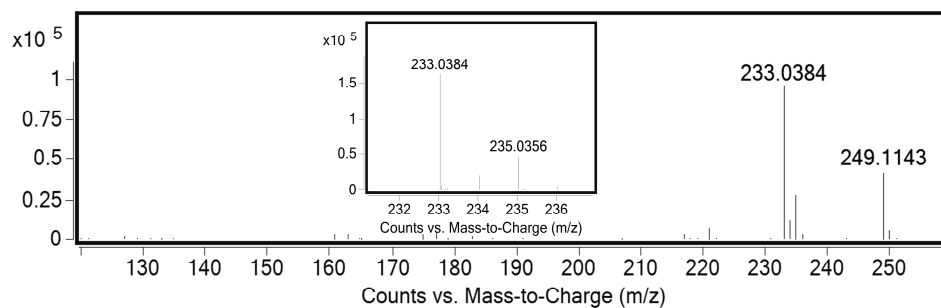
Figure S1. Mass spectra of chlorophene and its main ozonation by-products.
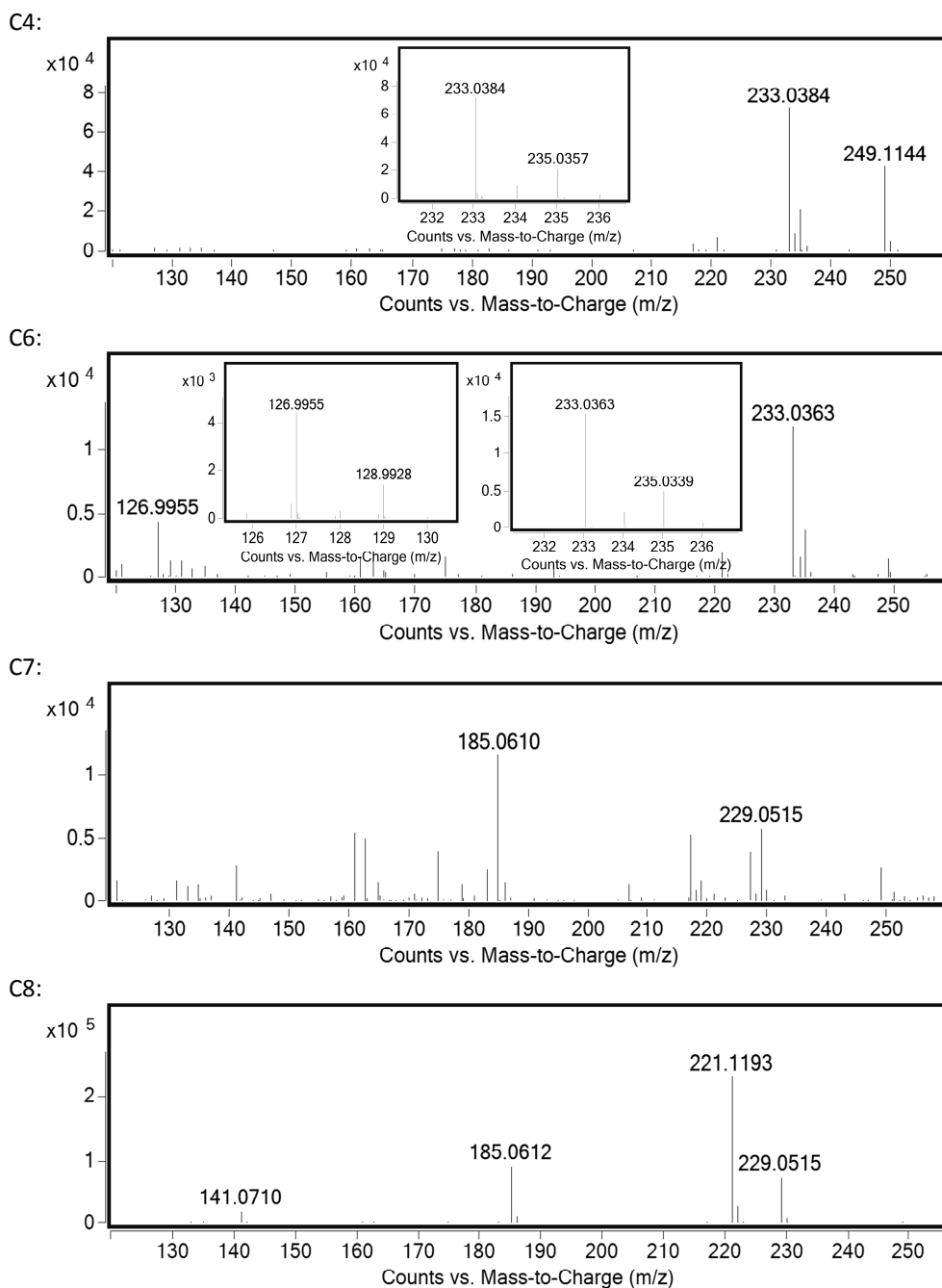
Figure S1 (cont.). Mass spectra of chlorophene and its main ozonation by-products.

C9:
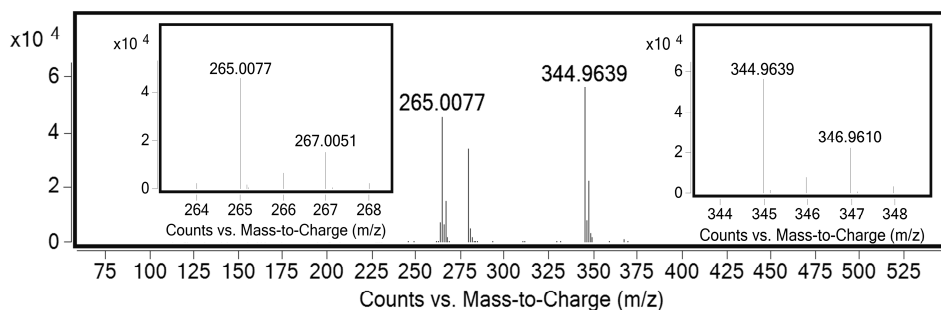
C10:
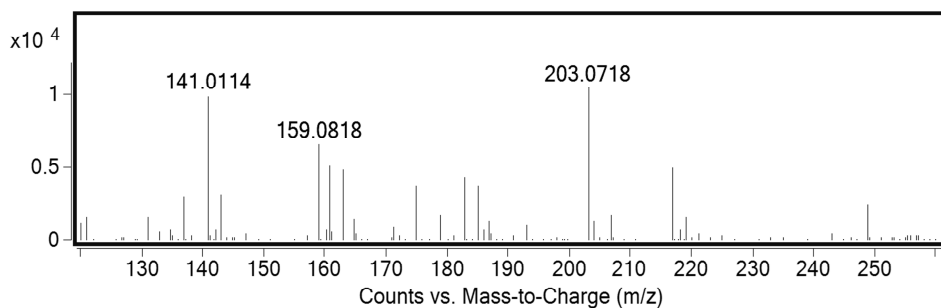
C11:
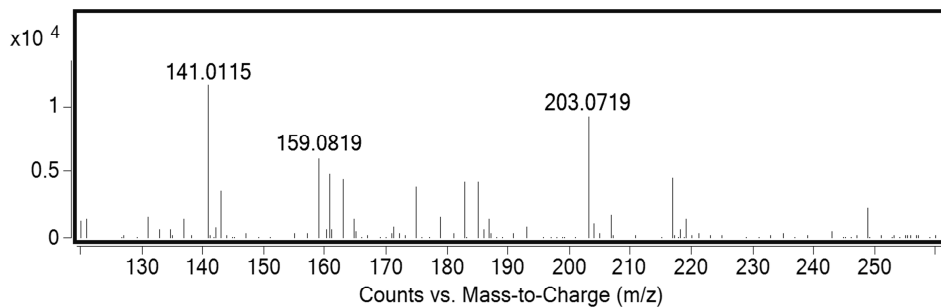
C12:
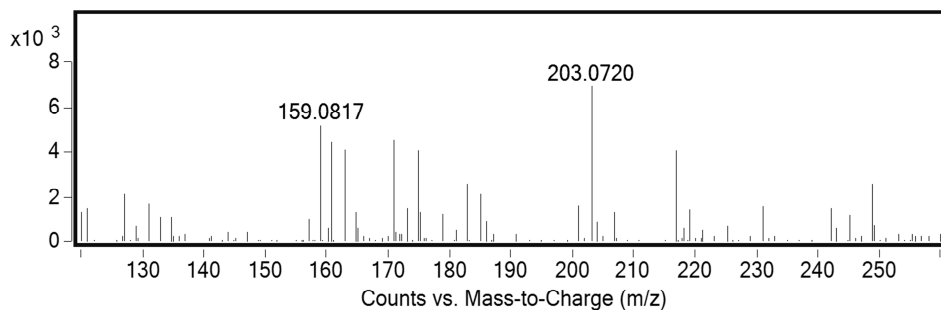
Figure S1 (cont.). Mass spectra of chlorophene and its main ozonation by-products.

C14:
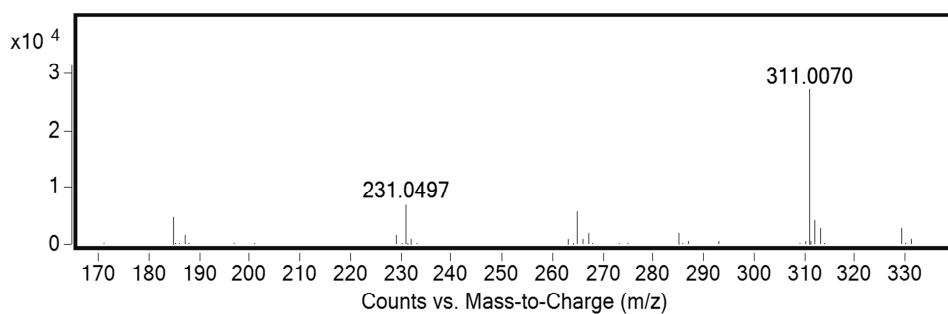
C15:
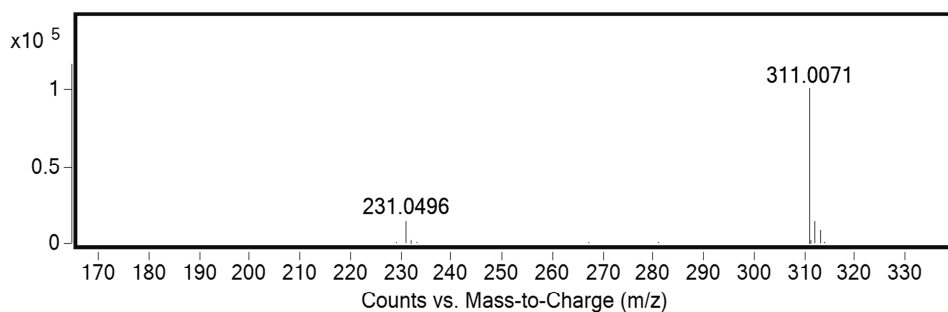
C16:
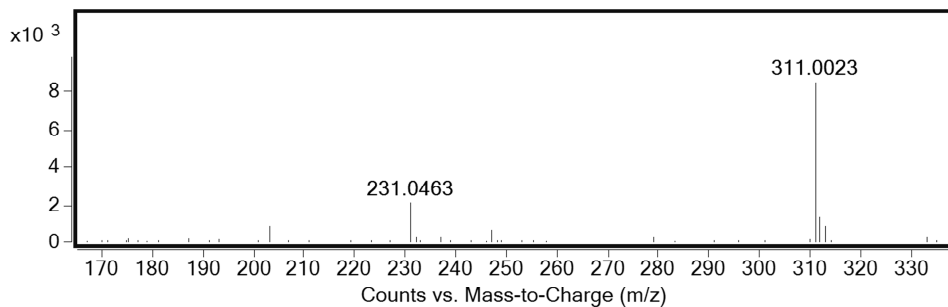
C17:
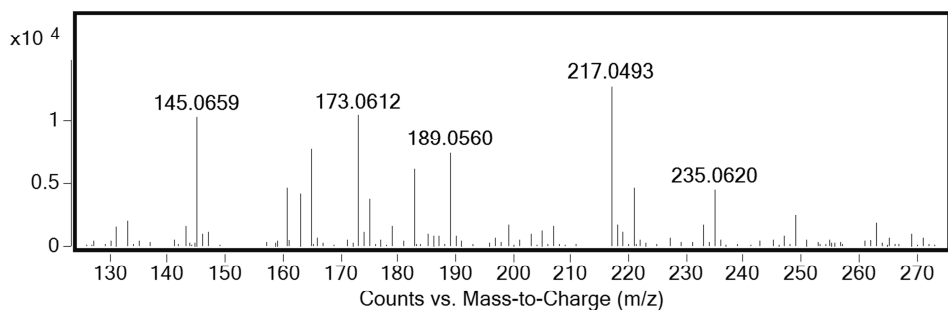
Figure S1 (cont.). Mass spectra of chlorophene and its main ozonation by-products.

C18:
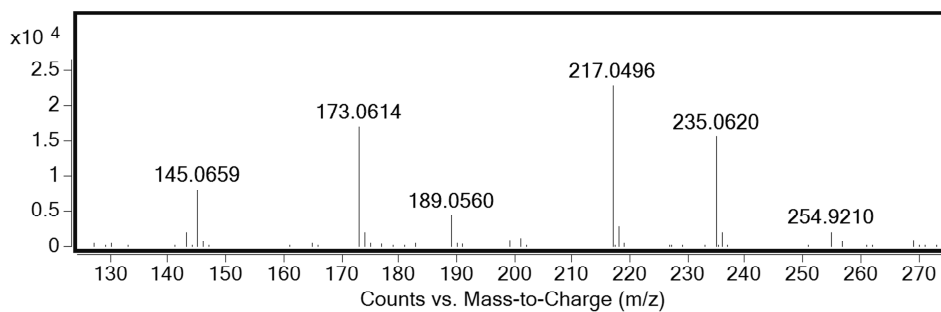
C19:
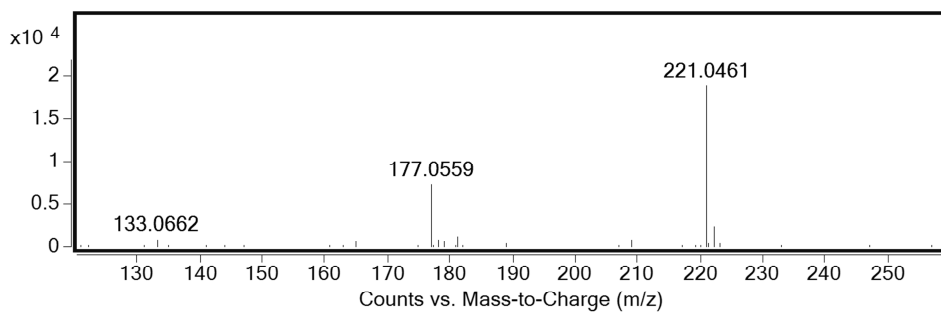
C20:
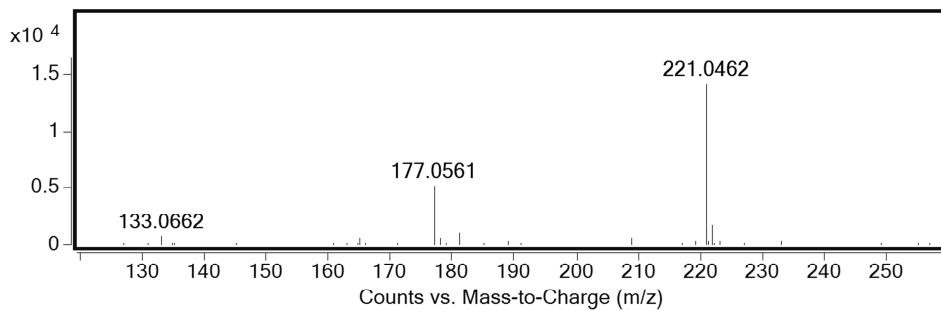
C21:
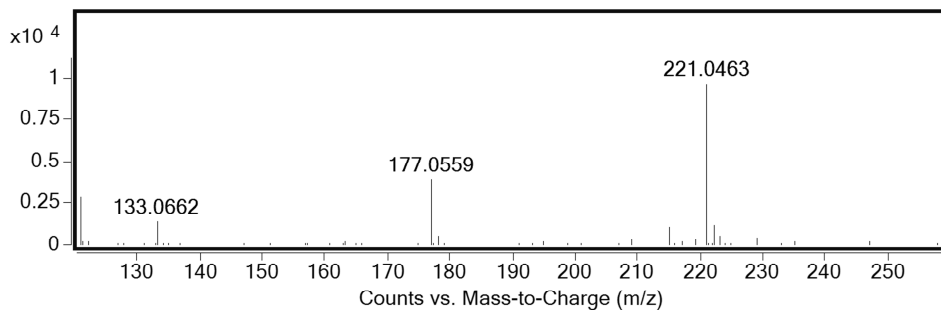
Figure S1 (cont.). Mass spectra of chlorophene and its main ozonation by-products.

C22:
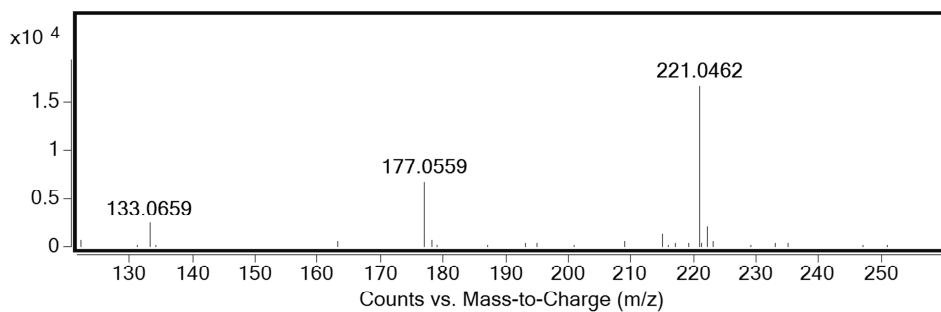
C23:
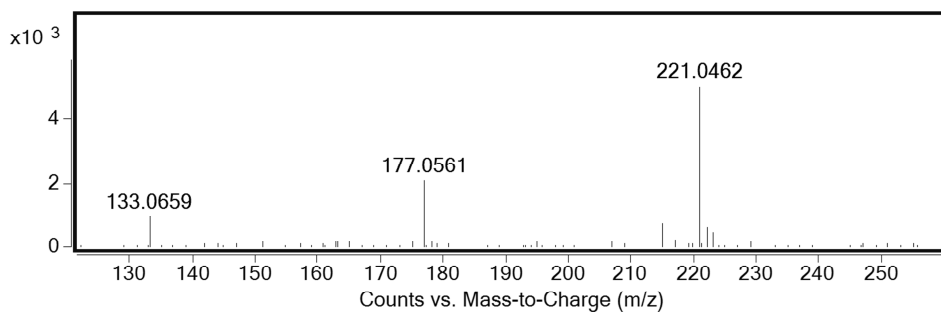
C24:
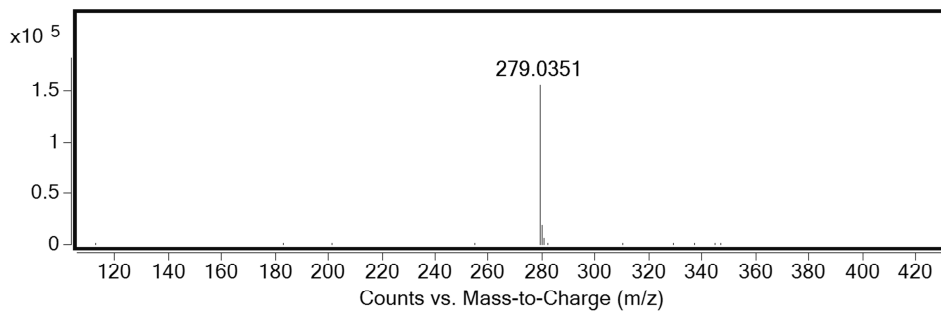
Figure S1 (cont.). Mass spectra of chlorophene and its main ozonation by-products.

3.6. Determination of the reaction rate constants and decomposition mechanisms of ozone with two model emerging contaminants: DEET and nortriptyline.

3.6. DETERMINATION OF THE REACTION RATE CONSTANTS AND DECOMPOSITION MECHANISMS OF OZONE WITH TWO MODEL EMERGING CONTAMINANTS: DEET AND NORTRIPTYLINE

F. Javier Benítez, Juan L. Acero, J. Francisco García†, Francisco J. Real, Gloria Roldan, Elena Rodríguez, Antonio Molina-Díaz†.

Departamento de Ingeniería Química, Universidad de Extremadura, Badajoz.

†Grupo de Investigación de Química Analítica, Universidad de Jaén, Jaén.

Two representative substances of the so-called emerging compounds group (ECs), N,N-diethyl-m-toluamide (DEET) and nortriptyline hydrochloride, were selected to be subjected to ozonation processes, which constitute promising technologies for the removal of hazardous pollutants. The kinetic study provided ozonation rate constants, with an average value of 0.123 ± 0.003 L mol^{-1} s^{-1} for DEET, which remained almost unaffected with the pH; while values varying from 2.40×10^3 to 472×10^3 L mol^{-1} s^{-1} for nortriptyline were deduced in the pH range 2-11. Because of the ionic nature of nortriptyline, the specific rate constants of the protonated and neutral species were determined, the values obtained being 2.1×10^3 and 4.3×10^5 L mol^{-1} s^{-1}, respectively. By means of liquid chromatography time-of-flight mass spectrometry analysis, the main by-products formed in the ozonation reactions were identified (14 for DEET and 27 for nortriptyline), and the evolution of their concentrations with reaction time were established. According to these compounds and their concentration profiles, the reaction mechanisms for the ozonation of both emerging contaminants were proposed and discussed. A decrease in the toxicity was also observed during ozonation of nortriptyline.

1. INTRODUCTION.

Chemical oxidation technologies are currently applied to the removal of recalcitrant pollutants present in waters because of the potential for the elimination of these substances. Among these oxidation systems, single oxidants such as UV irradiation, ozone, chlorine, and hydrogen peroxide, or combinations of these oxidants in the advanced oxidation processes, such as O_3/H_2O_2, UV/H_2O_2, Fenton/photo-Fenton systems, and UV/TiO_2 (Kim et al., 2009; Méndez-Arriaga et al., 2010). Recently, cavitation (Chakinala et al., 2009), a modern technique consisting of the formation, growth, and subsequent collapse of cavities that release large magnitudes of energy locally and generate strong oxidizing conditions has been incorporated to these oxidation processes. All of these systems have been frequently used with success and have demonstrated high effectiveness in the elimination of contaminants that are selectively oxidized to readily biodegradable and less toxic compounds (Klavarioti et al., 2009; Yuan et al., 2011). However, in some cases, these oxidants can generate potentially harmful by-products which could be very reactive towards some substances present in the water systems, as it has recently been pointed out (Magdeburg et al., 2012; Rivera-Utrilla et al., 2013).

Among these single oxidants, ozone constitutes an efficient agent for the purification of surface and drinking waters (Huber at al., 2003; Esplugas et al., 2007) because of its reactivity towards most of organic pollutants which are present in aquatic environments. As it is known, in addition to this direct reaction with most of the organic compounds, its self-decomposition produces OH radicals, which constitute a powerful oxidant. Accordingly, in an ozonation process both direct ozone and OH radical pathways must be considered, since molecular O_3 very selective, whereas OH radicals react indiscriminately with organic molecules (von Gunten, 2003; Rosenfeldt et al., 2006).

Recently, a new group of chemicals which are called emerging contaminants (ECs) has increased its presence in aquatic environments and represents an important source of pollution. This group includes different kinds of substances, such as pesticides, pharmaceuticals and personal care products, endocrine disruptors, industrial compounds, fragrances, water treatment by-products, flame retardants and surfactants, etc. (Stuart et

al., 2012). The denomination of emerging contaminants is due to the fact that most of these substances are still unregulated or in the process of being regulated. Because of their persistence in aquatic environments, some ECs may cause ecological harm and develope antimicrobial resistance. The health effects of small amounts of these agents on humans over a lifetime of exposure are unknown at this time. Municipal wastewater is a significant source of ECs in the environment because many of them are not removed completely in conventional wastewater treatment plants. The literature shows a wide range of many classes of ECs (e.g., antibiotics, betablockers, antiepileptics, liquid regulators, etc.) in wastewater effluents and receiving waters (Kasprzyk-Hordern et al., 2009). As a consequence of these problems, the elimination of ECs is currently pursued, and the use of chemical oxidation procedures could be effective technologies that are highly recommended for this objective.

Among the numerous substances included in this group, two emerging contaminants were selected in the present work for the study of their degradation by means of ozone. On the one hand, N,N-diethyl-m-toluamide or DEET is an active compound in insect repellents, commonly used for protection against insect bites. Contamination by DEET has been found in groundwater (Constanzo et al., 2007), surface streams, seawater, and even in drinking water treated by conventional water treatment systems (Stackelberg et al., 2004). It has been reported to have potential carcinogenic properties in human nasal mucosal cells (Tisch et al., 2002). On the other hand, the pharmaceutical nortriptyline HCl, which belongs to the group of tricyclic antidepressants (TCAs), is presently used as an effective treatment against depression since its introduction 50 years ago (Jorni et al., 2011). It has been detected at similar concentrations in WWTP effluents than in the influent samples (Langford and Thomas, 2009). This selection was made with the aim of considering two model compounds with a relevant toxic strength in the environment, that belong to two different representative families that are included into lists of priority emerging contaminants. Additionally, the literature provided very few studies about their degradation by chemical technologies.

Because of these facts, growing attention should be paid to the removal of both substances from waters in the production of drinking water, and chemical technologies

must be tested for this purpose. As a consequence, a wide research program was envisaged for the evaluation of chemical oxidants to eliminate of some selected ECs. Thus, in a previous works, a group of selected ECs (that included DEET and nortriptyline among others) was oxidized by means of UV radiation and the combination UV/H_2O_2 (Benitez et al., 2013), and by means of chlorine (Acero et al., 2013). The present study was focused in the use of ozone as oxidant agent. Thus, the first goal was to perform a kinetic study of the ozonation process of both substances, with the determination of rate constants in a wide pH range. In the second part, most of the by-products formed during the ozonation reactions are identified, and the degradation pathways in accordance to these by-products are proposed. Finally, some toxicity measurements were also conducted, which allows assessment of the evolution of the toxicity of the reaction mixtures through the ozonation process.

2. MATERIALS AND METHODS.

2.1. Ozonation experiments.

The first group of ozonation experiments was conducted with the aim of determining the rate constants for the direct reaction between ozone and each one of the two selected ECs. These experiments were carried out in homogeneous conditions, by mixing the solutions of ozone and the target compound. Thus, 1 µM solutions of DEET (DT) or nortriptyline hydrochloride (NH) were previously prepared by dissolving these compounds in a 250 mL glass reactor, and in the presence of 0.1 M tert-butyl alcohol, which was used as OH radical scavenger (Staehelin and Hoigne, 1985). An ozone stock solution was prepared by dissolving an ozone gas stream in ice-cooled ultra-pure water until saturation was reached.. The time required to reach dissolved ozone concentrations close to saturation (around 9×10^{-4} M for the operating temperature of the present study) was approximately 90 minutes. The initial ozone gas stream was produced by passing ultrapure oxygen gas through an ozone generator (Sander Labor-Ozonisator) at a constant flow rate of 40 L h^{-1}.

Every experiment was started by introducing into the reactor containing the EC solution the required volume of the saturated ozone solution to achieve an initial concentration of at least 10 μM in ozone. This excess of ozone with respect to DEET or norptriptyline allowed to reach experimental conditions of first-order kinetics, as will be explained later. At regular reaction times, sample aliquots were collected from the reactor in order to analyse the remaining concentration of the EC. All these experiments were carried out at a constant temperature of 20 $^{\circ}$C, while the pH was varied in the range 2-11 by using different phosphoric acid/phosphate buffers (0.05 M).

Exceptionally, the experiments of nortriptyline ozonation at pH 10 and 11 were conducted under different experimental conditions, because of the high reaction rate for these pHs which made impossible to directly follow the concentration of this substance with reaction time. In those cases, competition kinetics was applied, which needed the simultaneous presence of a reference compound. In the present work, this reference compound was metoprolol, and each experiment started by mixing solutions of nortriptyline 1 μM with metoprolol 1 μM into several 25 ml glass flasks, together with phosphoric acid/phosphate buffer required to reach the desired pH (10 or 11), and tert-butyl alcohol. Then, increasing volumes of the ozone stock solution were injected into each flask, according to the desired initial concentrations of ozone in the final mixture. After 1 h in a thermostatic bath at 20 °C, ozone was totally consumed and the remaining concentration of nortriptyline and metoprolol was measured in the solutions, which allowed to the determination of the rate constants.

The second group of ozonation experiments was performed with the objective of identifying the by-products generated during the ozonation reactions of these model ECs. The initial concentration tested was 10 mg L^{-1}. Neither buffers nor radical scavengers were used in these experiments in order to improve the Liquid Chromatography-Mass Spectra (LC-MS) analysis. The initial pH was 5.7 and decreased during the experiments to around 4.4. These experiments were carried out in heterogeneous conditions, by introducing an ozone gas stream (0.5 g m^{-3}) into the solution of DEET or nortriptyline through a gas-dispersion plate placed at the bottom of the reactor. During the reaction, at regular time

intervals, sample aliquots were collected from the reactor and were analysed for the identification of the intermediates present in the solutions.

2.2. Analytical methods.

According to the two types of ozonation experiments described, two different analytical methods were developed. Thus, in the homogeneous kinetic experiments, the concentrations of selected ECs and metoprolol were determined by High Performance Liquid Cromatography (HPLC), with a Waters chromatograph equipped with a 996 photodiode array detector and a Phenomenex Gemini C18 Column (5μm, 150mm × 3mm). The injection volume was 100 μL and the detection was made at 250 nm. A gradient mode was applied with acetonitrile and 25 mM formic acid as mobile-phase. The global flow rate was 0.2 mL min^{-1} and the column temperature was 20 ^{o}C. On the other hand, the ozone concentration of the stock solutions was determined directly by measuring its UV absorbance at 258 nm (ε=3150 L mol^{-1} cm^{-1}).

In the second group of ozonation experiments, those performed for the by-products identification, the procedure applied was similar to those previously reported (Robles-Molina et al., 2012; Martin de Vidales et al., 2012). Thus, an HPLC system comprising a binary pump, an autosampler and a degasser (Agilent Technologies 1290 Infinity) was used, with a XDB-C18 analytical column (1.8 μm, 50 mm x 4.6 mm). The separation of the different compounds was obtained by a mobile phase constituted by 0.1% formic acid and acetonitrile in gradient mode, with a flow rate of 0.5 mL min^{-1}. This procedure allowed to determining the relative abundances of each one of the model ECs and most of their intermediates generated during the reaction. The HPLC system was connected to a time-of-flight mass spectrometer (Agilent 6220 TOF) by means of an electrospray interface operated in either positive or negative ionization modes. The operating conditions were: capillary voltage, 4000 V(+)/3000 V(-); nebulizer pressure, 40 psig; drying gas flow rate, 9.0 L min^{-1}; gas temperature, 325 ^{o}C; skimmer voltage, 65 V; octapole 1 rf, 250 V; fragmentor voltages: 160, 200 and 240 V. LC–MS accurate mass spectra were recorded across the m/z range 50–1000 in positive ion mode, and 50–1100 in negative ion mode. The internal mass calibration was made automatically by using a dual-

nebulizer electrospray source with an automated calibrate delivery system. The calibrating solution contained the following internal reference masses: TFANH$_4$ (ammonium trifluoroacetate, C$_2$O$_2$F$_3$NH$_4$, at m/z 112.985587 in negative ion mode), purine (C$_5$H$_4$N$_4$, at m/z 121.050873 in positive ion mode), and HP-0921 (Hexakis-(1H,1H,3H-tetrafluoropropoxy) phosphazine, C$_{18}$H$_{18}$O$_6$N$_3$P$_3$F$_{24}$, at m/z 922.009798 in positive ion mode and m/z 1033.988109 in negative mode). The full scan mass spectra were recorded with an Agilent Mass Hunter Data Acquisition software (version B.04.00), and processed with an Agilent Mass Hunter Qualitative Analysis software (version B.04.00). For the identification and structure elucidation of the by-products, elemental compositions were obtained from accurate mass measurements of (de)protonated molecules and their characteristic fragment ions. Some specific ozonation reactions of the selected ECs described in literature, and other general ozonation reactions of organic compounds were also considered.

2.3. Toxicity measurements.

Final experiments were carried out for the determination of the toxicity evolution during the ozonation of DEET and nortriptyline. Initial concentration of ECs was maintained constant at 10 mg L^{-1}, and the pH value was 7. In these experiments, performed in heterogeneous conditions, sample aliquots were collected from the reactor at regular times, and the concentration of ECs was analysed by HPLC. At the same time, the toxicity was evaluated by using a Microtox Model 500 Toxicity Analyzer. This equipment measures the ability of the solution to inhibit the bioluminescence of the marine bacterium *Vibrio fischeri*, by determining the decay of the light emitted by the bacterium when it is exposed to toxic chemical compounds. The luminescence was recorded after 15 min of incubation at room temperature (20 ^{o}C), and the percentage of inhibition was then calculated.

3. RESULTS AND DISCUSSION.

3.1. Kinetic study.

The first group of ozonation experiments was carried at 20 ^{o}C and by varying the pH, with the aim of determining the apparent rate constant for the direct reaction between

ozone and each one of the selected ECs. As was mentioned, these experiments were performed in the presence of tert-butyl-alcohol, a scavenger of OH radicals (Staehelin and Hoigne, 1985). As it is known, free radicals can be generated from the ozone self-decomposition, which is enhanced by the increase of pH, and then, the reactions promoted by hydroxyl radical would contribute in a great extent at basic pH. Therefore, the presence of tert-butyl-alcohol assured that the ECs were only degraded by a direct attack of molecular ozone, while OH radicals contribution could be neglected.

It is widely described in the literature that the overall reaction of ozone with most of organic compounds follows second-order kinetics, and first order with respect to each reactant (von Gunten, 2003; Hoigne and Bader, 1983). In the present case, as the initial ozone concentration was much in excess with respect to DEET or nortriptyline (10 µM *vs*. 1 µM), the ozone concentration during each experiment was considered to remain almost constant. Then, the reaction rate can be reduced to pseudo-first-order kinetics with respect to the EC:

$$r_{O3} = -\frac{d\,[EC]}{dt} = k_{app}\,[O_3]\,[EC]_{tot} = k'\,[EC] \qquad (1)$$

where k_{app} is the second-order rate constant for the mentioned overall ozonation reaction based on the total concentration of the model EC (DEET or nortriptyline), and k' is the pseudo-first-order rate constant with respect to the emerging contaminant elimination. Equation (1) can be integrated, and after regression analysis of the terms ln ($[EC]_0/[EC]$ *vs* t, the rate constants k' were evaluated for each specific experiment. Then, by introducing the almost constant ozone concentration, the apparent second-order rate constants were determined (k_{DT} for DEET and k_{NH} for nortriptyline). Their values summarized in Table 1.

As was mentioned previously, the higher reactivity of nortriptyline at pH 10 and 11 did not permit the evaluation of its concentration at different times. Therefore, apparent rate constants were determined by competition kinetics, procedure initially proposed by Gurol and Nekouinaini (1984), and later widely used in other studies (Yao and Haag, 1991; Laat et al., 1996). It is based on the simultaneous oxidation of a reference compound, whose rate constant with the oxidant (ozone) is previously known, and a target compound

(nortryptiline in the present study). The model is described in detail elsewhere (Benitez et al., 2003), and its application leads to the following final expression:

$$\ln \frac{[NH]_0}{[NH]} = \frac{k_{NH}}{k_R} \ln \frac{[R]_0}{[R]}$$

(2)

where [NH] and [R] represent the concentrations of nortriptyline and the reference compound; and k_{NH} and k_R are the ozonation rate constants for the target and reference compounds, respectively. According to Equation (2), a regression analysis for the values of ln ([NH]$_0$/[NH]) and ln ([R]$_0$/[R]) provides the values of the rate constant ratios k_{NH}/k_R. Then, as the value of k_R is previously known, the rate constant k_{NH} can be easily evaluated. This method requires the fulfilment of an important condition: both substances, the target and reference compounds, must present reactivities towards ozone in the same order of magnitude. In the present study, metoprolol fulfils this condition and was used as reference compound. The rate constant for the reaction of metoprolol with ozone k_R at 20 ^{o}C has been previously determined (Benitez et al., 2009), being the values obtained 9.31 x10^4 and 1.25 x10^5 L mol^{-1} s^{-1} at pH 10 and 11, respectively.

Table 1. Apparent second-order rate constants for the reaction between DEET (k_{DT}) or nortriptyline (k_{NH}) and ozone at different pH values.

pH	k_{DT}, L mol^{-1} s^{-1}	k_{NH}x10^{-3}, L mol^{-1} s^{-1}
2	0.120 ± 0.005	2.40 ± 0.04
3	0.120 ± 0.004	2.34 ± 0.12
4	0.122 ± 0.011	2.28 ± 0.10
5	0.124 ± 0.011	1.94 ± 0.05
6	0.126 ± 0.031	2.25 ± 0.11
7	0.126 ± 0.006	2.73 ± 0.07
8	0.124 ± 0.008	3.48 ± 0.05
9	0.122 ± 0.004	17.3 ± 0.8
10	-	233 ± 11
11	-	472 ± 52

Some experiments described in the Experimental Section were performed for this specific objective, and the remaining concentrations of nortriptyline and metoprolol present in the samples were measured once ozone was totally consumed. The application of competition kinetics provided the apparent rate constants for nortriptyline at pH 10 and pH 11, values that are also depicted in Table 1 (233 x10^3 and 472 x10^3 L mol^{-1} s^{-1}, respectively).

As can be seen in Table 1, the k_{app} values for the ozonation reaction of DEET are fairly similar in the pH range of work 2-9, and an average value of 0.123 ± 0.003 L mol^{-1} s^{-1} can be proposed.. On the contrary, in the case of norptriptyline, it is also observed an almost constant k_{app} value in the pH range 2-8; but at pH>8, it occurred an important increase in the ozonation rate constants with the increase of pH. These results can be explained by considering the pK_a of both substances and previous results of ozonation reaction rates depending on the pH of work. As it has been reported (Hoigne and Bader, 1983; Gogate and Pandit, 2004), usually higher values of pH enhances the degradation rate of micropollutants ozonation, especially for those compounds with a pK_a value higher than the operating pH. Thus, in the case of DEET, with a pK_a value of 0.4, the operating pH does not exert any influence on the ozonation rate. However, in the case of nortriptyline with a pK_a of 10.2, the pH exerts a positive influence on the ozonation in the pH range 8-11. The results obtained for apparent rate constants for the reaction between ozone and norptriptyline (see Table 1) totally confirm these considerations. Then, it can be concluded that in the case of commercial operation, it is recommended to work at natural or slightly higher pH, in order to favor ozonation of micropollutants with pK_a above pH.

By considering the possibility of the presence in a water matrix of nortriptyline in its protonated or neutral forms depending on the pH of work, the overall ozonation reaction rate must be expressed as a function of the specific ozonation rate constants for both species in the form:

$$r_{O3} = k_{app} [O_3] [NH]_{tot} = k_1 [O_3] [NH^+] + k_2 [O_3] [NH] \qquad (3)$$

in this Equation (3), k_1 and k_2 represent the specific ozonation rate constants for the protonated and the neutral forms of nortriptyline, respectively. The usefulness of Equation (3) is as follows: if the rate constants k_1 and k_2 are known for any general compound (nortriptyline in this specific study), the global rate constant k_{app} can be theoretically evaluated; and subsequently, the global reaction rate r_{O3} can be predicted during the treatment of any surface or wastewater containing this pollutant substance at any pH. Therefore, the evaluation of both rate constants constitutes an interesting objective, and for this purpose, it must be taken into account the ratio of the protonated form to the neutral form, which is given by the degree of dissociation α. This parameter can be introduced into Equation (3), leading to:

$$k_{app} = \alpha \, k_1 + (1\text{-}\alpha) \, k_2 \tag{4}$$

At the same time, α is related to the pH by the dissociation constant K_a, by means of the expression:

$$\alpha = \frac{1}{1 + \dfrac{[H^+]}{K_a}} \tag{5}$$

In the present case, the introduction of the $pK_a=10.2$ value for nortriptyline into Equation (5) determines the α values for each specific pH. Then, and according to Equation (4), the application of a non-linear least squares regression analysis to the experimental values of k_{app} provided the evaluation of the intrinsic rate constants k_1 and k_2, being these values: 2.1×10^3 and 4.3×10^5 L mol^{-1} s^{-1}, respectively. These intrinsic rate constants k_1 and k_2 must be validated, and for this purpose, they were introduced into Equation (4), together with the values of α previously obtained from Equation (5), at each pH. The theoretically calculated k_{app} rate constants in this form were plotted in Figure 1 (lines) vs. pH, together with the experimental values (symbols) which were depicted in Table 1. As observed, there is a quite good agreement between calculated and experimental results, which confirms the goodness of the proposed model.
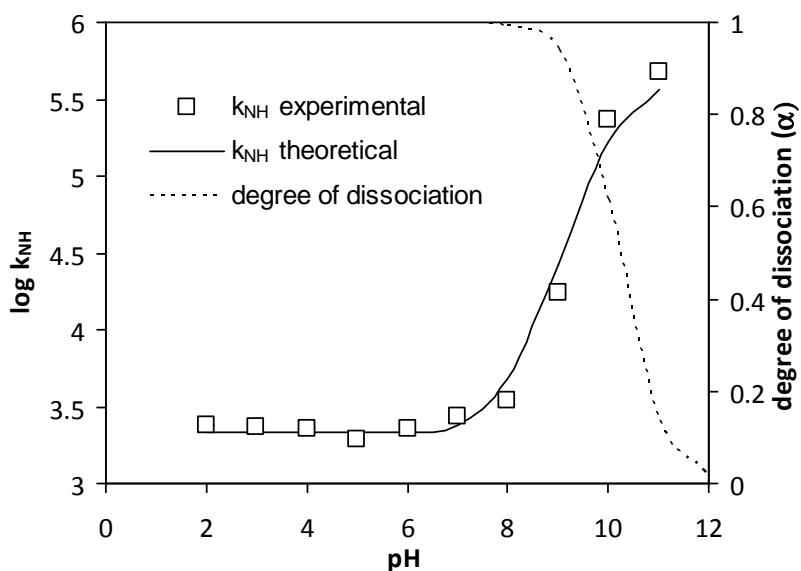
Figure 1. Apparent second-order rate constants (k_{NH}) for nortriptyline ozonation reaction and degree of dissociation at different pHs. Comparison of theoretical and experimental values or rate constants.

The low value of the rate constant for the reaction of DEET with molecular ozone indicates that in a real water treatment, where OH radicals can be generated from ozone decomposition and from the reaction of ozone with natural organic matter (NOM), the oxidation of DEET is performed mainly by OH radicals. However, nortriptyline reacts very fast with molecular ozone (rate constants in the order 10^3 to 10^5 L mol^{-1} s^{-1}), and therefore, its oxidation during a real water treatment is likely due to direct reactions with ozone.

3.2. Identification of by-products and ozonation pathways.

The intermediate by-products formed during the ozonation of DEET and norptriptyline were tentatively identified, since they could not be confirmed due to the lack of standards. Then, reaction pathways were proposed according to these intermediates generated. For the identification of ozonation by-products, samples of the ozonation reaction of both selected ECs were analyzed by LC-TOFMS. This approach provided accurate mass measurements of ions (m/z values) of the different compounds formed as well as the

subsequent elemental compositions and the Double Bond Equivalent (DBE) number, which informs about the double bonds and rings of the molecule. In-source collision induced dissociation (CID) fragmentation experiments (Robles-Molina et al., 2012), was also undertaken to assist the identification of the intermediates formed. For this purpose, three fragmentation voltages were applied (160, 200, and 240 V) in both positive and negative ionization modes, in order to find possible diagnostic ions which are common to a family of species. Multiple fragments ions were found for each by-product identified. For instance, Figure S1 of the Supporting Information shows the specific mass spectrum for the parent compound DEET, as well as its diagnostic ions identified. As most of them have been also found in most of its intermediates, it confirmed that the by-products contain part of the parent compound and have been generated from this initial substance.

Following this general procedure, Tables S1 and S2 of the Supporting Information include tentative structures proposed for all the by-products detected and identified in the ozonation processes (14 for DEET and 27 for nortriptyline, respectively) as well as the theoretical and experimental m/z values, the relative mass error in each case, and the DBE number. All by-products were identified with LC-TOFMS in the positive ionization mode for both DEET and nortriptyline. The low experimental relative mass errors obtained evidenced the high grade of confidence in the assignment of the elemental composition. In this sense, relative mass errors below 5 ppm are generally accepted for the verification of the elemental composition (Coelho et al., 2009).

Focusing specifically on the DEET ozonation, Figure 2 shows the evolution of the profiles for the parent compound and its major by-products formed, expressed as relative abundance of chromatographic areas (mean of two replicates) *vs* ozonation time. Due to the great number of by-products identified, those which were found in a minor extent (i.e., D1, D2, D3, D4, D5, D9 and D10) are not shown. Furthermore, the relative abundance of the parent compound DEET, which is in a much greater concentration, must be read in the right Y axis, while this abundance for the remaining compounds represented in Figure 2 must be read in the left Y axis. As observed in this Figure 2, DEET decreased continuously with reaction time, as could be expected. At the same time, a continuous formation during the whole ozonation process (around 2 h) occurred for the three main by-products (isomers D6

and D7; and compound D8) that were formed in a major extent. It must also be noted the formation of D13 which reached a maximum after 90 min, followed by a decrease in its concentration. The remaining by-products that are also shown in Figure 2 (D11, D12, and D14) presented continuous increases in their concentrations, but at much lower levels.

Figure 2. Quantitative analysis and time profiles of intermediate by-products detected during the ozonation of DEET. (Parent compound profile is represented in the right Y axis).

Bearing in mind these identified by-products and their distribution curves, the reaction mechanismproposed for DEET is shown in Figure 3. Since direct reactions with ozone are not relevant, DEET oxidation is mainly due to reactions with OH radicals. The first steps of DEET oxidation can occur through two possible main routes: by an attack of the hydroxyl radicals at the aromatic ring, or by a similar attack at the aliphatic chain. In the first case, the hydroxyl radicals attack at the aromatic ring of DEET could lead to the generation of a monohydroxylated DEET derivative, as it has been reported by Zhang and Lemley (2006), in a previous work which was focused in the degradation of DEET by anodic Fenton. Song et al. (2009), identified four isomers from the same attack at the aromatic ring during

the irradiation process of DEET; and Calza et al. (2011) also found the same four isomers during the photocatalytic treatment of this substance.

In the present study, six isomers have been identified for monohydroxy DEET (D2 to D7 in Table S1 of the Supporting Information and Figure 3, m/z 208.1332 and DBE 5) as a result of this radical attack. Thus, isomers D4 to D7 are the same compounds that were previously reported (Song et al., 2009; Calza et al., 2011) and they correspond to the different possible positions that can be occupied by the OH moiety in the aromatic ring. In addition, isomers D2 and D3 have been specifically detected in this study, although at a much lower concentrations, and were not previously reported. Specifically for D3, and based on its fragments found, it corresponded to the hydroxylation of the aliphatic chain: in effect, as it can be observed in Figure S2 of the Supporting Information which shows the mass spectrum of this by-product D3, the diagnostic ion with m/z 119 and molecular formula C_8H_6O was formed. Finally, the isomer D2 can be due to the hydroxylation of the methyl group. In all these cases, sodium adducts ($[M+Na]^+$) also appeared in their mass spectra, which confirmed the identity of the molecular ions.

In the second case, the OH radical attack at the aliphatic chain could occur through two possible different pathways. Firstly, by forming D1, which corresponds to N-acetyl-N-ethyl-m-toluenamide, with m/z 206.1175 (DBE 6). Figure S3 of the Supporting Information shows the mass spectrum for D1, and its diagnostic ions with m/z 164, 119 and 91. These diagnostic ions, and more specially that of m/z 164 confirms that the oxidation occurs in the alkyl chain. The previously referred works (Song et al., 2009; Calza et al., 2011), also identified this degradation by-product. A new hydroxylation step of D1 leads to the formation of D9 compound (with m/z 222.1124, DBE 6), which is followed by the generation of D12 (with m/z 238.1072, DBE 6): they correspond to the mono- and dihydroxylated derivatives of N-acetyl-N-ethyl-m-toluenamide. Both degradation by-products, D9 and D12, had also been identified (Calza et al., 2011). Moreover, the degradation product D9 could also be formed from isomers D2 to D7 by means of either oxidation of the aliphatic chain (D4 to D7) or aromatic ring (D2 and D3).

The second possible pathway of attack at the aliphatic chain could lead to the breakdown of the own aliphatic chain and the formation of by-product D8 (N-ethyl-m-toluenamide, with m/z 164.1071, and DBE 5). This compound perfectly matches with a diagnostic ion of DEET (see Figure S1 of the Supporting Information). Moreover, the diagnostic ions m/z 119.0516 and m/z 72.0447 also appear in the mass spectrum of D8 (figure not shown). Once again, Song et al. (2009), and Calza et al. (2011), found this by-product, even at a higher concentration, in their DEET photo-degradation studies.

Finally, the remaining degradation by-products identified (D10, D13, D14, and D11; most of them detected in much lower intensities), and according to the mechanism pathways proposed in Figure 3, could correspond to the opening of the aromatic ring, which is supported by the decrease to a value of 4 of the DBE parameter. Thus, the degradation by-product D10 (m/z 182.1175) can be explained by the breakdown of the aromatic ring of isomers D4 to D7. Later, the mono- and dihydroxylation of this intermediate D10 could lead to the formation of intermediate products D13 and D14 (with m/z 198.1125 and 214.1072, respectively). In a similar way, the formation of D11 (m/z 168.1018) from D8 could be explained by the loss of the alkyl chain and minor oxidation of aromatic ring. The opening of the aromatic ring was also proposed by Calza et al. (2011), for the formation of different by-products of DEET: specifically, two of those compounds reported matched perfectly with the degradation by-products D10 and D13 of the present study.
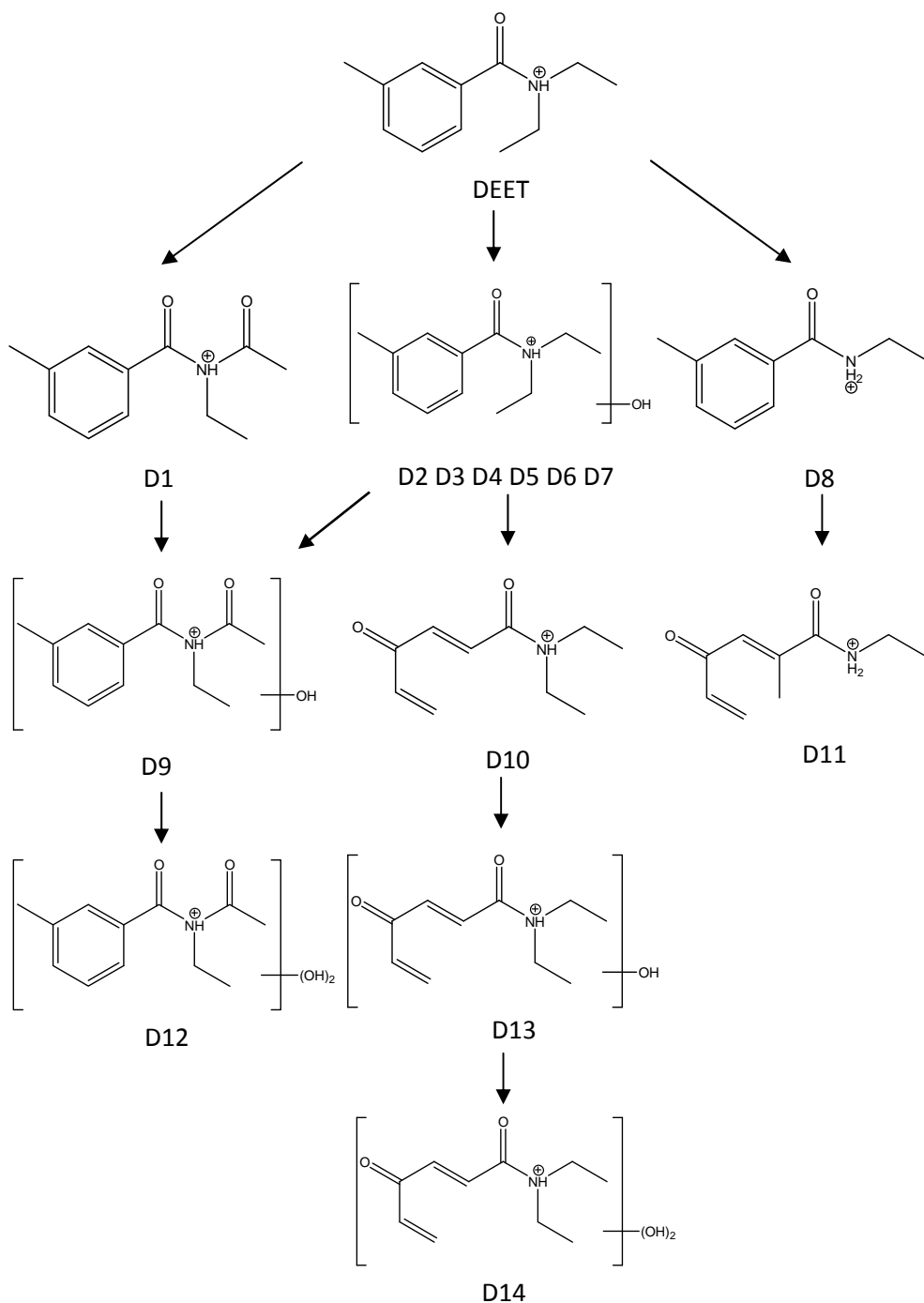
Figure 3. Reaction mechanism proposed for the ozonation of DEET.

The ozonation reaction of nortriptyline was studied in a similar way as for DEET. Thus, Figure 4 presents the time profiles for nortriptyline and its main by-products formed. Once again, it must be noted that the relative abundances of the parent compound nortriptyline and the major intermediate compound N1 must be read in the right Y axis, while the corresponding values for the remaining by-products (i. e., N2, N9, N11, N13, N16, N20, and N26) must be read in the left Y axis. The remaining intermediates identified and compiled in Table S2 of the Supporting Information are not represented in this Figure 4 since they gave much lower signals.

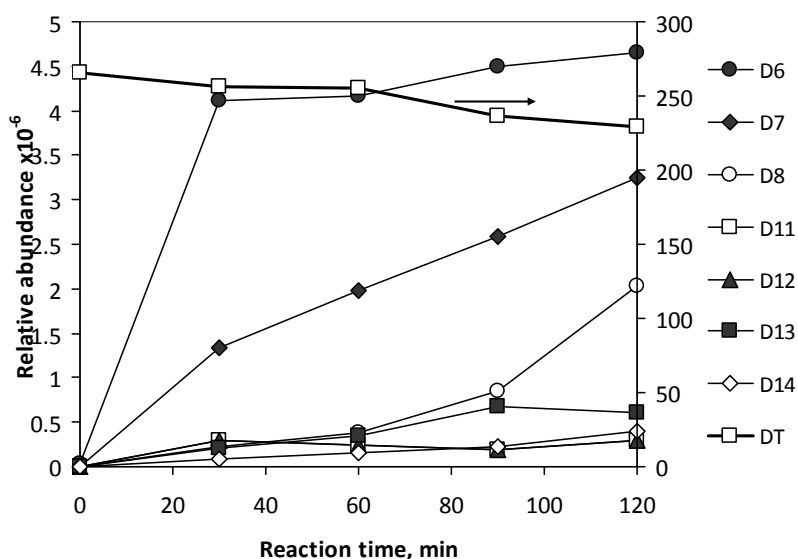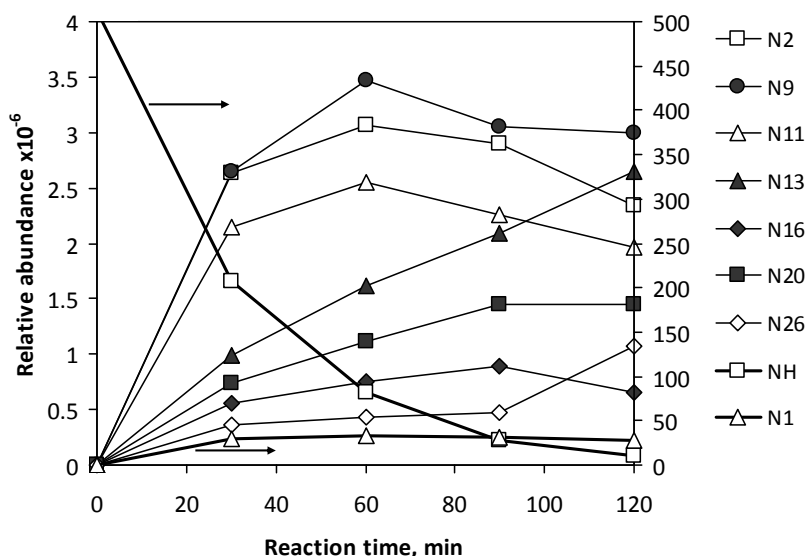**Figure 4. Quantitative analysis and time profiles of intermediate by-products detected during the ozonation of nortriptyline. (Parent compound and N1 by-product profiles are represented in the right Y axis).**

The observation of Figure 4 reveals that nortriptyline concentration decreased continuously through reaction time. Moreover, the by-products formed in higher extents followed the sequence: N1>N9>N2>N11>N20>N16. Initially, these by-products presented an increase in their abundance until a maximum value was reached (in the range 50-100 min, depending of each substance); and later, a period of decreasing abundance took place. On the contrary, intermediates N13 and N26 presented increased concentrations during the whole ozonation process (around 2 h).

According to these by-products generated and their relative abundances, it can be proposed that the mechanism of the reaction between nortriptyline and ozone takes place through the pathways shown in Figure 5. Thus, in a first step, the identified degradation products N1 and N2 (isomers with molecular formula $C_{19}H_{21}NO$, m/z 280.1696 and DBE 10) were formed and correspond to monohydroxylated nortriptyline. These isomers were the first and the third major degradation products found in this study, as has been discussed previously. Similarly, Linden et al. (2008) in their study focused on the metabolic degradation of amitriptyline, reported an initial formation of nortriptyline, and proposed that the hydroxyl group occupies one of the carbon atoms in the heptane ring, resulting in 10-hydroxynortriptyline. In the present study, the fragments found for each isomer support that the hydroxylation step did not occur in the aliphatic chain; however, the exact position occupied by the hydroxyl group cannot be confirmed.

A following hydroxylation step led to the formation of dihydroxylated nortriptyline, with molecular formula $C_{19}H_{21}NO_2$. In the present study, eight isomers have been identified for this intermediate (degradation products N3 to N10, with m/z 296.1645 and DBE 10), being N9 formed in a greater amount as commented before. Specifically, fragments found for isomers N3 to N9 showed that a water molecule was lost, and also, they revealed an increase in the DBE parameter (molecular formula $C_{19}H_{19}NO$, m/z 278.1539 and DBE 11), which indicates that the two hydroxylations occurred in adjacent carbon atoms. Therefore, the loss of this water molecule and the subsequent formation of a new double bond was a possibility. However, this fragment was not found for the degradation intermediate N10.

In next steps, the loss of the aliphatic chain in the degradation intermediates without hydroxylated aliphatic chain occurred. On the one hand, in the case of isomers N1 and N2, it led to the formation of N11 (with molecular formula $C_{15}H_{12}O$, m/z 209.0960 and DBE 10); and on the other hand, in the case of isomers N3 to N10, the by-product N12 (with molecular formula $C_{15}H_{12}O_2$, m/z 225.0914 and DBE 10) was formed. As a confirmation, the mass spectrum for the degradation product N12 (data not shown) provided a fragment that corresponded to the loss of a water molecule, which supports that the hydroxylation occurs in contiguous carbon atoms.

A new hydroxylation step can occur leading to the formation of isomers N13 and N14 (with molecular formula $C_{19}H_{21}NO_3$, m/z 312.16594 and DBE 10), which correspond to trihydroxylated nortriptyline. For both isomers, two fragments have been found with molecular formula $C_{17}H_{14}O_2$ and $C_{15}H_{12}O$, m/z 251.1071 and 209.0961, and DBE 11 and 10, respectively. Thus, Figure S4 of the Supporting Information shows, as an example, the mass spectrum for N13: the first fragment corresponds to the loss of the $-CHOHNH_2CH_3$ moiety, and therefore, one hydroxylation occurs in this section of the aliphatic chain. The second fragment involved the complete loss of the alkyl chain plus two oxygen atoms. Thus, these fragments support that two out of three hydroxylations occurred in the aliphatic chain.

A further hydroxylation step of trihydroxylated nortriptyline led to the formation of isomers N15 to N20 (with molecular formula $C_{19}H_{19}NO_4$, m/z 326.1387 and DBE 11). For these isomers, two fragments had been found (data not shown), with molecular formula $C_{19}H_{17}NO_3$ and $C_{17}H_{12}O_3$, m/z 308.1281 and 265.0859, and DBE 12. The first fragment supports that two hydroxylations occurred in contiguous carbon atoms, because its m/z was the result of a water molecule loss, and the DBE parameter was increased to a value of 12, just as discussed previously. Moreover, the second fragment agreed with the loss of the aliphatic chain $-CHOHNH_2CH_3$, and consequently, one of the hydroxylation steps occurred in this section of the chain. The increase in the value of DBE of isomers N15 to N20 can be justified by different possibilities: formation of a carbonyl group, or an epoxy group, or simply, a new double bound in the aliphatic chain or in the heptane ring (such as can be seen in Figure 5).

Finally, the loss of a water molecule in isomers N13 and N14 and the increase of one double bond lead to the by-products with molecular formula $C_{19}H_{19}NO_2$, m/z 294.1489 and DBE 11. Seven isomers have been identified, which are marked as by-products N21 to N27. In-source fragmentation technique was also applied for them, but no fragments were found. Once again, the generation of these isomers could be the result of the formation of a carbonyl group, an epoxy group, or even, the introductions of a new double bound in the aliphatic chain or in the heptane ring (as shown in Figure 5).
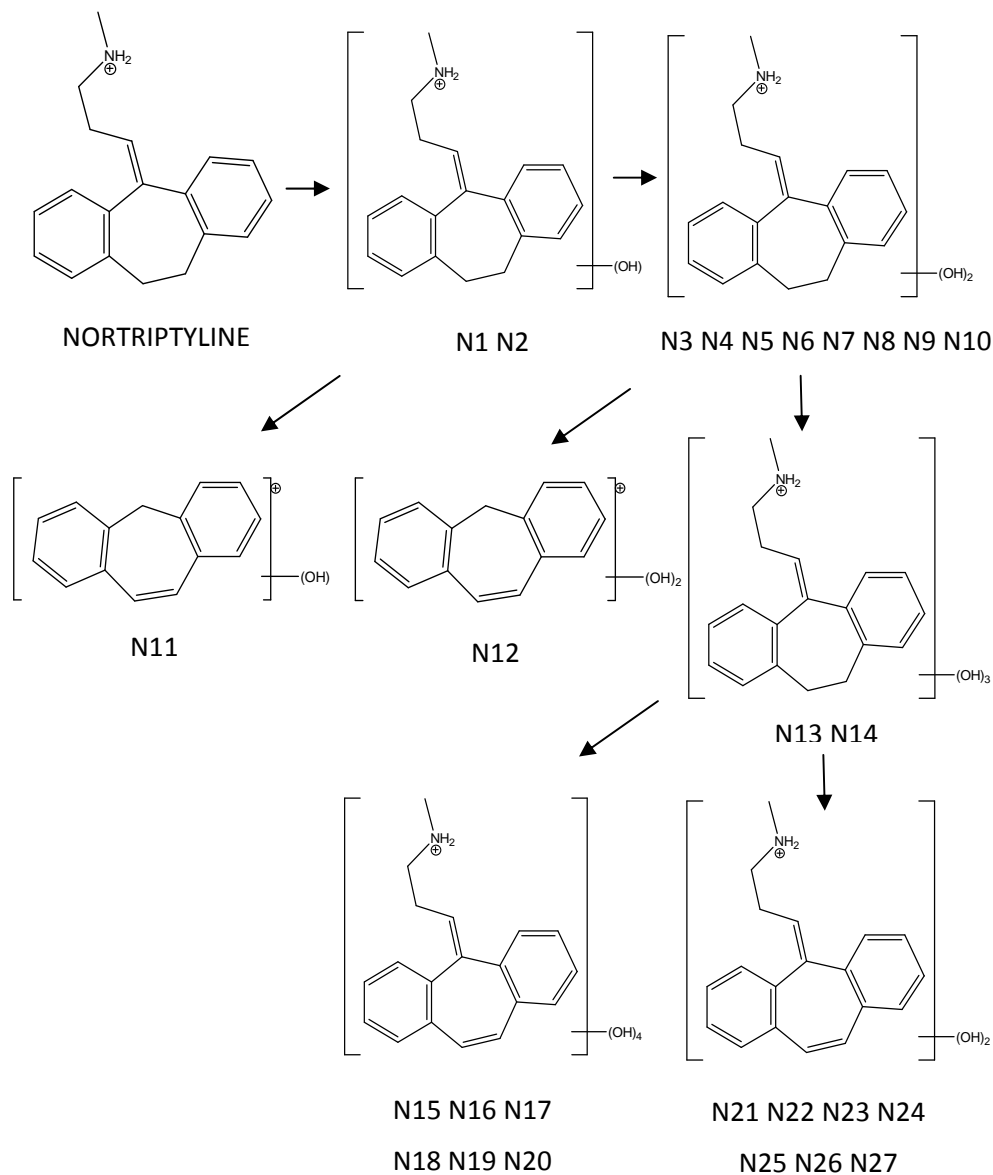
Figure 5. Reaction mechanism proposed for the ozonation of nortriptyline.

3.3. Toxicity measurements.

The evolution of the toxicity during the ozonation of DEET and nortriptyline was also studied in specific experiments performed for this purpose. Sample aliquots were periodically collected from the reactor and inoculated with the bacteria *Vibrio fischeri*, being the luminescence inhibition evaluated after 15 min. At the same time, the removal percentages of DEET and nortriptyline were also determined in each sample. Table 2 compiles the results obtained. As it is clearly observed, the removal of both compounds increased with reaction time. Thus, the degradation after 2 hours of ozonation occurred in a greater extent for nortriptyline (with a removal of 98%) than for DEET (with a removal around 14%), results that are consistent with the ozonation rate constants determined previously. However, a different evolution was observed for the luminescence inhibition percentage. As it is observed, a gradual decrease was obtained for the toxicity in the ozonation of NH, with a maximum value of 26.4% luminescence inhibition after 2 hours of reaction, which indicates that the ozonation process generated intermediate products less toxic than the parent compound. On the contrary, a moderate increase in toxicity up to 17% luminescence inhibition was obtained for DEET during the first period of reaction (60 min); and later, the toxicity remained almost constant for increasing DT removals (reaction times in the range 60-120 min). It seems to indicate that the by-products initially formed are more toxic than the parent compound, while those generated at more advanced reaction times presented a similar toxicity.

Table 2. Evolution of toxicity (percentage of inhibition of *Vibrio fischeri* luminescence after 15 min) and removal of DEET and nortriptyline during ozonation in ultrapure water at pH 7.

Reaction time, min	DEET		Nortriptyline	
	Luminiscence inhibition, %	X_{DT}, %	Luminiscence inhibition, %	X_{NH}, %
0	2.9	0	71.9	0
30	11.6	3.82	53.8	59.6
60	17.1	4.86	48.3	83.9
90	15.0	11.06	31.8	94.5
120	14.0	13.83	26.4	98.0

4. CONCLUSIONS.

The removal of emerging contaminants DEET and nortriptyline by using ozone as oxidant agent has been investigated in a wide pH rage. The rate constant for the ozonation of DEET remained almost constant in the pH range 2-9, its value being 0.123±0.003 L mol^{-1} s^{-1}. On the contrary the rate constants varied for nortriptyline between 2.40 x10^3 to 472 x10^3 L mol^{-1} s^{-1} at pH 2 and 11, respectively, as a consequence of its ionic nature, with a pK$_a$=10.2. A further evaluation led to determining the specific rate constants for the protonated and neutral species of this substance, being the values obtained 2.1 x10^3 and 4.3 x10^5 L mol^{-1} s^{-1}, respectively. Analysis by means of LC-TOFMS allowed the identification of 14 and 27 by-products for DEET and nortriptyline, respectively. The use of the whole information obtained in this identification process permits the proposal of general reaction mechanisms and pathways for the ozonation reaction of both selected emerging contaminants.

Although further experiments should be performed in real water matrices, according to the results of selected ECs degradation in ultrapure water, ozone is a good option for the oxidation of nortriptyline due to the high values of apparent rate constants and the decrease of toxicity. However, ozone is not a suitable oxidant for the abatement of DEET, mainly due to the low values of apparent rate constants.

REFERENCES

Acero, J.L.; Benítez, F.J.; Real, F.J.; Roldán, G.; Rodríguez, E. Chlorination and bromination kinetics of emerging contaminants in aqueous systems. Chem. Eng. J. **2013**, 219, 43-50.

Benitez, F.J.; Acero, J.L.; Real, F.J.; Garcia, J. Kinetics of photodegradation and ozonation of pentachlorophenol. Chemosphere **2003**, 51, 651-662.

Benítez, F.J.; Acero, J.L.; Real, F.J.; Roldán, G. Ozonation of pharmaceutical compounds: Rate constants and elimination in various water matrices. Chemosphere **2009**, 77, 53-59.

Benítez, F.J.; Acero, J.L.; Real, F.J.; Roldán, G.; Rodríguez, E. Photolysis of model emerging contaminants in ultra-pure water: Kinetics, by-products formation and degradation pathways. Water Res. **2013**, 47, 870-880.

Calza, P.; Medana, C.; Raso, E.; Giancotti, V.; Minero, C. N,N-diethyl-m-toluamide transformation in river water. Sci. Total Environ. **2011**, 409, 3894-3901.

Chakinala, A.G.; Gogate, P.R.; Burgess, A.E.; Bremner, D.H. Industrial wastewater treatment using hydrodynamic cavitation and heterogeneous advanced Fenton processing. Chem. Eng. J. **2009**, 152, 498-502.

Coelho, A.D.; Sans, C.; Agüera, A.; Gómez, M. J.; Esplugas, S.; Dezotti, M. Effects of ozone pre-treatment on diclofenac: Intermediates, biodegradability and toxicity assessment. Sci. Total Environ. **2009**, 407, 3572-3578.

Costanzo, S.D.; Watkinson, A.J.; Murby, E.J.; Kolpin, D.W.; Sandstrom, M.W. Is there a risk associated with the insect repellent DEET (N,N-diethyl-m-toluamide) commonly found in aquatic environments?. Sci. Total Environ. **2007**, 384, 214-220.

De Laat, J.; Maouala-Makata, P.; Dore, M. Rate constants for reactions of ozone and hydroxyl radicals with several phenyl-ureas and acetamides. Environ. Technol. **1996**, 17, 707-716.

Esplugas, S.; Bila, D.M.; Krause, L.G.T.; Dezotti, M. Ozonation and advanced oxidation technologies to remove endocrine disrupting chemicals (EDCs) and pharmaceuticals and personal care products (PPCPs) in water effluents. J. Hazard. Mater. **2007**, 149, 631-642.

Gogate, P.R.; Pandit, A.B.A review of imperative technologies for wastewater treatment I: oxidation technologies at ambient conditions. Adv. Environ. Res. **2004**, 8, 501-551.

Gurol, M.; Nekouinaini, S. Kinetic behavior of ozone in aqueous solutions of substituted phenols. Ind. Eng. Chem. Fund. **1984**, 23, 54-60.

Hoigne, J.; Bader, H. Rate constants of reactions of ozone with organic and inorganic compounds in water-I. Non-dissociating organic compounds. Water Res. **1983**, 17, 173-183.

Huber, M.M.; Canonica, S.; Park, G.; von Gunten, U. Oxidation of pharmaceuticals during ozonation and advanced oxidation processes (AOPs). Environ. Sci. Technol. **2003**, 37, 1016-1024.

Jornil, J.; Jensen, K.G.; Larsen, F.; Linnet, K. Risk assessment of accidental nortriptyline poisoning: The importance of cytochrome P450 for nortriptyline elimination investigated using a population-based pharmacokinetic simulator. Eur. J. Pharm. Sci. **2011**, 44, 265-272.

Karpel Vel Leitner, N.; Roshani, B. Kinetic of benzotriazole oxidation by ozone and hydroxyl radical. Water Res. **2010**, 44, 2058-2066.

Kasprzyk-Hordern, B.; Dinsdale, R.M.; Guwy, A.J. The removal of pharmaceuticals, personal care products,endocrine disruptors and illicit drugs during wastewater treatment and its impact on the quality of receiving waters. Water Res. **2009**, 43, 363-380.

Kim, I.; Yamashita, N.; Tanaka, H. Photodegradation of pharmaceuticals and personal care products during UV and UV/H_2O_2 treatments. Chemosphere **2009**, 77, 518-525.

Klavarioti, M.; Mantzavinos, D.; Kassinos, D. Removal of residual pharmaceuticals from aqueous systems by advanced oxidation processes. Environ. Int. **2009**, 35, 402-417.

Langford, K.H.; Thomas, K.V. Determination of pharmaceutical compounds in hospital effluents and their contribution to wastewater treatment works. Environ. Int. **2009**, 35, 766-770.

Linden, R.; Antunes, M.V.; Ziulkoski, A.L.; Wingert, M.; Tonello, P.; Tzvetkov, M.; Souto, A.A. Determination of Amitriptyline and its Main Metabolites in Human Plasma Samples using HPLC-DAD: Application to the Determination of Metabolic Ratios after Single Oral Dose of Amitriptyline. J. Braz. Chem. Soc. **2008**, 19, 35-41.

Magdeburg, A.; Stalter, D.; Oehlmann, J. Whole toxicity assessment at a wastewater treatment plant upgraded with a full-scale-post-ozonation using aquatic key species. Chemosphere **2012**, 88, 1008-1014.

Martín de Vidales, M.J.; Robles-Molina, J.; Domínguez-Romero, J.C.; Cañizares, P.; Sáez, C.; Molina-Díaz, A.; Rodrigo, M.A. Removal of sulfamethoxazole from waters and wastewaters by conductive-diamond electrochemical oxidation. J. Chem. Technol. Biotechnol. **2012**, 87, 1441-1449.

Méndez-Arriaga, F.; Esplugas, S.; Giménez, J. Degradation of the emerging contaminant ibuprofen in water by photo-Fenton. Water Res. **2010**, 44, 589-595.

Rivera-Utrilla, J.; Sánchez-Polo, M.; Ferro-García, M.A.; Prados-Joya, G.; Ocampo-Pérez, R. Pharmaceuticals as emerging contaminants and their removal from water. A review. Chemosphere **2013**, 93, 1268-1287.

Robles-Molina, J.M.; Martín de Vidales, M.J.; García-Reyes, J.F.; Cañizares, P.; Sáez, C.; Rodrigo, M.A.; Molina-Díaz, A. Conductive-diamond electrochemical oxidation of chlorpyrifos in wastewater and identification of its main degradation products by LC-TOFMS. Chemosphere **2012**, 89, 1169-1176.

Rosenfeldt, E.J.; Linden, K.G.; Canonica, S.; von Gunten, U. Comparison of the efficiency of OH radical formation during ozonation and the advanced oxidation processes O_3/H_2O_2 and UV/H_2O_2. Water Res. **2006**, 40, 3695-3704.

Song, W.; Cooper, W.J.; Peake, B.M.; Mezyk, S.P.; Nickelsen, M.G.; O'Shea, K.E. Free-radical-induced oxidative and reductive degradation of N,N'-diethyl-m-toluamide (DEET): Kinetic studies and degradation pathway. Water Res. **2009**, 43, 635-642.

Stackelberg, P.E.; Furlong, E.T.; Meyer, M.T.; Zaugg, S.D.; Henderson, A.K.; Reissman, D.B. Persistence of pharmaceutical compounds and other organic wastewater contaminants in a conventional drinking-water-treatment plant. Sci. Total Environ. **2004**, 329, 99-113.

Staehelin, J.; Hoigne, J. Decomposition of ozone in water in the presence of organic solutes acting as promoters and inhibitors of radical chain reactions. Environ. Sci. Technol. **1985**, 19, 1206-1213.

Stuart, M.; Lapworth, D.; Crane, E.; Hart, A. Review of risk from potential emerging contaminants in UK groundwater. Sci. Total Environ. **2012**, 416, 1-21.

Tisch, M.; Schmezer, P.; Faulde, M.; Groh, A.; Maier, H. Genotoxicity studies on permehtrin, DEET and diazinon in primary human nasal mucosal cells. Eur. Arch. Oto-rhino-l. **2002**, 259, 150-153.

von Gunten, U. Ozonation of drinking water. Part I. Oxidation kinetics and product formation. Water Res. **2003**, 37, 1443-1467.

Yao, D.C.C.; Haag, W.R. Rate constants for direct reactions of ozone with several drinking water contaminants. Water Res. **1991**, 25, 761-773.

Yuan, F.; Hu, C.; Hu, X.; Wei, D.; Chen, Y.; Qu, J. Photodegradation and toxicity changes of antibiotics in UV and UV/H_2O_2 process. J. Hazard. Mater. **2011**, 185, 1256-1263.

Zhang, H.; Lemley, A.T. Reaction mechanism and kinetic modeling of DEET degradation by flow-through anodic Fenton treatment (FAFT). Environ. Sci. Technol. **2006**, 40, 4488-4494.

SUPPLEMENTARY INFORMATION

Table S1. Degradation by-products identified in the ozonation of DEET.
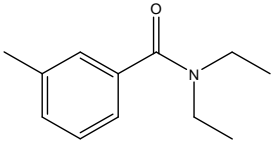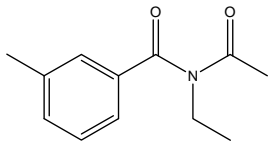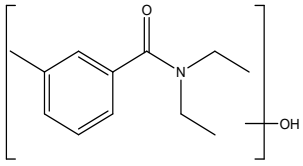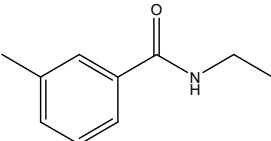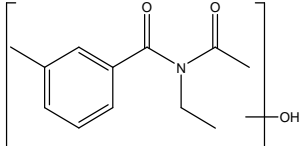
	R_t, min	Molecular Formula [M]	Theor. m/z	Exp. m/z	Error, ppm	DBE	Tentative structure [M]
DT	13.40	$C_{12}H_{17}NO$	192.1383	192.1378	2.62	5	
D1	10.36	$C_{12}H_{15}NO_2$	206.1176	206.1175	0.23	6	
D2	8.35			208.1329	1.64	5	
D3	9.06			208.1325	3.54	5	
D4	10.05	$C_{12}H_{17}NO_2$	208.1332	208.1327	2.64	5	
D5	10.30			208.1331	0.60	5	
D6	10.79			208.1329	1.58	5	
D7	12.28			208.1330	0.89	5	
D8	10.22	$C_{10}H_{13}NO$	164.1070	164.1071	-0.65	5	
D9	9.04	$C_{12}H_{15}NO_3$	222.1125	222.1124	0.50	6	

Table S1 (cont.). Degradation by-products identified in the ozonation of DEET.
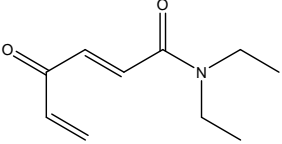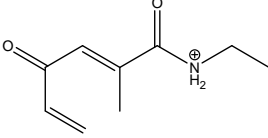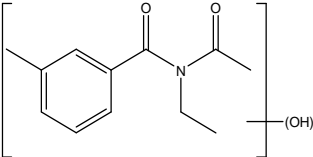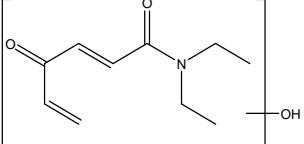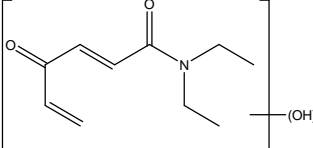
	R_t, min	Molecular Formula [M]	Theor. m/z	Exp. m/z	Error, ppm	DBE	Tentative structure [M]
D10	11.36	$C_{10}H_{15}NO_2$	182.1176	182.1175	0.16	4	
D11	9.14	$C_9H_{13}NO_2$	168.1019	168.1018	0.55	4	
D12	9.01	$C_{12}H_{15}NO_4$	238.1074	238.1072	0.96	6	
D13	7.12	$C_{10}H_{15}NO_3$	198.1125	198.1125	-0.06	4	
D14	6.63	$C_{10}H_{15}NO_4$	214.1074	214.1072	0.85	4	

Table S2. Degradation by-products identified in the ozonation of Nortriptyline.
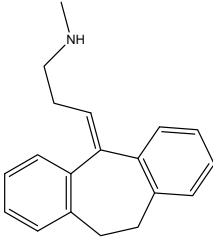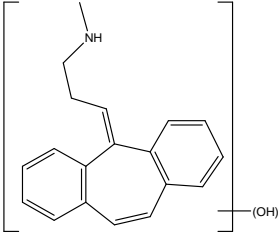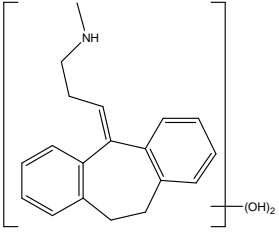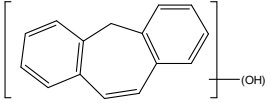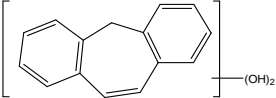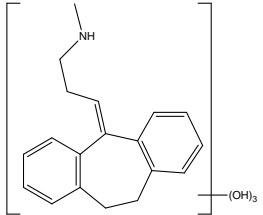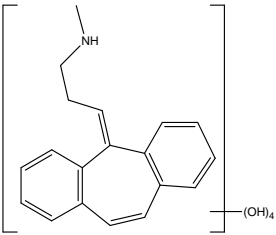
	R_t, min	Molecular Formula [M]	Theor. m/z	Exp. m/z	Error, ppm	DBE	Tentative structure [M]
NH	11.10	$C_{19}H_{21}N$	264.1747	264.1747	-0.21	10	
N1	9.92	$C_{19}H_{21}NO$	280.1696	280.1696	0.03	10	
N2	10.53			280.1785	-3.83	10	
N3	8.02			296.1645	0.09	10	
N4	8.28			296.1645	0.07	10	
N5	8.50			296.1644	0.42	10	
N6	8.67	$C_{19}H_{21}NO_2$	296.1645	296.1645	-0.12	10	
N7	8.85			296.1646	-0.39	10	
N8	8.97			296.1645	-0.06	10	
N9	9.24			296.1645	0.05	10	
N10	9.39			296.1644	0.21	10	
N11	17.85	$C_{15}H_{12}O$	209.0961	209.0960	0.28	10	

Table S2 (cont.). Degradation by-products identified in the ozonation of Nortriptyline.

	R_t, min	Molecular Formula [M]	Theor. m/z	Exp. m/z	Error, ppm	DBE	Tentative structure [M]
N12	12.85	$C_{15}H_{12}O_2$	225.0910	225.0914	0.68	10	
N13	7.55	$C_{19}H_{21}NO_3$	312.1594	312.1594	0.10	10	
N14	8.35			312.1595	-0.39	10	
N15	6.60	$C_{19}H_{19}NO_4$	326.1387	326.1381	1.87	11	
N16	6.94			326.1387	-0.37	11	
N17	7.32			326.1388	-0.25	11	
N18	7.71			326.1387	0.10	11	
N19	7.97			326.1386	0.09	11	
N20	8.15			326.1387	-0.07	11	
N21	7.37	$C_{19}H_{19}NO_2$	294.1489	294.1486	0.75	11	
N22	7.92			294.1489	-0.07	11	
N23	8.12			294.1488	0.19	11	
N24	8.90			294.1486	0.81	11	
N25	9.38			294.1489	-0.10	11	
N26	9.45			294.1487	0.29	11	
N27	9.79			294.1488	0.18	11	

m/z 72.0444

m/z 100.0757

m/z 164.1070

m/z 91.0544

m/z 119.0497
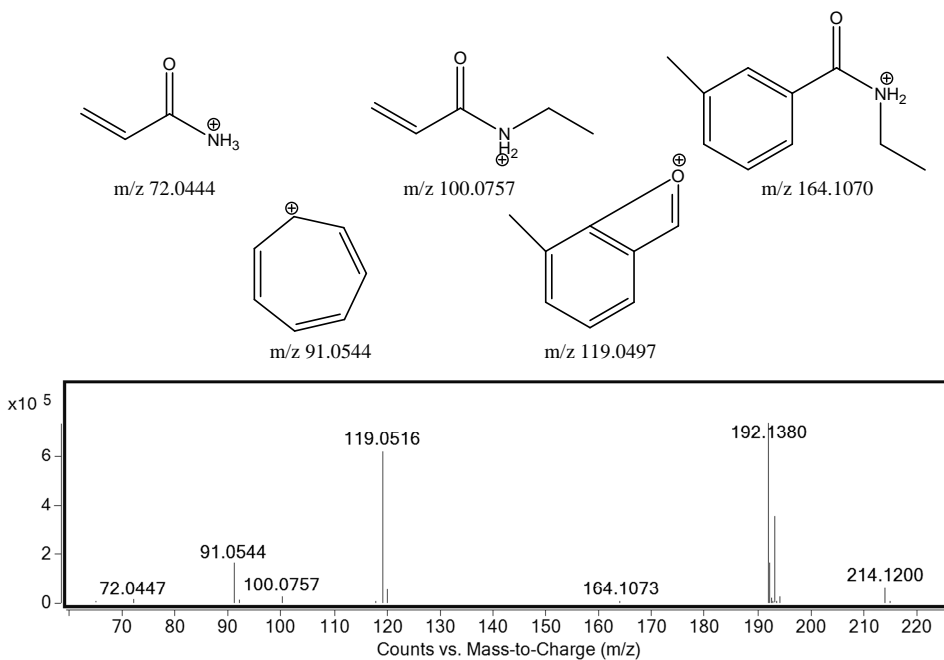
Figure S1. Mass Spectrum of DEET (fragmentor voltage 160V).
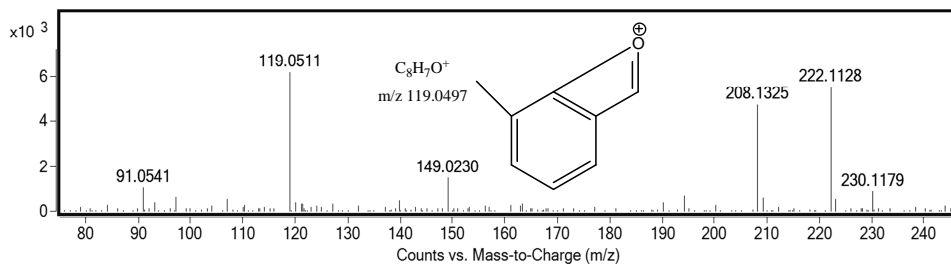
Figure S2. Mass spectrum of degradation by-product D3 formed during the ozonation of DEET (fragmentor voltage 200 V).
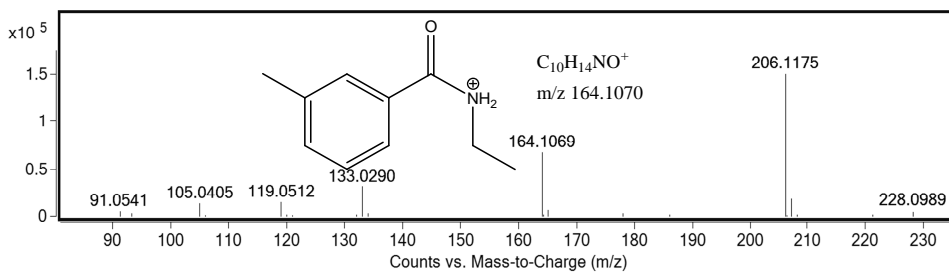
Figure S3. Mass spectrum of degradation by-product D1 formed during the ozonation of DEET (fragmentor voltage 200 V).
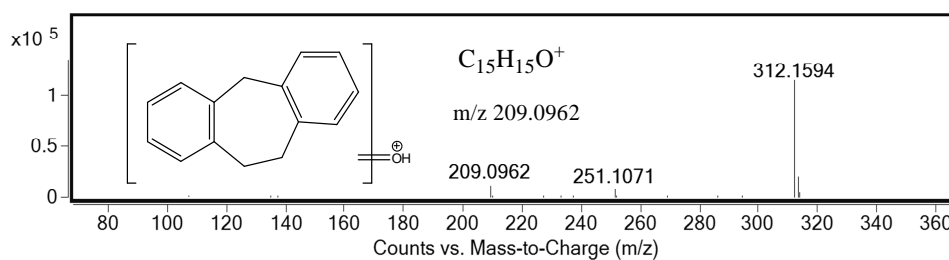
Figure S4. Mass spectrum of degradation by-product N13 formed during the ozonation of nortriptyline (fragmentor voltage 200 V)

3.7. Ozonation of benzotriazole and methylindole: kinetic modeling, identification of intermediates and reaction mechanisms.

3.7. OZONATION OF BENZOTRIAZOLE AND METHYLINDOLE: KINETIC MODELING, IDENTIFICATION OF INTERMEDIATES AND REACTION MECHANISMS

F. Javier Benítez, Juan L. Acero, Francisco J. Real, Gloria Roldan, Elena Rodríguez.

Departamento de Ingeniería Química, Universidad de Extremadura, Badajoz.

The ozonation of 1H-benzotriazole (BZ) and 3-methylindole (ML), two emerging contaminants that are frequently present in aquatic environments, was investigated. The experiments were performed with the contaminants (1µM) dissolved in ultrapure water. The kinetic study led to the determination of the apparent rate constants for the ozonation reactions. In the case of 1H-benzotriazole, these rate constants varied from 20.1 ± 0.4 M^{-1} s^{-1} at pH=3 to 2143 ± 23 M^{-1} s^{-1} at pH=10. Due to its acidic nature (pK$_a$=8.2), the degree of dissociation of this pollutant was determined at every pH of work, and the specific rate constants of the un-dissociated and dissociated species were evaluated, being the values of these rate constants 20.1 ± 2.0 and 2.0 ± 0.3 x 10^3 M^{-1} s^{-1}, respectively. On the contrary, 3-methylindole does not present acidic nature, and therefore, it can be proposed an average value for its rate constant of $4.90\pm0.7\times10^5$ M^{-1} s^{-1} in the whole pH range 3-10. Further experiments were performed to identify the main degradation byproducts (10 mg L^{-1} of contaminants, 0.023 g h^{-1} of ozone). Up to 8 intermediates formed in the ozonation of 3-methylindole were identified by LC-TOFMS, while 6 intermediates were identified in the ozonation of 1H-benzotriazole. By considering these intermediate compounds, the reaction mechanisms were proposed and discussed. Finally, evaluated rate constants allowed to predict and modeling the oxidation of these micropollutants in general aquatic systems.

1. INTRODUCTION.

1H-benzotriazole (BZ) and 3-methylindole (ML) are two chemicals that belong to a kind of micropollutants present in waters, usually called "emerging contaminants" (ECs), which at the present times are mostly unregulated or in process to be regulated. The term ECs includes a wide array of different compounds (as well as their metabolites and transformation products): pharmaceuticals and personal care products (PPCPs), pesticides, veterinary products, industrial compounds/by-products, food additives and engineered nano-materials. However, synthesis of new chemicals or changes in use and disposal of existing chemicals can create new sources of ECs (Stuart et al., 2012).

It is recognized that the effluents from municipal wastewater treatment plants (WWTPs) may be a significant source of ECs, because current treatment technologies are very often unable to entirely degrade such persistent substances. Consequently, they are accumulated in aquatic environments (Prieto-Rodriguez et al., 2012) and their elimination is currently pursued.

In addition to different kinds of treatments, the use of chemical oxidation procedures can constitute effective technologies for the removal of hazardous pollutants present in waters. Among these oxidation procedures, single oxidants such as UV irradiation, ozone, chlorine, and hydrogen peroxide, or combinations of these oxidants in the Advanced Oxidation Processes (AOPs), such as O_3/H_2O_2, UV/H_2O_2, Fenton/photo-Fenton systems, and UV/TiO_2, are frequently applied (Kim et al., 2009; Mohapatra et al., 2014). AOPs are characterized by an elevated production of OH radicals and have demonstrated high effectiveness in the oxidation of these compounds, leading to more biodegradable and less toxic intermediates (Klavarioti et al., 2009).

Specifically, ozone shows a great reactivity towards most of organic pollutants which are present in waters (Esplugas et al., 2007). In addition to its direct reaction with most of the organic compounds, ozone self-decomposition, preferently at high pH, generates OH radicals. Therefore, two oxidation pathways must be considered in an ozonation process: direct ozonation and OH radical reaction, being molecular O_3 very

selective, while OH radicals react indiscriminately with organic molecules (von Gunten, 2003).

Regarding to the selected ECs in this study, BZ is a well-known corrosion inhibitor for copper or silver materials, which has been widely utilized in cooling and hydraulic fluids, antifreezing products, aircraft deicer and anti-icer fluid (ADAF), as well as dishwasher detergents (Ding et al., 2010). This compound resists biodegradation and is only partially removed by conventional wastewater treatments (Reemstsma et al., 2010). By contrast, ozonation is an effective method to degrade BZ in waters (Weiss et al., 2006). Thus, rate constants for the ozonation reaction have been reported at pH 2 and 5 by Vel Leitner and Roshani (2010); and more recently Mawhinney et al. (2012) identified five transformation by-products formed in the ozonation reaction of BZ by Q-TOF MS technique, and proposed a reaction mechanism for the formation of three of these products. On the other hand, ML is used in pharmaceutical formulations, cosmetics, pesticides, disinfectants, agrochemicals and dyestuffs (Gu et al., 2002), and therefore, it constitutes a frequent pollutant substance in different waters. However, at the present times no information concerning the removal of ML by ozonation processes, or even conventional treatments, can be found in the literature.

According to these previous considerations, the present work was designed with the objective of establishing the effectiveness of the ozonation process in the removal of the ECs BZ and ML. For this purpose, ozonation rate constants for ML and BZ as a function of pH were determined. Additionally, the main intermediate products formed in this ozonation process were also identified; and finally, their respective reaction mechanisms were proposed.

2. MATERIALS AND METHODS.

2.1. Experimental procedures.

Two different groups of experiments were carried out in the ozonation of the selected ECs, all of them at $20 \pm 0.5\ °C$. The first group of experiments was conducted in homogeneous conditions, and with the aim to determine the rate constants of the

individual reactions of BZ and ML with ozone. Previously, an ozone stock solution was prepared by dissolving an ozone gas stream in ice-cooled ultra-pure water until saturation was reached (around 9×10^{-4} M of ozone). The initial ozone gas stream was produced by passing pure oxygen gas through an ozone generator (Sander Labor-Ozonisator, model 301.7) at a constant flow rate of 40 L h^{-1} and with an ozone production of 1.6 g h^{-1}. In this study, each micropollutant was individually dissolved (with an initial concentration of 1×10^{-6} M) in buffered ultrapure (UP) water and aliquots were poured into 25 mL flask reactors. The solution pH was adjusted to the desired value in the range 3-10 with phosphate buffer (0.05 M). These experiments were performed in presence of *tert*-butanol (0.01 M) as radical scavenger. According to the competition kinetic method described elsewhere (El Najjar et al., 2013; Dantas et al., 2007), it is also necesary the presence of a reference compound whose rate constant with ozone is previously known. This reference compound was also added to the solution and simultaneously oxidized with the selected EC (EC:reference compound molar ratio 1:1). The experiments were started after adding to the flask reactor the appropiate volume of an ozone stock solution to achieve the desired initial O$_3$ concentration (EC:ozone molar ratio was varied in the range 1:4 to 1:42). At different time intervals, samples were withdrawn from the flask reactors, and immediately, the O$_3$ present was quenched with sodium thiosulfate. These samples were ready for analysis, in order to determine the residual concentrations of the selected EC and the reference compound.

The second group of experiments for the identification of the intermediate products generated in the ozonation reaction was performed in heteregeneous conditions at 20 °C. The initial concentration of ECs dissolved in ultrapure water was 10 mg L^{-1}. In this case, the ozone gas stream produced in a Sander Labor-Ozonisator, model 300.5 (ozone production of 0.023 g h^{-1} at a constant flow rate of 40 L h^{-1}) was fed to the reaction vessel (350 mL). Neither buffers nor radical scavengers were used in these experiments. The initial pH was 5.6 and decreased during the experiments to around 5.0. Aqueous samples were withdrawn from the reactor at specific reaction intervals in order to analyze the parent compounds and the intermediates formed.

2.2. Analytical methods.

The concentrations of BZ, ML and the reference compound in the kinetic experiments were determined by means of an HPLC system, using a Waters Chromatograph equipped with a 996 Photodiode Array Detector and a Phenomenex Gemini C18 Column (5μm, 150mm × 3mm). The flow rate of the mobile phase, which consisted of acetonitrile as solvent A and formic acid aqueous solution (25 mM) as solvent B, was set at 0.2 mL min^{-1}. The linear gradient operated from 10% A to 90% A in 15 min. The wavelengths used for the quantification of the ECs were: 250 nm (BZ) and 280 nm (ML). Empower software was used for data acquisition and processing.

In the second group of experiments, intermediates formed during the ozonation of the selected ECs were independently determined by an HPLC equipment (Agilent 1290 Inffinity) connected to a time of-flight mass spectrometer (TOFMS, Agilent 6220 accurate mass TOF). HPLC system was equipped with a XDB-C$_{18}$ analytical column (1.8 μm, 50 mm x 4.6 mm). The mobile phase consisted of (A) Milli-Q water with 0.1% acetic acid, and (B) acetonitrile, which was run at a flow rate of 0.5 mL min^{-1}. The gradient was programmed as follows: 10% B for 3 min, increased to 100% at 25 min, and finally, it was held for 3 min. The column temperature was set at 35 °C. The mass spectrometer was operated under electrospray interface operating in either, positive and negative ionization modes at a fragmentor voltage of 160, 200 and 240 V with mass scan range of 50–1000 m/z. The ionization source conditions were listed as follows: a drying gas flow rate of 9 L min^{-1} at 325 °C, and a nebulizer pressure of 40 psig. The typical resolution was 9700 ± 500 full width at half maximum (FWHM) at a value of m/z 922. The full scan data were recorded with Agilent Mass Hunter Data Acquisition software (version B.04.00), and processed with Agilent Mass Hunter Qualitative Analysis software (version B.04.00). Samples were directly analyzed without previous treatment. The compounds were identified by retention times, comparison of the mass spectra with those from the literature data, and interpretation of the mass spectra.

3. RESULTS AND DISCUSSION.

3.1. Determination of rate constants for the reactions between ECs and ozone.

Competition kinetics method was used for the determination of the rate constants for the direct reaction between the selected emerging contaminants and ozone at different pH values. This model, initially proposed by Gurol and Nekouinaini (1984), and later widely used in other studies (Mawhinney et al., 2012; El Najjar et al., 2013), is useful for second-order kinetics, as occurs for ozonation of most organic compounds (Hoigne and Bader, 1983; Benitez et al., 2003). It is based on the simultaneous oxidation of a target compound (the selected ECs in the present case) and a reference compound, whose ozonation rate constants are previously known, and present similar reactivity towards ozone than the target compound. The development of the model, described in detail elsewhere (Benitez et al., 2003), leads to the final equation:
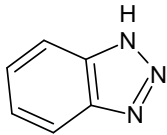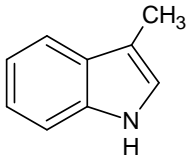
$$\ln\left(\frac{[T]}{[T]_0}\right) = \frac{k_{O3-T}}{k_{O3-R}}\ln\left(\frac{[R]}{[R]_0}\right) \tag{1}$$

where k_{O3-T} and k_{O3-R} are the rate constants for the target (T) and reference (R) compounds, respectively; and [T] and [R] their concentrations at different reaction times. In the present study, the pharmaceutical micropollutant metoprolol was selected as reference compound for BZ, and the pharmaceutical naproxen for ML, due to similar reactivities with these ECs towards ozone. The ozonation rate constants for these reference compounds were determined and reported in a previous work (Benitez et al., 2009).

The experiments performed provided the concentrations of the target and reference compounds, and a regression analysis of ln ([T]/[T]$_0$ vs. ln ([R]/[R]$_0$ led to the values of the k_{O3-T} /k_{O3-R} ratios. As the k_{O3-R} rate constants are previously known at different pH values (Benitez et al., 2009), the second-order rate constants k_{T-O3} for the ECs can be determined for each experiment. The final values of rate constants obtained for BZ and ML are compiled in Table 1. A search in the literature for similar reactions only provided a few values of rate constants for the ozonation of BZ. Thus, Karpel and Roshani (2010) reported

rate constants at pH 2 and 5, being the values obtained 18.4 and 22.0 $M^{-1} s^{-1}$ respectively. These results are quite similar to those found in the present work at the mentioned pHs.

Table 1. Second order rate constants (± standard deviation) for the reactions of molecular ozone with the selected compounds (T=20 ± 0.5 °C).

EC	pH	k_{O3-BZ}, $M^{-1} s^{-1}$	EC	pH	k_{O3-ML}, $M^{-1} s^{-1}$
1H-benzotriazole	3	20.1±0.4	3-methylindole	3	$(4.11±0.4)x10^5$
	4	20.4±0.5		4	$(4.26±0.4)x10^5$
	5	22.8±1.1		5	$(4.40±0.2)x10^5$
	6	32.6±0.6		6	$(5.67±0.8)x10^5$
	7	79.6±0.3		7	$(5.34±0.5)x10^5$
	8	398±14		8	$(5.32±0.4)x10^5$
	9	1942±10		9	$(4.93±0.4)x10^5$
	10	2143±23		10	$(5.21±0.7)x10^5$

Specifically for BZ, it can be seen in Table 1 that there is a reduced influence of pH on the ozonation rate constant k_{O3-BZ} in the pH range 3-6. However, increasing values of k_{O3-BZ} are observed when the pH was increased from 6 to 10. These results can be explained by taking into account the acidic nature of this substance, and the value of its pK_a. As previous works focused on the ozonation of dissociating substances reported (Hoigne and Bader, 1983; Gogate and Pandit, 2004) higher values of pH increased the oxidation rates, especially in the case of compounds with a pK_a higher than the operating pH. Specifically, BZ presents a value of pK_a=8.2, and the ozonation rate constants obtained totally confirm this trend, with the important increase of these rate constants in the pH range 6-10, values around its pK_a value.

By taking into account this dissociation effect, it is expected that BZ could be present in water matrices in its un-dissociated or dissociated forms, depending on the pH of the water. Then, the apparent ozonation reaction rate can be expressed as a function of the

specific ozonation rate constants of the un-dissociated and dissociated species (k_1 and k_2, respectively), in the form:

$$r_{O3} = k_{O3-BZ} \ [O_3] \ [BZ]_{tot} = k_1 \ [O_3] \ [BZ] + k_2 \ [O_3] \ [BZ^-] \qquad (2)$$

At this point, the goal is focused in the determination of both rate contants, by considering the degree of dissociation α, parameter which takes into account the ratio between the un-dissociated and dissociated species of BZ. The introduction of α into Equation (2) leads to the expression:

$$k_{O3-BZ} = \alpha \ k_1 + (1-\alpha) \ k_2 \qquad (3)$$

By using Equation (3), a non-linear least squares regression analysis was applied to the experimental values of k_{O3-BZ} and the calculated α values. The results led to the determination of the specific rate constants k_1 and k_2, whose values are: 20.1±2.0 and 2.0±0.3 x 10^3 M^{-1} s^{-1}, respectively. Once these rate constants are determined, the apparent rate constant for BZ can be theoretically evaluated for each pH by means of Equation (2); and consequently, the ozonation rate r_{O3} can be deduced for any water treatment at any pH.

On the contrary, as observed in Table 1, k_{O3-ML} rate constants for ML show an almost constant value for most of the pH range, with only a slight increase at lower pHs (3-4). It is in agreement with the fact that ML does not present acidic nature, and therefore, is characterized by the absence of any acid dissociation constant. Therefore, it can be proposed an average value of 4.90±0.7x10^5 M^{-1} s^{-1} in the pH range 3-10.

3.2. Identification of intermediate products and proposal of ozonation mechanisms.

In order to make a consistent proposal of the reaction mechanism for the ozonation reactions of the selected ECs, it is important to identify the intermediate products formed. This identification process was based on the accurate mass measurements of the samples that were analyzed by the LC-TOFMS equipment, as described in the Material and Methods Section. These measurements allow the proposal of

elemental compositions for molecular ions, as well as the characteristic of ion fragments, parameters that provide a high degree of confidence in the structure assignation. Moreover, mass accuracy, measured as the relative error (in ppm), was less than 5 units, as generally accepted for the verification of the elemental compositions (Coelho et al., 2009). The structure of the intermediates was proposed by taking into account the double bond and ring equivalents parameter (DBE), which provides information about the number of double bonds and rings that are present in the molecules.

Following this protocol, Tables 2 and 3 list the tentative molecular formula for all the degradation products detected and indentified (either, after positive or negative ionization) during the ozonation of ML and BZ. The experimental and calculated m/z values, molecular formula of the fragment ions, relative mass error, and values of DBE are included in Tables 2 and 3 as well.

Table 2. 3-Methylindole and its degradation products identified.

Compound	R_t, min	Molec. formula	Theor. m/z	Exp. m/z	Error, ppm	DBE
a) ESI+						
3-Methylindole	14.6	C_9H_9N	132.0808	132.0804	2.73	6
M1	13.39	C_9H_9NO	148.0757	148.0755	1.11	6
		C_8H_6NO	133.0522	133.0522	-0.04	6
		C_8H_9N	120.0808	120.0801	2.53	5
M2	13.75	C_9H_9NO	148.0757	148.0758	-0.51	6
		C_9H_9N	132.0808	132.0808	1.07	6
M3	9.23	$C_9H_9NO_2$	164.0706	164.0703	1.45	6
		C_8H_9NO	136.0757	136.0755	1.54	5
		C_8H_7N	118.0651	118.0650	0.21	6
		C_7H_6	91.0542	91.0546	-3.26	5
M4	3.77	$C_9H_{11}NO_2$	166.0863	166.0860	1.74	5
		C_9H_9NO	148.0757	148.0756	0.33	6
		C_9H_7N	130.0651	130.0647	3.28	7
		C_8H_9N	120.0808	120.0804	2.53	5

Table 2 (cont.). 3-Methylindole and its degradation products identified.

Compound	R_t, min	Molec. formula	Theor. m/z	Exp. m/z	Error, ppm	DBE
a) ESI+						
M5	6.38	$C_9H_9NO_3$	180.0655	180.0663	-3.18	6
		$C_8H_9NO_2$	152.0706	152.0704	1.36	5
		C_8H_7NO	134.0600	134.0597	1.86	6
		C_6H_7NO	110.0600	110.0603	-2.32	4
M6	8.27	C_8H_9NO	136.0757	136.0755	1.56	5
		C_7H_9N	108.0808	108.0806	1.64	4
		C_7H_6	91.0542	91.0542	0.39	5
M7	10.6	C_8H_9NO	136.0757	136.0757	0.24	5
		C_8H_7N	118.0651	118.0651	0.48	6
		C_7H_6	91.0542	91.0546	-3.30	5
M8	5.62	$C_8H_9NO_2$	152.0706	152.0703	2.05	5
		C_6H_7NO	110.0600	110.0599	1.29	4
		C_6H_5N	92.0495	92.0495	-0.65	5
a) ESI-						
M3	9.23	$C_9H_9NO_2$	162.0561	162.0561	-0.02	6
M5	6.38	$C_9H_9NO_3$	178.0510	178.0511	-0.60	6
		$C_8H_9NO_2$	150.0561	150.0560	0.21	5
M8	5.62	$C_8H_9NO_2$	150.0561	150.0563	-1.32	5
		C_6H_7NO	108.0455	108.0456	-0.92	4

In the case of the ozonation of ML, eight main intermediates were identified. Figure 1 shows the evolution of the concentration profiles for the parent compound and these major intermediates formed, being expressed as relative abundance of chromatographic areas *vs* ozonation time. As can be observed, ML decreased continuously with reaction time, reaching an almost total removal in 30 min of reaction. At the same time, the evolution of the relative abundances of the intermediates was as follows: most of them presented high concentrations after the first 30 min of ozonation, when ML was almost completely removed. It is worthy to note that the maximum concentration of these

intermediantes could be reached earlier, specially for M1 and M2. Compound M5 constitutes an exception, whose maximum relative abundance was reached for 60 min of reaction. After this, the concentration of M1, M2 and M4 decreased quickly, and were almost totally removed in 60 min. On the contrary, intermediates M3, M5, M6, M7 and M8 presented slight continuous decreases in their concentrations.
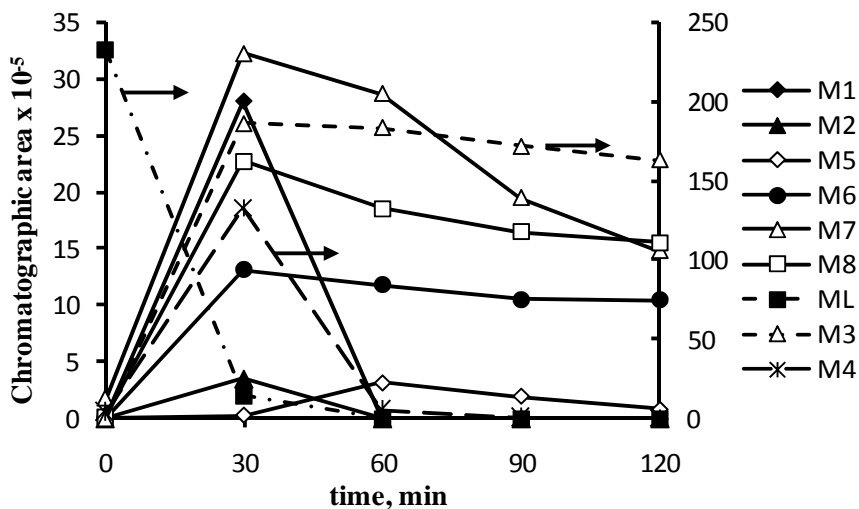
Figure 1. Relative abundance of 3-methylindole and its intermediates identified. (ML, M3 and M4 must be read in the right Y-axis. Rest of compounds in the left Y-axis).

In a similar way, the relative abundance profiles of BZ and its degradation products indentified are shown in Figure 2. Focusing in these profiles, the parent compound BZ continuously decreased during the whole ozonation process, and the removal after 120 min was 84%. At the same time, the concentration of intermediates increased continuously, especially B2, B4, B5 and B6. Generally speaking, this increase was more pronounced for all the intermediates identified after 90 min of reaction.
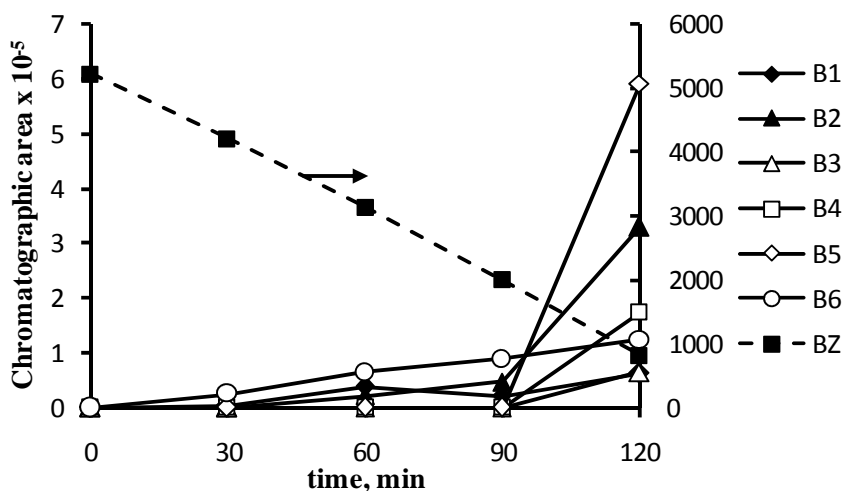
Figure 2. Relative abundance of benzotriazole and its degradation products identified. (BZ must be read in the right Y-axis. Rest of compounds in the left Y-axis).

Once the degradation intermediates in the ozonation process were tentatively identified, the next goal is the proposal of plausible reaction mechanisms. Thus, Figure 3 shows the proposed mechanism for the ozonation of ML. The ozonation of the parent compound leads to formation of degradation products M1 and M2, which are isomers with molecular formula C_9H_9NO and m/z 148.0757 (DBE=6). Different structures can be proposed depending on the reaction pathway and fragments ions found in their mass spectra. Thus, pathway I is based on the formation of the radical S1 and the compound S2 (3-methyleneindolenine), which formation was previously proposed by several authors in metabolic studies of 3-methylindole (D'Agostino et al., 2009; Kamel and Harriman, 2013). Later, this pathway I leads to the formation of the intermediate M1, which could be present in its enolic form (indole-3-carbinol); however, its fragment ion, with m/z 120.0801, agrees with the molecular formula C_8H_9N, and shows a loss of 28 ppm in the value of m/z, and a decrease on the value of DBE parameter from 6 to 5. This fact suggests that degradation product M1 has a carbonyl group in its molecular structure, which was lost after fragmentation.
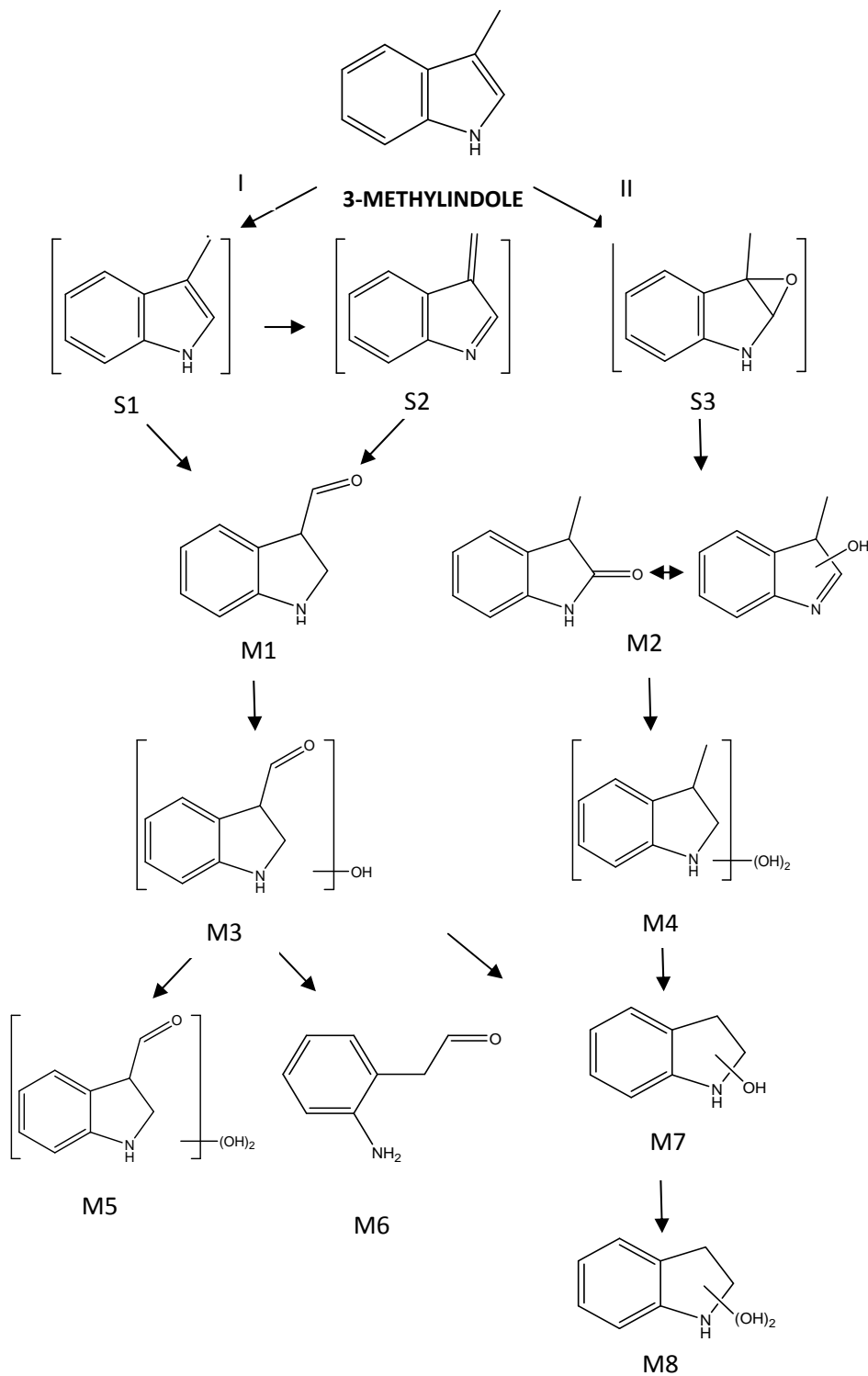
Figure 8. Proposed pathway for degradation of benzotriazole by ozonation.

On other hand, pathway II is based on the formation of the intermediate S3 (3-epoxy-3-methylindole), which later results in the intermediate M2 (3-methyloxindole), which is in equilibrium with its keto form. For this intermediate, the only fragment found matches with methylindole (that is, molecular formula C_9H_9N and m/z 132.0808). According to the fragment found in it mass spectra, it is not possible to elucidate which form of the keto-enolic equilibrium is predominant, as well as the exact position of the hydroxyl radical. By considering the molecular structures of M1 and M2, it can be assumed that these intermediates are the primary degradation by-products from molecular ozone attack to ML. Since the concentration of M1 is higher, pathway I may be favoured.

A second level of oxidation leads to the formation of intermediates M3 and M4. On one hand, M3 ($C_9H_9NO_2$), with m/z 164.0703 and DBE 6, is the most important intermediate, since it is formed to a greater extent, as a result of hydroxylation of intermediate M1. The assigned structure is supported by the fragments found in it mass spectrum (see Figure 4). Thus, the fragment with m/z 136.0755 (C_8H_9NO and DBE 5) suggests that a carbonyl group is lost (decrease of 28 in the value of m/z, and decrease of the DBE value from 6 to 5). Since M3 has a carbonyl group, it may be proposed that this compound is generated from the degradation of the isomer M1. The next fragment found with m/z 118.0650 (C_8H_7N and DBE 6) involves the loss of a water molecule and the formation of a new double bond (increase in DBE from 5 to 6). Finally, in this mass spectrum it can be seen a tropilium ion (C_7H_6 with m/z 91.0546), which is a typical fragment ion generated from the decomposition of aromatic compounds. It must be noted that this degradation product M3 was also identified in negative mode with m/z 162.0561.
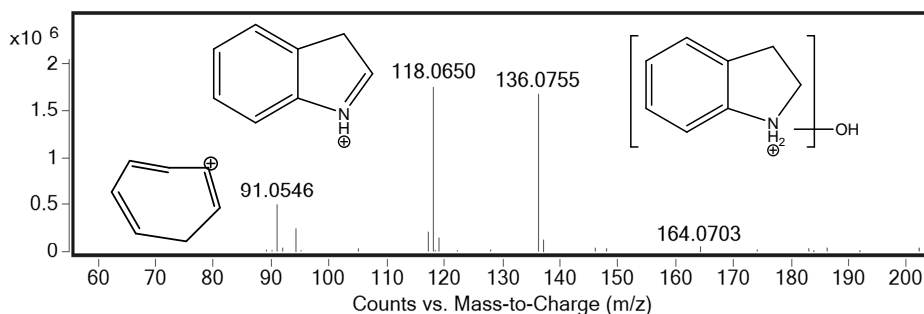
Figure 4. Mass spectrum of M3 (reaction time 30 minutes and voltage 200V).

On the other hand, the degradation product M4, with molecular formula $C_9H_{11}NO_2$ and m/z 166.0860, is mainly formed as a result of a hydroxylation of intermediate M2, with a decrease of the DBE parameter (from 6 to 5). Its mass spectrum reveales a fragment with m/z 148.0756, which corresponds to molecular formula C_9H_9NO and DBE 6 (see Table 2); that is, a molecule of water is lost, and consequently, a new double bound is formed, with the increase of DBE from 5 to 6.

Intermediate product identified as M5, with molecular formula $C_9H_9NO_3$, m/z 180.0663 and DBE 6, is formed from M3 in the next stage of degradation. Three fragments were found for this intermediate (see Figure 5). The first fragment, with molecular formula $C_8H_9NO_2$, m/z 152.0704 and DBE=5 supports that a carbonyl group is lost. The second fragment, with molecular formula C_8H_7NO, m/z 134.0597 and DBE=6 suggests that two hydroxylations take place in adjacent carbons; and consequently, a water molecule is lost, and a new double bound is formed, as the increase in the value of DBE parameter (from 5 to 6) demonstrates. Finally, the third fragment corresponds to a hydroxyl-aniline (C_6H_7NO, m/z 110.0603 and DBE 4). This degradation by-product M5, was also identified in both, negative and positive mode.
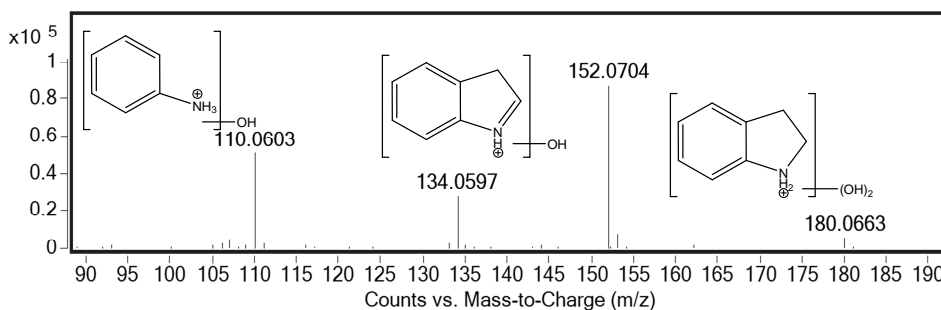
Figure 5. Mass spectrum of M5 (reaction time 60 minutes and voltage 200V).

It must be remarked that 9 C atoms remained constant in all the preceding intermediates identified. In contrast, the following identified degradation products show the loss of a carbon atom, as a consequence of further degradation steps. In effect, two new isomers were been identified, compounds M6 and M7, both with molecular formula C_8H_9NO, m/z 136.0757 and DBE 5. As can be seen in Figure 6, two fragments ions were found for isomer M6, which could be formed from M3: the fragment m/z 108.0806, and the

fragment m/z 91.0542, which corresponds to tropilium ion (C_7H_6). The formation of these fragments can be reasonably explained: M6 compound can lose a carbonyl group, resulting in the formation of the fragment with m/z 108.0806 (see structure in Figure 6), which at the same time, easily loses an ammonium group leading to the mentioned tropilium ion.
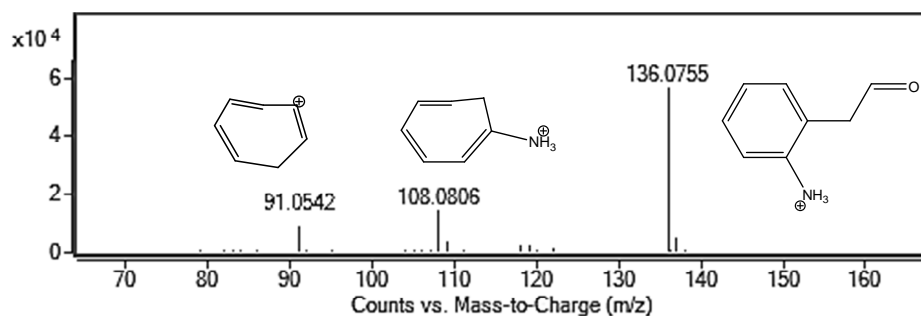
Figure 6. Mass spectrum of M6 (reaction time 60 minutes and voltage 200V).

In the case of isomer M7, a tropilium ion was also found (see Figure 7). The other fragment ion found, with m/z 118.0651 and molecular formula C_8H_7N, involves the loss of a water molecule, and therefore, an increase in the DBE parameter up to 6. This fact suggests that hydroxylation occurs on the pentane ring, and consequently, the loss of a water molecule leads to a new double bond, as well as increases the global aromaticity of the compound. M7 can also be formed from M3, by the loss of a carbonyl group; or from M4, by the loss of a methyl and a hydroxyl groups. Finally, a hydroxylation stage of M7 could lead to the formation of M8 (molecular formula $C_8H_9NO_2$, m/z 152.0703 and DBE 5).
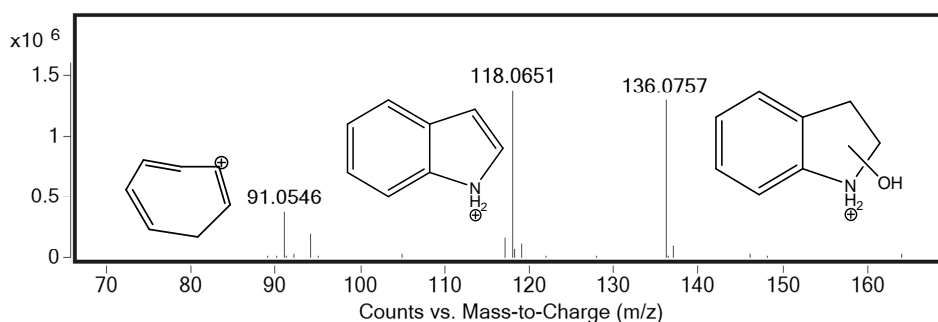
Figure 7. Mass spectrum of M7 (reaction time 60 minutes and voltage 200V).

Similarly, and focusing on the ozonation reaction of BZ, six degradation products were tentatively identified (see Table 3).

Table 3. Benzotriazole and its degradation products identified.

Compound	R_t, min	Molec. formula	Theor. m/z	Exp. m/z	Error, ppm	DBE
a) ESI+						
Benzotriazole	7.3	$C_6H_6N_3$	120.0556	120.0559	2.49	6
B1	3.71	$C_6H_5N_3O$	136.0505	136.0505	-0.33	6
		C_6H_5NO	108.0444	108.0450	5.15	5
B2	2.95	$C_6H_5N_3O$	136.0505	136.0503	-0.93	6
B3	1.83	$C_6H_5N_3O_2$	152.0453	152.0453	1.23	6
B4	1.39	$C_6H_5N_3O_3$	168.0404	168.0404	-0.23	6
B5	1.85	$C_6H_5N_3O_3$	168.0404	168.0402	-1.26	6
B6	1.34	$C_6H_7N_3O_3$	170.0560	170.0559	0.88	5
b) ESI-						
B1	3.71	$C_6H_5N_3O$	134.0349	134.0354	3.73	6
		C_6H_5NO	106.0298	106.0301	2.81	5
B2	2.95	$C_6H_5N_3O$	134.0349	134.0352	2.24	6

The proposed mechanism is shown in Figure 9, and basically consists in three hydroxylation stages. Firstly, a hydroxylation of the parent compound leads to the formation of the isomers B1 and B2, with molecular formula $C_6H_5N_3O$, m/z 136.0505 and DBE of 6. According to Asimakopoulos et al. (2013), a N-substitution in position "1" and a cycloaddition reaction on the benzene ring is favored in the case of BZ. Electrophilic substitutions occur preferentially at C4 and C7 positions, although substitution at C5 and C6 positions might also occur. Additionally, a N-substitution by an electron-donating group (as the hydroxyl group) increases the reactivity of the benzene ring. Thus, the N-substitution at position "1" by the hydroxyl group is highly favored in the ozonation process of benzotriazole, resulting in the formation of 1-OH-benzotriazole (1-OH-BZ). As two isomers were determined, it could be thought that the most abundant isomer corresponds to 1-OH-BZ; moreover, a fragment ion was found with m/z 108.0450 for the degradation by-product

B1, that corresponds to nitrosobenzene ion. This fact supports that degradation product B1 matches to 1-OH-BZ (see Figure 8). Both isomers were also identified in negative mode.
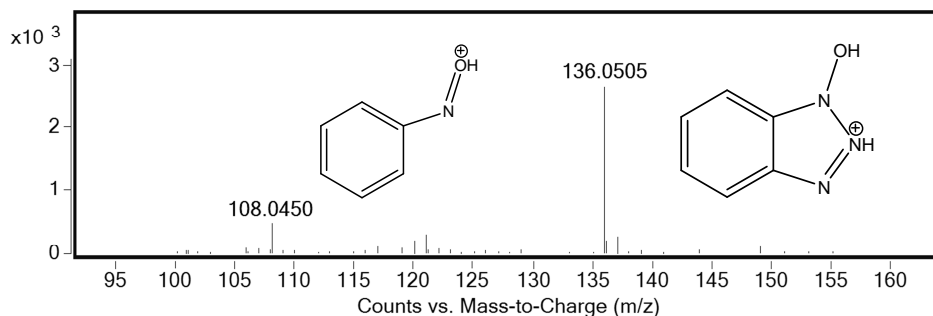
Figure 8. Mass spectrum of B1 (reaction time 120 minutes and voltage 200V).

A second hydroxylation stage leads to the formation of B3, with molecular formula $C_6H_5N_3O_2$, m/z 152.0453 and DBE of 6. Probably, this degradation product corresponds to 1,4-OH-BZ, or 1,7-OH-BZ, due to the reasons already discussed above. However, it could not be confirmed since no fragments were found for this substance.

Finally, the third hydroxylation step leads to the formation of isomers B4 and B5, and intermediate B6. These isomers B4 and B5 correspond to molecular formula $C_6H_5N_3O_3$, m/z 168.0404 and DBE of 6. Mass spectra do not show fragment ions; and therefore, exact position of hydroxyl groups could not be determined. It is proposed that these isomers are formed from the former intermediate B3, by means of a hydroxylation step. Finally, intermediate B6, with molecular formula $C_6H_5N_3O_3$ and m/z 170.0559, is also the result of a third hydroxylation step; but in this case, there is a decrease in the value of the DBE parameter (from 6 to 5). This fact indicates that this hydroxylation occurs with the loss of a double bond. However, it cannot be determined accurately where this loss occurs.

1-H-Benzotriazole

B1 B2

B3

B4 B5

B6
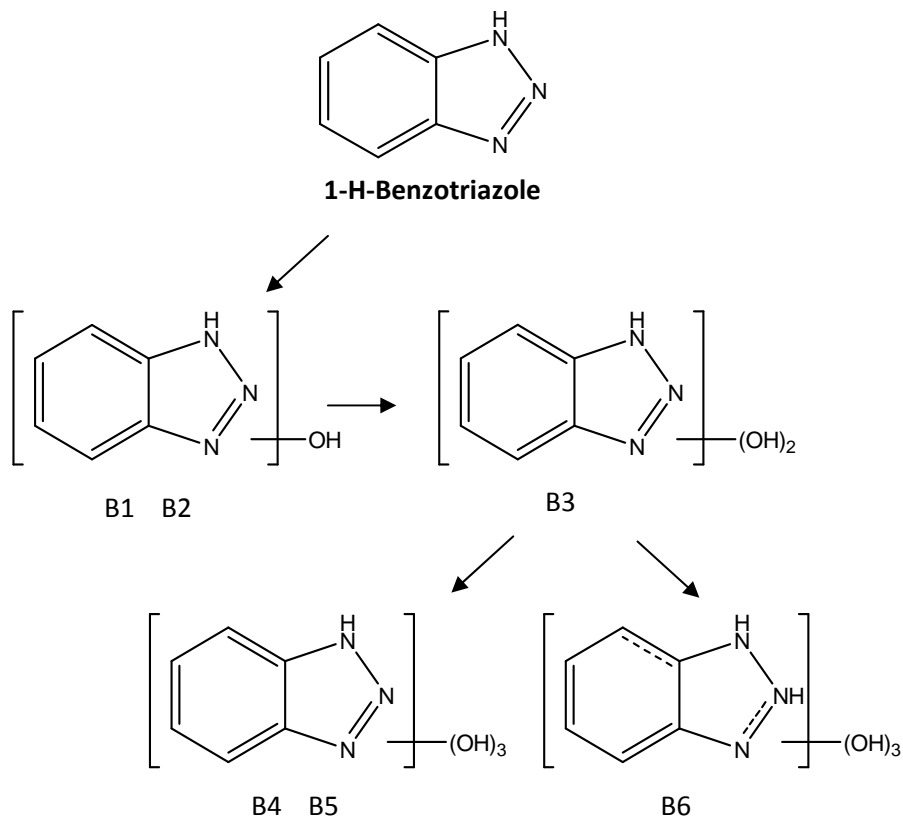
Figure 8. Proposed pathway for degradation of benzotriazole by ozonation.

3.3. Modeling the ozonation of the selected ECs in water systems.

The apparent rate constants determinated for the ozonation reactions of benzotriazole and methylindole are useful for predicting and modeling the oxidation of these micropollutants in a general aquatic systems where they are present. In ozonation processes, pollutants can be oxidized by direct molecular ozone, and also by the indirect attack of hydroxyl radicals generated *in situ* as a consequence of ozone self-decomposition, favoured at higher pHs, and by reactions of ozone with natural organic matter. Accordingly, the kinetics of the ozonation of a general micropollutant is the result of the contribution of both oxidants, molecular ozone and hydroxyl radicals; and therefore, the reaction rate can be expressed in the form:

$$-\frac{d[P]}{dt} = k_{OH-P}[OH][P] + k_{O_3-P}[O_3][P] \tag{4}$$

where k_{OH-P} and k_{O3-P} are the rate constants for the micropollutant reactions with OH radicals and ozone, respectively. The integration of this Equation (4) leads to the following expression:

$$\ln\left(\frac{[P]}{[P]_0}\right) = -(k_{OH-P}\int[OH]dt + k_{O3-P}\int[O_3]dt) \tag{5}$$

The modeling of the ozonation process of the selected ECs in a real water system can be conducted by applying Equation (5). However, for its application, in addition to the respective rate constants, the concentrations of O_3 and OH radicals are needed. While the ozone concentration can be directly followed with reaction time, the evolution of the OH radicals concentration through the reaction is a more complex problem, since there is no method for the direct measurement of the concentration of these species. In order to solve this situation, Elovitz and von Gunten (1999) proposed an experimental approach for the measurement of the transient OH radical concentrations during ozonation processes, by introducing the Rct parameter, which is defined as the ratio between OH radicals and O_3 exposures:

$$Rct = \frac{\int[OH]dt}{\int[O_3]dt} \tag{6}$$

The reported values of Rct in real waters are in the range 10^{-10}-10^{-6}, being these values affected by several factors, including pH, alkalinity and dissolved organic matter (Mawhinney et al., 2012; El Najjar et al., 2013; Elovitz and von Gunten, 1999). Substitution of Equation (6) in Equation (5) leads to:

$$\ln\left(\frac{[P]}{[P]_0}\right) = -\left(k_{OH-P}Rct + k_{O3-P}\right)\left(\int_0^t[O_3]dt\right) \tag{7}$$

Equation (7) was used to model ECs degradation in different water systems at pH 7. For this purpose, the values of k_{O3-P} were taken from Table 1, while the k_{OH-P} values were determined and reported in a recent work (Benitez et al., 2013), being: 8.24×10^9 M^{-1} s^{-1} for BZ and 5.57×10^9 M^{-1} s^{-1} for ML. On the other hand, two usual values reported for Rct in the literature (10^{-7} and 10^{-9}) were adopted in this case (El Najjar et al., 2013). Following this procedure, Figure 10a shows the decrease of ECs concentration as a function of ozone exposure, for both values of Rct. As can be observed, in the case of ML, the value adopted for Rct does not exert any influence on its concentration profile, which indicates that the radical pathway is not significant in this ozonation process, and ML oxidation mainly occurs through direct reactions with molecular ozone. On the contrary, the increase in the Rct parameter leads to a faster decrease of BZ concentration, which indicates that the radical pathway contributes significantly to the oxidation of BZ under water treatment conditions. Nevertheless, the removal of BZ is rather slow and a high ozone exposure is required.

On the other hand, the relative importance of each reaction pathway, direct ozonation and radical oxidation, can be also established. In effect, the fraction of P degraded by OH radicals can be expressed by Equation (8) (Dodd et al., 2006; Benner et al., 2008):

$$f_{OH} = \frac{k_{OH-P} \int_0^t [OH] dt}{k_{OH-P} \int_0^t [OH] dt + k_{O_3-P} \int_0^t [O_3] dt} = \frac{k_{OH-P} Rct}{k_{OH-P} Rct + k_{O_3-P}} \tag{8}$$

Specifically, Equation (8) was applied for different values of Rct in the range 10^{-1} - 10^{-11}, and Figure 10b shows the plott of this f_{OH} factor vs. Rct values for the ECs selected in this work. Obviously, the specific contribution of the direct ozonation reaction can be deduced by $1-f_{OH}$. According to these results, the direct ozone pathway predominates over the radical pathway in the oxidation of ML under natural water conditions (i.e. for Rct values below 10^{-7}). For BZ, the relative importance of the radical pathway depends on the characteristics of the natural water. Thus f_{OH} for ML varies from 1 at Rct$\approx 1 \times 10^{-6}$ to 0 at Rct$\approx 1 \times 10^{-10}$. This is a consequence of the reactivity of these substances with ozone, which is given by their rate constants summarized in Table 1.

a)
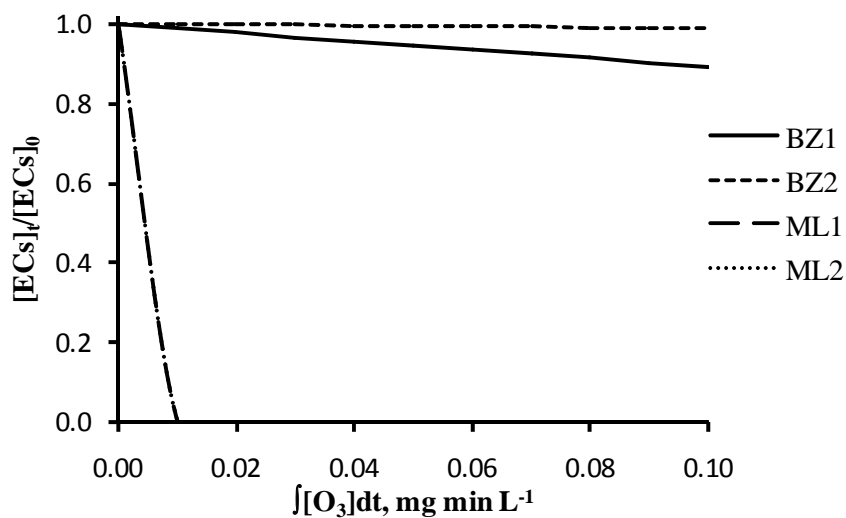
b)
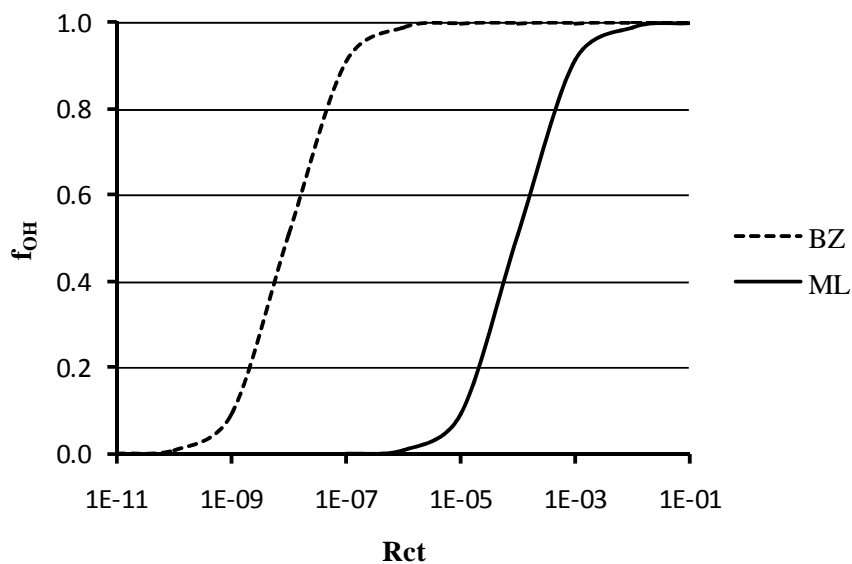
Figure 10. Contribution of OH radicals to ECs ozonation in real waters at pH 7. a) ECs removal at different ozone exposure. (BZ1 and ML1: Rct=10^{-7}; BZ2 and ML2: Rct=10^{-9}). b) Contribution of OH radical pathway at different Rct values.

REFERENCES

Asimakopoulos, A.G.; Wang, L.; Thomaidis, N.S.; Kannan, K. Benzotriazoles and benzothiazoles in human urine from several countries: A perspective on occurrence, biotransformation, and human exposure. Environ. Int. **2013**, 59, 274-281.

Benitez, F.J.; Acero, J.L.; Real, F.J.; Roldán, G.; Rodriguez, E. Modeling the photodegradation of emerging contaminants in waters by UV radiation and UV/H_2O_2 system. J. Environ. Sci. Health A. **2013**, 48, 120-128.

Benitez, F.J.; Acero, J.L.; Real, F.J.; Garcia, J. Kinetics of photodegradation and ozonation of pentachlorophenol. Chemosphere **2003**, 51, 651-662.

Benítez, F.J.; Acero, J.L.; Real, F.J.; Roldán, G. Ozonation of pharmaceutical compounds: Rate constants and elimination in various water matrices. Chemosphere **2009**, 77, 53-59.

Benner, J.; Salhi, E.; Ternes, T.; von Gunten, U. Ozonation of reverse osmosis concentrate: kinetics and efficiency of beta blocker oxidation. Water Res. **2008**, 42, 3003-3012.

Coelho, A.D.; Sans, C.; Agüera, A.; Gómez, M.J.; Esplugas, S.; Dezotti, M. Effects of ozone pre-treatment on diclofenac: Intermediates, biodegradability and toxicity assessment. Sci. Total Environ. **2009**, 407, 3572-3578.

D'Agostino, J.; Zhuo, X.; Shadid, M.; Morgan, D.G.; Zhang, X.; Humphreys, W.G.; Shu, Y.; Yost, G.S.; Ding, X. The pneumotoxin 3-methylindole is a substrate and a mechanism-based inactivator of CYP2A13, a human cytochrome P450 enzyme preferentially expressed in the respiratory tract. Drug Metab. Dispos. **2009**, 37, 2018-2027.

Dantas, R.F.; Canterino, M.; Marotta, R.; Sans, C.; Esplugas, S.; Andreozzi, R. Bezafibrate removal by means of ozonation: Primary intermediates, kinetics, and toxicity assessment. Water Res. **2007**, 41, 2525-2532.

Ding, Y.; Yang, C.; Zhu, L.; Zhang, J. Photoelectrochemical activity of liquid phase deposited TiO_2 film for degradation of benzotriazole. J. Hazard. Mat. **2010**, 175, 96-103.

Dodd, M.C.; Buffle, M.O.; von Gunten, U. Oxidation of antibacterial molecules by ozone: moiety-specific reaction kinetics and applications in ozone based wastewater treatment. Environ. Sci. Technol. **2006**, 40, 1969-1977.

El Najjar, N.H.; Touffet, A.; Deborde, M.; Journel, R.; Karpel Vel Leitner, N. Levofloxacin oxidation by ozone and hydroxyl radicals: Kinetic study, transformation products and toxicity. Chemosphere **2013**, 93, 604-611.

Elovitz, M.S.; von Gunten, U. Hydroxyl radical/ozone ratios during ozonation processes. I. The Rct concept. Ozone Sci. Eng. **1999**, 21, 239-260.

Esplugas, S.; Bila, D.M.; Krause, L.G.T.; Dezotti, M. Ozonation and advanced oxidation technologies to remove endocrine disrupting chemicals (EDCs) and pharmaceuticals and personal care products (PPCPs) in water effluents. J. Hazard. Mater. **2007**, 149, 631-642.

Gogate, P.R.; Pandit, A.B. A review of imperative technologies for wastewater treatment I: oxidation technologies at ambient conditions. Adv. Environ. Res. **2004**, 8, 501-551.

Gu, J-D.; Fan, Y.; Shi, H. Relationship between structures of substituted indolic compounds and their degradation by marine anaerobic microorganisms. Mar. Pollut. Bull. **2002**, 45, 379-384.

Gurol, M.; Nekouinaini, S. Kinetic behavior of ozone in aqueous solutions of substituted phenols. Ind. Eng. Chem. Fund. **1984**, 23, 54-60.

Hoigne, J.; Bader, H. Rate constants of reactions of ozone with organic and inorganic compounds in water-I. Non-dissociating organic compounds. Water Res. **1983**, 17, 173-183.

Kamel, A.; Harriman, S. Inhibition of cytochrome P450 enzymes and biochemical aspects of mechanism-based inactivation (MBI). Drug Discovery Today Tech. **2013**, 10,177-189.

Karpel Vel Leitner, N.; Roshani, B. Kinetic of benzotriazole oxidation by ozone and hydroxyl radical. Water Res. **2010**, 44, 2058-2066.

Kim, I.; Yamashita, N.; Tanaka, H. Photodegradation of pharmaceuticals and personal care products during UV and UV/H_2O_2 treatments. Chemosphere **2009**, 77, 518-525.

Klavarioti, M.; Mantzavinos, D.; Kassinos, D. Removal of residual pharmaceuticals from aqueous systems by advanced oxidation processes. Environ. Int. **2009**, 35, 402-417.

Mawhinney, D.B.; Vanderford, B.J.; Snyder, S.A. Transformation of 1H-Benzotriazole by ozone in aqueous solution. Environ. Sci. Technol. **2012**, 46, 7102-7111.

Mohapatra, D.P.; Brar, S.K.; Tyagi, R.D.; Picard, P.; Surampalli, R.Y. Analysis and advanced oxidation treatment of a persistent pharmaceutical compound in wastewater and wastewater sludge-carbamazepine Sci. Total Environ. **2014**, 470-471, 58-75.

Prieto-Rodriguez, L.; Miralles-Cuevas, S.; Oller, I.; Agüera, A.; Li Puma, G.; Malato, S. Treatment of emerging contaminants in wastewater treatment plants (WWTP) effluents by solar photocatalysis using low TiO_2 concentrations. J. Hazard. Mat. **2012**, 211, 131-137.

Reemtsma, T.; Miehe, U.; Duennbier, U.; Jekel, M. Polar pollutants in municipal wastewater and the water cycle: Occurrence and removal of benzotriazoles, Water Res. **2010**, 44, 596-604.

Stuart, M.; Lapworth, D.; Crane, E.; Hart, A. Review of risk from potential emerging contaminants in UK groundwater. Sci. Total Environ. **2012**, 416, 1-21.

von Gunten, U. Ozonation of drinking water. Part I. Oxidation kinetics and product formation. Water Res. **2003**, 37, 1443-1467.

Weiss, S.; Jakobs, J., Reemtsma, T. Discharge of three benzotriazole corrosion inhibitors with municipal wastewater and improvements by membrane bioreactor treatment and ozonation. Environ. Sci. Technol. **2006**, 40, 7193-7199.

3.8. The effectiveness of single oxidants and AOPs in the degradation of emerging contaminants in waters: a comparison study.

3.8. THE EFFECTIVENESS OF SINGLE OXIDANTS AND AOPS IN THE DEGRADATION OF EMERGING CONTAMINANTS IN WATERS: A COMPARISON STUDY

F. Javier Benítez, Juan L. Acero, Francisco J. Real, Gloria Roldan, Elena Rodríguez.

Departamento de Ingeniería Química, Universidad de Extremadura, Badajoz.

The effectiveness of single oxidants and several AOPs was studied for the degradation of five selected emerging contaminants: benzotriazole, N,N-diethyl-m-toluamide or DEET, chlorophene, 3-methylindole and nortriptyline HCl. First order rate constants and half-life times for the degradation of each compound in ultra-pure water were deduced and compared. The AOPs were later applied to the degradation of these ECs present in three real waters: public reservoir water, and two secondary effluents from municipal wastewater plants. The effect of the variables on the ECs elimination was established. Finally, a cost estimation based on the operating costs was established for the degradation of 3-methylindole by the single oxidants and AOPs tested.

1. INTRODUCTION.

The term emerging contaminants (ECs) is generally used for a large group of substances that constitute a new kind of aquatic pollutants. They include a wide array of different compounds: prescription and therapeutic drugs, veterinary drugs, dietary supplements, consumer products such as fragrances, topical agents such as cosmetics and sunscreens, laundry and cleaning products, etc. (Bolong et al., 2009). Nowadays, they have been increasingly detected in ground and surface waters and have the potential to cause known or suspected adverse ecological or human health effects (Stuart et al., 2012).

At present times, availability and quality of water constitutes an important problem in the world. Therefore, it is essential the optimization of resources, as well as the economically competitive reuse of waters in order to avoid environmental impacts (Klamerth et al., 2009). Within this general problem, numerous recent studies are found in the literature which are focused in the elimination, or at least partial degradation, of micro-pollutants in general and ECs in particular from waters. These studies find that conventional biological treatments and coagulation–flocculation processes have not obtained satisfactory results in the elimination of such as pollutants (Westheroff et al., 2005). Meanwhile, several researchs show a great interest in alternatives technologies, such as membrane operations (Dolar et al., 2012), adsorption (Rossner et al., 2009), chemical oxidations by single oxidants (Acero et al., 2010), and Advanced Oxidation Processes (AOPs) (Rodriguez et al., 2011; Prieto-Rodriguez et al., 2012; De la Cruz et al., 2012, etc.). Specifically, these AOPs have proved to be very efficient, because they generate hydroxyl radicals which are able to even mineralise most organic molecules, yielding CO_2 and inorganic ions as final products (Klamerth et al., 2010).

With these considerations in mind, a wide research study was designed for the removal from waters of five frequent ECs whose chemical structures are shown in Figure 1. The selected compounds were: Benzotriazole (BZ), an effective corrosion inhibitor for copper and iron, widely used in cooling and hydraulic fluids, antifreezing products, aircraft deicer and anti-ice fluid, dishwasher detergents, antifogging agents and intermediates for the synthesis of various chemicals (Ding et al., 2010); N,N-diethyl-m-toluamide or DEET (DT), major component of most topically applied insect repellents (Costanzo et al., 2007); chlorophene (CF), a widespread broad-spectrum antimicrobial pharmaceutical, commonly used in hospitals and households for general cleaning and disinfecting, as well as in industrial and farming environments as an active agent in disinfectant formulations (Sires et al., 2007); 3-methylindole (ML), used in the production of pharmaceuticals, cosmetics, pesticides, disinfectants, agrochemicals and dyestuffs (Gu et al., 2002); and the pharmaceutical nortriptyline HCl (NH), which belongs to the group of tricyclic antidepressants (TCAs).
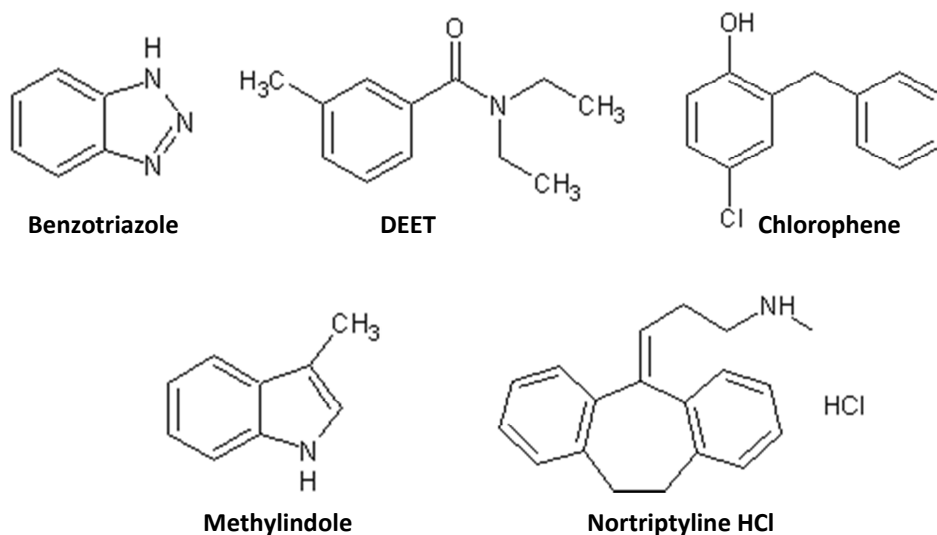
Figure 1. Chemical structures of the selected emerging contaminants.

Concretely, single oxidants (such as UV radiation and ozone) and several AOPs (Fenton's reagent, Fenton-like system, photo-Fenton system, and different combinations of UV radiation and ozone with H_2O_2, TiO_2, $S_2O_8^{2-}$, Fe (II) and Fe (III)), were tested in the present study for the removal of the above-mentioned ECs when they are individually dissolved in ultra-pure (UP) water, as well as simultaneously present in different water matrices. The main goals of this study were the establishment of the degradation levels reached for the ECs by each one of the oxidation systems tested, and the comparison of the efficiency of these different technologies. In a final stage, an approach to the estimation costs of these processes was conducted for ML, which was selected as model compound for this purpose.

2. MATERIALS AND METHODS.

2.1. Emerging contaminants, water matrices and analytical method.

The selected ECs were purchased from Sigma-Aldrich (Germany) of the highest purity available. Other chemicals used were of analytical grade or higher: ferrous sulfate heptahydrate, hydrated ferric perchlorate and sodium peroxodisulphate (from Fluka Chemika), hydrogen peroxide (35% by weight, from Sigma–Aldrich), and TiO_2 (P25 Degussa).

The UP water used in the individual oxidation reactions was Milli-Q grade. In the simultaneous oxidations of the selected ECs, three water matrices were used in order to reproduce realistic water treatment conditions: a natural water collected from the public reservoir "Peña del Aguila" (PA), located in the Extremadura Community, SW of Spain; and two secondary effluents from WWTPs corresponding to the cities of Badajoz (BA) and La Albuera (LA), also in the Extremadura Community. The main quality parameters of these water systems were characterized according to the Standard Methods (Clesceri et al., 1989) and their values are compiled in Table 1.

Table 1. Characterization of the water matrices used.

	PA	LA	BA
pH	7.4	7.9	8.3
Conductivity, μS cm^{-1}	80.2	570	550
A$_{254\,nm}$, cm^{-1}	0.187	0.041	0.245
COD, mg O$_2$ $^{-1}$	18	7	56
Alkalinity, mg CaCO$_3$ L^{-1}	30	335	325
TOC, mg L^{-1}	5.2	2.8	11.1
Total nitrogen, mg L^{-1}	1.51	21.3	35.5
Phosphorus, mg L^{-1}	0.041	0.156	1.76
Bromine, μg L^{-1}	n.d.	330	n.d.

The concentration of the five selected ECs were assayed by HPLC in a Waters Chromatograph equipped with a 996 Photodiode Array Detector and a Waters Phenomenex Gemini C18 Column (5 μm, 150 mm x 3 mm). Each run was performed in gradient mode with acetonitrile as mobile phase A and formic acid (2.5x10^{-2} M) as a mobile phase B, at a flow rate of 0.2 cm^3 min^{-1}. Each run started with an initial mobile-phase composition of 10% A, which was linearly increased to 30% A in 3 min, followed by another linear gradient to 40% A in 5 min, to 70% A in 4 min and 90% A in 5 min. Finally, the mobile-phase composition was maintained at 90% A for 5 min. A 5 min post-run time back to the initial mobile phase composition was used after each analysis. Detection was made at 250 nm for BZ, NH, and DT; and 280 nm for ML and CF.

2.2. Experimental procedures.

The first group of experiments, consisting in the individual oxidation of the selected ECs in UP water by UV radiation, ozone and AOPs, was carried out in a laboratory batch reactor. The initial concentration of each compound was established in 1 µM, and the temperature was maintained constant at the value of 20 ± 0.2 °C. The reacting medium was buffered in all experiments at the desired pH by adding a phosphoric acid/phosphate buffer (0.05 M). Rigorously, it could be expected that the phosphoric acid/phosphate buffer may act as an OH radical scavenger, but due to the low concentration used in this work, its contribution to the inhibition effect of OH radicals can be considered as negligible.

This experimental reactor was provided with the necessary elements for the development of the different processes. Specifically, in the photochemical decomposition alone and combined with other oxidant agents, a low pressure mercury vapor lamp (Heraeus TNN 15/32, 15 W) which emitted a monochromatic radiation at 254 nm was used, and it was located in the reactor in axial position inside a quartz sleeve. The value of incident photon flux at 254 nm (1.73×10^{-6} Einstein s^{-1}), was calculated on the basis of hydrogen peroxide actinometry experiments (Nicole et al., 1990), and the optical path length was 2.71 cm. On the other hand, in the experiments involving ozone, it was generated from pure oxygen (>99.9%) through an ozone generator (Sander, mod. 300.5), being the inlet stream monitored by an ozone Analyzer (mod. Ozomat GM). These ozonation experiments were carried out at 20 ^{o}C, with a global gas flow rate of 45 L h^{-1} that provided a ozone concentration of 0.7 g O_3 m^{-3} in the inlet gas stream. Finally, the catalysts concentration required for the AOPs (such us TiO_2, H_2O_2 and $S_2O_8^{2-}$) were added at the adequate dose at the beginning of each experiment. Specifically in the TiO_2 experiments, each sample was filtered through a 0.45 µm Millipore membrane filter before the chromatographic analysis was performed.

On the other hand, Fenton reagent and Fenton-Like experiments were conducted in 250 ml Erlenmeyer flasks. The required amounts of ferrous sulfate heptahydrate, hydrated ferric perchlorate, and hydrogen peroxide were added to the reactor, and the reacting mass was also maintained at a constant temperature of 20 ± 0.2 °C.

The second group of experiments was carried out with the EC mixtures dissolved in the three water systems above mentioned (PA, BA and LA) at 20 °C and at the natural pH of each water matrix. This set of experiments was performed in the same experimental reactor already described for the study of the individual ECs degradation in UP water. In all cases, sodium thiosulfate (0.1 M) was used to quench the reaction in the samples withdrawn from the reactor at regular time intervals.

3. RESULTS AND DISCUSSION.

3.1. Oxidation of ECs in UP water by direct photolysis and Fenton Reagent.

The degradation of the selected ECs (BZ, DT, CF, ML and NH) was firstly studied by means of UV radiation alone and by Fenton's Reagent in UP water at a constant temperature of 20 ^{o}C and at pH=3. In the photochemical experiments, the remaining pollutant concentrations obtained with reaction time were fitted to first order kinetics: for this purpose values of ln [EC]$_0$/[EC]) vs. reaction time were plotted, and regression coefficients above 0.99 were obtained in all cases. From the slopes of these straight lines, first order rate constants (k_{UV}) were determined and their values are summarized in Table 2 as well as the half-life time values ($t_{1/2}$). As it can be observed, the following order of reactivity is deduced: CF > BZ > ML > NH > DT.

Table 2. Degradation of ECs in UP water by UV radiation and Fenton Reagent.

Expt. UV-1			Expt. F-1		
ECs	k_{UV}, min^{-1}	$t_{1/2}$, min	ECs	k_F, min^{-1}	$t_{1/2}$, min
BZ	0.201	3.4	BZ	0.020	34.6
NH	0.066	10.5	NH	0.025	27.7
DT	0.014	49.5	DT	0.017	40.8
ML	0.097	7.1	ML	0.030	23.1
CF	0.292	2.4	CF	0.022	31.5

A similar oxidation study was carried out by using the Fenton reagent as oxidizing agent. Fenton's reaction follows a complex reaction mechanism widely described in the literature, which globally generates the very oxidizing hydroxyl radicals that attack and decompose the organic matter present in the reacting mass. In a simple approach, it can be considered that this reaction system also follows first order kinetics (Santos et al., 2011). Therefore, the remaining concentrations of each EC were adjusted to first order rate law, and the results obtained for these rate constants (k_F) are also shown in Table 2, as well as the $t_{1/2}$ values. As it is observed, ML and NH are the compounds with the highest rate of degradation by means of the hydroxyl radicals, followed by CF, BZ, and finally DT. However, from the values of these rate constants, it can be concluded that, with the exception of DT, the photodegradation process achieved a higher removal rate in comparison to the Fenton reagent process under the experimental conditions applied.

3.2. Oxidation of ECs in UP water by AOPs based in UV radiation and Fenton's Reagent.

Once the single photodegradation process was tested for the degradation of the selected ECs, this technique was later applied in combination with other reagents (H_2O_2, Fe^{2+}, Fe^{3+}, TiO_2, and $S_2O_8^{2-}$) in the so-called "Advanced Oxidation Processes" (AOPs). Several conditions were maintained constants in all these experiments: T=20 ^oC, pH=3 and initial concentrations of the ECs (1μM). Table 3 lists the combinations used and the experiments performed with the specific values of the operating conditions. In general terms, the oxidation mechanisms by the combinations of UV with different oxidant agents have been widely investigated, and it is generally proposed in a simple approach, that the overall degradation rate of an organic compound is the result of the contribution of two reaction pathways: the direct photolysis and the hydroxyl radical attack (Chelme-Ayala et al., 2010). Thus, this overall reaction rate may be expressed as follows:

$$-\frac{d[EC]}{dt} = k_{UV}[EC] + k_R[R^\bullet][EC] \qquad (1)$$

where [EC] and [R⁻] are the emerging contaminant and hydroxyl radical concentrations, respectively, and k_R is the second order rate constant for the reaction between these

radicals and the ECs. This second term indicates the relative relevance of the radical pathway in the global oxidation in each system; and indirectly measures the amount of radicals generated. As the radicals concentration can be assumed to be constant during the whole reaction, it can be proposed that $k_R' = k_R.[R^\cdot]$. By introducing k_R' into Equation (1), and after integration, it is deduced:

$$\ln \frac{[EC]_0}{[EC]} = k_{UV}t + k_R't = (k_{UV} + k_R')\,t = k_T t \tag{2}$$

According to Equation (2), the first order rate constant for the overall oxidation of each target compound (k_T) can be determined by representing plots of ln [EC]$_0$/[EC] versus reaction time. From the straight lines obtained, and after regression analysis (with regression coefficients $r^2 > 0.99$ in all cases), the slopes provide the k_T rate constants. Following this model, these k_T constants were evaluated and are depicted in Table 3, as well as the $t_{1/2}$ times. Later, the rate constant for the radical reaction (k_R') can be also deduced by substracting the previously known values of k_{UV} (Expt. UV-1 for each compound, values shown in Table 2). Following this procedure, the k_R' values were determined in all the experiments carried out, and are summarized in Table 3.

The observation of the rate constants obtained in these AOPs based on the use of UV radiation with different agents reveals some conclusions. Firstly, it is generally observed that, in most of the experiments, the contribution of the direct photolysis to the global degradation is higher than that of the radical pathway (values of k_{UP} vs. k_R), with the exception of the UV-TiO$_2$ system with higher TiO$_2$ concentration (Expt. UV-9); and both UV-S$_2$O$_8$$^{2-}$ systems (Expts. UV-10 and UV-11), where the radical pathway predominates over the direct photochemical reaction.

Table 3. **Degradation of ECs in UP water by AOPs based on the use of UV radiation.**

Expt.	AOP	EC	k_T, M^{-1} s^{-1}	k_R, M^{-1} s^{-1}	$t_{1/2}$, min
UV-2	UV-H$_2$O$_2$	BZ	0.217	0.016	3.2
		DT	0.073	0.004	9.5
		CF	0.004	0.000	49.5
		ML	0.103	0.006	6.7
		NH	0.312	0.020	2.2
UV-3	UV-H$_2$O$_2$	BZ	0.230	0.029	3.0
		DT	0.094	0.025	7.4
		CF	0.015	0.001	46.2
		ML	0.117	0.020	5.9
		NH	0.326	0.034	2.1
UV-4	UV-Fe^{2+}-H$_2$O$_2$	BZ	0.220	0.019	3.2
		DT	0.107	0.038	6.5
		CF	0.062	0.048	11.2
		ML	0.110	0.013	6.3
		NH	0.381	0.089	1.8
UV-5	UV-Fe^{2+}-H$_2$O$_2$	BZ	0.237	0.036	2.9
		DT	0.127	0.058	5.4
		CF	0.068	0.054	10.2
		ML	0.129	0.032	5.4
		NH	0.419	0.127	1.6
UV-6	UV-Fe^{3+}-H$_2$O$_2$	BZ	0.217	0.016	3.2
		DT	0.108	0.039	6.4
		CF	0.057	0.043	12.2
		ML	0.107	0.010	6.5
		NH	0.328	0.036	2.1

Operating conditions applied: UV-2: [H$_2$O$_2$]=5µM; UV-3: [H$_2$O$_2$]=10µM; UV-4: [H$_2$O$_2$]=10µM, [Fe^{2+}]=10µM; UV-5: [H$_2$O$_2$]=10µM, [Fe^{2+}]=15µM; UV-6: [H$_2$O$_2$]=10µM, [Fe^{3+}]=10µM.

Table 3 (cont.). Degradation of ECs in UP water by AOPs based on the use of UV radiation.

Expt.	AOP	EC	k_T, M^{-1} s^{-1}	k_R, M^{-1} s^{-1}	$t_{1/2}$, min
UV-7	**UV-Fe^{3+}-H$_2$O$_2$**	BZ	0.228	0.027	3.0
		DT	0.109	0.040	6.4
		CF	0.064	0.050	10.8
		ML	0.108	0.011	6.4
		NH	0.357	0.065	1.9
UV-8	**UV-TiO$_2$**	BZ	0.218	0.017	3.2
		DT	0.105	0.036	6.6
		CF	0.041	0.027	16.9
		ML	0.161	0.064	4.3
		NH	0.309	0.017	2.2
UV-9	**UV-TiO$_2$**	BZ	0.330	0.129	2.1
		DT	0.480	0.411	1.4
		CF	0.210	0.196	3.3
		ML	0.314	0.217	2.2
		NH	0.539	0.247	1.3
UV-10	**UV-S$_2$O$_8$$^{2-}$**	BZ	0.258	0.057	2.7
		DT	0.678	0.609	1.0
		CF	0.102	0.088	6.8
		ML	0.274	0.177	2.5
		NH	0.499	0.207	1.4
UV-11	**UV-S$_2$O$_8$$^{2-}$**	BZ	0.332	0.131	2.1
		DT	1.143	1.074	0.6
		CF	0.167	0.153	4.1
		ML	0.545	0.448	1.3
		NH	0.659	0.367	1.0

Operating conditions applied: UV-7: $[H_2O_2]$=10µM, $[Fe^{3+}]$=15µM; UV-8: $[TiO_2]$=0.001 g L^{-1}; UV-9: $[TiO_2]$=0.005 g L^{-1}; UV-10: $[S_2O_8^{2-}]$=250µM; UV-11: $[S_2O_8^{2-}]$=500µM.

It is also noteworthy that the presence of H_2O_2 (Expts. UV-2) only improves slightly the degradation rate of the ECs in comparison to the single UV radiation process (Expt. UV-1), due to a moderate production of OH radicals, which are generated by direct photolysis of water. This improvement is more significant when a higher initial concentration of H_2O_2 is used (Expt. UV-3). Similarly, the increases in the initial concentrations of Fe^{2+} (Expts. UV-4 and UV-5) and Fe^{3+} (Expts. UV-6 and UV-7) improve the degradation rates, as could be expected. Also, the increasing concentration of TiO_2 photocatalyst (Expts. UV-8 and UV-9) increases significantly the degradation of ECs, because the photo-oxidation of this semiconductor produces large amounts of oxidant radicals. However, an excess dose of TiO_2 may not improve the reaction, due to the fact that particles of TiO_2 reduce the interfacial area between the solution and the photocatalyst (San et al., 2002). Finally, the same positive effect of the increasing initial concentration is observed for the UV- $S_2O_8^{2-}$ combinations (Expts. UV-10 and UV-11).

The results in Table 3 also reveal that the most effective combination is the UV- $S_2O_8^{2-}$ process, which achieved a total oxidation of the target compounds in 10 minutes of reaction, as can be seen in Figure 2A. Prior experimental studies showed that persulfate oxidation reactions induce to the formation of $SO_4^{\cdot-}$ radicals, that can produce hydroxyl radicals. The ECs degradation by the UV-$S_2O_8^{2-}$ combined system may be described as a combination of direct photolysis and chemical reaction between ECs and $SO_4^{\cdot-}$ radicals or/and OH radicals. Thus, sodium persulfate is an alternative oxidant more effective than any other for "In Situ Chemical Oxidation" (ISCO) (Huang et al., 2002; Xie et al., 2012). Figure 2A also shows that the combination UV/H_2O_2 slightly improves the degradation rate of the single UV photodecomposition, as previously commented; this rate being significantly improved with the combination UV/TiO_2.

a)

b)

Figure 2a. Comparison of the effectiveness of oxidation systems based in UV radiation for NH (Expts: UV-1, UV-3, UV-9 and UV-11). Figure 2b. Comparison of the effectiveness of oxidation systems based in Fenton Reagent for BZ (Expts: F1, UV-5 and UV-7).

A similar comparison performed about the effectiveness of the AOPs applied which are based on the Fenton Reagent is shown in Figure 3B, and it reveals that the Photo-Fenton and Photo-Fenton-Like processes provide significant additional degradation rates of target compounds in comparison to the single Fenton Reagent system at the same operating conditions. These results may be due to the reactions promoted by OH radicals which are generated through different pathways in the mentioned combined systems.

a)

b)

c)

Figure 3. Influence of the water matrix nature on the pseudo-first-order contants obtained in the degradation of ECs by using different degradatioon systems.

a) Expt. A-1: UV ; b) Expt. A-2: UV-TiO$_2$; c) Expt. A-3: Fe^{2+}-H$_2$O$_2$.

d)

e)

f)

Figure 3 (cont.). Influence of the water matrix nature on the pseudo-first-order contants obtained in the degradation of ECs by using different degradatioon systems.

d) Expt. A-4: UV-Fe^{2+}-H$_2$O$_2$, e) Expt. A-5: O$_3$, f) Expt. A-6: O$_3$-H$_2$O$_2$.

3.3. Ozonation of ECs in UP water.

In a next stage, another group of experiments was performed at pHs 3 and 7 (Expt. O-1 and O-2 in Table 4) with the objective of evaluating the efficiency of single ozone in the degradation of these compounds. A first order kinetics was also applied, and the rate constants for the reaction (k_{O3}) were also evaluated and are listed in Table 4, as well as the half-life time values ($t_{1/2}$). As it is known, although less selective, ozonation processes are more efficient at alkaline pH, due to the contribution of the radical pathway, which is more significant at higher pH because of a greater generation of hydroxyl radicals. This fact is confirmed by the rate constant values shown in Table 4: the results indicate for both pH values that ML is the most reactive towards ozone, with much higher rates. On the contrary, BZ and DT presented the lower rate constants values, and CF and NH intermediate values, with the only difference that CF is more reactive than NH at pH=7, while the reactivity of NH is higher than CF at pH=3.

Table 4. Degradation of ECs in UP water by single ozone.

Expt. O-1 pH=3			Expt. O-2 pH=7		
ECs	k_{O3}, min^{-1}	$t_{1/2}$, min	ECs	k_{O3}, min^{-1}	$t_{1/2}$, min
BZ	0.025	27.7	BZ	0.076	9.1
NH	0.114	6.1	NH	0.115	6.0
DT	0.019	36.5	DT	0.078	8.9
ML	1.246	0.1	ML	2.641	0.3
CF	0.096	7.2	CF	0.240	2.9

3.4. Oxidation of ECs in ultrapure water by AOPs based on ozone.

In a similar way as occurred in the AOPs based in the use of UV radiation, several AOPs were applied to the degradation of the ECs by using ozone in combination with other oxidant agents. These experiments were conducted at pH=7 because of this pH is closer to the natural pH of most of the real water matrices. More specifically, the studied systems were O_3/UV, O_3/H_2O_2, $O_3/UV/H_2O_2$, O_3/TiO_2 and $O_3/UV/TiO_2$. Table 5 summarizes these

experiments and the operating conditions applied with the initial concentrations of hydrogen peroxide and titanium dioxide used.

Table 5. Degradation of ECs in UP water by AOPs based on the use of ozone.

Expt.	AOP	EC	k_T, M^{-1}·s^{-1}	k_R, M^{-1}·s^{-1}	$t_{1/2}$, min
O-3	O$_3$-UV	BZ	0.100	0.024	6.9
		DT	0.148	0.033	4.7
		CF	0.087	0.009	8.0
		ML	4.025	1.384	0.2
		NH	0.333	0.093	2.1
O-4	O$_3$-H$_2$O$_2$	BZ	0.131	0.055	5.3
		DT	0.170	0.055	4.1
		CF	0.089	0.011	7.8
		ML	4.233	1.592	0.2
		NH	0.340	0.100	2.0
O-5	O$_3$-UV-H$_2$O$_2$	BZ	0.338	0.262	2.1
		DT	0.422	0.307	1.6
		CF	0.325	0.247	2.1
		ML	4.708	2.067	0.1
		NH	1.030	0.790	0.7
O-6	O$_3$-TiO$_2$	BZ	0.164	0.088	4.2
		DT	0.201	0.086	3.4
		CF	0.156	0.078	4.5
		ML	4.038	1.397	0.2
		NH	0.363	0.123	1.9
O-7	O$_3$-UV-TiO$_2$	BZ	0.165	0.089	4.2
		DT	0.252	0.137	2.8
		CF	0.156	0.078	4.4
		ML	6.314	3.673	0.1
		NH	0.664	0.424	1.0

Operating conditions applied: O-4:[H$_2$O$_2$]=10mM; O-5:[H$_2$O$_2$]=10mM; O-6: [TiO$_2$]=0.001 g L^{-1}; O-7: [TiO$_2$]=0.001 g L^{-1}.

Once again, the kinetic of the ECs degradation may be globally described as the addition of the contributions of the direct ozonation and the radical pathway. According to this, and similarly to Eq. (1) the overall reaction rate can be expressed as follows:

$$-\frac{d[EC]}{dt} = k_{O_3}[EC] + k_R[EC] = (k_{O_3} + k_R)[EC] = k_T[EC] \qquad (3)$$

where k_{O3}, k_R, and k_T represent the corresponding reaction rate constants to these reactions. According to Equation (3), the application of the first order kinetic model provides the overall reaction constant (k_T), which values are listed in Table 5 together with the half-life time values $t_{1/2}$. At the same time, the kinetic rate constant for the OH radical attack to the pollutants (k_R) can be again obtained by subtracting from these constants (k_T), the direct ozonation rate constant (k_{O3}), and the resulting k_R values are also depicted in Table 5. Generally, it can be observed that the radical pathway, represented by the k_R constant, exerted a minor contribution to the global degradation in comparison to the direct ozonation (k_{O3}), with the exception of the combination $O_3/UV/H_2O_2$ where the efficiency of this pathway was significantly higher; and in the $O_3/UV/TiO_2$ system, with similar contributions of both pathways.

By individually considering the different compounds, ML reached a very high degradation rates in all these oxidant systems based on the use of ozone. On the contrary, DT usually showed a low reactivity towards ozone, while intermediates reactivities were deduced for the rest of the compounds. On the other hand, as could be expected, the presence of an additional oxidizing agent always improved the removal in comparison to the single ozonation process. Thus, the addition of UV radiation to single ozonation enhanced the overall oxidation reaction, due to the combination of three degradation pathways: direct ozonation, direct photolysis and decomposition by hydroxyl radicals. Similarly, the use of TiO_2 as catalyst in ozonation reaction provided an increase higher than a 20% in the elimination of the ECs.

In effect, TiO_2 catalyst promotes the occurrence of oxidative radicals, such as ozonide radicals, which later generate hydroxyl radicals. Furthermore, the additional presence of UV radiation in the O_3/TiO_2 process resulted in a higher production of hydroxyl

radicals This is due to the fact that titanium dioxide absorbs the UV radiation and forms electron-hole pairs which produce photoreduction and photoxidation reactions, respectively. Other ozone combinations with H_2O_2 and H_2O_2/UV also provide an increase in the ECs elimination by means of the radical pathway. Then, it can be concluded that the combination of oxidant agents exert synergistic effects that result in an increase in the oxidation of organic compounds in general, and the selected ECs in particular.

3.5. Oxidation of ECs in real waters by AOPs based in UV radiation and ozone.

To study the oxidation of the selected ECs in different real water systems by some of the AOPs previously tested in the degradation of the ECs in UP water, several degradation experiments at pH=7 were conducted with the simultaneous presence of these ECs in the three water matrices already described in the Experimental Section: a reservoir water (PA) and two secondary effluents from municipal WWTPs (BA and LA). Specifically, the oxidants used in this group of experiments were: single UV radiation (Expt. A-1), UV-TiO_2 (Expt. A-2, with $[TiO_2]_o$=0.001 g L^{-1}), Fe^{2+}-H_2O_2 and UV- Fe^{2+}-H_2O_2 (Expts. A-3 and A-4, with $[Fe^{2+}]_o$=$[H_2O_2]_o$=10µM in both cases), single O_3 (Expt. A-5), and combined O_3-H_2O_2 (Expt. A-6, with$[H_2O_2]$=10µM). Again, it was followed a first order kinetic model, and after regression analysis of the EC remaining concentrations vs. reaction time, the rate constants were evaluated for these processes. Figure 3 illustrate the results obtained.

Firstly, it can be observed in most of the oxidation systems tested some influence of the water matrix nature, with the general following oxidation rate sequence: LA>PA>BA. In effect, the higher degradation rate took place in the LA water as a consequence of its lower organic matter content (see Table 1). Even in some cases, the degradation reached in this LA water surpassed the values obtained in UP water, which may be attributable to the presence of some species dissolved in this water, such as bromide ions, which act as photosensitizer. On the contrary, in PA and BA waters, the rate constants decreased as a consequence of their higher contents in dissolved organic matter, because this matter consumes part of the oxidant in the degradation of other substances that could be present. At the same time, the DOM would also act as radiation filter, hindering the generation of hydroxyl radicals (Gomez-Pacheco et al., 2012).

Regarding the specific behavior of the selected ECs, it is observed that CF generally obtained the greatest degradation rates in the AOPs containing UV radiation and O_3 (Expts. A-1, A-2 and A-4 on one hand; and Expt. A-5 and A-6 on the other), but not in Expt. A-3 which was performed with Fenton reagent. At the same time, BZ and NH had intermediate values of rate constants, depending on the oxidation process tested. Specific attention must be paid for ML degradation, because different trends were observed for its rate constants: moderate or low values in the AOPs that used UV radiation (Expts. A-1, A-2 and A-4); higher values in the Fenton reagent process (Expt. A-3, Figure 3c), and a very much higher value in the ozonation processes (Expt. A-5 and A-6) in comparison to the rest of compounds: for that reason it is not represented in the corresponding Figures 3e and 3f. It must be remarked that these trends in the degradation rate of each compound in every process conducted reproduce most of the results obtained in the individual degradation of the ECs in UP water by the same oxidation systems.

As a global conclusion, the results confirmed that the oxidations by means of individual oxidants agents were considerably less favorable than the combination of oxidants. In particular, UV/TiO_2, O_3/H_2O_2, and Photo-Fenton systems provided higher removal rates of the selected compounds that are treated in this work. In the last times, several authors in different studies about the degradation of priority pollutants by single oxidants and AOPs have reported similar conclusions. Thus, Saritha et al. (2007) in the study of the degradation rate of 4-chloro-2-nitrophenol (4C-2NP) found the following order of reaction: UV/Fenton>UV/TiO_2>UV/H_2O_2>Fenton>H_2O_2>UV.

Once again, single oxidants reached lower elimination rates in comparison to any combined process. More recently, Gozzi et al. (2012), in the study about the degradation treatment of the herbicide chlorimuron-ethyl reported that ozonation was more efficient when was combined with UV-C and H_2O_2, while the photo-Fenton system showed the best results when compared to the other studied systems, achieving mineralization rates exceeding 85%, and proving to be an important technique for the treatment of wastewater containing micro-pollutants. This efficiency of the AOPs could be expected because several simultaneous reactions take place in these processes; among others, direct ozonation, direct photolysis and hydroxyl radical oxidation.

3.6. Cost estimation.

Cost estimation is an important issue in the treatment of any kind of waters. The costs of overall processes take into account the contributions of capital costs, operating costs, and the maintenance. An approach to an estimation of costs is made for the different treatments of this work applied to the degradation of one of the ECs studied. Thus, DT was specifically selected due to the fact that the results showed that it presented the higher resistance to the degradation. In this approach, the capital costs and replacement cost of UV lamp or ozone generator are excluded, and only operating costs, such as those of reagents and electricity consumption are considered.

On one hand, the estimation of the electrical consumptions of the UV lamp or the ozone generators is based on the determination of the electrical energy requirement per order (EE/O in kWh m^{-3}), parameter evaluated by means of the expression (Elmolla and Chaudhari, 2010; Mahamuni and Adewuyi, 2010):

$$EE/O = \frac{(P \cdot t \cdot 1000)}{\left(V \cdot 60 \cdot \log \dfrac{C_{ini}}{C_{fin}} \right)} \tag{4}$$

where P is the rated power (kW), t is the reaction time selected (min), V is the volume of water treated (L), and C_{ini} and C_{fin} are the initial and final concentrations of the pollutants (g L^{-1}). In this work, the selected time was the half-life time $t_{1/2}$, whose values were determined for each process and are reported in previous Tables; and consequently, $C_{fin}=(0.5) \cdot C_{ini}$. In addition, it is considered an average price of $0.10 per kWh for the industrial electricity. Both parameters provide the operating costs due to the electrical consumptions of the single UV radiation or the single ozonation processes, which values are shown in Table 6: 144 $ m^{-3} and 106 $ m^{-3}, respectively.

Table 6. Summary of estimation costs of various AOPs applied to the degradation of ML.

Process	Cost, $\cdot m^{-3}$	Process	Cost, $\cdot m^{-3}$
UV	144	$UV-S_2O_8^{2-}$	12
$UV-H_2O_2$	134	$O_3 (pH=7)$	106
$Fe^{2+}-H_2O_2$	0.003	O_3-UV	52
$Fe^{3+}-H_2O_2$	0.003	$O_3-H_2O_2$	23
$UV-Fe^{2+}-H_2O_2$	30	$O_3-UV-H_2O_2$	45
$UV-Fe^{3+}-H_2O_2$	32	O_3-TiO_2	6
$UV-TiO_2$	10	$O_3-UV-TiO_2$	26

To determining the operating costs of the AOPs tested, in addition to the electricity consumption of each process which values are also calculated by Equation (4), it is necessary to consider the costs of the reagents used in addition to UV radiation or ozone. For this purpose, Table 7 provides the average price per mass unit of these reagents. By taking into account the amount of every reagent consumed by each process, the cost per volume unit of treated water is deduced, values which are shown in Table 7. Finally, the sum of both contributions (electricity consumption plus reagent costs) provides the final operating costs of the AOPs tested, values that are also summarized in Table 6.

Table 7. Price of reagents used in the AOPs tested.

Reagent	Cost, $ kg^{-1}	Cost, $ m^{-3}
$FeSO_4.7H_2O$	0.95	2.64×10^{-3}
$Fe(ClO_4)_3.H_2O$	1.08	3.15×10^{-3}
$H_2O_2 (33\%)$	0.63	1.46×10^{-4}
TiO_2	3.00	1.50×10^{-2}
$Na_2S_2O_8$	2.40	1.20×10^{-3}

As seen in Table 6, under an economical point of view, the most economical choices are the Fenton reagent and Fenton-like system, due to the absence of electrical

energy in both processes. However, under a kinetic point of view these treatments present the lower degradation rates. On the contrary, operating costs of the photochemical processes are considerably higher, due to the electricity consumption of the UV lamp, although the presence of catalysts (such as H_2O_2, TiO_2, or even Fe(II) and Fe(III)) decreases these costs. Similarly, in the case of ozonation processes, single ozone presents higher costs, although great efficiency; and these costs decrease in the AOPs that use ozone in combination with additional oxidant agents (such as O_3/UV, O_3/H_2O_2, O_3/UV/H_2O_2, O_3/TiO_2 and O_3/UV/TiO_2).

Although an exact comparison of operating costs among the results obtained in this study and other results provided by the literature cannot be made because of the lack of similar studies focused in the chemical oxidation of these specific compounds, some results reported by several authors, that used similar chemical degradation processes but applied to different water matrices, can be mentioned. Thus, Saritha et al. (2007) conducted an estimation of costs for the treatments applied to the degradation of 4C-2NP, and they reported the following values (in $ m^{-3}): 250.5 for UV radiation; 5.8 for single H_2O_2; 58.6 for the combination UV/H_2O_2; 7.4 for the Fenton process; 28.7 for the combined UV/Fenton, and 78.5 for the combined UV/TiO_2. As observed, among all the treatment processes studied, operating costs of photo catalysis and UV are considerably more expensive than others. However, costs can be decreased considerably for photo catalytic treatments when solar light is used.

In the case of real wastewaters, Kestioglu et al. (2005) applied various treatments to the purification of an olive mill effluent (OME), such as acid cracking, chemical coagulation, adsorption and Advanced Oxidation Processes (AOPs). Specifically for the AOPs tested, the results revealed a cost of 12.62 $ m^{-3} for the O_3/UV combined system, and 13.17 $ m^{-3} for the H_2O_2/UV combined system. Finally, Durán et al. (2012) studied the operation costs of treating a real effluent from an integrated gasification combined cycle (IGCC) power station by a photo-Fenton process at an artificial UV pilot plant with the initial addition of H_2O_2, by a modified photo-Fenton process and by a ferrioxalate-assisted solar photo-Fenton process.

The results showed that the solar photo-Fenton system was economically feasible, being able to achieve up to 75% mineralization with a total cost of 6 $ m^{-3}. In conclusion, much different results are reported as a consequence of the different systems applied and different operating conditions used, but the general conclusions of this study prevail: lower costs in treatments with absence of electrical energy and higher operating costs in photochemical processes due to the electricity consumption of the UV lamp, although combined processes with the presence of catalysts can decrease these costs.

REFERENCES

Acero, J.L.; Benitez, F.J.; Real. F.J.; Roldan, G. Kinetics of aqueous chlorination of some pharmaceuticals and their elimination from water matrices. Water Res. **2010**, 44, 4158-4170.

Bolong, N.; Ismail, A.F.; Salim, M.R.; Matsuura, T. A review of the effects of emerging contaminants in wastewater and options for their removal. Desalination **2009**, 239, 229-246.

Chelme-Ayala, P.; Gamal El-Din, M.; Smith, D.W. Degradation of bromoxynil and trifluralin in natural water by direct photolysis and UV plus H_2O_2 Advanced Oxidation Process. Water Res. **2010**, 44, 2221-2228.

Clesceri, L.S.; Greenberg, A.E.; Trussell, R.R. Standard Methods for the Examination of Water and Wastewater, 17th ed., APHA, AWWA, WPCF, Washington DC, **1989**.

Costanzo, S.D.; Watkinson, A.J.; Murby, E.J.; Kolpin, D.W.; Sandstrom, M.W. Is there a risk associated with the insect repellent DEET (N,N-diethyl-m-toluamide) commonly found in aquatic environments?. Sci. Total Environ. **2007**, 384, 214-220.

De la Cruz, N.; Giménez, J.; Esplugas, S.; Grandjean, D.; de Alencastro, L.F.; Pulgarín, C. Degradation of 32 emergent contaminants by UV and neutral photo-fenton in domestic

wastewater effluent previously treated by activated sludge. Water Res. **2012**, 46, 1947-1957.

Ding, Y.; Yang, C.; Zhu, L.; Zhang, J. Photoelectrochemical activity of liquid phase deposited TiO_2 film for degradation of benzotriazole. J. Hazard. Mater. **2010**, 175, 96-103.

Dolar, D.; Gros, M.; Rodriguez-Mozaz, S.; Moreno, J.; Comas, J.; Rodriguez-Roda, I.; Barceló, D. Removal of emerging contaminants from municipal wastewater with an integrated membrane system, MBR–RO. J. Hazard. Mater. **2012**, 239, 64-69.

Durán, A.; Monteagudo, J.M.; San Martín, I. Photocatalytic treatment of an industrial effluent using artificial and solar UV radiation: An operational cost study on a pilot plant scale. J. Environ. Manage. **2012**, 98, 1-4.

Elmolla, E.S.; Chaudhari, M. Comparison of different advanced oxidation processes for treatment of antibiotic aqueous solution. Desalination **2010**, 256, 43-47.

Gomez-Pacheco, C.V.; Sanchez-Polo, M.; Rivera-Utrilla, J.; López-Peñalver, J.J. Tetracycline degradation in aqueous phase by ultraviolet radiation. Chem. Eng. J. **2012**, 187, 89-95.

Gozzi, F.; Machulek, A.; Ferreira, V.S.; Osugi, M.E.; Santos, A.P.F.; Nogueira, J.A.; Dantas, R.F.; Esplugas, S.; de Oliveira, S.C. Investigation of chlorimuron-ethyl degradation by Fenton, photo-Fenton and ozonation processes. Chem. Eng. J. **2012**, 210, 444-450.

Gu, J.D.; Fan, Y.; Shi, H. Relationship between structures of substituted indolic compounds and their degradation by marine anaerobic microorganisms. Mar. Poll. Bull. **2002**, 45, 379-384.

Huang, K.C.; Couttenye, R.A.; Hoag, G.E. Kinetics of heat assisted persulfate oxidation of methyl tert-butyl ether (MTBE). Chemosphere **2002**, 49, 413-420.

Kestioglu, K.; Yonar, T.; Azbar, N. Feasibility of physico-chemical treatment and Advanced Oxidation Processes (AOPs) as a means of pretreatment of olive mill effluent (OME). Proc. Biochem. **2005**, 40, 2409-2416.

Klamerth, N.; Miranda, N.; Malato, S.; Agüera, A.; Fernández-Alba, A.R.; Maldonado, M.I.; Coronado, J.M. Degradation of emerging contaminants at low concentrations in MWTPs effluents with mild solar photo-Fenton and TiO_2. Catal. Today **2009**, 144, 124-130.

Klamerth, N.; Rizzo, L.; Malato, S.; Maldonado, M.I.; Agüera, A.; Fernández-Alba, A.R. Degradation of fifteen emerging contaminants at $\mu g\ L^{-1}$ initial concentrations by mild solar photo-Fenton in MWTP effluents. Water Res. **2010**, 44, 545-554.

Mahamuni, N. N.; Adewuji, Y.G. Advanced oxidation processes (AOPs) involving ultrasound for waste water treatment: A review with emphasis on cost estimation. Ultrason. Sonochem. **2010**, 17, 990-1003.

Nicole, I.; De Laat, J.; Dore, M.; Duguet, J.P.; Bonnel, C. Utilisation du rayonnement ultraviolet dans le traitement des eaux: mesure du flux photonique par actinometrie chimique au peroxyde d'hydrogene. Water Res. **1990**, 24, 157-168.

Prieto-Rodriguez, L.; Miralles-Cuevas, S.; Oller, I.; Agüera, A.; Li Puma, G.; Malato, S. Treatment of emerging contaminants in wastewater treatment plants (WWTP) effluents by solar photocatalysis using low TiO_2 concentrations. J. Hazard. Mater. **2012**, 211, 131-137.

Rodriguez, S.; Santos, A.; Romero, A. Effectiveness of AOP's on abatement of emerging pollutants and their oxidation intermediates: Nicotine removal with Fenton's Reagent. Desalination. **2011**, 280, 108-113.

Rossner, A.; Snyder, S.A.; Knappe, D.R.U. Removal of emerging contaminants of concern by alternative adsorbents. Water Res. **2009**, 43, 3787-3796.

San, N.; Hatipoğlu, A.; Koçtürk, G.; Çınar, Z. Photocatalytic degradation of 4-nitrophenol in aqueous TiO_2 suspensions: Theoretical prediction of the intermediates. J. Photochem. Photobio. A: Chem. **2002**, 146, 189-197.

Santos, M.; Alves, A.; Madeira, L.M. Paraquat removal from water by oxidation Fenton's reagent. Chem. Engin. J. **2011**, 175, 279-290.

Saritha, P.; Aparna, C.; Himabindu, V.; Anjaneyulu, Y. Comparison of various advanced oxidation processes for the degradation of 4-chloro-2 nitrophenol. J. Hazard. Mater. **2007**, 149, 609-614.

Sirés, I.; Garrido, J.A.; Rodríguez, R.M.; Brillas, E.; Oturan, N.; Oturan, M.A. Catalytic behavior of the Fe^{3+}/Fe^{2+} system in the electro-Fenton degradation of the antimicrobial chlorophene. Appl. Catal. B: Environ. **2007**, 72, 382-394.

Stuart, M.; Lapworth, D.; Crane, E.; Hart, A. Review of risk from potential emerging contaminants in UK groundwater. Sci. Total Environ. **2012**, 416, 1-21.

Westerhoff, P.; Yoon, Y.; Snyder, S.; Wert, E. Fate of endocrine-disrupter, pharmaceuticals and personal care product chemicals during simulated drinking water treatment process. Environ. Sci. Technol. **2005**, 39, 6649-6663.

Xie, X.; Zhang, Y.; Huang, W.; Huang, S. Degradation kinetics and mechanism of aniline by heat-assisted persulfate oxidation. J. Environ. Sci. **2012**, 24, 821-826.

3.9. Influence of membrane, pH and water matrix properties on the retention of emerging contaminants by ultrafiltration and nanofiltration.

3.9. INFLUENCE OF MEMBRANE, PH AND WATER MATRIX PROPERTIES ON THE RETENTION OF EMERGING CONTAMINANTS BY ULTRAFILTRATION AND NANOFILTRATION

Juan L. Acero, F. Javier Benítez, Francisco J. Real, Elena Rodríguez.

Departamento de Ingeniería Química, Universidad de Extremadura, Badajoz.

The removal of five emerging contaminants (benzotriazole, DEET, chlorophene, 3-methylindole, and nortriptyline) dissolved in several water matrices by ultrafiltration and nanofiltration membranes has been investigated. The influence of some operating variables (nature and MWCO of the membranes, and pH) on the permeate flux and on the retention of the selected compounds was discussed. Pore blocking and cake layer formation probably dominated at the beginning of filtration, whereas cake layer formation was likely the dominant fouling mechanism at later stages, specially in presence of NOM and Ca^{2+}. The nanofiltration HL membrane was the most appropriate for the removal of the selected emerging contaminants, except for benzotriazole, which presented low retention. While adsorption is the main mechanism for micropollutants retention by UF filtration membranes, size exclusion and electrostatic repulsion at high pH are dominant in the case of NF membranes.The presence of natural organic matter increased retention likely due to compounds-humic acids interactions. However, the additional presence of Ca^{2+} decreased the contaminant removal probably due to reduced humic acids interaction sites. In addition, retention coefficients for parameters that measure the quality of the effluent were also evaluated, and the results revealed that the nanofiltration HL membrane is a feasible option for drinking water production, and for the purification of not very contaminated secondary effluents for reuse.

1. INTRODUCTION.

In recent years, an increasing attention has been paid to a wide group of numerous chemical substances, including pharmaceutically active compounds, endocrine disrupting compounds, and personal care products (Bolong et al., 2009). All of them are considered emerging contaminants (ECs), since they are still unregulated or in the process of being regulated. Wastewater treatment plant (WWTP) effluents are a major source of ECs in the environment, and they are found in wastewater effluents, surface water and treated drinking water (Ikehata et al., 2008; Kovalova et al., 2013; Nakada et al., 2007). Therefore, ECs constitute a potential risk for human health, since they can cause unexpected physiological consequences.

In general, their removal by conventional wastewater and drinking water processes has not been shown to be effective (Westerhoff et al., 2005; Stackelberg et al., 2004), and consequently, there is a need to investigate new technologies for their elimination. Due to this concern, different physical-chemical processes have been proposed as tertiary treatment of secondary effluents from municipal treatment plants, such as activated carbon adsorption (Kovalova et al., 2013; Snyder et al., 2007; Goren et al., 2008), advanced oxidation by ozone and hydroxyl radicals (Ikehata et al., 2008; Ternes et al., 2003; Huber et al., 2003) and photo-catalysis UV/TiO$_2$ (Al-Bastaki, 2004). More recently, membrane processes employing ultrafiltration (UF) and nanofiltration (NF) are increasingly used in wastewater reclamation and drinking water to remove micropollutants as well as natural organic matter (NOM) (Wintgens et al., 2005; Verliefde et al., 2007; Haberkamp et al., 2008; Wray et al., 2014; Anwar Sadmani et al., 2014). Retention of organic micropollutants by UF membranes is attributed to adsorption on the membrane during the early stages of filtration, or to interactions with the membrane fouling layer, and/or interactions with dissolved NOM in solution (Neale and Schafer, 2012). On the other hand, NF membranes remove organic solutes by three main mechanisms, i.e., size exclusion, electrostatic repulsion and adsorption (Chang et al., 2012). The presence of NOM contributes to NF membrane fouling, and may change the surface properties and therefore may affect the retention mechanism. In addition, the presence of cations can influence the interaction of compounds and NOM with each other as well as with the membrane surface

(Comerton et al., 2009). Although some studies have investigated the removal of ECs in presence of NOM and cations, some conflicting results were reported with respect to the influence of water matrix properties on ECs retention (Verliefde et al., 2007; Anwar Sadmani et al., 2014; Comerton et al., 2008). As a consequence, the complexity of fouling on retention mechanisms of ECs by UF and NF membranes needs further investigation.

The present research is focused in the assessment of the specific elimination of a group of five frequently found emerging contaminants in water systems by means of UF and NF membranes. The ECs selected were:benzotriazole (BZ), a well-known corrosion inhibitor for copper or silver material, widely used in cooling and hydraulic fluids, anti-freezing products, aircraft deicer and anti-ice fluid, and dishwasher detergents (Loos et al., 2009); N,N-diethyl-m-toluamide or DEET (DT), an active compound in insect repellents (Costanzo et al., 2007); chlorophene (CP), a widespread broad-spectrum antimicrobial pharmaceutical, used in hospitals and households for general cleaning and as active agent in disinfectant formulations (Boehmer et al., 2004); 3-methylindole (ML), used as perfume and synthesizing anti-inflammatory drug, antibiotic, dye, plant growth hormone, herbicide, muscular relaxant, respiratory inhibitor and heart stimulant medicaments (Wenhui et al., 2009); and the pharmaceutical nortriptylineHCl (NH), which belongs to the group of tricyclic antidepressants (TCAs), and used in treatments against depression (Langford et al., 2009).

In the first stage of this work the selected compounds were dissolved in ultrapure (UP) water, and in the second stage in different water matrices, including synthetic and real waters. Several objectives were pursued: the study of the evolution of the permeate flux with filtration time and volume retention factors; the establishment of the effect of several operating parameters (pH, and nature and molecular weight cut-off (MWCO) of the membranes)on the steady-state permeate flux; the evaluation of the partial contribution of the different membrane resistances; and the determination of retention coefficients and adsorbed mass for each EC, including the proposition of the main retention mechanisms. Finally, the influence of the water matrix properties (presence of natural organic matter and cations) was also investigated, since the additional presence of humic acids and cations might affect the permeate flux and therefore modify the retention coefficients and mechanisms.

2. MATERIALS AND METHODS.

2.1. Chemical and water matrices.

The five selected ECs were purchased from Sigma-Aldrich (Germany) and were of 99% purity or higher. Table 1 summarizes the selected compounds and their relevant physico-chemical properties related to the main removal mechanisms by membrane processes. Differences in hydrofobicity (expressed as log K_{ow}) and charge characteristics were chosen to enable assessment of the influence of hydrophobic interactions and charge on retention. The solutions used in this study were prepared by dissolving the ECs (1 µM of each) in UP water (from a Milli-Q system, Millipore Ibérica, Spain) or in synthetic water (SW) prepared from UP water buffered with 1 mM sodium bicarbonate and spiked with humic acids (Aldrich, 0-23 mg L^{-1}) as a surrogate NOM and calcium ions (0-1 mM). In addition, three real water matrices were used in order to reproduce realistic water treatment conditions: a surface water collected from the public reservoir "Peña del Aguila" (PA), located in the Extremadura Community, south-west of Spain; and two secondary effluents from WWTPs corresponding to the cities of Badajoz (BA) and La Albuera (LA), also in the Extremadura Community. These water samples were stored at 4 ^{o}C until use, and its main quality parameters are compiled in Table S1.

Table 1. Physico-chemical properties of model compounds.

Emerging contaminant	MW, g mol^{-1}	pK$_a$	Log k$_{ow}$
Benzotriazole	119.1	0.40 / 8.20	1.44
NortriptylineHCl	299.8	10.21	4.51
DEET	191.3	0.67	2.18
3-Methylindole	131.3	-	2.60
Chlorophene	218.7	9.81	4.18

2.2. Experimental equipment and membranes.

Ultrafiltration and nanofiltration experiments were conducted in a laboratory cross-flow mode filtration apparatus, supplied by CM-CELFA Membrantrenntechnik AG (Seewen, Switzerland), model P-28^{TM}. The equipment was constituted by a 500 mL pressurized storage vessel and a gear pump which fed the solution to the flat-sheet membrane module at the desired flow rates. The whole equipment is temperature controlled by means of a water stream at the desired temperature that circulated through an external jacket that surrounded the storage vessel. The transmembrane pressure (TMP) in the experiments was controlled by feeding nitrogen gas to the head of the storage vessel. The cumulative permeate volume was measured with a Mettler balance.

Several flat sheet commercial membranes provided by GE Osmonics (Florida, USA) were used, all of them with an effective surface area of 28 cm^2. They were three UF membranes, denoted PW, PT, and GK with MWCO of 20000, 5000, and 2000 Da, respectively; and three NF membranes, denoted CK, DK, and HL, with similar MWCOs, in the range 150–300 Da. Their main properties (material, MWCO and contact angle) are compiled in Table S2. More specifically, the GK membrane was made of thin film composite, with a cross-linked aromatic polyamide top layer; and the PT and PW membranes were of polyethersulfone. These three membranes are hydrophilic, specially the GK membrane with a lower value of contact angle (Park et al., 2007). On the other hand, DK and HL membranes were made of thin film composite (polypyperazinamide skin layer on a polyester support), and the CK membrane was of cellulose acetate. According to the determined and published data of contact angles (Verliefde et al., 2007; Jin et al., 2007), the CK membrane is hydrophobic, while DK and HL are hydrophilic. A new membrane was used in each experiment, rinsed with ultrapure water, and compacted by filtering ultrapure water during 2 hours before starting the filtration experiment.

2.3. Filtration experiments.

The filtration experiments were conducted in tangential cross-flow mode, and the operating method was batch concentration, in which the concentrate stream was flowed

back to the feed tank. During each experiment, temperature (20 $^{\circ}$C), tangential velocity (1 m s^{-1}) and TMP (3 bar for UF and 20 bar for NF) remained constant. The experiments performed with UP water were buffered at the desired pH with phosphate buffer (10 mM).

A standard operating protocol was followed, which was constituted by three steps: firstly, the new membrane was rinsed with UP water, and the permeate flux (J_{wi}) was measured with the aim of determining the membrane pure water permeability (PWP), which represents a main characteristic of a membrane. PWP was determined as the ratio between J_{wi} and the TMP of the experiment, and the average values obtained for the different membranes tested are summarized in Table S2. In a next step, the filtration of the selected ECs dissolved in UP water, synthetic water, or in the real water matrices (300 mL feed water volume with initial concentration of ECs of 1μM) took place. At regular time intervals, the permeate volume was measured with a balance in order to determine the permeate flux (J_v). Simultaneously, samples of this permeate stream were retired in order to analyze the content of the selected pollutants, as well as the global quality parameters in the water matrices (chemical oxygen demand (COD), UV absorbance at 254 nm (A_{254}), and total organic carbon (TOC)). These experiments lasted until a volume reduction factor of 3 was reached, collecting around 200 and 100 mL of permeate and concentrate, respectively. Once the filtration of emerging contaminants was finished, at the third step the feed tank was emptied and filled with UP water, and then the membrane was rinsed by circulating UP water inside the membrane module in order to remove the cake layer formed on the membrane surface. The final pure water flux (J_{wf}) was then measured in order to determine the irreversible membrane fouling.

2.4. Analytical methods.

The analytical methods for the characterization of the selected water matrices were followed according to the Standard Methods (Clesceri et al., 1989). TOC was determined using a total organic carbon analyzer TOC-multi N/C 3100 (Analytik Jena). Absorbance at 254 nm was measured in spectrophotometer Unicam Helios Beta. Conductivity and pH were measured using a multiparameter instrument Hanna HI 255. COD, total nitrogen and total phosphorus were determined by using Dr. Lange kits. On the

other hand, concentrations of the five selected ECs were assayed by HPLC in a Waters Chromatograph (Alliance 2695) equipped with a 2998 Photodiode Array Detector and a Phenomenex Gemini C18 column (5µm, 150mm×3mm). The analysis was performed in gradient mode with acetonitrile and 25 mM acid formic, at a flow rate of 0.2 mL min^{-1}. Further details about the analytical method are given elsewhere (Benitez et al., 2013). The injection volume was 100 µL in all cases. Detection was made at 250 nm for BZ, NH, and DT; and 280 nm for ML and CP.

2.5. Theoretical calculations.

The permeate volume (V_p) was continuously collected through each experiment, and the permeate flux (J_w in the case of UP water, or J_v in the aqueous solutions of ECs dissolved in UP water, synthetic water or real water matrices) was determined by using the expression:

$$J_w \text{ or } J_v = \frac{\Delta V_p}{\Delta t \ A} \tag{1}$$

where ΔV_p represents the cumulative permeate volume difference, Δt is the time difference and A is the membrane area.

The volume reduction factor (VRF) is defined as the ratio between the feed volume (V_f) and the retentate volume ($V_r = V_f - V_p$),and was calculated by using the equation:

$$VRF = \frac{V_f}{V_r} \tag{2}$$

Regarding to the resistances to the permate flux, the total hydraulic resistance (R_t) was evaluated from the permeate flux J_v, according to the general Darcy's law:

$$R_t = \frac{TMP}{\mu J_v} \tag{3}$$

where TMP is the transmembrane pressure, μ is the viscosity of the solution. This R_t is the result of several resistances in series:

$$R_t = R_m + R_f = R_m + R_{if} + R_{ef} \qquad (4)$$

where R_m is the intrinsic resistance of clean membrane, and R_f is the fouling resistance with two components, the internal (R_{if}) and external (R_{ef}) fouling. These resistances were determined following the procedure described elsewhere (Acero et al., 2010).

One of the best parameters which provide the efficiency of a membrane in a filtration process is the retention coefficient, which was determined for the selected ECs by the equation:

$$R = \frac{C_f - C_p}{C_f} \cdot 100 \qquad (5)$$

where C_f and C_p are the concentrations of each EC in the feed and permeate streams respectively. Similarly, retention coefficients were evaluated for the water quality parameters selected in the present work. For the specific case of COD, this coefficient was defined by the expression:

$$R_{COD} = \frac{COD_f - COD_p}{COD_p} \cdot 100 \qquad (6)$$

where COD_f and COD_p represent the COD in the feed and permeate streams respectively. Similar equations were used for TOC (R_{TOC}), and UV absorbance at 254 nm (R_{A254}).

The adsorption of contaminants onto the membrane surface and into the membrane pores was evaluated in order to assess the contribution of this mechanism to the global retention of the solutes by the selected membranes and to establish the retention mechanism for each specific compound. For this purpose, the adsorption percentage (AP) was determined by the expression (Yoon et al. 2006):

$$AP = \frac{(C_f V_f) - [(C_p V_p) + (C_r V_r)]}{C_f V_f} \cdot 100 \qquad (7)$$

where V_f, V_p, and V_r are the feed, permeate and retentate volumes; C_f, C_p, and C_r are the feed, permeate and retentate concentrations for each micropollutantmatrices

3.   RESULTS AND DISCUSSION.

3.1. Permeate flux, membrane fouling and analysis of resistances.

The filtration process of the selected ECs dissolved together in UP water was performed by using the UF and NF membranes already described, and by varying some operating conditions: characteristics of the membranes (MWCO, material, etc.), and pH. The experiments performed and the values of the operating conditions are summarized in Table 2. In addition, some experiments were carried out with the ECs dissolved in synthetic water and in the selected water matrices and subjected to both, UF with the PT membrane, and NF with the HL membrane. The criteria for selecting these UF and NF membranes were their better behaviour in terms of permeate flux, membrane fouling and retention of ECs. These experiments are summarized in Table 2 as well.

The evolution of J_v with VRF in some selected experiments is shown in Fig. 1. When UP water was used, there was an initial decrease in J_v (5-15% of J_{wi}) with the increase of VRF; and later, after a specific time, the flux remained almost constant. However, J_v decrease was more pronounced when synthetic or real waters were employed, and the time required to reach an almost constant value was higher than with UP water. The decay of J_v is a consequence of membrane fouling, which can be due to different causes, such as polarization concentration, cake layer formation, pore blocking, or adsorption of solutes onto the membrane. According to the shape of J_v and results found in previous studies (Maximous et al., 2009; Nghiem et al., 2010; Altapova et al., 2014), pore blocking and cake layer formation probably dominated at the beginning of filtration, whereas cake layer formation was likely dominant fouling mechanism at later stages. Polarization concentration could also contribute to membrane fouling, specially in experiments performed with UP water with very low foulant concentration. The almost constant permeate flux can be considered as the steady-state permeate flux (J_{vss}). Table 2 compiles the values of J_{vss} as well as the ratio J_{vss}/J_{wi} (ratio between the steady-state permeate flux for the solution containing the ECs and that corresponding to the filtration of UP water without solutes). Finally, the values of J_{wf}/J_{wi} were determined in order to evaluate the membrane flux recovery after washing with pure water, thus removing the external fouling. These values are also reported in Table 2 and provide an idea of internal membrane fouling.

Table 2. Filtration experiments performed with ECs dissolved in different water matrices (ultrapure water (UP), synthetic water (SW) and real water matrices (PA, LA and BA): operating conditions, steady-state permeate flux (J_{vss}), flux decay (J_{vss}/J_{wi}), and flux recovery (J_{wf}/J_{wi}).

Expt.	Membrane	TMP, bar	pH	TOC, mg L^{-1}	Ca^{2+}, mM	J_{vss}, L h^{-1} m^{-2}	J_{vss}/J_{wi}	J_{wf}/J_{wi}
UPUF-1	PW	3	6	-	-	377.6	0.87	0.98
UPUF-2	GK	3	5.8	-	-	10.1	0.89	0.96
UPUF-3	PT	3	5.5	-	-	87.3	0.97	0.98
UPUF-4	PT	3	7	-	-	87.8	0.95	0.98
UPUF-5	PT	3	8.5	-	-	82.8	0.93	0.99
UPUF-6	PT	3	10	-	-	83.9	0.92	0.98
UPNF-1	DK	20	5.5	-	-	30.5	0.85	0.88
UPNF-2	CK	20	5.7	-	-	40.1	0.98	0.98
UPNF-3	HL	20	5.5	-	-	188.2	0.96	0.98
UPNF-4	HL	20	7	-	-	187.1	0.91	0.99
UPNF-5	HL	20	8.5	-	-	171.3	0.84	0.98
UPNF-6	HL	20	10	-	-	167.7	0.84	0.99
SWUF-1	PT	3	7.2	12	-	79.5	0.86	0.97
SWUF-2	PT	3	7.3	12	1	70.3	0.79	0.88
SWUF-3	PT	3	7.3	23	1	67.1	0.73	0.81
SWNF-1	HL	20	7.3	12	-	155.8	0.82	0.98
SWNF-2	HL	20	7.3	12	1	19.0	0.10	0.91
SWNF-3	HL	20	7.4	23	1	18.9	0.10	0.79
PAUF	PT	3	7.2	6.8	-	75.2	0.96	0.98
LAUF	PT	3	8.1	2.6	-	84.5	0.95	0.98
BAUF	PT	3	8.6	19.0	-	69.8	0.74	0.85
PANF	HL	20	7.2	6.8	-	167.3	0.84	0.98
LANF	HL	20	8.1	2.3	-	153.6	0.80	0.97
BANF	HL	20	8.5	19.3	-	121.5	0.62	0.89
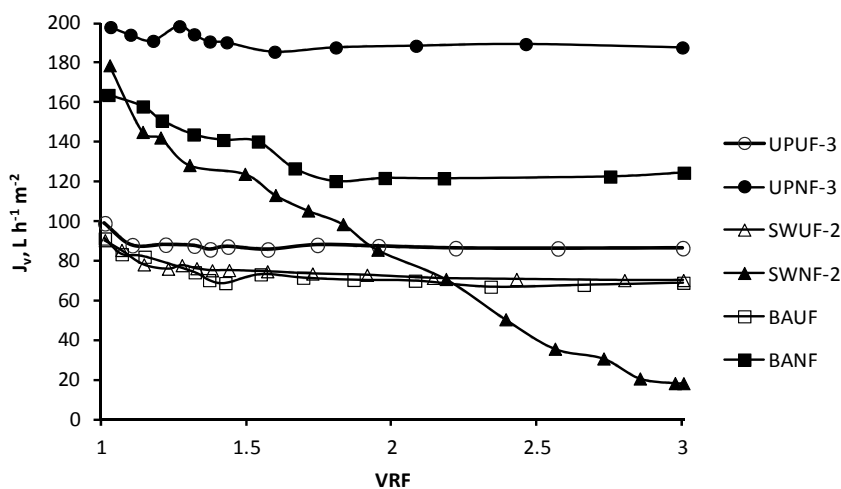
Figure 1. Evolution of the permeate flux with VRF during the filtration of micropollutants dissolved in UP water (Expts. UPUF-3 and UPNF-3), synthetic water (Expts. SWUF-2 and SWNF-2), and secondary effluent BA (Expts. BAUF and BANF). Experimental conditions detailed in Table 2.

The values of J_{vss} are affected by the characteristics of the membranes (MWCO, material, etc.), pH, and water matrix. With respect to the influence of the characteristics of the UF membranes, and although these membranes were different in materials, an influence of MWCO on J_{vss} can be deduced from the UF experiments compiled in Table 2 (Expts. UPUF-1 to UPUF-3). Thus, J_{vss} values were 10.1, 87.3 and 377.6 L h^{-1} m^{-2} for the membranes GK, PT, and PW (MWCOs of 2, 5 and 20 kDa, respectively), being this increase of the permeate flux likely due to the MWCO increased. On the contrary, in the NF process no conclusion could be drawn on the effect of the MWCO (Expts. UPNF-1 to UPNF-3), since the three membranes present similar pore sizes (in the range 150–300 Da). Nevertheless, a much higher permeate flux was obtained for the HL membrane, while the CK and DK membranes presented lower values, differences that can be attributed to the different nature of these membranes. Specifically, this sequence agrees with the results previously reported for the PWP of the membranes (see Table S2), with a significant higher value for the HL membrane and similar lower values for the DK and CK membranes. The best results for permeate flux and also for ECs retention (see below) were obtained for the UF membrane PT and the NF membrane HL. As a consequence, the remaining experiments

performed at different pH and with several water matrices were carried out with these membranes.

The influence of pH on the values of J_{vss} as well as on the ratio J_{vss}/J_{wi} is slightly negative. As can be observed in Table 2, a pH increase led to a decrease in the values of J_{vss} and an increase of the membrane fouling. An explanation for these results could be that a higher pH values, the negative zeta potential increase promotes stronger electrostatic interaction between dissociated functional groups of membrane material causing a pore constriction (Ribau Teixeira and Rosa, 2005; Lopez-Muñoz et al., 2009). Additional solute-membrane interactions could also be responsible for the fouling increase, as well as an increase of the osmotic pressure near the membrane surface (Ribau Teixeira et al., 2005).

The influence of the water matrix on J_{vss} can also be deduced from the results summarized in Table 2 as well as from Fig. 1. Thus, the permeate fluxes obtained with UP water at pH 7 (87.8 and 187.1 L h^{-1} m^{-2} for PT and HL membranes, respectively) were higher than those obtained with the different water matrices in similar experiments, especially in the NF process, where the flux decrease was more pronounced.

As pointed out above, the decrease in the permeate flux is a consequence of polarization concentration, pore blocking and formation of a cake layer on the membrane surface as well as adsorption of species (NOM and ions) onto the membrane. Consequently, a decrease of the effective pore size is caused, which leads to a decrease of the water flux. It can be appreciated in the experiments performed with synthetic waters that the presence of NOM led to a further decrease of the permeate flux as well as to a decrease of the ratio J_{vss}/J_{wi}. Furthermore, this decrease of the water flux was more pronounce in presence of both NOM and calcium ions. Certain compounds present in the NOM, mainly humic acids, are known to be hydrophobic, and therefore might be adsorb on the membrane due to hydrophobic interactions, being one of the major causes of NF fouling. Pore blocking can be caused by molecules with a size that is similar to the size of an important fraction of the pores. Such type of molecules can block the membrane pores efficiently, and thus the pores become unavailable for further filtration (Van der Bruggen et al., 1998). While internal pore adsorption is irreversible, pore blocking is partly reversed by

backwashing (Katsoufidou et al., 2005). Similarly, calcium ions are adsorbed onto the membrane surface and reduce its negative charge, which leads to a reduction of the membrane permeability and an increment of membrane-NOM interactions (Ribau Teixeira and Rosa, 2005). In addition, calcium ions can also contribute to the increase of the membrane hydrophobicity (Ribau Teixeira et al., 2005). In cake layer formation, foulants deposit on the particles that already block the pores and result in cake formation (Chang et al., 2012). At the same time, the formation of calcium complexes of humic acids could also contribute to cake layer formation. For these reasons, the extent of the membrane fouling was more important in the presence of both humic acids and calcium ions. Under these conditions, the main fouling mechanisms are an initial pore blocking stage (rapid fouling) followed by cake layer formation (slow fouling) (Chang et al., 2012). Furthermore, membrane fouling was lower in the case of the UF membrane PT with a MWCO of 5 kDa, since fouling of UF membranes in presence of NOM is more important for those membranes of higher MWCO (Neale and Schafer, 2012). The important fouling of the HL membrane in presence of NOM and Ca^{2+} is mainly due to cake layer formation, since this fouling is mostly reversible and could be removed by rinsing with UP water, as can be deduced from the values of J_{wf}/J_{wi} summarized in Table 2.

Additionally, among the real waters investigated, the trend observed for J_{vss} and J_{vss}/J_{wi} was: PA ≈ LA > BA. The higher content of NOM in the secondary effluent BA (values of UV absorbance, TOC and DOC in Table S1) led to lower J_{vss} values due to the reasons given above. On the other hand, the results obtained for the reservoir water PA and the secondary effluent LA are rather similar. Compared to PA water, LA presents less NOM but higher inorganic matter content (from the values of conductivity and alkalinity summarized in Table S1). Although a limited membrane fouling could be expected from the low NOM content in LA secondary effluent, the presence of cations could enhance the formation of complexes with NOM and thus increase membrane fouling as mentioned above.

The permeate flux decline discussed is a consequence of the resistances found by the solutions to pass through the membranes during the filtration processes. Then, this decline can be analysed by means of the resistance in series model (equations (3) and (4)). The values obtained for these resistances in all the experiments are summarized in Table 3,

which also shows the partial contribution of the fouling resistance to the total resistance, represented by the ratio $(R_f/R_t) \times 100$.

Table 3. Resistances obtained in the filtration of ECs dissolved in different water matrices at VRF=3. Experimental conditions in Table 2.

Expt.	Membrane	$R_m \times 10^{-13}$, m^{-1}	$R_t \times 10^{-13}$, m^{-1}	$R_f \times 10^{-13}$, m^{-1}	$R_{ef} \times 10^{-13}$, m^{-1}	$R_{if} \times 10^{-13}$, m^{-1}	$(R_f/R_t) \times 100$, %
UPUF-1	PW	0.25	0.29	0.04	0.03	0.01	11.2
UPUF-2	GK	9.45	10.7	1.21	0.81	0.40	11.4
UPUF-3	PT	1.21	1.27	0.06	0.03	0.03	4.7
UPUF-4	PT	1.16	1.23	0.07	0.04	0.03	5.3
UPUF-5	PT	1.23	1.30	0.07	0.06	0.01	5.4
UPUF-6	PT	1.18	1.29	0.11	0.08	0.03	8.2
UPNF-1	DK	20.1	23.6	3.51	0.75	2.76	14.9
UPNF-2	CK	16.8	17.9	1.14	0.27	0.87	6.3
UPNF-3	HL	3.65	3.83	0.18	0.09	0.09	4.5
UPNF-4	HL	3.51	3.85	0.34	0.30	0.04	8.8
UPNF-5	HL	3.54	4.20	0.66	0.59	0.07	15.7
UPNF-6	HL	3.60	4.30	0.70	0.69	0.01	16.2
SWUF-1	PT	1.16	1.35	0.19	0.16	0.03	14.3
SWUF-2	PT	1.21	1.54	0.33	0.17	0.16	21.4
SWUF-3	PT	1.18	1.61	0.43	0.16	0.27	26.6
SWNF-1	HL	3.80	4.62	0.82	0.72	0.10	17.7
SWNF-2	HL	3.71	37.8	34.1	33.7	0.35	90.2
SWNF-3	HL	3.64	37.9	34.3	33.3	0.97	90.4
PAUF	PT	1.23	1.43	0.14	0.08	0.06	9.8
LAUF	PT	1.21	1.27	0.06	0.04	0.02	5.0
BAUF	PT	1.14	1.55	0.41	0.21	0.20	26.2
PANF	HL	3.63	4.30	0.67	0.58	0.09	15.6
LANF	HL	3.74	4.69	0.95	0.83	0.12	20.3
BANF	HL	3.49	5.86	2.37	1.65	0.72	40.4

In the experiments performed with UP water, R_f was much smaller than R_m for the different membrane tested, which confirms that the membrane fouling is low in these experiments performed with ECs dissolved in UP water. However, in the experiments carried out with synthetic and real waters, a significant increase was appreciated for the partial contribution of R_f to R_t, specially for the NF process. It should be noted that $R_f > R_m$ in the NF experiments performed with synthetic water containing NOM and Ca^{2+}.

When the ECs were dissolved in UP water, the values of R_f were higher in the NF process than in the UF process, which indicates that NF membranes were more sensitive to fouling. Moreover, greater flux decrease values were obtained in the UF membranes with lower MWCO: thus, the GK membrane (2 kDa) presented the highest value of R_f within UF membranes. Although the MWCO of the selected NF membranes was similar, the HL membrane presented the lowest values of fouling resistance. With respect to the contribution of internal and external components to the total fouling, R_{ef} was higher than R_{if} for the selected UF membranes and also for the NF HL membrane. These results indicate that polarization concentration and cake layer formation contribute to a higher extent to fouling that pore blocking and contaminants adsorption onto the membrane, especially in the case of the hydrophilic membrane HL. However, R_{if} was higher than R_{ef} for the NF membranes CK and DK, which can be explained by the higher contribution of pore blocking rather than adsorption, since the adsorption percentages are similar for the three NF membranes.

The pH influence on membrane fouling is negative, specially for the HL membrane (Expts. UPNF-3 to UPNF-6 in Table 3). This higher membrane fouling at greater pH is due to the increment of the external fouling, and therefore the formation of the cake layer is favoured at high pH. These results can be explained by the reduction of the pore size and also by the enhanced solute-membrane interactions at high pH (Lopez-Muñoz et al., 2009; Ribau Teixeira et al., 2005).

During the filtration of synthetic waters, the additional presence of humic acids and calcium ions also increased R_t and R_f due to the adsorption of NOM and Ca^{2+} onto the membrane as well as to the formation of calcium complexes of humic acids as explained

above. Thus, the initial concentration of humic acids as well as the additional presence calcium ions led to a moderate increase of R_{if}. Nevertheless, the highest increment for the different resistances was obtained for R_{ef} in the case of the NF HL membrane (Expts. SWNF-2 and SWNF-3), which is due to the cake layer formation enhancement in presence of both humic acids and Ca^{2+}. These results corroborate that cake layer formation is the dominant fouling mechanism for the NF membrane in presence of NOM-Ca complexes.

With respect to the filtration of surface water and secondary effluents, the main increase in the values of R_f with respect to UP water filtration was obtained for the secondary effluent from Badajoz (BA), which is the most contaminated within the selected real water matrices. As can be observed in Table 3, both R_{if} and R_{ef} were higher for real waters than for UP water, which can be explained by the contribution of the different fouling mechanisms commented above (adsorption, pore blocking and cake layer formation) in presence of organic and inorganic matter (specially for the secondary effluent BA).

3.2. Retention and adsorption of emerging contaminants.

The retention coefficients relate the concentration of a specific substance in the permeate stream with its concentration in the feed stream, and were determined by using Eq. (5). In general, R coefficients decreased slightly with the increase in VRF, and consequently with processing time. This decay is representative of filtration processes in batch concentration mode. In effect, the increase of VRF or water recovery leads to an increase of the concentration of ECs in the feed solution which facilitates their transport through the membrane.

The values of the retention coefficients of the ECs at steady-state conditions (VRF=3) in all the UF and NF experiments carried out cover a wide range, because there are several membrane characteristics and solute properties that affect the retention (MW, molecular size, pK_a, log K_{ow}, dipole moment, etc.) by different mechanisms (adsorption, steric hindrance, electrostatic repulsion, etc.). In general terms, the retention of ECs by NF membranes was slightly higher than by UF membranes, as can be observed in Fig. 2, which

represents the R coefficients for the selected ECs in experiments carried out with the six membranes tested (Expts. UPUF-1 to UPUF-3, and UPNF-1 to UPNF-3). The highest retentions were obtained with the UF PT membrane and with the NF HL membrane.
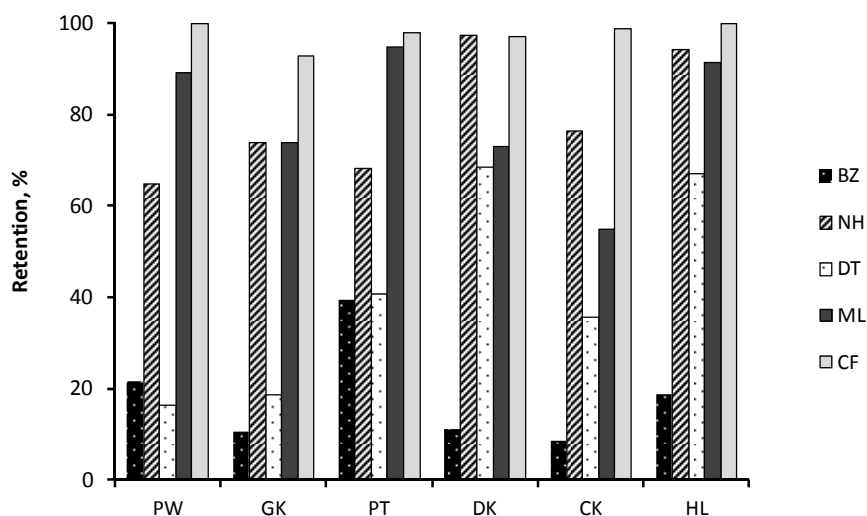
Figure 2. Influence of the MWCO and nature of some UF and NF membranes on the retention of emerging compounds at VRF=3 (Expts. UPUF-1 to UPUF-3 and UPNF-1 to UPNF-3 in Table 2).

The retention coefficients obtained for the selected ECs in the experiments performed with the UF membranes followed the sequence CP > ML > NH > DT > BZ (Fig. 2). According to these results, adsorption should be the main mechanism responsible for retention of ECs by UF membranes rather than size exclusion, since the MWCO of these membranes is much higher than the molecular weight of the selected pollutants. Thus, the highest values of retention coefficients with UF membranes were obtained for CP, which is a hydrophobic compound according to the values of log K_{ow} summarized in Table 1. Although NH is also a hydrophobic compound (log K_{ow}=4.51), at acidic pH is partially protonated (pK_a=10.21). The hydrophobicity of ionisable compounds can be determined as log D= log K_{ow} – log (1+10(pK_a-pH)), being the value for NH of 1.40 at pH 7. Therefore, the hydrophobic character of NH decreases at lower pH, and thus its adsorption is hindered. BZ presents the lowest MW (119.1 g mol^{-1}) and is the most hydrophilic compound, and

therefore adsorbed only partially onto the membranes, so that its retention is rather low. However, the retentions obtained with NF membranes followed the trend: CP > NH > ML > DT > BZ (Fig. 2). Therefore, other mechanisms such as size exclusion must also contribute efficiently to the retention of ECs by NF membranes. Thus, the retention coefficients obtained for NH, the EC with the highest MW (299.8 g mol^{-1}), were higher than those of ML. At the same time, the retention of BZ was lower with NF membranes (MWCO of 150-300 Da) than with UF membranes, since this contaminant has a MW lower than the MWCO of the selected NF membranes and is hardly adsorbed on NF membranes. In addition, the CK membrane provided lower retentions than DK and HL membranes, which can be due to its higher pore size (Benitez et al., 2010). Therefore, retention of ECs by NF membranes is controlled by a combination of adsorption, size exclusion, and even electrostatic repulsion specially when pH > pK$_a$ (Chang et al., 2012).

The adsorption percentages (AP) of the selected compounds on UF and NF membranes determined by Eq. (7) are summarized in Table S7. In most of the experiments, the values of AP followed the sequence CP > ML > NH > DT > BZ, accordingly with the hydrophobic character of selected ECs, since adsorption is strongly correlated with log K$_{ow}$ (Comerton et al., 2008). Within the UF membranes, the highest values of AP were obtained for the PT membrane, which is the most hydrophobic membrane according to the values of contact angle detailed in Table S2. One could expect higher values of AP for the hydrophobic NF membrane CK (contact angle of 70°). However, the values of AP are very similar to those of the hydrophilic NF membranes HL and DK, which can be explained by the higher pore size of the membrane CK (Benitez et al., 2010), or by the fact that adsorption is not the dominant mechanism for micropollutant retention with NF membranes. In addition, the values of AP for the NF membranes were lower than their corresponding values of R and also lower than the values of AP for the UF membranes. These results confirm that adsorption is not the main mechanism for emerging contaminants retention with NF membranes.

Figures 3 and 4 depict the values of R and AP, respectively, obtained for the selected ECs in experiments carried out with UP water at different pH. The variation of pH exerted slightly different influence on the retention of ECs in the UF process with the PT

membrane (Expts. UPUF-3 to UPUF-6) and in the NF process with the HL membrane (Expts.UPNF-3 to UPNF-6), as can be appreciated in Fig. 3. Thus, the retention of BZ (pK$_a$=8.20) decreased at high pH (Fig. 3A), which is due to the hindered adsorption of the anionic species. However, the retention of BZ increased with pH in the case of the NF membrane HL (Fig. 3B), which can be explained by the contribution of the electrostatic repulsion mechanism to the global retention of BZ. CP, which is also negatively charged at high pH (pK$_a$=9.81), was almost completely rejected at any pH, and therefore, the influence of this variable was not appreciable. At the same time, the values of AP for these compounds (BZ and CP) decreased at high pH, as can be appreciated in Fig. 4A and 4B for PT and HL membranes respectively. As pH increases, the concentration of negatively charged species also increases, and their hydrophobic character decreases (log D decreases versus log K$_{ow}$), being their adsorption on the membranes hindered. On the other hand, the values of AP for NH increased with pH, as well as the retention by the PT membrane, as could be expected from the deprotonation of this compound at high pH (pK$_a$=10.21), being the neutral species more easily adsorbed. Finally, the values of R and AP for DT and ML remained fairly constants with the variation of pH, as corresponds to non ionic compounds in the investigated pH range. These results can be justified if adsorption is the main mechanism responsible for micropollutants retention by UF membranes, being the adsorption of neutral species more favourable (Yoon et al., 2006). Instead, for the NF HL membrane, in addition to size exclusion and partially to adsorption, electrostatic repulsion must contribute efficiently to the retention of negative species at high pH, while the retention of neutral compounds remains fairly independent on pH.
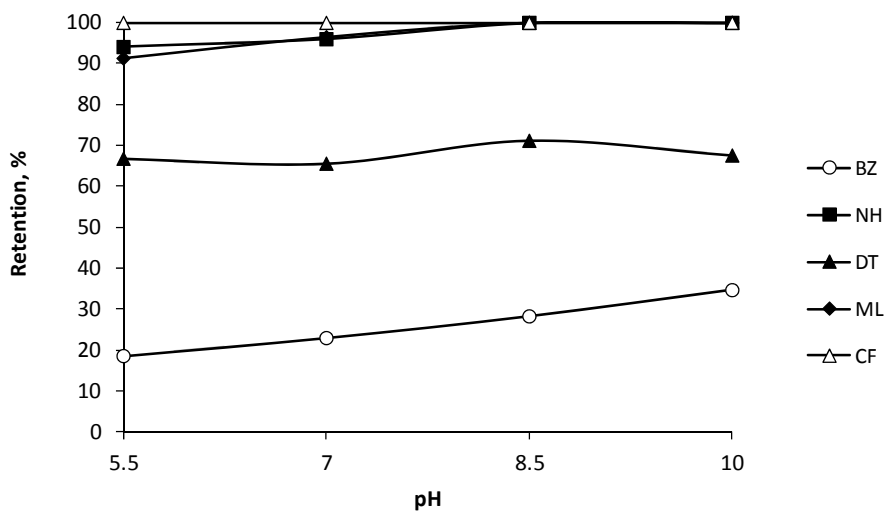
Figure 3. Retention of selected micropollutants obtained in experiments performed at different pH with (A) the UF PT membrane (Expts. UPUF-3 to UPUF-6) and (B) the NF HL membrane (Expts. UPNF-3 to UPNF-6). Experimental conditions detailed in Table 2.
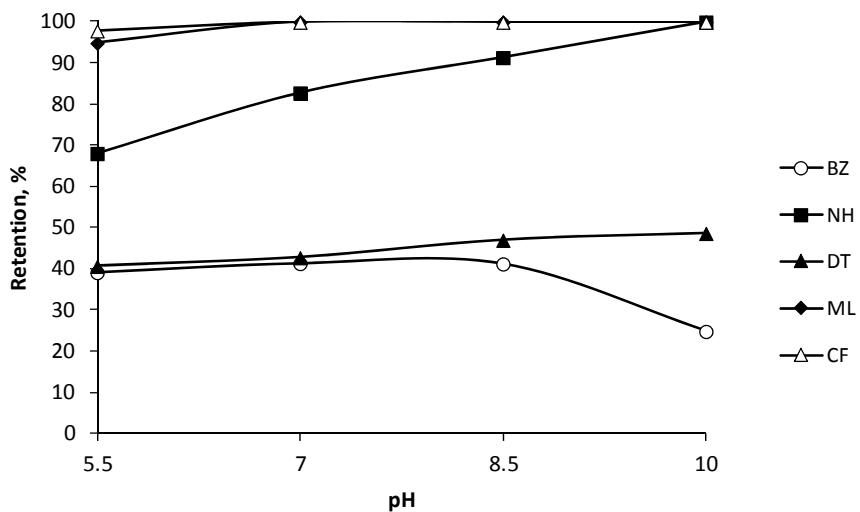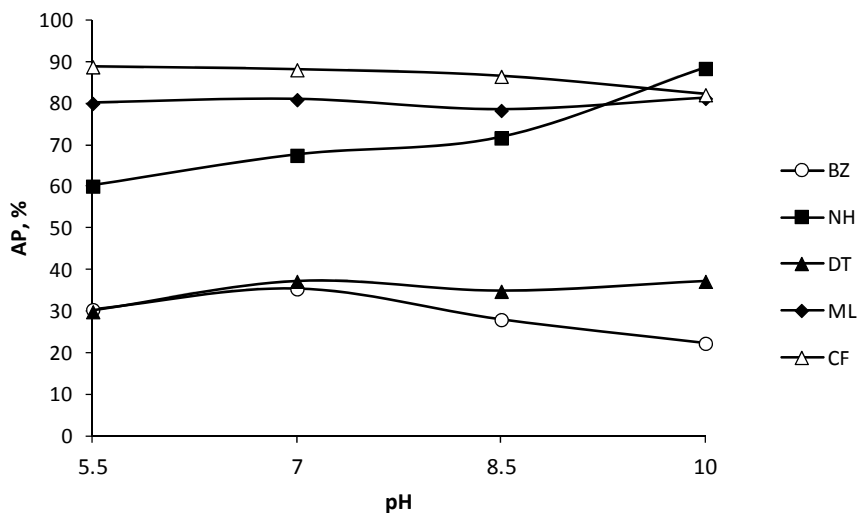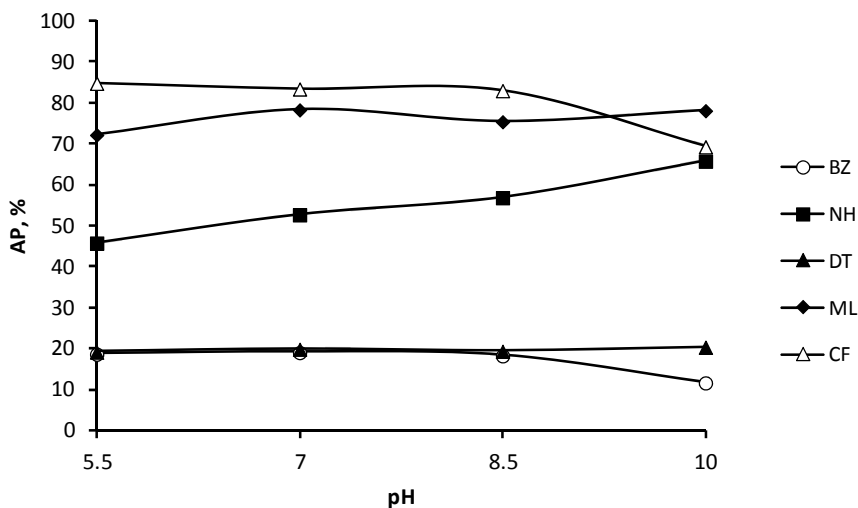
A)

B)

Figure 4. Adsorption percentages (AP) for each selected micropollutant obtained in experiments performed at different pH with (A) the UF PT membrane (Expts. UPUF-3 to UPUF-6) and (B) the NF HL membrane (Expts. UPNF-3 to UPNF-6). Experimental conditions detailed in Table 2.

In order to establish the influence of the water matrix constituents on the retention of the investigated ECs, the results obtained in the filtration of synthetic waters and real waters in experiments performed with the UF PT and the NF HL membrane are depicted in Fig. 5A and 5B, respectively. Compared to the results obtained with UP water, the presence of NOM (Expts. SWUF-1 and SWNF-1) enhanced slightly the retention of the selected ECs. However, the additional presence of calcium ions (Expts. SWUF-2 and SWNF-2) exerted a negative effect on the retention of these contaminants with UF and NF membranes. Finally, a slight increase of retentions was observed when the concentration of humic acids was increased from 12 to 23 g L^{-1} in presence of the same amount of Ca^{2+} (1mM, Expts. SWUF-3 and SWNF-3). Contaminants removal enhancement in presence of NOM might be due to the formation of macromolecular complexes with NOM functional groups (size exclusion and adsorption) and/or increased level of charge density induced by NOM in "pseudo-complexes" (electrostatic repulsion) (Anwar Sadmani et al., 2014; Comerton et al., 2008). In addition, the fouling layer may act as a more selective secondary membrane capable of retaining larger molecular weight and hydrophobic micropollutants (Wray et al., 2014). However, the additional presence of divalent cations transform the flexible, linear humic molecules to a rigid, compact, and coiled conformation by forming metal-humic complexes and reducing the negative charges of humic carboxylic functional groups (Li and Elimelech, 2004). Therefore, increases in divalent cation concentration cause NOM macromolecular conformation changes and may alter the distribution of sites for compound association, resulting in a reduction of compound-NOM complexation (Comerton et al., 2009), and as a consequence, ECs retention is hindered.

Finally, by considering the nature of the real water matrices, the retention coefficients for a specific compound reveal that slightly higher retentions were obtained in the secondary effluent BA, while lower values were obtained in the reservoir water PA and the secondary effluent LA (Fig. 5A and 5B). These results can be explained since the secondary effluent BA, with higher NOM content, induces higher membrane fouling in comparison to the reservoir water PA and the secondary effluent LA, with lower NOM content; and this membrane fouling decreases the pore size and increases the ECs

retention. Additionally, contaminants interactions with the organic matter present in the water matrix itself might increase ECs retention as commented above.

A)
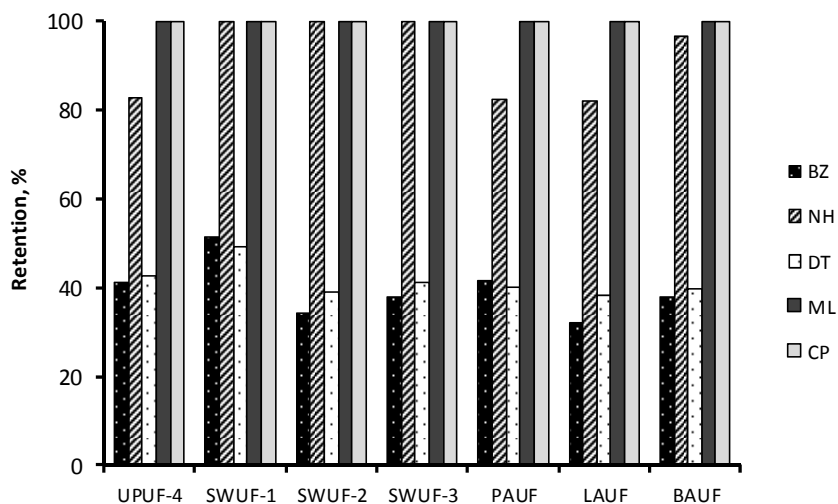
B)
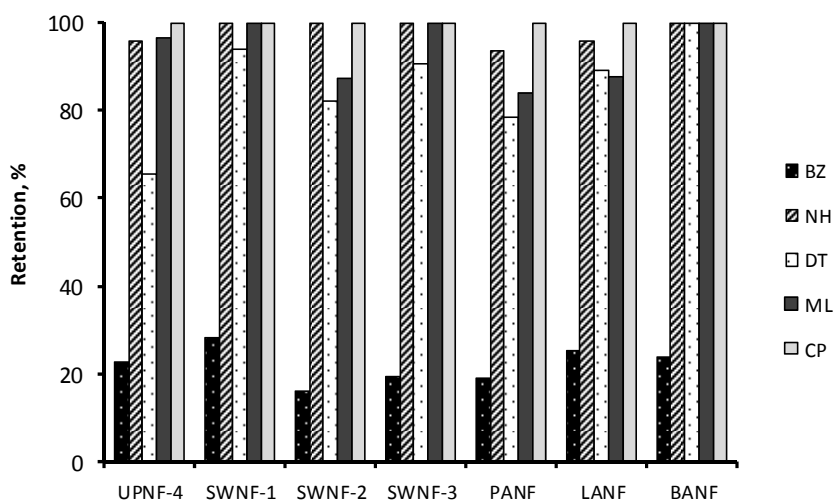
Figure 5. Influence of water matrix composition on retention of selected micropollutants in experiments performed with (A) the UF PT membrane and (B) the NF HL membrane. Experimental conditions detailed in Table 2.

In addition to the retention coefficients for the specific compounds, the effectiveness of the filtration processes for the elimination of the organic matter present in different water matrices can be also evaluated by the retention coefficients referred to the water quality parameters selected in the present work: absorbance at 254 nm (A_{254}), COD, and TOC. These coefficients were evaluated by means of Eq. (6), and the values obtained for VRF=3 are summarized in Table 4. In general terms, lower removals were obtained in the UF process (in the range 39-91% for A_{254}, 4-72% for COD and 7-82% for TOC) than in the NF process (in the range 67-99% for A_{254}, 45-81% for COD and 72-91% for TOC), as could be expected for membranes with much lower MWCO. Therefore, size exclusion must be the main retention mechanism for high MW compounds. In addition, the retention of these parameters followed the sequence: A_{254}> TOC > COD. Absorbance at 254 nm retention was higher than COD or TOC retention since UV absorbance at 254 nm is mainly due to aromatic/hydrophobic compounds that might be absorbed on the membranes, whereas COD or TOC measure the concentration of overall compounds.

Table 4. Retention coefficients obtained for several quality parameters in the filtration of synthetic and real waters with the UF PT and NF HL membranes (VRF=3).

Expt.	R_{A254}, %	R_{COD}, %	R_{TOC}, %
SWUF-1	91.1	71.7	82.4
SWUF-2	87.1	63.4	74.5
SWUF-3	87.3	71.9	80.7
SWNF-1	98.8	77.8	91.4
SWNF-2	96.7	74.8	90.6
SWNF-3	99.1	81.3	91.2
PAUF	68.4	48.7	55.4
LAUF	39.2	3.9	7.1
BAUF	50.9	44.4	48.2
PANF	91.0	76.4	83.2
LANF	67.3	45.2	72.7
BANF	90.4	74.1	86.5

The presence of humic acids and calcium ions in synthetic waters led to a high retention of the selected parameters (Table 4) due to the formation of complexes and adsorption on the membranes as commented above. COD and TOC retention was slightly lower when Ca^{2+} was present in addition to humic acids (compare Expts. SWUF-2 and SWUF-1 or Expts.SWNF-2 and SWNF-1) due to the different configuration of metal-humic complexes and the reduced negative charges of humic carboxylic functional groups. With respect to the real water matrices, the lowest values of retention coefficients for the investigated water quality parameters were obtained for the secondary effluent LA, which is probably due to its low content of organic matter. In addition, the retention of COD and TOC in LA water with the UF PT membrane was very low, which is an indication that the NOM present in this secondary effluent has a MW not very high.

4. CONCLUSIONS.

According to the results obtained in the UF and NF experiments of five emerging contaminants, flux decline was higher when the ECs were dissolved in synthetic and real water matrices as a consequence of membrane fouling. The pH effect on the permeate flux was negative due to stronger electrostatic interaction between dissociated functional groups of membrane material causing a pore constriction. Among fouling mechanisms, pore blocking and cake layer formation probably dominated at the beginning of filtration, whereas cake layer formation was likely the dominant fouling mechanism at later stages. The important fouling of the NF HL membrane in presence of NOM and Ca^{2+} is mainly due to cake layer formation, since this fouling is mostly external and reversible.

Under a point of view of the retention coefficients, the nanofiltration HL membrane was the most appropriate for the removal of the selected emerging contaminants from the waters tested, excepting benzotriazole. The effect of pH on the retention of negatively charged compounds was negative for UF membranes (due to the decrease of adsorption at high pH) and slightly positive for NF membranes (because of electrostatic repulsion at high pH). While adsorption is the main retention mechanism for UF membranes, size exclusion and electrostatic repulsion of negative species at high pH are also responsible for micropollutant retention by NF membranes. These results can be

extrapolated to UF and NF processes applied to environmental water samples with very low concentration of emerging contaminants (in the order of $\mu g\ L^{-1}$ to $ng\ L^{-1}$).

With respect to the selected membranes, and taking into account permeate fluxes and retentions, PT and HL membranes, among UF and NF membranes respectively, provided the best results for the retention of micropollutants at high permeate fluxes and with lower fouling. Additionally, the NF HL membrane also provided high retentions for COD and TOC (around 80%) and aromatic compounds (around 90%). It must be noticed that the significant removal of NOM, especially hydrophobic and aromatic compounds, reduces the disinfection by-products formation potential in the final water. Therefore, the HL membrane is adequate for natural water treatment to produce drinking water and for the purification of not very contaminated secondary effluents for reuse.

REFERENCES

Acero, J.L.; Benitez, F.J.; Leal, A.I.; Real, F.J.; Teva, F. Membrane filtration technologies applied to municipal secondary effluents for potential reuse. J. Hazard. Mater. **2010**, 177, 390-398.

Al-Bastaki, N.M. Performance of advanced methods for treatment of wastewater: UV/TiO_2, RO and UF. Chem. Eng. Process. **2004**, 43, 935-940.

Altapova, A.; Kim, E-S.; Dong, S.; Sun, N.; Chelme-Ayala, P.; Gamal El-Din, M. Treatment of oil sands process-affected water with ceramic ultrafiltration membrane: Effects of operating conditions on membrane performance. Sep. Purif. Technol. **2014**, 122, 170-182.

Anwar Sadmani, A.H.M.; Andrews, R.C.; Bagley, D.M. Nanofiltration of pharmaceutically active compounds as a function of compound interactions with DOM fractions and cations in natural water. Sep. Purif. Technol. **2014**, 122, 462-471.

Benitez, F.J.; Acero, J.L.; Real, F.J.; Garcia, C. Combination of chemical oxidation-membrane filtration processes for the elimination of phenyl-ureas in water matrices. J. Chem. Technol. Biotechnol. **2009**, 84, 1883-1893.

Benitez, F.J.; Acero, J.L.; Real, F.J.; Roldan, G.; Rodriguez, E. Photolysis of model emerging contaminants in ultra-pure water: kinetics, by-products formation and degradation pathways. Water Res. **2013**, 47, 870-880.

Boehmer, W.; Ruedel, H.; Wenzel, A.; Schröeter-Kermani, C. Retrospective monitoring of triclosan and methyl-triclosan in fish: Results from the german environmental specimen bank. Organohalogen. Comp. **2004**, 66, 1489-1494.

Bolong, N.; Ismail, A.F.; Salim, M.R.; Matsuura, T. A review of the effects of emerging contaminants in wastewater and options for their removal. Desalination **2009**, 239, 229-246.

Chang, E-E.; Chang, U-C.; Liang, C-H.; Huang, C-P.; Chiang, P-C. Identifying the rejection mechanism for nanofiltration membranes fouled by humic acids and calcium ions exemplified by acetaminophen, sulfamethoxazole, and triclosan. J. Hazard. Mater. **2012**, 221, 19-27.

Clesceri, L.S.; Greenberg, A.E.; Trussell, R.R. Standard Methods for the Examination of Water and Wastewater, 17th ed., APHA, AWWA, WPCF, Washington, DC, 1989.

Comerton, A.M.; Andrews, R.C.; Bagley, D.M. The influence of natural organic matter and cations on the rejection of endocrine disrupting and pharmaceutically active compounds by nanofiltration. Water Res. **2009**, 43, 613-622.

Comerton, A.M.; Andrews, R.C.; Bagley, D.M.; Hao, C. The rejection of endocrine disrupting and pharmaceutically active compounds by NF and RO membranes as a function of compound and water matrix properties. J. Membr. Sci. **2008**, 313, 323-335.

Costanzo, S.D.; Watkinson, A.J.; Murby, E.J.; Kolpin, D.W.; Sandstrom, M.W. Is there a risk associated with the insect repellent DEET (N,N-diethyl-m-toluamide) commonly found in aquatic environments?. Sci. Total Environ. **2007**, 384, 214-220.

Goren, U.; Aharoni, A.; Kummel, M.; Messalen, R.; Mukmenev, I.; Brenner, A.; Gitis, V. Role of membrane pore size in tertiary flocculation/adsorption/ultrafiltration treatment of municipal wastewater. Sep. Purif. Technol. **2008**, 61, 193-203.

Haberkamp, J.; Ernst, M.; Bockelmann, U.; Szewzyk, U.; Jekel, M. Complexity of ultrafiltration membrane fouling caused by macromolecular dissolved organic compounds in secondary effluents. Water Res. **2008**, 42, 3153-3161.

Huber, M.M.; Canonica, S.; Park, G-Y.; von Gunten, U. Oxidation of pharmaceuticals during ozonation and advanced oxidation processes. Environ. Sci. Technol. **2003**, 37, 1016-1024.

Ikehata, K.; Gamal El-Din, M.; Snyder, S.A. Ozonation and advanced oxidation treatment of emerging organic pollutants in water and wastewater. Ozone Sci. Eng. **2008**, 30, 21-26.

Jin, X.; Hu, J.; Ong, S.L. Influence of dissolved organic matter on estrone removal by NF membranes and the role of their structure. Water Res. **2007**, 41, 3077-3088.

Katsoufidou, K.; Yiantsios, S.G.; Karabelas, A.J. A study of ultrafiltration membrane fouling by humic acids and flux recovery by backwashing: Experiments and modelling. J. Memb. Sci. **2005**, 266, 40-50.

Kovalova, L.; Siegrist, H.; von Gunten, U.; Eugster, J.; Hagenbuch, M.; Wittmer, A.; Moser, R.; McArdell, C.S. Elimination of micropollutants during post-treatment of hospital wastewater with powdered activated carbon, ozone and UV. Environ. Sci. Technol. **2013**, 47, 7899-7908.

Langford, K.H.; Thomas, K.V. Determination of pharmaceutical compounds in hospital effluents and their contribution to wastewater treatment works. Environ. Int. **2009**, 35, 766-770.

Li, Q.; Elimelech, M. Organic fouling and chemical cleaning of nanofiltration membranes: measurements and mechanisms. Environ. Sci. Technol. **2004**, 38, 4683-4693.

Loos, R.; Gawlik, B.M.; Locoro, G.; Rimaviciute, E.; Contini, S.; Bidoglio, G. EU wide survey of polar organic persistent pollutants in European river waters. Environ. Pollut. **2009**, 157, 561-568.

López-Muñoz, M.J.; Sotto, A.; Arsuaga, J.M.; Van der Bruggen, B. Influence of membrane, solute and solution properties on the retention of phenolic compounds in aqueous solution by nanofiltration membranes. Sep. Purif. Technol. **2009**, 66, 194-201.

Maximous, N.; Nakhla, G.; Wan, W. Comparative assessment of hydrophilic membrane fouling in wastewater applications. J. Membr. Sci. **2009**, 339, 93-99.

Nakada, N.; Komori, K.; Suzuki, Y.; Konishi, C.; Houwa, I.; Tanaka, H. Occurrence of 70 pharmaceutical and personal care products in Tone River basin in Japan. Water Sci. Technol. **2007**, 56, 133-40.

Neale, P.A.; Schafer, A.I. Quantification of solute-solute interactions in steroidal hormone removal by ultrafiltration membranes. Sep. Purif. Technol. **2012**, 90, 31-38.

Nghiem, L.D.; Coleman, P.J.; Espendiller, C. Mechanisms underlying the effects of membrane fouling on the nanofiltration of trace organic contaminants. Desalination **2010**, 250, 682-687.

Park, N.; Lee, Y.; Lee, S.; Cho, J. Removal of taste and odor model compound (2,4,6-trichloroanisole) by tight ultrafiltration membranes. Desalination **2007**, 212, 28-36.

Ribau Teixeira, M.; Rosa, M.J. Microcystins removal by nanofiltration membranes. Sep. Purif. Technol. **2005**, 46, 192-201.

Ribau Teixeira, M.; Rosa, M.J.; Nystrom, M. The role of membrane charge on nanofiltration. J. Membr. Sci. **2005**, 265, 160-166.

Snyder, S.A.; Adham, S.; Redding, A.M.; Cannon, F.S.; De Carolis, J.; Oppenheimer, J.; Wert, E.C.; Yoon, Y. Role of membranes and activated carbon in the removal of endocrine disruptors and pharmaceuticals. Desalination **2007**, 202, 156-181.

Stackelberg, P.E.; Furlong, E.T.; Meyer, M.T.; Zaugg, S.D.; Henderson, A.K.; Reissman, D.B. Persistence of pharmaceutical compounds and other organic wastewater contaminants in a conventional drinking-water-treatment plant. Sci. Total Environ. **2004**, 329, 99-113.

Ternes, T.A.; Stuber, J.; Hermann, N.; Mc Dowell, D.; Ried, A.; Kampman, M.; Teiser, B. Ozonation: a tool for removal of pharmaceuticals, contrast media and musk fragrances from wastewater?. Water Res. **2003**, 37, 1976-1982.

Van der Bruggen, B.; Shaep, J.; Maes, W.; Wilms, D.; Vandecasteele, C. Nanofiltration as a treatment method for the removal of pesticides from ground waters. Desalination **1998**, 117, 139-147.

Verliefde, A.R.D.; Heijman, S.G.J.; Cornelissen, E.R.; Amy, G.; Van der Bruggen, B.; Van Dijk, J.C. Influence of electrostatic interactions on the rejection with NF and assessment of the removal efficiency during NF/GAC treatment of pharmaceutically active compounds. Water Res. **2007**, 41, 3227-3240.

Wenhui, L.; Xinghai, L.; Dongyan, L.; Lei, S.; Qi, S. Vapor-phase synthesis of 3-Methylindole over Fe-, Co-, or Ni-promoted Ag/SiO_2. Chin. J. Catal. **2009**, 30, 1287-1290.

Westerhoff, P.; Yoon, Y.; Snyder, S.; Wert, E. Fate of endocrine-disruptor, pharmaceutical, and personal care product chemicals during simulated drinking water treatment processes. Environ. Sci. Technol. **2005**, 39, 6649-6663.

Wintgens, T.; Melin, T.; Schafer, A.; Khan, S.; Muston, S.; Bixio, D.; Thoeye, C. The role of membrane processes in municipal wastewater reclamation and reuse. Desalination **2005**, 178, 1-11.

Wray, H.E.; Andrews, R.C.; Bérubé, P.R. Surface shear stress and retention of emerging contaminants during ultrafiltration for drinking water treatment. Sep. Purif. Technol. **2014**, 122, 183-191.

Yoon, Y.; Westerhoff, P.; Snyder, S.A.; Wert, E.C. Nanofiltration and ultrafiltration of endocrine disrupting compounds, pharmaceuticals and personal care products. J. Membr. Sci. **2006**, 270, 88-100.

SUPPLEMENTARY INFORMATION

Table S1. Characterization of the selected real water matrices.

	PA	LA	BA
pH	7.2	8.1	8.5
Conductivity, $\mu S\ cm^{-1}$	68.6	538	546
$A_{254\ nm}$, cm^{-1}	0.190	0.054	0.286
COD, mg $O_2\ L^{-1}$	24	12.4	53
Alkalinity, mg $CaCO_3\ L^{-1}$	30	335	325
TOC, mg L^{-1}	6.8	2.5	19.2
Total nitrogen, mg N L^{-1}	1.51	21.3	35.5
Total phosphorus, mg P L^{-1}	0.041	0.156	1.76

Table S2. Properties of target membranes (material, MWCO, pH range, and salt rejection provided by manufacturer). Pure water permeability (PWP) values were determined at 20 ^{o}C.

Membrane	Material	MWCO, Da	pH	$MgSO_4$ rejection, %	Contact angle, ^{o}	PWP, $L\ h^{-1}\ m^{-2}\ bar^{-1}$
PW	PES	20000	2-11		50±3	141.4
PT	PES	5000	2-11		53±2	29.7±1.5
GK	TF	2000	2-11		44±3	3.8
CK	CA	150-300	2-8	92	70±3	2.1
DK	TF	150-300	2-11	98	31±3	1.8
HL	TF	150-300	3-9	98	30±3	10.2±0.3

Table S3. Adsorption percentages (AP, %) of ECs in filtration experiments performed with UP water at VRF=3. Experimental conditions in Table 4.

Expt.	Membrane	pH	BZ	NH	DT	ML	CP
UPUF-1	PW	6	16.9	50.3	13.8	65.2	80.9
UPUF-2	GK	5.8	10.6	64.5	15.1	60.9	82.9
UPUF-3	PT	5.5	31.5	60.2	30.2	80.1	88.9
UPUF-4	PT	7.0	35.5	67.6	37.3	81.0	88.2
UPUF- 5	PT	8.5	28.1	71.8	34.9	78.4	86.6
UPUF-6	PT	10	22.4	88.5	37.3	81.3	82.2
UPNF-1	DK	5.5	7.9	70.9	17.6	59.1	84.1
UPNF-2	CK	5.7	8.2	71.4	19.0	44.9	86.6
UPNF-3	HL	5.5	18.8	45.9	19.3	72.3	84.9
UPNF-4	HL	7.0	19.2	52.8	20.0	78.4	83.5
UPNF- 5	HL	8.5	18.4	57.0	19.5	75.5	83.1
UPNF-6	HL	10	11.8	65.9	20.5	78.2	69.4

3.10. Investigating the removal of five emerging contaminants from secondary effluent by powdered activated carbon/ultrafiltration hybrid process.

3.10. INVESTIGATING THE REMOVAL OF FIVE EMERGING CONTAMINANTS FROM SECONDARY EFFLUENT BY POWDERED ACTIVATED CARBON/ULTRAFILTRATION HYBRID PROCESS

Elena Rodríguez, †Margarida Campinas, †Maria João Rosa, Juan L. Acero.

Departamento de Ingeniería Química, Universidad de Extremadura, Badajoz.

†Unidade de Qualidade e Tratamento de Águas, Laboratório Nacional de Engenharia Civil, Lisboa.

In preparation.

Hybrid system PAC/UF has been investigated to remove NOM and/or five emerging contaminants (benzotriazole, DEET, chlorophene, 3-methylindole, and nortriptyline) dissolved in several water matrices. Firstly, simultaneous removal of emerging contaminants by different doses of two PACs was investigated, and the sequence of removal obtained was benzotriazole < DEET < 3-methylindole < nortriptyline < chlorophene, accordingly with their hydrophobicity and aromaticity. Once the most appropriate dose and PAC was established, PAC/UF experiments were carried out with the selected water matrices and the influence of NOM was investigated. PAC addition did not affect the permeate flux during the subsequent UF step, independently of water matrix employed, but significantly increased the removal of ECs. In real waters, PAC/UF process resulted a plausible option for the removal of chlorophene, nortriptyline and methylindole (elimination above 95%); but not very effective for the removal benzotriazole and DEET (elimination around 60%).

1. INTRODUCTION.

In the last two decades, many reports have demonstrated that pharmaceuticals, personal care products and endocrine disrupting chemicals are ubiquitous contaminants in wastewater effluents at low concentrations (Kolpin et al., 2002; Stackelberg et al., 2004). Many of these compounds, as well as other organic pollutants (such as pesticides, fuel additives, plasticizers, etc.), are included in the so-called category of "emerging contaminants". Their presence indicates a failure in the removal of these compounds in conventional water treatment plants (Ternes and Hirsch, 2000) and constitutes a negative impact on the quality of natural water and unknown toxicological effects with potential risk for human health. Due to their long persistence in water systems, more powerful specific wastewater treatments have been tested with success in the removal of refractory pollutants, involving chemical oxidation and physical separation techniques.

Among the physical treatments used for the purification of surface waters and wastewaters, membrane separation processes have gradually gained popularity because they effectively remove a wide variety of contaminants from raw waters. Specifically, ultrafiltration (UF) and nanofiltration (NF) membranes constitute an effective technology to eliminate micropollutants with molecular weights larger than 200 Da by size exclusion and membrane-solute interactions (e.g. electrostatic and hydrophobic) (Kim et al., 2007; Campinas et al., 2013). However, two main disadvantages are found in the direct application of UF for the treatment of secondary effluents: the low retention of organic pollutants and the fouling of membranes, which constitutes one of the critical issues in membrane technology for water and wastewater treatment (Liu et al., 2010). The possible decrease of the permeate flux by membrane fouling caused by humic acids can be mitigated by the use of hybrid processes or by pretreating the raw water prior to the filtration process (Campinas and Rosa, 2010). Thus, hybrid adsorption/low-pressure membrane systems with powdered activated carbon (PAC)/micro- or ultrafiltration membranes have proven to be a promising option for improving the removal of ECs while enabling to control the irreversible membrane fouling (Stoquart et al., 2012; Lowenberg et al., 2014; Secondes et al., 2014). Challenges of hybrid systems are the adsorbent's selection and optimization, process design and membrane fouling control (Stoquart et al., 2012).

Previous studies of PAC/UF have focused on the removal of NOM and/or individual or binary mixtures of emerging contaminants, but hardly any studies have studied removal of mixtures of micropollutants by PAC/UF process.

With these considerations in mind, the elimination of emerging contaminants that could be contained in an effluent from a municipal WWTP, as well as the removal of the natural organic matter (NOM) also present in the effluent were investigated. The ECs selected were: benzotriazole (BZ), a well known corrosion inhibitor for copper or silver material, widely used in cooling and hydraulic fluids, anti-freezing products, aircraft deicer and anti-ice fluid, and dishwasher detergents (Loos et al., 2009); N,N-diethyl-m-toluamide or DEET (DT), an active compound in insect repellents (Constanzo et al., 2007); chlorophene (CP), a widespread broad-spectrum antimicrobial pharmaceutical, used in hospitals and households for general cleaning and as active agent in disinfectant formulations (Boehmer et al., 2004); 3-methylindole (ML), used as perfume and synthesizing anti-inflammatory drug, antibiotic, dye, plant growth hormone, herbicide, muscular relaxant, respiratory inhibitor and heart stimulant medicaments (Wenhui et al., 2009); and the pharmaceutical nortriptyline HCl (NH), which belongs to the group of tricyclic antidepressants (TCAs), and used in treatments against depression (Langford et al., 2009).

The present work focuses on the elimination of these selected emerging contaminants from a WWTP effluent by applying the PAC/UF process. The main objective was to evaluate the effect of the adsorption pre-treatment on the single UF process in terms of membrane fouling and permeate flux, as well as on the elimination of the selected emerging contaminants and NOM present in the WWTP effluent.
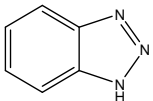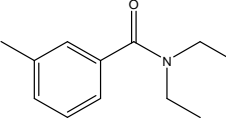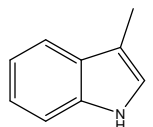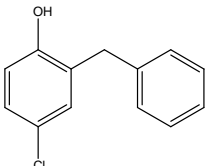
2. MATERIALS AND METHODS.

2.1. Emerging contaminants.

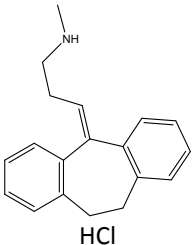The five selected ECs were purchased from Sigma-Aldrich (Germany) and were of 99% purity or higher. Table 1 summarizes the selected compounds and their relevant physico-chemical properties, listed by hydrophobic character (i.e. log D) at pH work. The

solutions used in this study were prepared by dissolving the ECs (1 µM of each) in UP water (from a Milli-Q system).

Table 1. Physico-chemical characteristics of selected contaminants.

EC	Structure	Molecular formula	Log k_{ow}	Log D pH 7-7.5	Charge at pH 7	Minimal/ maximal length, Å[1]	MW, g mol^{-1}
BZ		$C_6H_5N_3$	1.44	1.42-1.39	n	3.4/8.2	119.1
NH		$C_{19}H_{21}NO \cdot$ HCl	4.51	1.40-1.80	+	9.1/12.7	299.8
DT		$C_{12}H_{17}NO$	2.18	2.18	n	8.7/11.1	191.3
ML		C_9H_9N	2.60	2.60	n	4.8/9.1	131.3
CP		$C_{13}H_{11}ClO$	4.18	4.18	n	6.7/11.1	218.7

[1] Properties predicted by ChemAxon.

2.2. Water matrices.

Different water matrices were employed in the present study with the aim of evaluating the influence of nature of NOM in PAC/UF process: DS, WW1 and WW2. DS was prepared as deionized water with addition of $CaCl_2$, $NaHCO_3$ and NaCl to achieve similar

hardness, alkalinity and conductivity of the other water matrices but without organic matter, whereas WW1 and WW2 were prepare from secondary effluent of WWTP Beirolas (Lisbon) following the next procedure. Approximately 240 L of secondary effluent from WWTP Beirolas were undergone a process of microfiltration: concentrate obtained not was employed in this study and permeate obtained was subjected to a nanofiltration process. Permeate of nanofiltration process (MW<300) was stored in sterile bottles at 4 °C and concentrate was frozen (MW>300). Before each run, NF concentrate was thawed and it was left to reach room temperature. Required volumes of NF permeate and NF concentrate were mixed until the desires ratios to prepare water matrix with different kind of natural organic matter: WW1 was prepared as 16% concentrate NF and 84% permeate NF (major composition MW<300) while WW2 was prepared as 16% concentrate NF and 84% DS (in essence MW>300).

Table 2. Characterization of water matrices employed.

	WW1	WW2
pH	7.4 ± 0.4	7.1 ± 0.2
DOC, mg L^{-1}	3.0 ± 0.6	0.31 ± 0.02
Electrical conductivity, uS cm^{-1}	1432 ± 116	1109 ± 202
Hardness, mg $CaCO_3$ L^{-1}	370	114 ± 29
Abs $_{254\,nm}$, m^{-1}	11.614 ± 0.273	0.702 ± 0.161
Abs $_{436\,nm}$, m^{-1}	1.004 ± 0.035	-
SUVA, L m^{-1} mg C^{-1}	3.8	2.3
NOM composition, %		
Strongly hydrophobic	71.2	27.7
Moderately hydrophobic	14.0	37.1
Charged hydrophilic	10.5	5.4
Neutral hydrophilic	4.3	29.8

2.3. Adsorbents.

Two commercial PACs were selected for the present studies: PAC Norit SAE super and PAC Norit SA Super. The textural characterization and point of zero charge (pH_{pzc}) of

those PACs are presented in Table 3. The textural characterization was analyzed by nitrogen and carbon dioxide adsorption isotherms and the pHpzc was determined by mass titration following the methods proposed by Moreno-Castilla et al. (2000) and Noh and Schwarz (1989). Surface of PAC is always charged due to the presence of acidic and basic functional groups on pore surfaces. The pHpzc identifies the pH at which the net surface charge of the carbon is zero; i.e., at this pH there are as many positively as negatively charged surface functional groups. In this study, since water matrices pH is lower than the pH_{pzc}, the net charge of the active carbons surface is positive.

Table 3. PACs characterization.

PAC	Diameter, μm	S_{BET} m^2g^{-1}	A_{ext} m^2g^{-1}	A_{micro} m^2g^{-1}	V_{tot} cm^3g^{-1}	V_{micro} cm^3g^{-1}	V_{mes} cm^3g^{-1}	$V_{micro\,1}^{ry}$ cm^3g^{-1}	pH_{pzc}
SAE super	15	1093	265	666	0.791	0.397	0.394	0.267	9.9
SA super	10-20	1156	261	697	0.892	0.491	0.401	0.280	11.3

S_{BET}-surface area; A_{ext}-external area (mesopore+macropore); A_{micro}-micropore area; V_{tot}-total pore volume; V_{micro}-total micropore volume; V_{mes}-mesopore volume; $V_{micro\,1ry}$-primary micropore volume.

Both PACs present similar area (surface area, external and micropore area). Nevertheless, SA Super has largest total pore volume concretely, higher micropore volume. PAC having higher amount of micropores (with size approaching the dimensions of the target molecules) showed higher adsorption capacity, due to higher adsorption energies resulting from multiple contact points between the PAC and molecules.

2.4. UF lab-scale installation.

UF experiments used a hollow-fibre cellulose acetate membrane from Aquasource (inside-out configuration) previously used in other PAC/UF studies. This UF hydrophilic membrane has a cut-off of 100 kDa. The module has 16 fibres, 1.1 m length and 0.93 mm internal diameter, with a total surface area of 0.05 m^2. The manufacturer recommends a maximum UF pressure of 1.5 bar and a maximum backflushing pressure of 2.5 bar. The module was mounted in a bench-scale apparatus including a feed tank (FT), a positive

displacement pump, two manometers (P1, P2), one flow meter (Flm), a permeate tank (PT) and the valves and tubing involved in the backwashing and in the recirculating loop (V1–V5) (Fig.1). The module was operated under the inside-out configuration during the filtration cycles and membrane flushing, and under outside-in flow during backwashing.
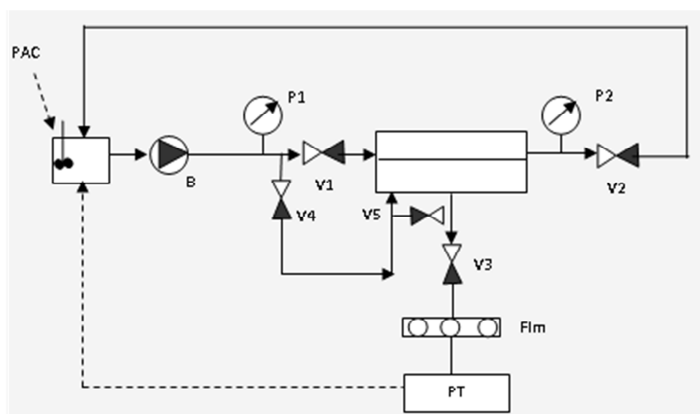
Figure 1. Flow diagram of the UF system. FT-stirred feed tank; B-positive displacement pump; P-manometers; Flm-flow meter; PT-permeate tank; V1, V4, V5- valves for backwashing; V2-concentrate valve; V3-permeate valve.

2.5. Experiments.

PAC Kinetics

Batch tests with efficient mixing were conducted in a jar-test apparatus with 6 positions (Flocumatic, Selecta). Prior to its addition to the solutions, PAC was soaked overnight in ultrapure water to allow for complete wetting of the pores. Samples were taken at predetermined intervals over a 3-h period (3, 5, 10, 30, 60, 120 and 180 minutes of contact) and filtered through a 0.7 µm glass fibre filter (GF-F Whatman) for PAC particles retention. Identical mixing (200 rpm), water volume (500 mL) and temperature conditions (19-21°C) were applied to all batch reactors. Dose PAC employed varied between 3-15 mg L^{-1}.

UF runs

All the UF experiments were performed in a cross-flow filtration mode. Time-depending fouling runs were performed, with the concentrate and the permeate being recycled back to the feed tank during two hours at a constant transmembrane pressure of 0.9 bar. The positive displacement pump provided the necessary pressure and recirculation, and a variable-frequency drive allowed adjusting the cross-flow velocity in the hollow-fibres. Permeate flow rate and temperature were periodically measured and, whenever necessary, transmembrane pressure was adjusted by manual control of the concentrate valve. At given time intervals (2, 15, 30, 60, 90, and 120 minutes of filtration) permeate samples were collected.

In PAC/UF experiments, PAC was directly added to the feed tank, which was continuously stirred at 150 rpm. The total mass of PAC was always added at the beginning of the filtration cycle, and was only discarded at the end of the run.

At the end of each experiment, membranes were backwashed and flushed. Backwashing lasted 1 min. with a 5 mg L^{-1} (as Cl_2) sodium hypochlorite solution to inhibit the biological activity on the UF system, and flushing was performed with deionised water during 5 min.

Normalised flux, as a function of time was used as the membrane fouling indicator. Normalised fluxes were calculated as the ratio of solution flux over the pure water flux before starting the run. All flux values were corrected to a constant temperature (20°C) using Crozes et al. (1997) equation, $J_{20} = J_T e^{-0.0239 (T-20)}$, which is based on the variation of water viscosity with temperature, and where J_{20} is the flux (L $min^{-1}m^{-2}$) at 20°C, T is the temperature (°C) and J_T is the flux (L $min^{-1}m^{-2}$) at temperature T.

2.6. Analytical methods.

Samples were analysed for pH at 20°C (WTW 340 pH meter), electrical conductivity at 25°C, (Crison GLP 32 conductimeter), total and dissolved organic carbon (TOC, DOC) (measured as non-purgeable organic carbon by high temperature combustion method in a

Shimadzu TOC 5000A) and/or UV absorbance (UV/VIS spectrophotometer-Beckman DU 640B) at 254 nm and 436 nm. The nature of NOM was assessed through UV_{254nm} absorbance and SUVA parameter, computed by UV_{254nm}/DOC.

Concentrations of the five selected ECs were assayed by HPLC in a Waters Chromatograph (Alliance 2695) equipped with a 2998 Photodiode Array Detector and a Phenomenex Gemini C18 column (5μm, 150mm×3mm). The analysis was performed in gradient mode with acetonitrile and 25 mM acid formic, at a flow rate of 0.2 mL min^{-1}. Further details about the analytical method are given elsewhere (Benitez et al., 2013). The injection volume was 100 μL in all cases. Detection was made at 250 nm for BZ, NH, and DT; and 280 nm for ML and CP.

Rapid NOM fraction method developed by Chow et al. (2004) was used for the characterization of NOM. Following this method, three contiguous glass columns were set up in serial. Each column was filled with different resin in order DAX-8, XAD-4 and IRA-958, respectively. The resins were used to separate the NOM into four different portions: strongly hydrophobic, moderately hydrophobic, charged hydrophilic and neutral hydrophilic. Feed samples and samples of the effluent after passing resins were collected for DOC analysis.

3.   RESULTS AND DISCUSSION.

3.1. Adsorption of NOM and ECs on PACs.

In the first stage of this study, initial jar tests were carried out to investigate the adsorption of NOM by both PACs in absence of ECs. Figure 2 shows the changes in the water quality during the jar tests for WW1 matrix with different initial dose of both PACs. As expected, an increase in the PAC dose resulted in a significant improvement in the quality of the clarified water as a result of the decreases in UV_{254nm}, colour (UV_{436nm}) and DOC. Comparing both PACs, SA Super showed higher adsorption of hydrophobic NOM than SAE Super, since the reduction of UV_{254nm} was more significant than that of DOC when SA Super was used. Thus, for contact time in the range 3-180 minutes, SA rejected 9-16% and 14-27% of DOC with initial doses of 7 and 15 mg L^{-1} respectively, whereas SAE rejected 1-14 y 18-

22% of DOC with the same doses. Regarding UV254nm, while SA rejected 14-29% and 21-51% when 7 and 15 mg L^{-1} were used, SAE rejected only 10-20% and 13-37% for 7 and 15 mg L^{-1}, respectively.
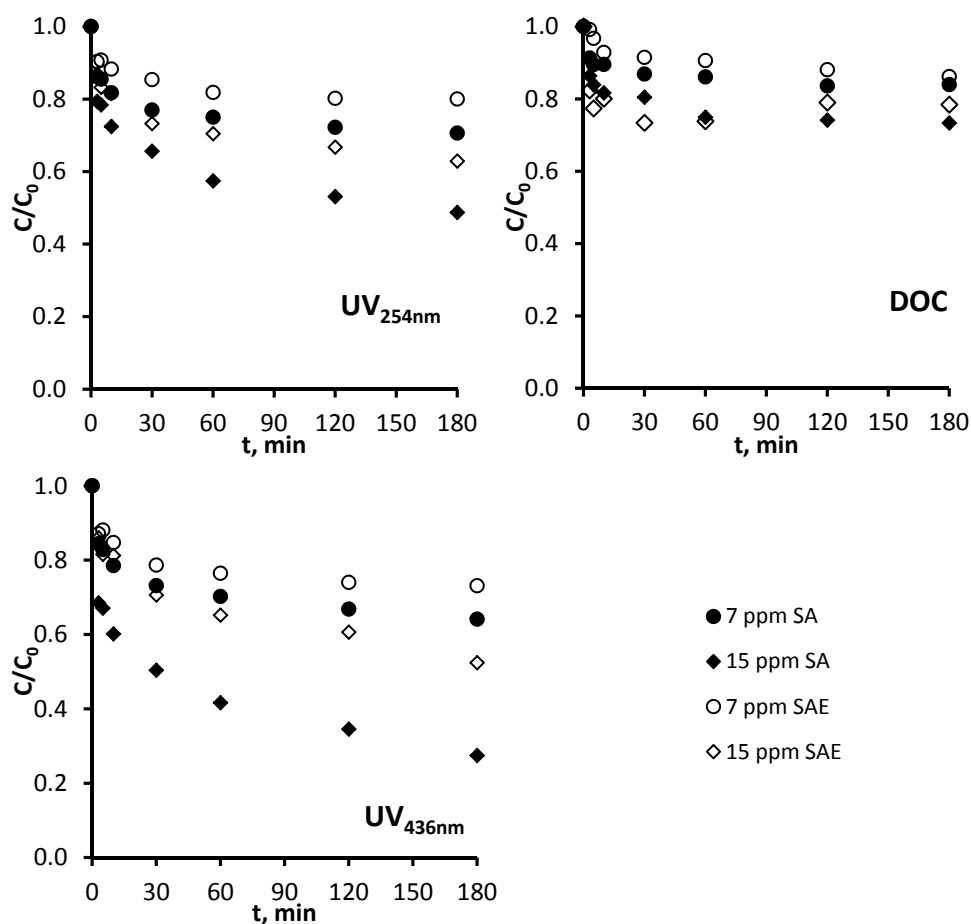
Figure 2. Evolution of normalised values of DOC, UV$_{254}$ y UV$_{436}$ during adsorption kinetics experiments performed with WW1 water matrix.

With respect to adsorption kinetics, not significant differences were found between both PACs since their mesopore volume is similar (Table 3). The main difference between both activated carbons is the secondary micropore volume, which may determine differences in the adsorption equilibrium of smaller adsorbates, such as emerging contaminants.

Later, adsorption kinetics of a mixture of selected emerging contaminants in presence and absence of NOM was tested for five doses and two different PACs in a couple of water matrices (DS and WW1). In absence of NOM, adsorption rate sequence of emerging contaminants was BZ<DT<ML<NH<CP (Figure 3). This sequence is almost in agreement with their hydrophobicity, which can be evaluated as the octanol/water partition coefficient (k_{ow}, usually expressed in log scale). The values of log K_{ow} summarized in Table 1 follows the order: BZ<DT<ML<CP<NH. Therefore, NH presents a discrepancy between adsorption and log K_{ow} sequences. Organic compounds contain ionisable functional groups and can ionise to become either negatively or positively charged depending on pH. To take into account this pH dependence, hydrophobicity was also calculated as log D $_{(pH)}$ = log k_{ow} − log $(1+10^{(pH-pKa)})$ in the pH range 7.0-7.5, and the resulting values are included in Table 1. Once again, the sequence of removal of ECs matched with their hydrophobicity as log D (BZ<NH<DT<ML<CP), with exception of NH. Most of selected contaminants are neutral and hydrophobic, thus the values of log k_{ow} are equal to those of log D. However, NH is positively charged at neutral pH, which affects to the calculation of log D, being the value different to that of log k_{ow}. Since adsorption is favorable for neutral substances (Nguyen et al., 2013), the positive charge of NH limits its adsorption due to repulsive interactions with the positive surface of PACs (values of pH_{pzc} in Table 3). In addition, NH size (Table 1) could also hinder its adsorption on both PACs. According to these considerations, NH adsorption was higher than expected. A possible reason to explain the significant adsorption of NH is its aromatic character, since NH presents the highest value of molar extinction coefficient at 254 nm of the selected ECs (7058 M^{-1} cm^{-1} vs. 5083, 2725, 1641 and 1350 M^{-1} cm^{-1} for BZ, ML, DT and CP respectively, Benitez et al. 2013). Therefore, adsorption rate sequence of emerging contaminants (BZ<DT<ML<NH<CP) can be explained by considering their hydrophobicity and aromatic character. Previous studies (De Ridder et al., 2010; Dickenson and Drewes, 2010) also found that adsorption of solutes with low log D value was favoured by the presence of functional groups capable of forming hydrogen bonds or by aromaticity allowing the formation of pi-pi bonds.
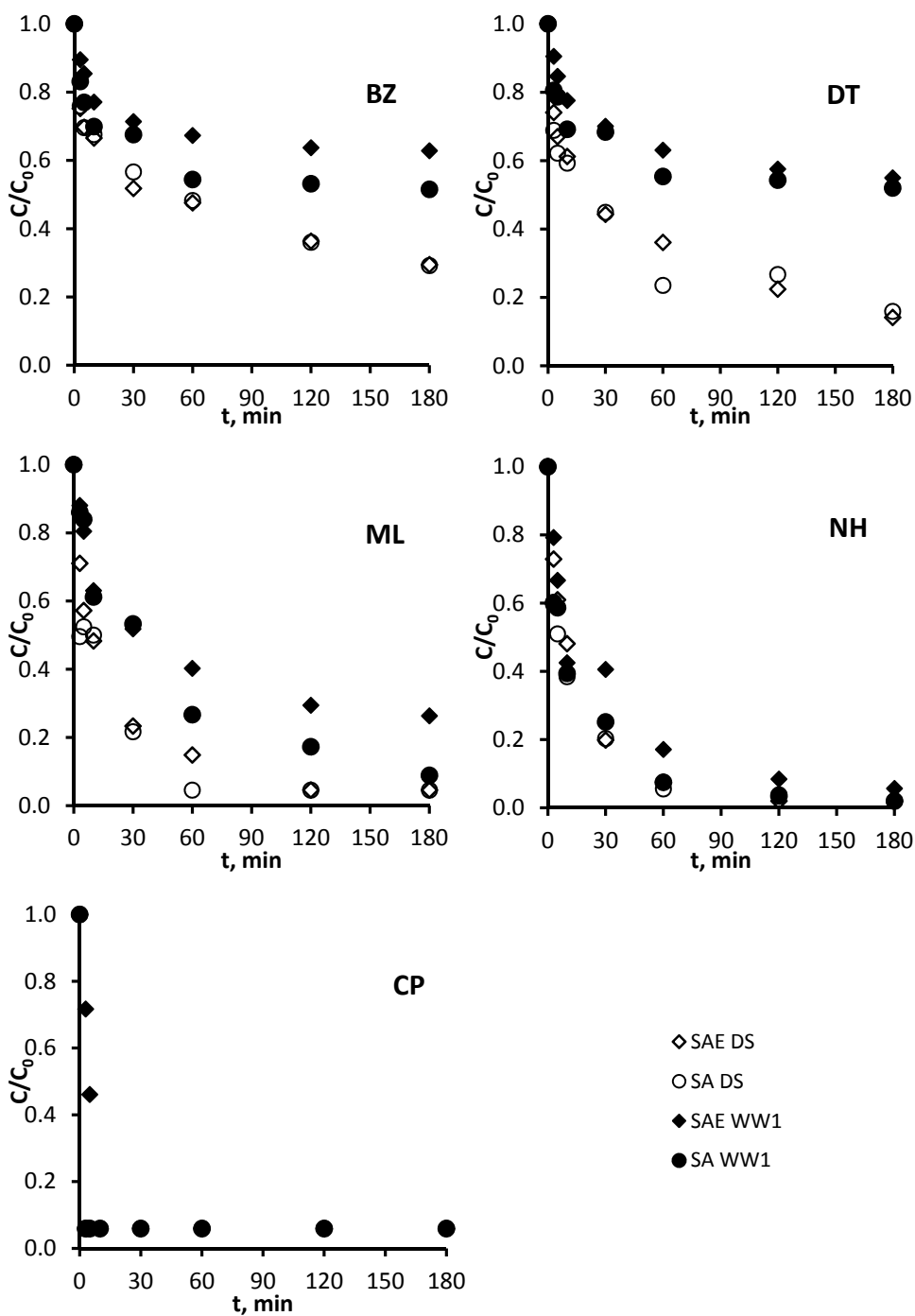
Figure 3. Evolution of normalized concentration of ECs during adsorption experiments performed with DS and WW1 water matrices. PAC dose of 10 mg L^{-1}.

The influence of the water matrix on ECs adsorption can be deduced from Figure 3. For example, comparing the results obtained in DS and WW1 water matrices, within a contact time of 2 hours the removal of BZ decreased from 64 to 47% with SAE and from 64 to 37% with SA. However, no effect of the selected water matrix on CP and NH adsorption was observed. Therefore, in presence of NOM, those emerging contaminants more hydrophobic (CP and NH) did not show competition effect with NOM, whereas less hydrophobic compounds (BZ, DT and ML) were indeed affected. In addition to competition effects with contaminants, the presence of NOM can also bock pores within the activated carbon structure, thus decreasing its efficacy (Snyder et al., 2007). As mentioned above, major NOM adsorbed was hydrophobic, and should present similar hydrophobicity to the less adsorbed emerging contaminants. In addition, the smallest selected contaminants, BZ and ML, exhibited different behaviour in competition with NOM depending on the PAC used, reaching higher rejection when SA was employed. SA presents more secondary micropores volume than SAE, and thus NOM competition is stronger in these secondary micropores of SA, which facilitates BZ and ML adsorption.

In the case of both PACs employed, adsorption of selected emerging contaminants was better related with log k_{ow} than with molar volume as can be seen in Figure 4 for PAC SA Super. This trend was also observed in the PAC/UF processes (detailed in Section 3.2). As a consequence, for both processes, PAC and PAC/UF, retention of pollutants is not associated to their size but to their hydrophobicity. Thus, BZ and DT showed very similar behaviour in WW1 in terms of both kinetics and adsorption capacity. However, although NH adsorption kinetics was slower than CP as explained above, their final adsorption capacities were similar. Therefore, the adsorption capacity or a certain EC is mainly related to its hydrophobic character.
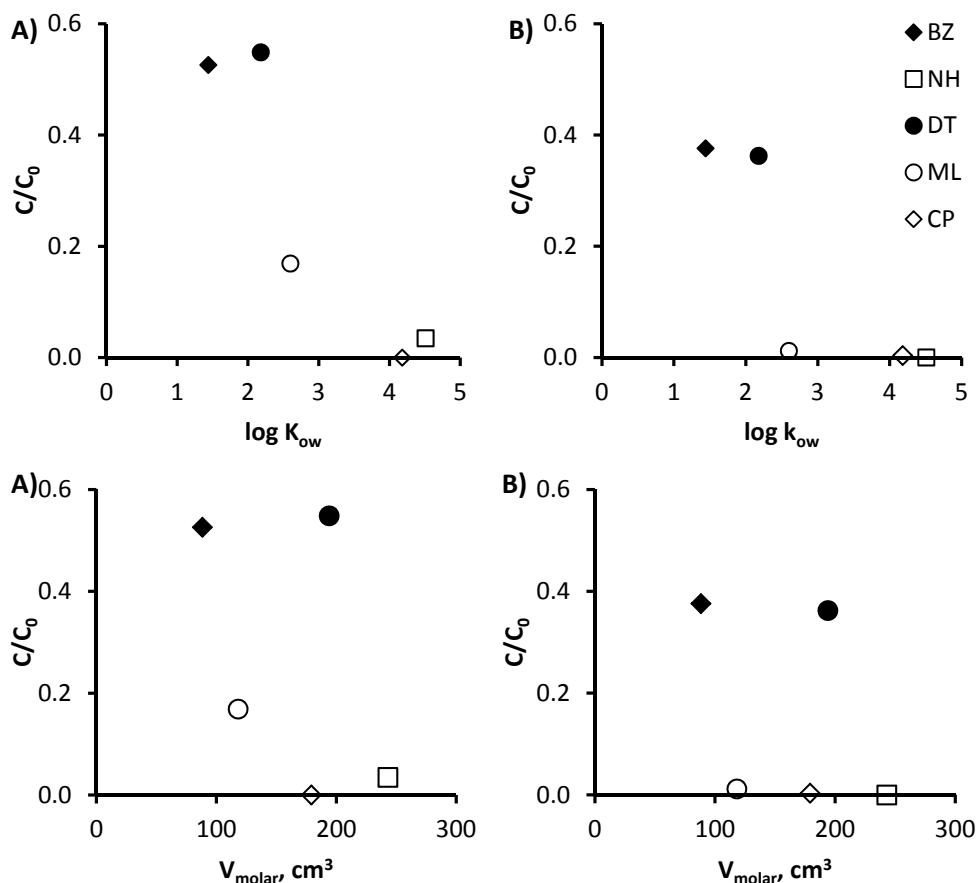
Figure 4. Normalized concentration of ECs vs. log k_{ow} and vs. molar volume after PAC (A) and PAC/UF (B) kinetic experiments performed in the same operating conditions (10 mg L^{-1} of SA Super and WW1 water matrix).

Figure 5 shows the evolution of the normalized concentration of BZ and CP with different PACs doses in WW1 matrix. These two compounds were selected as examples of low and high adsorption capacity, respectively. The results obtained for the remaining ECs is depicted in Fig. S1. Thus, for those emerging contaminants easily adsorbed such as CP or NH, equilibrium was reached at very short contact time independently of the dose employed in the range 10-15 mg L^{-1}. However, when the dose was less than 7 mg L^{-1}, kinetics was slower and the time required to reach the equilibrium was higher for lower PAC dose. On the other hand, for less adsorbed contaminants, i.e. BZ, DT and ML, increasing PAC dose in the full range 3-15 mg L^{-1} implicated faster adsorption. Based on these results,

10 mg L^{-1} was the selected dose to be employed in PAC/UF runs, as a compromise between removal of ECs and operating cost. Similarly, previous studies (Margot et al., 2013; Lowenber et al., 2014) found that a PAC dose between 10 and 20 mg L^{-1} was enough to efficiently remove micropollutants in typical concentration ranges from municipal secondary effluents by the PAC/UF process. In case of peak load of contaminants with high concentration, the PAC dosage can be increased, a supporting coagulant dose of Fe^{3+} could be added. Nevertheless, higher PAC dose can be used during secondary effluent from a WWTP if the main goal is the reduction of TOC. Thus, Goren et al. (2008) found an optimal PAC dose of 0.6 g L^{-1} in the treatment of a secondary effluent, leading to a significant reduction of TOC, especially of low molecular weight organic compounds up to 500 Da.
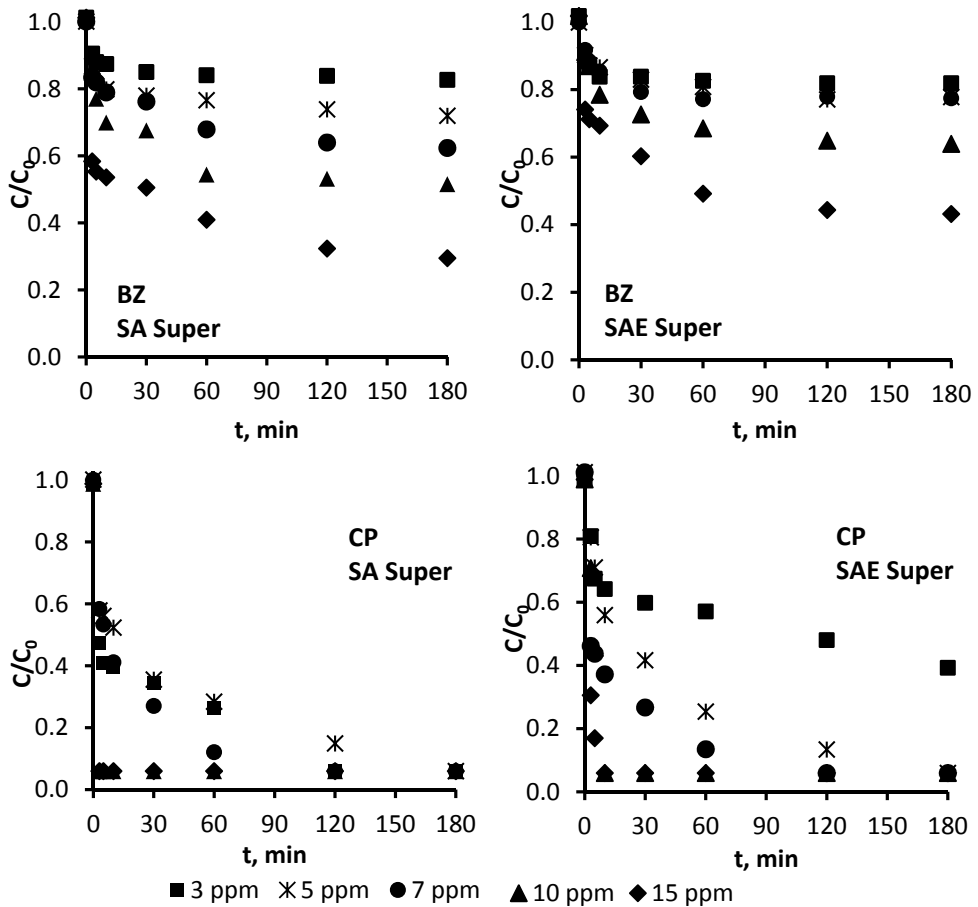
Figure 5. Evolution of normalized concentration of BZ and CP during PAC adsorption in experiments performed with WW1 water matrix.

3.2. PAC/UF runs.

Variations in the permeate flux obtained during the ultrafiltration of different water matrices (with and without addition of PAC) as a function of time are presented in Fig. 6. In spite of different characteristics of NOM, in terms of load and nature (MW and hydrophobicity), significantly differences in permeate flux were not found (standard deviation < 5%). Furthermore, addition of PAC did not affect the permeate flux during PAC/UF runs. These results agree with previous findings that the permeate flux was not influenced by addition of PAC to ultrafiltration processes employing hydrophilic membranes. PAC particles should be large enough to avoid membrane fouling through pore blocking. Thus, PAC could form a porous layer that allows the passage of water without increasing the resistance (Campinas and Rosa, 2010).
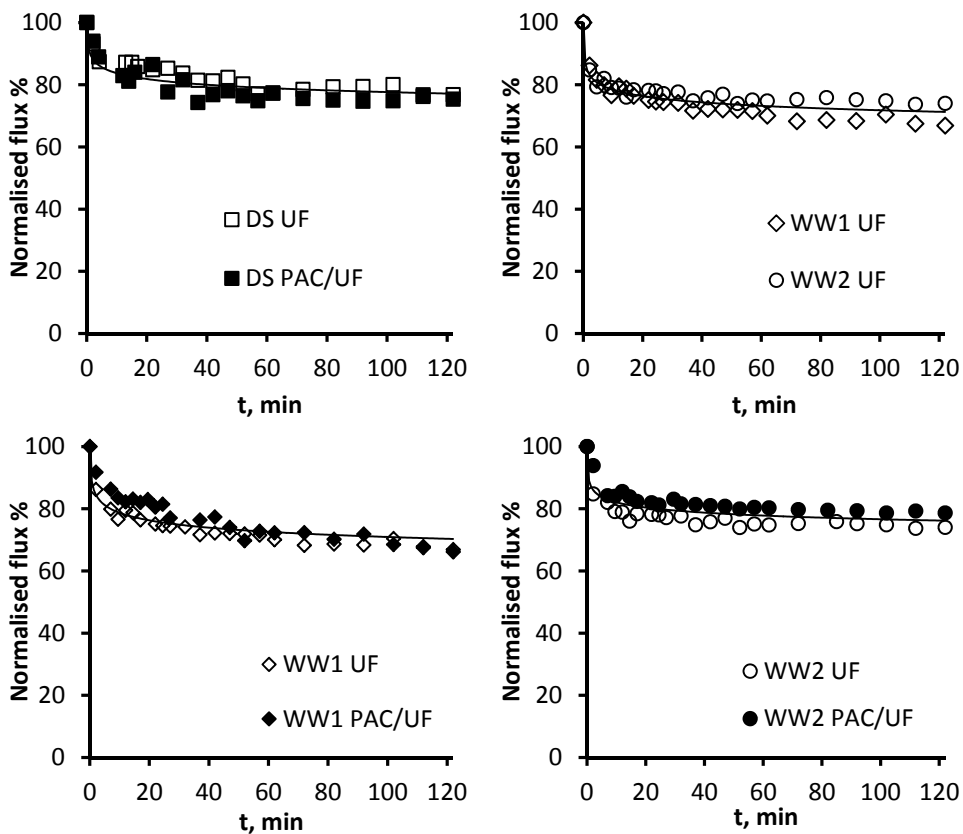
Figure 6. Evolution of normalized flux in UF and PAC/UF runs with different water matrices.

In order to assess the feasibility of this process for the removal of different kind of organic matter, permeate was analysed for different NOM fractions: strongly hydrophobic (SH), moderately hydrophobic (MH), charged hydrophilic (CH) and neutral hydrophilic (NH). From the results shown in Fig. 7A, it can be concluded that the UF process did not retain any kind of NOM, while the PAC/UF process resulted efficient in the rejection of NOM with strongly hydrophobic character, especially in water matrices with higher content of NOM (i.e., higher DOC). When WW1 was employed, the presence of emerging contaminants did not implicate significant changes in the composition of feed and permeate, since the contribution of these contaminants to total organic matter was not relevant. Therefore, the reduction of DOC was mainly due to the adsorption of hydrophobic NOM present in the water matrix onto the PAC.

However, the contribution of ECs to the different fractions of organic matter present in WW2 was important, due to the low NOM content of this matrix. As can be observed in Figure 7b, for removal of ECs in WW2 by PAC/UF, higher changes occurred in the composition of permeate due to removal of emerging contaminants. Thus, an almost complete disappearance of strongly hydrophobic organic matter was observed, which corresponds practically with the removal of hydrophobic ECs. As commented above, hydrophobic ECs were easily adsorbed onto the PAC.
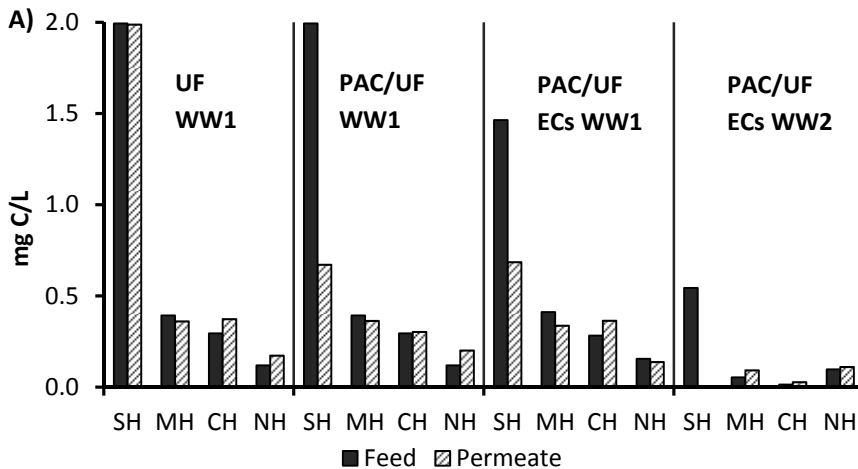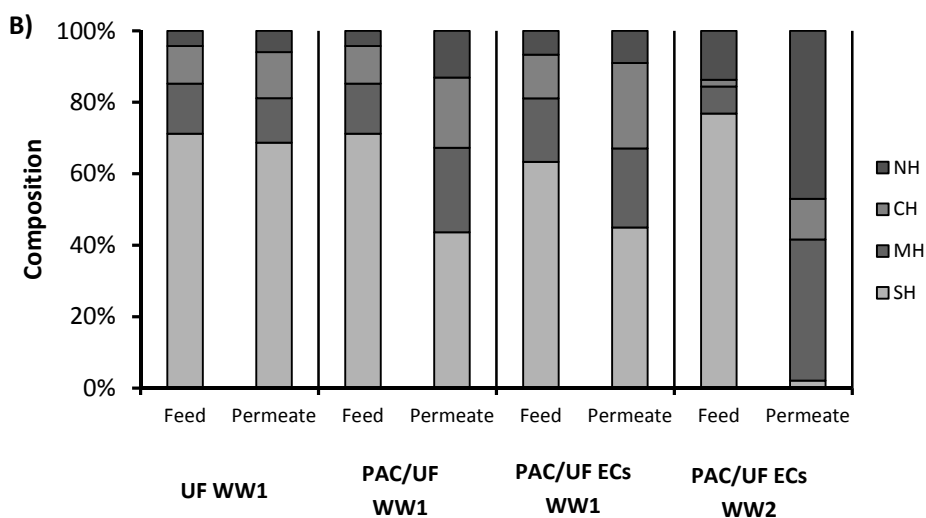
Figure 7. Characterization of NOM fractions in UF and PAC/UF experiments at the end of 2-h filtration cycle. SH: strongly hydrophobic; MH: moderately hydrophobic; CH: charged hydrophilic; and NH: neutral hydrophilic.

The rejection of contaminants in the UF process by different mechanisms (adsorption, steric hindrance, electrostatic repulsion) is affected by several membrane characteristics and solute properties (MW, molecular size, pK_a, log D, dipole moment). Two selected emerging contaminants, chlorophene and methylindole, were almost totally removed (rejection higher than 95%) only by ultrafiltration process, i.e. without PAC addition, when the water matrix employed was DS (Fig. 8). However, nortriptyline was removed only around 40% and the most hydrophilic compounds, benzotriazole and DEET, were removed only 30% and 13%, respectively. Previous studies indicated that the influence of ultrafiltration on the removal of hydrophilic microcontaminants is expected to be negligible due to the relatively high molecular weight cut-off of the membrane (100-300 kDa), compared to the molecular weight of micropollutants (< 1 kDa) (Snyder et al., 2007 and Yoon et al., 2007). Thus, since the MWCO of the membrane employed was much higher than the size of the molecules, it could be thought that retention was not due to steric factors and may be due mainly to adsorption phenomena onto the membrane surface (Comerton et al. (2007), Secondes et al. (2014). Consequently, CP and ML were the most

rejected ECs due to their hydrophobic character (see Table 1) while the lower rejection of
NH, DT and BZ can be attributed to their less hydrophobicity at pH 7.
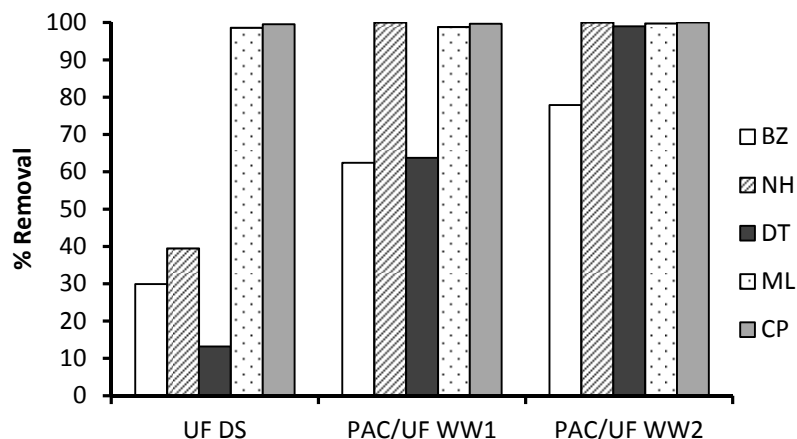
**Figure 8. Percentage of removal of each selected emerging contaminant by UF and
PAC/UF in different water matrices after 120 min. PAC SA Super 10 mg L^{-1}.**

When the combined PAC/UF process was used, the removal sequence was similar
to that obtained with PAC alone, i.e. BZ<DT<ML≈NH≈CP. Therefore, the influence of the
ECs' characteristics prevails and adsorption seems to be the predominant mechanism for
contaminants removal in the PAC/UF process (Secondes et al., 2014). The addition of PAC to
UF runs improved considerably the elimination of selected contaminants, especially for less
hydrophobic compounds, i.e. NH, BZ and DT (Fig. 8 and 9). The best rejection of
contaminants was found when WW2 water was employed, since competition effect of
natural organic matter was lower. In addition, as can be seen in Figure 9, emerging
contaminants BZ and DT presented similar kinetics and retention when PAC as well as
PAC/UF processes were applied (see also Fig. 3). Nevertheless, the PAC/UF system allowed
reaching 20% extra removal of both BZ and DT. In the case of NH, PAC/UF system allowed
its total removal with faster kinetics. These results highlight the advantages of the PAC/UF
process for removal of emerging contaminants. Adsorption on both PAC and membrane
surface plays an important role in this combined process and constitutes the major
retention mechanism for emerging compounds, with minor contribution of the size

exclusion mechanism, since the MWCO of the membrane is much higher than the MW of the selected pollutants.
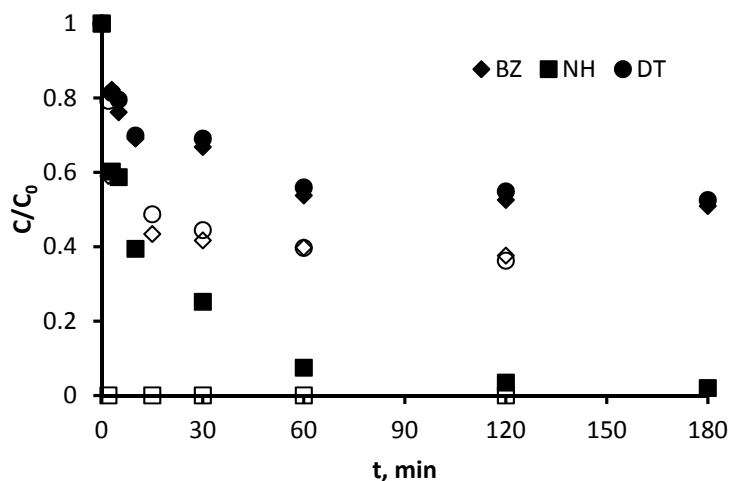
Figure 9. Evolution of normalised concentration of BZ, DT and NH in PAC (solid symbols) and PAC/UF (white symbol) in WW1 using 10 mg L^{-1} SA Super.

It should be noted that with the selected dose of 10 mg L^{-1}, total rejection of ML, NH and CP was reached in both water matrices WW1 and WW2. In addition, when WW2 was used, DT was also totally removed and rejection above 75% was obtained for BZ, i.e. the least hydrophobic compound studied. In the case of higher competition with NOM (WW1 matrix), removal of DT and BZ decreased, although remaining above 60%. As a consequence, higher content of NOM exerts a negative effect on contaminants removal. A plausible option to achieve the desired removal of contaminants by the PAC/UF process in presence of high content of NOM is to increase the PAC dose. Thus, this combined process could generate a final effluent practically free of emerging contaminants which could be reused in several applications.

4. CONCLUSIONS

The results of the adsorption and adsorption combined with UF processes of the five emerging contaminants selected (1-H-benzotriazole, N,N-diethyl-m-toluamide or DEET,

chlorophene, 3-methylindole, and nortriptyline HCl) allowed the following conclusions to be drawn:

i.   Comparing both PACs, SA Super shows better rejection of hydrophobic NOM than SAE Super, as well as slightly better removal of ECs.

ii. The single adsorption process of selected ECs in DS and WW1 water matrices revealed the sequence of removal BZ<DT<ML<NH<CF, accordingly with their hydrophobicity and aromaticity.

iii. A PAC dose of 10 mg L^{-1} was selected as a compromise between removal of ECs and NOM and required dosage.

iv. PAC addition did not affect the permeate flux during PAC/UF runs, independently of water matrix employed.

v.   The PAC/UF process significantly increased the removal of ECs over single UF. The sequence of retention of ECs matches with that previously obtained for single adsorption, which indicates that activated carbon plays a significant role in the removal of ECs by the PAC/UF process.

vi. The combination PAC/UF constitutes an interesting option for the removal of ECs and treatment of secondary effluents, leading to a final effluent with good quality to be reused.

REFERENCES

Benitez, F.J.; Acero, J.L.; Real, F.J.; Roldan, G.; Rodriguez, E. Photolysis of model emerging contaminants in ultra-pure water: kinetics, by-products formation and degradation pathways. Water Res. **2013**, 47, 870-880.

Boehmer, W.; Ruedel, H.; Wenzel, A.; Schröeter-Kermani, C. Retrospective monitoring of triclosan and methyl-triclosan in fish: Results from the german environmental specimen bank. Organohalogen. Comp. **2004**, 66, 1489-1494.

Campinas, M.; Rosa, M.J. Assessing PAC contribution to the NOM fouling control in PAC/UF systems. Water Res. **2010**, 44, 1636-1644.

Campinas, M.; Viegas, R.M.C.; Rosa, M.J. Modelling and understanding the competitive adsorption of microcystins and tannic acid. Water Res. **2013**, 47, 5690-5699.

Chow, C.K.W.; Fabris, R.; Drikas, M. Rapid fractionation technique to characterise natural organic matter for the optimisation of water treatment process. J. Water SRT Aqua **2004**, 53, 85-92.

Comerton, A.M.; Andrews, R.C.; Bagley, D.M.; Yang, P. Membrane adsorption of endocrine disrupting compounds and pharmaceutically active compounds, J. Membr. Sci. **2007**, 303, 267-277.

Costanzo, S.D.; Watkinson, A.J.; Murby, E.J.; Kolpin, D.W.; Sandstrom, M.W. Is there a risk associated with the insect repellent DEET (N,N-diethyl-m-toluamide) commonly found in aquatic environments?. Sci. Total Environ. **2007**, 384, 214-220.

Crozes, G.F.; Jacangelo, J.G.; Anselme, C.; Laine, J.M. Impact of ultrafiltration operating conditions on membrane irreversible fouling. J. Membr. Sci. **1997**, 124, 63-76

De Ridder, D.J.; Villacorte, L.; Verliefde, A.R.D.; Verberk, J.Q.J.C.; Heijman, S.G.J.; Amy, G.L.; van Dijk, J.C. Modeling equilibrium adsorption of organic micropollutants onto activated carbon. Water Res. **2010**, 44, 3077-3086.

Dickenson, E.R.V.; Drewes, J.E. Quantitative structure property relationships for the adsorption of pharmaceuticals onto activated carbon. Water Sci. Technol. **2010**, 62, 2270-2276.

Goren, U.; Aharoni, A.; Kummel, M.; Messalem, R.; Mukmenev, I.; Brenner, A.; Gitis, V. Role of membrane pore size in tertiary flocculation/adsorption/ultrafiltration treatment of municipal wastewater. Sep. Purif. Technol. **2008**, 61, 193-203.

Kim, H-A.; Choi, J-H.; Takizawa, S. Comparison of initial filtration resistance by pretreatment processes in the nanofiltration for drinking water treatment. Sep. Purif. Technol. **2007**, 56, 354-362.

Kolpin, D.W.; Furlong, E.T.; Meyer, M.T.; Thurman, E.M.; Zaugg, S.D.; Barber, L.B.; Buxton, H.T. Pharmaceuticals, hormones, and other organic wastewater contaminants in U.S. streams, 1999-2000: a national reconnaissance, Environ. Sci. Technol. **2002**, 36, 1202-1211.

Langford, K.H.; Thomas, K.V. Determination of pharmaceutical compounds in hospital effluents and their contribution to wastewater treatment works. Environ. Int. **2009**, 35, 766-770.

Liu, C.; Chen, W.; Cao, Z.; van Merkenstein, R. Removal of algogenic organic matter by miex (R) pre-treatment and its effect on fouling in ultrafiltration. Fresenius Environ. Bulletin **2010**, 19, 3118-3124.

Loos, R.; Gawlik, B.M.; Locoro, G.; Rimaviciute, E.; Contini, S.; Bidoglio, G. EU wide survey of polar organic persistent pollutants in European river waters. Environ. Pollut. **2009**, 157, 561-568.

Löwenberg, J.; Zenker, A.; Baggenstos, M.; Koch, G.; Kazner, C.; Wintgens, T. Comparison of two PAC/UF processes for the removal of micropollutants from wastewater treatment plant effluent: Process performance and removal efficiency. Water Res. **2014**, 56, 26-36.

Margot, J.; Kienle, C.; Magnet, A.; Weil, M.; Rossi, L.; Felippe de Alencastro, L.; Abegglen, C.; Thonney, D.; Chevre, N.; Schärer, N.; Barry, D.A. Treatment of micropollutants in municipal wastewater: ozone or powdered activated carbon. Sci. Total Environ. **2013**, 461, 480-498.

Moreno-Castilla, C.; López, Ramón M.; Carrasco-Marín, F. Changes in surface chemistry of activated carbons by wet oxidation. Carbon **2000**, 38, 1995-2001.

Nguyen, L.N.; Hai, F.I.; Kang, J.; Price, W.E.; Nghiem, L.D. Coupling granular activated carbon adsorption with membrane bioreactor treatment for trace organic contaminant removal: Breakthrough behaviour of persistent and hydrophilic compounds. J. Environ. Manag. **2013**, 119, 173-181.

Noh, J.S.; Schwarz, J.A. Estimation of the point of zero charge of simple oxides by mass titration. J. Colloid. Interface Sci. **1989**, 130, 157-164.

Secondes, M.F.N.; Naddeo, V.; Belgiorno, V.; Ballesteros Jr., F. Removal of emerging contaminants by simultaneous application of membrane ultrafiltration, activated carbon adsorption, and ultrasound irradiation. J. Hazard. Mat. **2014**, 264, 342-349.

Snyder, S.A.; Adham, S.; Redding, A.M.; Cannon, F.S.; De Carolis, J.; Oppenheimer, J.; Wert, E.C.; Yoon, Y. Role of membranes and activated carbon in the removal of endocrine disruptors and pharmaceuticals. Desalination **2007**, 202, 156-181.

Stackelberg, P.E.; Furlong, E.T.; Meyer, M.T.; Zaugg, S.D.; Henderson, A.K.; Reissman, D.B. Persistence of pharmaceutical compounds and other organic wastewater contaminants in a conventional drinking-water-treatment plant. Sci. Total Environ. **2004**, 329, 99-113.

Stoquart, C.; Servais, P.; Bérubé, P.R.; Barbeau, B. Hybrid Membrane Processes using activated carbon treatment for drinking water: A review. J. Membr. Sci. **2012**, 411, 1-12.

Ternes, T. A.; Hirsch, R. Occurrence and behavior of X-ray contrast media in sewage facilities and the aquatic environment. Environ. Sci. Technol. **2000**, 34, 2741-2748.

Wenhui, L.; Xinghai, L.; Dongyan, L.; Lei, S.; Qi, S. Vapor-phase synthesis of 3-Methylindole over Fe-, Co-, or Ni-promoted Ag/SiO$_2$. Chin. J. Catal. **2009**, 30, 1287-1290.

Yoon, Y.; Westerhoff, P.; Snyder, S.A.; Wert, E.C.; Yoon, J. Removal of endocrine disrupting compounds and pharmaceuticals by nanofiltration and ultrafiltration membranes. Desalination **2007**, 202, 16-23.
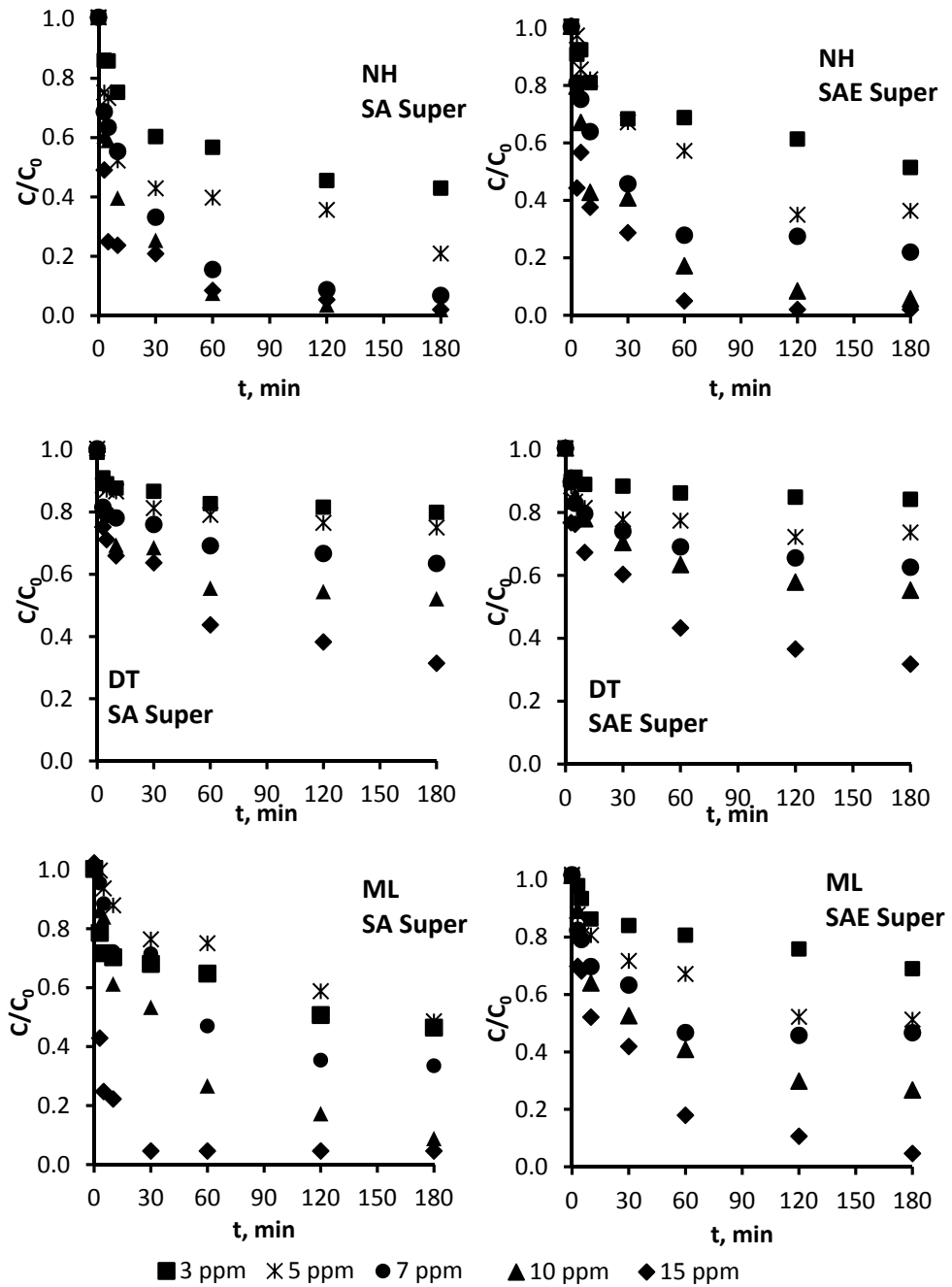
SUPPLEMENTARY INFORMATION

Figure S1. Evolution of normalized concentration of NH, DT and ML during PAC adsorption in experiments performed with WW1.

3.11. Elimination of selected emerging contaminants by the combination of membrane filtration and chemical oxidation processes.

3.11. ELIMINATION OF SELECTED EMERGING CONTAMINANTS BY THE COMBINATION OF MEMBRANE FILTRATION AND CHEMICAL OXIDATION PROCESSES

Juan L. Acero, F. Javier Benítez, Francisco J. Real and Elena Rodríguez.

Departamento de Ingeniería Química, Universidad de Extremadura, Badajoz.

The elimination of five selected emerging contaminants (1-H-benzotriazole, DEET, chlorophene, 3-methylindole, and nortriptyline HCl) dissolved in different water matrices (surface water and secondary effluents) was carried out by sequential membrane filtration and chemical oxidation processes. First, a membrane filtration (ultrafiltration (UF) or nanofiltration (NF)) pre-treatment was conducted, and both permeate and retentate were afterwards treated by chemical oxidation, using ozone or chlorine. The application of UF and specially of NF provided a large volume of permeate, whose quality can be improved by a chemical treatment to completely remove residual contaminants except 1-H-benzotriazole. Chlorination and specially ozonation have demonstrated to be effective for the reduction of emerging contaminants in the concentrated stream, thus generating an effluent that might be recycled to the activated sludge treatment in the WWTP. In a second group of experiments, a chemical oxidation pre-treatment (by using ozone, chlorine, O_3/H_2O_2, UV radiation or UV/H_2O_2) was applied followed by a nanofiltration process. Results of removals and rejection coefficients for the emerging contaminants showed that the chemical pre-treatment exerted a positive influence on the subsequent NF process, not only in terms of ECs removal but also of DOC reduction. While global removals higher than 97% were reached for DEET, chlorophene, 3-methylindole, and nortriptyline HCl, lower values were obtained for 1-H-benzotriazole, specially for chlorine pre-treatment, and in those mater matrices with high content of natural organic matter. Therefore, both

sequential treatments are promising to remove the selected micropullutants while reducing the chlorine doses needed to achieve final water disinfection.

1. INTRODUCTION.

Increasing public health concern has grown in relation to a new group of micropollutants present in water systems, since little is known about their potential effects in humans and animals. They are commonly known as Emerging Contaminants (ECs), because they are still unregulated or in the process of being regulated. This group of contaminants is constituted by numerous chemical substances, including pesticides, pharmaceuticals and personal care products, industrial compounds, fragrances, water treatment by-products, flame retardants and surfactants (Heberer, 2002). Currently, the presence of these substances in surface and ground waters, and even in drinking water, is increasing (Sim et al., 2011; Tijani et al., 2013), being their main source municipal wastewater treatment plants (WWTP) effluents. It is recognized that WWTP technologies are very often unable to entirely degrade such persistent substances (Jelic et al., 2011). Consequently, their elimination from waters, together with other priority pollutants, is an important goal in environmental technology.

For this purpose, common agents used in chemical oxidation processes are chlorine, hydrogen peroxide, ozone, UV radiation, as well as the combination of these oxidants in the so-called Advanced Oxidation Processes (AOPs), which are characterized by the generation of free radicals, such as hydroxyl radicals. Specifically, chlorine has been widely applied in water treatments due to its low cost, generally formulated as hypochlorite (Sharma, 2008). Ozone is a very powerful oxidant for water and wastewater treatment, because it reacts with the organic matter by two different pathways: through direct oxidation, as molecular ozone; and through indirect reaction, by generating hydroxyl radicals (Staehelin and Hoigne, 1985). At the same time, UV radiation is a common method for disinfecting drinking water, which also induces phototransformations of organic pollutants (Canonica et al., 2008). Additionally, the presence of hydrogen peroxide combined with ozone or UV radiation is a very frequent AOP used for the oxidation of refractory organic compounds (Rivera-Utrilla et al., 2013; Tijani et al., 2014).

On the other hand, among the physical treatments also used for the purification of surface waters and wastewaters, membrane separation processes have gradually gained popularity because they effectively remove a wide variety of contaminants. Specifically, ultrafiltration (UF) and nanofiltration (NF) membranes constitute an effective technology to eliminate micropollutants with molecular weights larger than 200 Da, as well as ions (Kim et al., 2007; Wray et al., 2014; Anwar Sadmani et al., 2014). However, an important drawback of membrane processes is the generation of the concentrated stream or retentate. Possibilities to treat or to discharge the retentate include reuse, further treatment by removal of contaminants, incineration, direct or indirect discharge in surface water, direct or indirect discharge in groundwater and landfilling (van der Bruggen et al., 2008).

As these conventional chemical and physical processes are not effective enough to reach the total removal of some contaminants, alternative advanced technologies for tertiary treatment of WWTP effluents are increasingly being tested. Thus, in the latest years, several studies have tested the elimination of organic micropollutants in water treatments by using different combinations of physical treatments and chemical oxidation (Illueca-Muñoz et al., 2008; Saquib et al., 2010; Dolar et al., 2013; James et al., 2014). The application of AOPs to treat the retentate generated in membrane processes has also been investigated (Perez-Gonzalez et al., 2012). However, as most of the studies were based mainly on natural organic matter removal, the literature focused on the elimination of ECs from wastewater and surface waters by combined treatments involving membrane filtration and chemical oxidation is rather scarce.

Accordingly, the aim of the present investigation was to apply combinations of chemical treatments and membrane processes for the elimination of five selected ECs when they are present in three water matrices: surface water from a reservoir and two effluents from WWTP. These compounds are: 1-H-benzotriazole (BZ), N,N-diethyl-m-toluamide or DEET (DT), chlorophene (CP), 3-methylindole (ML), and nortriptyline HCl (NH), which are frequently found in surface waters and wastewaters (Costanzo et al., 2007; Langford et al., 2009; Loos et al., 2009). Specifically, two sequences have been studied: in the first one, each water matrix containing the five ECs was subjected to a membrane filtration stage (UF and NF); and later, both resulting streams, permeate and retentate, were treated in a

chemical oxidation stage (by using ozone and chlorine). The inverse sequence, which consisted in a chemical oxidation stage by using ozone, chlorine, UV radiation, and the AOPs UV/H_2O_2 and O_3/H_2O_2 followed by a NF stage, was also investigated. In all these treatments, the partial contribution of the different stages on the removals of ECs was established. In addition, the global removals for each combined treatment were also determined with the aim of establishing the efficiency of each sequence tested. Finally the effect of the water matrix on each sequence was also investigated.

2. MATERIALS AND METHODS.

2.1. Emerging contaminants, water systems and membranes.

The five selected ECs were supplied by Sigma Co. (Germany), with the highest purity available. Table 1 summarizes the selected compounds and their relevant physico-chemical properties. These micropollutants were dissolved in three different water systems: a surface water (denoted SW) that was collected from the reservoir "Peña del Aguila" (Extremadura Community, south-west Spain); and two secondary effluents from two municipal WWTP, located at Badajoz (denoted BA) and La Albuera (denoted LA), both cities also in the Extremadura Community. These water samples were filtered within 24 h after sampling and stored at 4 °C until use. They were analysed and their main quality parameters are shown in Table 2.

Table 1. Physico-chemical properties of selected ECs.

Emerging contaminant	MW, g mol^{-1}	pK$_a$	Log k$_{ow}$
1-H-benzotriazole	119.1	0.40 / 8.20	1.44
Nortriptyline HCl	299.8	10.21	4.51
DEET	191.3	0.67	2.18
3-methylindole	131.3	-	2.60
Chlorophene	218.7	9.81	4.18

Table 2. Characteristics of the water matrices used.

	SW	LA	BA
pH	7.4	7.9	8.3
Conductivity, μS cm^{-1}	80.2	570	550
A$_{254\ nm}$, cm^{-1}	0.187	0.041	0.245
COD, mg O$_2$ L^{-1}	24	12.4	53
Alkalinity, mg CaCO$_3$ L^{-1}	30	335	325
DOC, mg L^{-1}	6.8	2.5	19.2
Total nitrogen, mg L^{-1}	1.51	21.3	35.5
Phosphorus, mg L^{-1}	0.041	0.156	1.76

The membranes used were commercial flat-sheet membranes provided by GE Osmonics, Inc. (Florida, USA), with an effective surface area of 28 cm^2. The UF membrane used (PT) had a molecular weight cut-off (MWCO) of 5000 Da, was made of polyethersulfone, and presented hydrophobic character. On the contrary, the NF membrane (HL) had a MWCO in the range 150-300 Da, was made of thin film polyamide composite, and presented a hydrophilic character. The values of hydraulic permeability for PT and HL membranes were 29.7 and 10.2 L h^{-1} m^{-2} bar^{-1}, respectively.

2.2. Experimental procedures and analysis.

Regarding to the chemical oxidation treatments, the temperature was kept constant at 20±0.5 ^{o}C in all cases, and the pH was the natural value of the water system used. Specifically, ozonation experiments were carried out in homogeneous conditions. Mixtures of the five ECs selected (together with the probe compound p-chlorobenzoic acid (pCBA)) dissolved in the three water matrices tested were introduced into 25 mL flask reactors. On the other hand, ozone stock solutions were generated by dissolving an ozone-oxygen gas stream in ice-cooled ultra-pure (UP) water until saturation was reached. Each run was initiated by injecting into the reaction flask containing the EC solution the necessary amount of the ozone stock solution to achieve the desired initial ozone concentration (0-7.5 mg L^{-1}). After ozone was totally consumed, residual concentrations of

ECs and pCBA were analyzed. Hydrogen peroxide (50 µM) was additionally added to some experiments.

In the chlorination experiments, a stock solution of hypochlorous acid of 10^{-3} M was initially prepared. Each experiment was initiated by injecting the adequate amount of chlorine into the flask reactors containing the ECs solution in order to reach the desired initial chlorine concentration (0-10.7 mg L^{-1}). Once chlorine was totally consumed, the remaining concentrations of ECs were analyzed.

The photochemical treatment of waters containing the selected ECs was carried out in a 500 cm^3 cylindrical glass reactor at a constant temperature of 20±0.5 °C. The radiation source used was a low pressure mercury vapor lamp (Hanau TNN 15/32, electrical power 15 W), which emitted monochromatic radiation at 254 nm. This lamp was placed axially within the reactor and covered by a quartz sleeve. Once kept constant the temperature of the reacting mass inside the reactor, the UV lamp was switched on and the reaction started. Some experiments were carried out in presence of H_2O_2 (50 µM). Samples were regularly withdrawn from the reactor for ECs analysis.

Regarding to the membrane filtration stages (UF or NF), the experiments were conducted in a laboratory cross-flow membrane filtration unit supplied by CM-CELFA Membrantechnik AG, model P-28™ (Seewen, Switzerland), which was described in detail in a previous research (Benitez et al., 2011). It basically consisted in a 500 mL pressurized storage vessel with a device containing the membrane. The temperature and tangential velocity were kept constant at 20±0.5 °C and 1 m s^{-1}, respectively, and the experiments were performed at the natural pH of the waters (around 7.5-8). The transmembrane pressure (TMP) was fixed at 3 bar for UF experiments and 20 bar for NF ones. A new membrane was used for each experiment.

A batch concentration mode was applied to carry out the filtration experiments, being the permeate stream collected separately, and the retentate stream recycled to the feed tank. The experiments were performed with 300 mL of solution containing the mixture of ECs. The filtration process was carried out until getting a volume of permeate equal to two thirds of the initial volume of the wastewater fed. Then, samples of feed, retentate and

permeate streams were simultaneously collected and the EC concentrations were analyzed in these samples.

In the first stage of every combined process, membrane filtration or chemical oxidation treatment, the initial concentration of each EC was fixed at 1 µM. The concentrations of the five selected ECs and p-CBA (when used as a probe compound) were determined by HPLC, using a Waters Chromatograph (Alliance 2695) equipped with a 2998 Photodiode Array Detector and a Phenomenex Gemini C18 Column (5µm, 150mm×3mm). The analysis was performed in gradient mode with acetonitrile and 25 mM acid formic, at a flow rate of 0.2 mL min^{-1} and at a column temperature of 20 ^{o}C. The volume of injection was of 100 µL in all cases. Detection was made at 250 nm for BZ, NH, DT, and pCBA; and 280 nm for ML and CP. In addition, ozone concentration in the stock solutions was determined directly by measuring their UV absorbance at 258 nm (ε=3150 L mol^{-1} cm^{-1}); chlorine stock solution was analyzed spectrophotometrically in presence of excess of iodide to form triiodide (ε at 351 nm: 25700 L mol^{-1} cm^{-1}) according to the procedure described by Bichsel and von Gunten (1999); and dissolved organic carbon content (DOC) was analyzed in a Multi N/C Analytik Jena TOC analyzer, by using the non-purgeable organic carbon method.

3. RESULTS AND DISCUSSION.

3.1. Filtration pre-treatment followed by chemical oxidation treatment.

The removal of selected ECs by the combination of a membrane filtration pre-treatment followed by a chemical oxidation treatment (chlorine or ozone) was firstly investigated. Focusing on the filtration pre-treatment (UF with the PT membrane and NF with the HL membrane), the efficiency of a membrane filtration process can be evaluated by the amount of ECs rejected by the membrane. Thus, the rejection coefficient (f) for each compound is defined by the expression:

$$f = \frac{[EC]_F - [EC]_P}{[EC]_F} \cdot 100 \tag{1}$$

being [EC]$_F$ and [EC]$_P$ the concentration of each EC in the feed and permeate streams respectively.

The values of the rejection coefficients obtained in the single filtration experiments for the three selected water matrices are compiled in Table 3. Two facts are clearly observed in these rejection coefficients: firstly, both single filtration processes (UF or NF) totally eliminated CP and ML in the three water matrices tested. For the remaining ECs, high eliminations were generally obtained for NH, intermediate for DT and low for BZ. And secondly, it is noted that higher rejection coefficients were obtained for every water system when using the NF HL membrane in comparison to the UF PT membrane, with the exception of BZ. Adsorption should be the main mechanism responsible for rejection of ECs by the hydrophobic UF PT membrane, since the MWCO of this membrane (5000 Da) is much higher than the molecular weight of the selected pollutants. However, other mechanisms such as size exclusion must contribute efficiently to the retention of ECs by the hydrophilic NF HL membrane with MWCO of 150-300 Da. BZ presents the lowest MW (119.1 g mol^{-1}) and is the most hydrophilic compound; thus, BZ is adsorbed only partially onto the PT membrane and is poorly retained by size exclusion with the HL membrane.

Table 3. Rejection coefficients obtained in the filtration pre-treatment (UF or NF) of selected water matrices (SW, LA and BA).

Treatment	f_{BZ}, %	f_{NH}, %	f_{DT}, %	f_{ML}, %	f_{CP}, %	f_{DOC}, %
SW-UF	44.3	81.2	40.5	100	100	40.6
SW-NF	27.7	93.3	92.9	100	100	67.9
LA-UF	33.9	83.8	41.7	100	100	12.7
LA-NF	29.1	96.3	91.2	100	100	53.9
BA-UF	49.1	83.2	45.8	100	100	56.0
BA-NF	28.8	100	100	100	100	84.3

Finally, the results obtained show slightly higher rejection coefficients in the secondary effluent BA than in the secondary effluent LA and in the surface water (SW), which can be explained by a slightly greater fouling caused on the membrane by the adsorption and pore blocking of natural organic matter (NOM), which is present in a major extent in the secondary effluent BA. This membrane fouling decreased the pore size and increased the ECs retention (Wray et al., 2014). In addition, contaminants removal

enhancement in presence of NOM might be due to the formation of macromolecular complexes with NOM functional groups (size exclusion and adsorption) and/or increased level of charge density induced by NOM in "pseudo-complexes" (electrostatic repulsion) (Comerton et al., 2008; Anwar Sadmani et al., 2014).

In addition to the rejection coefficients for the specific compounds, the effectiveness of the filtration processes for the elimination of the organic matter present in different water matrices was also evaluated by the rejection coefficients referred to the dissolved organic carbon. The values obtained for DOC removal at the end of the membrane stage are also summarized in Table 3. In general terms, lower removals were obtained in the UF process (in the range 12-56%) than in the NF process (in the range 54-84%), as could be expected for membranes with much lower MWCO. Therefore, size exclusion must be the main retention mechanism for high MW compounds. The lowest values of rejection coefficients were obtained for the secondary effluent LA, which is probably due to its low content of organic matter. In addition, the retention of DOC in LA water with the UF PT membrane was very low, which is an indication that the NOM present in this secondary effluent has a rather low MW after extended aeration secondary treatment.

Once the single membrane filtration pre-treatment was carried out, both effluents, permeate and retentate, were subjected to chemical oxidation processes by means of chlorine and ozone. Due to the different concentrations of ECs obtained in both, permeate and retentate streams, different oxidant doses were used for each effluent, and the results are discussed separately.

Focusing firstly on the permeate streams, different experiments were carried out by adding certain doses of ozone (up to 3.75 mg L^{-1}) or chlorine (up to 5 mg L^{-1}) to the permeates obtained in the filtration of the selected water matrices. At the same time, parallel oxidation experiments were performed with the water matrices, without any filtration stage, for comparative purposes. The residual concentration of each EC was analyzed after complete oxidant consumption. It must be noted that CP and ML were not present in these permeates and therefore their oxidation could not be investigated. The

results obtained for the residual concentrations of DT and BZ in the experiments carried out with SW water are depicted in Fig. 1 (Fig. 1A for chlorine and Fig. 1B for ozone). Although lower initial concentration of ECs could be expected in the NF permeate, the concentration of BZ was higher than in the UF permeate because of the reasons commented above. It can be observed in Fig. 1 that the removals of BZ and DT with both oxidants were higher in the permeate obtained in the NF process, which is due to its lower content of NOM (higher oxidant stability). In addition, ozone is a much more efficient oxidant for the removal of BZ and DT than chlorine. Thus, while both ECs were completely eliminated with around 3 mg L^{-1} of ozone, only DT could be removed by chlorine from the permeate obtained in the NF process, which is due to its very low concentration. Similar tendencies were obtained for the remaining water matrices. These results can be explained by the higher apparent rate constants of selected ECs with ozone (Benitez et al., 2013a,b; Benitez et al., 2014) than with chlorine (Acero et al., 2013). Furthermore, reactions of BZ and DT with OH radicals might be also considered. As von Gunten (2003) pointed out, an important source of OH radicals is the reaction between ozone and the organic matter present in a real water, being these substances promoters of a chain mechanism for the decomposition of ozone into OH radicals.

Figure 1. Concentration profiles of BZ and DT during a) chlorination of permeates obtained after the filtration pre-treatment (UF or NF) of SW water.
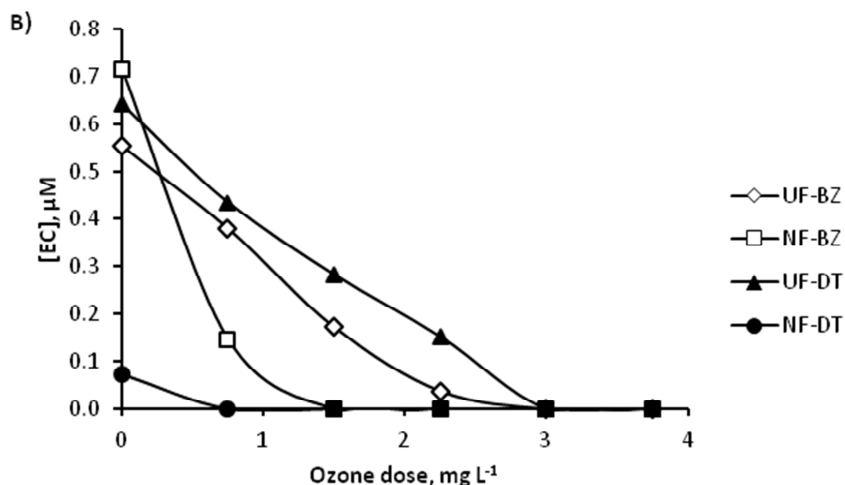
Figure 1 (cont.). Concentration profiles of BZ and DT during b) ozonation of permeates obtained after the filtration pre-treatment (UF or NF) of SW water.

Specifically for the chemical oxidation stages, the removals of ECs were quantified by the conversions obtained after applying different oxidant doses:

$$X_{EC} = \frac{[EC]_0 - [EC]_f}{[EC]_0} \cdot 100 \qquad (2)$$

where $[EC]_0$ and $[EC]_f$ represent the measured initial and final concentrations for each EC. This equation can be also applied to evaluate the global removal in the sequential process.

Table 3 provides the global removals (XEC) for each EC in some selected combined experiments performed with a specific dose of chlorine or ozone (0.75 mg L^{-1}). This table also includes those removals obtained in the two experiments carried out with each water matrix consisting in the single chlorination or ozonation stage, and without filtration pre-treatment (experiments Cl$_2$ and O$_3$).

Considering the results obtained in the single oxidation experiments without a previous filtration stage, the sequence of conversions obtained for both oxidants was ML > CP > NH > BZ > DT, which exactly agrees with the sequence of reaction rate constants of these ECs with both chlorine and ozone. Thus, apparent second order rate constants for the

chlorination of this group of ECs at several pHs have been published (Acero et al., 2013), being the values at pH 8 of 1.82×10^3, 79.8, 0.57, 0.14 and 4.41×10^{-4} M^{-1} s^{-1} for ML, CP, NH, BZ and DT, respectively. Similarly, apparent rate constants for the ozonation of these compounds have also been published previously (Benitez et al., 2013a,b; Benitez et al., 2014): 5.34×10^5, 9.39×10^3, 3.48×10^3, 398 and 0.12 M^{-1} s^{-1} for ML, CP, NH, BZ and DT, respectively, at pH 8. It must be noted that ozonation of water matrices might lead to the formation of OH radicals which also react with ECs, and could contribute significantly to the removal of ozone-refractory compounds such as DT. Furthermore, from the values of conversions and rate contants, ozone is a better oxidant than chlorine for the elimination of this group of contaminants. Thus, considering single oxidation experiments, while ML can be removed to a great extend by low doses of either chlorine or ozone, intermediate doses are required for the elimination of CP and NH. However, BZ and DT can be only partially oxidized with the doses of chlorine or ozone tipically applied in water treatment. In addition, the removals obtained in the single oxidation process show the following trend among each type of water matrix: LA > SW > BA. This sequence can be explained by the amount of NOM present in each water matrix (Table 2), which consumes part of the oxidant in competition with the ECs.

According to the results summarized in Table 4, the comparison of global removals obtained for BZ, NH and DT in any of the sequential processes (UF of NF followed by chemical oxidation), with those of the single oxidation process (Expts. Cl_2 and O_3) reveals that any combination provided higher eliminations than the single oxidation stage. In general, high conversions were obtained for the ECs, specially in the case of the pre-treated water with the NF process, which reached almost total removal of selected ECs. The low content of organic matter in the NF permeate led to a decrease of chlorine and ozone consumption (higher oxidant stability), thus favouring the oxidation of ECs. Nevertheless, partial eliminations of DT with the combination UF and chemical oxidation and of BZ with both investigated combinations were reached, accordingly with the low retention and reactivity of these pollutants. These results confirm the goodness of a filtration pre-treatment, specially NF, followed by an oxidation treatment of the resulting permeate for

the removal of ECs from secondary effluents to be reused and from drinking water sources. In addition, the final effluent is disinfected after the chemical process.

Table 4. Global removals obtained after single oxidation of selected water matrices (SW, LA and BA) and after filtration pre-treatment (UF or NF) followed by chemical oxidation of permeates. Initial dose of chlorine or ozone: 0.75 mg L^{-1}.

Treatment	X_{BZ}, %	X_{NH}, %	X_{DT}, %	X_{ML}, %	X_{CP}, %	X_{DOC}, %*
SW-Cl$_2$	1.9	12.7	1.4	83.7	24.2	3.5
SW-O$_3$	24.9	26.8	19.5	68.0	52.7	5.2
SW-UF-Cl$_2$	45.7	100	41.5	100	100	64.9
SW-UF-O$_3$	62.5	100	56.7	100	100	70.4
SW-NF-Cl$_2$	30.1	100	100	100	100	84.7
SW-NF-O$_3$	55.4	100	100	100	100	93.2
LA-Cl$_2$	3.2	39.0	1.7	94.9	63.5	2.3
LA-O$_3$	26.2	55.9	23.5	86.8	80.2	3.0
LA-UF-Cl$_2$	35.5	84.8	43.1	100	100	19.5
LA-UF-O$_3$	41.1	90.6	44.7	100	100	23.5
LA-NF-Cl$_2$	29.6	100	100	100	100	57.5
LA-NF-O$_3$	67.5	100	100	100	100	65.2
BA-Cl$_2$	2.2	13.5	0.8	52.5	15.6	3.7
BA-O$_3$	10.4	15.5	8.9	32.7	24.9	5.3
BA-UF-Cl$_2$	49.7	84.1	47.2	100	100	57.5
BA-UF-O$_3$	57.1	100	51.4	100	100	59.9
BA-NF-Cl$_2$	30.0	100	100	100	100	90.3
BA-NF-O$_3$	45.8	100	100	100	100	92.4

Finally, the global removals of ECs were similar in the different water matrices investigated. Although the presence of NOM in the water matrices could benefit the retention of ECs in the filtration step as commented above, its presence exerted a negative influence on the subsequent chemical oxidation.

With respect to the reduction of organic matter expressed as DOC, it can be appreciated in Table 4 that this reduction was rather low in the single oxidation experiments. As a consequence, oxidation of water matrices with ozone or chlorine led to the formation of intermediate oxidation products but not to mineralization. However, the global reduction of DOC after the sequential process was even higher than that obtained in the filtration pre-treatment. Values of DOC obtained after both stages of the sequential process for BA water are depicted in Fig. 2. In general, slightly higher DOC reductions were obtained with ozone than with chlorine, since ozone is a stronger oxidant. In addition, higher removal of DOC was reached in the permeate obtained with the NF membrane, which can be explained by its lower MWCO. Finally, the global conversions of DOC in the combined experiments carried out are summarized in Table 4, reaching values higher than 90% with the sequential treatment NF+ozone applied to some water matrices. The influence of the water matrix on DOC removal was similar to that commented for the filtration pre-treatment; that is higher removals for the secondary effluent BA and for SW water, and lower removals for the secondary effluent LA, as corresponds to their organic matter content.
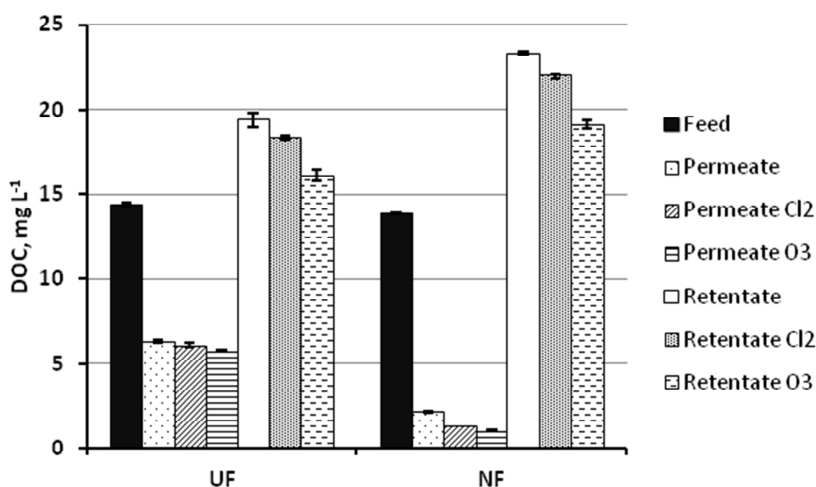

Figure 2. DOC values of feed, permeate and retentate samples after filtration pre-treatment of BA water, and of chlorination and ozonation treated samples of permeate and retentate. Chlorine dose applied to permeate and retentate: 5 and 10.5 mg L^{-1}, respectively. Ozone dose applied to permeate and retentate: 3.75 and 7.5 mg L^{-1}, respectively.

Regarding to the retentate streams obtained in the filtration pre-treatment (UF and NF), different experiments were carried out by adding certain doses of ozone (up to 7.5 mg L^{-1}) or chlorine (up to 10.7 mg L^{-1}) to the retentate obtained in the filtration of the selected water matrices. The evolution of the concentration of the selected ECs in the filtration pre-treatment (feed and retentate obtained in UF and NF processes) and subsequent chemical oxidation of retentates with different doses of chlorine and ozone is depicted in Fig. 3 for SW water taken as an example. It can be observed that micropollutant concentration in the resulting UF retentate was even lower than in the feed stream. These results can be explained by the adsorption of ECs on the UF membrane surface, which confirms that adsorption is the main mechanism for ECs retention with the UF PT membrane. However, only CP and ML concentrations were lower in the NF retentate than in the feed stream, as corresponds to their hydrophobic character at pH around 8. On the other hand, NH and DT concentrations were higher in the NF retentate, since these compounds are hydrophilic at pH 8 and therefore poorly adsorbed. Finally the concentration of BZ was similar in feed and retentate streams, which is due to its hydrophilic character and low retention with the NF HL membrane. These results also confirm that the main mechanism responsible for the retention of selected ECs on the NF HL membrane is size exclusion, with a certain participation of adsorption. Similar tendencies were obtained for LA and BA waters.
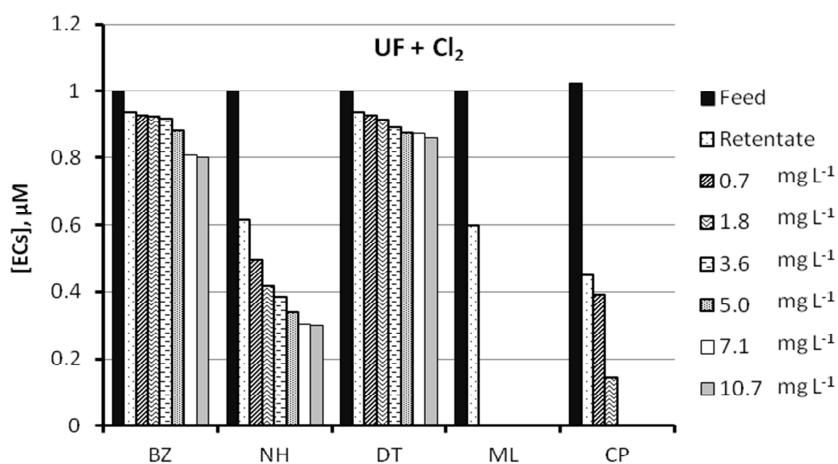

Figure 3. Residual concentration of ECs after oxidation treatment (chlorination or ozonation) of retentates obtained in the filtration pre-treatment (UF or NF) of SW water.
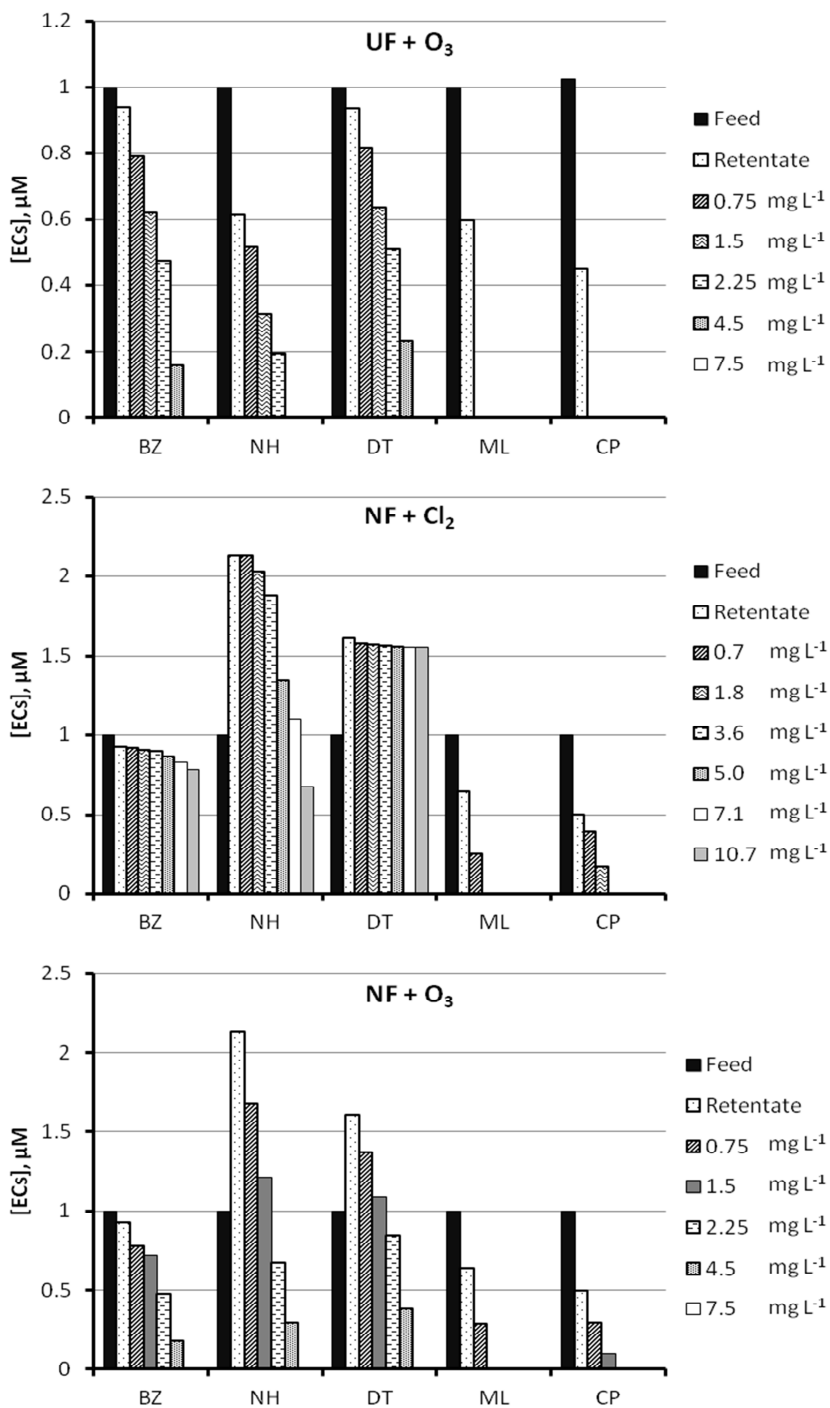
Figure 3 (cont.). Residual concentration of ECs after oxidation treatment (chlorination or ozonation) of retentates obtained in the filtration pre-treatment (UF or NF) of SW water.

It can also be observed in Fig. 3 a continuous decrease of EC concentration with increasing the oxidant dose. The removals reached for each EC (X_{EC}) after total oxidant consumption in the chemical treatment of investigated retentates are summarized in Table 5 for a specific dose of chlorine (5.0 mg L^{-1}) and ozone (2.25 mg L^{-1}) taken as example. Similar conclusions can be deduced for the oxidation of ECs in retentates to those of the oxidation in permeates. Thus, ozone is a more powerful oxidant than chlorine, and a significant removal of ECs could be reached only by ozone. The reactivity sequence was ML > CP > NH > BZ > DT for both oxidants, according to the values of apparent rate constants for the reaction of these ECs with chlorine and ozone. With respect to the removals reached in the different water matrices, the sequence was LA > SW > BA as corresponds with the organic matter content. Finally, the elimination of ECs was higher in the retentate obtained in the UF process than in the NF process, specially for slow-reacting compounds such as BZ and DT, which can be explained by the lower organic matter content of the UF retentate. As a consequence, higher oxidant doses are required to reach the removal of ECs from the retentate generated by NF membranes. Nevertheless, if a secondary effluent is being treated by this combined process and the appropriate oxidant dose is applied to the retentate generated in the filtration stage, a final effluent with very low concentration of ECs can be obtained. This final effluent might be recycled to the activated sludge treatment in the WWTP or discharged in surface water (direct or indirect via sewage systems) or in groundwater (van der Bruggen et al, 2008).

With respect to the reduction of DOC during the chemical oxidation of retentates, it can be observed in Fig. 2 for BA water that this reduction was relatively low when chlorine was applied (less than 10% with a chlorine dose of 10.7 mg L^{-1}). However, this DOC reduction was slightly higher when ozone was applied, and removals up to 20% were obtained for an ozone dose of 7.5 mg L^{-1}. Therefore, although a high removal of ECs from the retentate stream can be reached, the mineralization level is limited.

Table 5. Elimination of ECs reached in the chemical oxidation of retentates when 5.0 and 2.25 mg L^{-1} of chlorine or ozone, respectively, were applied to the retentante generated in the filtration pre-treatment (UF or NF) of selected water matrices (SW, LA and BA).

Treatment	X_{BZ}, %	X_{NH}, %	X_{DT}, %	X_{ML}, %	X_{CP}, %
SW-UF-Cl$_2$	5.9	45.0	6.4	100	100
SW-UF-O$_3$	49.5	68.5	45.6	100	100
SW-NF-Cl$_2$	3.9	12.6	1.6	100	100
SW-NF-O$_3$	48.6	69.2	47.7	100	100
LA-UF-Cl$_2$	17.1	70.3	12.7	100	100
LA-UF-O$_3$	84.5	100	55.7	100	100
LA-NF-Cl$_2$	10.7	55.4	8.6	100	100
LA-NF-O$_3$	63.8	100	39.5	100	100
BA-UF-Cl$_2$	4.3	22.2	3.7	100	54.4
BA-UF-O$_3$	20.9	24.1	11.7	100	100
BA-NF-Cl$_2$	2.3	9.9	0.5	65.3	35.3
BA-NF-O$_3$	11.2	17.4	8.8	100	84.3

In addition, the contributions of direct and radical pathways, f_{O3} and f_{OH}, to the removal of ECs were evaluated in the ozonation experiments. For this purpose, a procedure initially proposed by Elovitz and von Gunten (1999), and lately applied by Benitez et al. (2014), allowed the determination of the specific contribution of the radical pathway, f_{OH}, by using a probe compound, which reacts quickly with OH radicals and negligibly with O$_3$. pCBA was selected in this study as the probe compound, due to the fact that its rate constant with ozone is negligible, while with OH radicals is 5×10^9 M^{-1} s^{-1} (Buxton et al., 1988). In these experiments, pCBA was dissolved together with the ECs in the selected water systems. Thus, f_{OH} is calculated by Eq (3):

$$f_{OH} = \frac{\dfrac{k_{OH-EC}}{k_{OH-pCBA}} \ \ln\left(\dfrac{[pCBA]_t}{[pCBA_0]}\right)}{\ln\left(\dfrac{[EC]_t}{[EC]_0}\right)} \qquad (3)$$

In this Eq. (3), pCBA and EC refer to the probe compound, pCBA, and the different ECs. The rate constants for the reaction of selected ECs with OH radicals were determined in a previous work (10.87×10^9, 8.47×10^9, 8.24×10^9, 7.51×10^9 and 5.57×10^9 M^{-1} s^{-1} for NH, CP, BZ, DT and ML, respectively (Benitez et al., 2013c)). Following this procedure, Eq. (3) was applied to the results obtained in the ozonation of permeates (only for BZ and DT) and retentates, being the time 0 considered after filtration pre-treatment and time t when the total ozone depletion was reached. With the values of f_{OH} obtained, the values of f_{O3} can be easily determined by the expression: $f_{O3} = 1 - f_{OH}$. The average values obtained for f_{OH} were 0.93±0.05, 0.83±0.05, 0.65±0.08, 0.21±0.04, and 0.10±0.04 for DT, BZ, NH, CP and ML, respectively. According to these values of f_{OH}, it can be appreciated that BZ and DT are mainly oxidized by OH radical reactions, while ML and CP are mainly degraded by direct reactions with molecular ozone. According to the procedure proposed, the rank observed for f_{OH} should be inversely related to the ratio k_{O3-EC}/k_{OH-EC} at pH 8, being this ratio 9.55×10^{-5}, 1.11×10^{-6}, 3.20×10^{-7}, 4.83×10^{-8}, and 1.60×10^{-11} for ML, CP, NH, BZ, and DT, respectively. Therefore, it can be appreciated that this rank is fulfilled, which means that the higher ozonation rate constant at pH 8 of these compounds, the greater direct O_3 oxidation pathway contribution during real water ozonation.

The application of UF and specially of NF to secondary effluents provides a large volume of permeate, which can be directly reused as such or after a chemical treatment to remove residual contaminants, and a concentrated stream that requires further treatment. Chlorination and specially ozonation have demonstrated to be effective for the reduction of emerging contaminants in the concentrated stream, thus generating an effluent that might be recycled to the activated sludge treatment in the WWTP. In addition, ozonation decreases NOM fractions with high MW by breaking the larger molecules (Linlin et al., 2011), leading to higher proportions of low molecular weight compounds which are more biodegradable (Jansen et al., 2006), thus favoring the biological degradation of the resulting effluent. Additional advantages of this sequential process, due to the reduction in the volume of retentate to be treated, are lower treatment times and more efficient reagent consumption (Perez-Gonzalez et al., 2012).

3.2. Chemical oxidation pre-treatment followed by nanofiltration.

In this second phase, experiments consisting in sequential chemical pre-treatment (UV radiation, chlorine, ozone, and the combinations UV radiation plus H_2O_2 and ozone plus H_2O_2) and nanofiltration were conducted. Nanofiltration (HL membrane with TMP=20 bar) was selected because, with the exception of BZ, it showed higher efficiency for the elimination of ECs from water matrices. In addition, oxidation of NOM leads to lower molecular weight compounds, which would not be retained by a UF membrane. Initial doses of oxidants applied in the chemical pre-treatment were 2.25 and 3.5 mg L^{-1} for ozone and chlorine, respectively. The photodegradation experiments lasted 30 min. Hydrogen peroxide (50 µM) was added in some experiments (UV/H_2O_2 and O_3/H_2O_2).

With respect to the removals obtained for each EC in the chemical oxidation pre-treatments, CP and ML were totally eliminated, as a consequence of their high reactivity with the oxidant agents used. Focusing on the three remaining ECs, Fig. 4 shows the residual concentrations obtained after the pre-treatment step as well as after the subsequent NF stage, for the three selected water matrices. In general terms, the sequence of conversions obtained for the ECs included in Fig. 4 was NH > BZ > DT, which exactly agrees with the sequence of reaction rate constants of these ECs with both chlorine and ozone, as commented above. However, this disappearance rate sequence is not in complete agreement with the sequence of quantum yields for NH, BZ and DT obtained in the photodegradation of these ECs in UP water (Benitez et al., 2013c). In effect, NH presented a slightly higher disappearance rate than BZ, while the quantum yields were 29×10^{-3} mol Einstein^{-1} for BZ and 14×10^{-3} mol Einstein^{-1} for NH. This result can be explained by taking into account that the photolysis of NOM could induce the formation of OH radicals and rate constant of the reaction with OH radicals is higher for NH than for BZ (10.87×10^9 *vs.* 8.24×10^9 M^{-1} s^{-1}). Thus, the elimination sequence in the combination UV/H_2O_2, where both direct photolysis and OH radical reaction have to be considered, was NH > BZ > DT.
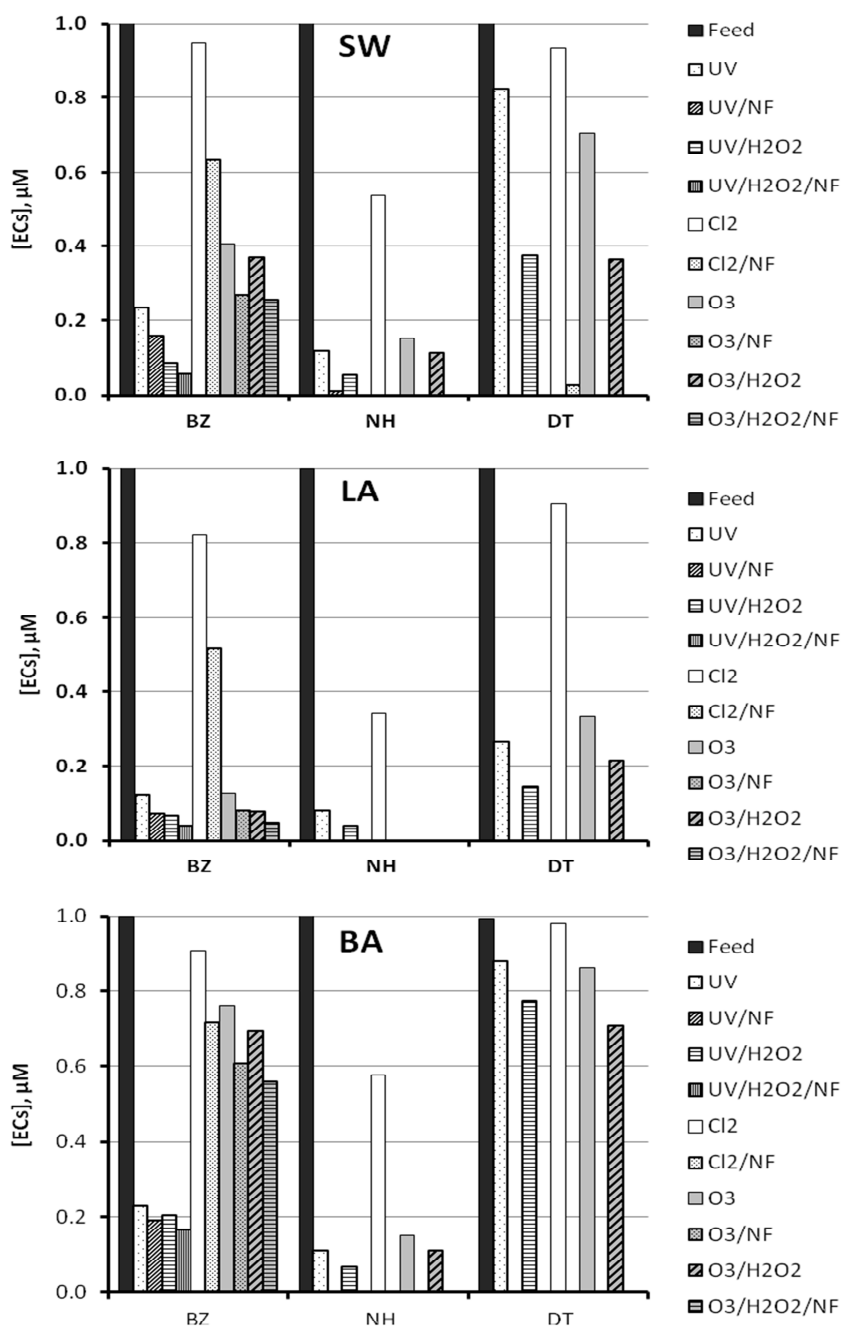
Figure 4. Residual concentration of ECs after chemical pre-treatment (UV irradiation, UV/H$_2$O$_2$, chlorination, ozonation or O$_3$/H$_2$O$_2$) and after the sequential chemical oxidation and NF treatment applied to selected water matrices (SW, LA, BA). UV irradiation time- 30 min; chlorine dose-3.5 mg L^{-1}; ozone dose-2.25 mg L^{-1}; hydrogen peroxide dose-50 µM.

According to the results depicted in Fig. 4, the UV/H$_2$O$_2$ system was usually the most efficient pre-treatment under the conditions of work, followed nearly by UV radiation, O$_3$/H$_2$O$_2$ system, ozonation, and finally, chlorination, which was the least effective oxidation process. Therefore, it is confirmed that the addition of hydrogen peroxide to UV radiation or ozone promoted the radical pathway, a supplementary way for the degradation of the selected ECs. Moreover, it is generally observed lower residual concentration after the chemical pre-treatment when ECs were dissolved in LA water than in SW or BA water. This effect is due to the amount of dissolved organic matter present in each water matrix, which competes with the ECs in the consumption of UV radiation, chlorine, ozone or hydroxyl radicals. Therefore, the efficiency of the selected chemical pre-treatments was inversely proportional to the amount of NOM present in the water. Additionally, the reduction of organic matter expressed as DOC was rather low in the different chemical pre-treatments.

The effluents of the chemical oxidation pre-treatment, with the remaining ECs concentration depicted in Fig. 4, constituted the feed stream for the NF process. The residual concentration of ECs in the resulting permeate stream are also shown in Fig. 4. The efficiency of this NF stage was evaluated by the rejection coefficients, which were defined by Eq. (1). The values obtained for each EC in this group of experiments are summarized in Table 6. Due to the total elimination of CP and ML in the preceding oxidation pre-treatment, it was not possible to determine the corresponding rejection coefficients for these compounds in this second stage. Additionally, the rejection coefficients obtained in the NF experiments directly performed with the selected water matrices without chemical pre-treatment are included in Table 3 (Expts. SW-NF, LA-NF and BA-NF).

In general, the results compiled in Table 6 reveal high rejection coefficients for NH and DT, with values above 90% in all cases. However, the retention of BZ was rather low, with values in the range 16-42% depending mainly on the type of water, which is due to its low MW and hydrophilic character. These rejection coefficients were similar or slightly higher than those obtained in the NF of water matrices without pre-treatment (Table 3), except for BZ in BA water. The size exclusion is likely the main rejection mechanism for ECs with the NF HL membrane, while the physico-chemical interactions and electrostatic repulsion/attraction

probably had influence on the rejection of the smaller photodegradation and oxidation products (Dolar et al., 2013).

Table 6. Rejection coefficients obtained in the NF stage and global conversions reached after the combination of chemical pre-treatment and NF process.

Type of water	Pre-treatment	Rejection coefficients			Global conversions		
		f_{BZ}, %	f_{NH}, %	f_{DT}, %	X_{BZ}, %	X_{NH}, %	X_{DT}, %
SW	UV	31.9	89.8	100	84.1	98.4	100
	UV/H_2O_2	33.1	93.9	100	94.4	99.5	100
	Cl_2	33.2	98.8	96.7	37.1	99.3	97.4
	O_3	33.8	96.5	100	73.3	99.5	100
	O_3/H_2O_2	31.1	95.3	100	74.6	99.5	100
LA	UV	41.8	100	100	92.8	100	100
	UV/H_2O_2	39.4	100	100	96.0	100	100
	Cl_2	37.4	100	100	48.8	100	100
	O_3	36.5	-	100	92.0	100	100
	O_3/H_2O_2	36.6	-	100	95.1	100	100
BA	UV	16.7	100	100	81.1	100	100
	UV/H_2O_2	18.6	100	100	83.5	100	100
	Cl_2	21.2	100	100	28.7	100	100
	O_3	20.2	100	100	39.6	100	100
	O_3/H_2O_2	19.5	100	100	46.2	100	100

The total effectiveness of the combined process, globally considered, can be appreciated in Table 6, which also summarizes the final values obtained for the removals of the selected ECs, once both stages, chemical oxidation pre-treatment and NF process, were completed. It should be noted that CP and ML were completely removed in the pre-treatment. According to these results, global reductions higher than 95% were reached for CP, ML, NH and DT when the combined process was applied. The exception was BZ, which presented lower removals, specially with chlorine pre-treatment, and in those mater matrices

with high content of NOM such as BA water. Nevertheless, BZ global removal was above 80% when UV irradiation or the combination UV/H_2O_2 was applied as a pre-treatment. On the other hand, global removal of BZ with ozone pre-treatment depended on the water matrix composition, being lower in those waters with higher NOM content. Additionally, it must be also remarked the increases obtained in these global reductions by this sequence, in comparison to the single NF experiments of waters without any chemical pre-treatment (Table 3).

The evolution of DOC in this combined treatment was also evaluated, being the global removals depicted in Fig. 5. Thus, higher DOC removals were obtained for SW and BA waters (around 90%) than for LA water (in the range 70-80%), which can be due to the low DOC content of LA water (Table 2). In addition, it can be appreciated that the additional presence of H_2O_2 in the chemical pre-treatment enhanced slightly the removal of DOC due to the greater participation of OH radicals. In any case, DOC reduction by this combined treatment was higher than when single NF was applied, which highlights the positive influence of the chemical pre-treatment.
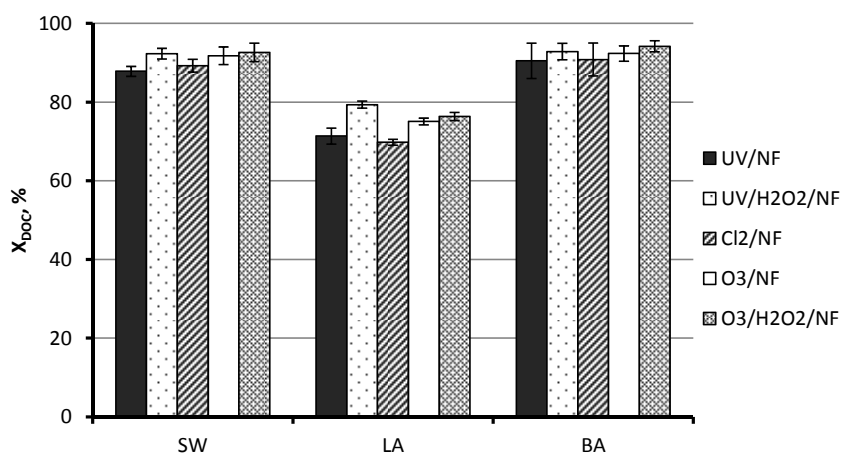

Figure 5. Removal of DOC after chemical pre-treatment followed by nanofiltration (HL membrane) of selected water matrices. UV irradiation time-30 min; chlorine dose-3.5 mg L^{-1}; ozone dose-2.25 mg L^{-1}; hydrogen peroxide dose-50 µM.

Therefore, the application of a chemical pre-treatment (ozone, UV irradiation or their combination with H_2O_2) exerts a positive influence on the subsequent NF process, not only in terms of ECs removal but also of DOC reduction. In addition, the NF process could remove some of the oxidation products formed in the chemical pre-treatment, some of which could be even more toxic than the parent compounds (Dolar et al., 2013; Sanches et al., 2013). The permeate thus generated has a good quality to be reused in many applications and the retentate might have better quality and higher biodegradability (Jansen et al., 2006) than without chemical pre-treatment, and therefore the need to further treat/dispose this retentate and the respective costs are also likely to decrease. An additional advantage of this combined process is that the chemical pre-treatment usually reduces membrane fouling in the later filtration stage (Van Geluwe et al., 2010).

4. CONCLUSIONS.

In this research, sequential chemical oxidation and filtration treatments were tested for the elimination of five selected emerging contaminants from different water matrices (one surface water and two secondary effluents). The application of UF and specially of NF pre-treatment provided a large volume of permeate with low amounts of NH, DT and BZ. The subsequent chemical treatment led to a further removal of residual ECs and DOC from the permeate, generating practically clean water (complete removal of ML, CP, NH and DT from the NF permeate). In addition, chlorination and specially ozonation have demonstrated to be effective for the reduction of emerging contaminants in the concentrated stream, thus generating an effluent that is prone to be easily purified by activated sludge in case it is recirculated back to the activated sludge treatment in WWTPs. Although the presence of NOM in the water matrices could benefit the retention of ECs in the filtration step, its presence exerted a negative influence on the subsequent chemical oxidation. The sequence of conversions obtained for both oxidants was ML > CP > NH > BZ > DT, which exactly agrees with the sequence of reaction rate constants of these ECs with both chlorine and ozone.

In the sequence chemical oxidation (UV radiation, UV/H_2O_2, ozone, O_3/H_2O_2 or chlorine) followed by NF, results of removals and rejection coefficients for the selected ECs

showed that the pre-treatment exerted a positive influence on the subsequent NF process, not only in terms of ECs removal but also of DOC reduction. Thus, while global removals higher than 97% were reached for ML, CP, NH and DT, lower values were obtained for BZ, specially for chlorine pre-treatment, and in those mater matrices with high content of natural organic matter. The NF treatment generated a permeate with good quality to be reused in many applications and a retentate with better quality and higher biodegradability than without chemical pre-treatment. Therefore, the need to further treat/dispose this retentate and the respective costs are likely to decrease.

By only considering an efficiency point of view, and without economic considerations, both sequences (UF or NF followed by chemical oxidation and chemical oxidation followed by NF) provided high levels of elimination for the selected ECs, as well as for DOC. Therefore, both sequential treatments are promising to remove the selected micropullutants while reducing the chlorine doses needed to achieve final water disinfection, thus decreasing also the formation of disinfection-byproducts.

REFERENCES

Acero, J.L.; Benítez, F.J.; Real, F.J.; Roldán, G.; Rodríguez, E. Chlorination and bromination kinetics of emerging contaminants in aqueous systems. Chem. Eng. J. **2013**, 219, 43-50.

Anwar Sadmani, A.H.M.; Andrews, R.C.; Bagley, D.M. Nanofiltration of pharmaceutically active compounds as a function of compound interactions with DOM fractions and cations in natural water. Sep. Purif. Technol. **2014**, 122, 462-471.

Benitez, F.J.; Acero, J.L.; Garcia-Reyes, F.J.; Real, F.J.; Roldán, G.; Rodriguez, E.; Molina-Diaz, A. Oxidation of chlorophene by ozonation: kinetics, identification of by-products and reaction pathways. Chem. Eng. J. **2013a**, 230, 447-455.

Benitez, F.J.; Acero, J.L.; Garcia-Reyes, F.J.; Real, F.J.; Roldán, G.; Rodriguez, E.; Molina-Diaz, A. Determination of the reaction rate constants and decomposition mechanisms of ozone

with two model emerging contaminants: DEET and nortriptyline. Ind. Eng. Chem. Res. **2013b**, 52, 17064-17073.

Benitez, F.J.; Acero, J.L.; Real, F.J.; Roldan, G.; Rodriguez, E. Ultrafiltration and nanofiltration membranes applied to the removal of the pharmaceuticals amoxicillin, naproxen, metoprolol and phenacetin from water. J. Chem. Technol. Biotechnol. **2011**, 86, 858-866.

Benitez, F.J.; Acero, J.L.; Real, F.J.; Roldán, G.; Rodriguez, E. Modeling the photodegradation of emerging contaminants in waters by UV radiation and UV/H_2O_2 system. J. Environ. Sci. Health A: Tox. Hazard. Subst. Environ. Eng. **2013c**, 48, 120-128.

Benitez, F.J.; Acero, J.L.; Real, F.J.; Roldán, G.; Rodriguez, E. Ozonation of benzotriazole and methylindole: Kinetic modeling, identification of intermediates and reaction mechanisms. J. Hazard. Mat. **2015**, 282, 224-232.

Bichsel, Y.; von Gunten, U. Determination of iodine and iodate by ion chromatography with postcolumn reaction and UV/visible detection. Anal. Chem. **1999**, 71, 34-38.

Buxton, G.V.; Greenstock, C.L.; Helman, W.P.; Ross. A.B. Critical review of rate constants for oxidation of hydrated electrons, hydrogen atoms and hydroxyl radicals (AOH/AO$^-$) in aqueous solutions. J. Phys. Chem. Ref. Data **1988**, 17, 513-886.

Canonica, S.; Meunier, L.; von Gunten, U. Phototransformation of selected pharmaceuticals during UV treatment of drinking water. Water Res. **2008**, 42, 121-128.

Comerton, A.M.; Andrews, R.C.; Bagley, D.M.; Hao, C. The rejection of endocrine disrupting and pharmaceutically active compounds by NF and RO membranes as a function of compound and water matrix properties. J. Membr. Sci. **2008**, 313, 323-335.

Costanzo, S.D.; Watkinson, A.J.; Murby, E.J.; Kolpin, D.W.; Sandstrom, M.W. Is there a risk associated with the insect repellent DEET (N,N-diethyl-m-toluamide) commonly found in aquatic environments?. Sci. Total Environ. **2007**, 384, 214-220.

Dolar, D.; Kosutic, K.; Perisa, M.; Babic, S. Photolysis of enrofloxacin and removal of its photodegradation products from water by reverse osmosis and nanofiltration membranes. Sep. Purif. Technol. **2013**, 115, 1-8.

Elovitz, M.S.; von Gunten, U. Hydroxyl radical/ozone ratios during ozonation processes. I. The R_{ct} concept. Ozone Sci. Eng. **1999**, 21, 239-260.

Heberer, T. Occurrence, fate and removal of pharmaceutical residues in the aquatic environment: a review of recent research data. Toxicol. Lett. **2002**, 131, 5-17.

Illueca-Muñoz, J.; Mendoza-Roca, J.A.; Iborra-Clar, A.; Bes-Pia, A.; Fajardo-Montañana, V.; Martinez-Francisco, F.J.; Bernacer-Bonora, I. Study of different alternatives of tertiary treatments for wastewater reclamation to optimize the water quality for irrigation reuse. Desalination **2008**, 222, 222-229.

James, C.P.; Germain, E.; Judd, S. Micropollutant removal by advanced oxidation of microfiltered secondary effluent for water reuse. Sep. Purif. Technol. **2014**, 127, 77-83.

Jansen, R.H.S.; Zwijnenburg, A.; van der Meer, W.G.J.; Wessling, M. Outside-in trimming of humic substances during ozonation in a membrane contactor. Environ. Sci. Technol. **2006**, 40, 6460-6465.

Jelic, A.; Gros, M.; Ginebreda, A.; Cespedes-Sanchez, R.; Ventura, F.; Petrovic, M.; Barcelo, D. Occurrence, partition and removal of pharmaceuticals in sewage water and sludge during wastewater treatment. Water Res. **2011**, 45, 1165-1176.

Kim, H.-A.; Choi, J-H.; Takizawa, S. Comparison of initial filtration resistance by pretreatment processes in the nanofiltration for drinking water treatment. Sep. Purif. Technol. **2007**, 56, 354-362.

Langford, K.H.; Thomas, K.V. Determination of pharmaceutical compounds in hospital effluents and their contribution to wastewater treatment works. Environ. Int. **2009**, 35, 766-770.

Linlin, W.; Xuan, Z.; Meng, Z. Removal of organic matter in municipal effluent with ozonation, slow sand filtration and nanofiltration as high quality pre-treatment option for artificial groundwater recharge. Chemosphere **2011**, 83, 693-699.

Loos, R.; Gawlik, B.M.; Locoro, G.; Rimaviciute, E.; Contini, S.; Bidoglio, G. EU wide survey of polar organic persistent pollutants in European river waters. Environ. Pollut. **2009**, 157, 561-568.

Perez-Gonzalez, A.; Urtiaga, A.M.; Ibañez, R.; Ortiz, I. State of the art and review on the tratment technologies of water reverse osmosis concentrates. Water Res. **2012**, 46, 267-283.

Rivera-Utrilla, J.; Sánchez-Polo, M.; Ferro-García, M.A.; Prados-Joya, G.; Ocampo-Pérez, R. Pharmaceuticals as emerging contaminants and their removal from water. A review. Chemosphere **2013**, 93, 1268-1287.

Sanches, S.; Penetra, A., Rodrigues, A.; Cardoso, V.V.; Ferreira, E.; Benoliel, M.J.; Barreto Crespo, M.T.; Crespo, J.G.; Pereira, V.J. Removal of pesticides from water combining low pressure UV photolysis with nanofiltration. Sep. Purif. Technol. **2013**, 115, 73-82.

Saquib, M.; Vinckier, C.; Van der Bruggen, B. The effect of UF on the efficiency of O_3/H_2O_2 for the removal of organics from surface water. Desalination **2010**, 260, 39-42.

Sharma, V.K. Oxidative transformation of environmental pharmaceuticals by Cl_2, ClO_2, O_3, and Fe (VI): Kinetics assessment. Chemosphere **2008**, 73, 1379-1386.

Sim, W-J.; Lee, J-W.; Lee, E-S.; Shin, S-K.; Hwang, S-R.; Oh, J-E. Occurrence and distribution of pharmaceuticals in wastewater from households, livestock farms, hospitals and pharmaceutical manufactures. Chemosphere **2011**, 82, 179-186.

Staehelin, J.; Hoigne, J. Decomposition of ozone in water in the presence of organic solutes acting as promoters and inhibitors of radical chain reactions. Environ. Sci. Technol. **1985**, 19, 1206-1213.

Tijani, O.J.; Fatoba, O.O.; Madzivire, G.; Petrik, L.F. A Review of combined advanced oxidation technologies for the removal of organic pollutants from water. Water Air Soil Pollut. **2014**, 225, 2102-2132.

Tijani, O.J.; Fatoba, O.O.; Petrik, L.F. A review of pharmaceuticals and endocrine-disrupting compounds: sources, effects, removal and detections. Water Air Soil Pollut. **2013**, 224, 1770-1809.

Van der Bruggen, B.; Manttari, M.; Nystrom M. Drawbacks of applying nanofiltration and how to avoid them: a review. Sep. Purif. Technol. **2008**, 63, 251-263.

Van Geluwe, S.; Vinckier, C.; Bobu, E.; Trandafir, C.; Vanelslander, J.; Braeken, L.; Van der Bruggen, B. Eightfold increased membrane flux of NF 270 by O_3 oxidation of natural humic acids without deteriorated permeate quality. J. Chem. Technol. Biotechnol. **2010**, 85, 1480-1488.

von Gunten, U. Ozonation of drinking water. Part I. Oxidation kinetics and product formation. Water Res. **2003**, 37, 1443-1467.

Wray, H.E.; Andrews, R.C.; Bérubé, P.R. Surface shear stress and retention of emerging contaminants during ultrafiltration for drinking water treatment. Sep. Purif. Technol. **2014**, 122, 183-191.

4. CONCLUSIONS/CONCLUSIONES

CONCLUSIONS

The results obtained from the present Ph.D. Thesis work, focused on the removal of selected emerging contaminants dissolved in different water matrices by means of physico-chemical treatments, have permitted to establish the following general conclusions:

o   UVC radiation and the individual chemical oxidants used (ozone, chlorine and bromine) are adequate for the removal of methylindole, chlorophene and nortriptyline hydrochloride, and to a certain extent, for benzotriazole. However, these processes are not effective options for DEET removal. The following reactivity order for the individual oxidants is deduced: ozone > bromine > chlorine. Thus, the highest removals of contaminants under conditions typically applied in water treatment were reached with ozone.

o   The advanced oxidation processes used in this research were effective in the removal of four of five selected contaminants (chlorophene, methylindole, and nortriptyline hydrochloride, and in a lesser extent, benzotriazole). However, DEET, which is the most refractory compound toward such processes, could not be efficiently removed. Concretely, advanced oxidation processes based on ozone were the most efficient treatments to remove the selected compounds from natural waters. Other AOPs, such as UV/TiO_2 and UV/H_2O_2, were also effective to eliminate the emerging contaminants from water matrices, due to the important generation of OH radicals.

o   The efficiency of these oxidation processes was also influenced by the characteristics of the water matrices investigated. In general, a decrease in the degradation level of contaminants was observed in waters with higher NOM content. Such NOM competes with contaminants in the oxidation reactions and thus increases the consumption of oxidants.

o Numerous by-products were generated in the degradation reactions of selected contaminants with UVC and ozone. The application of the kinetic data determined in this work, as well as the results derived from the study of identification of by-products and toxicity analysis, offers valuable information in order to elucidate the most adequate process at real scale. In addition, an economical study is also necessary to assess the overall process cost.

o Membrane technologies used in this research were effective in the removal of the selected contaminants, specially for chlorophene, methylindole and nortriptyline hydrochloride, being a suitable technique for this purpose in water treatment plants. However, a lower retention of benzotriazole was observed, which difficult the application of membrane technologies for its removal.

o The main retention mechanism of emerging contaminants with UF membranes was adsorption. Among all the UF membranes used, the most efficient was the PT membrane (5 kDa). In the nanofiltration process, size exclusion and electrostatic repulsion at high pH were the dominant retention mechanisms, being the HL membrane the most efficient for contaminants and NOM removal. In addition, the presence of NOM increased the retention of emerging contaminants, probably due to their interaction with humic acids.

o The application of the PAC/UF process enhanced the removals reached by single ultrafiltration, not affecting significantly the permeate flux in any of the water matrices employed. The sequence of retention of the emerging contaminants obtained was: benzotriazole < DEET < methylindole < nortriptyline hydrochloride < chlorophene, which corresponds with their hydrophobic character and aromaticity.

o With respect to the sequential application of different physico-chemical processes, a chemical pre-treatment followed by NF led to higher elimination levels of emerging contaminants and NOM. The best results were reached when the sequential processes UV/NF, UV/H_2O_2/NF and O_3/NF were applied, which produced a high quality final effluent. In addition, the chemical pre-treatment decreased the membrane fouling in the subsequent filtration step. This sequence

could be an alternative to the ozonation step followed by activated carbon used in real drinking water plants.

o   The sequence constituted by a NF step followed by the oxidation of the resulting permeate led also to a final effluent free of contaminants except benzotriazole. The sequence UF/chemical oxidation resulted in a total removal of nortriptyline hydrochloride, methylindole and chlorophene, but not of benzotriazole and DEET. The reduction of TOC in these combined processes was also significant. Another advantage of this sequence is that the oxidation step is applied only to the permeate fraction, and as a result, a final effluent with good quality is obtained, which can be reused to many applications.

o   The retentate stream generated after the filtration step could be treated adequately by means of a chemical oxidation process with ozone. The resulting effluent, practically free of emerging contaminants and with higher biodegradability, can be recirculated to the biological process in case of urban wastewater treatment plants.

o   The final choice of the most adequate treatment for the removal of the selected emerging contaminants from aquatic systems will depend on several factors: the characteristics of the water matrix and the nature of pollutants which are present in the aqueous system, the global cost of installation and oxidizing reagents to be employed, as well as on the by-products generated and their toxicity. Therefore, a detailed economical study is required to determine the most appropriate treatment train.

CONCLUSIONES

Los resultados obtenidos en este trabajo de investigación, centrado en la eliminación de diversos contaminantes emergentes seleccionados y disueltos en diferentes matrices acuosas mediante procesos físico-químicos, han permitido establecer las siguientes conclusiones generales:

o   Tanto la radiación UVC como los agentes oxidantes individuales utilizados (ozono, cloro y bromo) son adecuados para eliminar metilindol, clorofeno y nortriptilina clorhidrato, pero resultan moderadamente apropiados para la eliminación de benzotriazol y muy poco adecuados para la eliminación de DEET. Se deduce el siguiente orden de reactividades de tales oxidantes individuales: ozono > bromo > cloro. Concretamente, ozono fue el oxidante que mostró eliminaciones superiores de los contaminantes cuando se aplicaron condiciones típicas del tratamiento de aguas.

o   Por su parte, los procesos de oxidación avanzada empleados fueron efectivos en la eliminación de cuatro de estos cinco contaminantes modelo (clorofeno, metilindol, nortriptilina clorhidrato y en menor medida benzotriazol), pero no para DEET, que fue el compuesto más refractario a la acción de tales procesos. Concretamente, aquellos procesos basados en el uso de ozono resultaron ser los más eficaces en las aguas reales. Asimismo, otros POAs, como UV/TiO_2 y UV/H_2O_2, fueron también efectivos para la eliminación de los contaminantes seleccionados, debido a la importante generación de radicales OH.

o   La eficacia de los procesos de oxidación se vio también influida por las matrices acuosas empleadas, observándose un descenso en la degradación de contaminantes cuanto mayor era el contenido de materia orgánica disuelta en las mismas. Dicha materia orgánica compite con los contaminantes en las reacciones de oxidación y aumenta así el consumo de los oxidantes.

o Se ha formado una amplia gama de subproductos en las reacciones de degradación de los contaminantes mediante radiación UVC y ozono. La aplicación de los datos cinéticos determinados en este trabajo, así como los resultados del estudio de los subproductos identificados y los análisis de toxicidad, constituyen una información valiosa para dilucidar el tratamiento químico más adecuado a llevar a cabo escala real, en cuya decisión también habrá que tener en cuenta el coste global del proceso, que se determinará mediante el correspondiente estudio económico.

o Las tecnologías de membrana usadas en esta investigación fueron efectivas en la eliminación de la mayoría de los contaminantes emergentes seleccionados, especialmente para clorofeno, metilindol y nortriptilina clorhidrato, siendo por tanto aptas para ser usadas con este fin en plantas de tratamiento de agua. Sin embargo, el nivel de retención de benzotrialzol resultó ser muy bajo, lo que dificulta la aplicación de la filtración mediante membranas para su eliminación.

o El principal mecanismo de retención de los contaminantes en ultrafiltración fue la adsorción, siendo la membrana PT (5 kDa) la más eficaz entre las estudiadas. Por su parte, en nanofiltración, la exclusión molecular y las repulsiones electrostáticas a elevados valores de pH son los mecanismos de retención dominantes, siendo la membrana HL la más eficaz, tanto para la retención de los contaminantes seleccionados como de la materia orgánica. Además, la presencia de NOM incrementó la retención de los compuestos, probablemente debido a la interacción de estos con los ácidos húmicos.

o El empleo del proceso combinado PAC/UF proporcionó una mayor eficacia en la retención de los compuestos seleccionados, no afectando significativamente al flujo de permeado en ninguna de las matrices empleadas. La secuencia de retención de los contaminantes en este proceso fue: benzotriazol < DEET < metilindol < nortriptilina clorhidrato < clorofeno, la cual se corresponde con el carácter hidrófobo y con la aromaticidad de los compuestos.

o En cuanto a la combinación de diferentes técnicas físico-químicas de forma secuencial, la aplicación de una etapa previa de oxidación química y un posterior

tratamiento de nanofiltración de la solución resultante resultó muy eficaz en la eliminación de contaminantes y de NOM. Los mejores resultados se obtuvieron al aplicar los tratamientos UV/NF, UV/H_2O_2/NF y O_3/NF, los cuales generan un efluente final de elevada calidad y disminuyen el ensuciamiento de la membrana en la posterior etapa de filtración. Esta secuencia de tratamientos podría ser una alternativa a las etapas de ozonación seguida de adsorción sobre carbón activado que se emplean en la actualidad en un gran número de plantas de potabilización.

o Por su parte, la secuencia constituida por una etapa de NF seguida de oxidación química del permeado proporcionó un efluente exento de contaminantes emergentes, excepto de benzotriazol. Asimismo, en el proceso secuencial de una etapa de UF seguida de oxidación del permeado se logró la eliminación total de nortriptilina, metilindol y clorofeno, pero no de benzotriazol y DEET. La reducción de TOC en estos procesos secuenciales fue asimismo significativa. En esta secuencia, la etapa química solo se aplicaría a la fracción del permeado, generando un efluente de gran calidad apto para ser reutilizado en diversos usos.

o La corriente de retenido generada tras la etapa de filtración puede ser tratada adecuadamente mediante una etapa de oxidación química con ozono. El efluente resultante, prácticamente exento de contaminantes emergentes y con una mayor biodegradabilidad, puede ser recirculado al tratamiento secundario en el caso de depuración de aguas residuales urbanas.

o Finalmente, se concluye que la elección final del tratamiento más adecuado para la eliminación de los contaminantes emergentes seleccionados presentes en matrices acuosas dependerá de múltiples factores: características del agua a tratar y de los contaminantes específicos presentes en la misma, coste global de las instalaciones necesarias y de los agentes oxidantes a emplear, así como de la generación de intermedios de reacción y su toxicidad. En consecuencia, resulta imprescindible realizar un detallado estudio económico para determinar la secuencia de tratamiento óptima en cada caso.

5. PUBLICACIONES

PUBLICACIONES

Benítez, F.J.; Acero, J.L.; Real, F.J.; Roldán, G.; Rodríguez, E. Photolysis of model emerging contaminants in ultra-pure water: Kinetics, by-products formation and degradation pathways. Water Res. **2013**, 47, 870-880.

Benítez, F.J.; Acero, J.L.; Real, F.J.; Roldán, G.; Rodríguez, E. Modeling the photodegradation of emerging contaminants in waters by UV radiation and UV/H_2O_2 system. J. Environ. Sci. Health A. **2013**, 48, 120-128.

Acero, J.L.; Benítez, F.J.; Real, F.J.; Roldán, G.; Rodríguez, E. Chlorination and bromination kinetics of emerging contaminants in aqueous systems. Chem. Eng. J. **2013**, 219, 43-50.

Benítez, F.J.; Acero, J.L.; García-Reyes, F.J.; Real, F.J.; Roldán, G.; Rodriguez, E; Molina-Diaz, A. Determination of the reaction rate constants and decomposition mechanisms of ozone with two model emerging contaminants: DEET and nortriptyline. Ind. Eng. Chem. Res. **2013**, 52, 17064-17073.

Benítez, F.J.; Acero, J.L.; García-Reyes, F.J.; Real, F.J.; Roldán, G.; Rodriguez, E; Molina-Diaz, A. Oxidation of chlorophene by ozonation: Kinetics, identification of by-products and reaction pathways. Chem. Eng. J. **2013**, 230, 447-455.

Benítez, F.J.; Acero, J.L.; Real, F.J.; Roldán, G.; Rodríguez, E. Ozonation of benzotriazole and methylindole: kinetic modeling, identification of intermediates and reaction mechanisms. J. Hazard. Mat. **2015**, 282, 224-232.

Benítez, F.J.; Acero, J.L.; Real, F.J.; Roldán, G.; Rodríguez, E. The effectiveness of single oxidants and AOPs in the degradation of emerging contaminants in waters: a comparison study. Ozone Sci. Eng. **2013**, 35, 263-272.

Photolysis of model emerging contaminants in ultra-pure water: Kinetics, by-products formation and degradation pathways

F. Javier Benitez*, Juan L. Acero, Francisco J. Real, Gloria Roldan, Elena Rodriguez

Departamento de Ingeniería Química, Universidad de Extremadura, Facultad de Ciencias, 06071 Badajoz, Spain

ARTICLE INFO

ABSTRACT

The photolysis of five frequent emerging contaminants (Benzotriazole, Chlorophene, N,N-diethyl-m-toluamide or DEET, Methylindole, and Nortriptyline HCl) was investigated in ultra-pure water under monochromatic ultraviolet radiation at 254 nm and by a combination of UV and hydrogen peroxide. The results revealed that the photolysis rates followed first-order kinetics, with rate constant values depending on the nature of the specific compound, the pH, and the presence or absence of the scavenger tert-butanol. Quantum yields were also determined and values in the range of $53.8 \times 10^{-3} - 9.4 \times 10^{-3}$ mol E^{-1} for Benzotriazole, $525 \times 10^{-3} - 469 \times 10^{-3}$ mol E^{-1} for Chlorophene, $2.8 \times 10^{-3} - 0.9 \times 10^{-3}$ mol E^{-1} for DEET, $108 \times 10^{-3} - 165 \times 10^{-3}$ mol E^{-1} for Methylindole, and $13.8 \times 10^{-3} - 15.0 \times 10^{-3}$ mol E^{-1} for Nortriptyline were obtained. The study also found that the UV/H₂O₂ process enhanced the oxidation rate in comparison to direct photolysis. High-performance liquid chromatography coupled to electrospray ionization quadrupole time-of-flight mass spectrometry (HPLC-ESI-QTOF-MS) technique was applied to the concentrations evaluation and further identification of the parent compounds and their by-products, which allowed the proposal of the degradation pathways for each compound. Finally, in order to assess the aquatic toxicity in the photo-degradation of these compounds, the *Vibrio fischeri* acute toxicity test was used, and the results indicated an initial increase of this parameter in all cases, followed by a decrease in the specific case of Benzotriazole, DEET, Methylindole, and Chlorophene.

1. Introduction

The so-called emerging contaminants (ECs) is a wide group of numerous chemical substances, that includes prescription and therapeutic drugs (pharmaceuticals), veterinary drugs, dietary supplements, consumer products such as fragrances, topical agents such as cosmetics and sunscreens (personal care products), laundry and cleaning products, flame retardants, corrosion inhibitors, etc. Once they are consumed by humans for personal health or cosmetic reasons, and also, by agribusiness to enhance growth or health of livestock, they are incorporated into the water environment in a variety of ways. Their presence in water effluents is mainly attributed to their incomplete removal through conventional methods in wastewater treatment plants (Suárez et al., 2008), and consequently, these compounds are increasingly found in water systems (Nakada et al., 2007), affecting the quality of drinking water supplies (Heberer, 2002). Therefore, a public health concern has recently increased in relation to this problem, since little is known about potential effects of these

Taylor & Francis
Taylor & Francis Group

Modeling the photodegradation of emerging contaminants in waters by UV radiation and UV/H$_2$O$_2$ system

F. JAVIER BENITEZ, JUAN L. ACERO, FRANCISCO J. REAL, GLORIA ROLDAN and ELENA RODRIGUEZ

Departamento de Ingeniería Química, Universidad de Extremadura, Badajoz, Spain

Five emerging contaminants (1-H-Benzotriazole, N,N-diethyl-m-toluamide or DEET, Chlorophene, 3-Methylindole, and Nortriptyline HCl), frequently found in surface waters and wastewaters, were selected to be photooxidized in several water matrices. Previous degradation experiments of these compounds individually dissolved in ultra pure water were performed by using UV radiation at 254 nm and the Fenton's reagent. These oxidation systems allowed the determination of the quantum yields and the rate constants for the radical reaction between each compound and hydroxyl radicals. Later, the simultaneous photodegradation of mixtures of the selected ECs in several types of water (ultrapure water, reservoir water, and two effluents from WWTPs) was carried out and a kinetic study was conducted. A model is proposed for the ECs elimination, and the theoretically calculated concentrations with this model agreed well with the experimental results obtained, which confirmed that it constitutes an excellent tool to predict the elimination of these compounds in waters.

Keywords: Emerging contaminants (ECs), UV radiation, quantum yields and radical rate constants, natural waters, prediction of elimination.

Introduction

Emerging contaminants (ECs) constitute a diverse group of numerous chemical substances that include nanomaterials, pesticides, pharmaceuticals and personal care products, industrial compounds, fragrances water treatment by-products, flame retardants and surfactants, etc.[1] These products have been labelled as emerging contaminants, which means that they are still unregulated or in the process of being regulated. They are frequently found in treated wastewater, surface and ground waters, and even in drinking water,[2,3] although their main source is through municipal sewage, because it is recognized that wastewater treatment plant technologies are very often unable to entirely degrade such persistent substances. Consequently, they accumulate in the aquatic environment where they may cause ecological risk,[4] such as interferences with endocrine system of higher organisms, micro-biological resistance and accumulation in soil, plants and animals.[5]

An increasing public health concern has grown in relation to these compounds, since little is known about their potential effects in humans and animals; and their elimination from waters, together with other priority pollutants,

is an emerging issue in environmental technology. Consequently, alternative advanced technologies for tertiary treatment of WWTP effluents are necessary. In this way, single oxidation treatments and advanced oxidation processes (AOPs) have been proposed as valuable methods for the elimination of persistent organic compounds, because unselective hydroxyl radicals are able to promote organic matter oxidation at high reaction rates.

Among the chemical procedures tested, UV radiation is very effective and widely applied to induce photoreactions of organic pollutants in advanced water treatment technologies for groundwater and drinking water remediation.[6] For this purpose, mercury lamps emitting at 254 nm are the UV sources most commonly used. Additionally, the use of UV radiation in combination with hydrogen peroxide is also a very promising technique for the oxidative degradation of organic compounds. In that case, the UV radiation dissociates H$_2$O$_2$ and generates hydroxyl radicals which can oxidize organic compounds more effectively.[7]

Although some information on the removal of ECs using UV radiation is reported in the literature,[8, 9] this information is not abundant, even nonexistent for some specific substances. With these considerations in mind, the present study was designed with the main objective to investigate the degradation, during single UV and combined UV/H$_2$O$_2$ treatments, of five selected ECs commonly found in water environments. These ECs, whose

Address correspondence to F. Javier Benitez, Departamento de Ingeniería Química, Universidad de Extremadura, Badajoz, Spain; E-mail: javben@unex.es

Chlorination and bromination kinetics of emerging contaminants in aqueous systems

Juan L. Acero *, F. Javier Benitez, Francisco J. Real, Gloria Roldan, Elena Rodriguez

Universidad de Extremadura, Departamento de Ingeniería Química, 06006 Badajoz, Spain

HIGHLIGHTS

► Chlorination and bromination kinetics of emerging contaminants was investigated.
► Apparent rate constants were pH dependent and the primary oxidant species was HOCl.
► Chlorine was specially efficient for the removal of 3-Methylindole and Chlorophene.
► The additional presence of bromide enhanced slightly the chlorination of ECs.

ABSTRACT

Second-order rate reaction constants of micropollutants with chlorine are essential for evaluating their removal efficiencies from water during chlorine disinfection. In this study, the reactions of five selected emerging contaminants with unavailable kinetic data (Benzotriazole, N,N-diethyl-m-toluamide or DEET, Chlorophene, 3-Methylindole, and Nortriptyline HCl) with chlorine and bromine have been investigated, and their apparent second-order rate constants have been determined as a function of the pH. For the chlorination process, the intrinsic rate constants for the elementary reactions of the ionized and neutral species were also evaluated. The sequence of reaction rates was Methylindole > Chlorophene > Nortriptyline HCl > Benzotriazole > DEET. The bromination of the selected emerging contaminants in ultra-pure water provided exactly the same sequence of reaction rates as in the chlorination process, although higher values of rate constants. The efficiency of the chlorination process for the degradation of these ECs when present in several aqueous systems (surface water from a public reservoir, and two effluents from municipal wastewater treatment plants) was investigated. During wastewater or drinking water treatment, chlorine is a good option for the degradation of Methylindole, and in a lower extent for Chlorophene and Nortriptyline. However, it is not a suitable oxidant for the abatement of Benzotriazole and DEET. Finally, chlorination in the presence of bromide revealed that low bromide concentrations enhanced slightly the degradation of the selected compounds during chlorine oxidation.

© 2013 Elsevier B.V. All rights reserved.

1. Introduction

Chemical oxidants are commonly used in water treatments because of their potential for destruction of micropollutants. Some of the oxidation systems include UV radiation, ozonation, and advanced oxidation processes (AOPs), such as O_3/H_2O_2, UV/H_2O_2 or Fenton's reagent. Most of these AOPs have demonstrated high effectiveness in the degradation of organic compounds present in water systems which are oxidized to readily biodegradable and less toxic compounds [1]. Although less reactive than ozone, chlorine (Cl_2) as gaseous chlorine or hypochlorite has also been

frequently used in water treatments [2,3]. Chlorine hydrolyzes in water and forms hypochlorous acid:

$$Cl_2 + H_2O \rightarrow HOCl + Cl^- + H^+ \tag{1}$$

Moreover, hypochlorous acid is a weak acid that dissociates in aqueous solutions:

$$HOCl \iff ClO^- + H^+ \tag{2}$$

This equilibrium presents a dissociation constant $K_{HOCl} = 2.9 \times 10^{-8}$ ($pK_a = 7.54$ at 25 °C). In the pH range 6–9 (typical of water treatment conditions), hypochlorous acid and hypochlorite are the main chlorine species present [3]. Besides its low cost, the great advantage of chlorine is the reaction with numerous inorganic and organic micropollutants present in waters. However, its main

Taylor & Francis
Taylor & Francis Group

The Effectiveness of Single Oxidants and AOPs in the Degradation of Emerging Contaminants in Waters: A Comparison Study

F. Javier Benitez, Juan L. Acero, Francisco J. Real, Gloria Roldán, and Elena Rodríguez

Departamento de Ingeniería Química, Universidad de Extremadura, Badajoz 06006, Spain

The effectiveness of single oxidants and several AOPs was studied for the degradation of five selected emerging contaminants: Benzotriazole, N,N-diethyl-m-toluamide or DEET, Chlorophene, 3-Methylindole and Nortriptyline HCl. First-order rate constants and half-life times for the degradation of each compound in ultra-pure water were deduced and compared. The AOPs were later applied to the degradation of these ECs present in three real waters: public reservoir water, and two secondary effluents from municipal wastewater plants. The effect of the variables on the ECs elimination was established. Finally, a cost estimation based on the operating costs was established for the degradation of 3-Methylindole by the single oxidants and AOPs tested.

Keywords   Ozone, UV Radiation, AOPs, Emerging Contaminants, Rate Constants, Real Waters, Costs Estimation

INTRODUCTION

The term emerging contaminants (ECs) is generally used for a large group of substances that constitute a new kind of aquatic pollutants. They include a wide array of different compounds: prescription and therapeutic drugs, veterinary drugs, dietary supplements, consumer products such as fragrances, topical agents such as cosmetics and sunscreens, laundry and cleaning products, etc. (Bolong et al. 2009). Nowadays, they have been increasingly detected in groundwaters and surface waters and have the potential to cause known or suspected adverse ecological or human health effects (Stuart et al. 2012).

At present times, availability and quality of water constitutes an important problem in the world. Therefore, it is essential the optimization of resources, as well as the economically competitive reuse of waters in order to avoid environmental

impacts (Klamerth et al. 2009). Within this general problem, numerous recent studies are found in the literature which are focused in the elimination, or at least partial degradation, of micropollutants in general and ECs in particular from waters. These studies find that conventional biological treatments and coagulation–flocculation processes have not obtained satisfactory results in the elimination of such as pollutants (Westerhoff et al. 2005). Meanwhile, several researchers have shown great interest in alternatives technologies, such as membrane operations (Dolar et al. 2012), adsorption (Rossner et al. 2009), chemical oxidations by single oxidants (Acero et al. 2010), and Advanced Oxidation Processes (AOPs) (De la Cruz et al. 2012; Prieto-Rodriguez et al. 2012; Rodriguez et al. 2011; etc.). Specifically, these AOPs have proved to be very efficient, because they generate hydroxyl radicals, which are able to even mineralize most organic molecules, yielding CO_2 and inorganic ions as final products (Klamerth et al. 2010).

With these considerations in mind, a wide research study was designed for the removal from waters of five frequent ECs whose chemical structures are shown in Figure 1. The selected compounds were: Benzotriazole (BZ), an effective corrosion inhibitor for copper and iron, widely used in cooling and hydraulic fluids, antifreezing products, aircraft deicer and anti-ice fluid, dishwasher detergents, antifogging agents and intermediates for the synthesis of various chemicals (Ding et al. 2010); N,N-diethyl-m-toluamide or DEET (DT), major component of most topically applied insect repellents (Costanzo et al. 2007); Chlorophene (CF), a widespread broad-spectrum antimicrobial pharmaceutical, commonly used in hospitals and households for general cleaning and disinfecting, as well as in industrial and farming environments as an active agent in disinfectant formulations (Sires et al. 2007); 3-Methylindole (ML), used in the production of pharmaceuticals, cosmetics, pesticides, disinfectants, agrochemicals and dyestuffs (Gu et al. 2002); and

CrossMark

Oxidation of chlorophene by ozonation: Kinetics, identification of by-products and reaction pathways

F.J. Benitez [a,*], J.L. Acero [a], J.F. Garcia-Reyes [b], F.J. Real [a], G. Roldan [a], E. Rodriguez [a], A. Molina-Díaz [b]

[a] Chemical Engineering Department, University of Extremadura, 06006 Badajoz, Spain
[b] Analytical Chemistry Research Group, University of Jaén, 23071 Jaén, Spain

HIGHLIGHTS

- Ozonation of chlorophene, a model emerging contaminants (ECs) is investigated.
- Apparent second order rate constants are determined for each pH of work.
- 24 Intermediates by-products are indentified.
- The degradation pathways are proposed for the ozonation reaction.
- Toxicity measurements show a decrease in the pollutant content of the water.

ARTICLE INFO

ABSTRACT

The ozonation of chlorophene, an emerging contaminant frequently present in aquatic systems because of its numerous uses nowadays, is studied. The kinetic experiments allowed the determination of the apparent rate constants for its reaction with ozone in the pH range 3–11. The rate constants values obtained varied from 1.67×10^3 L mol^{-1} s^{-1} at pH = 3 to 1.82×10^5 L mol^{-1} s^{-1} at pH = 11. As a consequence of its acidic nature (pK_a = 9.81), the degree of dissociation of this pollutant was determined at every pH of work, and the specific rate constants of the neutral and anionic species were evaluated, being these rate constants $k_1 = 2.8 \times 10^3$ L mol^{-1} s^{-1} and $k_2 = 2.5 \times 10^5$ L mol^{-1} s^{-1}. Up to 24 by-products formed in the ozonation reaction were identified by liquid chromatography/mass spectrometry using a high-resolution time of flight analyzer (LC-TOFMS). From these intermediates identified, the degradation pathways are proposed and discussed. Toxicity measurements of the ozonated chlorophene solutions revealed that these by-products are less toxic than the parent compound.

© 2013 Elsevier B.V. All rights reserved.

1. Introduction

Emerging contaminants (ECs) is a wide group of chemical substances, that includes prescription and therapeutic drugs (pharmaceuticals), veterinary drugs, dietary supplements, consumer products, cosmetics and sunscreens (personal care products), laundry and cleaning products, and corrosion inhibitors. One of these ECs is chlorophene, a halogenated phenolic compound that presents multiple applications: in personal care, in household products for general cleaning and disinfecting, as antimicrobial substance, and as an active agent in disinfectant formulations in industrial and farming environments [1–3]. Due to these numerous usages, it is inevitably discharged into aquatic systems in the environment, Similarly to the rest of chlorophenols, it is toxic and poorly biodegradable, and therefore, remains for long periods in

the environment, in both, soils and waters [4]. Chlorophene concentrations of 50 mg L^{-1} have been found in activated sludge sewage systems, as well as 10 µg L^{-1} in sewage treatment plant effluent and rivers [5].

In order to avoid the accumulation in the environment of ECs in general, and chlorophene in particular, there is an increasing interest in developing new technologies for their removal. Specifically for the elimination of chlorophene from waters, several studies can be found in the literature, which are focused in the degradation of this compound by a variety of chemical procedures, such as oxidation by manganese oxides [2], oxidation by the combined system Fe^{3+}/Fe^{2+} [5] or photochemical degradation [4]. More recently, two studies focused on the chemical degradation of five model ECs, including chlorophene, by UV radiation by itself or combined with H$_2$O$_2$ [6], and by chlorine [7], have been reported.

Inside this general field of work, focused on the application of chemical oxidation processes, other different oxidation technologies are recommended to be tested for the elimination of this

---

* Corresponding author. Tel.: +34 924289384; fax: +34 924289385.
  E-mail address: javben@unex.es (F.J. Benitez).

I&EC research
Industrial & Engineering Chemistry Research

Determination of the Reaction Rate Constants and Decomposition Mechanisms of Ozone with Two Model Emerging Contaminants: DEET and Nortriptyline

F. Javier Benitez,*,[†] Juan L. Acero,[†] Juan F. Garcia-Reyes,[‡] Francisco J. Real,[†] Gloria Roldan,[†] Elena Rodriguez,[†] and Antonio Molina-Díaz[‡]

[†]Chemical Engineering Department, Universidad de Extremadura, Badajoz 06006, Spain
[‡]Analytical Chemistry Research Group, Universidad de Jaen, Jaen 23071, Spain

Ⓢ Supporting Information

ABSTRACT: Two representative substances of the so-called emerging compounds group (ECs), N,N-diethyl-m-toluamide (DEET) and nortriptyline hydrochloride, were selected to be subjected to ozonation processes, which constitute promising technologies for the removal of hazardous pollutants. The kinetic study provided ozonation rate constants, with an average value of 0.123 ± 0.003 $L \cdot mol^{-1} \cdot s^{-1}$ for DEET, which remained almost unaffected with the pH; while values varying from 2.40×10^3 to 472×10^3 $L \cdot mol^{-1} \cdot s^{-1}$ for nortriptyline were deduced in the pH range 2−11. Because of the ionic nature of nortriptyline, the specific rate constants of the protonated and neutral species were determined, the values obtained being 2.1×10^3 and 4.3×10^5 $L \cdot mol^{-1} \cdot s^{-1}$, respectively. By means of liquid chromatography time-of-flight mass spectrometry analysis, the main byproducts formed in the ozonation reactions were identified (14 for DEET and 27 for nortriptyline), and the evolution of their concentrations with reaction time were established. According to these compounds and their concentration profiles, the reaction mechanisms for the ozonation of both emerging contaminants were proposed and discussed. A decrease in the toxicity was also observed during ozonation of nortriptyline.

1. INTRODUCTION

Chemical oxidation technologies are currently applied to the removal of recalcitrant pollutants present in waters because of the potential for the elimination of these substances. Among these oxidation systems, are single oxidants such as UV irradiation, ozone, chlorine, and hydrogen peroxide, or combinations of these oxidants in the advanced oxidation processes, such as O_3/H_2O_2, UV/H_2O_2, Fenton/photo-Fenton systems, and UV/TiO_2.[1,2] Recently, cavitation,[3] a modern technique consisting of the formation, growth, and subsequent collapse of cavities that release large magnitudes of energy locally and generate strong oxidizing conditions has been incorporated to these oxidation processes. All of these systems have been frequently used with success and have demonstrated high effectiveness in the elimination of contaminants that are selectively oxidized to readily biodegradable and less toxic compounds.[4,5] However, in some cases, these oxidants can generate potentially harmful byproducts which could be very reactive toward some substances present in the water systems, as it has recently been pointed out.[6,7]

Among these single oxidants, ozone constitutes an efficient agent for the purification of surface and drinking waters,[8,9] because of its reactivity toward most organic pollutants which are present in aquatic environments. As it is known, in addition to this direct reaction with most of the organic compounds, its self-decomposition produces OH radicals, which constitute a powerful oxidant. Accordingly, in an ozonation process both direct ozone and OH radical pathways must be considered, since molecular O_3 is very selective, whereas OH radicals react indiscriminately with organic molecules.[10,11]

Recently, a new group of chemicals which are called emerging contaminants (ECs) has increased its presence in aquatic environments and represents an important source of pollution. This group includes different kinds of substances, such as pesticides, pharmaceuticals, and personal care products, endocrine disruptors, industrial compounds, fragrances, water treatment byproducts, flame retardants, and surfactants, etc.[12] The domination of emerging contaminants is due to the fact that most of these substances are still unregulated or in the process of being regulated. Because of their persistence in aquatic environments, some ECs may cause ecological harm and develop antimicrobial resistance. The health effects of small amounts of these agents on humans over a lifetime of exposure are unknown at this time. Municipal wastewater is a significant source of ECs in the environment because many of them are not removed completely in conventional wastewater treatment plants. The literature shows a wide range of many classes of ECs (e.g., antibiotics, betablockers, antiepileptics, liquid regulators, etc.) in wastewater effluents and receiving waters.[13] As a consequence of these problems, the elimination of ECs is currently pursued, and the use of chemical oxidation procedures could be effective technologies that are highly recommended for this objective.

Among the numerous substances included in this group, two emerging contaminants were selected in the present work for

Ozonation of benzotriazole and methylindole: Kinetic modeling, identification of intermediates and reaction mechanisms

CrossMark

F. Javier Benitez*, Juan L. Acero, Francisco J. Real, Gloria Roldán, Elena Rodríguez

Departamento de Ingeniería Química, Universidad de Extremadura, Avenida de Elvas S/N, 06006 Badajoz, Spain

HIGHLIGHTS

- The ozonation of ECs benzotriazole and methylindole, is investigated.
- Apparent second order rate constants are determined in the pH range 3–10.
- Eight intermediates for benzotriazole and six intermediates for methylindole are identified.
- Degradation pathway mechanisms are proposed for the ozonation reactions.
- The ozonation reactions in water systems are modeled.

ARTICLE INFO

ABSTRACT

The ozonation of $1H$-benzotriazole (BZ) and 3-methylindole (ML), two emerging contaminants that are frequently present in aquatic environments, was investigated. The experiments were performed with the contaminants (1 μM) dissolved in ultrapure water. The kinetic study led to the determination of the apparent rate constants for the ozonation reactions. In the case of $1H$-benzotriazole, these rate constants varied from $20.1 \pm 0.4 \, M^{-1} \, s^{-1}$ at pH = 3 to $2143 \pm 23 \, M^{-1} \, s^{-1}$ at pH = 10. Due to its acidic nature ($pK_a = 8.2$), the degree of dissociation of this pollutant was determined at every pH of work, and the specific rate constants of the un-dissociated and dissociated species were evaluated, being the values of these rate constants 20.1 ± 2.0 and $2.0 \pm 0.3 \times 10^3 \, M^{-1} \, s^{-1}$, respectively. On the contrary, 3-methylindole does not present acidic nature, and therefore, it can be proposed an average value for its rate constant of $4.90 \pm 0.7 \times 10^5 \, M^{-1} \, s^{-1}$ in the whole pH range 3–10. Further experiments were performed to identify the main degradation byproducts (10 mg L^{-1} of contaminants, 0.023 g h^{-1} of ozone). Up to 8 intermediates formed in the ozonation of 3-methylindole were identified by LC–TOFMS, while 6 intermediates were identified in the ozonation of $1H$-benzotriazole. By considering these intermediate compounds, the reaction mechanisms were proposed and discussed. Finally, evaluated rate constants allowed to predict and modeling the oxidation of these micropollutants in general aquatic systems.

© 2014 Elsevier B.V. All rights reserved.

1. Introduction

$1H$-benzotriazole (BZ) and 3-methylindole (ML) are two chemicals that belong to a kind of micropollutants present in waters, usually called "emerging contaminants" (ECs), which at the present times are mostly unregulated or in process to be regulated. The term ECs includes a wide array of different compounds (as well as their metabolites and transformation products): pharmaceuticals and personal care products (PPCPs), pesticides, veterinary products, industrial compounds/by-products, food additives and engineered nano-materials. However, synthesis of new chemicals or changes in use and disposal of existing chemicals can create new sources of ECs [1].

It is recognized that the effluents from municipal wastewater treatment plants (WWTPs) may be a significant source of ECs, because current treatment technologies are very often unable to entirely degrade such persistent substances. Consequently, they are accumulated in aquatic environments [2], and their elimination is currently pursued.

In addition to different kinds of treatments, the use of chemical oxidation procedures can constitute effective technologies for the removal of hazardous pollutants present in waters. Among these oxidation procedures, single oxidants such as UV irradiation, ozone, chlorine, and hydrogen peroxide, or combinations of these oxidants in the Advanced Oxidation Processes (AOPs), such as O_3/H_2O_2, UV/H_2O_2, Fenton/photo-Fenton systems, and UV/TiO_2,

* Corresponding author. Tel.: +34 924289384; fax: +34 924289385.
  E-mail address: javben@unex.es (F.J. Benitez).